European Commission | Horizon 2020 European Union funding for Research & Innovation

Technical Shortfalls for Pan European Power System with High Levels of Renewable Generation

D2.4

EU-SysFlex

PROGRAMME	H2020 COMPETITIVE LOW CARBON ENERGY 2017-2-SMART-GRIDS
GRANT AGREEMENT NUMBER	773505
PROJECT ACRONYM	EU-SysFlex
DOCUMENT	D2.4
TYPE (DISTRIBUTION LEVEL)	☒ Public ☐ Confidential ☐ Restricted
DATE OF DELIVERY	April 2020
STATUS AND VERSION	V0.3
NUMBER OF PAGES	292
Work Package / TASK RELATED	WP2 / Task 2.4
Work Package / TASK RESPONSIBLE	Sheila Nolan (EirGrid) / Hassan Qazi (EirGrid)
AUTHOR (S)	Hassan Qazi (EirGrid), Peter Wall (EirGrid), Jeff Kelliher (EirGrid), Sheila Nolan (EirGrid), David Corcoran (EirGrid), Dianne Favennec (EirGrid), Daniel McSwiggan (SONI), Jacek Wasilewski (PSEi), Artur Mirowski (PSEi), Mateusz Skwarski (PSEi), Josselin Fournel (EDF), Gregorie Prime (EDF), Jussi Ikäheimo (VTT), Hannele Holttinen (VTT), Michał Kłos (NCNR), Endika Urresti Padrón (NCNR), Nuno Fulgêncio (INESCTEC), Carlos Moreira (INESCTEC), Bernardo Silva (INESCTEC), Marius Stiller (INNOGY)

DOCUMENT HISTORY

VERSION	ISSUE DATE	CONTENT AND CHANGES
0.1	18th February 2020	First version
0.2	20th March 2020	Second version - Changes proposed through internal review by Technical Manager
0.3	7th April 2020	Third version – For submission to the PMB
1	20th April 2020	Final version – For submission to the European Commission, minor changes proposed through the review from the PMB.

DOCUMENT APPROVERS

PARTNER	APPROVER
EirGrid	Sheila Nolan WP2 leader
EDF	Marie-Ann Evans Technical Manager
EirGrid, EDF, SONI, VITO, innogy, Elering, EDP, EURACTIV, Zabala	EU-SysFlex Project Management Board
EirGrid	John Lowry, Project Coordinator upon PMB review

TABLE OF CONTENTS

LIST OF FIGURES

LIST OF TABLES

ABBREVIATIONS AND ACRONYMS

AC	Alternating Current
ADN	Active Distribution Network
ADS	Active Distribution System
aFRR	automatic Frequency Restoration Reserve
APE	Automated PLEXOS Extraction tool
ASCC	Automatic Sequencing Short Circuit Calculation
BAU	Business as Usual
BESS	Battery Energy Storage Systems
CCGT	Combined Cycle Gas Turbine
CCT	Critical Clearing Time
CE	Continental Europe
CHP	Combined Heat and Power
DC	Direct Current
DER	Distributed Energy Resources
DR	Distributed renewables
DSM	Demand-Side Management
DSO	Distributed System Operator
EHV	Extra High Voltage
ENTSO-E	European Network of Transmission System Operators for Electricity
EOC	Enhanced Operational Capabilities
EPC	Emergency Power Control
EPSO	Evolutionary Particle Swarm Optimization
ET	Energy transition
EU	European Union
EV	Electrical Vehicle
FCR	Frequency Containment Reserve
FCR-D	Frequency Containment Reserve - Disturbances (in Nordic system)
FCR-N	Frequency Containment Reserve - Normal operation (in Nordic system)
FFR	Fast Frequency Reserve
FRR	Frequency Restoration Reserve
FRT	Fault Ride Through
GG	Going Green
HS	High solar
HV	High Voltage
HVDC	High Voltage Direct Current
IEC	International Electrotechnical Commission
IEEE	Institute of Electrical and Electronics Engineers
LCL	Low Carbon Living
LFG	Landfill Gas
LFSM	Limited Frequency Sensitivity Mode
LFSM-O	Limited Frequency Sensitivity Mode for Overfrequencies
LFSM-U	Limited Frequency Sensitivity Mode for Underfrequencies
LSI	Largest Single Infeed

LVRT	Low Voltage Ride-Through
MARUN	Market Run
mFRR	manual Frequency Restoration Reserve
MV	Medium Voltage
NI	Northern Ireland
OCGT	Open Cycle Gas Turbine
OFGS	Over Frequency Generating Scheduling Scheme
PCC	Point of Common Coupling
PL	Poland
PLL	Phase Lock Loop
POR	Primary Operating Reserve
PPM	Power Park Module
PSAT	Powerflow and Short-circuit Assessment Tool
PSRP	Power System Restoration Plan
PSS	Power System Stabiliser
PST	Phase Shift Transformer
PV	Photovoltaic
RA	Renewable Ambition
RES	Renewable Energy Sources
RES-E	Renewable Energy Sources of Electricity
RfG	Requirements for Generators
RMS	Root Mean Square
RoCoF	Rate of Change of Frequency
SE	Steady Evolution
SGM	Synchronous Power Generating Module
SNSP	Systems Non-Synchronous Penetration
SOR	Secondary Operating Reserve
TSAT	Transient Security Assessment Tool
TSO	Transmission System Operator
TSSPS	Transmission System Security Planning Standard
UC/ED	Unit Commitment and Economic Dispatch
UCTE	Union for the Coordination of Transmission of Electricity
VRES	Variable Renewable Energy Sources
VSAT	Voltage Security Assessment Tool
WP	Work Package
WSAT	Wind Security Assessment Tool

EXECUTIVE SUMMARY

The goal of the EU-SysFlex project is to enable the European power system to integrate, in a secure and sustainable way, high levels of renewable energy sources, and through this meet future decarbonisation objectives, e.g. to enable over 50 % of electrical demand to be met by renewable energy sources. Enabling this transition toward a decarbonised society requires the integration of high levels of variable non-synchronous renewable generation, such as wind and solar, and a significant increase in the electrification of heating and transport.

Work Package 2 of EU-SysFlex deals with identifying the scarcities that will be faced by the European power system when operating with high levels of renewable generation (Task 2.4), evaluating the market issues and financial gaps occurring with these high levels of renewables (Task 2.5), and proposing and assessing viable mitigation strategies for these scarcities (Task 2.6). A scarcity can be loosely defined as a shortage of something that the power system has traditionally had in good supply; for example, inertia is a commonly cited scarcity in high renewable systems. Task 2.1 reviewed state of the art literature to identify the potential scarcities and grouped these into five categories (the sixth category, system adequacy, was addressed in the scenario building task): frequency stability, voltage stability, rotor angle stability, congestion, and restoration, and Task 2.4 followed this structure.

This report describes the detailed technical power system studies performed for Task 2.4 and the scarcities identified. These studies were scenario driven and employed the scenarios developed in Task 2.2 and the models developed in Task 2.3. Each scenario represents a high level vision of the future for the system under study and entails a plant portfolio, network configuration and annual renewable energy generation level. Scenario driven studies capture the variations in system configuration, plant portfolio and system demand by analysing a selected set of representative snapshots for each scenario (intra scenario analysis), where a snapshot is a selected hour of operation that captures an extreme or characteristic element of system operation (e.g. peak demand or peak renewable). Then the results for different scenarios can be compared to perform inter scenario analysis. Intra scenario analysis can be used to assess the conditions under which a scarcity emerges and inter scenario analysis can be used to determine if this scarcity is inevitable or if it is linked to one specific vision of the future.

The varying nature of the synchronous systems considered within EU-SysFlex (Ireland and Northern Ireland, the Nordic system and the synchronised Continental European system) means that not all systems can, or should, be studied for all scarcities. The assessment of scarcities is power system specific. To this end, studies have been performed for the following combinations of system and scarcity: a detailed model of the Ireland and Northern Ireland power system (all scarcities), a detailed model of the Polish transmission system that is connected to an approximate model of neighbouring countries (voltage and rotor angle), a reduced six nodes model of continental Europe (frequency), a simplified frequency stability model of the Nordic system (frequency), and a subset of the Continental European system (congestion).

The high level outcomes of these studies are summarised below. Where appropriate, the scarcities are separated into localised scarcities, which occur for a specific subset of operating conditions, and global scarcities, which occur for almost all operating conditions.

A direct and widely reported consequence of increasing levels of non-synchronous generation (wind and PV - variable RES generation, which is Power Electronics Interfaced to the system) is a decline in power system rotational energy or system inertia, leading to higher RoCoF values. It has been shown for the continental European system that the increase in RoCoF at higher penetration levels is notably more significant for particular parts of the system. Although RoCoF values are generally below 1 Hz/s in most continental Europe countries after a reference incident (-3GW in France, i.e. tripping of the 2 largest nuclear plants, and -2GW in the other zones), there are some cases in the Iberian Peninsula where RoCoF values reach 1.3 Hz/s. Thus, there is a localised scarcity emerging.

Several configurations of system split have also been simulated leading to very high power unbalances, up to 30 GW in some extreme cases. In such conditions, RoCoF higher than 1 or 2 Hz/s can be observed regularly which can endanger severely the continental European power system stability. In the Nordic system no issue related to inertia was identified, with maximum RoCoF of 0.4 Hz/s, although a trend toward reduced inertia was observed. The Ireland and Northern Ireland power system exhibited a clear global inertia scarcity, which was so severe that it had to be managed through a RoCoF constraint of 1 Hz/s in the production cost model before performing other studies.

A second consequence of reduced inertia and increased RoCoF is that frequency containment reserves have less time in which to limit the frequency nadir/zenith to the acceptable range, which can potentially result in a lack of, and therefore a scarcity of, effective reserve. Studies for the Continental European system show that the frequency nadirs after the loss of a large generating unit in each area decrease as penetration levels in the corresponding area increase; however, all nadirs remain above the threshold for load shedding. The Iberian Peninsula is the worst affected, with a nadir of 49.25 Hz for a 2 GW loss for the highest penetration snapshot. It happens because it is less interconnected with the rest of the continental power system, and it has low regional inertia due to the high penetration of non-synchronous generation.

This vulnerability is further exposed under system separation events. As such, there is no global scarcity of reserve at European level for a dimensioning event, but a localised scarcity may emerge due to diminished dynamic coupling. Furthermore, European system split events usually lead to extremely low nadirs. These low nadirs under system split events are not related to any reserve scarcity given that such imbalances can only be managed by defence plan actions such as load shedding or LFSM-O mechanisms. In some cases, especially for both Iberian and Italian splits, the activation of these mechanisms is still insufficient to avoid black out situations.

In the Ireland and Northern Ireland power system a RoCoF limit and a minimum level of fast frequency reserve were incorporated into the production cost model. As such, the two most significant frequency stability scarcities had mitigation applied to them prior to performing the studies. These studies revealed no relationship between penetration levels and frequency nadirs and this is driven by the fact that, in the presence of fast reserves, the nadir is dominated by the volume of fast reserve and not the inertia. Whilst some cases did have nadirs below the load shedding threshold, these cases occurred because of inadequacies in the scheduling of reserve (when existing policy is applied in 2030) and not due to any intrinsic scarcity. These studies have shown the effectiveness of a RoCoF constraint and fast reserve in mitigating scarcities in Ireland and Northern Ireland. Studies for the Nordic system indicated no scarcity in reserve.

The Polish and Ireland & Northern Ireland power systems, for which steady state voltage regulation was studied, exhibit a scarcity at higher non-synchronous renewable penetrations. In addition to this, the Ireland and Northern Ireland system exhibits a clear deterioration of fault levels and a dynamic voltage regulation scarcity. However, it is to be noted that the model utilised for the Continental European system is characterised by various levels of modelling detail for various regions, with the Polish system modelled with a high level of detail. Furthermore, the cases analysed have been pre-selected using various criteria such as minimum inertia, minimum reactive margin and maximum load across various component regions, as opposed to analysing all potential system configurations. The levels of RES for a specific system operating condition differ across the various sub-systems of continental Europe. Therefore a lack of potential scarcity can either be due to the snapshot selection approach, modelling deficiencies, choice of the representative system within continental Europe or the level of variable renewable generation considered.

Rotor angle stability analysis has been carried out for the Continental Europe (using the detailed model of the Polish system) and Ireland and Northern Ireland power systems. The analysis was based upon time domain simulations of a short circuit event and stability was assessed using rotor angle deviations, critical clearing times and oscillation damping. The studies performed show no scarcity in stability margin in either system, when assessed through critical clearing times for faults that are cleared by primary protection operation. However, a localised scarcity exists when certain faults are cleared by the slower backup protection. These cases are driven by specific combinations of contingencies, unit commitments and the generator's pre-fault conditions and not the overall penetration level. Furthermore, it should be noted that in these studies it is assumed that the fault current observed would be sufficient for protection relays to pick up, i.e. the protection relay is not modelled and breakers are simply opened by predefined simulation events. With the scarcity in short circuit current reported here, this assumption should be verified and where necessary, protection settings/design may need to be modified or minimum fault currents ensured. Therefore, an effective action for this scarcity in stability margin is to mitigate the localised scarcity of short circuit current through a system service.

Oscillation damping presents a global scarcity in both the Continental European studies and the Ireland and Northern Ireland studies. This scarcity does not correlate to vRES penetration level and may be particularly worthy of further study as system models tend to have higher damping than reality. Furthermore, the study

performed for the Continental system did not capture the impact of this reduced damping on inter-area oscillations. As such modes of oscillation are already known to exist in the Continental system, the impact of this damping scarcity on these modes should be assessed in the future, as poorly damped inter area modes can contribute to system separation events. This scarcity can be mitigated by developing a damping requirement and associated system service, which would ensure that the system had appropriate damping at a range of frequencies of oscillation.

The Ireland and Northern Ireland system was assessed for a scarcity in synchronising torque and a small subset of contingencies exhibited angular instability that caused a generator to slip a pole. This reveals a localised scarcity in synchronising torque and occurred regardless of scenario, with no relationship to penetration level. No global scarcity was observed in the Ireland and Northern Ireland studies (which would manifest as inter area oscillations and in the worst case system separation) and the system has no particular recent history of exhibiting such behaviour. This scarcity could be mitigated through a service that ensures any generator synchronised to the system had a sufficient level of synchronising torque to the other generators synchronised to the system.

Congestion was assessed from two perspectives; unscheduled flows in the Continental European system and thermal congestion in the Ireland and Northern Ireland power system. Studies for a subset of the continental European system identified that with increasing renewable penetration levels there is a scarcity in managing these unscheduled flows. This scarcity is driven by the tendency for renewable energy sources to be localized in particular parts of the system, which increases the likelihood of loop flows occurring when these localised resources serve remote domestic demand. Without mitigation, this scarcity is likely to cause unscheduled flows on certain corridors to exceed the acceptable level of 30 % of capacity. The study of congestion for the Ireland and Northern Ireland system assessed the N-1 loading of transmission assets and revealed a global scarcity in thermal capacity that is also driven by the location of renewable energy sources. Specifically, many renewable energy sources are installed in parts of the system where there was traditionally little generation or demand and, as such, sufficient transmission infrastructure is not in place to transfer the generated power to load centres. Overloads are observed at low penetration levels and the occurrence and magnitude of thermal overloads increases with penetration level. These scarcities could be mitigated through a service that incentivises real-time power flow control resources or where justifiable construction of new transmission assets.

Power system restoration is a critical function that operators must provide to ensure that a system can recover from catastrophic failure. The restoration plan for Ireland and Northern Ireland was assessed and it was concluded that, whilst several black start units will be decommissioned, there will be sufficient black start units to support bottom up restoration plans and there will be new voltage source HVDC interconnectors that can provide additional sources for top down restoration. However, the availability of black start units must be managed more actively to mitigate the risk of delayed restoration, due to the increased likelihood that black start units will be cold or off. Furthermore, its cranking paths must be reassessed due to the loss of multiple target generators, which are synchronous machines that support the restoration process. The opportunity exists to replace some of these target generators with non-synchronous resources or storage, which would require more variable and

flexible restoration plans to manage the variability of these resources. Restoration plans were not assessed for the other synchronous areas under study as all scenarios indicated a high level of black start resources would still be available.

Whilst scarcities are more clearly apparent for the Ireland and Northern Ireland power system than in the Continental European system, it does not mean the absence of technical scarcities in Continental Europe. The appearance (or otherwise) of scarcities for the Continental system is highly influenced by the focus area (Poland in this Task), snapshots, variable renewable penetration levels and contingencies. Furthermore, the reduced model used here may not capture the complex interaction between the focus area and the rest of the Continental system for certain parts of the analysis presented (e.g. transient stability or inter area oscillations). In addition, dedicated studies showed that Continental Europe is particularly at risk when system splits occur, especially when inertia is low and cross-border flows prior to events are high. However, the probability of such events, induced by cascade disconnections of interconnectors between two European blocks, is low and should be assessed, in particular when these disconnections correspond to DC interconnectors (HVDC lines).

The analysis of the Continental European and Nordic systems clearly demonstrate technical scarcities associated with certain domains of system stability (e.g. voltage control), while highlighting emerging scarcities for others (e.g. frequency control and congestion). These scarcities are indicators of the evolution of system needs due to changes in the system generation portfolio and the stress this will place upon existing operational practices and policies. These scarcities are more evident for the Ireland and Northern Ireland system, which manifest technical scarcities across multiple categories of system stability for the scenarios analysed, and in the case of frequency stability required pre-emptive mitigation to enable worthwhile studies. The mitigation measures applied for these frequency stability studies are an example of how effective mitigation can be implemented through appropriate constraints and the design of appropriate and targeted system services, underpinned by appropriate financial and regulatory arrangements. The extent of the effectiveness of such services will be examined in Task 2.6.

1. INTRODUCTION

The EU-SysFlex project seeks to enable the European power system to integrate high levels of renewable energy sources and to meet future power system decarbonisation objectives. One of the primary goals of the project is to examine the pan-European power system with at least 50% of electricity demand on an annual basis being met by renewable energy sources (RES-E). The transition towards a decarbonised power system considers increasing levels of variable non-synchronous renewable technologies such as wind and solar.

In the context of the EU-SysFlex project, high levels of renewable generation are considered to be installed thereby meeting at least 50% of the total annual electricity demand. As hydro power potential has largely been deployed in many regions, and biomass growth is limited by supply constraints and sustainability concerns, much of the growth in renewable energy is assumed to come from variable non-synchronous renewables in the EU-SysFlex scenarios. In addition to developments in renewable electricity, there is also a trend towards sector coupling with, for example, increased electrification of heat and transport, which is seen to be an enabler of the power system transition. While this is clearly an advantage and an opportunity, this can also create challenges for the transmission and distribution networks. Distribution networks in particular were not designed for accommodating embedded generation and this can lead to the need for expensive infrastructure investment.

Transitioning from power systems which have traditionally been dominated by large synchronous generating units to power systems with high levels of variable non-synchronous renewable technologies has been shown to result in technical challenges for balancing and operating power systems safely and reliably. This is due to the non-synchronous nature of renewable technologies as well as the variable nature of the underlying resources.
Work package 2 (WP2) is focussed on the development of new approaches for system operation with high levels of variable output renewable generation resources. The first output of WP2 was Deliverable 2.1 [1] which detailed the outcomes of a comprehensive review of the literature. A number of key potential technical scarcities associated with integration of variable non-synchronous generation and the associated displacement of conventional synchronous generation were identified. These scarcities, if not mitigated, could severely impact the security and stability of the power system of the future. Addressing and mitigating these scarcities is at the heart of the EU-SysFlex project.

WP2 forms a crucial starting point for the EU-SysFlex project. It entails detailed technical power system simulations of the European power system with high levels of renewable generation as well as high levels of electrification, with a view to identifying potential technical scarcities. This is supplemented by financial & economic analysis of various scenarios that form the basis of the technical analysis. Task 2.4 deals with the detailed technical analysis to identify scarcities in high renewable energy-based power systems.

1.1 TASK 2.4 WITHIN EU SYSFLEX

As mentioned above, the first deliverable of WP2 was completed as a literature review of System Scarcities at high levels of renewable generation [1]. Deliverable 2.1 divided the technical scarcities from the literature into a number of categories (the sixth category identified, system adequacy, is not analysed within T2.4):

- Frequency stability
- Voltage stability
- Rotor Angle stability
- Network Congestion
- System Restoration

These five categories provide a general framework within which technical scarcities and challenges are being assessed in detail in Task 2.4. However, to perform a robust and detailed technical analysis, it was first necessary to develop scenarios and models. Thus, Task 2.2 defined a set of pragmatic and ambitious scenarios for renewable generation deployment in Europe [2], while Task 2.3 developed detailed models to simulate technical scarcities on the European system.

Task 2.2 defined central Core Scenarios as well as Network Sensitivities [2]. The Network Sensitivities are additional scenarios that are complementary and supplementary to the Core Scenarios and are used to assess more specific technical scarcities in certain part of the European power system.

In Task 2.3, detailed models developed and methodologies specified to enable the assessment of technical scarcities. These included Unit Commitment and Economic Dispatch (UC/ED) models, frequency stability models, network models and a suite of tools for performing quasi steady-state and time domain simulations. Furthermore, the study settings, stimuli and snapshot selection were also dealt with in Task 2.3.

Task 2.4 employs the scenarios and the models to perform detailed simulations to determine the technical shortfalls of future power systems. In addition to identification of technical scarcities in future power systems, WP2 also seeks to perform techno-economic analysis using production cost modelling to assess, among other things, the levels of revenues available to fund large scale deployment of renewables. This takes place in Task 2.5.

The outcomes of Task 2.4 in terms of technical scarcities at high renewable generation levels provide input to a number of other critical aspects, necessary for secure system operation. These aspects include the mitigation measures for the identified technical scarcities (Task 2.6), system service product/market design to deploy system services within the regulatory framework (WP3). Task 2.4 is therefore critical to be able to formulate an over-arching future roadmap to enable power system decarbonisation.

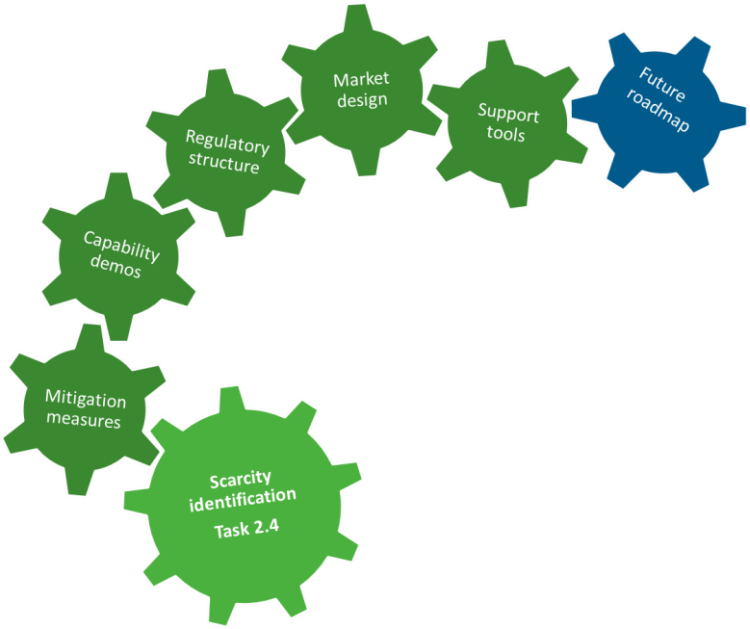

FIGURE 1-1: OVERVIEW OF TASK 2.4 WITHIN SYSFLEX PROJECT

1.2 SCOPE & OBJECTIVE

The main objective of Task 2.4 is to perform detailed technical analysis to assess the potential existence of the technical scarcities, within the framework outlines by literature review in Task 2.1, in a 2030 power system with high levels of renewables.

1.3 REPORT OUTLINE

The report starts with a brief review of the generic methodology used for all types of analysis, and provides sufficient context for the reader to comprehend the results presented in subsequent chapters. Chapter 2 to Chapter 6 entail analysis on specific categories of system stability, with a view towards identifying relevant technical scarcities. For each of these chapters, subsections are created to present the results relevant to the system (Continental Europe, Ireland & Northern Ireland, and Nordic). Chapter 2 focusses on frequency stability, Chapter 3 deals with voltage stability (steady state & dynamic), and analysis and results relevant to rotor angle stability are presented in Chapter 4, followed by Congestion and system restoration in Chapter 5 & 6. Chapter 7 presents the overall conclusions of the report.

1.4 METHODOLOGY

The philosophy of the analysis conducted in EU-SysFlex project under Task 2.4 is underpinned by an investigation of potential scarcities in 2030 on the pan-European system. The uncertainty regarding system configuration, plant portfolio and system demand has been catered for, through analysing multiple scenarios for each category of system stability. In order to ensure the evaluation of a wide variety of potential system snapshots, while

considering computational efficiency, the most relevant snapshots that highly susceptible to potential system scarcities are identified. Based on the computational requirements owing to the models and analysis type, all possible snapshots or a subset of most interesting snapshots has been evaluated. Using specific individual stimuli for each type of analysis, the simulations have been conducted. Finally, the outcome of individual studies have been analysed and evaluated against stability indices detailed in deliverable 2.3, within the context of model limitations to draw conclusions regarding the technical scarcities of the system, as shown in [3].

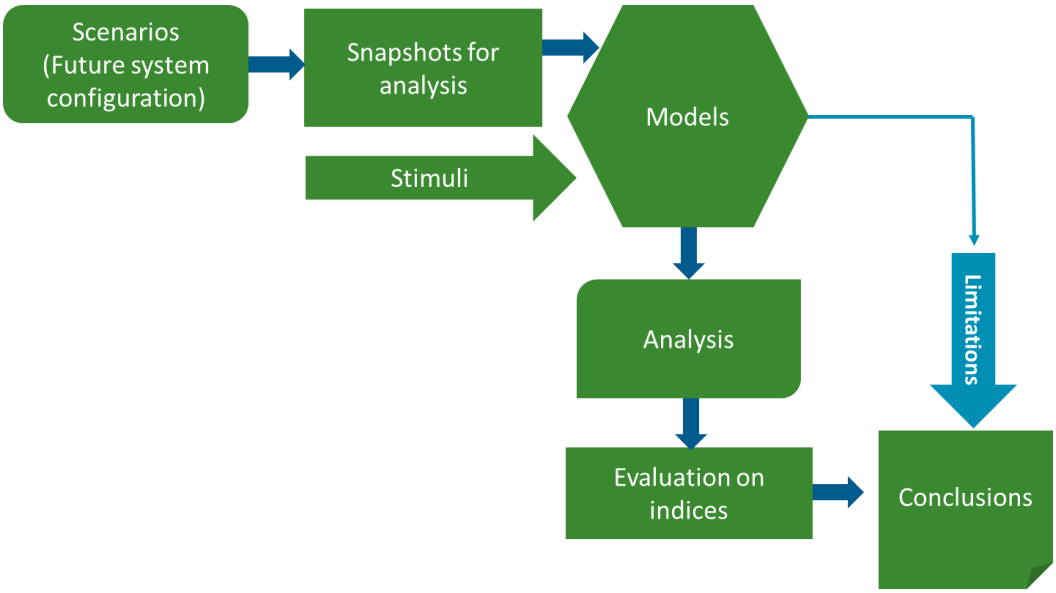

FIGURE 1-2: HIGH LEVEL OVERVIEW OF GENERIC EVALUATION METHODOLOGY

A brief description of the scenarios, snapshots, stimuli and analysis setup for every jurisdiction of 2030 pan-European system are described below.

1.5 EVALUATED SCENARIOS

The scenarios represent high level visions of each evaluated jurisdiction of the pan-European power system. Each scenario entails a plant portfolio, network configuration and annual renewable energy generation level (as represented by the fraction of system load met by renewable energy sources (RES-E)). Two core scenarios were developed for the EU-SysFlex project: Energy Transition with over 50% RES over Europe and Renewable Ambition over 60% RES, additional scenarios were added to study the impact on specific systems. With the exception of system restoration, each category of system stability has been assessed across various power systems, while the evaluated scenarios also differ across the categories. The variation in scenarios represents most relevant scenarios to be investigated for respective power systems and stability categories. For example, the LCL scenario (Low Carbon Living) for Ireland and Northern Ireland system entails >70% RES-E levels, in line with the 2030 renewable energy targets for this system, while SE (Steady Evolution) has lower RES-E levels, thereby enabling a useful comparison for the system level impacts of decarbonisation. Further details, regarding the scenarios shown in Table 1-1, are available in deliverable D2.2 [2]. In view of the level of detail used for the analysis regarding the

Ireland and Northern Ireland power system for D2.4, the analysis is focussed on the LCL & SE scenarios as opposed to the two core scenarios.

TABLE 1-1: OVERVIEW OF EVALUATED SCENARIOS

Category	Power System	Evaluated scenarios
Frequency Stability and Control	Ireland & Northern Ireland	Low carbon living (LCL) Steady evolution (SE)
	Continental Europe	Energy transition (ET) Renewable ambition (RA)
	Nordic system	Energy transition (ET) Renewable ambition (RA) High solar (HS)
Voltage Control	Ireland & Northern Ireland	Low carbon living (LCL) Steady evolution (SE)
	Continental Europe	Energy transition (ET) Going Green (GG) Distributed renewables (DR)
Rotor Angle Stability	Ireland & Northern Ireland	Low carbon living (LCL) Steady evolution (SE)
	Continental Europe	Energy transition (ET) Going Green (GG) Distributed renewables (DR)
Congestion	Ireland & Northern Ireland	Low carbon living (LCL) Steady evolution (SE)
	Continental Europe	Energy transition (ET) Going Green (GG) Distributed renewables (DR)
System restoration	Ireland & Northern Ireland	Low carbon living (LCL)

1.6 STIMULI & ANALYSIS METHODS

The analysis conducted under Task 2.4 focusses primarily on load flow studies, time domain simulations and critical analysis of pre-existing operation practices. Various categories of system stability are evaluated in accordance with one of the aforementioned analysis methods. Furthermore, a large number of system snapshots has been analysed in majority of individual analysis categories; however where applicable, the analysis has been limited to selected system snapshots for computational efficiency reasons. The individual snapshots for analysis, where applicable are selected in a systematic manner to reveal potential technical scarcities at higher levels of renewable generation, details regarding snapshot selection are given in the relevant sections of this report. Table

1-2 provides an overview of stimuli, analysis methods and study types considered. Further details on the rationale for consideration of various study types, analysis methods and stimuli is provided in deliver D2.3 [3].

TABLE 1-2: OVERVIEW OF STIMULI AND ANALYSIS METHODS

Category	Power System	Stimuli & analysis method	Study type
Frequency Stability and Control	Ireland & Northern Ireland	Time domain simulation - Loss of infeed - Loss of outfeed/export Economic dispatch analysis	Every 7th hour across the year Every hour across the year
	Continental Europe	Time domain simulation - Interconnected incidents - System splits	Every hour across the year
	Nordic system	Time domain simulation - Interconnected incidents	Every hour across the year
Voltage Control	Ireland & Northern Ireland	Load flow analysis: - Intact system - N – 1 faults Time domain simulation: - Short circuit faults	Every hour across the year Selected snapshots
	Continental Europe	Load flow analysis: - Intact system - N – 1 faults Time domain simulation: - Short circuit faults	Selected snapshots Selected snapshots
Rotor Angle Stability	Ireland & Northern Ireland	Time domain simulation: - Short circuit faults	Selected snapshots
	Continental Europe	Time domain simulation: - Short circuit faults	Selected snapshots
Congestion	Ireland & Northern Ireland	Load flow analysis: - Intact system - N – 1 faults	Every hour across the years
	Continental Europe	Load flow analysis: - Intact system	Selected snapshots
System restoration	Ireland & Northern Ireland	Assessment of restoration plan	N-A

1.6.1 SNAPSHOT SELECTION

1.6.1.1 CONTINENTAL SYSTEM VOLTAGE AND TRANSIENT STABILITY EVALUATION

Three generation capacity scenarios have been considered in the voltage and transient stability studies. In conjunction with EU-SysFlex Energy Transition[1], two Network Sensitivities have been taken into account – Going Green and Distributed Renewables [2] [3].

The operational snapshots on national level have been found with the use of EDF CONTINENTAL model and consider the following three criteria:

- Minimum inertia in the power system (abbreviation ““Min_Inertia”” is used in further part of report)
- Maximum power demand (abbreviation “Max_Load” is used in further part of report)
- Minimum power reactive margins for the synchronous generation (abbreviation “Min_Reactive” is used in further part of report).

The following sets (perimeters) of countries have been considered in order to find particular operation snapshots:

Poland (abbreviation “/1” used in further part of report)
Poland and Germany (abbreviation “/2” used in further part of report)
Poland, Germany, Austria, Czech Republic, Slovakia and Hungary (abbreviation “/3” used in further part of report)
All countries in CE, only for “Min_Inertia” and Max_Load (abbreviation “/4” used in further part of report)
An additional snapshot has been obtained meeting the criterion of maximum SNSP (“Max_SNSP”) in the whole CE (“/4”).
Selected and aggregated data obtained from EDF’s Unit Commitment Model for Energy Transition capacity scenario are shown in Annex: Table 11-1 - Table 11-4. The annual FCR and aFRR values forecasted in 2029/2030 are presented in Annex: Table 11-5.
Looking at the dispatching results in the national level for Energy Transition capacity scenario one can observe that:

- Minimum of inertia occurs in different days when different perimeter is considered. For PL the snapshot occurs in one of January nights, while for wider perimeter, the operation scenario represents an hour in June. In total, three snapshots have been taken into consideration;
- Maximum of load occurs almost in the same time moment (end of November in afternoon) for all considered perimeters. In total, two snapshots have been taken into consideration;
- Minimum of reactive power margin in synchronous generation occurs in PL in same time as minimum of inertia. In total, two snapshots have been taken into consideration;

[1] An attempt has been made to extrapolate the results from EU-SysFlex Energy Transition core scenario and its network sensitivities to the conditions determined in Renewable Ambition scenario.

- Maximum $SNSP$ in CE equals 62.4% and it has been obtained for the noon in one of June's day. Just one snapshot has been taken into consideration.

TABLE 1-3: SUMMARY OF STUDY CASES ANALYSED IN VOLTAGE AND TRANSIENT STABILITY STUDIES FOR THE SUB-NETWORK OF THE PAN-EUROPEAN POWER SYSTEM

Criterion \ Perimeter	PL (1)	PL+DE (2)	PL+DE+AU+CZ+SK+HU (3)	all CE (4)
Energy Transition				
maximum load	ET/Max_Load/1	ET/Max_Load/2/3/4		
minimum inertia	ET/"Min_Inertia"/1	ET/"Min_Inertia"/2	ET/"Min_Inertia"/3/4	
minimum power reactive margins for the SGM	ET/Min_Reactive/1/2		ET/Min_Reactive/3/4	
Going Green				
maximum load	GG/Max_Load/1	GG/Max_Load/2/3/4		
minimum inertia	GG/"Min_Inertia"/1	GG/"Min_Inertia"/2	GG/"Min_Inertia"/3/4	
minimum power reactive margins for the SGM	GG/Min_Reactive/1/2		GG/Min_Reactive/3/4	
Distributed Renewables				
maximum load	DR/Max_Load/1	DR/Max_Load/2/3/4		
minimum inertia	DR/"Min_Inertia"/1	DR/"Min_Inertia"/2	DR/"Min_Inertia"/3/4	
minimum power reactive margins for the SGM	DR/Min_Reactive/1/2		DR/Min_Reactive/3/4	
maximum $SNSP$	DR/Max_SNSP/4 (extra case considered only in rotor angle stability studies)			

In total, twenty-one basic study cases (including considered capacity scenarios, snapshots and perimeters) have been prepared to further study the voltage control and rotor angle stability issues. The case based on maximum $SNSP$ has been treated as an extra-case and foreseen to consider only in the rotor angle stability studies. All the analysed study cases are summarised in Table 1-3.

1.6.1.2 CONTINENTAL SYSTEM CROSS BORDER CONGESTION MANAGEMENT

The same study cases as in the previous section 1.6.1.1 were examined for the cross border congestion management analysis except for the maximum $SNSP$ case.

1.6.1.3 IRELAND AND NORTHERN IRELAND POWER SYSTEM DYNAMIC VOLTAGE AND TRANSIENT STABILITY EVALUATION

Due to a large number of snapshots constituting the two scenarios under consideration, running dynamic simulations with a complete dynamic model and using a large number of contingencies for analysis becomes computationally intensive. In order to maximise the benefits of such an analysis, the most relevant snapshots across the two scenarios have been identified for further analysis. The choice of snapshots should be dictated by the variation of factors that are most likely to influence transient stability. Here, the factors selected are the three most significant factors that are the basis of constraints under existing operational policy but are not constrained in the cases studied here:

1) SNSP level: SNSP level indicates the fraction of generation which is comprised of renewable generation devoid of inherent synchronising torque capability. Traditionally higher SNSP level is likely to yield a more vulnerable snapshots. It is however to be noted that the SNSP level does not represent the system load level. For an identical SNSP level, the available synchronising torque from conventional generation can vary significantly, if the load levels are non-identical. It can therefore be concluded that SNSP level alone is not a sufficient indicator of potential transient stability issues.

2) System inertia: As indicated previously, for an identical level the generation inertia can vary. Inertia and system load is particularly important for transient stability, as the critical clearing time for a unit is highly influence by the inertia of such unit. Traditionally in a single machine infinite bus configuration a higher inertia level is indicative of a slower acceleration resulting in a reduced area of acceleration, thereby making it more likely to maintain synchronism. Similar to SNSP level, system inertia alone is not an adequate measure of likely transient stability, as lower inertia levels can correspond to lower system load and hence lightly loaded units and less stressed system.

3) Location of synchronous generation: The electrical distance between various synchronous generations is an indicator of available synchronising torque in the system, with higher synchronising torque resulting in better transient stability. A better dispersion of synchronous units across the system yields better reactive injection during a fault, thereby reducing resulting in an improved dynamic voltage support during a fault, and directly influencing the transient stability.

The first two criteria are simple to apply as they are measureable, system level values. In contrast, a single value cannot be applied to the location of synchronous generation; existing policy on ensuring appropriate dispersion is

instead a complex set of rules on appropriate running arrangements that are sensitive to topology and demand levels. Here, the total number of units in Dublin and Northern Ireland is used as a rough measure of the dispersion of synchronous units, as these are two remote load centres in the All Island system.

Based upon these three measures, snapshots can then be selected to reflect the extremes within the range of possible combinations of each measure. The preferred means by which to do this is to define high and low limits for each measure and then select a subset of the hours that reflect the eight combinations of high and low for each of the three measures. Each of these combinations is a different 'type' of case and the analysis presented in this report is grouped by type, as presented in Table 1-4.

Given the variation in each measure between the scenarios, the high and low limits are not consistent between the scenarios. Instead, each scenario has its own high and low limits, to ensure the range of extremes is reflected and these are discussed in the following section. This variation does mean that the types for each scenario are not directly comparable and the degree of variation is discussed in the comparison section.

TABLE 1-4: GROUPING OF SNAPSHOTS FOR ANALYSIS

Type ID	SNSP level	Units in NI & Dublin	Inertia
Type 1	Low	High	High
Type 2	High	Low	Low
Type 3	Low	Low	Low
Type 4	Low	High	Low
Type 5	Low	Low	High
Type 6	High	High	High
Type 7	High	High	Low
Type 8	High	Low	High

Snapshots were selected and grouped by type by applying high/low limits to each measure, with 5 snapshots selected to represent each type for each scenario (with the exception of Type 7 for low carbon lining where only one snapshot complied to the requirements. The selection of snapshots across the two considered scenarios is visualised in Figure 1-3 & Figure 1-4. Further details regarding the selected snapshots across the two scenarios are given in ANNEX I.

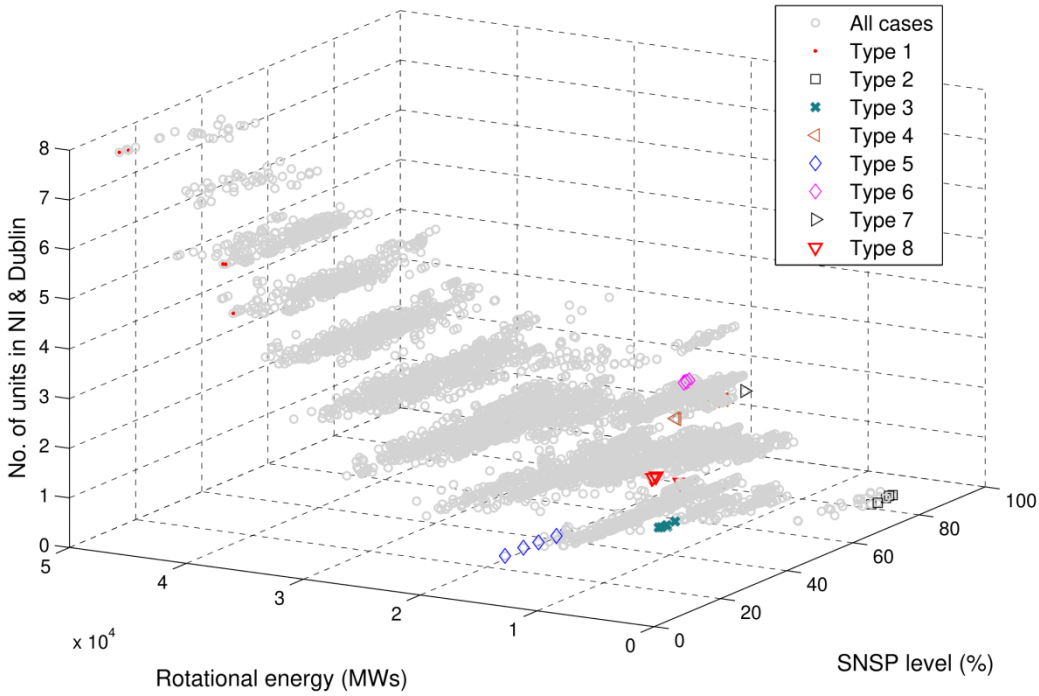

FIGURE 1-3: LOW CARBON LIVING SCENARIO - SNAPSHOT GROUPING BY TYPE

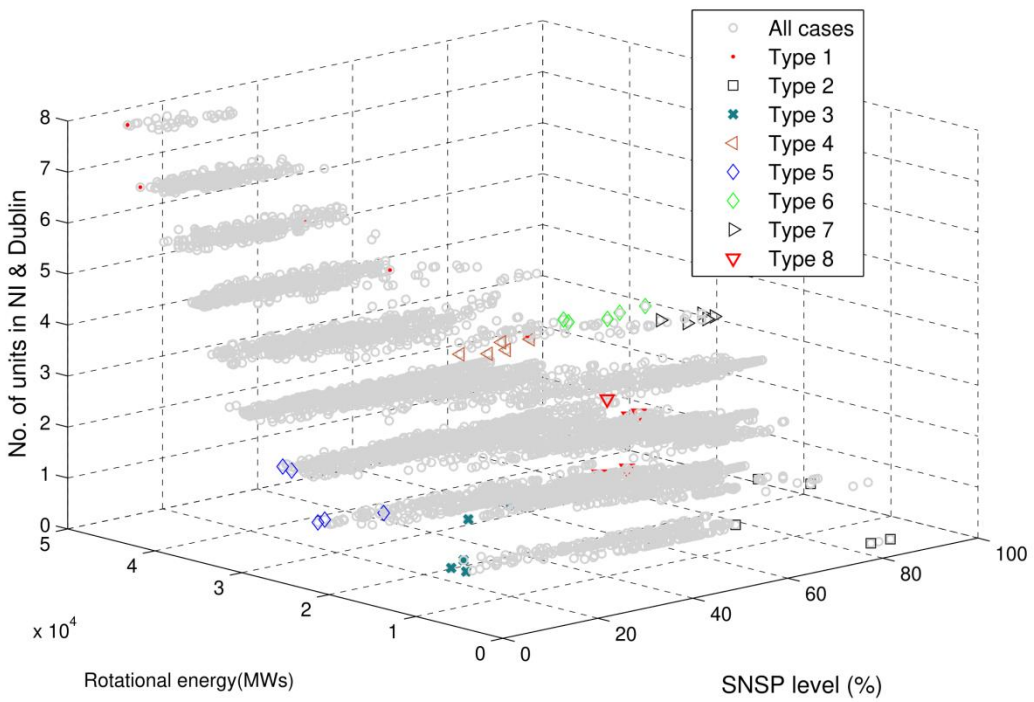

FIGURE 1-4: STEADY EVOLUTION SCENARIO - SNAPSHOT GROUPING BY TYPE

2. FREQUENCY STABILITY & CONTROL (CONTINENTAL EUROPE, IRELAND AND NORTHERN IRELAND, AND NORDIC POWER SYSTEMS)

Frequency stability is the ability of a power system to maintain steady state frequency, following a severe system event, resulting in a significant imbalance between generation and load [4]. Large imbalances are caused by severe system disturbances, such as large load or generation tripping, tripping of HVDC interconnectors, or system splits. It is anticipated, and it has been acknowledged in the literature and in Deliverable D2.1 of EU-SysFlex [1], that frequency stability will decline in the future with the transition to a power system with high levels of non-synchronous renewables. This section explores the frequency stability of first the Continental, or pan European power system, followed by the Nordic power system and finally the Ireland and Northern Ireland power system.

2.1 CONTINENTAL EUROPE

2.1.1 FREQUENCY STABILITY TIME DOMAIN SIMULATIONS

Several assumptions and limitations need to be highlighted, as they could impact the results analysis:

- Only six electrical nodes are considered in PALADYN, which is not sufficient to precisely calculate the power flows exchanged between European zones. Furthermore, the impedances that link the six zones are based on the current grid, and not on prospective detailed Continental Europe power system models.
- Voltage and reactive power are not considered, due to the DC approximation. However, after an incident such as the loss of a generation unit, the voltage experiences large local variations, which can impact frequency (for example, loads could react to voltage variations, leading to a frequency deviation). This effect is not captured by PALADYN, which supposes that at a Continental Europe scale, the local variations of voltage after an incident can be neglected. This hypothesis may not be valid on system split configurations for the small separated zones.
- PALADYN considers a limited number of generation technologies, and provides an average dynamic response. A better accuracy would be reached using a single model for each unit/plant.
- An assumption is made that storage and VRES dynamic response follow FCR requirements, meaning that half of the reserve is delivered in 15 seconds, and all the reserve in 30 seconds. This choice was made because there is no incentive today to provide a faster response. Therefore, the storage and VRES owners are not required to use the full potential of their resources in providing this fast response.
- There are still in Continental Europe large volumes of decentralized generators (mainly wind and solar) which have frequency disconnection settings in ranges between 49.5 Hz and 50.5 Hz [5]. These settings are far from the RfG targets (47.5 Hz and 51.5 Hz) and therefore endanger the system in case of large frequency deviations. This issue is supposed to be resolved in the long term and is not taken into account in that study.

- In all the presented simulations, system splits imply the disconnection of both AC and DC interconnectors, which could be deemed as a pessimistic assumption. Indeed, DC links could be controlled in order to remain connected in case of system splits. This possibility could reduce drastically the severity of the splits consequences and is to be thoroughly explored.

In order to assess the impacts of resultant energy imbalances on the power system, Normative Incidents have been defined by ENTSO-E, one for interconnected operation and one for system split. These are employed here for assessing the frequency stability of the Continental power system and are defined as follows:

- Interconnected operation: The reference incident for interconnected operation in Continental Europe is the tripping of two of the largest generating facilities connected to the same busbar. The reference incident, which defines the required primary reserves in the system, is 3 GW. Many years of interconnected operation show that this normative contingency is appropriate. No load shedding is allowed during the normal system operation [6].
- System split: As system splits are not predictable, the size of the islands and the amount of the imbalance may vary considerably. Future system reinforcements and deployment of generation technologies will increase the power exchanges throughout Europe. As a result, a system split could lead to higher imbalances. From this perspective, the maximum RoCoF criteria could be set to 2 Hz/s by ENTSO-E. System split scenarios have been identified by ENTSO-E as the most severe events [6], compared with tripping of loads, HVDC-links, and generation during interconnected operation.

PALADYN is used in EU-SysFlex Task 2.4 to simulate both reference incidents for interconnected operation and system splits with several zones having to absorb high imbalances for the Continental European power system. Each Normative Incident is assessed and reported separately, below. The key indicators for this part of the analysis are the frequency nadir and zenith, the RoCoF, and the frequency rise/drop duration index. For each Normative Incident, each of these indicators is dealt with individually.

2.1.1.1 INTERCONNECTED INCIDENTS

The reference incident corresponds to the loss of the two largest generation units in a zone. In most zones, except France, the largest generating unit has installed capacity of around 1 GW. In France, the largest generation unit averages 1.5 GW. Therefore, in the PALADYN simulations, incidents of 2 GW were simulated everywhere, and additional 3 GW incidents were simulated for France only. The “Balkans + Turkey” zone is modelled with historical data, as it did not seem relevant to achieve dynamic simulations in this perimeter. Consequently, the resultant number of simulations is more than 87600 simulations[2].

[2] 5 zones × 8760 hours × 2 scenarios ≈ 87600 simulations

2.1.1.1.1 ANALYSIS OF FREQUENCY NADIR VALUES

Firstly, the Energy Transition scenario was simulated (around 50,000 simulations). To assess the impact of vRES penetration on the frequency nadir values, a classification of the results is given. The mean frequency nadirs are given for each zone and for each range of System Non Synchronous Penetration (SNSP). The SNSP is calculated as follows:

$$SNSP(\%) = \frac{Non\ Synchronous\ Generation + Net\ Interconnector\ Imports}{Demand + Net\ Interconnector\ Exports}\ x\ 100 \qquad \text{(Eq. 2-1)}$$

The results are given in Table 2-1. From this table, several observations are made:

- Firstly, the behaviours of zones are different. In the Iberian Peninsula, and to a lesser extent in Italy, the mean nadir values are much lower than the other zones. This can be explained by the fact that these zones have lower inertia, and they have low levels of interconnection with the rest of Europe.
- For the "weakest" zones, the impact of SNSP on nadir values is visible: in Iberian Peninsula, the frequency drop is 60% higher (in average) when the SNSP value is above 80%, compared to SNSP values under 10%. In the strongest zones, the impact of SNSP is not visible: these zones are highly interconnected and maintain sufficient inertia levels.

TABLE 2-1: ENERGY TRANSITION SCENARIO - MEAN NADIR VALUES [HZ] FOR THE LOSS OF 2 GW IN EACH ZONE, DEPENDING ON THE RANGE OF SNSP

Level of SNSP [%]	Iberian peninsula	France	Germany + neighbours	Poland + neighbours	Italy
[0%; 10%]	49.80	49.86	49.87	49.86	49.85
[10%; 20%]	49.79	49.86	49.87	49.86	49.85
[20%; 30%]	49.77	49.87	49.87	49.,86	49.85
[30%; 40%]	49.75	49.87	49.87	49.86	49.85
[40%; 50%]	49.74	49.87	49.87		49.84
[50%; 60%]	49.74	49.87	49.87		49.84
[60%; 70%]	49.74		49.87		
[70%; 80%]	49.71		49.87		
[80%; 90%]	49.68				
[90%; 100%]					

Figure 2-1 and Figure 2-2 show the impact of SNSP and load (or demand) on frequency nadir values in Iberian Peninsula and in France, respectively, for each hour of the year. The red dots correspond to the lowest frequency nadir values observed. While they nadir values correspond to hours with high SNSP in the Iberian Peninsula, nadir values are more correlated with load in France. High loads imply that there is a large number of generating units

online providing electricity. On the contrary, in periods of low demand, only a few units are online (excluding import and export). In zones with a high levels of renewables (such as the Iberian Peninsula), during periods of low demand and high SNSP, there are only a few synchronous machines remaining on the system. Therefore, the inertia of the system is very low. In addition, as the Iberian Peninsula is weakly connected to the rest of the system, it does not take advantage of quick power contributions from other zones. This leads to low nadir values under those conditions. In zones with less capacity in variable renewables (such as France), the maximal SNSP values are around 55%. At these levels of SNSP, similar to the Iberian Peninsula, periods of low demand are the worst cases because the local inertia is lowest.

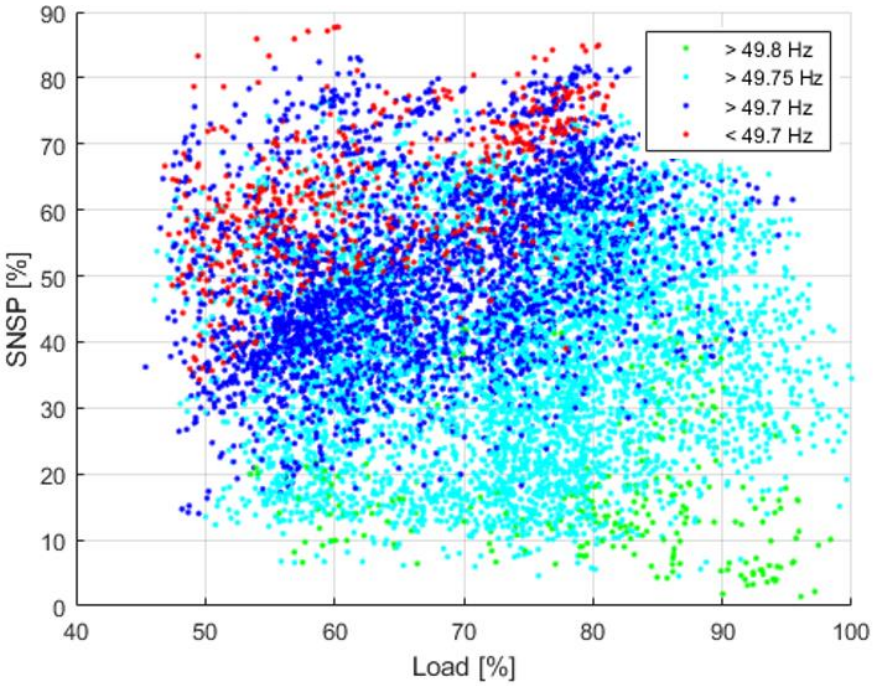

FIGURE 2-1: ENERGY TRANSITION SCENARIO - 2 GW INCIDENT IN IBERIAN PENINSULA, IMPACT OF LOAD AND SNSP ON NADIR VALUES

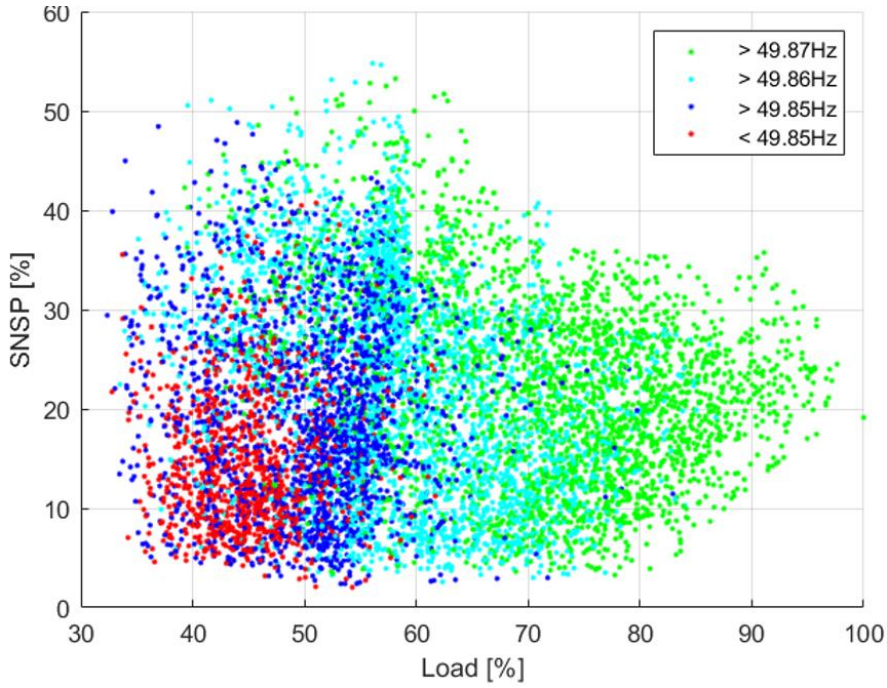

FIGURE 2-2: ENERGY TRANSITION SCENARIO - 2 GW INCIDENT IN FRANCE, IMPACT OF LOAD AND SNSP ON NADIR VALUES

In France, the 3 GW incident was also simulated. It leads to the same observation, however with lower frequency nadir values. This is shown in Figure 2-3.

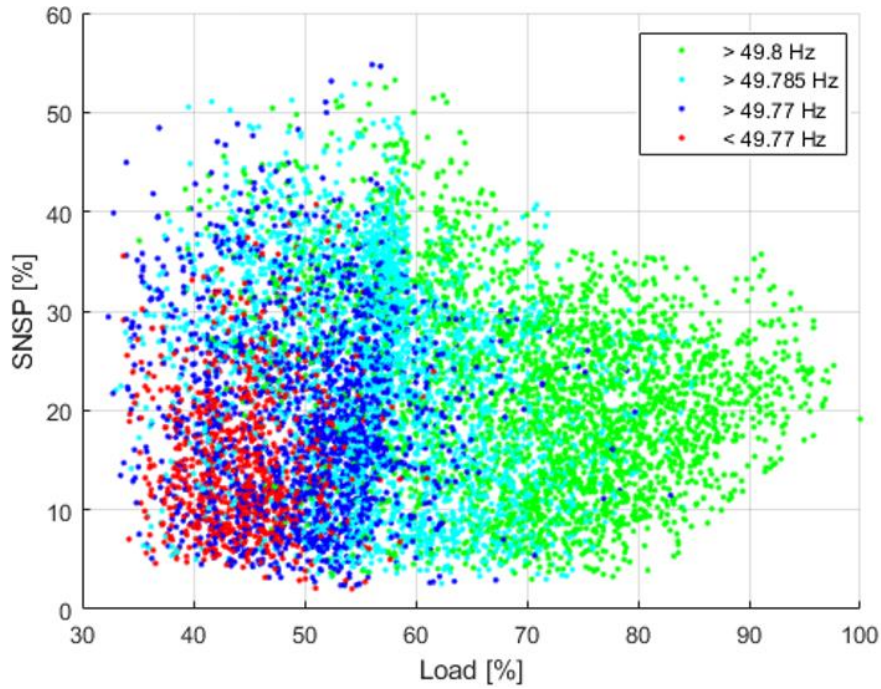

FIGURE 2-3: ENERGY TRANSITION SCENARIO - 3 GW INCIDENT IN FRANCE, IMPACT OF LOAD AND SNSP ON NADIR VALUES

TABLE 2-2: RENEWABLE AMBITION SCENARIO - MEAN NADIR VALUES [HZ] FOR THE LOSS OF 2 GW IN EACH ZONE, DEPENDING ON THE RANGE OF SNSP

Level of SNSP [%]	Iberian peninsula	France	Germany + neighbours	Poland + neighbours	Italy
[0%; 10%]		49.86	49.86	49.85	49.85
[10%; 20%]	49.78	49.85	49.86	49.86	49.85
[20%; 30%]	49.76	49.85	49.86	49.86	49.85
[30%; 40%]	49.75	49.86	49.86	49.86	49.85
[40%; 50%]	49.73	49.86	49.87	49.86	49.85
[50%; 60%]	49.70	49.87	49.87	49.86	49.85
[60%; 70%]	49.67	49.87	49.87	49.86	49.85
[70%; 80%]	49.64	49.86	49.86		49.84
[80%; 90%]	49.59	49.85			49.84
[90%; 100%]	49.56				

The Renewable Ambition scenario was also simulated. The mean local frequency nadir (Hz) values for the loss of 2 GW in each zone are provided in Table 2-2. The levels of SNSP reach higher values compared to Energy Transition. In the Iberian Peninsula, SNSP levels > 90% are reached during several hours in the year. The correlation between frequency stability and SNSP is still valid in Iberian Peninsula (and to some extent in Italy), whereas in the other zones the mean nadir values are not correlated with SNSP. Figure 2-4 shows the impact of load and SNSP on frequency nadir values in Iberian Peninsula. A clear correlation is observed with SNSP, as red dots (frequency nadirs below 49.6 Hz) occur at SNSP levels above 65%.

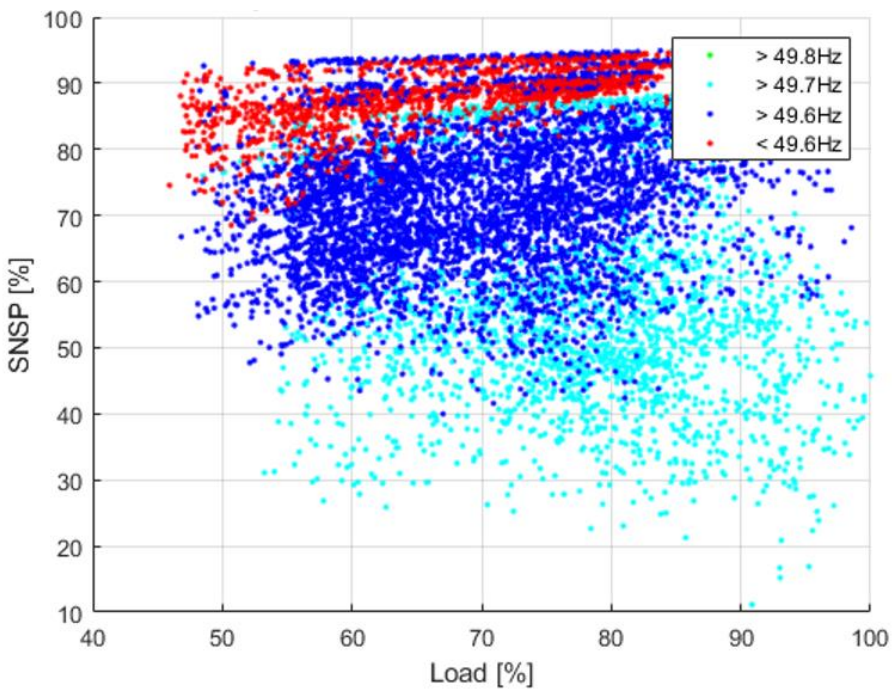

FIGURE 2-4: RENEWABLE AMBITION SCENARIO - 2 GW INCIDENT IN IBERIAN PENINSULA, IMPACT OF LOAD AND SNSP ON NADIR VALUES

A similar graph was created for France (Figure 2-5). Again, it can be seen that the correlation between frequency nadir and load is much more visible than with the SNSP level.

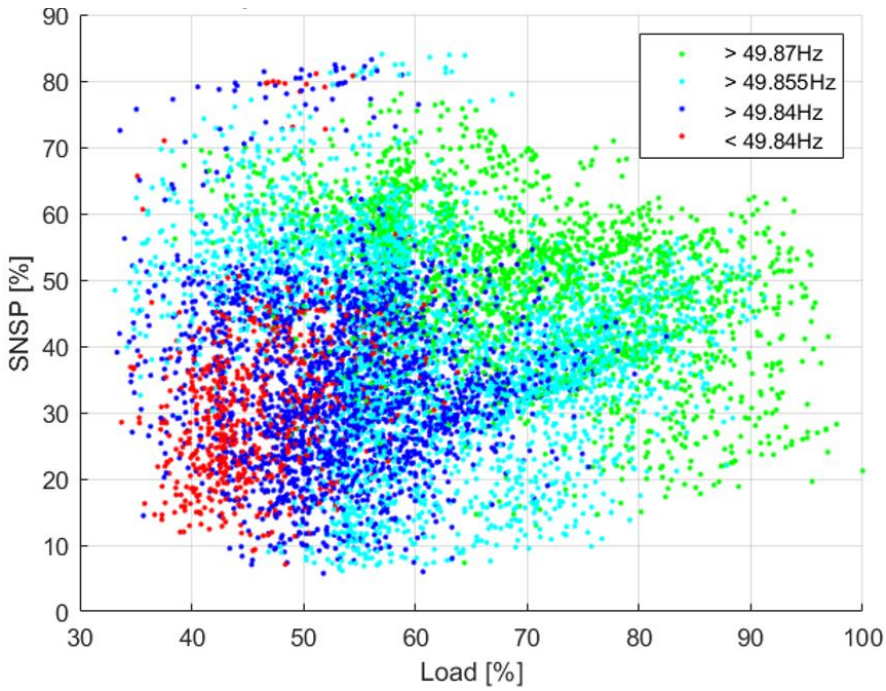

FIGURE 2-5: RENEWABLE AMBITION SCENARIO - 2 GW INCIDENT IN FRANCE, IMPACT OF LOAD AND SNSP ON NADIR VALUES

For the 3 GW incident, the same correlations are observed (see Figure 2-6). Figure 2-7 shows the monotonic function of nadir values in Iberian Peninsula, where the most extreme situations occur. Renewable Ambition leads to lower nadir values than Energy Transition, with minimal values around 49.35 Hz. Load shedding is not needed, as frequency stays above its activation threshold of 49 Hz.

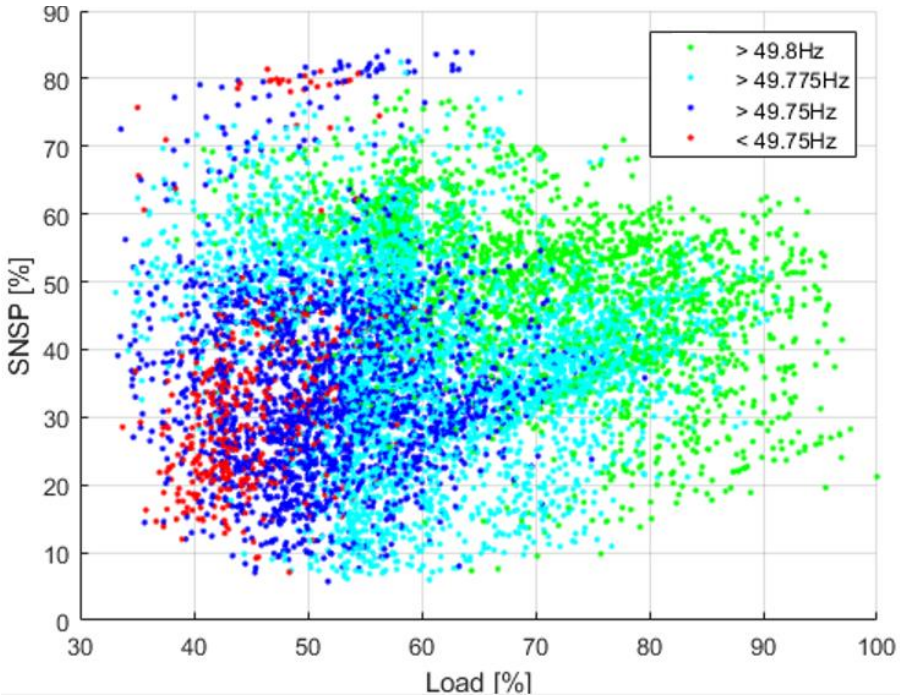

FIGURE 2-6: RENEWABLE AMBITION SCENARIO - 3 GW INCIDENT IN FRANCE, IMPACT OF LOAD AND SNSP ON NADIR VALUES

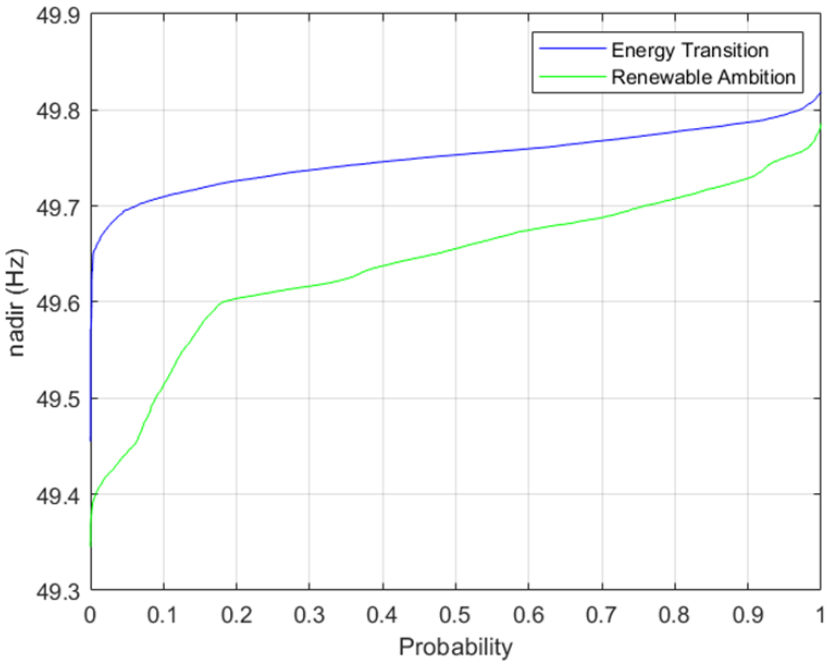

FIGURE 2-7: NADIR MONOTONIC FUNCTION FOR THE LOSS OF 2 GW IN IBERIAN PENINSULA

2.1.1.1.2 ANALYSIS OF ROCOF VALUES

The analysis provided above was repeated to assess local RoCoF values (Hz/s) for the loss of 2 GW in each zone.

The Energy Transition scenario results are shown first: the mean RoCoF values are shown in Table 2-3, depending on the SNSP level. Contrary to the frequency nadir values, RoCoF values are correlated with SNSP levels in almost all zones (except in France). This correlation is logical because the RoCoF is directly dependant on the inertia level. Figure 2-8 shows the impact of load and SNSP on RoCoF values in Iberian Peninsula. Two correlations are observed, as the worst RoCoF values happen at low load and with high SNSP levels.

A similar graph for France shows that RoCoF is mainly correlated with the load, and not with the SNSP levels (Figure 2-9).

For the 3 GW incident in France, a similar observation is made (Figure 2-10).

TABLE 2-3: ENERGY TRANSITION SCENARIO - MEAN ROCOF VALUES [HZ/S] FOR THE LOSS OF 2 GW IN EACH ZONE, DEPENDING ON THE RANGE OF SNSP

Level of SNSP [%]	Iberian peninsula	France	Germany + neighbours	Poland + neighbours	Italy
[0%; 10%]	0.24	0.11	0.07	0.16	0.21
[10%; 20%]	0.27	0.11	0.08	0.17	0.25
[20%; 30%]	0.31	0.11	0.08	0.19	0.27
[30%; 40%]	0.36	0.11	0.08	0.20	0.30
[40%; 50%]	0.39	0.12	0.09		0.32
[50%; 60%]	0.40	0.11	0.09		0.40
[60%; 70%]	0.42		0.10		
[70%; 80%]	0.49		0.10		
[80%; 90%]	0.58				
[90%; 100%]					

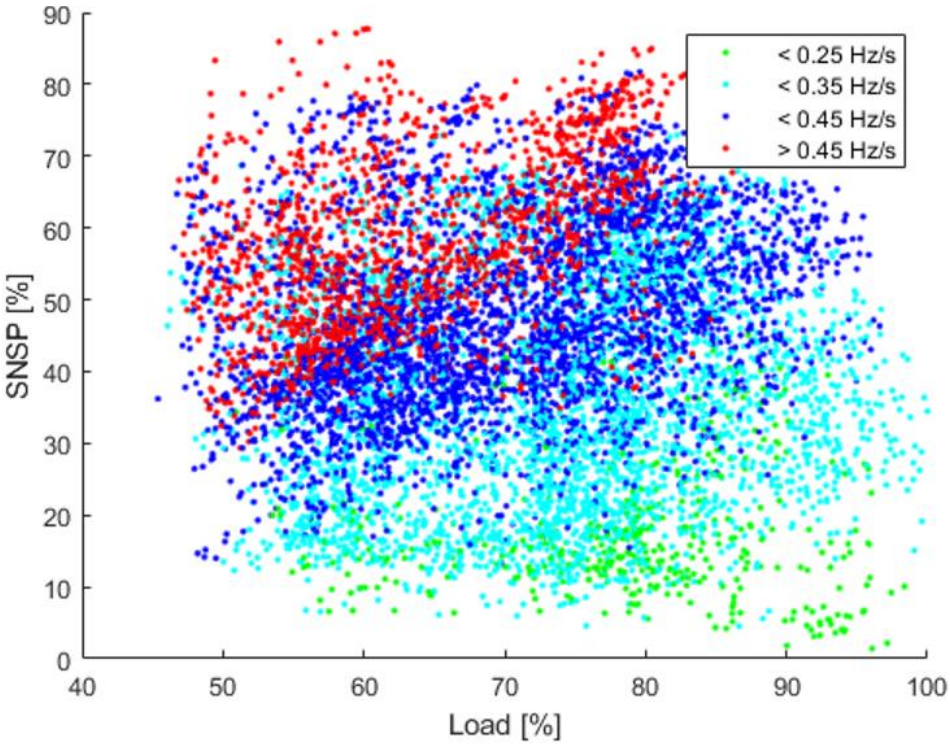

FIGURE 2-8: ENERGY TRANSITION SCENARIO - 2 GW INCIDENT IN IBERIAN PENINSULA, IMPACT OF LOAD AND SNSP ON ROCOF VALUES

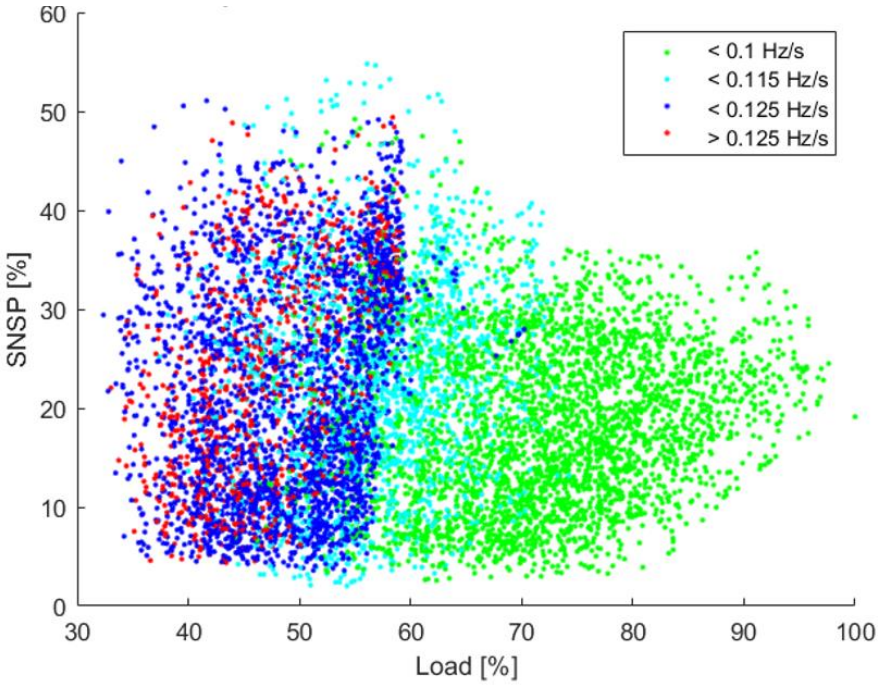

FIGURE 2-9: ENERGY TRANSITION SCENARIO - 2 GW INCIDENT IN FRANCE, IMPACT OF LOAD AND SNSP ON ROCOF VALUES

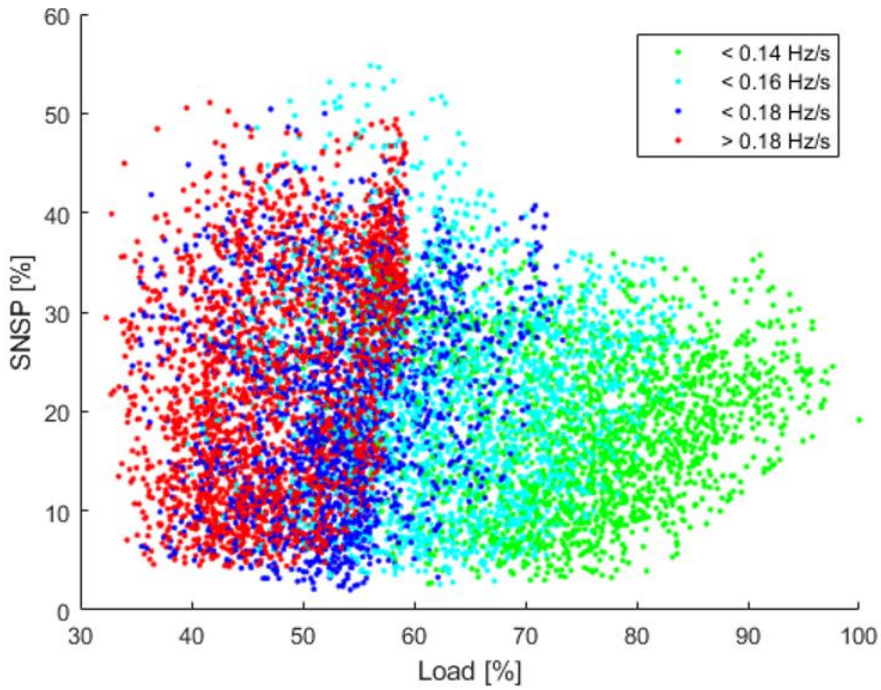

FIGURE 2-10: ENERGY TRANSITION SCENARIO - 3 GW INCIDENT IN FRANCE, IMPACT OF LOAD AND SNSP ON ROCOF VALUES

For the Renewable Ambition scenario, the mean local RoCoF values for the loss of 2 GW in each zone reach higher values than in the Energy Transition scenario. The impact of SNSP on RoCoF is visible in every zone, even France at SNSP above 70% (Table 2-4).

TABLE 2-4: RENEWABLE AMBITION SCENARIO - MEAN ROCOF VALUES [HZ/S] FOR THE LOSS OF 2 GW IN EACH ZONE, DEPENDING ON THE RANGE OF SNSP

Level of SNSP [%]	Iberian peninsula	France	Germany + neighbours	Poland + neighbours	Italy
[0%; 10%]		0.12	0.07	0.14	0.17
[10%; 20%]	0.30	0.12	0.08	0.15	0.18
[20%; 30%]	0.34	0.12	0.08	0.15	0.20
[30%; 40%]	0.37	0.12	0.09	0.17	0.22
[40%; 50%]	0.43	0.12	0.09	0.19	0.24
[50%; 60%]	0.51	0.12	0.10	0.20	0.26
[60%; 70%]	0.61	0.12	0.10	0.20	0.29
[70%; 80%]	0.70	0.14	0.11		0.33
[80%; 90%]	0.81	0.18			0.33
[90%; 100%]	0.87				

Figure 2-11 shows the correlations between load, SNSP and RoCoF values. RoCoF values above 1 Hz/s are frequently observed at SNSP levels above 75%.

Figure 2-12 shows a similar graph in France. The high SNSP levels lead to high RoCoF values. However, some high RoCoF values are also observed at lower SNSP levels. The same graph for the 3 GW incident in France shows the same pattern: some RoCoF values are observed at high SNSP values, but not all of them (Figure 2-13).

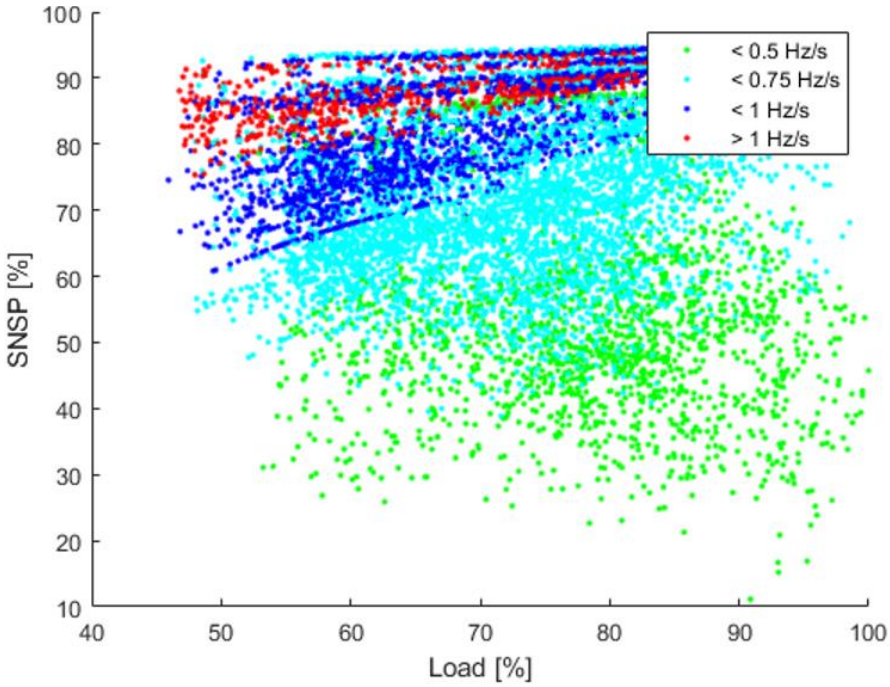

FIGURE 2-11: RENEWABLE AMBITION SCENARIO - 2 GW INCIDENT IN IBERIAN PENINSULA, IMPACT OF LOAD AND SNSP ON ROCOF VALUES

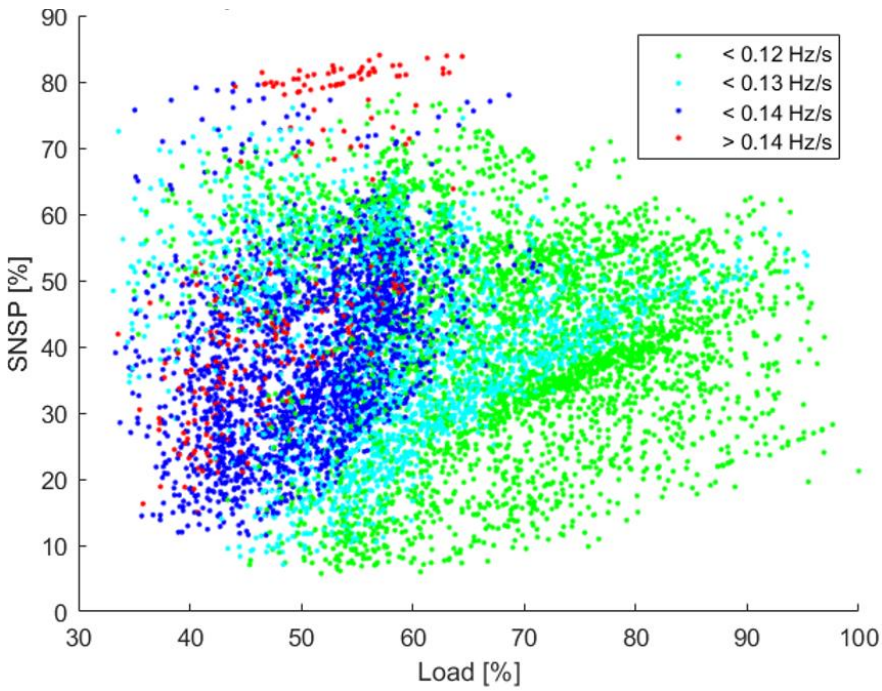

FIGURE 2-12: RENEWABLE AMBITION SCENARIO - 2 GW INCIDENT IN FRANCE, IMPACT OF LOAD AND SNSP ON ROCOF VALUES

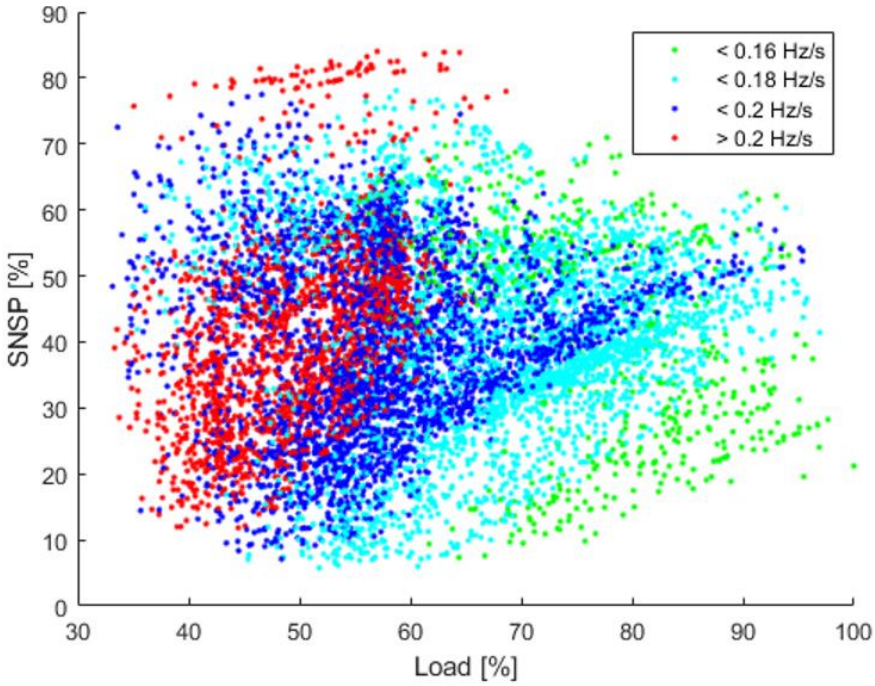

FIGURE 2-13: RENEWABLE AMBITION SCENARIO - 3 GW INCIDENT IN FRANCE, IMPACT OF LOAD AND SNSP ON ROCOF VALUES

Figure 2-14 shows the monotonic functions of RoCoF values in Iberian Peninsula, where the highest values are reached. Renewable Ambition leads to higher RoCoF values than Energy Transition. Renewable Ambition leads to RoCoF values above 1 Hz/s around 10% of the time. The most extreme cases are around 1.3 Hz/s.

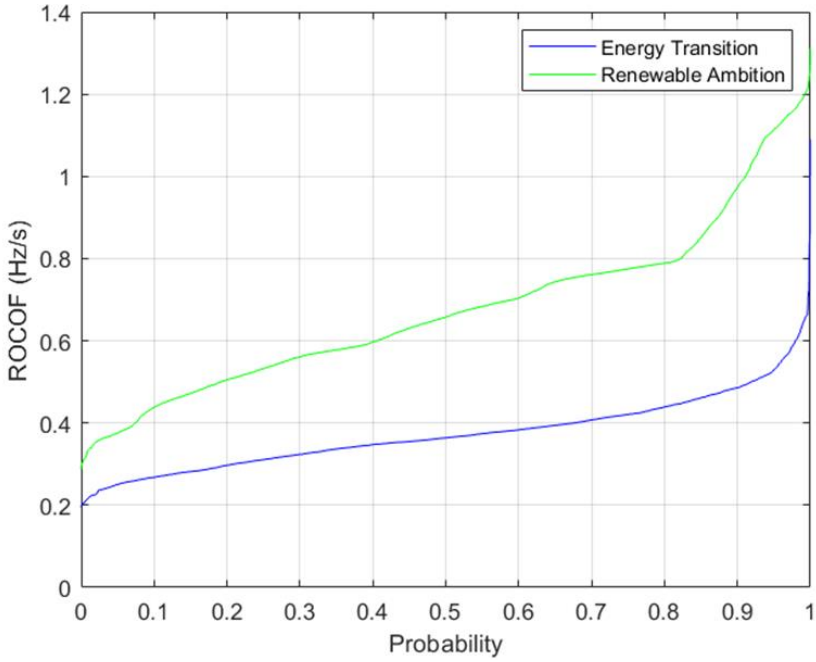

FIGURE 2-14: ROCOF MONOTONIC FUNCTION FOR THE LOSS OF 2 GW IN IBERIAN PENINSULA

Some of the simulations above were run with very high SNSP, which reached more that 70-80% in France, Italy and Germany & neighbors, and at times more than 90% for the Iberian Peninsula. It is worth assessing whether the frequency nadir and RoCoF results indicate that the European stability limits are reached or not. In the Table 2-5, the percentage of hours with extreme frequency nadir or RoCoF values are given. The colours highlight the events that occur frequently.

TABLE 2-5: SUMMARY OF THE RESULTS ON INTERCONNECTED INCIDENTS

Reference loss	Energy Transition		Renewable Ambition	
	NADIR < 49 Hz	ROCOF > 1 Hz /s	NADIR < 49 Hz	ROCOF > 1 Hz /s
East	0%	0%	0%	0
Iberian Peninsula	0%	< 1%	0%	~ 9%
Italy	0%	0%	0%	0%
France	0%	0%	0%	0%
Germany & Neighbours	0%	0%	0%	0%

<2%
<15%
>15%

As can be seen, for all the zones apart from the Iberian Peninsula, frequency nadir values do not seem to be an issue, as they do not deviate from what ENTSO-E currently considers as theoretically achievable in case of the reference loss of generation. In particular, the UCTE report [7] highlights that with unfavorable but current system conditions, the frequency might reach 49.2 Hz following the 3 GW loss. The EU-SysFlex results are compatible with this analysis.

The results from Task 2.4 reveal that the Iberian Peninsula is the weakest zone because of its large integration of renewables and its weaker connection to the rest of Europe. However, frequency nadir values seem to be manageable as they always stay above 49.3 Hz, far from the first load-shedding levels (49 Hz).

Nevertheless, as these frequency nadir levels are rarely reached currently, large efforts may be required in order to ensure that all generators and loads connected to the grid can withstand these frequency deviations. Future work should consider what modifications of generators are needed. In particular, retrofit actions described in ENTSO-E report [5] must be achieved.

The maximal local RoCoF values can exceed 1 Hz/s and can reach 1.3 Hz/s. These values can be problematic as very few systems can currently run with such high levels of RoCoF. In particular, the grid codes of Great-Britain and Ireland and Northern Ireland stipulate that generating assets shall withstand RoCoF values up to 1 Hz/s (calculated over 500 ms time period). This value was the result of many years of discussion and consultation between the different stakeholders.

In Continental Europe, ENTSO-E proposed [8] to set 2 Hz/s (calculated over a 500 ms time frame) but there are still some doubt as to whether manufacturers could fulfill this requirement, and if they could do so with

acceptable costs [9]. Furthermore, new requirements on RoCoF withstand capabilities introduced through the RfG Code only apply to the new generators. For all these reasons, it is considered that RoCoF higher than 1 Hz/s raise concerns.

Analysis suggests that controlling the RoCoF values, particularly in the Iberian Peninsula, is vital. Solutions will have to be found. Restricting the SNSP in the Iberian Peninsula or incentivising alternatives for providing inertia (Synchronous condensers, Grid Forming control of the Renewables) are possible mitigations.

2.1.1.2 SYSTEM SPLITS

According to ENTSO-E, system splits can be more challenging than interconnected incidents for frequency stability [6]. Three configurations are studied for the EU-SysFlex simulations:

- A separation of the Iberian Peninsula from the rest of Continental Europe.
- A separation of Italy from the rest of Continental Europe (situation similar to 2003 Italian incident [10])
- A split of Continental Europe into three zones (situation similar to the 2006 system split [11]).

The first two cases were chosen because the Iberian Peninsula and Italy are electrical peninsulas with high levels of vRES. The last case corresponds to a situation that has happened in the past and could happen again in the future.

The objective of this part of the study is to assess the impact of a system split, which is simulated for all hours of the year, for both Energy Transition and Renewable Ambition scenarios. In case of a split, the separated zones need to absorb the power imbalances that correspond to the power flows at their borders when the split occurs.

Each of the three configurations are assessed and discussed separately.

2.1.1.2.1 IBERIAN PENINSULA

The first case considered is the separation of the Iberian Peninsula from the rest of Continental Europe (Figure 2-15). Figure 2-16 shows, for both scenarios, the monotonic function of the imbalances at the France-Spain border. These imbalances can reach +/- 8 GW for Energy Transition and +/- 12 GW for Renewable Ambition, due to the development of interconnections between France and Spain. In addition, Energy Transition is not symmetrical, whereas Renewable Ambition is. This implies that the over-frequencies and under-frequencies will also not be symmetrical in the results. The Figure 2-17 shows the magnitude of those imbalances as a percentage of the load.

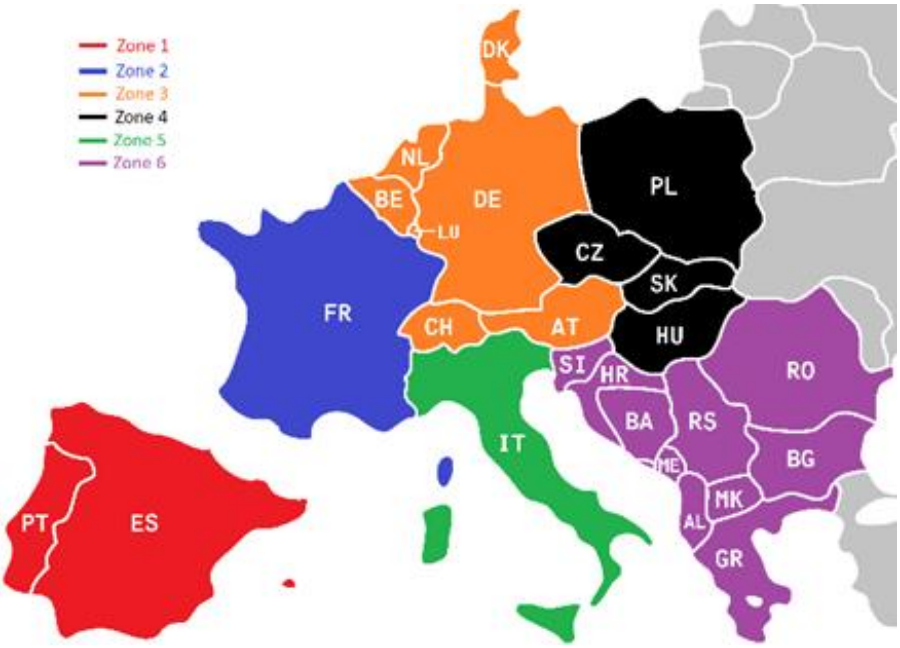

FIGURE 2-15: SEPARATION OF THE IBERIAN PENINSULA FROM THE REST OF CONTINENTAL EUROPE

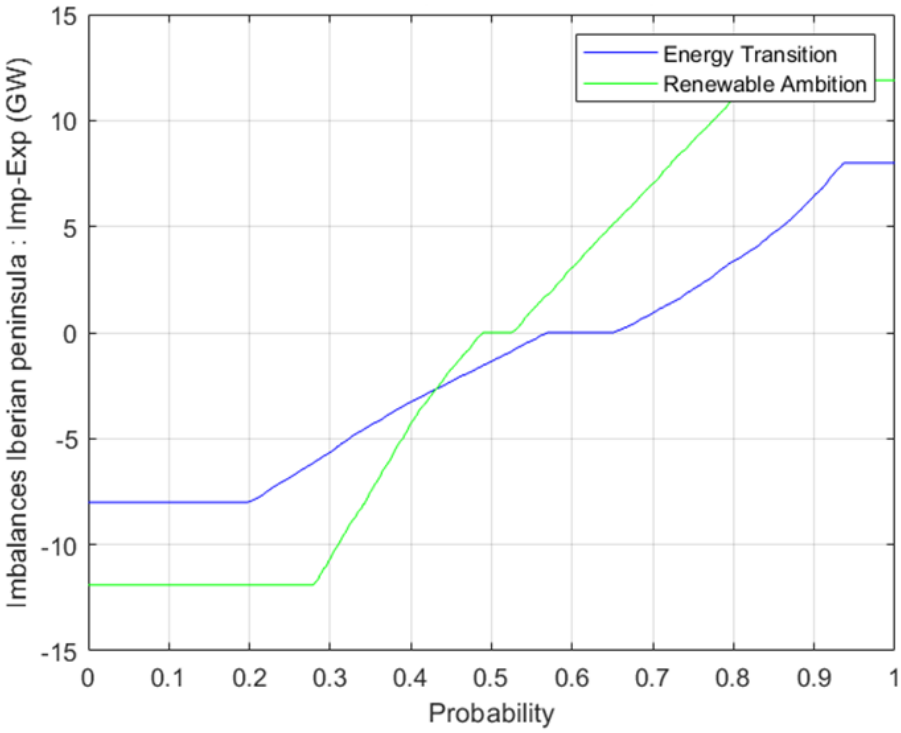

FIGURE 2-16: MONOTONIC FUNCTION OF THE IMBALANCES FOR THE IBERIAN PENINSULA (POSITIVE VALUES MEAN IBERIAN PENINSULA IS IMPORTING)

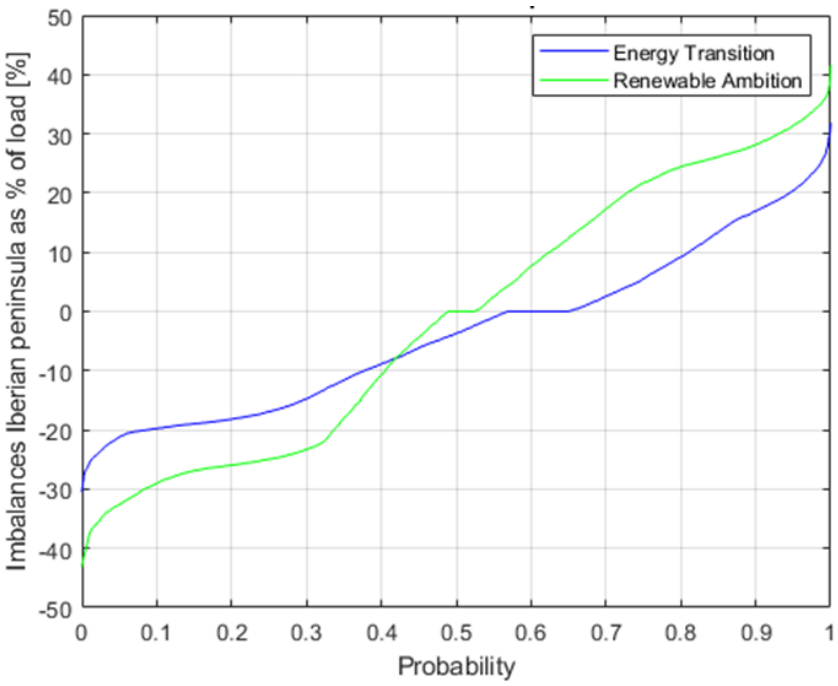

FIGURE 2-17: MONOTONIC FUNCTION OF THE IMBALANCES FOR THE IBERIAN PENINSULA [% OF LOAD]

The most extreme imbalances correspond to 30% of the instantaneous load with Energy Transition, and 40% of the instantaneous load with Renewable Ambition. The ENTSO-E value of 40% imbalance between the generation and the load, as a consequence of a system split [6], seems credible. However, this would appear to be very unlikely given that it only occurs in the Renewable Ambition scenario and for very few hours of the year. The indicators of frequency stability employed for the analysis of system splits are the same as those used previously for interconnected incidents: nadir (and zeniths, when the imbalances are positive) and RoCoF values. Activated load shedding and Limited Frequency Sensitivity Mode for Over-frequencies (LFSM-O) power are levers which can be used to mitigate the frequency drop/rise and so these are also utilised as indicators in the analysis. As with the analysis on interconnected incidents, each indicator is dealt with individually.

Figure 2-18 shows the monotonic function of frequency nadir values in Iberian Peninsula for both scenarios. Nadir values are much more extreme than for interconnected incidents, which is logical because the imbalances are much higher. Frequency nadir values as low as 46 Hz are observed for a few hours in Renewable Ambition. This corresponds to situations of blackout, because FCR, load sensitivity to frequency and even load shedding (activated progressively between 49 Hz and 48 Hz) were not sufficient and fast enough to avoid the frequency collapse. Moreover, generators are not required to remain connected to the grid in case of frequency lower than 47.5 Hz (as defined for instance in RfG). This means that frequencies lower than 47.5 Hz are considered to mean that the system is in a state of black-out.

The monotonic function of load shedding for both scenarios is shown in Figure 2-19. Load shedding is activated in almost 50% of cases in both scenarios. However, the magnitude of the load shedding is much higher in Renewable Ambition (more than 25 GW in some cases). The load shedding action is effective in stopping the frequency drop.

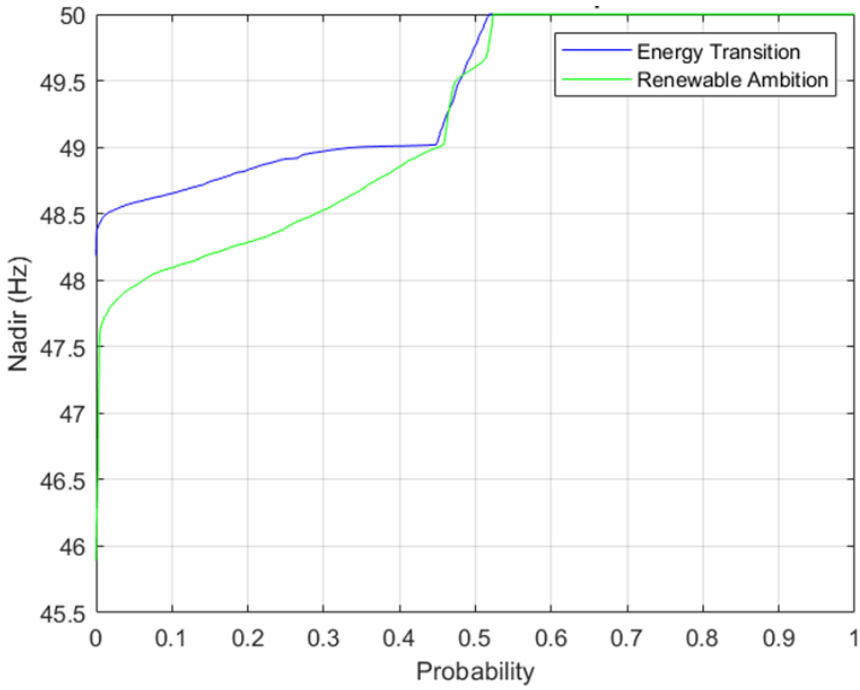

FIGURE 2-18: MONOTONIC FUNCTION OF NADIR VALUES IN IBERIAN PENINSULA AFTER THE SPLIT WITH THE REST OF CONTINENTAL EUROPE

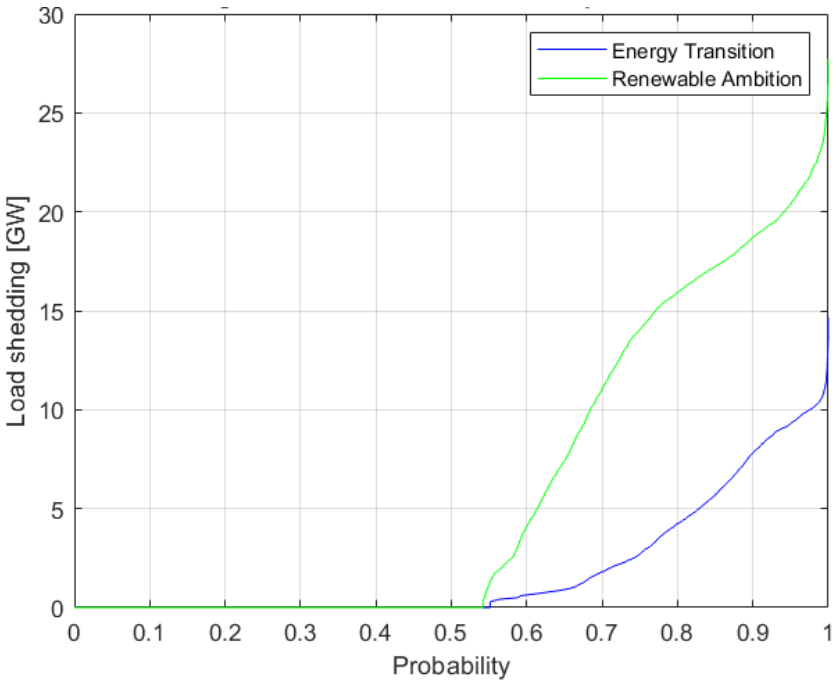

FIGURE 2-19: MONOTONIC FUNCTION OF LOAD SHEDDING IN IBERIAN PENINSULA AFTER THE SPLIT WITH THE REST OF CONTINENTAL EUROPE

Frequency zenith values also reach extreme values (Figure 2-20), especially in the Renewable Ambition scenario where zeniths of up to 53 Hz are possible. In those cases, the activation of LFSM-O was insufficient in maintaining the frequency below 51.5 Hz, which is critical frequency, above which the generators start to disconnect. Figure 2-21 shows the values of LFSM-O activated for both scenarios. In the worst cases of Renewable Ambition, 17 GW of LFSM-O are activated.

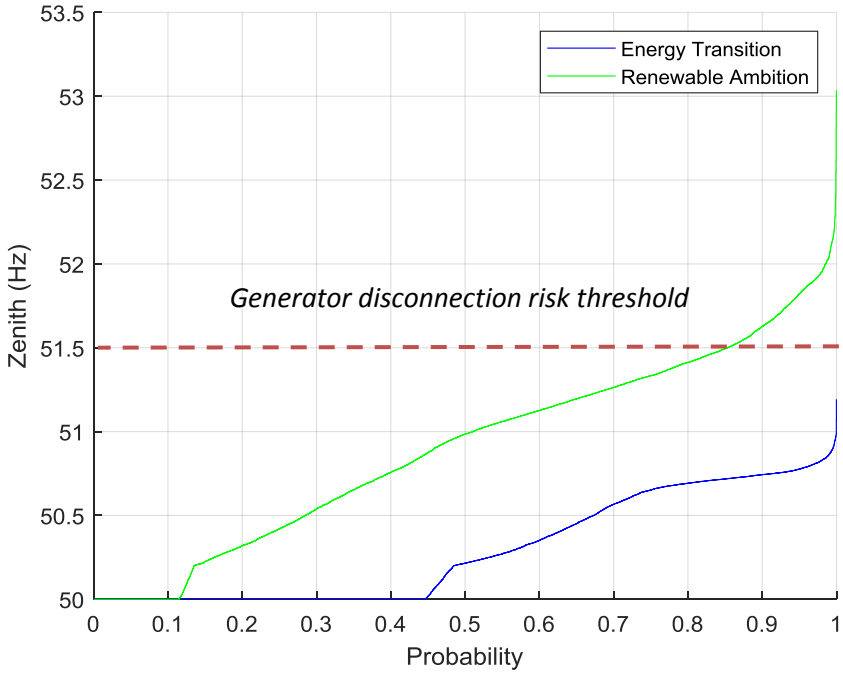

FIGURE 2-20: MONOTONIC FUNCTION OF ZENITH VALUES IN IBERIAN PENINSULA AFTER THE SPLIT WITH THE REST OF CONTINENTAL EUROPE

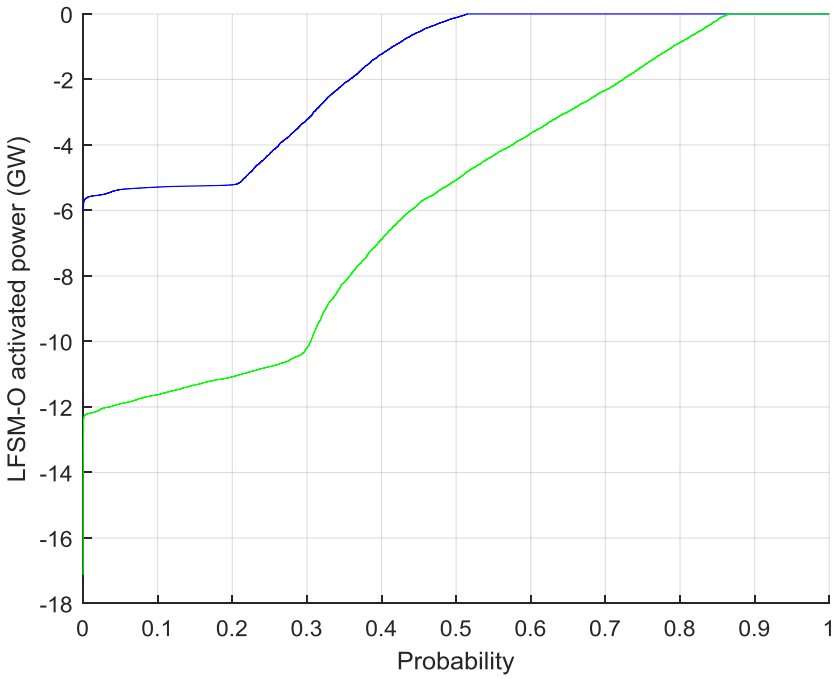

FIGURE 2-21: MONOTONIC FUNCTION OF LFSM-O ACTIVATED IN IBERIAN PENINSULA AFTER THE SPLIT WITH THE REST OF CONTINENTAL EUROPE

It is worth noting that RfG do not force the generators to stay connected to the grid if the frequency goes above 51.5Hz. That consideration raises the question of how the system behaves once 51.5 Hz is reached. The will be discussed later in this document.

The monotonic function of RoCoF values is shown in Figure 2-22. RoCoF values are much more extreme than for interconnected incidents. RoCoF values > 2 Hz/s are much more frequent in the Renewable Ambition scenario (65% of situations, vs. 5% of situations for Energy Transition. The different colored areas in Figure 2-22 highlight the situations where the system is endangered. The analysis indicates that the Iberian Peninsula splits would black-out in many situations.

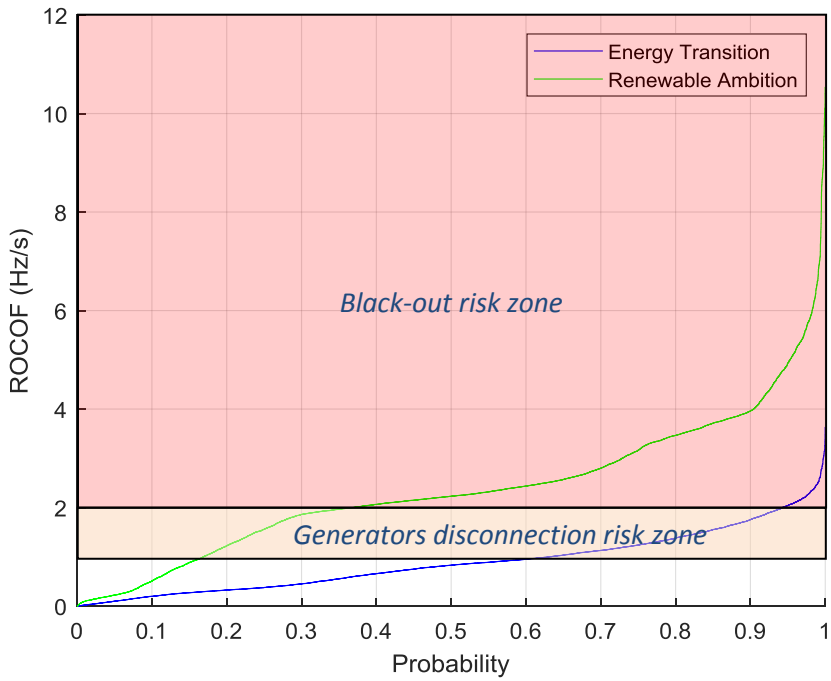

FIGURE 2-22: MONOTONIC FUNCTION OF ROCOF VALUES IN IBERIAN PENINSULA AFTER THE SPLIT WITH THE REST OF CONTINENTAL EUROPE

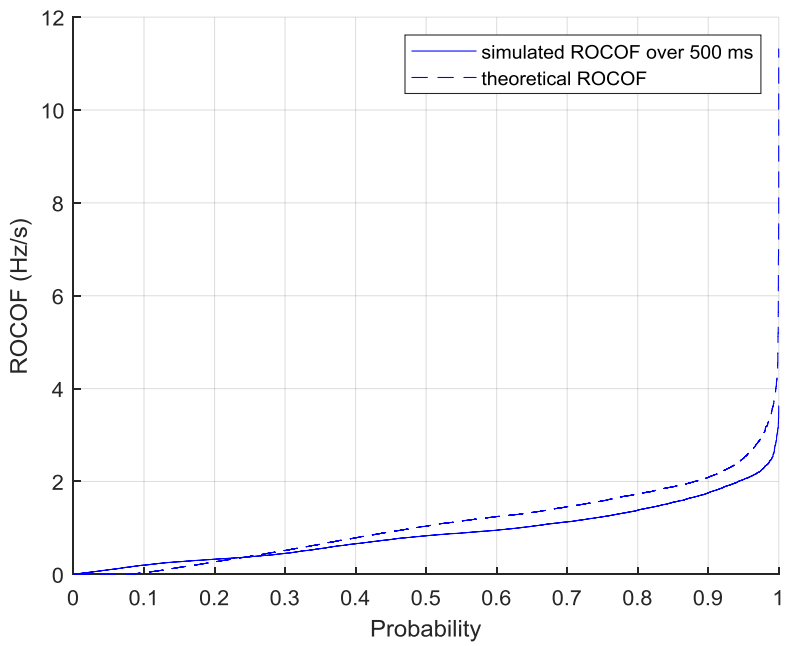

FIGURE 2-23: COMPARISON OF SIMULATED AND THEORETICAL ROCOF VALUES IN IBERIAN PENINSULA AFTER THE SPLIT WITH THE REST OF CONTINENTAL EUROPE FOR THE ENERGY TRANSITION SCENARIO

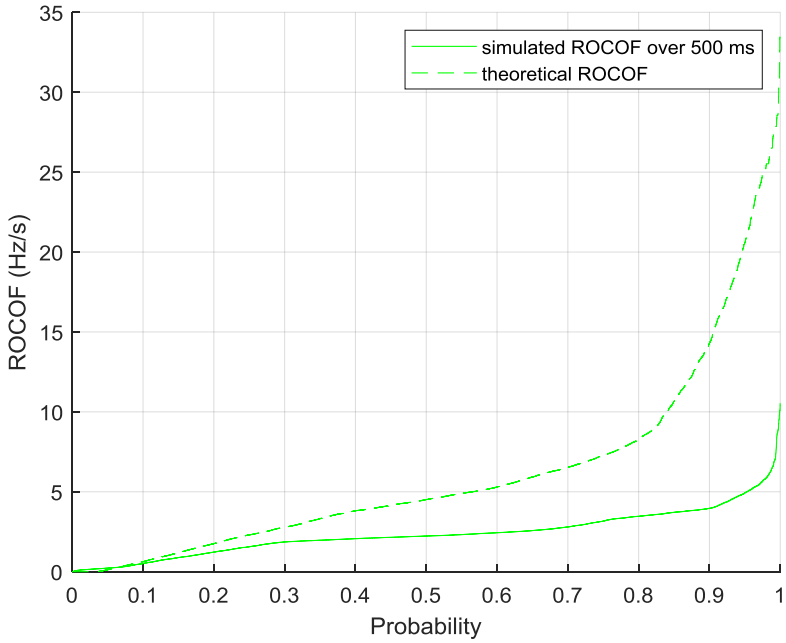

FIGURE 2-24: COMPARISON OF SIMULATED AND THEORETICAL ROCOF VALUES IN IBERIAN PENINSULA AFTER THE SPLIT WITH THE REST OF CONTINENTAL EUROPE FOR THE RENEWABLE AMBITION SCENARIO

Those RoCoF values are calculated over a 500 ms time period, as explained previously. Figure 2-23 and Figure 2-24 compare those simulated values with the theoretical RoCoF values. Some differences can be observed between theoretical and simulated RoCoF, especially for maximal values. These differences mainly highlight the impact of calculating the RoCoF over a 500 ms period in the simulations.

2.1.1.2.2 ITALY

The second case considered is the separation of Italy from the rest of Continental Europe (Figure 2-25).

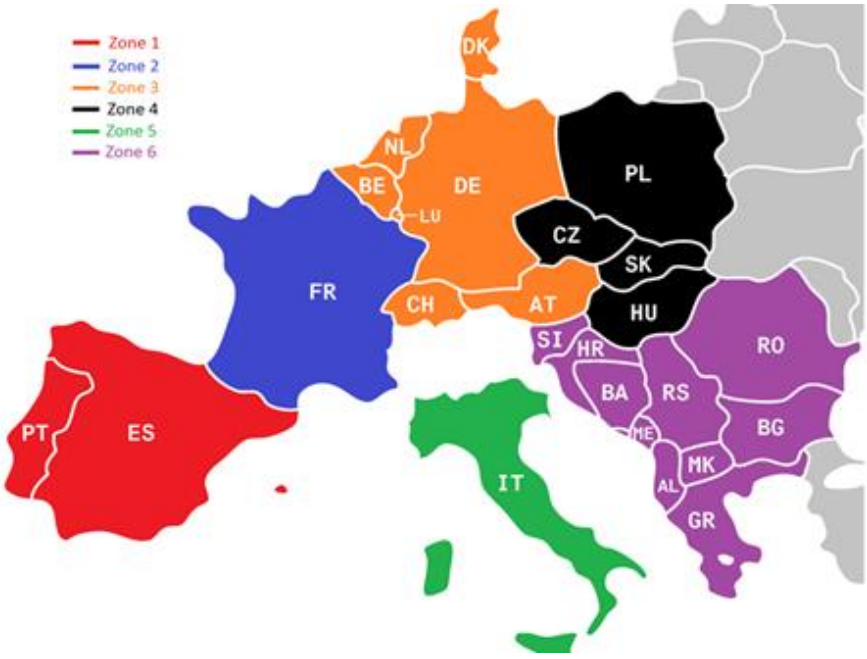

FIGURE 2-25: SEPARATION OF ITALY FROM THE REST OF CONTINENTAL EUROPE

Figure 2-26 shows, for both scenarios, the monotonic function of the imbalances at the Italian borders. Italy is importing 90% of the time with Energy Transition and 65% with Renewable Ambition. Maximal imports are much bigger than exports, up to +18 GW with Renewable Ambition.

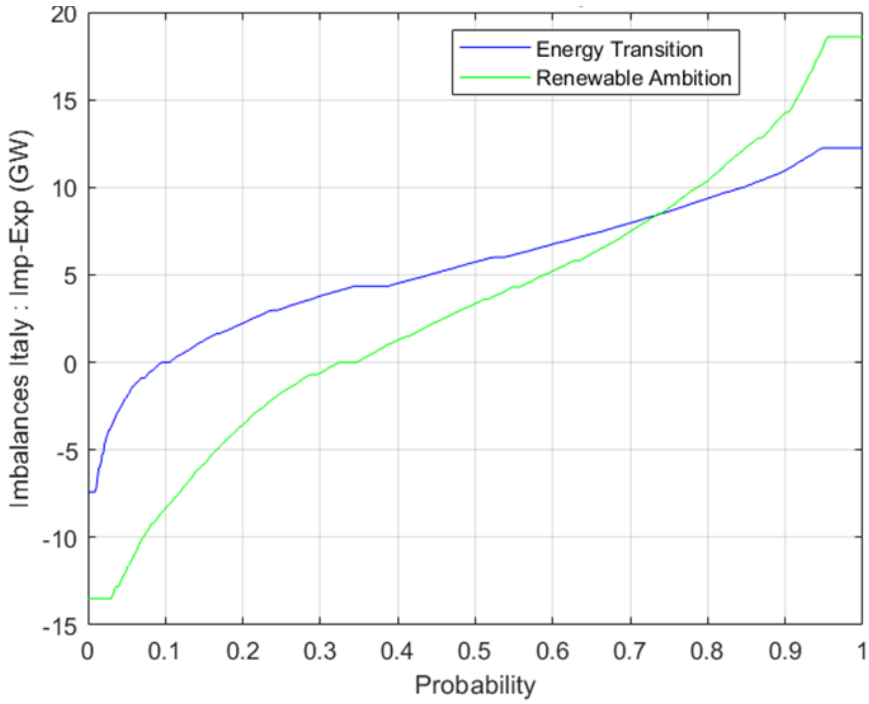

FIGURE 2-26: MONOTONIC FUNCTION OF THE IMBALANCES FOR ITALY

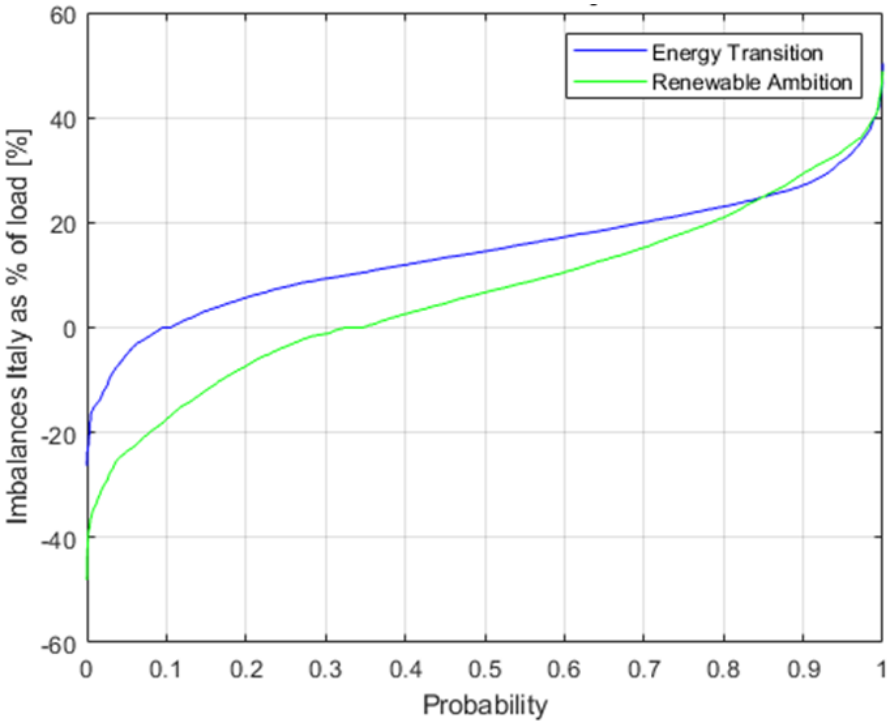

FIGURE 2-27: MONOTONIC FUNCTION OF THE IMBALANCES FOR ITALY [% OF LOAD]

Figure 2-27 shows the magnitude of those imbalances as a percentage of the load. Regarding imports, the maximum is almost the same for both scenarios, close to 50%. For exports, Renewable Ambition leads to bigger imbalances (around 50% too, vs. 25% for Energy Transition). Similarly to the Iberian case, the possibility to face imbalances between the generation and load which could amount to 40% is real, even though very unlikely.

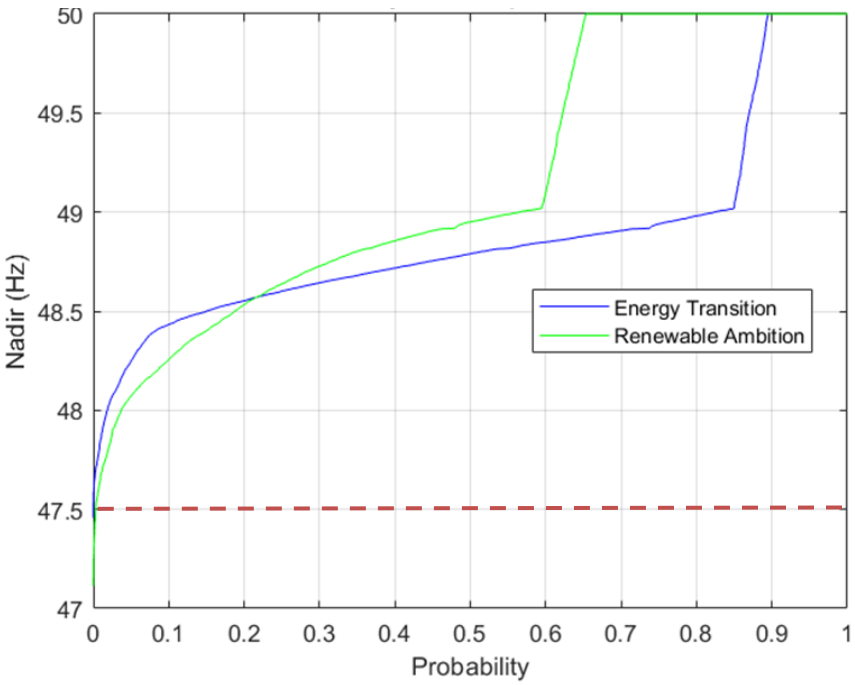

FIGURE 2-28: MONOTONIC FUNCTION OF NADIR VALUES IN ITALY AFTER THE SPLIT WITH THE REST OF CONTINENTAL EUROPE

Figure 2-28 shows the monotonic function of frequency nadir values in Italy for both scenarios. Nadir values lower than 49 Hz (which is the threshold for load shedding), are more frequent in Energy Transition, due to the distribution of imbalances (Italy is importing almost all the time). Very few cases of frequency below the critical level of 47.5 Hz occur.

Figure 2-29 shows the load shed for both scenarios. Load shedding is needed more often with Energy Transition, due to the distribution of imbalances. However, Renewable Ambition leads to higher load shed for the most extreme cases.

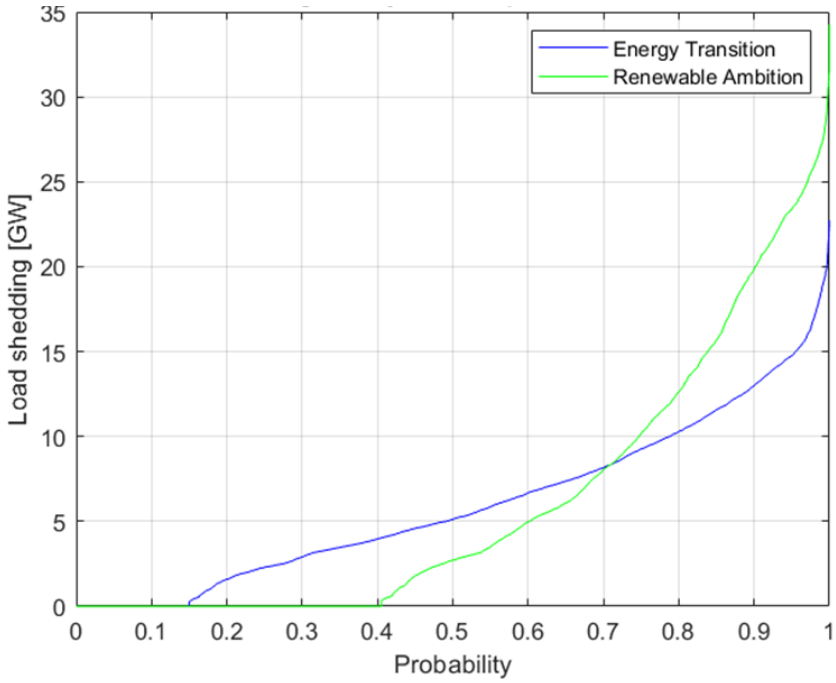

FIGURE 2-29: MONOTONIC FUNCTION OF LOAD SHEDDING IN ITALY AFTER THE SPLIT WITH THE REST OF CONTINENTAL EUROPE

Figure 2-30 shows the monotonic function of frequency zeniths. High frequency zeniths are observed, with Renewable Ambition being slightly worse than Energy Transition. Several problematic cases with frequencies higher than 51.5Hz occur in both scenarios. Those high zenith values are obtained even with the activation of high LFSM-O activations for Renewable Ambition (Figure 2-31).

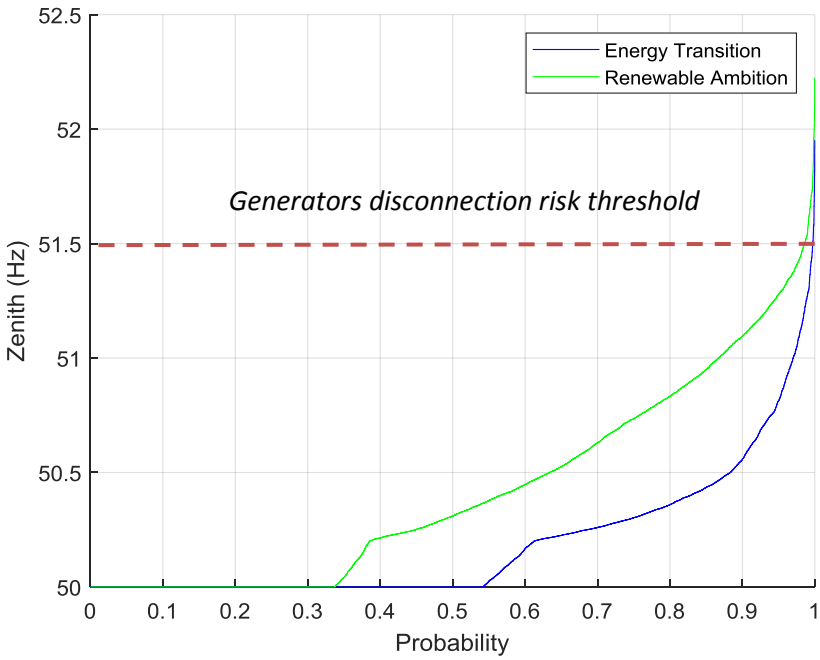

FIGURE 2-30: MONOTONIC FUNCTION OF ZENITH VALUES IN ITALY AFTER THE SPLIT WITH THE REST OF CONTINENTAL EUROPE

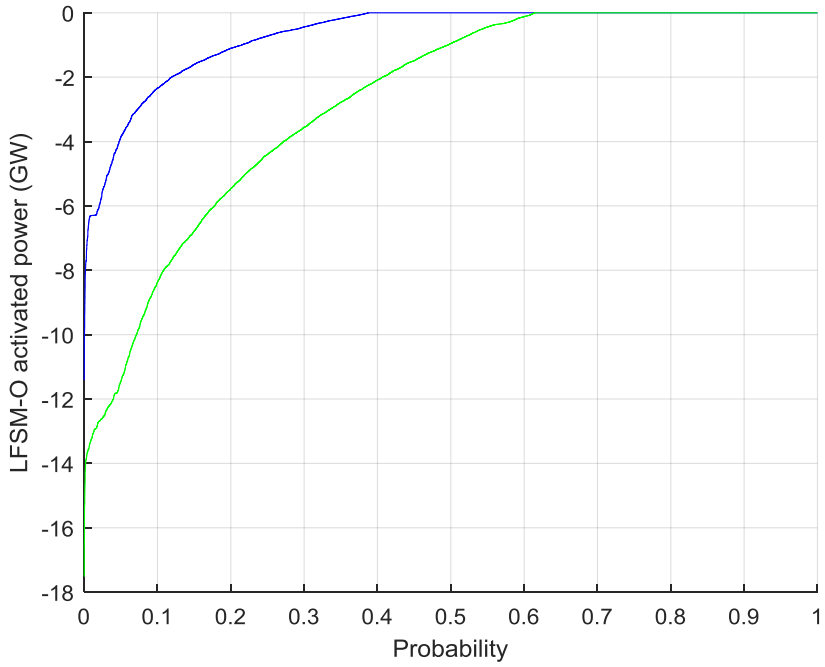

FIGURE 2-31: MONOTONIC FUNCTION OF LFSM-O ACTIVATED IN ITALY AFTER THE SPLIT WITH THE REST OF CONTINENTAL EUROPE

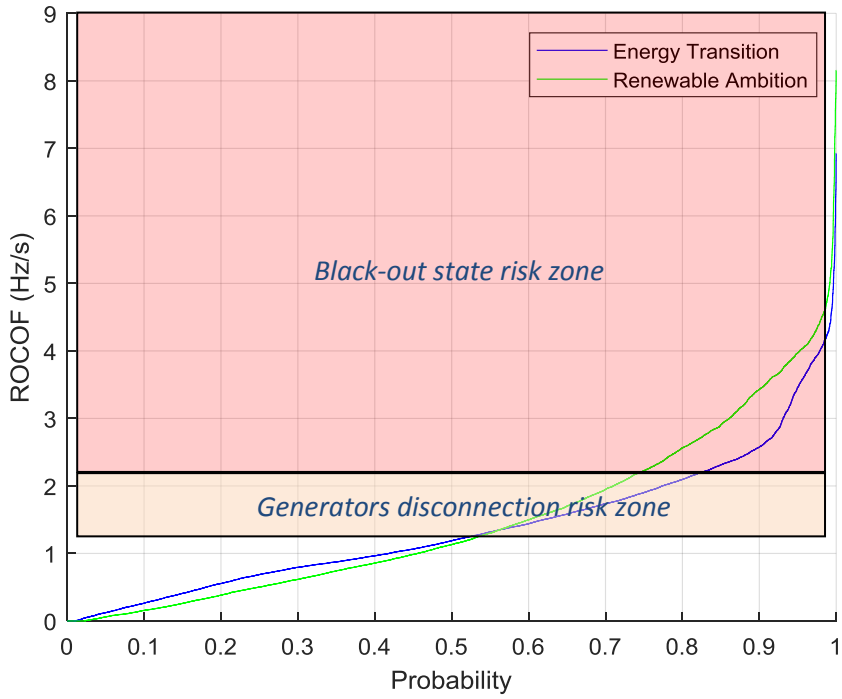

FIGURE 2-32: MONOTONIC FUNCTION OF ROCOF VALUES IN ITALY AFTER THE SPLIT WITH THE REST OF CONTINENTAL EUROPE

Finally, Figure 2-32 shows the monotonic function of RoCoF values. They can reach values > 6 Hz/s for both scenarios, in the hours when inertia is very low in Italy. The threshold of 2 Hz/s is reached for 25% (Energy Transition) to 30% (Renewable Ambition) of hours. The observation of high Zenith and RoCoF values raise concerns about the Italian system stability in the case of system splitting events, as critical thresholds (51.Hz and especially RoCoF > 1 or 2 Hz/s) are breached regularly. Figure 2-33 and Figure 2-34 compare the theoretical and

simulated RoCoF values for both Energy Transition and Renewable Ambition scenarios. For the most extreme cases, the simulated RoCoF values are lower than the theoretical ones.

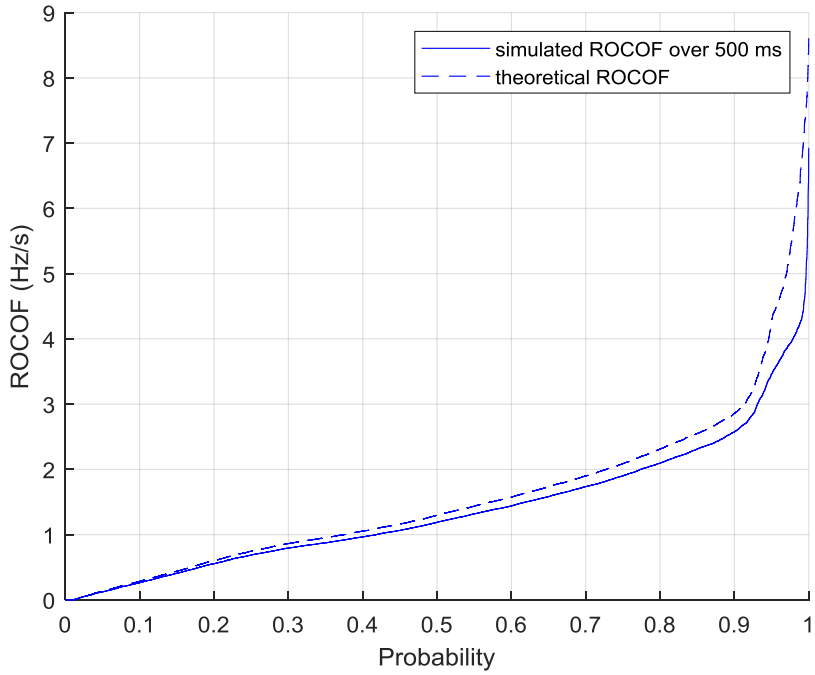

FIGURE 2-33: COMPARISON OF SIMULATED AND THEORETICAL ROCOF VALUES IN ITALY AFTER THE SPLIT WITH THE REST OF CONTINENTAL EUROPE FOR THE ENERGY TRANSITION SCENARIO

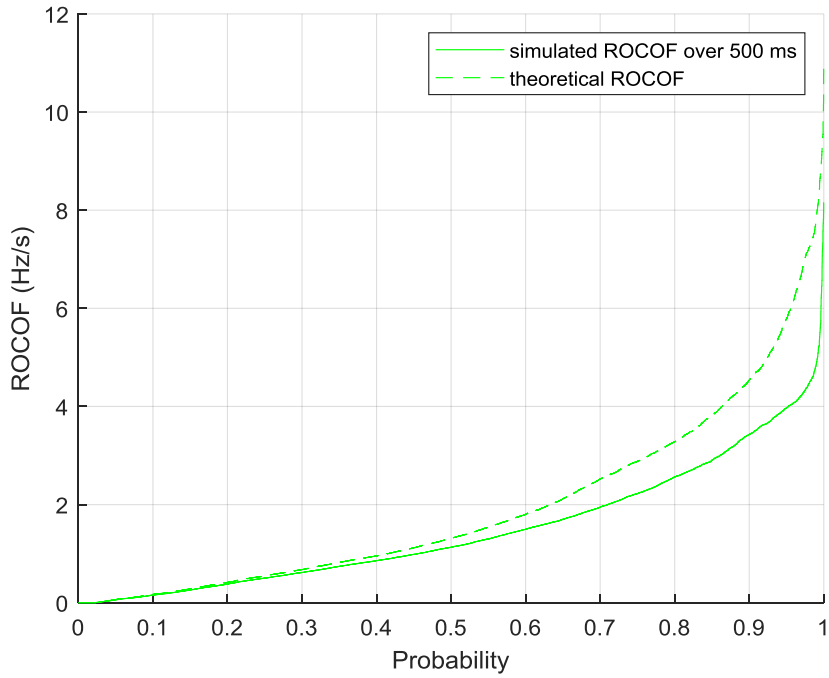

FIGURE 2-34: COMPARISON OF SIMULATED AND THEORETICAL ROCOF VALUES IN ITALY AFTER THE SPLIT WITH THE REST OF CONTINENTAL EUROPE FOR THE RENEWABLE AMBITION SCENARIO

2.1.1.2.3 3 ZONES SPLIT

The final case considered in this part of the analysis on frequency stability is the split of Continental Europe into three zones (Figure 2-35), which is close to what happened in 2006 [11].

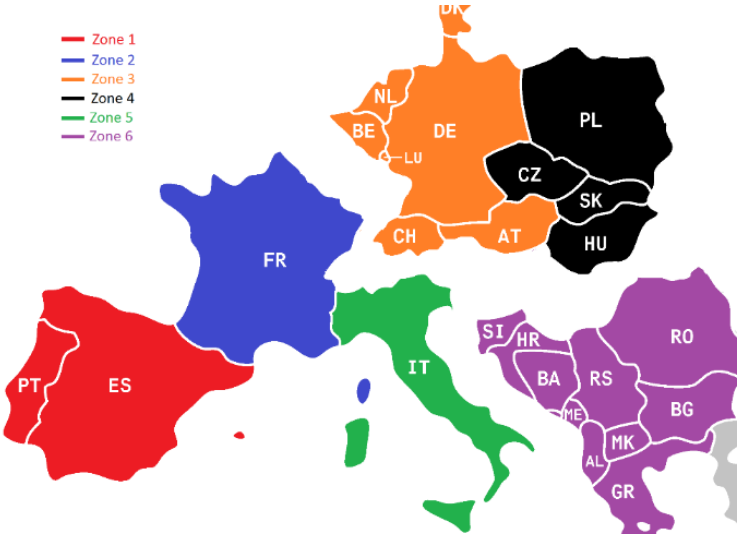

FIGURE 2-35: SEPARATION OF CONTINENTAL EUROPE INTO THREE ZONES – SIMULATED CASE

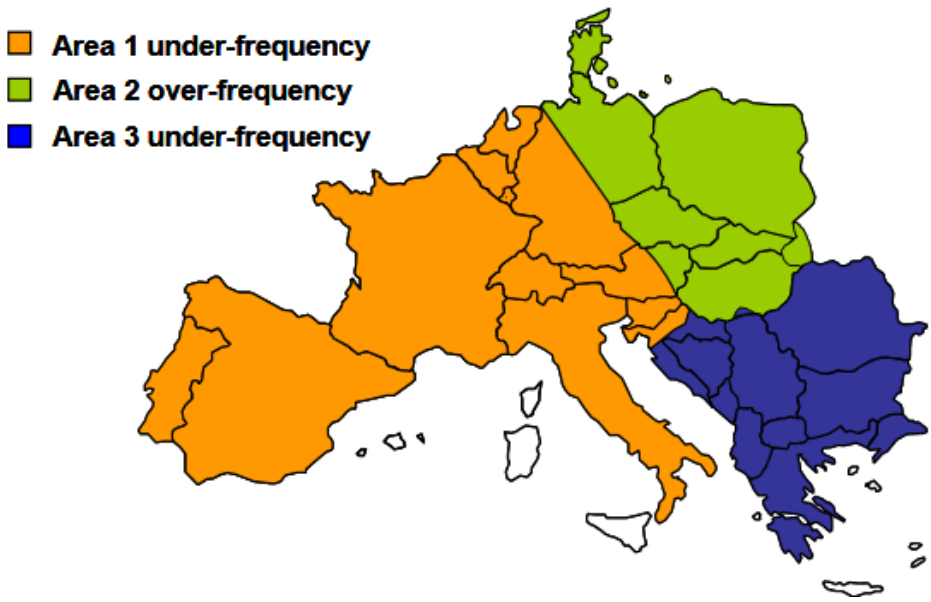

FIGURE 2-36: SEPARATION OF CONTINENTAL EUROPE INTO THREE ZONES – 2006 EVENT [11]

The results for two zones will be studied: the zone containing the Iberian Peninsula, Italy and France (called the "West Zone"), and the zone "North and East" that contains Germany, Belgium, the Netherlands, Denmark, Luxembourg, Switzerland, Austria, Poland, Czech Republic, Slovakia and Hungary. The third zone containing the Balkans countries will not be considered because the input data for this zone are less accurate.

The imbalances for France and the Iberian Peninsula can be observed on Figure 2-37. For Energy Transition, this zone is exporting 85% of the time, and 60% of the time with Renewable Ambition.

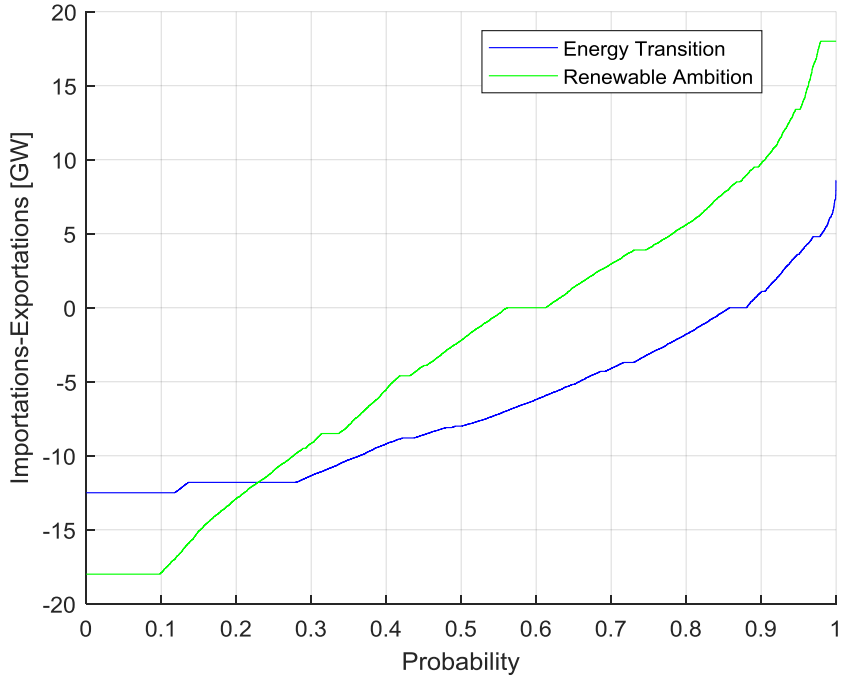

FIGURE 2-37: MONOTONIC FUNCTION OF THE IMBALANCES FOR THE WEST ZONE

Maximum imbalances of +/- 18 GW are observed, which is the same order of magnitude of the imbalance which affected the West Zone in 2006. Indeed, even though the initial imbalance after the system split in 2006 was around 9 GW, almost 11 GW of decentralized generators in the West part disconnected because of adverse setting of protections [11].

The same monotonic function is shown on Figure 2-38 for the North and East zone. The imports and exports are symmetrical for, whereas in Energy Transition there are imports 75% of the time and the magnitude of these imports are lower.

The possible imbalances that the North + East zone could face in the case of a system split event are higher than for the West zone, given that the flows with the Balkans will be interrupted at the same time. For both of the separated zones, the Renewable Ambition maximum imbalances are higher than for the Energy Transition because higher interconnection capacities are expected to be operational in the Renewable Ambition scenario.

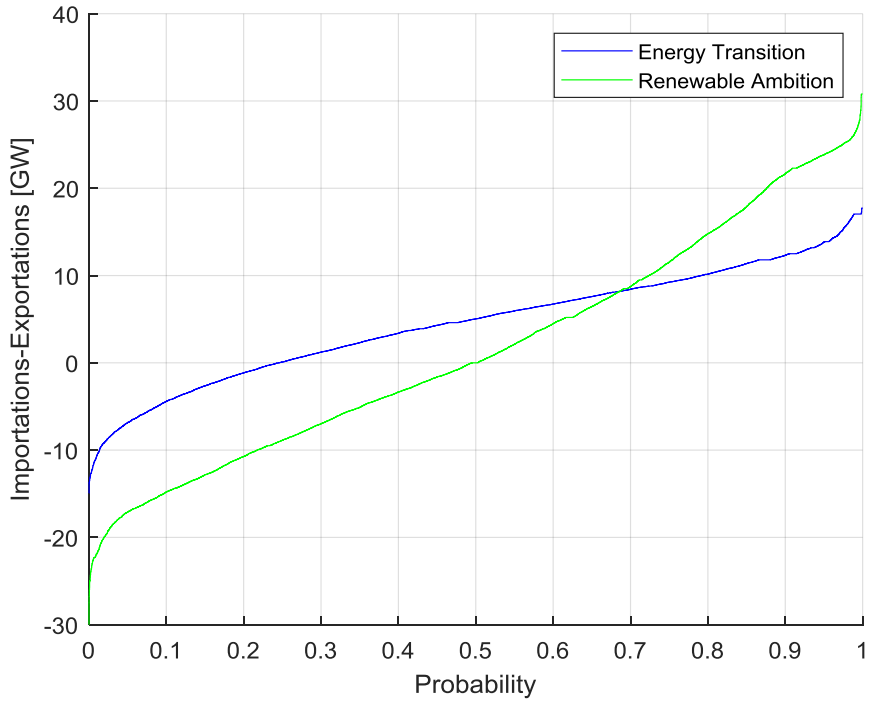

FIGURE 2-38: MONOTONIC FUNCTION OF THE IMBALANCES FOR ZONE NORTH AND EAST

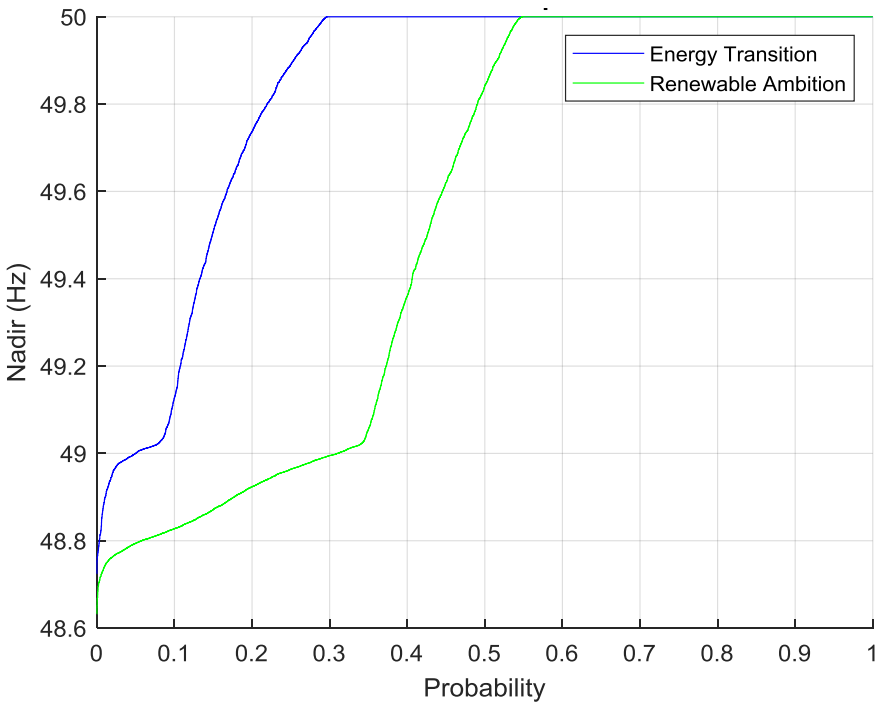

FIGURE 2-39: MONOTONIC FUNCTION OF NADIR VALUES IN THE WEST ZONE AFTER THE SPLIT OF CONTINENTAL EUROPE INTO THREE ZONES

Figure 2-39 and Figure 2-40 show the monotonic functions of nadir values for both scenarios, for France and for the North and East zone, respectively. Nadir values lower than 49 Hz (which is the threshold for load shedding) are more frequent with Renewable Ambition in France, but it is the contrary for North and East zone. The lowest

values reached are around 48.7 Hz in both zones, which does not correspond to black out situations. The activation of load shedding is sufficient to avoid higher frequency drops. The European system seems to be resilient in this configuration of system splits in term of frequency nadir.

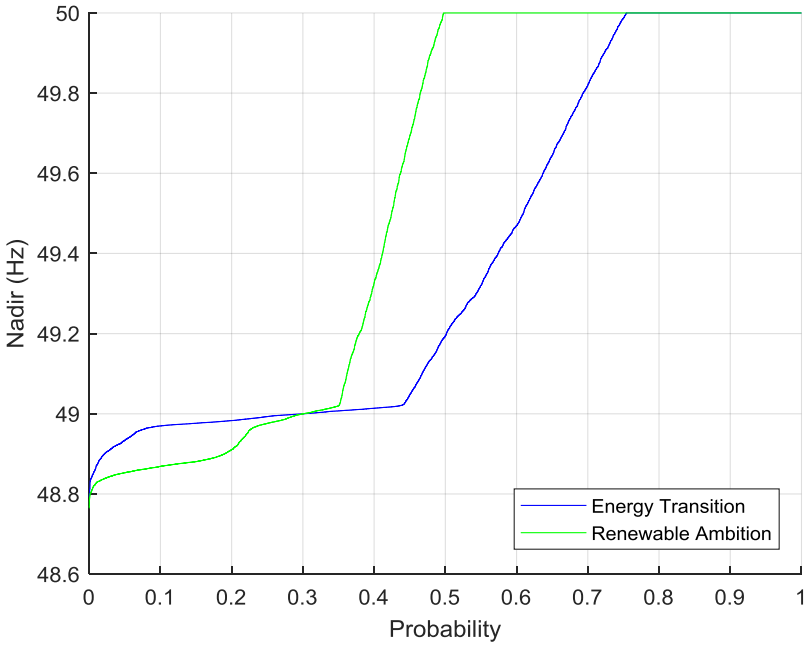

FIGURE 2-40: MONOTONIC FUNCTION OF NADIR VALUES IN NORTH AND EAST ZONE AFTER THE SPLIT OF CONTINENTAL EUROPE INTO THREE ZONES

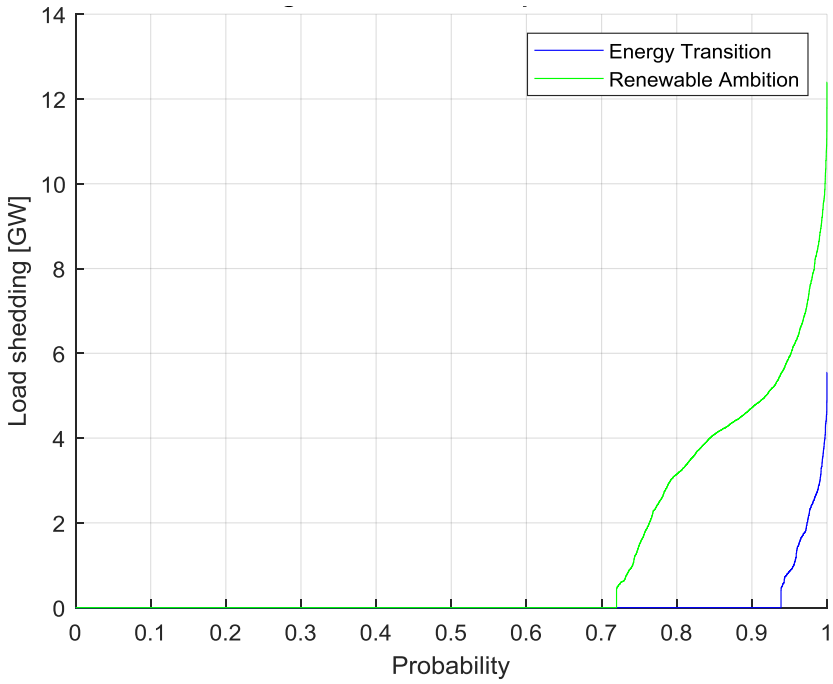

FIGURE 2-41: MONOTONIC FUNCTION OF LOAD SHEDDING IN FRANCE AFTER THE SPLIT OF CONTINENTAL EUROPE INTO THREE ZONES

The amount of load shedding in both zones is given in Figure 2-41 and Figure 2-42. The values are much higher in North and East zone, which is logical because the imbalances in this zone are higher.

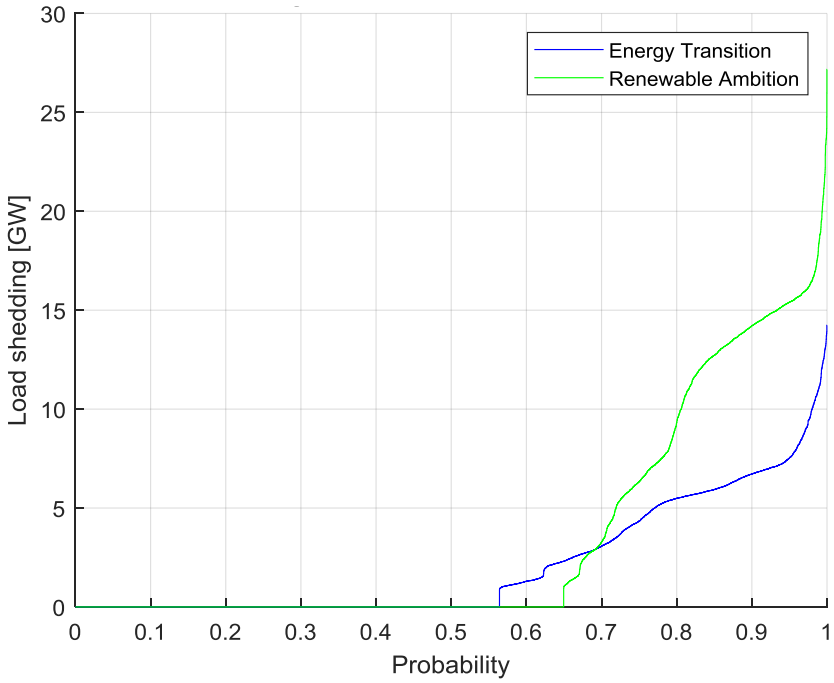

FIGURE 2-42: MONOTONIC FUNCTION OF LOAD SHEDDING IN THE NORTH AND EAST ZONE AFTER THE SPLIT OF CONTINENTAL EUROPE INTO THREE ZONES

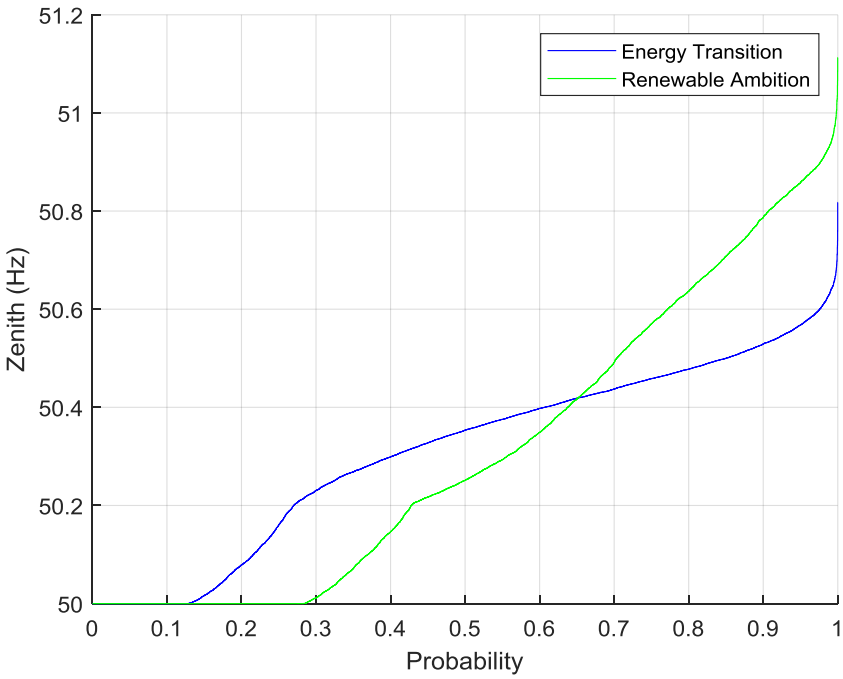

FIGURE 2-43: MONOTONIC FUNCTION OF ZENITH VALUES IN WEST ZONE AFTER THE SPLIT OF CONTINENTAL EUROPE INTO THREE ZONES

The analysis of frequency zenith values is shown on Figure 2-43 and Figure 2-44. The highest frequencies are obtained with the Renewable Ambition scenario. Values around 51 Hz are observed, which would not be critical for the system.

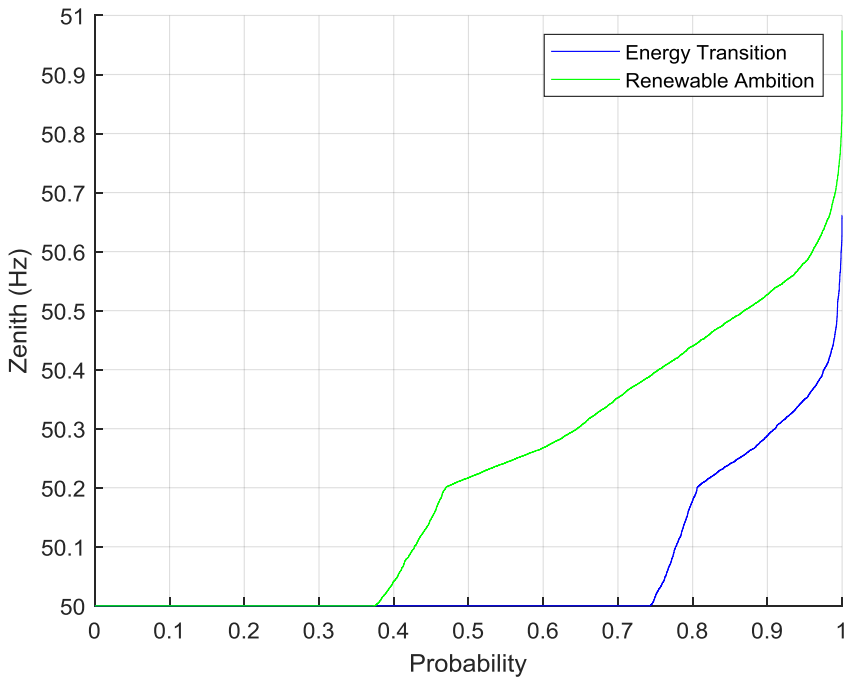

FIGURE 2-44: MONOTONIC FUNCTION OF ZENITH VALUES IN ZONE NORTH AND EAST AFTER THE SPLIT OF CONTINENTAL EUROPE INTO THREE ZONES

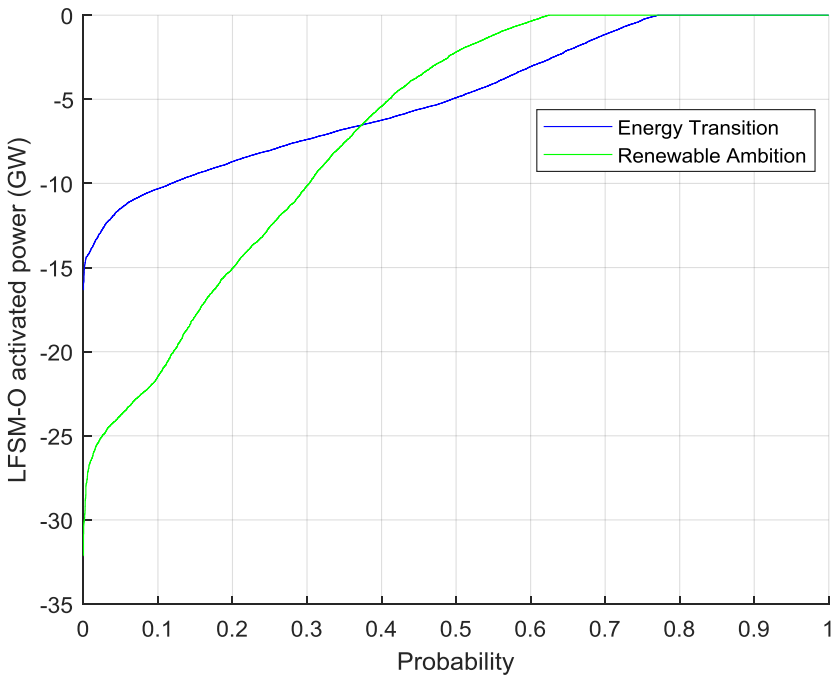

FIGURE 2-45: MONOTONIC FUNCTION OF LFSM-O ACTIVATED IN ZONE WEST AFTER THE SPLIT OF CONTINENTAL EUROPE INTO THREE ZONES

The activated LFSM-O power is given in Figure 2-45 and Figure 2-46 for the two zones.

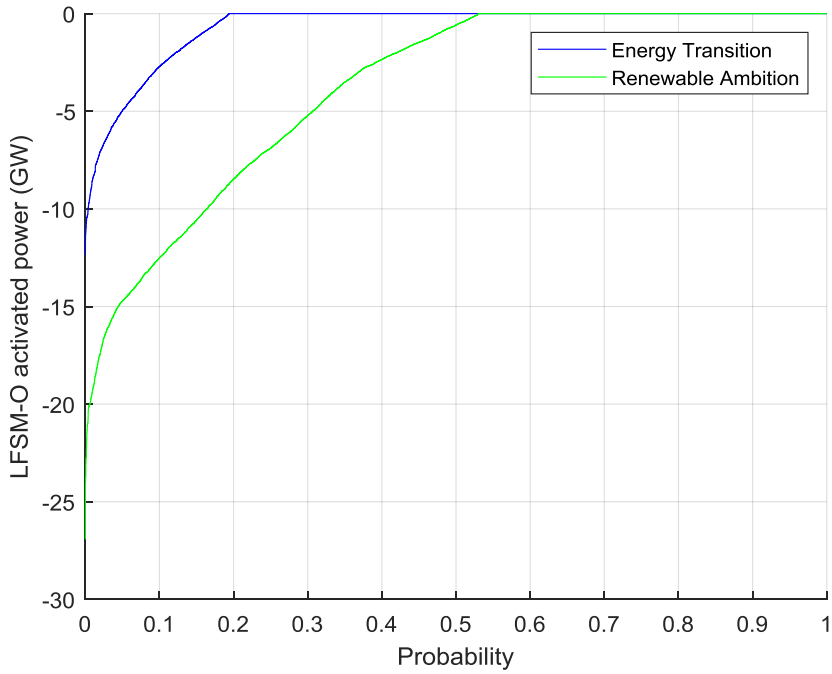

FIGURE 2-46: MONOTONIC FUNCTION OF LFSM-O ACTIVATED IN ZONE NORTH AND EAST AFTER THE SPLIT OF CONTINENTAL EUROPE INTO THREE ZONES

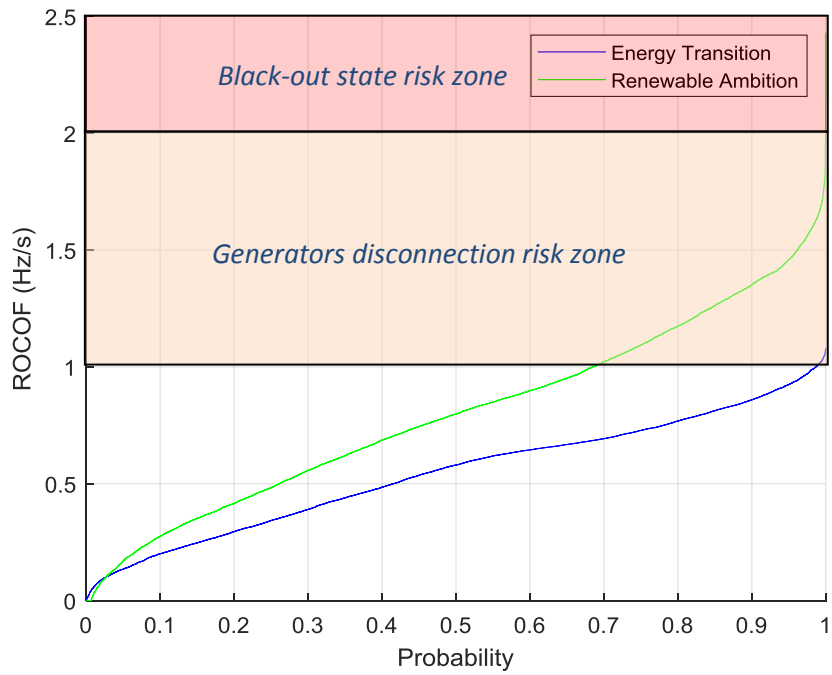

FIGURE 2-47: MONOTONIC FUNCTION OF ROCOF VALUES IN ZONE NORTH AFTER THE SPLIT OF CONTINENTAL EUROPE INTO THREE ZONES

Finally, RoCoF values can be observed in the two zones in Figure 2-47 and Figure 2-47. Renewable Ambition leads to a few RoCoF values higher than 2 Hz/s in both zones. Energy Transition shows maximum RoCoF values that are much more limited, just above 1 Hz/s.

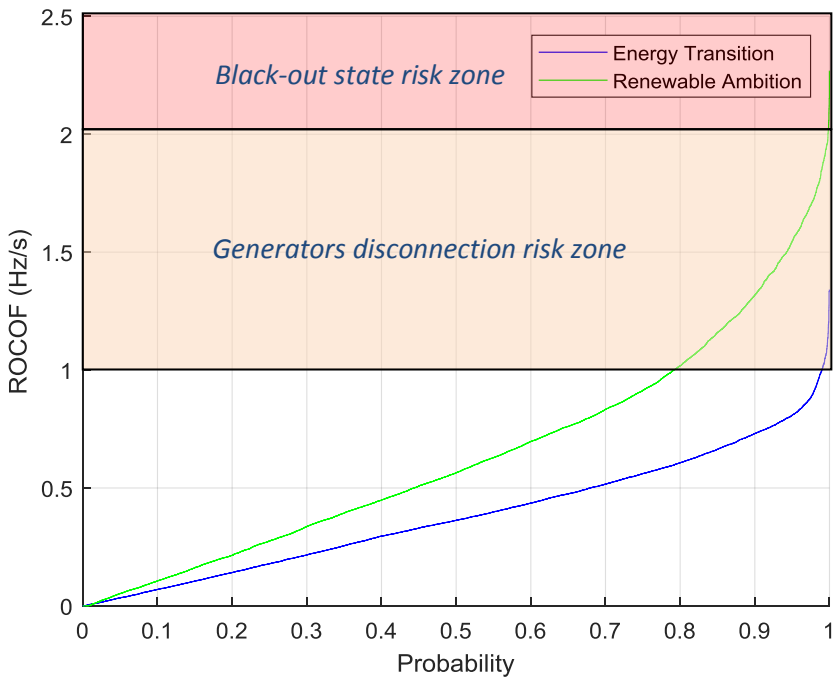

FIGURE 2-48: MONOTONIC FUNCTION OF ROCOF VALUES IN NORTH AND EAST ZONE AFTER THE SPLIT OF CONTINENTAL EUROPE INTO THREE ZONES

The observation of zenith and RoCoF values raises concerns about the European system stability in the case of splitting events, as critical thresholds (51.6Hz and RoCoF > 1 or 2 Hz/s) can be breached, especially in the Renewable Ambition scenario.

As expected, system split event entail instantaneous imbalances much higher than the reference incidents. The classical frequency control mechanisms are consequently insufficient to cope with such incidents and the system stability must rely on defensive actions, such as LFSM-O/U and load shedding.

In general, the same trends can be observed for the three system split cases, even though the results are exacerbated for the splits of the Iberian Peninsula and Italy, compared to the "Europe in 3" split case. The possible imbalances between zones are higher in Renewable Ambition than in Energy Transition, due to the higher levels of interconnection in Renewable Ambition. It was observed that in Renewable Ambition, all system's split cases endangered the system stability. The following Table 2-6 summarises the main trends.

The load shedding mechanism, as modelled in that study, was globally able to maintain the frequency above 47.5 Hz. There were, however, a few cases for all configurations where the 47.5 Hz threshold was crossed.

As for zenith values, the study reveals that the LFSM-O, as modelled, was not always sufficient to maintain frequency below 51.5 Hz, which is the critical level for the European power system. In 2006, the East zone (Area 3) faced a 9 GW positive imbalance which drove up the frequency to 51.4 Hz and caused some massive disconnections which finally stabilized the frequency to 50.4 Hz. Figure 2-49, taken from [11] depicts this stabilizing effect.

TABLE 2-6: SUMMARY OF THE RESULTS ON SYSTEM SPLITS (% OF SIMULATIONS)

Splitting event	Energy Transition			Renewable Ambition		
	NADIR < 47.5 Hz	ZENITH > 51.5 Hz	ROCOF > 1 Hz /s	NADIR < 47.5 Hz	ZENITH > 51.5 Hz	ROCOF > 1 Hz /s
Iberian Peninsula	0%	0%	~ 38%	< 1%	~ 15%	~ 85 %
Italy	< 1%	< 1%	~ 58%	< 1%	~ 2%	~ 49%
Europe in 3	0%	0%	~ 1%	0%	0%	~ 26%

<2%
<15%
>15%

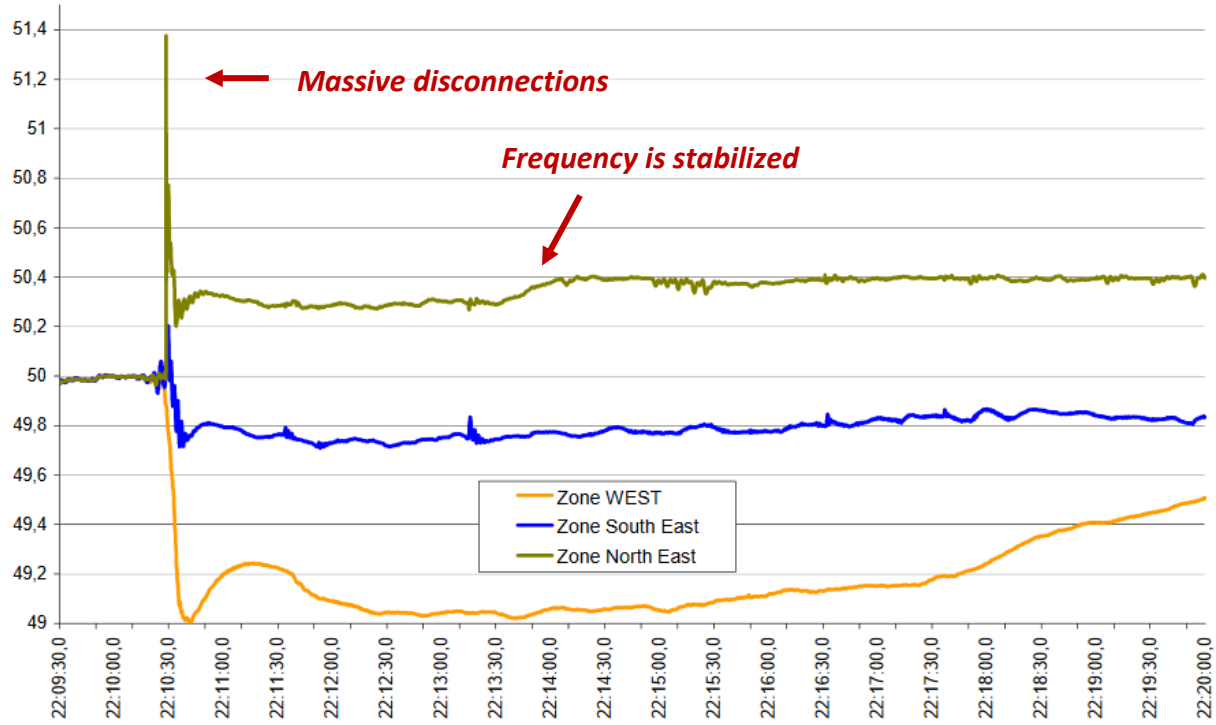

FIGURE 2-49: BEHAVIOUR OF EUROPEAN FREQUENCIES DURING THE 2006 SYSTEM SPLIT [11]

These disconnections appeared to be the ultimate way to ensure the frequency stability. The question is whether these massive disconnections would be progressive enough in the future and would therefore keep their beneficial effect, or, because of a generic common mode, they would affect most part of the generators at the same time and would result in a system black-out. To address this question, it is important to highlight that high RoCoF values could contribute to more generators being disconnected at the same time because the frequency could largely exceed 51.5 Hz before the disconnections happen. RoCoF values reach the critical threshold (1 Hz or 2 Hz) in:

- Many cases for both the Iberian Peninsula and the Italian events (between 38% and 85% of the cases, depending on the zone and the scenario considered)
- Fewer cases for “Europe in 3” split (26% in Renewable Ambition and 1% in Energy Transition). As explained before, these values seem to be problematic due to the possibility of large generation disconnections.

2.1.2 AFRR SIZING

The automatic Frequency Restoration Reserve (aFRR) is the active power reserve used to restore system frequency to its nominal value (50 Hz) and the power balance between areas to the scheduled value. This reserve is activated to take over from the Frequency Containment Reserve (FCR). In Task 2.4 of EU-SysFlex, the OPIUM methodology was used to assess the needs of aFRR for Energy Transition and Renewable Ambition. Detailed results are provided in [12]. For more information on the methodology underpinning OPIUM, the reader is directed to EU-SysFlex Deliverable 2.3 [3].

The methodology was first calibrated for the French and the German systems. For both of these countries, reliable 15 minutes or 30 minutes data was available [13] and it was therefore possible to reproduce current French and German aFRR values. The French calibration process is described in [12]. As a pragmatic approach, it was assumed that in each zone, the forecasted accuracy level for renewable generation resources and consumption matches the current French and German levels which were assessed during the calibration stage. More precisely, German PV accuracy levels have been used (standard deviation (STD) can reach 0.07% of installed capacity), as well as French wind and demand accuracy levels (STD can reach 1.2% of installed wind capacity and consumption STD is set to 0.66 MW per TWh of annual consumption). Although based on German and French data, each uncertainty source is zone-specific, and depends on factors such as the level of installed RES capacities, the yearly demand profiles, the wind conditions and the cloud cover.

OPIUM runs with a predefined risk level to take into account the different practices applied by TSOs. The lower a TSO set this risk level, the lower is the probability for the TSO to run out of aFRR [14]. Three risk levels have been considered in that study:

- 1%, the minimal level required by SOGL and the level which enables reproduction of the French aFRR volume during the calibration step (it's worth mentioning that currently RTE does not use probabilistic approach and do not consider any explicit risk level [12]),
- 0.1%, the current Belgian TSO target [15],
- 0.025%, the current German TSOs target) [14].

The OPIUM methodology yields downward and upward aFRR requirements. However, for simplicity purposes, the analysis which follows only addresses the upward margin. Figure 2-50 and Figure 2-51 show the mean upward margins for the Energy Transition and Renewable Ambition, respectively and for several different risk levels (1%, 0.01% and 0.025%). The current amounts of aFRR[3] are given for illustrative purposes only. Any comparison should be performed carefully given that operational aFRR volumes can take into account factors other than consumption and renewables uncertainty, such as deterministic deviations [16] and operational practices.

[3] Based on ENTSO-E Transparency data

On the x axis, the abbreviations correspond to the following countries:

- FRA: France,
- IBR: Spain and Portugal,
- ITA: Italy,
- EAST: Poland, Czech Republic and Slovakia,
- NTH: Germany, Belgium, Luxemburg, Netherlands, Denmark, Switzerland and Austria.

As can be seen, the aFRR requirement rises significantly in both scenarios. For the North zone (NTH), the current aFRR level is already quite high due to the current methods used at least in Germany and Belgium. In both of these countries, probabilistic approaches are already used (RES uncertainty is consequently already taken into account) with very low risk levels (0.05% in Germany and 0.1% in Belgium). This leads to a unique aFRR requirement for a long period of time (e.g. 3 months in Germany). This “static” application of the probabilistic approach results in sizing the aFFR regarding the worst possible conditions the system can experience. With a dynamic sizing (as is the case in OPIUM), the aFRR value is frequently updated depending on the system conditions (wind and solar, demand levels, etc.). Such a dynamic approach has the advantage of sizing less aFRR volume in most cases.

The results can be compared according to the scenario chosen or the risk level. It appears that the risk level plays a significant role. With the 0.025% risk level, some rare events such as power plant outages become more visible. This effect is particularly visible for the East zone (EAST), due to its large conventional power plant fleet.

However, no simple rule can be derived from the results, as the uncertainties are country-specific, and the results depend on how the different sources of uncertainty may or may not interact with one another. For instance, for a given risk level, the evolution of aFRR requirements from Energy Transition to Renewable Ambition is more pronounced in France than in other zones, whereas the increase in wind capacity is similar in the North, and even smaller for PV. In France, the evolution is mainly explained by the fact that the wind, demand and solar uncertainties turn out to be higher at the same time, in the middle of the day.

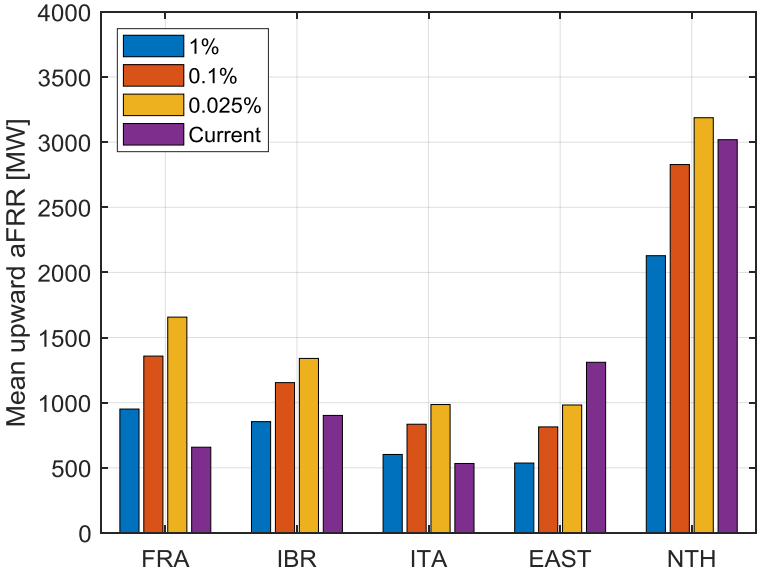

FIGURE 2-50: EVOLUTION OF MEAN UPWARD MARGINS IN EUROPE CONSIDERING ENERGY TRANSITION SCENARIO AND SEVERAL RISK LEVELS

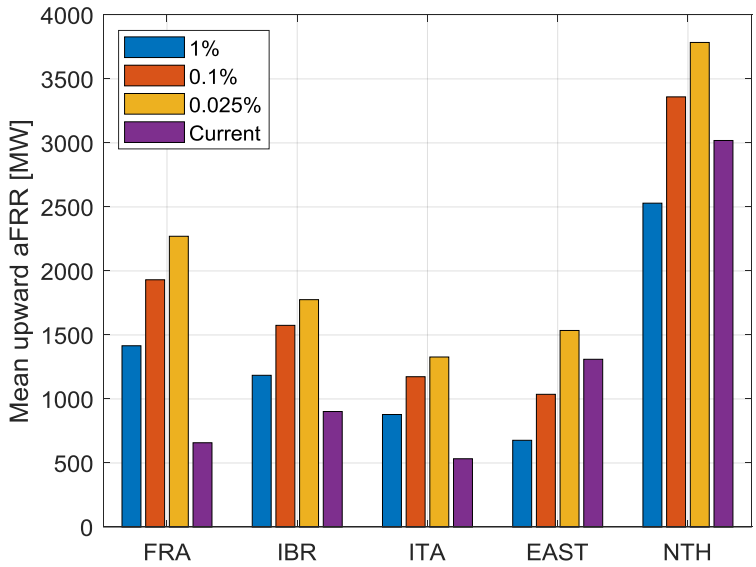

FIGURE 2-51: EVOLUTION OF MEAN UPWARD MARGINS IN EUROPE CONSIDERING RENEWABLE AMBITION SCENARIO AND SEVERAL RISK LEVELS

To complete the previous analysis, it is of interest to consider duration curves instead of mean values for the three different risk levels since the mean value cannot provide insight on the extreme values reached (Figure 2-52, Figure 2-53 and Figure 2-54).

From the figures, it can be seen that the annual variability of the hourly aFRR requirement increases with the insertion of vRES. Indeed, the difference between minimum and maximum values is bigger for North, than it is in Iberia and in France, followed by Italy and East. It demonstrates that areas with high RES installed capacities can

experience situations of very high uncertainty contrary to the areas with lower RES capacities. The difference between maximum and minimum aFRR sizes are given in
Table 2-7 Table 2-7, for the three risk levels chosen and the Renewable Ambition scenario.

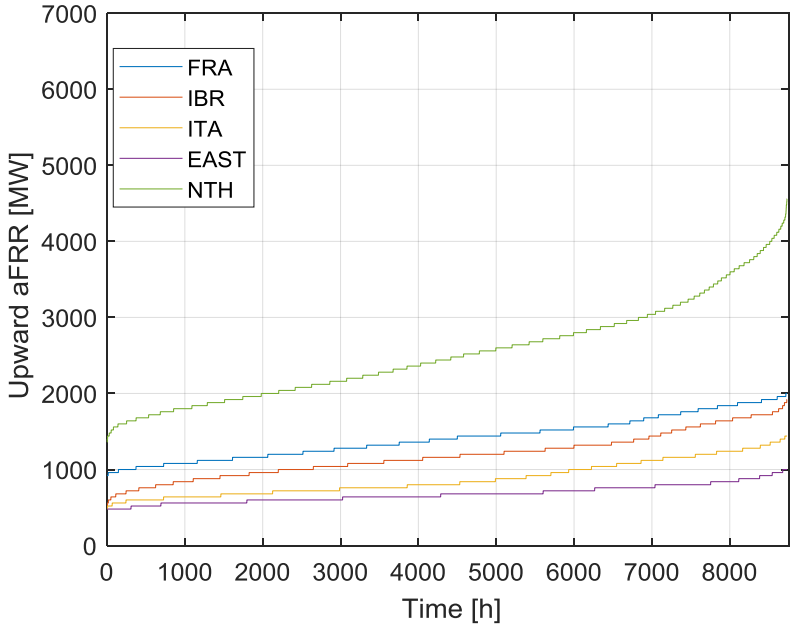

FIGURE 2-52: AFRR DURATION CURVES, RENEWABLE AMBITION, RISK LEVEL = 1%

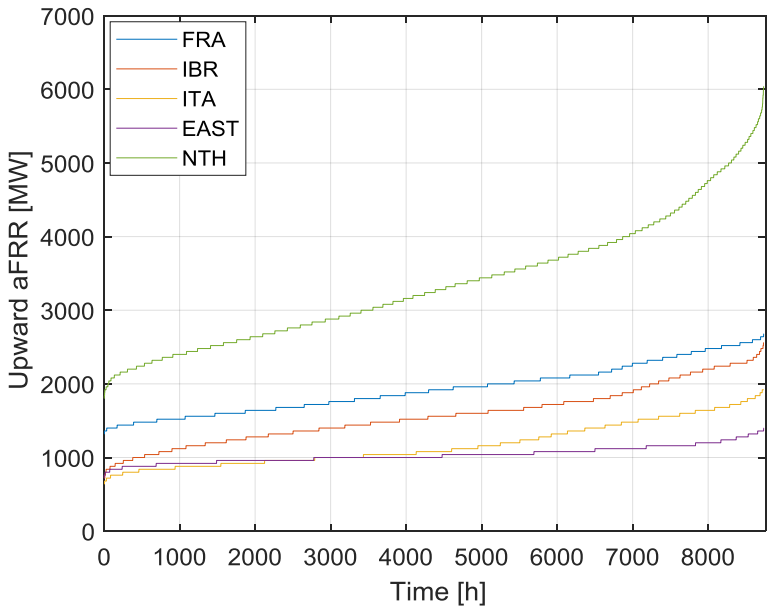

FIGURE 2-53: AFRR DURATION CURVES, RENEWABLE AMBITION, RISK LEVEL = 0.1%

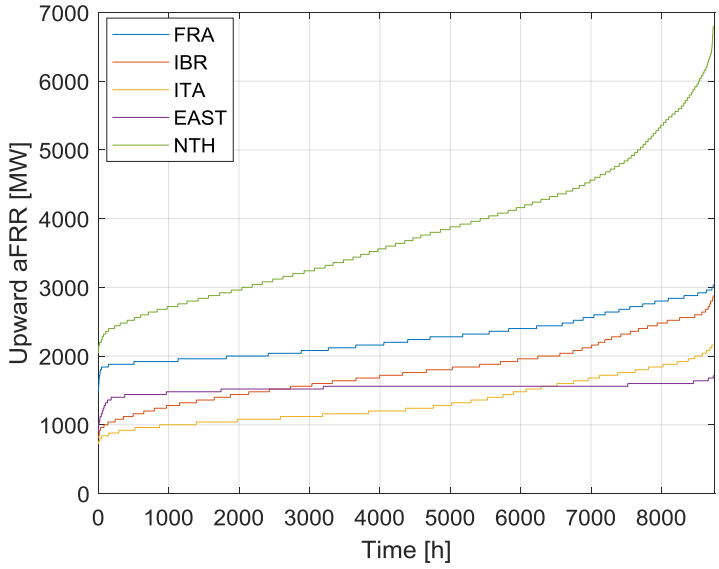

FIGURE 2-54: AFRR DURATION CURVES, RENEWABLE AMBITION, RISK LEVEL = 0.025%

TABLE 2-7: SPREAD (MAX - MIN) OF AFRR SIZES FOR RENEWABLE AMBITION SCENARIO AT DIFFERENT RISK LEVELS

Zone	max aFRR - min aFRR [MW]		
	1%	0.1%	0.025%
North	3200	4200	4760
Italy	920	1280	1440
France	1080	1360	1560
East	520	680	840
Iberian Peninsula	1400	1840	2080

Even though the average values of North aFRR would not increase in the long run, extreme values of aFRR could be more than twice as much as the current values.

The level of frequency quality does not solely depend on aFRR volumes but also on a set of TSO practices and policies (FCR volumes and features, aFRR & mFRR volumes and features, imbalance nettings and algorithms for cross-border activation in the short-term future etc.) and other dynamic parameters (such as the load-frequency and the load-voltage sensitivities, the system inertia etc.). All things considered, the adequacy of aFRR requirement (and hence the risk level) could be checked by using dynamic models to simulate the system frequency over a long period of time (several days at least).

For all zones in the Continental system, apart from the Iberian Peninsula, frequency nadir values for interconnected system analysis do not seem to be an issue, as they do not deviate from what ENTSO-E currently considers as theoretically achievable in case of the reference loss of generation. Even in the Iberian Peninsula, which is the weakest zone because of its large integration of variable renewables and its weaker connection to the rest of Europe, frequency nadir values seem to be manageable as they always stay above 49.3 Hz, far from the first load-shedding levels (49 Hz). RoCoF on the other hand could be more problematic than nadirs as the maximal local RoCoF values identified can exceed 1 Hz/s and can reach 1.3 Hz/ and very few systems can currently run with such high levels of RoCoF.

System split analysis indicates that classical frequency control mechanisms are insufficient for dealing with such events; load shedding was required to maintain frequency.

Analysis was also conducted on automatic Frequency Restoration Reserve requirements. It was found that the transition to higher penetrations of variable renewables results in a higher requirement for automatic Frequency Restoration Reserve and the annual variability requirement also increases.

2.2 IRELAND & NORTHERN IRELAND POWER SYSTEM

2.2.1 THE IRELAND AND NORTHERN IRELAND POWER SYSTEM

As outlined in the EU-SysFlex D2.2 report [2], Network Sensitivities were developed to stress the Ireland and Northern Ireland power system and were leveraged from work completed as part of Tomorrow's Energy Scenarios 2017 [17]. Across the Network Sensitivities for Ireland and Northern Ireland, the installed renewable generation capacities for the Ireland and Northern Ireland power system vary between about 9,000 MW and 15,000 MW by 2030. The generation portfolios corresponding to the Network Sensitivities that are the focus on the analysis for Ireland and Northern Ireland in this task are detailed in Table 2-8. For additional detail on these scenarios, the reader is directed to the EU-SysFlex D2.2 report [2].

2.2.2 PRODUCTION COST SIMULATION MODEL FOR IRELAND AND NORTHERN IRELAND

PLEXOS is a widely utilised tool for Unit Commitment and Economic Dispatch problems, both within industry and in academia. UCED is an hourly cost minimisation problem. The algorithm in PLEXOS determines the least cost manner in which to schedule generation to meet demand for each hour of the simulation, whilst being subject to a number of operating constraints. As part of Task 2.3, EirGrid and SONI created many UCED models for the Ireland and Northern Ireland power system in PLEXOS. These models corresponded to the various scenarios and network sensitivities (Steady Evolution and Low Carbon Living) which have been detailed in D2.2 of EU-SysFlex [2].

TABLE 2-8: IRELAND AND NORTHERN IRELAND PORTFOLIOS

Installed Capacity by Fuel Type (MW_e)	IE and NI Network Sensitivities	
	Steady Evolution	Low Carbon Living
Gas	5657	5207
Distillate Oil or Heavy Fuel Oil	389	273
Conventional Fuel Generation	6096	5530
Wind (Onshore)	6678	7040
Wind (Offshore)	700	3000
Wind-Total	7378	10040
Hydro	237	237
Biomass/LFG (including Biomass CHP)	487	847
Solar PV	900	3916
Ocean (Wave/Tidal)	50	98
Renewable Generation	9052	15188
Pumped Storage	292	652
Small Scale Battery Storage	200	500
Large Scale Battery Storage	350	1300
DSM	500	750
DC Interconnection	1650	2150
Conventional CHP or waste	290	309

The two most significant constraints when evaluating the operation of the transmission system in Ireland and Northern Ireland power system in a 2030 timeframe are System Non-Synchronous Penetration (SNSP) and maximum instantaneous Rate of Change of Frequency (RoCoF).

A constraint is included explicitly in the PLEXOS model to calculate SNSP and limit the SNSP. The current SNSP limit on the Ireland and Northern Ireland power system is 65%, with a goal of reaching 75% by 2020. By 2030 it is envisaged that this SNSP limit will be either increased to approximately 90% or will be completely removed.

A second constraint which is explicitly implemented into PLEXOS is a Rate of Change of Frequency (RoCoF) constraint which calculates the maximum instantaneous RoCoF which would be seen on the system for the loss of any infeed on the system. The N-1 RoCoF constraint is calculated as:

$$ROCOF = \frac{f^{nom}.\max\{p_t\}}{2.(System\ Inertia)} \qquad \text{(Eq. 2-2)}$$

where f^{nom} is the nominal frequency (i.e. 50Hz) and $\max\{p_t\}$ is the largest potential contingency at time *t*.

The current RoCoF limit on the Ireland and Northern Ireland power system is 0.5 Hz/s measured over a 500ms timeframe. This is to be increased to 1 Hz/s in 2020. It is highly unlikely that the RoCoF limit on the Irish power

system will be increased above 1Hz/s by 2030. Thus, the 1Hz/s RoCoF, as will be discussed later, is included in all simulations apart from, of course, the unconstrained market run. The ability to implement this RoCoF constraint in PLEXOS allows for the scheduling of additional inertia on the power system to ensure the maximum instantaneous RoCoF limit is not breached.

In addition, at present for system stability reasons, current operational policy requires that a minimum number of large conventional generating units are online at all times [18]. In order to accommodate greater levels of non-synchronous renewable generation, the minimum number of units constraint will have to be lowered. This, however, will expose a number of technical scarcities that will need to be surmounted, scarcities which are being investigated in Task 2.4.

Analyses of production costs are performed for the Network Sensitives. In addition, two key cases relating to operational policies are described below:

- 2030 Market Run (MARUN): This is a case set up to simulate the energy only market. There are no system operating constraints incorporated into the model. It is these simulations that are used to perform the financial analysis.
- 2030 Business as Usual (BAU): This represents 2020 operational policies including a maximum SNSP limit of 75% and a RoCoF limit of 1Hz/s. In addition it is required that a minimum of 7 large synchronous generator units are online at all times and in specific geographical locations. There are also operating reserve requirement constraints included in the model.
- 2030 Enhanced Operational Capabilities (EOC): It is assumed that the technical scarcities can be mitigated through provision of system services and that these services are provided by the range of different technologies in the portfolio. These services are modelled by assuming enhanced operational capability of the power system. This enhanced operational capability is modelled by removing the 75% SNSP limit as well as the requirement that a minimum number of large synchronous generators must be online in each time period. The RoCoF limit of 1 Hz/s is not removed as it is not envisaged that this will change in the near future. The operating reserve requirements continue to be included in the model; findings from Task 2.1 show that there will continue to be a significant requirement for carrying additional capacity in the form of operating reserves and in many cases this requirement will actually increase.

This information is summarised below in Table 2-9:

TABLE 2-9: SUMMARY OF CASES FOR EXAMINATION IN THE PRODUCTION COST SIMULATIONS

Case	SNSP Limit	RoCoF Limit	Operating Reserve	Min. Units
2030 Market Run (MARUN)	-	-	-	-
2030 Business as Usual (BAU)	75%	1 Hz/s	Yes	7
2030 Enhanced Operating Capability (EOC)	-	1 Hz/s	Yes	-

2.2.3 PRODUCTION COST SIMULATION RESULTS FOR THE IRELAND & NORTHERN IRELAND POWER SYSTEM

Employing PLEXOS, in conjunction with the Automated PLEXOS Extraction (APE) tool, analysis on the SNSP, inertia levels and result potential RoCoF values is conducted. To put the analysis in context, it is worth briefly discussing curtailment and dispatch-down.

Dispatch-down refers to the amount of wind energy that is available but cannot be accommodated. In Ireland and Northern Ireland, dispatch-down due to overall power system limitations is referred to as curtailment, while dispatch-down due to local network limitations is considered a constraint [19]. A distinction should also be made between dispatch-down due to power system limitations and dispatch-down for energy balance reasons. For example, variable renewable dispatch-down for energy balance reasons is analogous to dispatching down a conventional generator because demand levels have decreased from one interval to the next; there are no system constraints impeding the accommodation of wind generation, only the balance of energy in the market.
In Deliverable 2.5 of EU-SysFlex, additional analysis is conducted on dispatch-down levels and curtailment levels. The important finding from Task 2.5 is that as wind levels increase so too do dispatch-down levels for energy balance reasons. It is also found in Deliverable 2.5 that that continuing with Business As Usual operational constraints and policies (see Table 2-9 above) whilst also increasing the level of wind, dispatch-down levels for renewables will increase, potentially to levels that are unacceptable from the point of view of investment in variable renewable technologies. However, Deliverable 2.5 shows that by adopting system services, it is possible to move towards a more enhanced system operating regime. Doing so permits a reduction in curtailment levels. This is one of the primary drivers behind the need to transition to enhanced operation.

The current SNSP limit on the power system of Ireland and Northern Ireland is 65%. In order to be in a position to accommodate much higher penetrations of variable renewable generation on the Ireland and Northern Ireland power system, predominately wind, and minimizing the levels of dispatch-down and curtailment, it is necessary to remove, or at the very least move, the SNSP limit. Transitioning to operating a power system with very high SNSP levels represents a significant paradigm shift in system operation. The alternative is high levels of curtailment and the inability to meet the newly set government renewable target of 70% RES-E in Ireland by 2030.

If Business As Usual operational policies are not changed over the next decade, the SNSP limit in 2030 could be a binding constraint for up to 25% of the calendar year, as illustrated by the dotted line in Figure 2-55. In such cases, this would entail curtailment of renewables during those hours, as a number of large conventional units will need to be committed to keep the SNSP level below the 75% limit, reducing the headroom on the system to accommodate non-synchronous variable renewable generation.

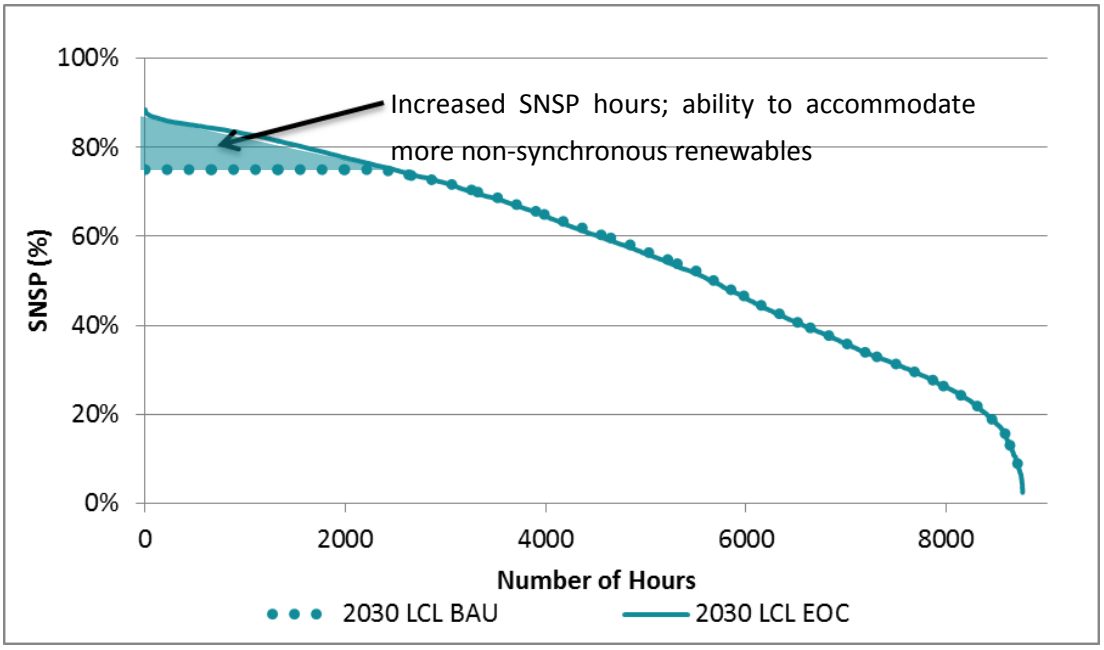

FIGURE 2-55: SNSP DURATION CURVE FOR LOW CARBON LIVING SNSP DURATION CURVE (BUSINESS AS USUAL (BAU) -V- ENHANCED OPERATING CAPABILTY (EOC))

However, by adopting system services, and thus having a portfolio with enhanced operating capability, it may be possible to remove the SNSP limit. This would then enable accommodation of more non-synchronous variable renewables and a reduction in curtailment. Moving to an enhanced operating regime results in a greater than 4% increase in annual wind production.

A comparison of two different 2030 scenarios is presented in Figure 2-56. As can be seen, the Steady Evolution (SE) scenario has, on average lower SNSP levels in comparison to the Low Carbon Living (LCL) scenario. This is not surprising given that there is about 7 GW of wind capacity installed in Steady Evolution (SE) but 10 GW of wind capacity in the Low Carbon Living (LCL) scenario.

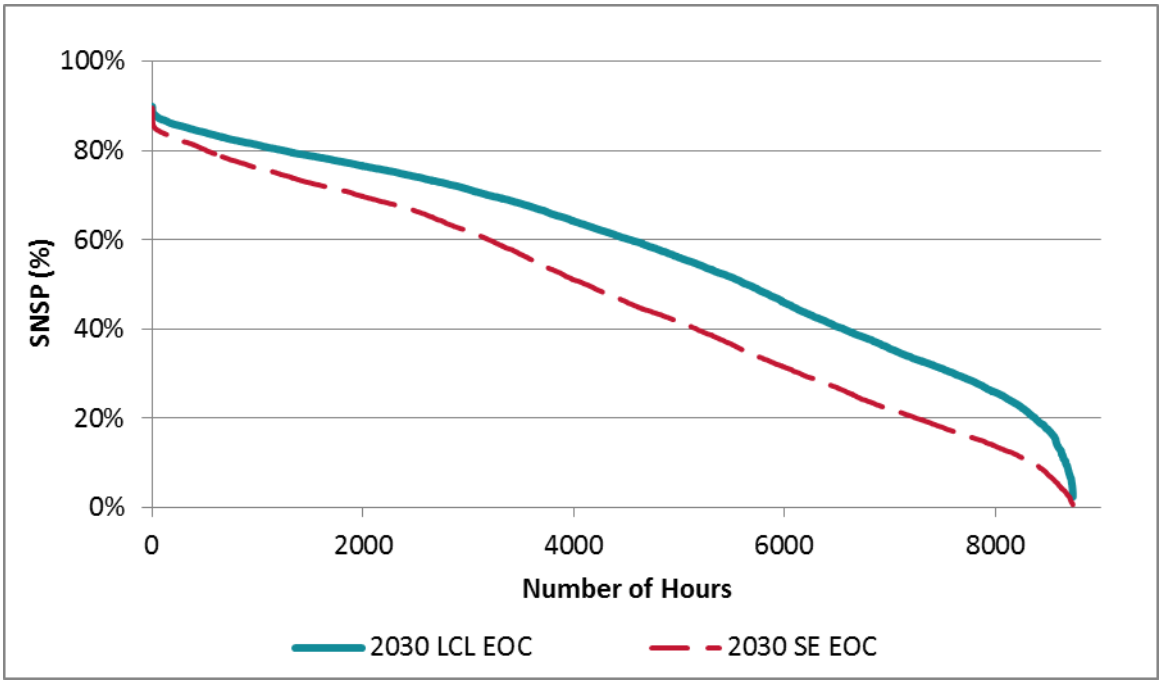

FIGURE 2-56: SNSP DURATION FOR LOW CARBON LIVING ENHANCED OPERATING CAPABILTY (EOC)-V- STEADY EVOLUTION ENHANCED OPERATING CAPABILTY (EOC)

If the system is to be operated at these high levels of SNSP, there will be technical challenges that will first need to be surmounted. One of these challenges relates to operating a power system with very low levels of inertia. Low inertia levels can have serious consequences for system operation and frequency stability. Synchronous inertia response is required to arrest the change in system frequency in the time frame immediately following a system disturbance such as the loss of a large generating unit or other infeed/export. Without sufficient levels of inertia, and thus synchronous inertial response capability, the system frequency can decline very rapidly, i.e. the rate of change of frequency (RoCoF) can be high.

Indeed, in the unconstrained dispatch (2030 LCL MARUN) , it was found that these low levels of system inertia lead to potential RoCoFs that far exceed 1Hz/s, the RoCoF standard in Ireland and Northern Ireland from 2020 onwards (see Figure 2-57). Increasing the penetration of non-synchronous generation leads to a marked increase in potential RoCoFs in the transition to a 2030 power system with high levels of non-synchronous variable renewable generation. As such high levels of RoCoF are wholly unacceptable, it was necessary to include a mitigation; a RoCoF Limit. Thus in the analysis which follows, there is a 1 Hz/s RoCoF limit included in the dispatches.

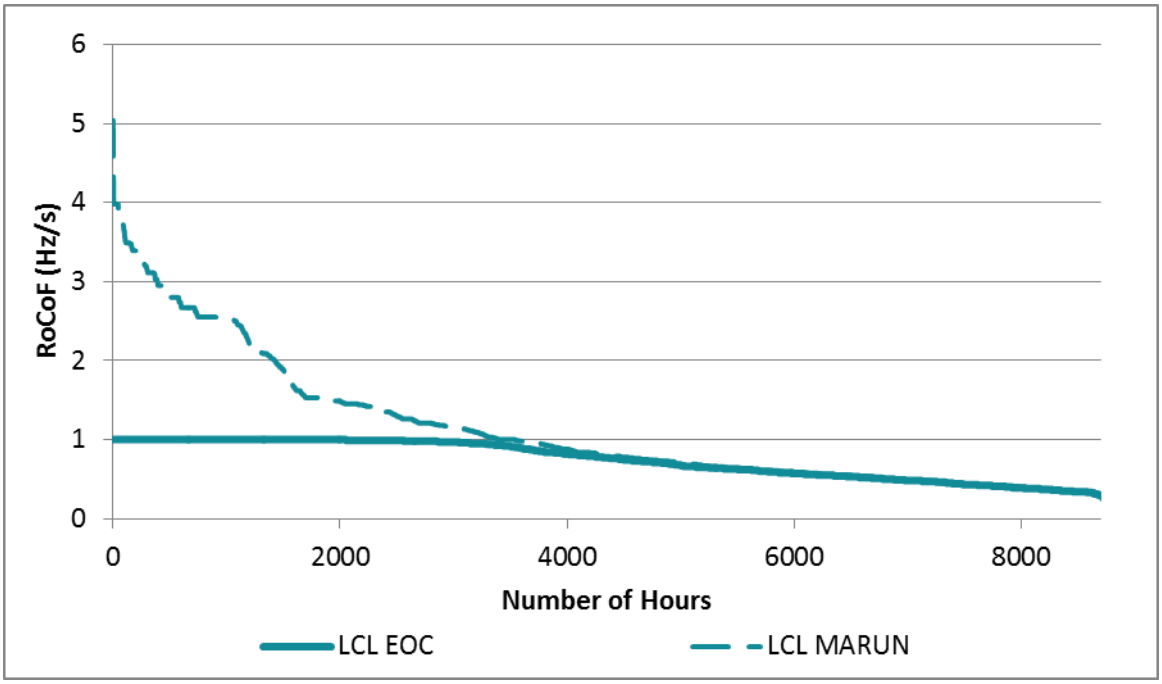

FIGURE 2-57: ROCOF DURATION CURVE FOR LOW CARBON LIVING ENHANCED OPERATING CAPABILTY (EOC)-V- MARKET RUN SIMULATION (MARUN)

It should be noted that in the Unit Commitment and Economic Dispatch algorithm there are two ways in which to satisfy this RoCoF limit and keep the RoCoF to 1Hz/s: a) by committing more conventional generators to increase the system kinetic energy or b) by reducing the largest infeed or $\max\{p_t\}$. In some extreme situations, it has been found that at times of low demand and high wind generation it is possible to satisfy the RoCoF constraint with a very low system inertia value. These cases are represented in Figure 2-59 by the sharp decrease in inertia levels for the EOC case. These are very extreme cases and represent a limitation of dispatch analysis in isolation. Such extreme hours require considerable, detailed examination to assess the transient stability of the power system.

A comparison of the two different 2030 scenarios is presented in
Figure 2-58. As can be seen, the Steady Evolution (SE) scenario has lower potential RoCoF in comparison to the Low Carbon Living (LCL) scenario. The main reason for this is due to the fact there is a large additional interconnector included in the Low Carbon Living (LCL) portfolio, which becomes the new largest single infeed (or dimensioning incident) resulting in higher potential RoCoF.

The results presented in Figure 2-59 are by no means an indication that it is anticipated that the power system will be operated at such low levels of inertia in 2030. It does however succeed in highlighting that there is potential for rotor angle stability issues during these hours. Rotor angle stability is dealt with in a separate chapter later in this report. It can also be seen in
Figure 2-59 that, apart from a number of extreme hours, inertia levels in the 2030 LCL EOC case are above 17.5 GWs for the vast majority of the year, in line with operational policy transition plans.

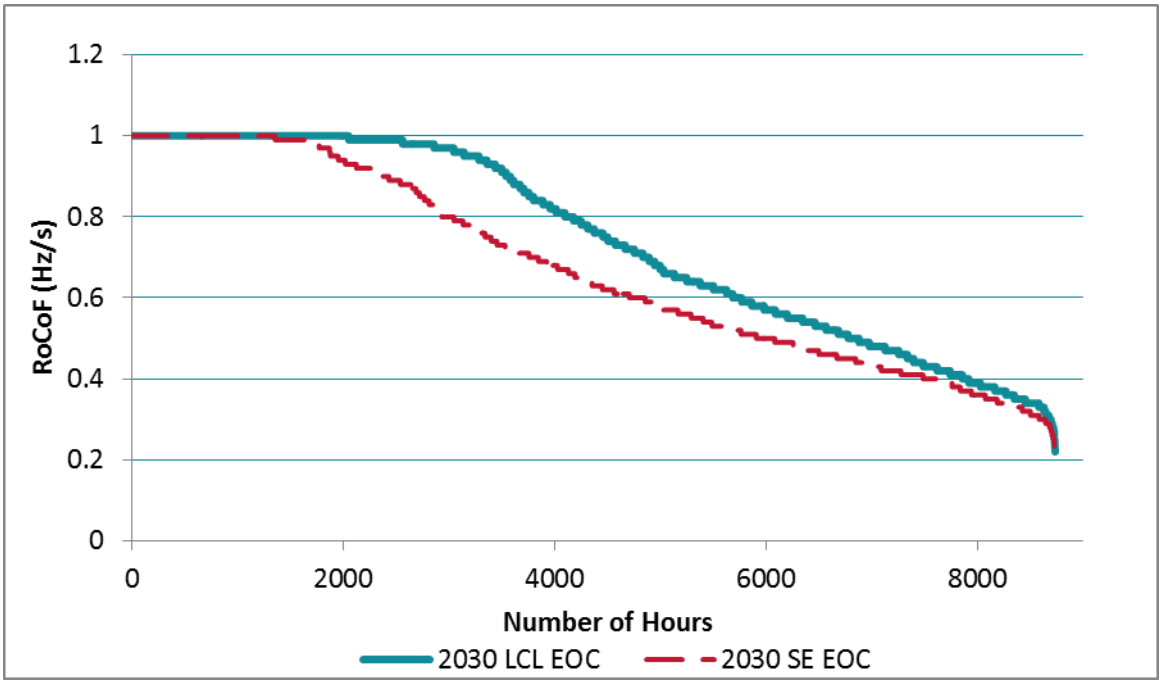

FIGURE 2-58: ROCOF COMPARISON BETWEEN LOW CARBON LIVING AND STEADY EVOLUTION (ENHANCED OPERATING CAPABILTY EOC))

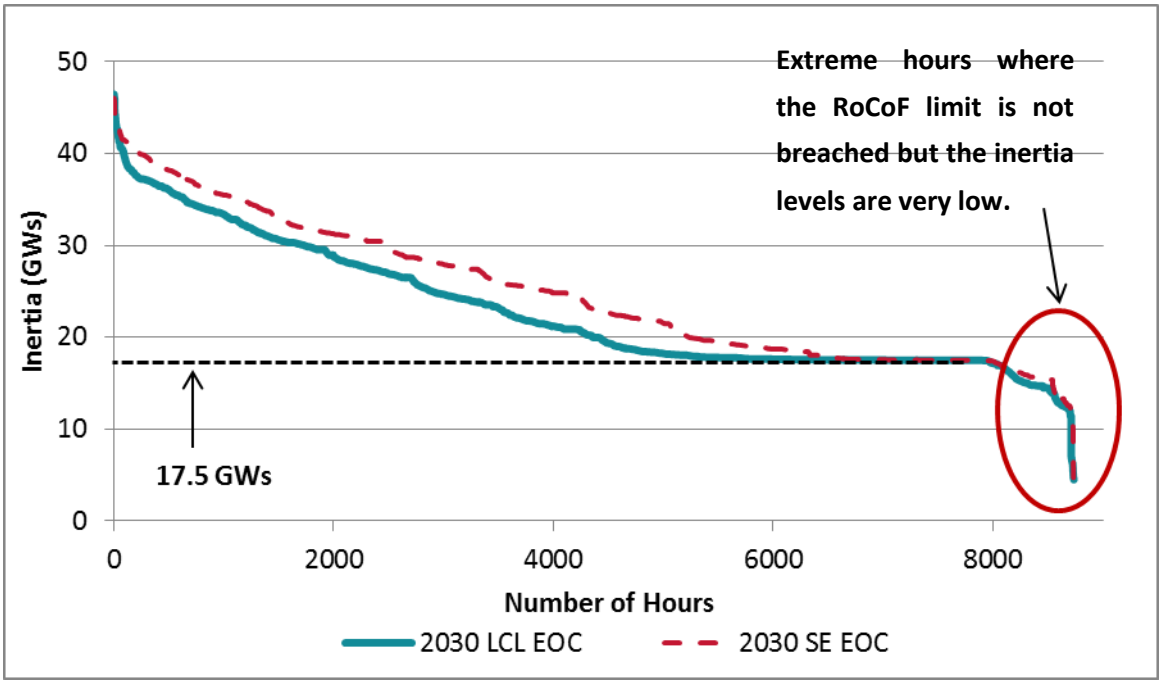

FIGURE 2-59: INERTIA LEVEL COMPARISON BETWEEN LOW CARBON LIVING AND STEADY EVOLUTION (ENHANCED OPERATING CAPABILTY (EOC))

2.2.4 TIME DOMAIN SIMULATIONS FOR THE IRELAND & NORTHERN IRELAND POWER SYSTEM

A reduction in system inertia and potential changes to the dimensioning incidents in the future, as discussed in the previous section, coupled with a changing reserve portfolio can have significant impacts on system frequency stability and expected frequency profiles. Time domain simulations have been carried out to examine the effects of these changes on system stability and to identify potential system scarcities which may require mitigation measures.

The study on the Ireland and Northern Ireland power system is informed by unit commitment schedules acquired through using PLEXOS for every hour of 2030 across the two scenarios for Ireland and Northern Ireland, namely Low Carbon Living (LCL) and Steady Evolution (SE). LCL generally envisages a higher level of RES-E, compared to SE, along with the difference in reserve portfolios. Further details on the individual scenarios are available in Task 2.2 report.

As highlighted in Task 2.3, a single frequency model (SMF) is used for frequency stability analysis; this is due to the computational efficiency of such a model. Due to the tight meshing and relatively low impedance between the nodes and regular model validation across system wide PMU measurements, a single bus model is a suitable approximation for the bulk system, from a frequency stability point of view. It is therefore suitable to use such a model for a high level indicative analysis of frequency stability to identify the frequency stability trends. The analysis has been carried out for every 7th hour of the year for both the scenarios under consideration to ensure sufficient variability of system conditions. As per the methodology highlighted in the Task 2.3 report, loss of largest infeed and loss of largest outfeed have been used as stimuli to investigate the system response during under and over frequency events. The system performance has been categorised using a combination of maximum frequency deviation (nadir/zenith) and the suitability, or otherwise, of the observed frequency profile.

The following assumptions have been made for the time domain simulations, providing a context for the interpretation of the results:

1. The maximum rate of change of frequency (RoCoF) has been limited to 1 Hz/s using specific constraints during the scheduling procedure (see previous section), therefore a mitigating measure for the lack of system inertia has been assumed to be in place
2. System operational settings (dead-bands, reserve, magnitudes etc.) for the resources existing currently as well as in future are kept in line with current operational practices
3. Variable output renewable resources (such as wind & solar generation) are assumed to provide no contribution towards frequency regulation. This assumption has been made to highlight potential system scarcities
4. Load inertia and load frequency sensitivity has been ignored to obtain conservative results

5. An over-frequency generation shedding scheme is assumed to be in place as a mitigating measure for excessive over-frequency deviations. Similarly, under-frequency load shedding is assumed to be in place for the simulations
6. Non-synchronous resources such as battery energy storage systems (BESS) and demand response participate in reserve provision within the frame-work of current system service in Ireland and Northern Ireland
7. Current system services are assumed to be in place in the future (FFR, POR & SOR etc.). It has also been assumed that reserve resources strive to maximise their reserve payments by delivering services in line with the scalar definitions for fast frequency response product, as defined for the Ireland and Northern Ireland power system.

2.2.5 UNDER-FREQUENCY STABILITY ANALYSIS FOR THE IRELAND & NORTHERN IRELAND POWER SYSTEM

Under-frequency stability analysis refers to the stability evaluation of the system following the loss of largest infeed, thereby creating a shortage of generation versus system load causing the system frequency to decline. The extent of the frequency deviation from the nominal value, following a deficiency of generation, is influenced by the size of the infeed loss, the available system inertia and the magnitude & speed of reserve provision. The analysis has been carried out for both the future scenarios, i.e. Low Carbon Living and Steady Evolution

LOW CARBON LIVING SCENARIO:

The Low Carbon Living (LCL) scenario entails a higher annual RES-E level (>70% annual energy consumption) with an increased number of interconnectors and a higher penetration of battery energy storage systems. The loss of the largest infeed simulations for the LCL scenario produces the results shown in Figure 2-60.

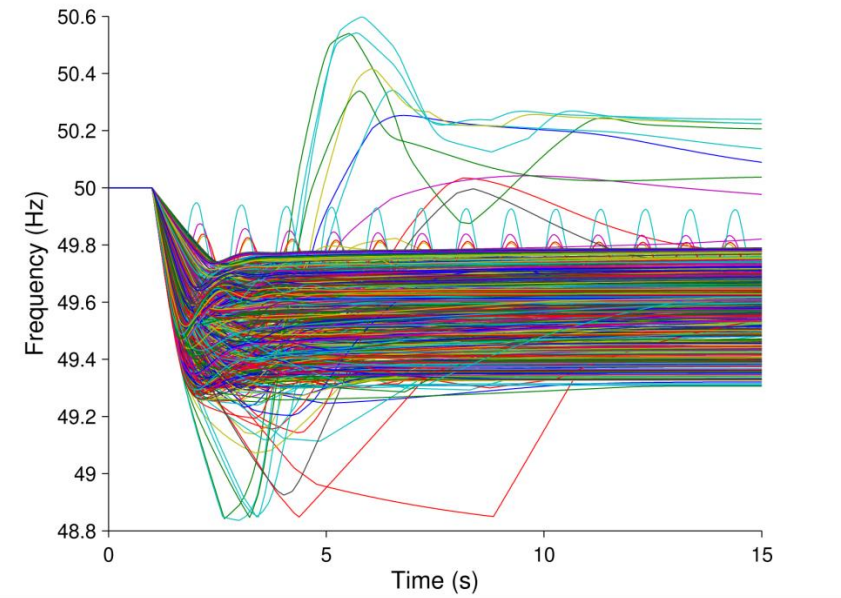

FIGURE 2-60: FREQUENCY PROFILE FOR LOW CARBON LIVING SCENARIO FOLLOWING INFEED LOSS

It can be seen that there are a few cases (0.6%) whereby the system frequency deviates below acceptable levels (49 Hz) and triggers involuntary load shedding. The triggering of load shedding for some of the cases results in a subsequent frequency zenith exceeding 50 Hz and the triggering of the over-frequency generation shedding scheme. Similarly, it can be seen that there are some cases whereby the system frequency oscillates following the loss of largest infeed. Apart from these cases, the majority of the frequency profiles demonstrate an acceptable level for the frequency nadir and post contingency steady state error. The average frequency nadir is 49.52 Hz.

The frequency profile for hour 1380 (see Figure 2-61) exhibits the triggering of load shedding and subsequent frequency overshoot. The synchronous machines in this snapshot have an aggregate rotational energy of 17.4 GWs and the largest infeed loss in this hour is 700 MW.

Due to the presence of excessive static reserve resource, consisting of pumped hydro units and static demand response in the snapshot under-consideration (652 MW) and comparatively smaller magnitude of fast dynamic reserves (HVDC interconnection & battery storage), a frequency overshoot is observed. This occurs because upon the 700 MW infeed loss, the frequency declines and attains a frequency nadir prior to the response of static reserve resources owing to the long response times associated with these resources (~1 second). These response times for static resources are in-line with the TSO experience of system operation and reserve contracts. As the frequency recovers, the static resources inject step reserves resulting in a frequency overshoot. This phenomenon can be seen in Figure 2-61.

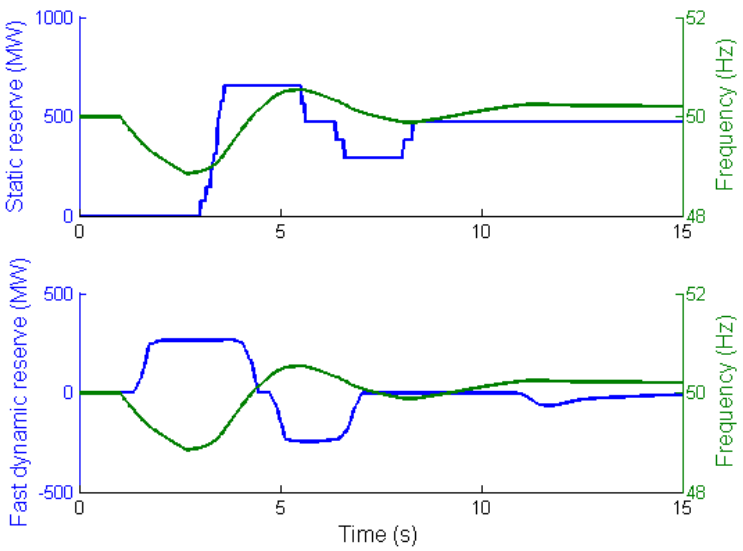

FIGURE 2-61: FREQUENCY AND RESERVE PROVISION FOR HOUR 1380

The over-shoot occurs due to a comparatively large (compared to the magnitude of the infeed loss) and relatively slow responding static reserve being triggered. With increasing static reserve levels and reducing system inertia levels, the static reserve needs to be carefully managed. This can be done either by curtailing the available static reserve magnitude and/or retuning the under-frequency load shedding magnitude.

Hour 4530 has an aggregate synchronous rotational energy of 4.5 GWs with a relatively small infeed loss (100 MW). The magnitude of available fast dynamic reserve from HVDC interconnectors and BESS is 400 MW. The fast acting dynamic reserves react quickly to arrest system frequency and can continuously modulate their power output in response to a change in system frequency. Tuning these resources in an aggressive manner (small deadband and small droop equivalent values) results in a quicker arrest of frequency and thereby a smaller nadir.

However, in the case that the aggregate fast dynamic reserve magnitude is comparable or greater than the infeed loss, in an appropriately low inertia system, an oscillatory response can develop due to excessively large responses to an infeed loss, as can be seen in Figure 2-62. This primarily occurs due to the reserve magnitude being larger than the infeed loss and due to the response delays of the reserve resources. In these simulations, the response delays have been informed by the current operational data for fast responsive resources. For BESS, the response delay has been assumed to be ~200 ms.

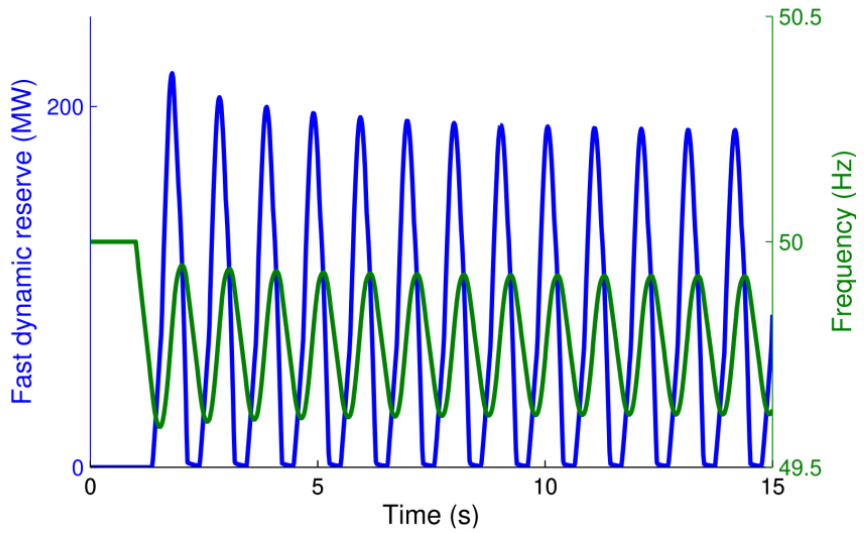

FIGURE 2-62: OSCILLATORY BHEVIOR IN HOUR 4530

It is to be noted that due to the excessive availability of BESS reserve in LCL scenario, a BESS reserve curtailment logic has been implemented, whereby the maximum magnitude of BESS reserve in an hour has been assumed to be no more than the magnitude of largest infeed. In the absence of this assumption a very large number of cases exhibit an oscillatory behaviour in the frequency profile. There is a correlation of such a behaviour with the system inertia, whereby a high inertia system is less likely to oscillate and more likely to damp any prevailing oscillations. Curtailing the magnitude of BESS reserve is in line with EirGrid and SONI's FFR service structure, whereby the grid controller has the option to curtail BESS response by activating one of the pre-programed modes of response for each battery (modes represent varying levels of response magnitude and response trigger settings).

There is no clear correlation between increasing renewable generation represented by SNSP levels and system frequency nadir. Generally, an increase in renewable generation levels is characterised by a decline in system

inertia and thereby higher frequency deviations following a demand-generation imbalance. Counterintuitively, the increasing SNSP levels seem to result in improved frequency nadir as can be seen in Figure 2-63.

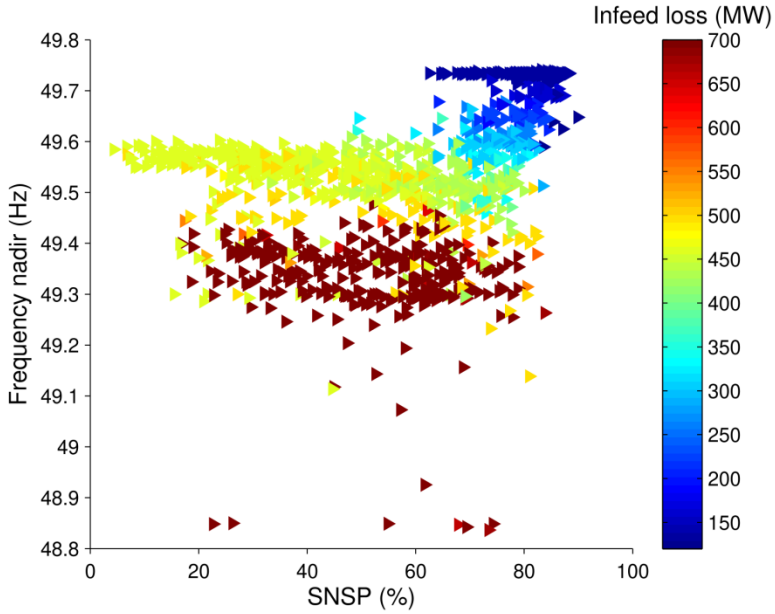

FIGURE 2-63: LCL - FREQUENCY NADIR VS SNSP & INFEED LOSS MAGNITUDE

It can also be seen in the figure, that the frequency nadir is directly correlated with the infeed loss magnitude (MW). There appears to be a trend, whereby as renewable levels increase beyond 70% SNSP, the size of the largest infeed loss tends to become smaller and thereby results in small frequency nadirs. This occurs due to more conventional generation being pushed towards minimum generation levels to accommodate renewable generation at high SNSP levels.

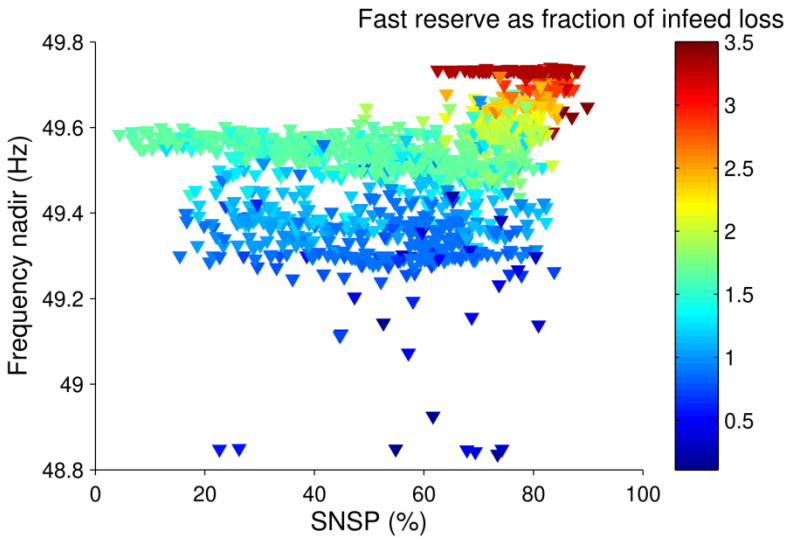

FIGURE 2-64: LCL - FREQUENCY NADIR VS SNSP & FAST RESERVE MAGNITUDE

The trend can be further explained by considering the availability of fast reserves (HVDC interconnectors and BESS) as a fraction of infeed loss. It is evident in Figure 2-64 that for the cases where the available fast reserves form a larger fraction of infeed loss, the frequency nadir is higher and vice-versa. It is particularly relevant to note that cases above 60% SNSP with a similar infeed loss volume and SNSP values have varying frequency nadirs owing to the varying levels of fast reserve magnitude available. The higher the fast reserve magnitude that is available, the better the frequency nadirs.

It can therefore be concluded that the availability of fast acting reserve at low inertia situations is vital for obtaining higher frequency nadirs. It can further be concluded that adequate level of frequency stability is maintained if the volume of fast acting reserve is equivalent to that of infeed loss, indicating that the speed of response for fast acting reserves compensates for faster frequency decline owing to lower system inertia levels.

STEADY EVOLUTION SCENARIO

The Steady Evolution (SE) scenario entails a comparatively (relative to LCL) lower level of annual RES-E, a smaller magnitude of HVDC interconnection and a smaller magnitude of BESS. The loss of the largest infeed simulation for the SE scenario produces the frequency profiles shown in Figure 2-65Figure 2-65: FREQUENCY PROFILE FOR Steady evolution scenario following infeed lossFigure. It can be seen that there is a significant number (4% snapshots) of frequency profiles with frequency nadir lower than 49 Hz, and such cases require load shedding activation to arrest the frequency decline. It can also be seen that there are no significant frequency over-shoots during frequency recovery. This is primarily due to the absence of an additional 360 MW of pumped storage step response which is available in the LCL scenario. It is also to be noted that the level of HVDC interconnection and thereby the associated fast dynamic reserve (75 MW) in SE scenario is lower than in LCL. The value of average frequency nadir for the SE scenario is 49.42 Hz.

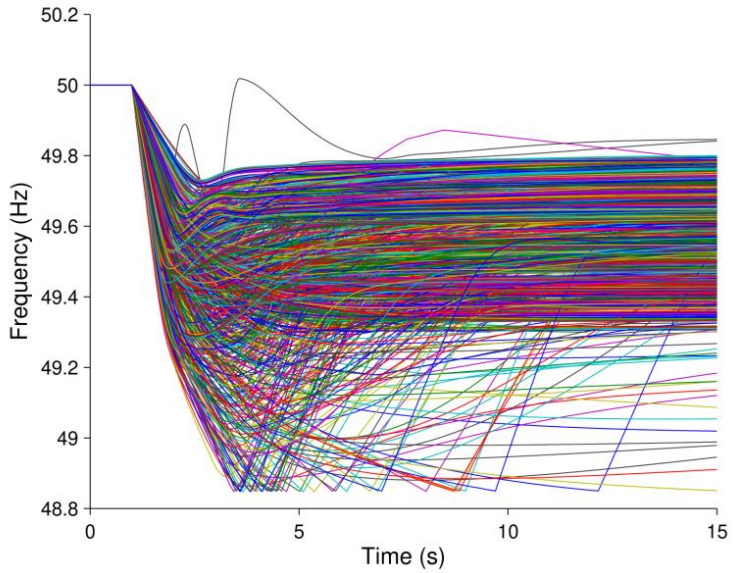

FIGURE 2-65: FREQUENCY PROFILE FOR STEADY EVOLUTION SCENARIO FOLLOWING INFEED LOSSFIGURE

Generally in the SE scenario, the level of fast acting dynamic reserve with the potential to offset the effects of a lower system inertia and faster frequency dynamics is lower than in LCL. The absence of adequate fast acting dynamic reserve exposes a potential issue with regards to the maintaining current reserve scheduling magnitude despite a changing reserve portfolio. Currently the Ireland and Northern Ireland system is scheduled with POR magnitude equating to 75% of largest infeed values. With the current system conditions and reserve portfolio, this practice has been proven to be effective.

For a fundamentally changed system inertia and reserve portfolio, as represented by SE & LCL scenarios in 2030, it has been assumed that POR is scheduled as 75% of largest infeed, while FFR service is scheduled to 47% of largest infeed value. Hour 5461 serves as a suitable example to question this scheduling practice, with an aggregate rotational energy of synchronous units equal to 27.3 GWs, SNSP level of 32% and infeed loss magnitude of 700 MW. As per the scheduling practice, the FFR magnitude available is 69% of infeed loss (488 MW), while POR available is 78% of infeed loss (550 MW). However, the majority of reserve resources making up the FFR and POR reserve portfolio consist of resources with a droop equivalent, substantially smaller than 4%. The net effect of this smaller droop equivalent is that these resources provide exactly as much reserve as contracted, since the contracted reserve values are required at relatively high frequency levels. These reserve resources include BESS and HVDC interconnectors and demand response. For hour 5461, these resources constitute 97% of scheduled FFR and 88% of scheduled POR magnitude, resulting in the initial infeed loss magnitude (700 MW), not being recovered by the reserves. The frequency profile therefore drifts downwards, until arrested by load shedding, causing substantially lower frequency nadirs.

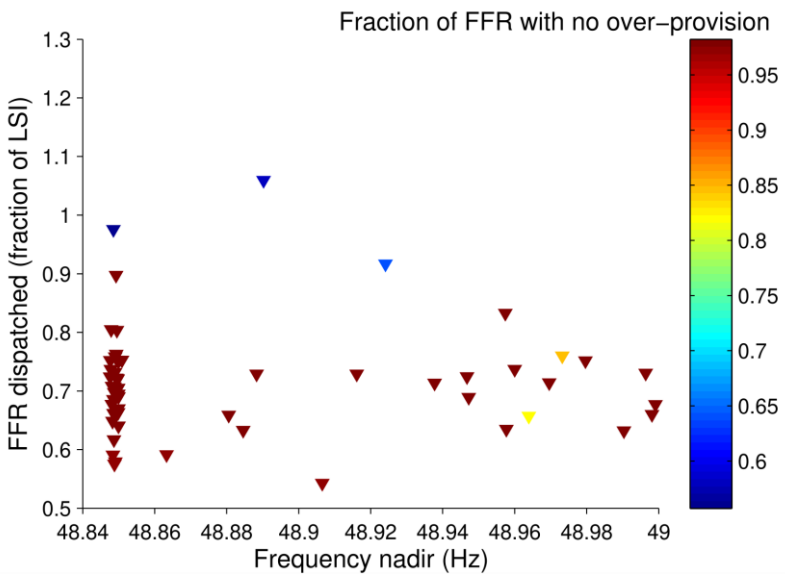

FIGURE 2-66: INADEQUACY OF DISPATCHED RESERVE MAGNTIUDE (SNAPSHOTS WITH NADIRS < 49 HZ)

The aforementioned trend is visible across all the snapshots with substantially low frequency nadirs (<49 Hz). As seen in Figure 2-66, there is a clear trend among the low frequency nadir cases, whereby, a substantial magnitude of dispatched FFR consists of resources with no over-provision of reserves, thereby resulting in worse frequency nadirs. The analysis shows that there is a need to redefine the reserve magnitude requirements for both POR and

FFR services while recognising the nature of available reserve. Traditionally for the Ireland and Northern Ireland power system, the 75% of LSI POR requirement is adequate owing to the over-provision (beyond the contracted value) of reserve from conventional resources operating at 4% droop.

Similar to LCL scenario, there is very little correlation between the increasing SNSP levels and frequency nadirs. The primary factor determining the frequency nadir is the infeed loss magnitude as shown in Figure 2-67. In contrast with the LCL scenario, a larger proportion of snapshots have SNSP levels lower than 60%. The over-arching trend of higher SNSP levels and smaller infeed loss magnitudes is also visible.

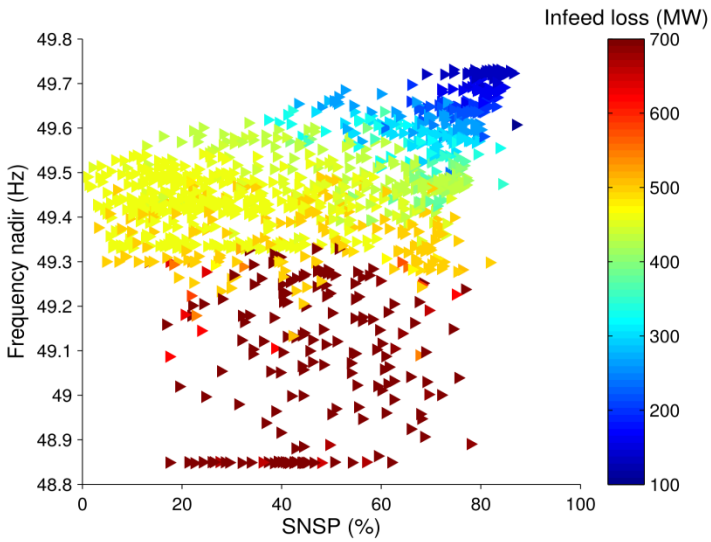

FIGURE 2-67: SE - FREQUENCY NADIR VS SNSP & INFEED LOSS MAGNITUDE

Similar to LCL, the availability of fast reserve as fraction of infeed loss simulated appears to be a major factor in determining the frequency nadirs, with higher availability of fast reserves combined with smaller infeed loss resulting in better frequency nadirs, Figure 2-68.

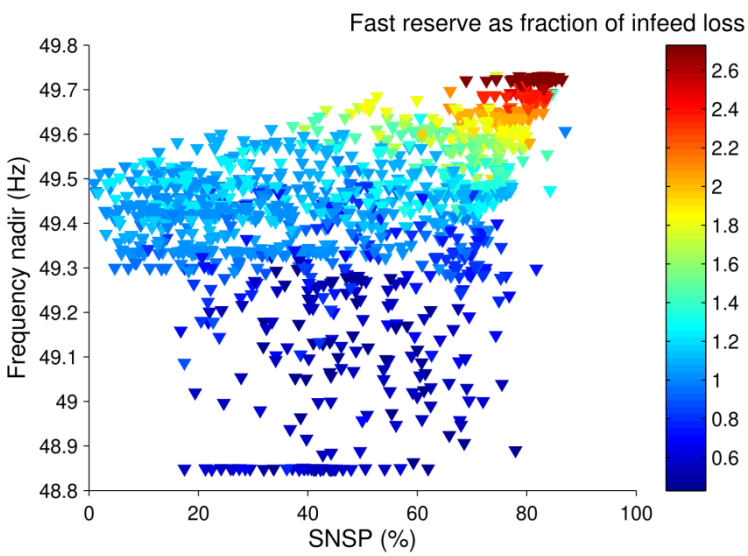

FIGURE 2-68: SE - FREQUENCY NADIR VS SNSP & FAST RESERVE MAGNITUDE

The cluster of nadirs below 49 Hz across various SNSP levels, present in SE scenario is due to the FFR and POR scheduling requirements and due to a majority of reserves providing exact contracted magnitudes, while operating at small droop equivalents, as evidenced in Figure 2-66.

2.2.6 OVER-FREQUENCY STABILITY ANALYSIS FOR THE IRELAND & NORTHERN IRELAND POWER SYSTEM

Traditionally, the loss of an infeed has been the focus of frequency stability phenomena for the Ireland & Northern Ireland power system. However, with increasing levels of renewable generation and increased interconnection levels, the loss of a HVDC interconnection at full export becomes a credible threat to the system and therefore needs to be evaluated. For over-frequency stability simulations, the loss of largest export value on the interconnectors has been simulated and the system response evaluated. For some of the simulated snapshots, there is no export on interconnectors and hence no outfeed loss for these snapshots has been considered. The evaluation has been carried out for both LCL and SE scenarios.

LOW CARBON LIVING SCENARIO:

The Low Carbon Living scenario is characterised by higher levels of RES-E, larger number of BESS resources and higher levels of HVDC interconnection. For over-frequency situations, the Ireland and Northern Ireland power system employs an over-frequency generation shedding scheme, which sheds various magnitudes of wind generation on pre-specified over-frequency magnitudes, shedding about 881 MW between 50.5 to 50.75 Hz. Therefore, 50.75 Hz is considered in these simulations as the highest acceptable value of frequency zenith, as 1000 MW of distribution network connected wind is assumed to be involuntarily disconnected at 50.8 Hz. This relatively large magnitude of disconnection can lead to an under-frequency following the over-frequency event.

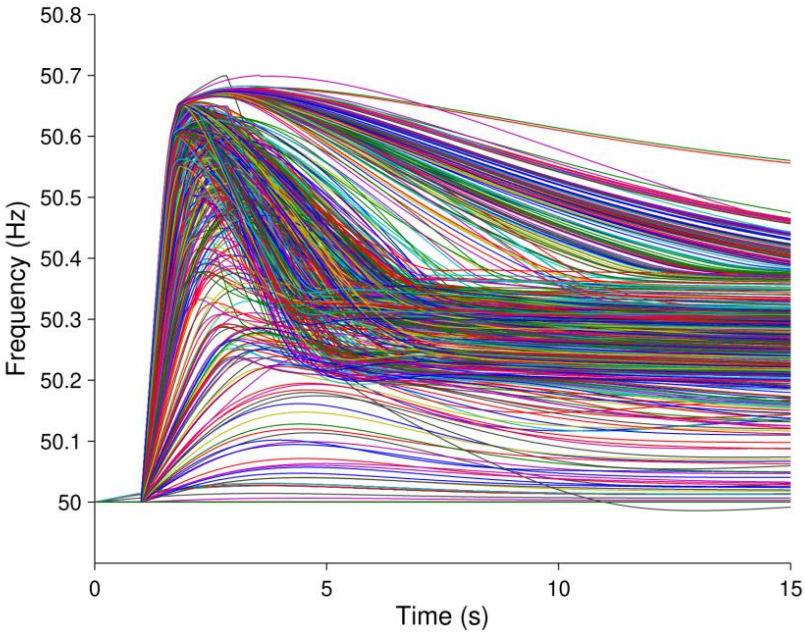

FIGURE 2-69: FREQUENCY PROFILE FOR LOW CARBON LIVING SCENARIO FOLLOWING OUTFEED LOSS

The time domain frequency simulation profiles for LCL are shown in Figure 2-69. It can be observed that the frequency zeniths stay below the highest acceptable zenith of 50.75 Hz. There is no under-frequency following the activation of OFGS scheme indicating that the magnitude and trip settings for OFGS are appropriate. It is to be noted that fast acting reserves from interconnectors are assumed to respond in a dynamic manner by altering the flow on HVDC links according to the frequency deviation. The relatively improved security of over-frequency profiles for LCL compared to the under-frequency profiles is primarily due to the activation of OFGS at a frequency deviation of 0.5 Hz above nominal frequency.

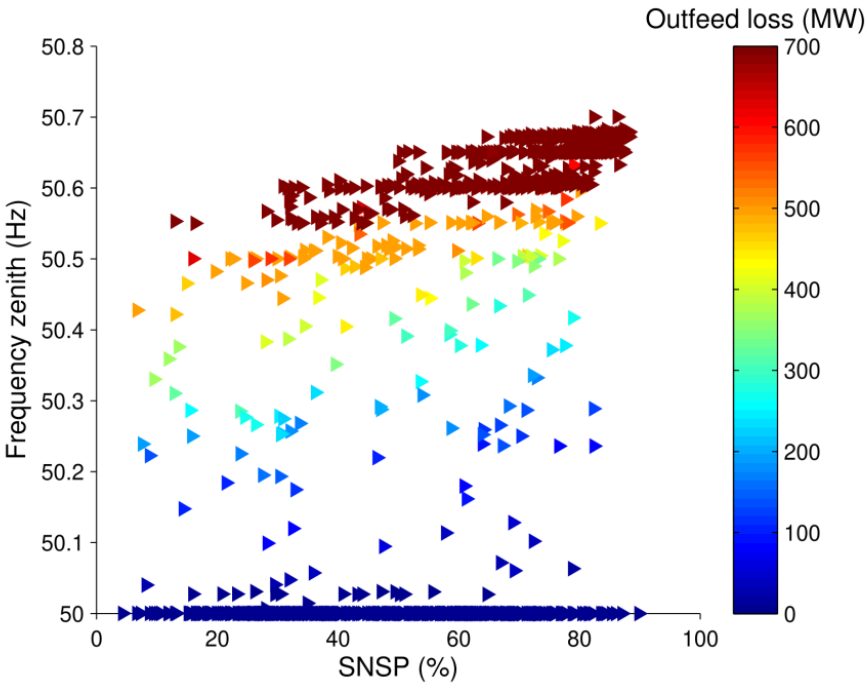

FIGURE 2-70: LCL - FREQUENCY ZENITH VS SNSP & OUTFEED LOSS MAGNITUDE

In contrast with the under-frequency profiles, there is a clear co-relation between increasing SNSP levels and worsening frequency zeniths. However, the underlying primary influencing factor is the same i.e. the magnitude of imbalance. It can be seen that as the SNSP level increases, so does the level of export, thereby increasing the initial active power imbalance initiating the frequency event. As the level of renewable generation increases, the interconnector export levels increase correspondingly, as shown in Figure 2-70.

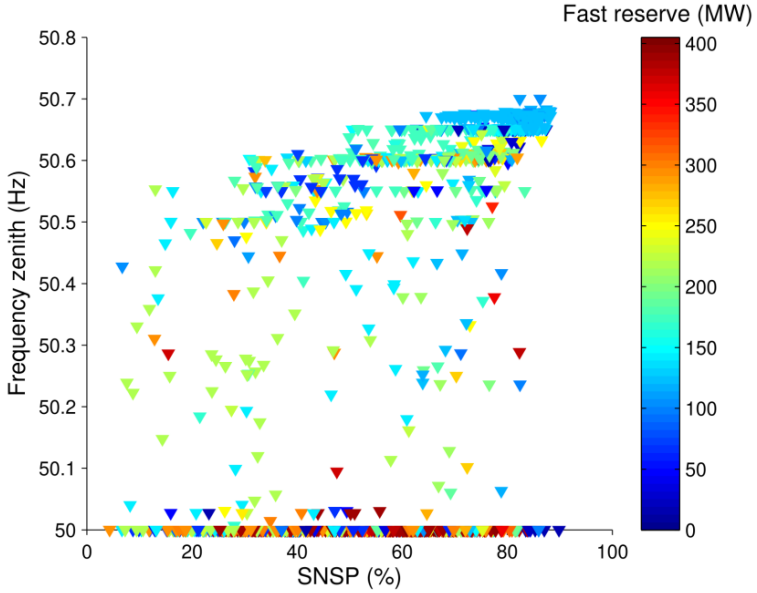

FIGURE 2-71: LCL - FREQUENCY ZENITH VS SNSP & FAST RESERVE MAGNITUDE

Furthermore, at higher SNSP levels, a smaller number of conventional generators are likely to be online with ever decreasing levels of foot-room to accommodate higher levels of renewable generation. In addition, most interconnectors are very close to full export levels, with very little capacity available to accommodate additional export following the loss of an export link. This is demonstrated in Figure 2-71 whereby there is a trend of reduced fast reserve levels and higher outfeed loss at increasing SNSP levels, resulting in higher frequency zenith values. It is to be noted that 15% of BESS magnitude available for under-frequency reserve provision, participates in over-frequency reserve provision. This is in line with the current mechanism of BESS reserve participation in ancillary services in Ireland and Northern Ireland. Furthermore, the effectiveness of over-frequency generation shedding scheme can be demonstrated by Figure 2-72 whereby a cluster of high frequency zeniths forms around 50.7 Hz due to the start of OFGS activation at 50.5 Hz, with the highest frequency zenith occurring at 50.70 and a mean zenith of 50.30 Hz.

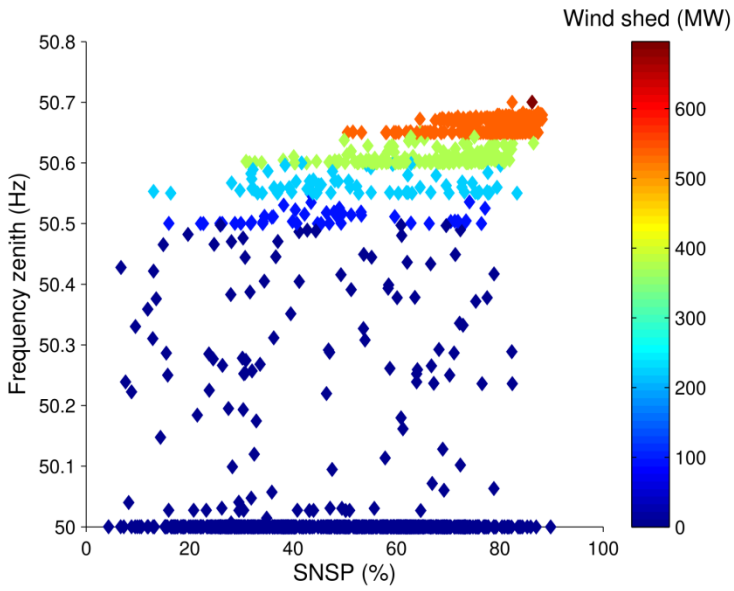

FIGURE 2-72: LCL - FREQUENCY ZENITH VS SNSP & OVER FREQUENCY WIND SHEDDING

STEADY EVOLUTION SCENARIO

Frequency profile evaluation for the SE scenario following the loss of the largest export/outfeed is not materially different to the LCL scenario. Similar to LCL, the frequency zeniths stay below 50.8 Hz and the frequency profiles do not exhibit an under-frequency dip following reserve activation for curtailing excessive over-frequency deviations. Due to the relatively smaller magnitudes of BESS activated for over-frequency events (15% of magnitude activated for an under-frequency event), there is no substantial difference between the frequency profiles for the SE and LCL scenarios, as fast reserve from BESS is the major difference between the two scenarios, which fully comes in to play for under-frequency simulations. The major factor influencing the frequency zeniths is the OFGS scheme, with the magnitude of wind required to trip being available for both the scenarios (SE and LCL).

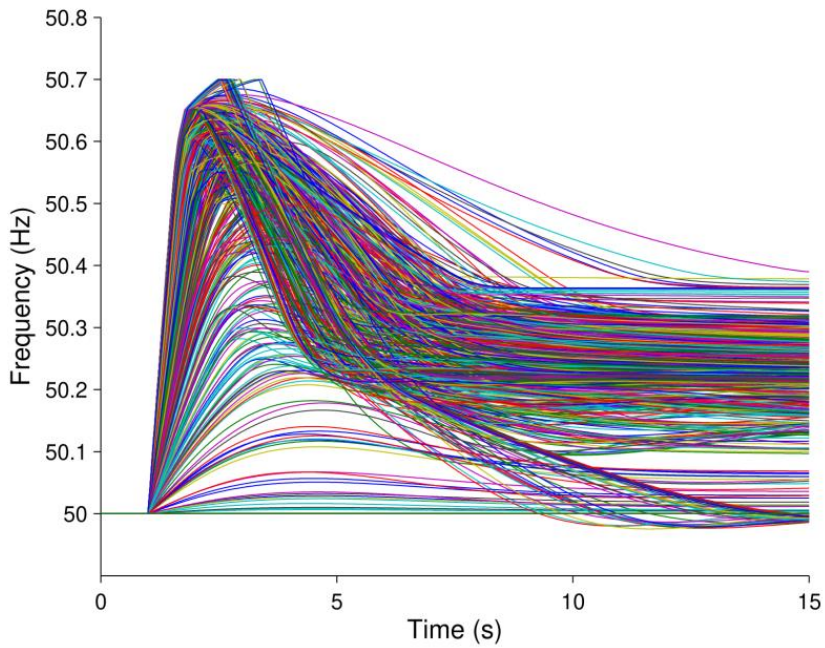

FIGURE 2-73: FREQUENCY PROFILE FOR STEADY EVOLUTION SCENARIO FOLLOWING OUTFEED LOSS

There is a correlation observed between the SNSP levels and higher frequency zeniths, primarily driven by higher export magnitudes at higher SNSP levels as shown in Figure 2-74 and also by the availability of fast acting reserves to mitigate over-frequency excursions as shown in Figure 2-75. It can be noted that the maximum available fast acting reserve for SE is smaller than LCL due to lower levels of HVDC interconnection. The OFGS scheme proves to be an effective measure to arrest excessive over-frequency excursions and acts as a key resource in ensuring frequency stability in the event of a high magnitude export loss.

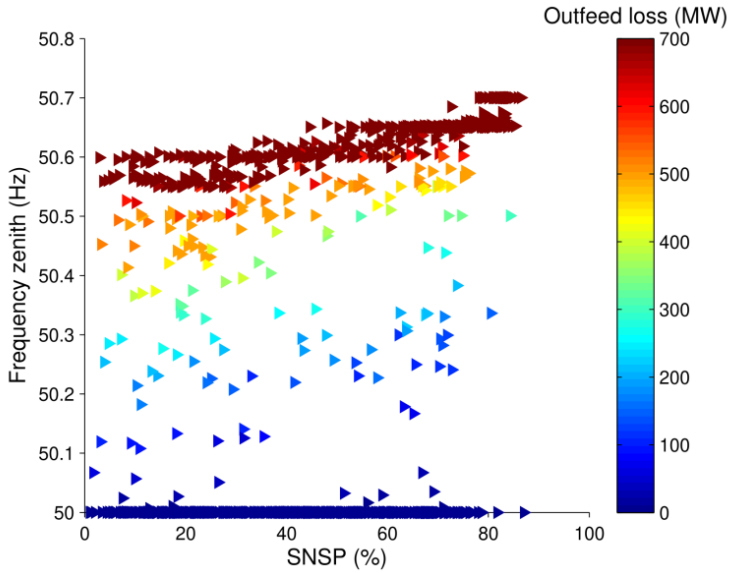

FIGURE 2-74: SE - FREQUENCY ZENITH VS SNSP & OUTFEED LOSS MAGNITUDE

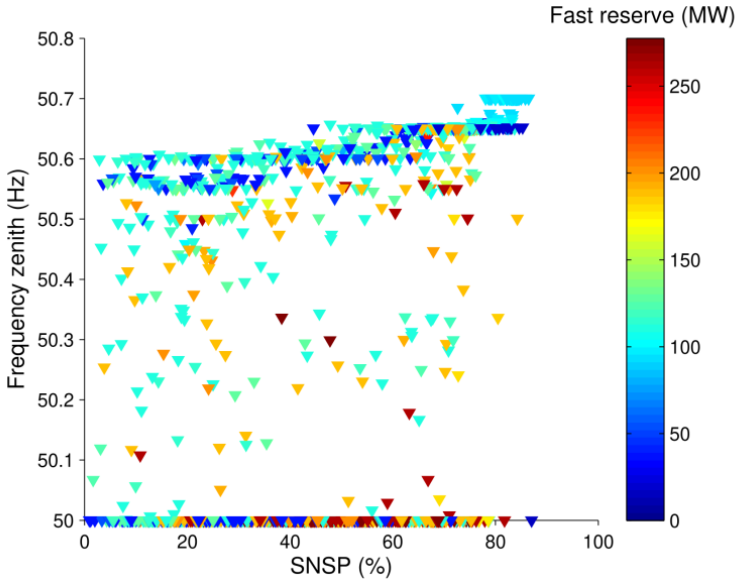

FIGURE 2-75: SE - FREQUENCY ZENITH VS SNSP & FAST RESERVE MAGNITUDE

A comparison between the two simulated scenarios establishes that there are likely to be substantial changes in the degree of system stability, based on the available reserve portfolio and hence the quality of reserve, even at identical SNSP/renewable generation levels. LCL contains a higher percentage of snapshots with higher renewable energy levels and lower inertia, making the frequency stability dynamics quicker. This is evidenced by the mean time to frequency deviation for both infeed and outfeed loss events, Table 2-10. The mean time to maximum frequency deviation for the SE scenario is distorted slightly due to a number of cases with insufficient reserve provision, delaying the occurrence of a frequency nadir.

TABLE 2-10: COMPARISON OF LCL AND SE SCENARIOS

	Infeed loss – LCL	**Infeed loss – SE**	**Outfeed loss – LCL**	**Outfeed loss – SE**
Mean maximum frequency deviation (Hz)	49.52	49.42	50.57	50.57
Mean time to maximum frequency deviation (s)	1.76	3.54	1.60	1.76
Mean steady state error (Hz)	0.38	0.43	0.28	0.22

It can be seen in Figure 2-76 that LCL has a higher distribution of frequency nadirs around 49.7 to 49.8 Hz, due to a relatively higher number of cases with high SNSP levels and thereby smaller infeed loss volumes. However, subsequent distribution of frequency nadirs with snapshot accumulations around 49.5 Hz in case of LCL are due to a higher availability of fast acting dynamic reserve (BESS and HVDC interconnection) compared to the SE scenario. A high number of snapshots in SE accumulating at below 49 Hz levels are indicative of insufficient reserve being dispatched coupled with the insufficient fast dynamic reserve to offset reserve dispatch volumes, contrary to LCL scenario.

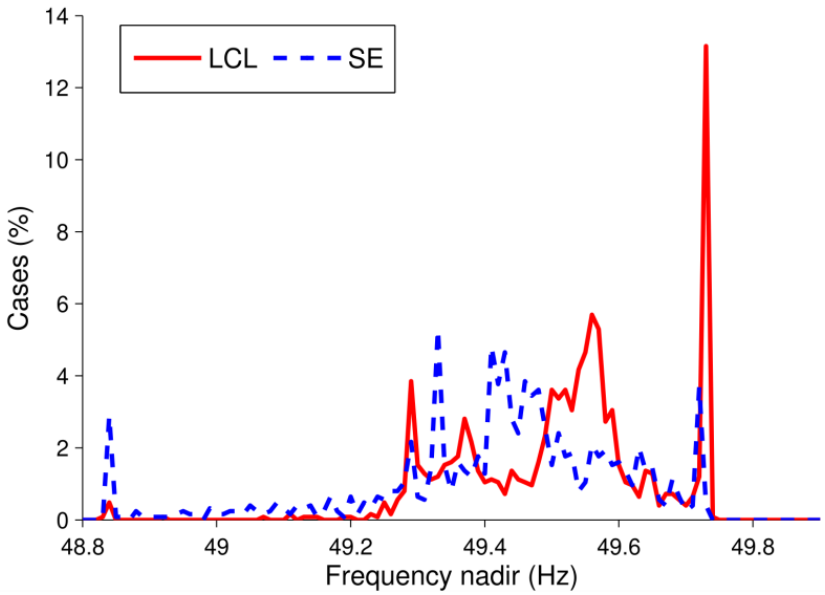

FIGURE 2-76: FREQUENCY NADIR COMPARISON

Under-frequency issues such as oscillations and frequency overshoots occurring in LCL are absent in SE due to the absence of a substantial BESS resource and excessive static (step response) reserve. However, the insufficient reserve issue leading to low frequency nadirs, occurs in both SE and LCL. That being said, the frequency of occurrence is much higher in SE as opposed to LCL due to excessive fast dynamic reserve availability in LCL.

There is no substantial difference between the over-frequency responses between the two scenarios, with the exception of time to frequency zenith, indicative of lower inertia levels in LCL as compared to SE. The dominant factor in arresting the frequency excursions in over-frequency scenarios is the OFGS scheme which remains

uniform across the two scenarios. Hence the result is similar frequency zenith distributions across the two scenarios.

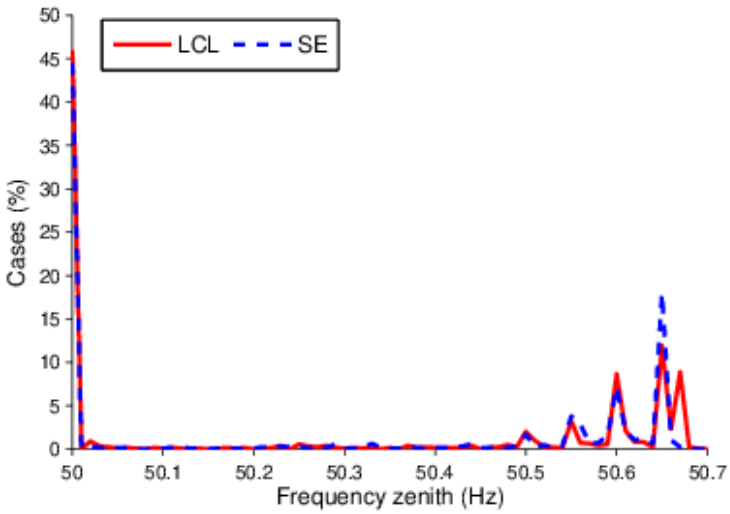

FIGURE 2-77: FREQUENCY ZENITH COMPARISON

Reducing system inertia levels requires a more careful management response from relatively slow static energy resources. The faster frequency dynamics at low inertia levels can cause reserve provision to misalign with the frequency trajectory, resulting in frequency overshoots. With reducing system inertia levels and increasing magnitudes of fast reserve resources, the magnitude and response settings of fast dynamic reserve resources must be managed in accordance with the magnitude of the dimensioning event.

Even with the management of responsive magnitudes against infeed loss, there can be situations whereby a smaller infeed loss can trigger oscillatory behaviour due to reserve magnitudes exceeding the infeed loss and the associated response time of reserve provision. The smaller the response time for fast acting reserve resources, the lesser the likelihood of oscillations.

Increasing SNSP levels is most likely to be accompanied by reducing infeed loss magnitudes, thereby naturally mitigating the effects of smaller system inertia. For the simulated cases in the LCL scenario, the availability of fast acting reserves from HVDC interconnection and BESS plays a dominant role in maintaining frequency stability following the loss of largest infeed, by offsetting the effect of faster system dynamics. Increasing SNSP levels is accompanied by increasing export levels and hence outfeed loss magnitudes, which result in lager frequency deviations following a contingency. There is a clear correlation between increased SNSP and frequency zenith.

Increasing SNSP levels are therefore more likely to influence system over-frequency profiles compared to the under-frequency profiles. Power systems with differing levels of fast dynamic reserves may exhibit different degrees of frequency security at identical SNSP, load and inertia levels, whereby a system with a reserve portfolio dominated by fast acting resources is more likely to offset potential frequency security issues, in general.

For the Ireland and Northern Ireland power system, in the LCL scenario, in general a scarcity with regards to fast acting reserves has not been observed due to the abundant volumes of fast dynamic reserve available. It is to be noted that the provision of FFR has been considered in these simulations. The current design of FFR service mandates the delivery of contracted reserve magnitude within 2s, while incentivising faster response times. A key assumption in the simulations undertaken has been the delivery of FFR from HVDC interconnection and BESS within the milliseconds timeframe in line with the incentivisation mechanism. It is therefore concluded that with regards to the LCL scenario, a faster reserve product is assumed to be implicitly delivered owing to the assumed effectiveness of the incentivisation mechanisms of the current FFR product. In the event of non-effectiveness of the incentives for faster reserve delivery, a new faster reserve product may be required to ensure system frequency security.

For under-frequency situations, an issue has been identified with regards to the validity of current reserve dispatch levels in 2030 across the two scenarios. The practice of scheduling 75% of largest infeed loss as primary reserve, no longer guarantees system security, due to changing reserve portfolios. As the system is dominated by fast acting reserves operating at substantially smaller droop equivalent settings, which provide exactly as much reserve as contracted, the POR requirements need to be increased.

Similarly, the FFR requirements assumed in these simulations need to be revised in line with the magnitude of fast acting reserve available. Furthermore, it has been identified that there is a need to carefully manage the trigger settings of static (step response) reserve, if a significant volume is available (as in the LCL scenario) and consider its knock-on effects on the settings of pre-existing load shedding schemes. It has also been identified that at times of low infeed loss and small inertia levels and with significant magnitudes of highly responsive fast acting reserve, oscillations may develop in system frequency, requiring the TSO to have the ability to adjust the magnitude and response settings (deadband, droop equivalent) of these resources.

Over-frequency situations appear to be less concerning than the under-frequency events from frequency security point of view, providing the expected reserve can effectively be available, due to the general availability of higher foot-room on conventional generation. There is however a very close correlation between increasing SNSP levels and increasing frequency zeniths. The OFGS scheme currently in place for the Ireland and Northern Ireland system proves effective at arresting over-frequency excursions without any detrimental impacts to the frequency profile subsequent to its activation.

2.3 NORDIC POWER SYSTEM

The frequency response was calculated for all hours of the year for the three scenarios defined for the Nordic system in Deliverable D2.2 [2]. The scenarios are the two Core Scenarios, Energy Transition and Renewable Ambition, and one Network Sensitivity, High Solar. The High Solar scenario resembles the Energy Transition scenario except for much higher solar PV capacities.

2.3.1 METHODOLOGY

The Frequency Stability Model simulates the grid frequency in the case of sudden disconnection of large generator or HVDC transmission line between the Nordic synchronous area and other synchronous areas. In other words, N-1 contingency analysis is performed to assess frequency stability. All generators within the Nordic synchronous area are assumed to remain synchronised. What this means is that system splits within the Nordic synchronous area are not simulated. Considering the high transmission capacities between different countries and bidding zones in the Nordic area, in most cases frequency stability cannot not be maintained in the case of a system split event.

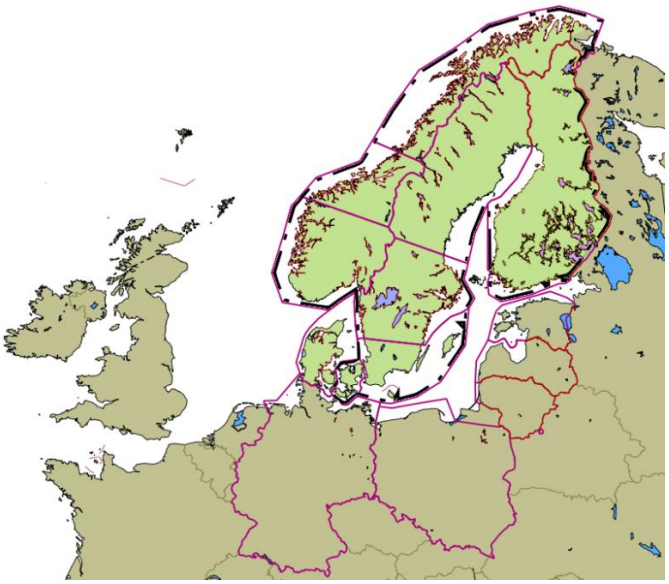

FIGURE 2-78: THE SIMULATED REGION (NORDIC SYNCHRONOUS AREA) IS SHOWN HERE BY DASHED LINE

Figure 2-79 shows the model framework used in this analysis. The Wilmar joint market model and the Stossch hydro-scheduling model are the same models which have also been used in EU-SysFlex Task 2.5 analyses. They run with rolling horizon and hourly resolution (varying resolution for the Stossch model). They provide inputs to the Frequency Stability Model, which runs on the Simulink platform. The main inputs are:

- Online capacity of each aggregated plant
- Average hourly power generation of each aggregated plant
- The reserve capacities for each reserve type provided by each aggregated plant. In some cases the aggregated plants may be individual generators but in most cases they group together several generators of the same type in the same geographical zone.

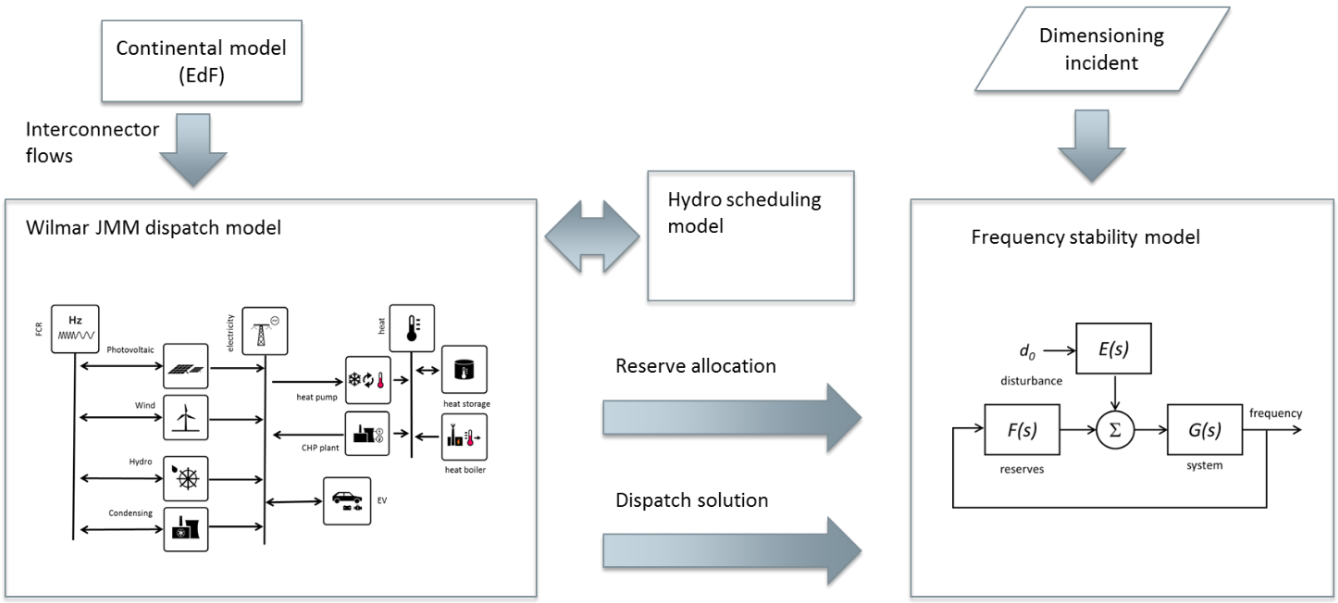

FIGURE 2-79: THE MODEL FRAMEWORK USED TO ANALYZE FREQUENCY STABILITY IN THE NORDIC SYSTEM.

The frequency stability model has been implemented on the Mathworks Simulink platform and contains response models for several plants types. Their responses are superposed to find the total system response. In this simulation the following plant types were included: hydro power, wind power, solar PV, steam and gas turbines, heat pumps, electric vehicles and aggregated industrial loads.

In addition to the plant characteristics, the requirements for the specific reserve product will affect the response. The main reserve product used in this simulation is the Frequency Containment Reserve for Disturbances (FCR-D). Frequency Containment Reserve for Normal operation (FCR-N) is also included. At the moment new requirements are being prepared for Nordic FCR and the first draft was published in 2017 [20]. These draft requirements are used in the analysis presented here. Currently, the performance requirement in terms of activation time for FCR-D product is 30s (with 50 % activation in 5s). The draft requirement proposes a stricter performance requirement. However, the requirements can still change before they are adopted during the first half of the decade. The fast frequency reserve FRR, which will be introduced in 2020 was not included in the base case. However, some plant models such as aggregated industrial loads were configured in the sensitivity analysis so that they comply with the draft requirements set for FRR (e.g. activation time at most 1.3 s) [21].

Some of these response models, e.g. heat pumps and EV, are rather generic because the response greatly depends on the specific communication and automation technology used for the control. It is difficult to predict the exact performance of the control solutions in 2030. For hydro power, which together with demand response has been the most important provider of FCR-D, the classical model of hydro turbine [22] was used. This represents the turbine and penstock with transfer function:

$$T(s) = \frac{-T_w s + 1}{0.5T_w s + 1} \quad \text{(Eq. 2-3)}$$

where T_w is the so called water starting time and represents the response delay due to the great masses of flowing water. According to Agneholm *et al*. [23] the majority of Nordic hydropower has T_w less than 1.2 s with small minority of plants reaching 1.8 s. As it is not necessary to use all plants for FCR-D, T_w = 1.0 s was used here as a base case value.

In addition to the response models for the reserve providing plants, a response model for the rest of the power system is needed. The grid transfer function G(s) is based on the Swing equation as shown below in Eq. 2.

$$\mathrm{G(s)} = \frac{\mathrm{f_0}}{\mathrm{H_s S_n s + D f_0}} \quad \text{(Eq. 2-4)}$$

The swing equation utilises parameters for the system kinetic energy and frequency dependency of load. The system kinetic energy is calculated based on the scheduled online capacities, which are produced by the Wilmar JMM unit commitment and economic dispatch model. For some generator types, notably hydro power, online capacities are produced but they must be estimated from the real power output as in (Eq. 2-5). In (Eq. 2-5), H is the inertia coefficient, P real power output, cosθ power factor, and λ the ratio of real power output to online capacity in terms of real power. For power factor cosθ = 0.9 was assumed for all production types. λ = 0.8 was used for hydro power shows the used inertia constants.

$$W_{kin} = \frac{H \cdot P}{cos\theta \cdot \lambda} \quad \text{(Eq. 2-5)}$$

TABLE 2-11: AVERAGE INERTIA CONSTANTS USED FOR DIFFERENT GENERATOR TYPES [24].

Generator type	Inertia constant *H* (s)
Hydro power	3
Nuclear power	6.3
Other thermal	4

Frequency dependency of load is somewhat time variant depending on what loads are connected and of course it is proportional to the demand at each hour. Ørum *et al*. [25] use the coefficient *D*=0.9.

2.3.2 ASSUMPTIONS

The dimensioning incident for this analysis was assumed to be the loss of 1400 MW. In practise, this can be a HVDC interconnector or a nuclear plant. It should be noted that the Olkiluoto 3 plant, which will start operation in 2021, has a net capacity of approximately 1600 MW. However, a separate system protection reserve, which is

dedicated to Olkiluoto 3, has been developed, which will reduce the impact on the grid. The capacity of this reserve is approximately 350 MW and can be activated in 200 ms.

Nordlink HVDC cable presents a dimensioning incident of 1400 MW and Oskarshamn 3 plant also 1400 MW. The power loss is assumed to be instantaneous, which is a conservative assumption. After the incident, system kinetic energy is reduced when the tripping unit is a nuclear power plant. This was an assumption in the simulation. If the tripping unit were HVDC link, system kinetic energy is not reduced and the results would be correspondingly less dramatic.

2.3.3 RESULTS

2.3.3.1 KINETIC ENERGY/ INERTIA

In 2017 the estimated Nordic system kinetic energy minimum and maximum values were approximately 120 GWs and 280 GWs, respectively. Figure 2-80 shows box plots of the simulated kinetic energy values in the studied scenarios. It can be noticed that these are normal operation values where the contribution of the tripping unit has not been subtracted. The maximum value clearly increases in all scenarios due to increased generation capacity assumptions in the portfolios. However, the low end of the distribution is the most interesting from the point of view of identifying technical scarcities. The results can be compared with Ørum *et al*. [26] where the future minimum kinetic energy in 2025 was estimated to be approximately 110 GWs. Figure 2-81 shows the average kinetic energy by month in the Energy Transition scenario. The lowest values are found in June and July when load is lowest and thus there are fewer generators online.

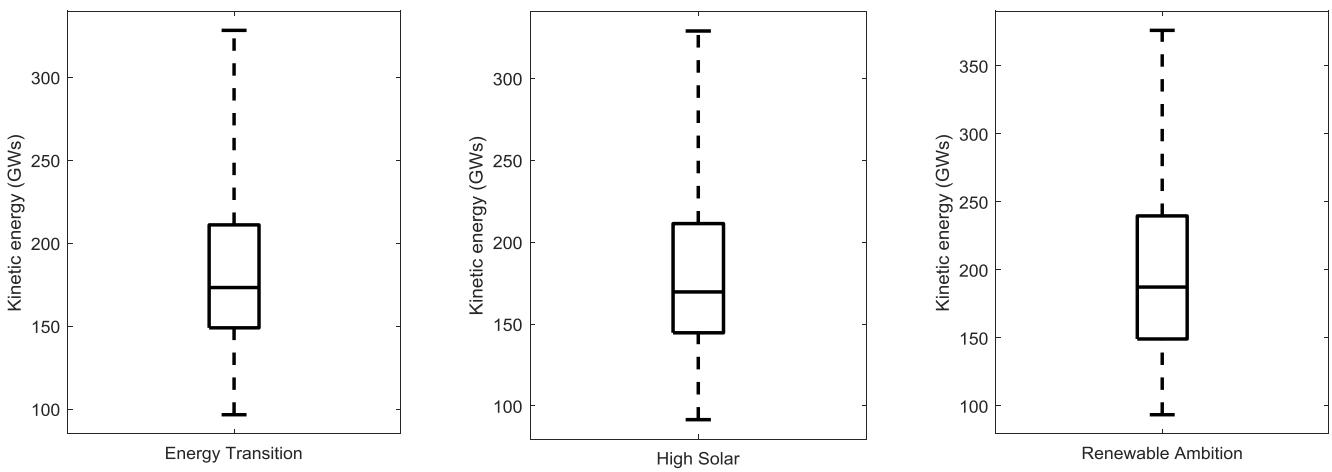

FIGURE 2-80: KINETIC ENERGY IN THE NORDIC SYSTEM. FOR EACH BOX, THE CENTRAL MARK INDICATES THE MEDIAN, AND THE BOTTOM AND TOP EDGES OF THE BOX INDICATE THE 25TH AND 75TH PERCENTILES, RESPECTIVELY. THE WHISKERS INDICATE MINIMUM AND MAXIMUM KINETIC ENERGY VALUES

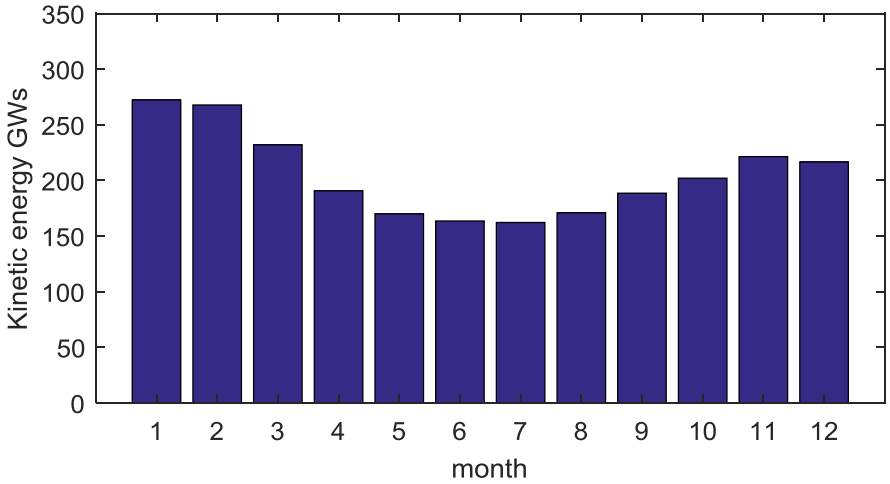

FIGURE 2-81: AVERAGE KINETIC ENERGY IN THE NORDIC SYSTEM IN ENERGY TRANSITION SCENARIO, GROUPED ACCORDING TO MONTH

2.3.3.2 FREQUENCY NADIR

Frequency nadirs (the minimum frequency during the simulated event) were recorded for 8760 hours of the simulated year. The frequency nadir may change from hour to hour due to varying kinetic energy of the power system, which depends on the online capacity, and different allocation of frequency containment reserve (FCR), which affects the reserve response. Figure 2-82 shows statistical box plots for frequency nadir in the three different scenarios. The lowest nadir is slightly lower in High Solar scenario, due to the lower net load and lower system kinetic energy during some sunny hours. In comparison to this, low frequency nadir is not a problem in the Renewable Ambition scenario. The variance of the frequency nadir is a bit higher in Renewable Ambition. This is explained by the need to run high amounts of thermal generation at certain times, due to increased total demand.

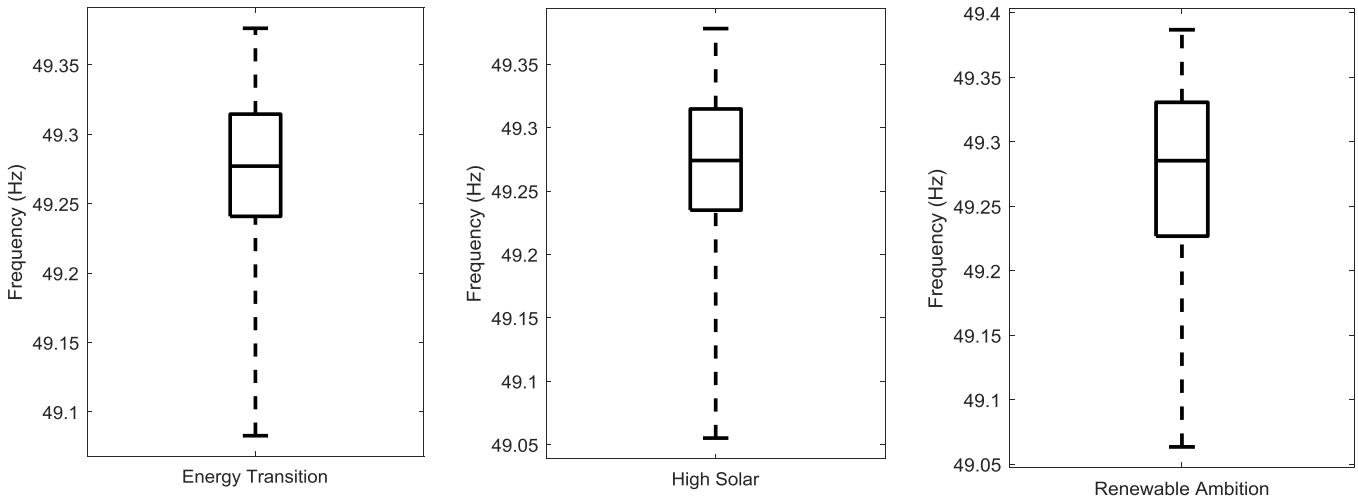

FIGURE 2-82: FREQUENCY NADIR IN THE NORDIC SYSTEM. ON EACH BOX, THE CENTRAL MARK INDICATES THE MEDIAN, AND THE BOTTOM AND TOP EDGES OF THE BOX INDICATE THE 25TH AND 75TH PERCENTILES, RESPECTIVELY. THE WHISKERS INDICATE MINIMUM AND MAXIMUM FREQUENCY NADIR VALUES

The dependency of the frequency nadir on different variables will be analysed next.

Figure 2-83 shows the average frequency nadir in the interconnected event grouped according to hour of day. It is clearly visible that the frequency drop is the highest at night during low demand and lowest in the evening during high demand. A similar pattern is visible at monthly level in Figure 2-84, where the frequency drop is the highest during the summer months when demand is low. Similar diurnal and annual patterns are visible also in the other scenarios (not shown).

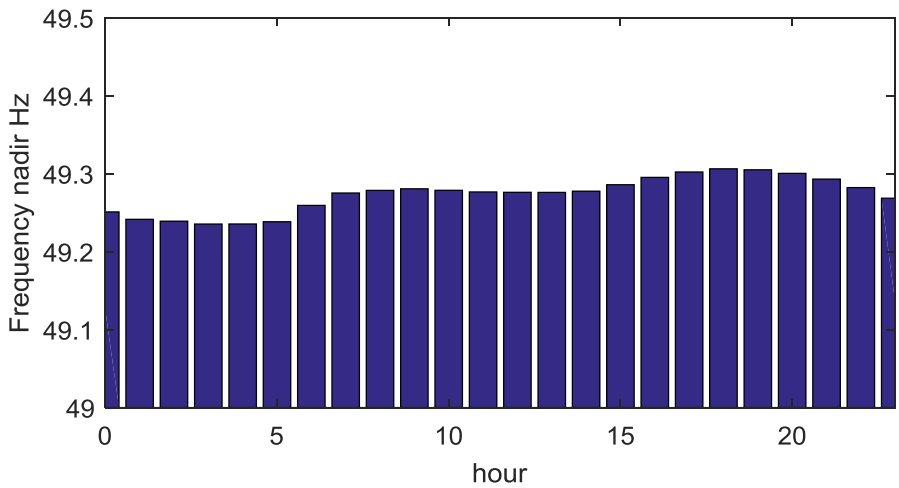

FIGURE 2-83: AVERAGE FREQUENCY NADIR IN THE NORDIC SYSTEM IN ENERGY TRANSITION SCENARIO, GROUPED ACCORDING TO HOUR OF DAY.

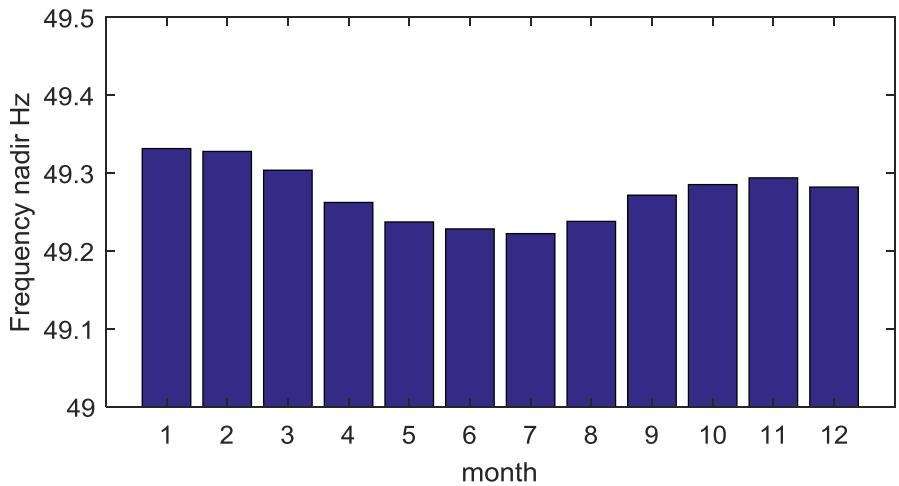

FIGURE 2-84: AVERAGE FREQUENCY NADIR IN THE NORDIC SYSTEM IN ENERGY TRANSITION SCENARIO, GROUPED ACCORDING TO MONTH.

The frequency drop compared to the estimated system inertia is illustrated in Figure 2-84. A clear dependency is visible which is shown more clearly in Figure 2-85. Frequency nadir in the interconnected incident is, to high degree, dependent upon the system kinetic energy. The reason is that in the simulation most of the FCR-D reserve is provided by hydro power and there is not much variation in reserve provision.

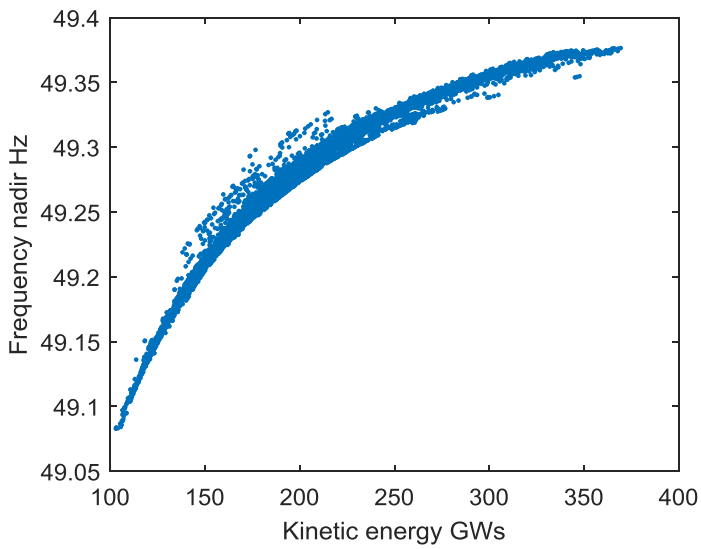

FIGURE 2-85: RELATIONSHIP BETWEEN THE FREQUENCY NADIR AND SYSTEM KINETIC ENERGY IN THE NORDIC SYSTEM IN ENERGY TRANSITION SCENARIO.

2.3.3.3 RATE OF CHANGE OF FREQUENCY

RoCoF is currently not of major concern in the Nordic synchronous area. The results of the analysis here also show that in the scenarios being examined RoCoF is not likely to be a problem in 2030. There are no official RoCoF limits in the Nordic system at present but for example on the Ireland and Northern Ireland power system the current RoCoF limit is 0.5 Hz/s measured over a 500 ms timeframe and is set to rise to 1Hz/s over the coming years. Figure 2-86 Figure shows box plots of the RoCoF in the three analysed scenarios. It is seen that the maximum RoCoF does not approach 0.5 Hz/s.

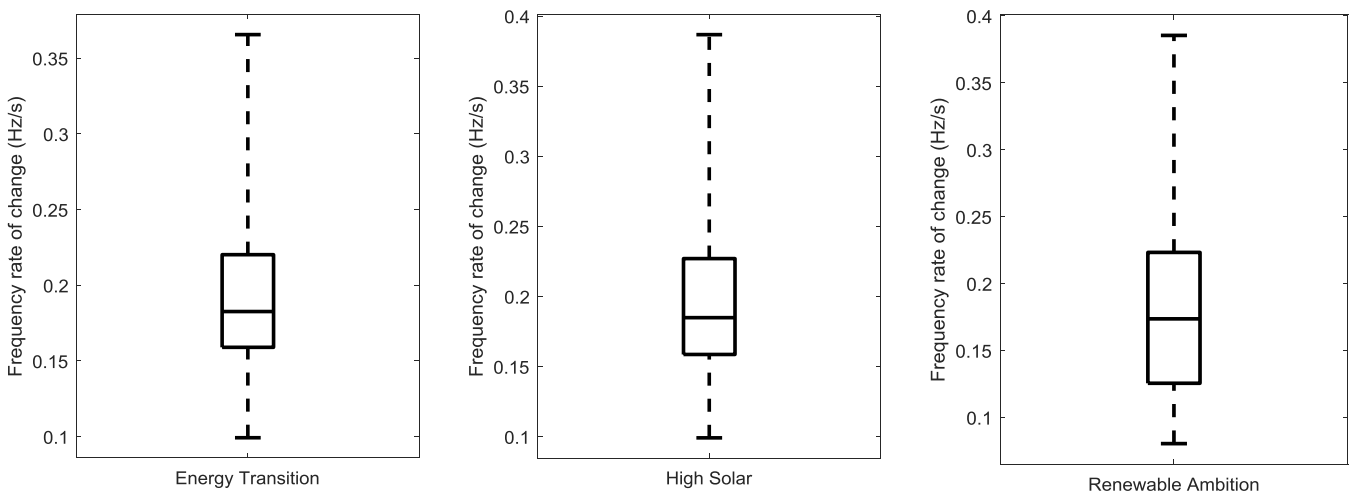

FIGURE 2-86: RATE OF CHANGE OF FREQUENCY IN THE NORDIC SYSTEM IN THE THREE ANALYZED SCENARIOS

2.3.3.4 SENSITIVITY ANALYSIS

As mentioned above, there is a certain distribution in the response delay experienced by different Nordic hydropower plants, depending e.g. on penstock construction. The water starting time parameter describes this delay and the reference value for it was T_w = 1.0 s. Due to the fact that for some plants this value has been estimated to be higher, a sensitivity with T_w = 1.2 s was run, without changing the hydro governor parameters. Figure 2-87 shows the frequency nadir result for the most critical scenario, High Solar. A decrease of approximately 40 mHz can be seen.

Fast Frequency Reserve (FFR) has been planned [27] as a solution to improve frequency stability in low-inertia situations. FFR is a faster reserve category than both FCR-D and FCR-N. The technical requirements include e.g. the aspects of full activation time, trigger frequency, support duration and deactivation behaviour. Three trigger frequencies have been defined, 49.7 Hz, 49.6 Hz and 49.5 Hz. Full activation time decreases with the trigger frequency.

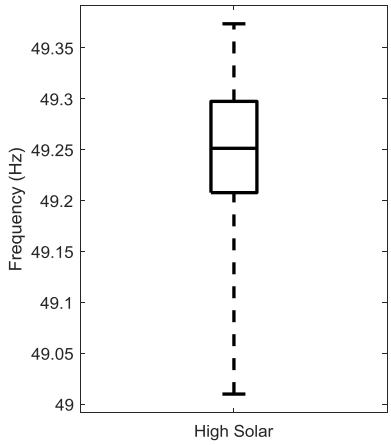

FIGURE 2-87: FREQUENCY NADIR IN THE NORDIC SYSTEM USING HIGHER WATER STARTING TIME T_w.

It is possible to study the effects of FRR in the Nordic scenarios. The setup in this sensitivity analysis required the exclusion of 100 MW of aggregated loads from the FCR-D reserve category and moving them to the FFR category. FFR was then further increased. Figure 2-88 shows the results of the sensitivity analysis. It can be seen that the minimum frequency nadir is slightly increased when FFR is added. The increase is approximately 60 mHz from the base case to the case where 200 MW of FFR is present.

TABLE 2-12: PARAMETERS FOR THE SIMULATED FFR

Parameter	Value
Trigger frequency	49.7 Hz
Full activation time	1.3 s

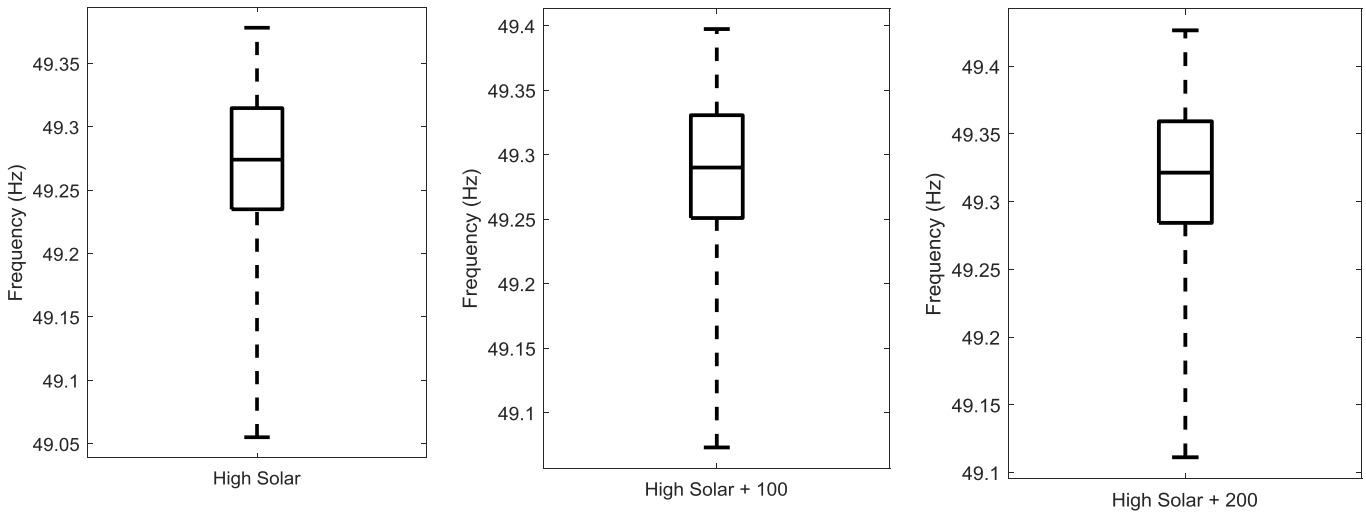

FIGURE 2-88: FREQUENCY NADIR IN THE NORDIC SYSTEM IN THE HIGH SOLAR SCENARIO WHEN FFR IS ADDED. THE LEFTMOST FIGURE SHOWS THE ORIGINAL DISTRIBUTION FOR THE HIGH SOLAR SCENARIO. THE CENTER GRAPH SHOWS THE CASE WITH 100 MW FFR CAPACITY ADDED AND THE RIGHT GRAPH THE CASE WITH 200 MW FFR CAPACITY ADDED

Emergency power control (EPC) is a service which can be provided by all types of HVDC links. In the base case no EPC through the HVDC links between the Nordic system and other synchronous grids was included. The base case was conservative in this respect because if the HVDC link is already using its full capacity for energy market operations, EPC activation is not possible. A sensitivity case was analysed where a number of EPC controls have been included. Table 2-13 shows the settings for the simulated EPC under-frequency controls. In reality there can be 1–3 steps for each HVDC link. Here only the most important ones were selected.

TABLE 2-13: PARAMETERS FOR THE SIMULATED HVDC EMERGENCY POWER CONTROL [25]

HVCD link	Trigger frequency (Hz)	Ramp rate (MW/s)	Capacity (MW)	Time delay (s)
Kontiskan 2	49.5	200	150	0.05
Baltic Cable	49.55	100	150	0.5
Swepol	49.4	100	150	0.5
NordBalt	49.4	990	150	0.5

Figure 2-89 shows the frequency nadir in the High Solar scenario when the listed EPC controls were included. Compared to the base case the minimum frequency nadir increases approximately 70 mHz.

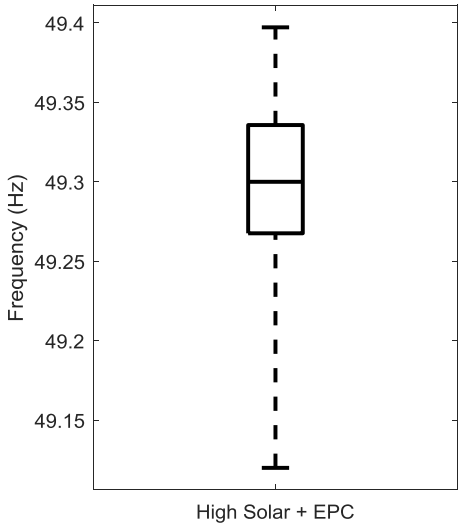

FIGURE 2-89: FREQUENCY NADIR IN THE NORDIC SYSTEM IN THE HIGH SOLAR SCENARIO WHEN EMERGENCY POWER CONTROL HAS BEEN ADDED.

2.3.3.5 CONCLUSIONS FOR THE NORDIC POWER SYSTEM ANALYSIS

The analysis shows that frequency stability could be maintained in the Nordic system in the Core Scenarios and in the Nordic Network Sensitivity for the dimensioning interconnected incident concerned. The frequency nadir could be maintained above 49.0 Hz in all cases and the rates of change of frequency remained within safe range. However, the margin for frequency nadir was very low. Very little differences could be seen between the three analysed scenarios in terms of these indicators. This can be attributed to the fact that the differences in vRES energy penetration between the scenarios are relatively small. As expected, the High Solar scenario manifested more aggressive frequency behaviour. For the Renewable Ambition scenario the indicators were similar to High Solar.

2.4 SUMMARY & CONCLUSIONS

This chapter has outlined that, with the transition to high levels of variable renewable generation, the frequency stability of the European power system will, in general, decline. However, this decline is likely to be to a different extent depending on the jurisdiction and operating conditions in questions. Furthermore, and perhaps most importantly, it is anticipated that effective measures can be taken to mitigate against this decline.

Different operating conditions for the pan-European power system were explored, including interconnected system operation and system split conditions. For an intact Continental power system, it has been shown that frequency nadirs following the loss of a large generating unit in each jurisdiction decline as SNSP levels in that jurisdiction increase. It should be noted, however, that all the frequency nadirs recorded for the intact system are above the threshold for activation of load shedding. The Iberian Peninsula is the worst affected, where, for the highest renewable scenario, the loss of 2 GW of generation in the peninsula has been shown to lead to nadirs

around 49.35 Hz. This is a result of the fact that the Iberian Peninsula is weakly interconnected with the rest of the Continental power system and has low system inertia due to the high penetration of variable renewable generation.

Furthermore, it has been shown for the Continental system that with higher SNSP and lower inertial response, there is a tendency towards higher local RoCoF values. The impact of SNSP levels on RoCoF values is observed in every zone considered, and this impact is much more visible above a certain level of penetration in the strongest zones (70% to 75%). There is an indication that RoCoF values as high as 1.3 Hz/s could be reached in the Iberian Peninsula.

Examination of frequency stability on the Ireland and Northern Ireland power system paints a similar picture to the pan-European power system. It was found that in a 2030 power system with SNSP levels approaching 90%, RoCoFs can be excessive. Consequently, it was decided to put a mitigation in place early in the study; a 1 Hz/s RoCoF constraint is included in the scheduling simulations. Therefore a mitigating measure for the lack of system inertia has been assumed to be in place and it is found that, similar to the Continental system results, the majority of cases examined experience nadirs above the load shedding threshold. It is interesting to note that there is no clear correlation between SNSP levels and frequency nadirs. This is because as SNSP levels increase there is a trend towards smaller dimensioning incidents, in order to satisfy the RoCoF constraint.

While it was found in the Ireland and Northern Ireland analysis that there are some frequency nadirs below load shedding levels, there are mitigations currently available such as a change in dispatched reserve magnitude. The results indicate that the higher the fast reserve magnitude that is available, the higher the frequency nadirs. A general finding is that to maintain frequency stability, the volume of fast acting reserves should be equal to the magnitude of the dimensioning incident. In cases where there is insufficient fast acting dynamic reserve capability in the generation portfolio, lower frequency nadirs for the Ireland and Northern Ireland power system are observed. This is because, as the portfolio changes, there is increasing reliance on non-conventional generators (batteries, IC and demand-side units) which have smaller droop equivalents to provide the needed reserve response. These resources provide precisely their contracted volumes and no more and the result is that the dimensioning incident causes lower frequency nadirs that can only be arrested by load shedding. This indicates that the practice of scheduling 75% of largest infeed loss (dimensioning incident) as primary reserve, no longer guarantees system security, due to changing reserve portfolio.

In contrast to the inertia levels in the Ireland and Northern Ireland power system, in general, the upper inertia levels in the Nordic power system are increasing due to increasing capacity in the scenarios. However, during some hours, typically at night and during the summer when demand is low and depending on the dispatch schedule, the Nordic power system could experience inertia levels that are lower than current inertia levels due to displacement of conventional generation by non-synchronous resources. These lower inertia levels lead to, similar to the other systems examined, lower frequency nadirs. That being said, even in the highest variable renewable scenario, these nadir levels are never below the load shedding threshold. It is acknowledged however,

that there are certain measures that could be implemented to improve nadir margin above the critical level. This includes the Fast Frequency Reserve, which is already being adopted. On the other hand, however, unlike the Ireland and Northern Ireland power system and certain jurisdictions in the Continental power system, RoCoF has been deemed to not be a serious issue for the Nordic power system in 2030, with RoCoF values never rising above 0.4 Hz/s.

While the importance of fast reserves is clearly demonstrated for the Ireland and Northern Ireland power system and the benefit of fast reserves in the Nordic power system have been illustrated, it should be noted that the analysis for the Continental European power system did not consider fast reserves. Consequently, no overarching conclusions about fast reserves in Continental Europe can be drawn. What can be concluded, however, is that future analysis, potentially in EU-SysFlex Task 2.6, should explore the need for fast reserves, particularly for the Iberian Peninsula, where low frequency nadirs and high RoCoF values have been identified in the studies.

While it has been demonstrated across all the systems examined that frequency nadirs are trending downwards as inertia levels decrease, and RoCoF values are projected to increase compared to current levels, the scarcities are not limited to exist during under-frequency event; over-frequency could also pose a problem, though to a lesser extent. It has been shown that in the Ireland and Northern Ireland power system higher frequency zeniths are possible. However is has also been demonstrated that the current over-frequency generation shedding scheme employed on the Ireland and Northern Ireland power system is affective at maintaining the frequency zenith below the threshold of 50.75 Hz and, just as importantly, is also effective in avoiding under-frequency following activation of the scheme.

There is also an additional problem identified in Ireland and Northern Ireland in that if there are considerable amounts of static reserve that responds to under-frequency too slowly, overshoots could be possible and there is potential for oscillatory behaviour. This clearly indicates that static reserve needs to be managed carefully. Similarly, it was discovered that if the magnitude of the available fast dynamic reserve is comparable to the magnitude of the dimensioning incident, oscillatory behaviour is also possible. Again, there is a need to carefully manage the levels of dynamic reserve that are available.

System split events for the Continental power system were also examined. Unsurprisingly, the frequency stability indicators are much more extreme than for interconnected incidents and the traditional frequency control mechanisms are insufficient to cope with such incidents. Under system split conditions, the system stability relies on LFSM-O/U and load shedding. It was observed that, for all three Continental power system split events studied, the frequency stability of the system is endangered. However, for example, in the case of the Iberian Peninsula disconnecting from the remainder of the Continental system, frequency nadirs in the peninsula could fall as low as 46 Hz, well under the load shedding threshold, and such a situation corresponds to a blackout event as generators are not obliged to remain connected at such low frequencies. Similarly, extreme frequency zeniths of 53 Hz in the Iberian Peninsula could be possible if the Iberian Peninsula is disconnected, while RoCoF values greater than 2 Hz/s are more likely, also leading to generator disconnections. The probability of such extreme

events is however very low and should be assessed in future work. Moreover, the split events simulated in that study assume that DC links also disconnected, which is questionable. Again this is an area that requires further detailed analysis.

3. VOLTAGE CONTROL

In order to maintain system voltage within acceptable levels both in steady state and during a transient, the system must be operated in a suitable operating condition. The operating condition, corresponds to both active power transfers and the magnitude of available reactive support. The reactive support entails the relatively slower voltage regulation during steady state as well as fast reactive current injection during a contingency. In this chapter, both these areas are dealt with for the continental European system, as well as the Ireland & Northern Ireland power system.

3.1 CONTINENTAL EUROPE

For the analysis presented in this section, all network contingencies have been assumed in Polish power system owing to the detailed representation of power grid used for Poland (e.g. type of busbar systems, double-circuit line representation, detailed data of power generation units, lack of 110 kV distribution grid) [28]. Furthermore, preliminary analysis has demonstrated absence of any issues relevant to steady state voltage regulation for EHV network both in Poland and in the rest of the countries in Continental Europe that were considered part of this analysis. Therefore, the analysis in this section has been focused on 110 kV network in Poland, especially the nodes to which passive and active radial distribution systems are connected. The analysis presented covers the steady state voltage deviations and short circuit levels, P-V and Q-V analysis. Furthermore, time domain simulations are carried out to investigate the dynamic voltage regulation.

Owing to the large magnitude of data produced as an outcome of steady state analysis (due to the large number of nodes and faults), a filter mechanism to determine the most interesting cases for further investigation is warranted. The strategy used to carry out such filtering is the following (Figure 3-1):

- Under steady-state operating conditions (N-0), steady-state voltage levels at the 110 kV nodes cannot be lower than 0.95 p.u. or higher than 1.05 p.u. (see Table 3-1). If voltage levels at the terminals are outside these upper and lower bounds, further voltage control analysis is necessary.
- If this system is in a contingency state (N-1), steady-state voltage levels at 110 kV nodes should not decline below 0.9 p.u. or rise above 1.1 p.u. (Table 3-2). If the voltage levels fall outside these thresholds, further voltage stability analysis has to be considered
- For contingency states (N-1), after the switching of certain elements in the grid, if the relative percentage voltage change compared to the (N-0) state at the 110 kV nodes is above 6%, further voltage stability analysis is recommended.
- In steady state (N-0) conditions, the voltage stability assessment should be carried out based on the V-P and V-Q linear sensitivities. The aim of this step is to indicate which 110 kV nodes have relatively high sensitivity factors and thus require further stability analysis. It is expected that some 110 kV nodes may be highly voltage-sensitive, but steady-state voltage in the worst (N-1) contingency may only be slightly above 0.9 p.u.

- 110 kV nodes which don't meet the simplified voltage stability criterion (based on the calculation of initial three-phase short-circuit power in (N-0) and (N-1) states) are considered to require further analysis;
- P-V curves are calculated for those 110 kV nodes which are nominated for further voltage stability analysis. The voltage stability margin is then calculated and evaluated (according to permissible values in Table 3-1 and Table 3-2). Prior to this, power system areas representing active power transfer have to be identified;
- Q-V curves are calculated for those 110 kV nodes which are nominated for further voltage stability analysis. Both reactive power reserve and voltage stability limits are calculated and evaluated;
- Due to the high uncertainty of impedance representing MV and LV network in the active distribution system equivalent, the relevant sensitivity analysis has to be performed together with evaluation on the steady-state results.

Based on the PSE standard [28], permissible voltage levels are presented in Table 3-1 and Table 3-2:

TABLE 3-1: PERMISSIBLE VOLTAGE LEVELS FOR THE EHV AND 110 KV NODES IN THE (N-0) CONDITION.

Nominal voltage of bus	**400 kV**	**220 kV**	**110 kV**
EHV and 110 kV nodes, to which generation units are connected and 110 kV nodes directly supplied from the EHV/110 kV transformers	1,0—1,05	1,0—1,1	1,0—1,1
other EHV and 110 kV nodes	0,95—1,05	0,95—1,1	0,95—1,1

TABLE 3-2: PERMISSIBLE VOLTAGE LEVELS FOR THE EHV AND 110 KV NODES IN THE (N-1) CONDITIONS.

Nominal voltage of bus	**400 kV**	**220 kV**	**110 kV**
EHV and 110 kV nodes, to which generation units are connected and 110 kV nodes directly supplied from the EHV/110 kV transformers	0,95—1,05	0,95—1,1	1,0—1,1
other EHV and 110 kV nodes	0,90—1,05	0,90—1,1	0,90—1,1

The aforementioned strategy for analysis is shown in Figure 3-1, in the diagram form. All the calculations have been performed with the use of DIgSILENT PowerFactory software.

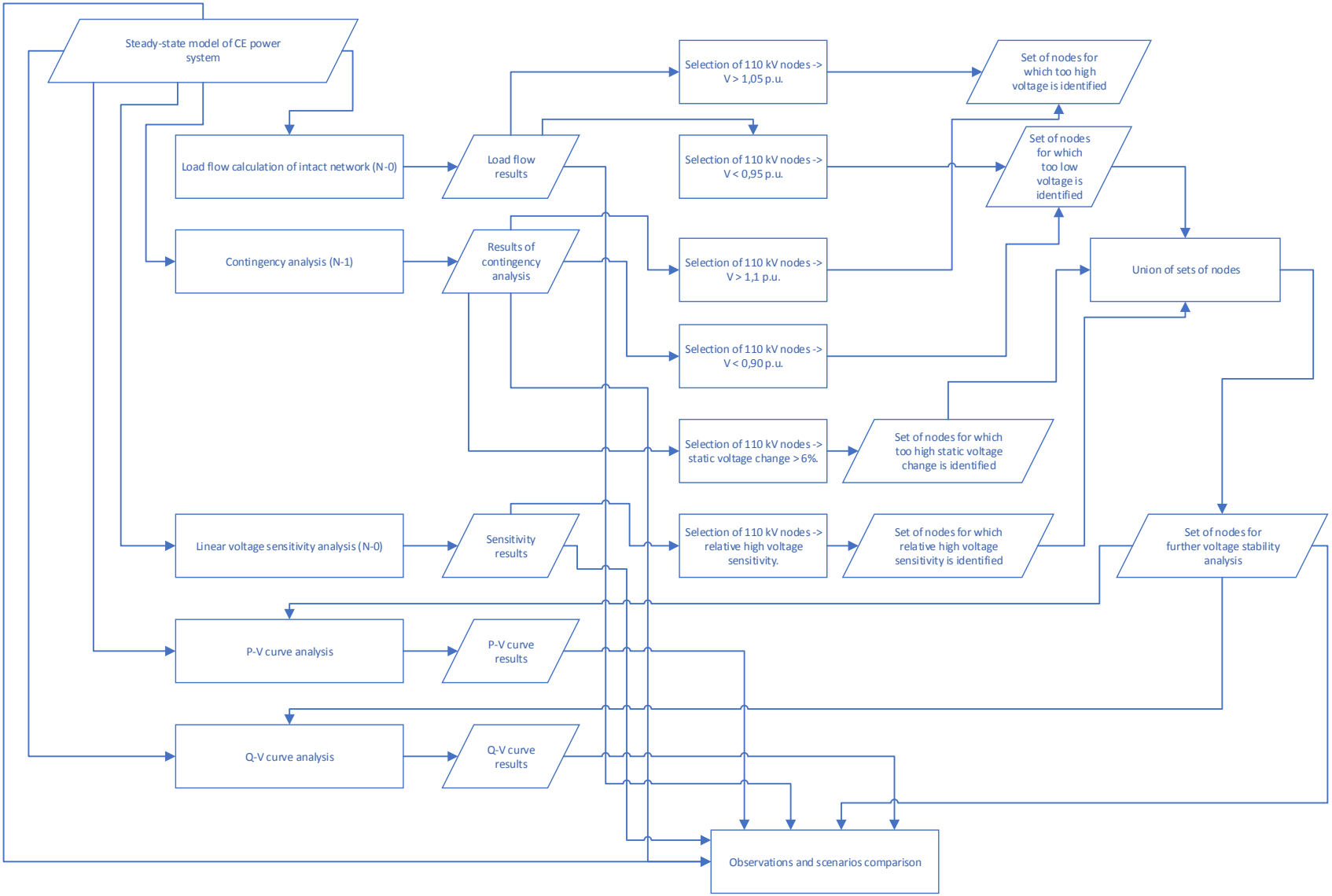

FIGURE 3-1: PROPOSED ALGORITHM OF THE STEADY-STATE VOLTAGE CONTROL ANALYSIS

3.1.1 VOLTAGE DEVIATIONS

The steady state voltage deviation analysis has been carried out on each of the snapshots identified and described in 1.6.1.1, the results presented are for 110 kV Polish network. The SNSP referred to henceforth in this section is the global CE system SNSP.

Figure 3-2 and Figure 3-3 show that that the problems of low voltage levels occur particularly in the "Max_Load" case (with relatively low SNSP). Under-voltage issues are visible across all scenarios for "Max_Load" conditions. Also, in certain ""Min_Inertia"" and "Min_Reactive" cases, problems with under-voltage have been identified. The highest number of 110 kV nodes for which the voltage is below 0.9 p.u. are observed for the Going Green scenario. For the same scenario, the minimum voltage value is observed in one of the post-contingency states (in the "Max_Load" operational case). Figure 3-2 shows that the impact of reduced voltage regulation due to higher RES generation becomes apparent at high load conditions. The reactive power demand (both from load and network side) determines whether voltage problems may occur in the power network. Participation of renewables is a secondary factor having an impact on the under-voltage issue.

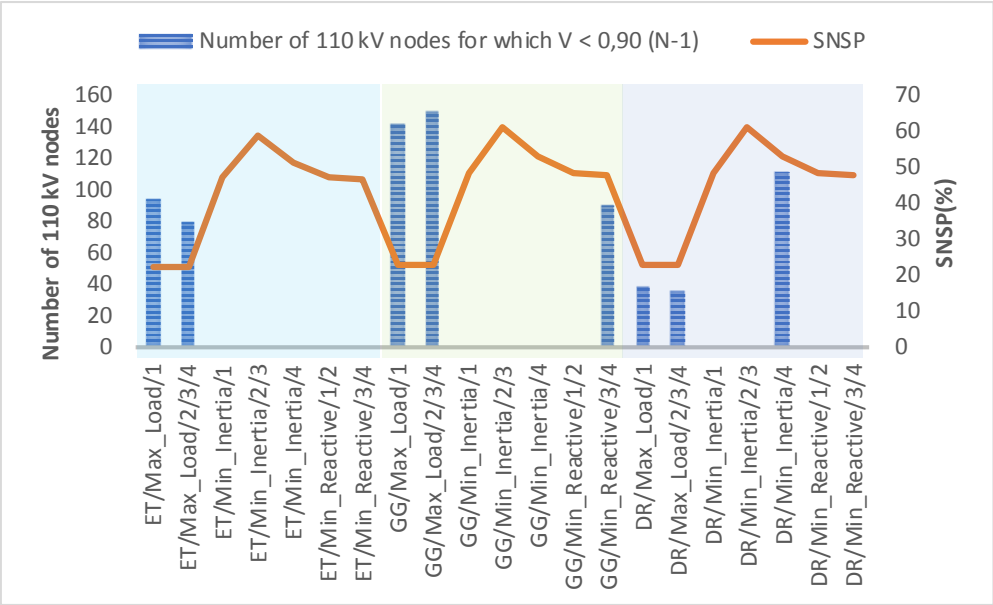

FIGURE 3-2: SNSP AND NUMBER OF 110 KV NODES FOR WHICH V < 0.90 P.U. (N-1)

This project has received funding from the European Union's Horizon 2020 research and innovation programme under grant agreement No 773505.

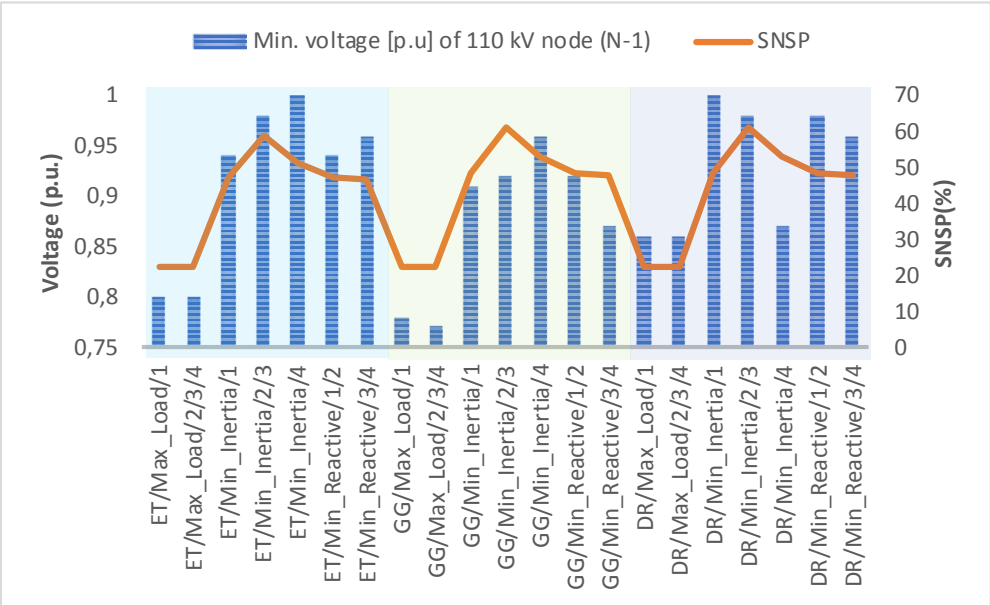

FIGURE 3-3: SNSP AND MIN. VOLTAGE [P.U.] OF 110 KV NODES (N-1)

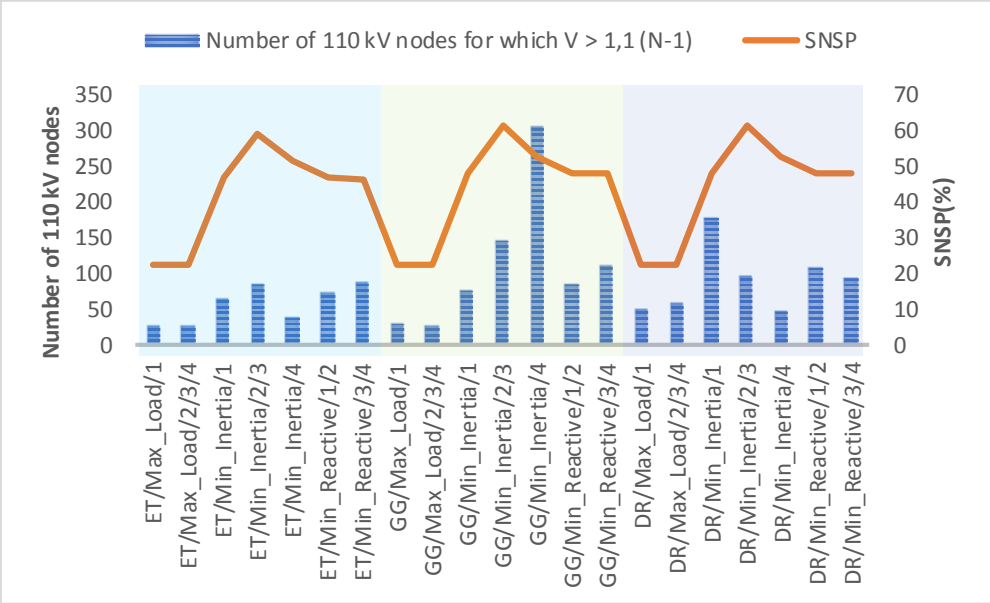

FIGURE 3-4: SNSP AND NUMBER OF 110 KV NODES FOR WHICH V > 1.1 P.U. (N-1)

Over-voltage deviations show a similar trend (Figure 3-4 and Figure 3-5). For over-voltage deviations "Min_Inertia" and "Min_Reactive" snapshots show increased over-voltage deviations, although this issue is observed across all snapshots and scenarios. The assumptions relating to the RES capacity in Poland in Going Green and Distributed Renewables scenarios results in a significant number of 110 kV nodes for which the voltage is above 1.1 p.u. The highest numbers of nodes with over-voltage issues correspond to the Going Green scenario. The highest values of over-voltage at 110 kV nodes are observed in the Distributed Renewables scenario. There is a significant correlation between the problems with high voltage and higher level of renewables, especially in the Going Green and Distributed Renewables scenarios. As mentioned earlier, the key factor affecting steady-state

voltage issues is the power demand. Due to the fact that “Min_Inertia” and “Min_Reactive” snapshots are much close to the minimum load time, more over-voltage problems can be observed.

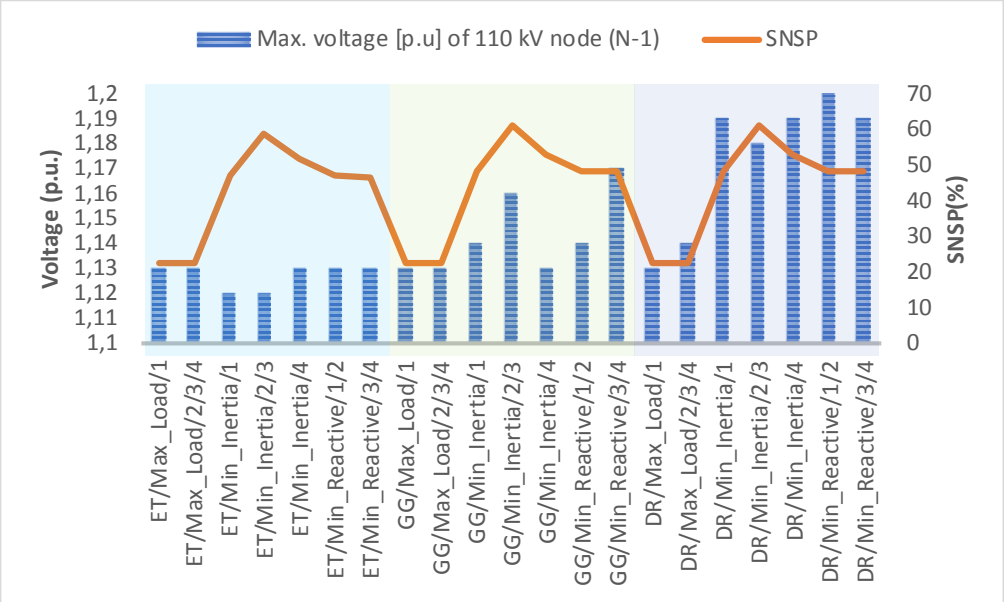

FIGURE 3-5: SNSP AND MAX. VOLTAGE [P.U.] OF 110 KV NODES (N-1).

Figure 3-6 & Figure 3-7 show that in the Energy Transition scenario the static voltage change is more significant when there is relatively low RES generation in the power system (“Max_Load” operational case). The increasing renewables capacity in the Going Green scenario causes more cases with voltage changes Δ > 6%. RES mainly connected to 110 kV network change the flows in lines and therefore, change in reactive power consumption by lines. Some lines may be highly loaded while some are lightly-loaded. As a result, an outage of the former makes 110 kV nodes more sensitive on the voltage change. In turn, the Distributed Renewables scenario seems to mitigate this problem to some extent. It can be also identified that the higher the level of renewables generation the lower the magnitude of the problems with the static voltage change. Some exceptions from this rule of thumb could be expected as well. RES generation as well as power demand contribute to the high volatility of power flows in 110 kV, which may cause under- and over-voltage states as well as high static voltage change in case of contingencies.

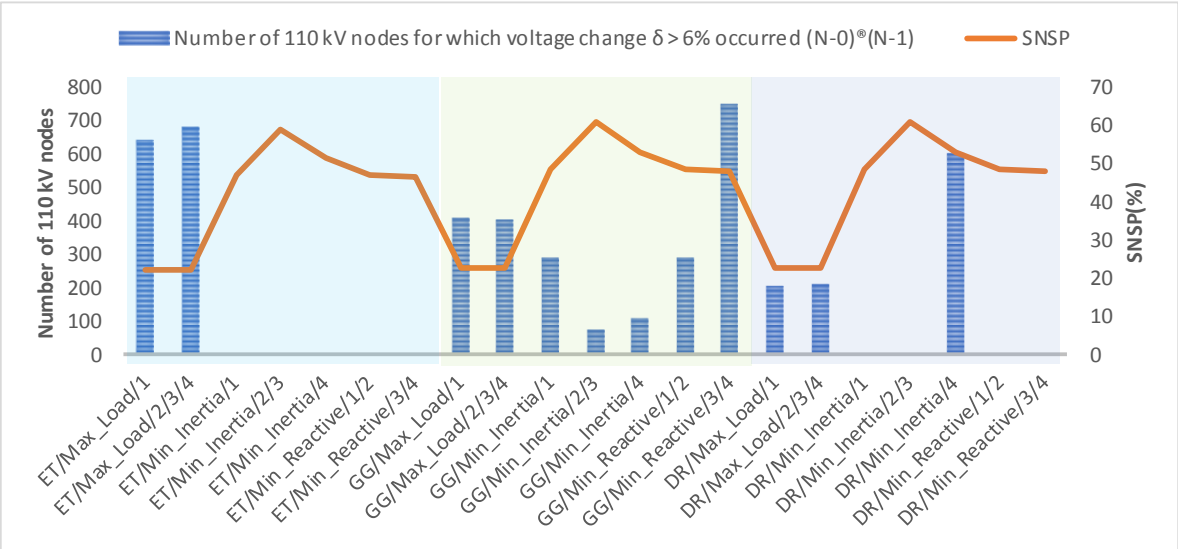

FIGURE 3-6: SNSP AND NUMBER OF 110 KV NODES FOR WHICH VOLTAGE CHANGE Δ > 6% (N-0)→(N-1).

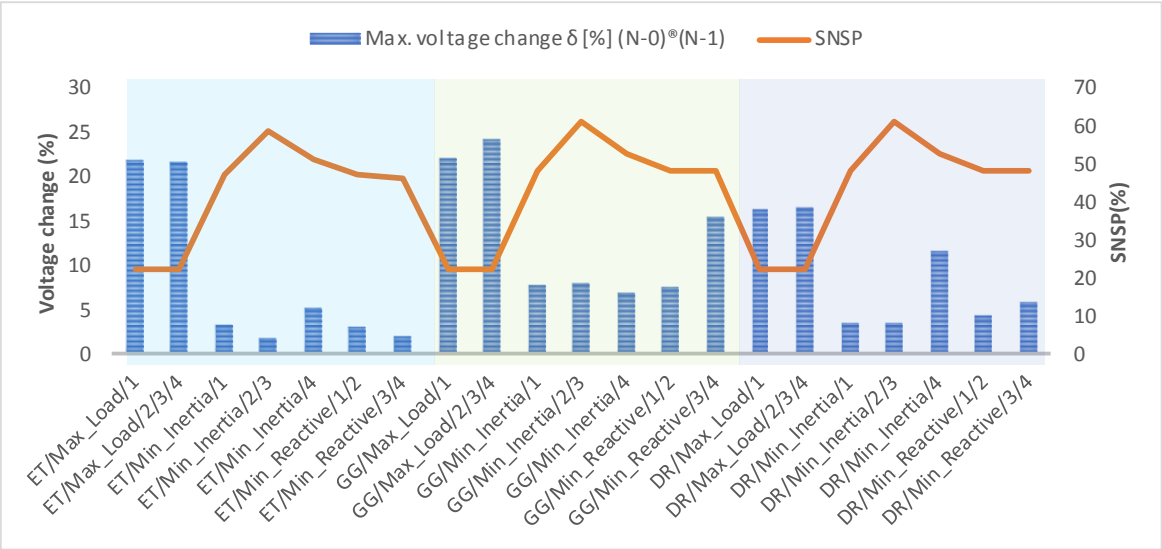

FIGURE 3-7: SNSP AND MAX. VOLTAGE CHANGE Δ [%] (N-0)→(N-1).

In addition to the quantitative analysis of voltage issues, the spatial dispersion of the problematic 110 kV nodes has also been analysed. Considering the problems with low voltage levels in the contingency state (Figure 3-8), it can be seen that higher RES level causes not only changes in the number and magnitude of voltage deviations but also shifts the problem from one location to another. For instance, when the "Max_Load" operation case is considered, the nodes for which the voltage is below 0.9 p.u. (N-1) occur mainly in central and South-West Poland. When RES generation increases, the voltage problems are shifted to the North-East and the North-West parts of the Polish power system in the Going Green and Distributed Renewables scenarios, respectively.

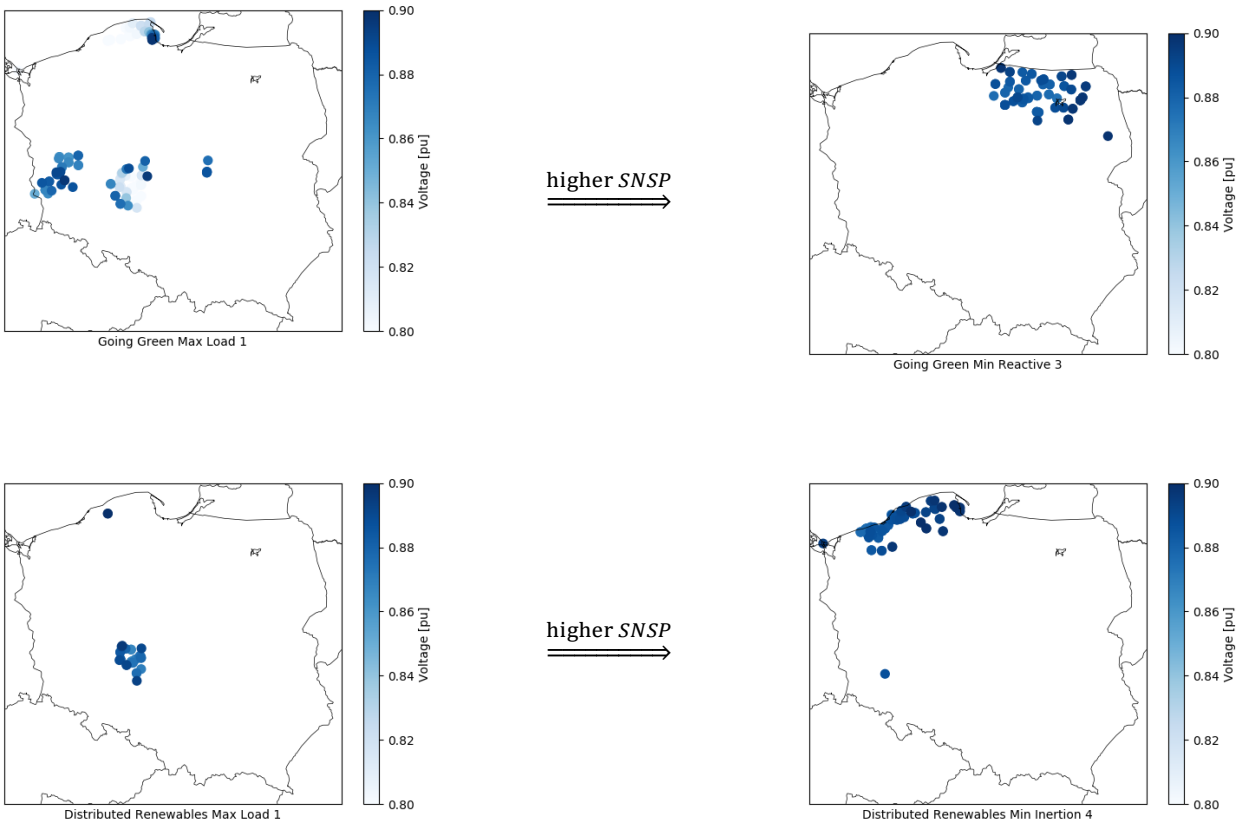

FIGURE 3-8: SPATIAL DISTRIBUTION OF 110 KV NODES IN WHICH VOLTAGE LEVEL DECREASES BELOW THE LEVEL OF 0.90 P.U. (FOR CONTINGENCY (N-1)) – SELECTED CAPACITY AND OPERATIONAL CASES.

Figure 3-9, demonstrates the spatial distribution of over-voltage issues. It can be seen that that increasing RES impacts upon the magnitude of voltage values without causing significant changes in spatial distribution for the distributed renewables scenario. On the other hand, in Going Green scenario, the over-voltage spatial distribution occurring at high load ("Max_Load" operation case) may spread into other areas of the power system.

As mentioned earlier, the highest static voltage changes have been observed for the "Max_Load" operational cases. The most significant problems are located especially in Northern Poland near Gdańsk as well as in the central/West of Poland (see Figure 3-10). When the power system operates with higher RES, it can be observed that the spatial relocation of static voltage can bring problems into other areas of Poland.

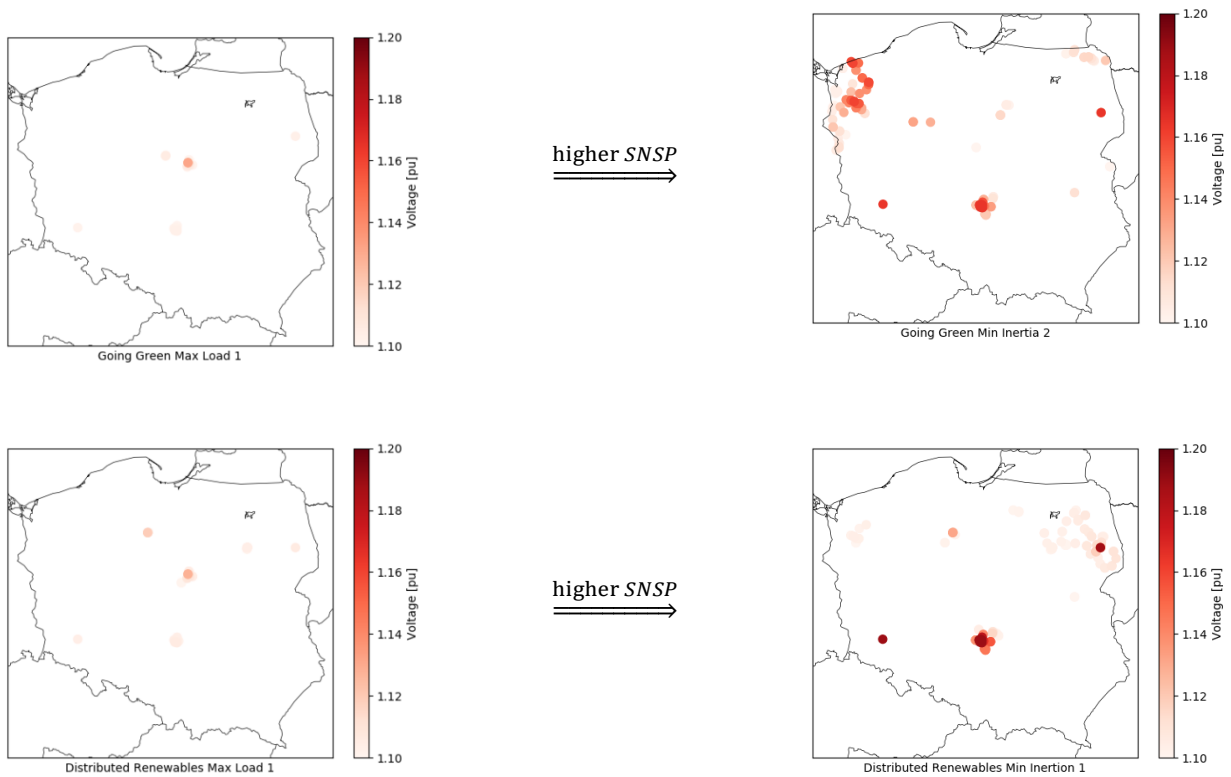

FIGURE 3-9: SPATIAL DISTRIBUTION OF 110 KV NODES IN WHICH VOLTAGE LEVEL INCREASES ABOVE THE LEVEL OF 1.10 P.U. (FOR CONTINGENCY (N-1)) – SELECTED CAPACITY AND OPERATIONAL CASES.

The overall results of steady-state voltage analysis have shown that steady state voltage control is generally an issue. Some of the identified problems could be mitigated by change in network configuration (no-cost network resources), while the others may need additional reactive power control resources (both shunts and DER connected to 110 kV network). A quantitative assessment of mitigation measures requires further detailed studies including close cooperation with Polish DSOs and assuming hour-by hour approach. The obtained results do not give a clear premise to draw a general conclusion whether moving some RES capacity to the radial distribution network can either worsen or improve the voltage control due to locational nature of this phenomenon.

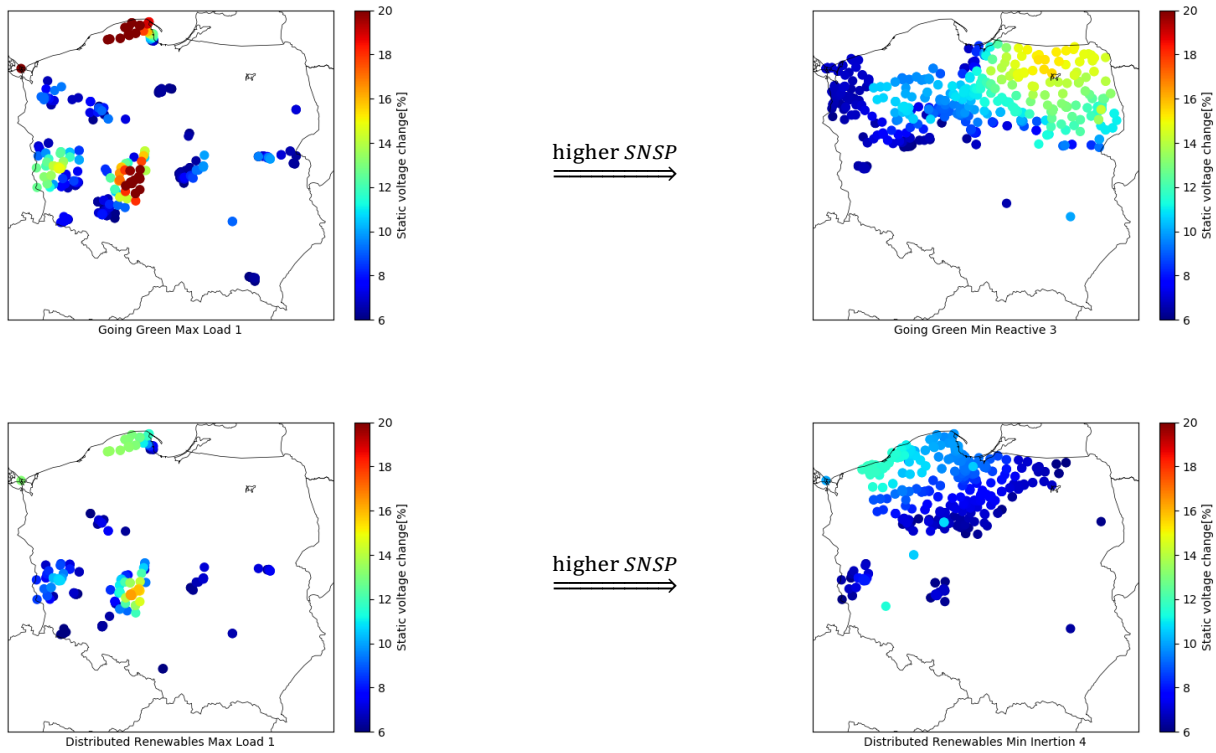

FIGURE 3-10: SPATIAL DISTRIBUTION OF 110 KV NODES IN WHICH THE VOLTAGE STATIC CHANGE INCREASED ABOVE 6% – SELECTED CAPACITY AND OPERATIONAL CASES.

3.1.2 VOLTAGE LINEAR SENSITIVITIES

As mentioned in [3], the linear voltage sensitivity analysis is a useful approach enabling assessment of local voltage stability. Linearization of the load flow equations in the vicinity of the operation point leads to the system of equations:

$$\begin{bmatrix}\Delta\mathbf{p}\\ \Delta\mathbf{q}\end{bmatrix} = \begin{bmatrix}\mathbf{J}_{P\theta} & \mathbf{J}_{PV}\\ \mathbf{J}_{Q\theta} & \mathbf{J}_{QV}\end{bmatrix}\begin{bmatrix}\Delta\boldsymbol{\theta}\\ \Delta\mathbf{v}\end{bmatrix} \qquad \text{(Eq. 3-1)}$$

where $\Delta\mathbf{p}$ is the vector representing the change of active power between system nodes, $\Delta\mathbf{q}$ is the vector representing the change reactive power between system nodes, $\Delta\boldsymbol{\theta}$ is the vector representing the change of the voltage angle between system nodes and $\Delta\mathbf{v}$ is the vector representing the change of the voltage magnitude between system nodes.

The Jacobian matrix $\mathbf{J}$ indicates the sensitivities between bus voltage changes and power flow changes, $\partial V / \partial P$ and $\partial V / \partial Q$, respectively. Thus, voltage stability is affected by both the P and Q injected or consumed at power network nodes.

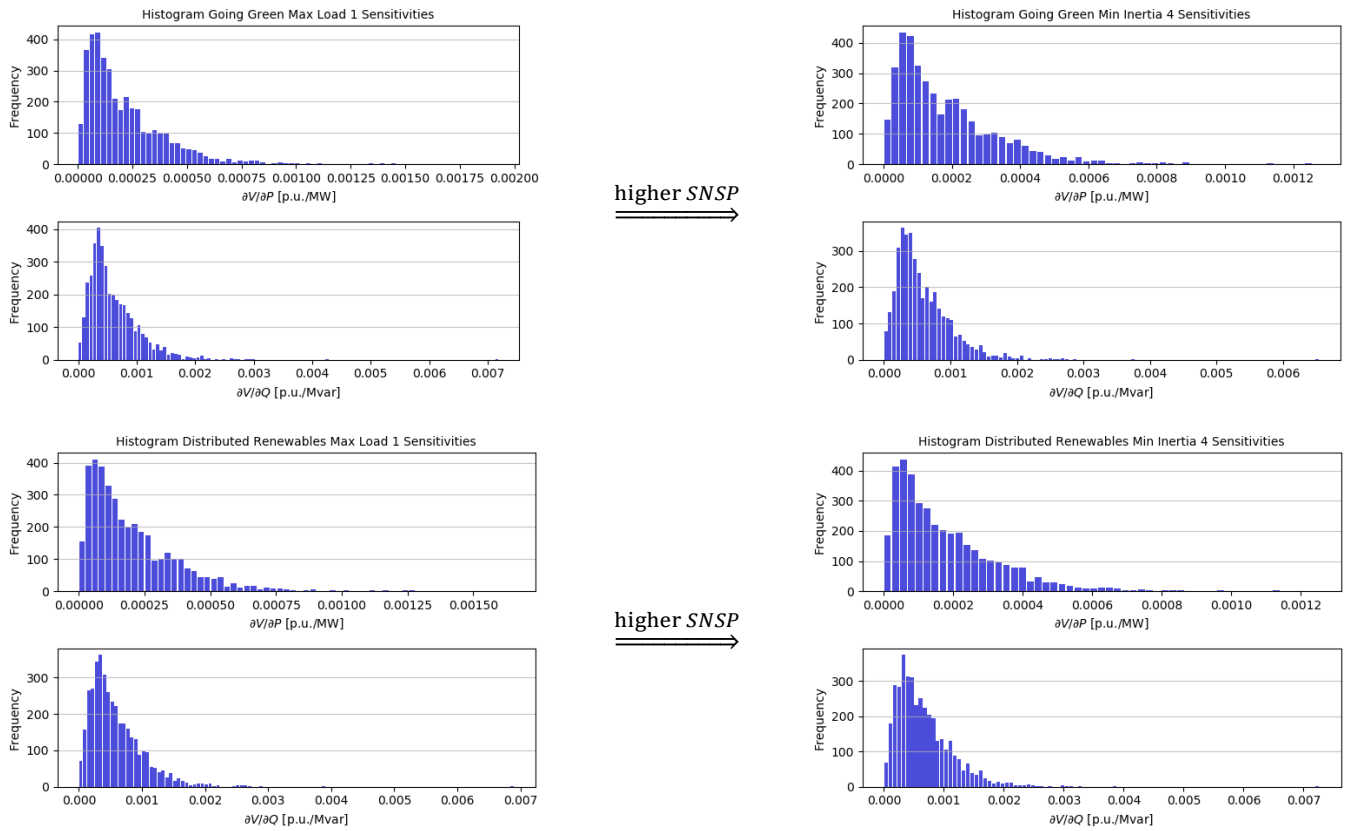

FIGURE 3-11: HISTOGRAMS OF VOLTAGE LINEAR SENSITIVITIES – SELECTED CAPACITY AND OPERATIONAL CASES.

Sensitivity analysis has been carried out for an intact network in order to indicate the susceptible 110 kV load buses. Figure 3-11 presents the resultant histograms for selected scenarios and operational cases. Negative values for the Jacobian matrix J have not been observed, suggesting that all the operation points of the power system are locally stable. For both capacity scenarios, going from “Max_Load” to “Min_Inertia” (increasing RES levels) operational cases the histograms seem to lean to the right. It means that higher RES generation and decreasing load cause higher voltage sensitivities values and therefore more voltage volatility in some of the 110 kV nodes.

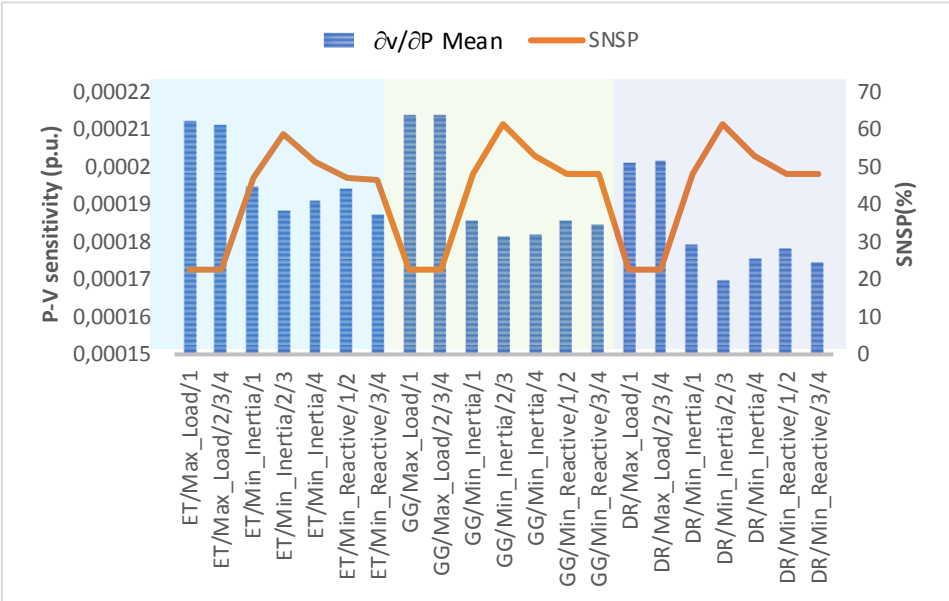

FIGURE 3-12 SNSP AND MEAN VALUES OF $\partial V/\partial P$ SENSITIVITIES

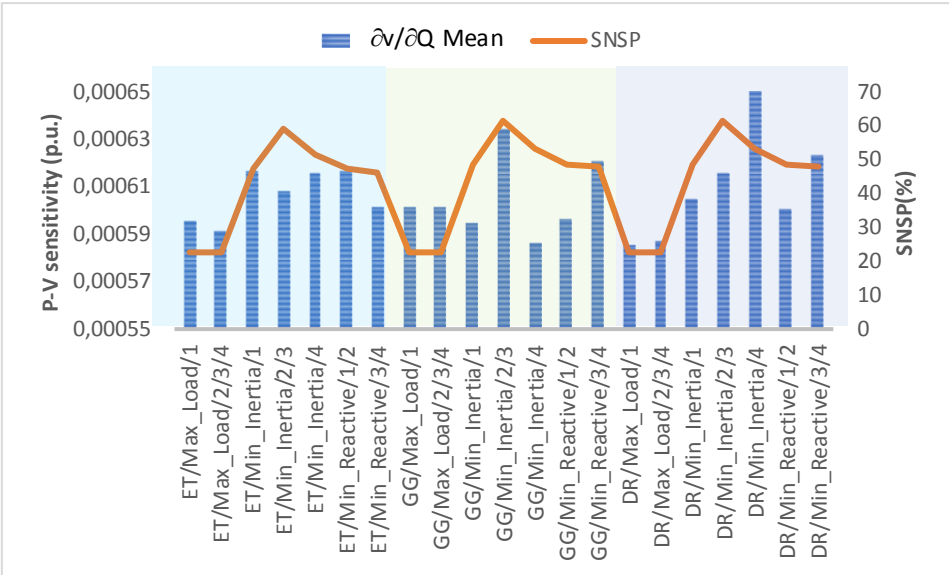

FIGURE 3-13: SNSP AND MEAN VALUES OF $\partial V/\partial Q$ SENSITIVITIES.

Additionally, mean values[4] of linear voltage sensitivities calculated for all capacity and operational cases in relation to the achieved SNSP are presented in Figure 3-12 and Figure 3-13.

A relatively high correlation between mean values of $\partial V/\partial P$ sensitivities and SNSP can be observed in Figure 3-13. Higher participation of RES in covering demand results in the voltage being more sensitive to fluctuations in active power demand. Looking at the mean values for $\partial V/\partial Q$ as a function of SNSP indicates that the correlation is not high, especially in Going Green and Distributed Renewables. In these scenarios, the highest $\partial V/\partial Q$ values

[4] Mean of all analysed 110 kV nodes

occur in the "Min_Inertia" operation cases (with high $SNSP$). It is worth emphasising that $\partial V / \partial Q$ and $\partial V / \partial P$ have the opposite characteristics in relation to $SNSP$.

Identification of 110 kV nodes prone to the voltage changes is based on the criterion as follows:

$$\frac{\partial \mathrm{V}}{\partial \mathrm{P}} > 0{,}0006 \text{ (p.u/MW)} \qquad \text{(Eq. 3-2)}$$

$$\frac{\partial \mathrm{V}}{\partial \mathrm{Q}} > 0{,}002 \text{ (p.u/Mvar)} \qquad \text{(Eq. 3-3)}$$

The aforementioned $\partial V / \partial P$ and $\partial V / \partial Q$ margins have been chosen due to the fact that all tails in the obtained histograms start from these points. A set of 110 kV nodes which fulfilled the above conditions is mostly contained in the set identified based on contingency analysis conditions.

The presented analysis has shown that increasing SNSP, as a function of load and RES generation, the voltage sensitivity increases as well.

3.1.3 SHORT-CIRCUIT LEVELS

Three-phase short-circuit power and currents have been calculated for the Polish power system for both (N-0) and (N-1) states, for all operational cases and for all scenarios, based on IEC 60909 standard [29]. The detailed results are presented in Annex: Table 11-6 and Table 11-7.

For the intact network, the minimum initial short circuit currents have been obtained in 110 kV nodes. The short circuit currents are the lowest for Going Green scenario (see Figure 3-14). The minimum short circuit currents in relation to the operational cases and SNSP are shown in Figure 3-15 . As can be seen, the Going Green and Distributed Renewables scenarios have lower short circuit currents relative to Energy Transition scenario examined. The difference between the short-circuit current for Going Green and Distributed Renewables results from the slightly different nodal distribution of conventional unit for both capacity scenarios. This makes both scenarios not precisely comparable themselves from the short-circuit level point of view.

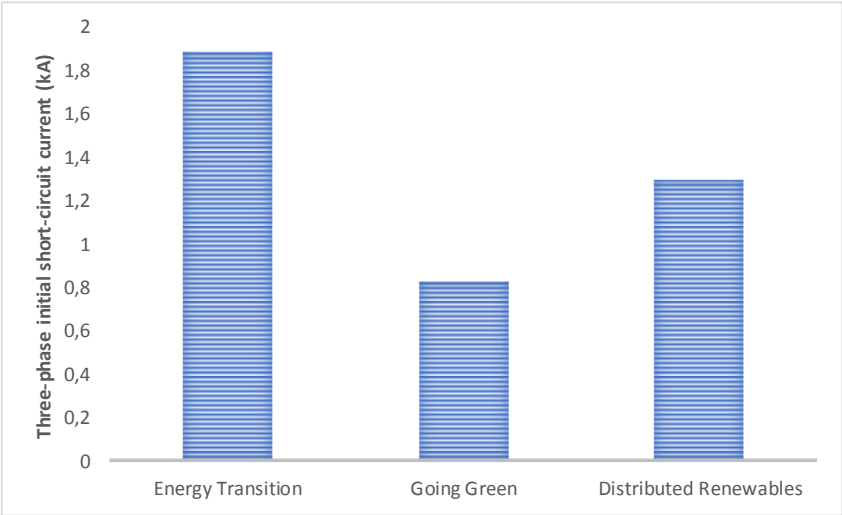

FIGURE 3-14: MINIMUM OBSERVED THREE-PHASE SHORT-CIRCUIT CURRENT IN THE ANALYSED CAPACITY SCENARIOS (INTACT NETWORK).

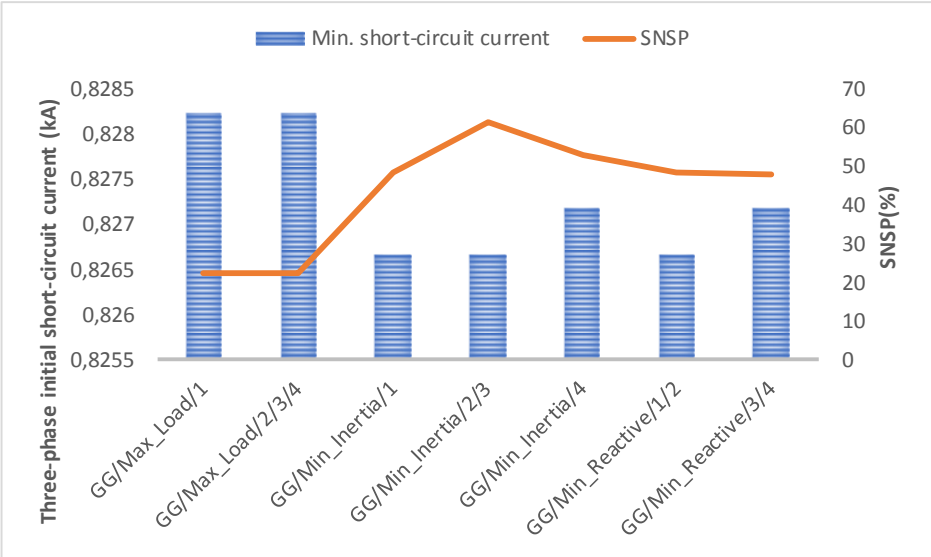

FIGURE 3-15: SNSP AND MINIMUM OBSERVED THREE-PHASE SHORT-CIRCUIT CURRENT IN GOING GREEN CAPACITY SCENARIO (INTACT NETWORK).

One can observe a relatively low spread of short-circuit current with the significant negative correlation between SNSP and short-circuit current level. The relatively smaller number of conventional units operating in the Going Green and Distributed Renewables scenarios is the main cause of reduced short-circuit level.

For analysis of (N-1) states, critical contingencies have been chosen as the contingencies that cause voltage levels decline below 0.90 p.u. and cause a change in voltage static greater than 6%. Similar to the intact network, analysis, minimum initial short circuit currents have been obtained in 110 kV nodes. Going Green is also the worst scenario under contingency conditions (Figure 3-16), but no significant changes have been observed when different operational cases are considered. This means that, in a contingency state, the change in the power

network topology could stiffen the short-circuit current level at the 110 kV network and would make the short-circuit current levels less dependent of renewable generation.

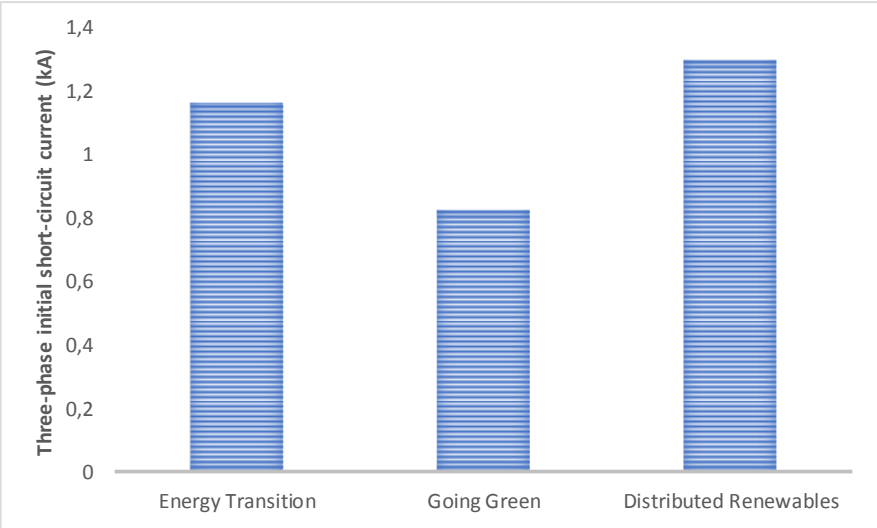

FIGURE 3-16: MINIMUM OBSERVED THREE-PHASE SHORT-CIRCUIT CURRENT IN THE ANALYSED CAPACITY SCENARIOS (FOR CONTINGENCY (N-1)).

In both N-0 and N-1 states, all the calculated short-circuit currents are above the required minimum value 0.5 kA, which is specified in PSE standard [28].

Considering contingency (N-1) states, three-phase short-circuit power has been used in a simplified method to assess conditions for voltage stability at 110 kV nodes. Assuming that the power system is represented by a voltage source equivalent including short-circuit reactance, a load supply can be ensured with a required voltage stability margin [22]. This is described in Equation X:

$$S_{\mathrm{k}}^{''} \geq 2k_V(1+\sin\varphi)S_{\mathrm{load}} \qquad \text{(Eq. 3-4)}$$

where $S_{\mathrm{k}}^{''}$ is the three-phase short-circuit power, S_{load} and φ are the apparent power of load and its angle, respectively, and $\mathrm{k_V} = 1.1$ which is the required voltage stability margin.

Figure 3-17 presents both the required and the delivered short-circuit power values in the worst cases for the particular scenarios. The difference between the delivered and required values can be interpreted as a short-circuit power margin. All of the obtained margin values have a positive sign indicating that the simplified voltage stability condition (Eq. 3-4) is met. From Figure 3-17, it can be seen that higher RES capacity scenario exhibit a significantly lower stability margin. The lowest stability margin for Going Green capacity scenario results from the slightly different synchronous generation distribution in the transmission network.

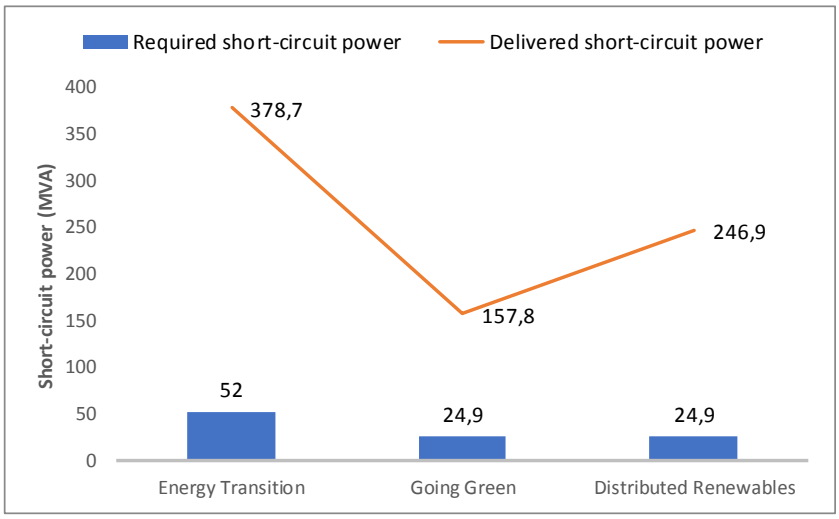

FIGURE 3-17: WORST CASES FOR REQUIRED AND DELIVERED SHORT-CIRCUIT POWER VALUES (FOR ANALYSED CAPACITY SCENARIOS AND CONTINGENCY (N-1)).

Summarizing, this analysis has shown that reducing conventional generation as in assumed scenarios does not yield a short-circuit current level issue. The difference between short-circuit levels for analysed capacity and operation scenarios are noticeable, but not critical.

3.1.4 VOLTAGE STABILITY ANALYSIS

Based on the results of voltage deviations (Section 3.1.1), sensitivity (Section 3.1.2) and short-circuit (Section 3.1.3) analysis, a number of network zones in the Polish power system have been identified in order to perform further voltage stability studies (P-V and Q-V curve analysis). A zone has been selected as a critical one if it contains at least one 110 kV node where voltage conditions resulting from the missing reactive power are not met. The zones denoted as critical ones and nominated to further voltage stability analysis are presented in Annex: Table 11-8, together with the map of 110 kV nodes and corresponding zones (Annex: Figure 11-1).

The Going Green scenario has highest number of identified zones in which voltage stability problems are expected. For all “Max_Load” operational cases, at least one critical zone has been identified.

3.1.4.1 P-V CURVES

The decreased synchronous generation as well as identified lack of steady-state voltage regulation margin in the vicinity of high loaded areas (urban or industrial especially) causes both active and reactive power transfer from remote generation sources. This could make the under-voltage problems deepening. It is necessary to assess how far is the voltage stability equilibrium.

The Voltage stability margins in Polish part of CE power system have been assessed with the use of the Power-Voltage (P-V) Curve method. The idea is to calculate the voltage levels at 110 kV nodes located in the selected

zones for (N-0) and (N-1) states. The voltage is a function of active power in this area from operational point up to the loss of load flow convergence. The real and reactive power of the load is iteratively increased step by step while the cos φ parameter is kept constant. As mentioned in Machowski (2008) [22], such a simplified approach may be sufficient in power system planning studies. More advanced techniques exist, such as continuation power flow, which enable identification of stable operational point located behind the loss of convergence point [22] [30].

The voltage stability margin will be calculated as follows:

$$k_V = \frac{P_{\max} - P_0}{P_{\max}} \qquad \text{(Eq. 3-5)}$$

The criteria for voltage stability margin are given in Table 3-3.

TABLE 3-3: PERMISSIBLE VALUES OF VOLTAGE STABILITY MARGIN [3].

Contingency	Voltage stability margin
None	10%
Loss of any element such as: **one generator, one line (including double-circuit), one transformer, one HVDC pole**	5%
Loss of busbar system (section) in a substation	2.5%

It has been assumed that the initial positions of on-load tap changers (OLTC) in transformers are constant. An opportunity to change them has been reserved for when the criterion of voltage stability margin could not be met (OLTC's are fixed).

In order to assess the voltage stability margin based on P-V curves, the power system areas have been divided into following groups:

- Polish power system area,
- Five districts of Polish regional TSO's control centres,
- Critical zones in Polish power system.

Since no specified method for selection of P-V Curves areas has been established, the aforementioned set of load areas has identified as a natural area levels for the analysis.

3.1.4.1.1 POLISH POWER SYSTEM AREA

The first type of area considered for P-V curve analysis is the Polish Power System. Voltage stability margins have been calculated for all investigated scenarios and operational cases, including (N-0) and (N-1) states. For the purpose of (N-1) analysis the most critical contingency has been identified.

The obtained results of voltage stability margins calculated for Polish power system in (N-0) and (N-1) have been presented Figure 3-18.

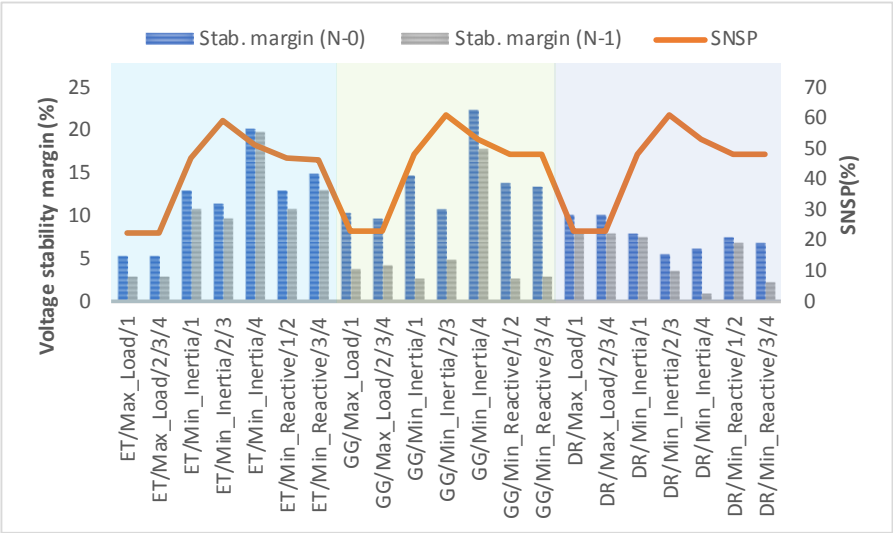

FIGURE 3-18: SNSP AND VOLTAGE STABILITY MARGINS CALCULATED FOR POLISH POWER SYSTEM.

Looking at Figure 3-18 one can observe relatively poor margin for Energy Transition /"Max_Load" scenarios in the intact network state. In these cases, some 110 kV lines are highly loaded which significantly increase the local reactive power consumption.

As can be also seen in Figure 3-18, relatively high correlations between voltage stability margin and the load level occur in the Energy Transition and Going Green scenarios (the lower load, the higher the voltage stability margin). A secondary factor having impact to increasing the voltage stability margin is the renewables generation which change the load in power network elements. The aforementioned dependence of voltage stability margin is not observed for the Distributed Renewables scenario. In that case, relatively low values of the voltage stability margin have been obtained. Distributed Renewables /"Min_Inertia"/4 (minimum inertia caught for whole CE power system) is the case for which a very low voltage stability margin has been observed (below 2.5%). Such a case occurs when one of the crucial 400 kV overhead line located in the north-western Poland is out of service. In Distributed Renewables scenario, for that location, the distance between load and generation (both synchronous and nonsynchronous) is more remote than for other capacity scenarios.

3.1.4.1.2 DISTRICTS OF POLISH REGIONAL TSO'S CONTROL CENTRES

The Polish transmission power system is divided into five areas (synchronously connected). Each of them is controlled by regional operational centres coordinated by the national operation centre. The individual district areas have specific features related to load density, renewables and conventional generation density and power network topology. This makes an obvious choice to select them as the load areas for P-V curves analysis These five districts of Polish regional TSO's control centres are:

1. ODM Warszawa (ODM 1),
2. ODM Radom (ODM 2),
3. ODM Katowice (ODM 3),
4. ODM Poznań (ODM 4),
5. ODM Bydgoszcz (ODM 5).

The location of the aforementioned districts in Poland is shown in Figure 3-19.

For particular scenarios and operational cases as well as investigated TSO's districts, the most critical zone has been selected5 including a contingency resulting in the worst voltage conditions (see Annex: Table 11-8. It should be noted that significant renewables capacity is located in ODM 4 and ODM 5. Figure 3-20 and Figure 3-21 present the obtained results of voltage stability margins calculated for districts of Polish regional TSO's control centres. In order to obtain the P-V Curves, the load was increasing in particular ODMs individually.

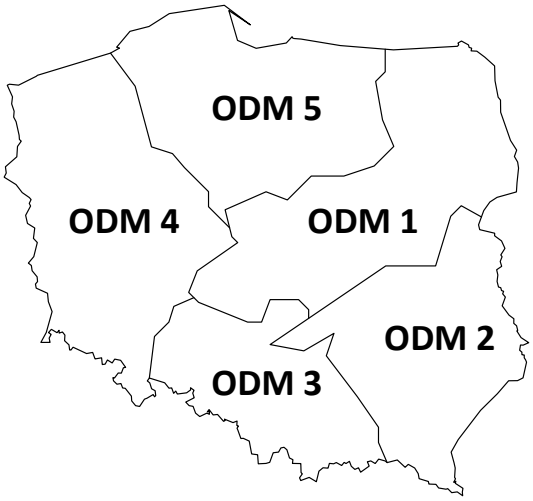

FIGURE 3-19: APPROXIMATE LOCATION OF DISTRICTS OF POLISH REGIONAL TSO'S CONTROL CENTRES.

Comparing both Figure 3-20 and Figure 3-21 with Figure 3-18, similar trends of the voltage stability margin can be seen.

[5] A zone in Polish power system belongs to only one district of districts for Polish regional TSO's control centres.

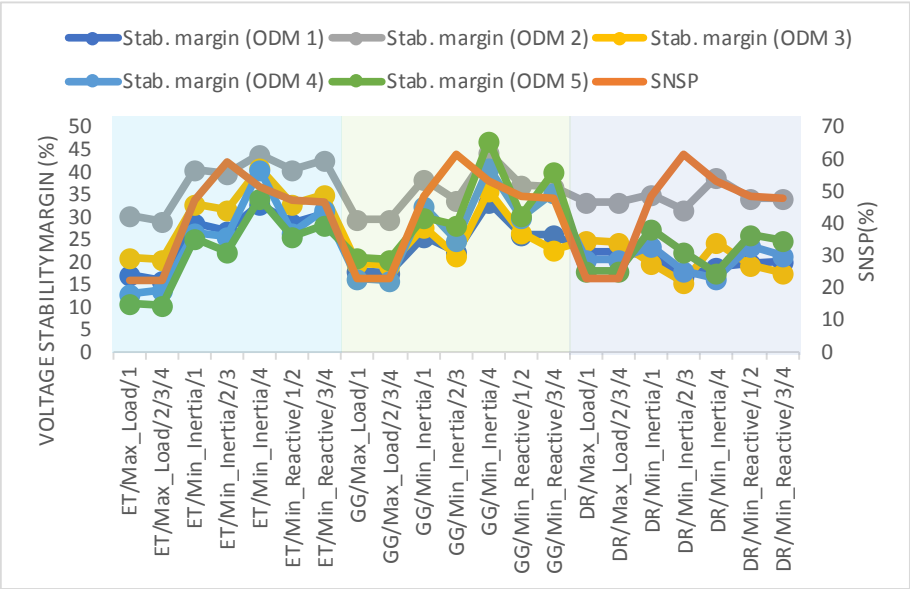

FIGURE 3-20: SNSP AND VOLTAGE STABILITY MARGINS CALCULATED FOR DISTRICTS OF POLISH REGIONAL TSO'S CONTROL CENTRES (N-0).

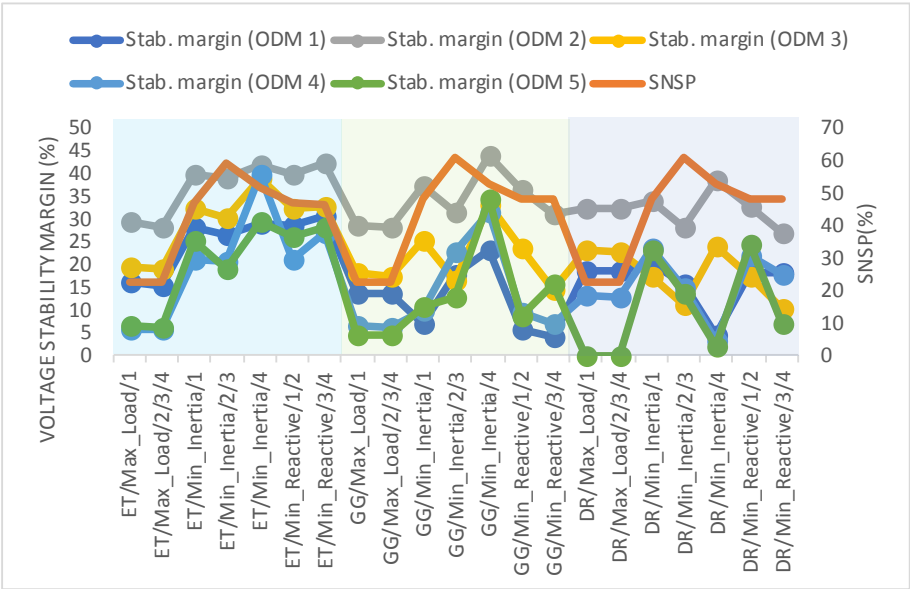

FIGURE 3-21: SNSP AND VOLTAGE STABILITY MARGINS CALCULATED FOR DISTRICTS OF POLISH REGIONAL TSO'S CONTROL CENTRES (N-1).

In (N-0) state (see Figure 3-20), the lowest values of voltage stability margin occur for the Energy Transition scenario and "Max_Load" operational cases. Minimum voltage stability margin is observed in ODM 5. In this case, a heavily loaded transmission system plays a crucial role for voltage stability conditions in particular power system areas. When Going Green and Distributed Renewables are considered, lower reactive power capability in generation is compensated by even lower reactive power demand by transmission equipment. It should be noted that for the Distributed Renewables scenario the voltage stability margin for ""Min_Inertia"" is lower than for "Max_Load" operational case. Such a situation is observed in ODM 1 and ODM 3. In general, no scarcities are observed for intact power network.

For (N-1) states there are two cases in which divergence of the load flow has been obtained (see Figure 3-21). These cases are Distributed Renewables /"Max_Load"/1 and Distributed Renewables /"Max_Load"/2/3/4. The contingency causing such problems is an outage of 400 kV busbar (740) located in ODM 5. Furthermore, it has been not possible to achieve convergence when changing tap positions using OLTC. Very low values of voltage stability margins can be observed for Distributed Renewables /"Min_Inertia"/4. For ODM 1, ODM 4 and ODM 5, voltage stability margins are 4.3%, 3.2% and 2.0% respectively. The latter value is below the permissible margin, as in Table 3-3. This shows that districts having remote generation (both conventional and renewable) are characterised by lower voltage stability margins.

3.1.4.1.3 CRITICAL ZONES

Table 3-4 and Table 3-5 present the calculation results of P-V curves when critical zones are considered. Such zones are smaller than ODMs, but they are also administrative regions. Not all the zones in Poland have been selected, but only those, in which steady-state voltage control problems are expected (identified in previous subsections). Only the worst cases have been presented for particular capacity and operational cases. Additionally, cases in which the voltage stability margins have been identified below permissible values are presented in Table 3-5.

TABLE 3-4: SELECTED P-V CURVE RESULTS FOR CRITICAL ZONES (N-0).

Scenario name	Critical zone	Number of analysed nodes	Initial active power [MW]	Maximum active power [MW]	Voltage stability margin [%]	The weakest 110 kV node	Critical voltage for the weakest node [p.u.]
ET/Max_Load/1	42	161	1706.7	2237.4	23.7	42505	0.737
ET/Max_Load/2/3/4	54	147	965.3	1262.3	23.5	54475	0.780
GG/Max_Load /1	42	161	1706.7	2366.1	27.9	42505	0.644
GG/Max_Load /2/3/4	17	138	750.9	1049.9	28.5	17220	0.656
GG/"Min_Inertia"/1	54	147	965.3	1733.3	44.3	54470	0.798
GG/"Min_Inertia"/4	17	138	750.9	1426.9	47.4	17260	0.675
GG/Min_Reactive/1/2	54	147	965.3	1741.3	44.6	54470	0.803
GG/Min_Reactive/3/4	17	138	750.9	1257.9	40.3	17260	0.744
DR/Max_Load/1	54	147	965.3	1402.1	31.2	54475	0.678
DR/Max_Load/2/3/4	54	147	965.3	1402.1	31.2	54475	0.689
DR/"Min_Inertia"/4	42	161	1706.7	2498.7	31.7	42022	0.753

TABLE 3-5: SELECTED P-V CURVE RESULTS FOR CRITICAL ZONES (N-1).

Scenario name	Critical zone	Number of analysed nodes	Initial active power [MW]	Maximum active power [MW]	Voltage stability margin [%]	The weakest 110 kV node	Critical voltage for the weakest node [p.u.]
ET/Max_Load/1	52	78	641.1	707.1	10.3	52270	0.906
ET/Max_Load/2/3/4	51	106	752.0	834.0	10.9	51100	0.900
GG/Max_Load /1	49	49	435.6	525.9	17.2	49010	0.619
GG/Max_Load /2/3/4	49	49	435.6	525.9	17.2	49010	0.634
GG/"Min_Inertia"/1	54	147	965.3	1261.3	23.5	54475	0.839
GG/"Min_Inertia"/2/3	49	49	435.6	762.4	42.9	49010	0.592
GG/"Min_Inertia"/4	17	138	750.9	1192.9	37.1	17865	0.740
GG/Min_Reactive/1/2	54	147	965.3	1157.3	16.6	54470	0.825
GG/Min_Reactive/3/4	17	138	750.9	828.9	9.4	17415	0.832
DR/Max_Load/1	49	49	435.6	579.6	24.8	49010	0.629
DR/Max_Load/2/3/4	54	147	No convergence in the load flow				
	49	49	435.6	579.6	24.8	49010	0.630
	54	147	No convergence in the load flow				
DR/"Min_Inertia"/1	42	161	1706.7	1825.5	6.5	42470	0.860

For (N-0) intact network, no voltage stability scarcities are observed. The lowest values of voltage stability margin have been obtained in three zones (17, 42 and 54) which belong to districts ODM 1, ODM 4 and ODM 5 respectively (see Figure 3-19). In this case, the obtained values of stability margins are relatively high compared to those, calculated for the other power system districts.

For (N-1) states, the load flow divergence occurs for Distributed Renewables /"Max_Load"/2/3/4 and zone 54 is considered a critical one. Such problems result from the same contingency as in district areas P-V calculation (see Figure 3-21). As in (N-0) calculations, obtained values of stability margins are relatively high compared to those calculated for the other power system districts. The zone 54 is the one which is supplied from the farthest located sources.

As an example, P-V curves obtained for one of the zones is presented in Figure 3-22.

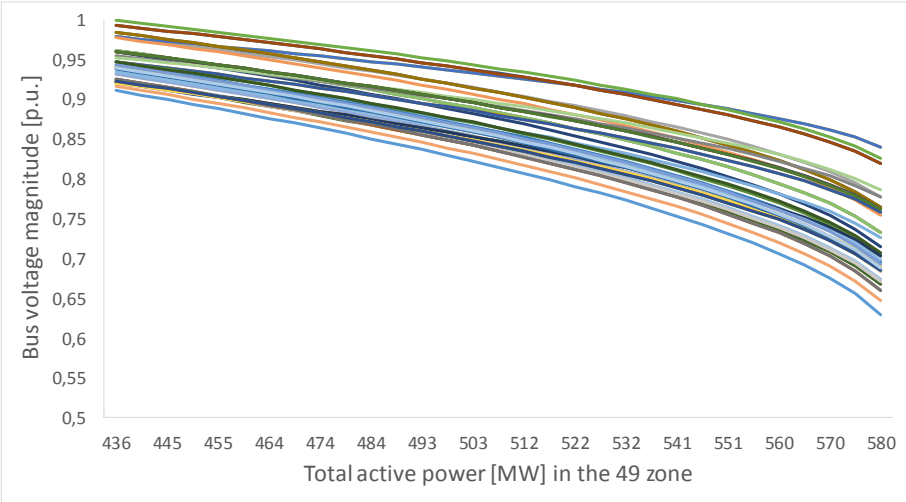

FIGURE 3-22: P-V CURVES OBTAINED FOR ZONE 49 IN DR/MAX_LOAD/2/3/4 SCENARIO.

3.1.4.2 **Q-V CURVES**

Q-V curves present the relationship between the reactive power injected into a power network node and the nodal voltage level [4] [22] [30]. Q-V characteristics are determined by the connection of a fictitious reactive power resource with zero real power to the analysed node. Additional reactive power is generated/consumed at the bus based on the voltage control mode.

For all scenarios and operational cases, the weakest 110 kV nodes (based on the results of the voltage sensitivity analysis) have been identified within all the critical zones. Only (N-1) contingency states for various snapshots are analysed for the purpose of Q-V curve calculation.

In Figure 3-23, an example of a Q-V curve is presented. Two parameters are then investigated:

- Required reactive power reserve
- Voltage stability limits (an absorption reactive power distance from zero to the bifurcation point).

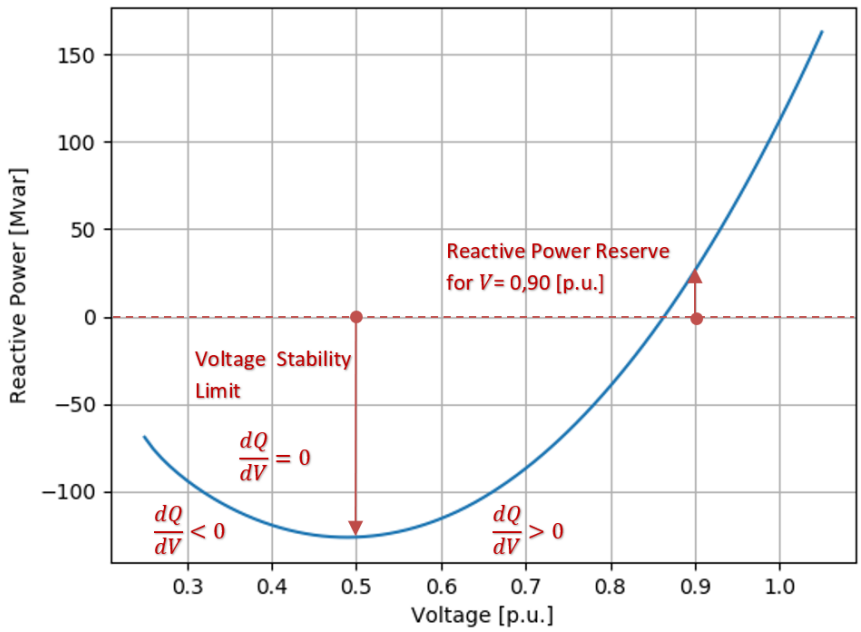

FIGURE 3-23: Q-V CURVE OBTAINED FOR DR/MAX_LOAD/1 AND ITS BASIC PARAMETERS.

Table 3-6 presents the results of Q-V curve analysis for all investigated scenarios and operational cases.

TABLE 3-6: Q-V RESULTS FOR (N-1) STATES.

Scenario name	Critical zone	The weakest 110 kV node	Reactive power reserve [Mvar]	Reactive power limit [Mvar]
ET/Max_Load/1	41	41311	11.8	-155.8
	42	42495	18.9	-140.1
	43	43500	71.0	-92.0
	49	49010	10.3	-76.9
	53	53150	11.4	-37.1
	54	54015	12.6	-66.3
ET/Max_Load/2/3/4	14	14070	0.8	-40.1
	41	41311	11.3	-156.8
	42	42495	14.4	-144.7
	43	43500	69.3	-93.1
	49	49010	0.3	-85.1
	53	53150	12.5	-36.5
	54	54015	14.6	-65.2
GG/Max_Load /1	14	14070	4.8	-35.3
	41	41311	19.6	-136.0
	42	42495	23.6	-126.5
	43	43500	79.5	-75.4
	48	48115	6.1	-84.9

	49	49010	20.1	-69.3
	53	53150	26.2	-28.7
	54	54015	39.0	-48.2
GG/Max_Load/2/3/4	14	14070	5.1	-35.1
	41	41311	24.2	-129.8
	42	42495	34.5	-116.4
	43	43500	84.7	-70.9
	48	48115	6.6	-84.7
	49	49010	19.9	-69.5
	53	53150	25.6	-29.1
	54	54015	38.1	-49.0
GG/Min_Reactive/3/4	17	17415	9.2	-63.5
	55	55430	9.8	-73.1
	57	57130	8.8	-94.3
DR/Max_Load/1	43	43500	26.2	-126.4
	53	53150	No convergence in the load flow	
DR/Max_Load/2/3/4	43	43500	28.0	-124.8
DR/"Min_Inertia"/4	53	53415	6.1	-31.5
	54	54470	2.2	-34.8
	56	56070	21.7	-33.4

Positive values of reactive power reserve requirement indicate a lack of reactive generation. High demand for the leading reactive power has been observed for bus number 43500 (in zone 43). The highest reactive power reserve value occurs for the Going Green scenario, while for Distributed Renewables it is relatively low. Minimum value of reactive power limit has been obtained for bus number 53150 (in zone 53) in the Going Green capacity scenario.

It should however be emphasised that for the Distributed Renewables scenario load flow divergence has been identified which means that there is a negative reactive power limit causing an instable operation point. Such problems occur when the P-V curves for the critical zones are analysed (see Section 3.1.4.1.3). The load flow divergence is caused by the outage of a 400 kV busbar (busbar 740) (see Table 11-8: Critical zones identified for each capacity and operation scenario.). Q-V curves obtained for bus number 53150 in (N-1) states are shown in Figure 3-24.

In general, the scenarios characterized by high RES capacity entail a higher risk of nodal voltage in-stability.

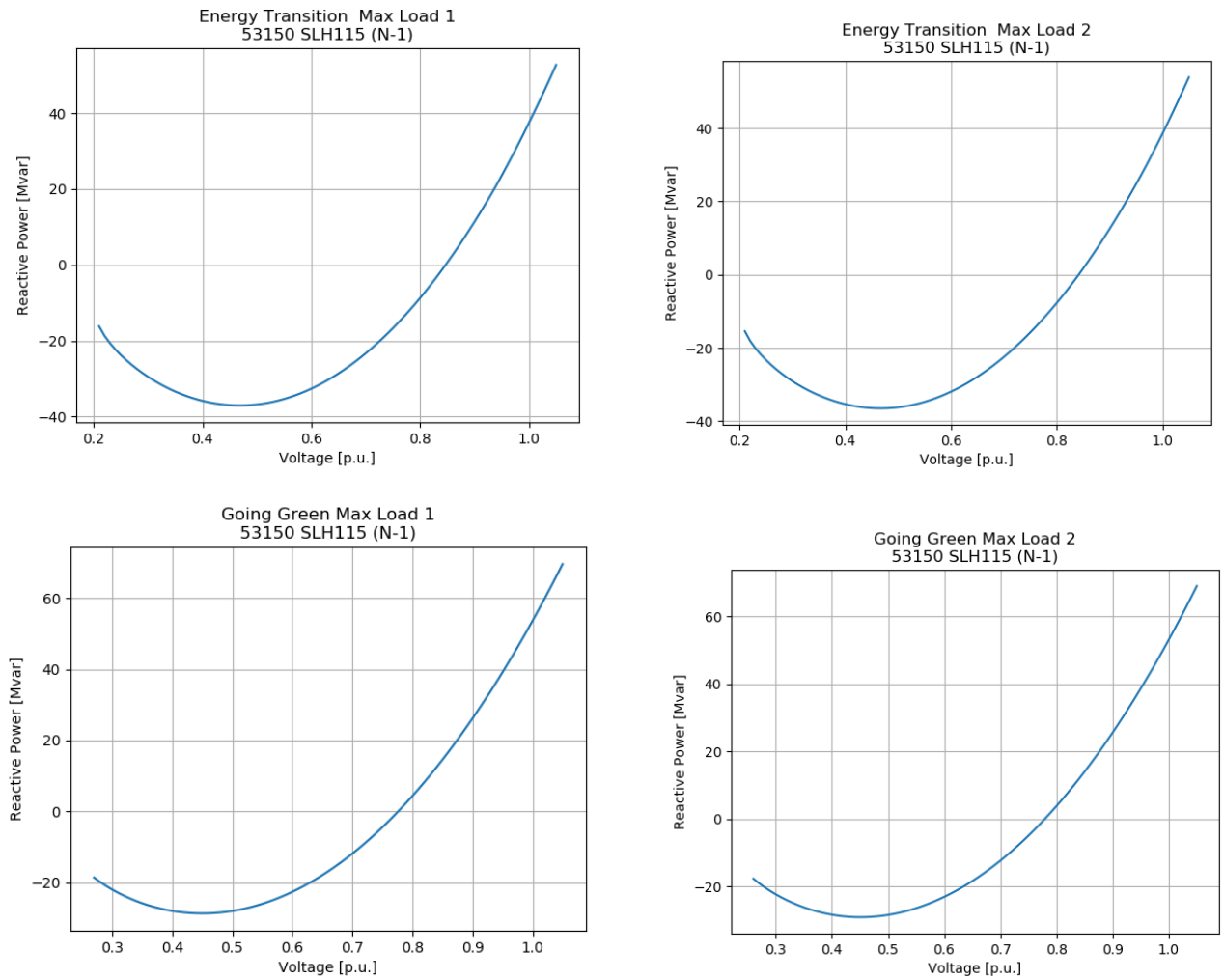

FIGURE 3-24: Q-V CURVES FOR ONE OF THE ANALYSED 110 KV NODES.

3.1.5 DYNAMIC VOLTAGE CONTROL

Low Voltage Ride-Through (LVRT) profiles have been analysed based on the time-domain simulations performed alongside the transient rotor angle stability analysis, which is discussed in a separate chapter in this report. The obtained voltage waveforms have been compared with the LVRT profiles required as per the Polish implementation of the RFG network code, which have been presented in detail in [3].

For the purposes of Fault Ride Through (FRT) analysis including SGMs (Synchronous Power Generating Modules), a set of 150 ms self-clearing close 3-phase short circuit in transmission lines leading out of a power plant station have been assumed. As regards the non-synchronous generation units, such as large-scale PPMs, it has been assumed that it is appropriate to analyse 150 ms self-clearing 3 phase short circuits at the point of common connection (PCC) of the PPM.

In order to assess how outages may influence the LVRT capability of non-synchronous generators, critical contingencies identified in the voltage control analyses, also have been applied to the pre-fault power system operation state. A set of the largest PPMs within the whole Polish power system and selected two critical zones regarding steady-state voltage stability, have been selected for the test simulations.

As a result of the analysis, no LVRT requirement violations have been observed in the transient analysis. Figure 3-25 and Figure 3-26 present the transient voltage response in one of the investigated EHV busbars to which the synchronous generators are connected via unit transformers and lines. The FRT plots are shown for three operational cases ("Max_Load", ""Min_Inertia"" and "Min_Reactive") for Poland only. Figure 3-25 and Figure 3-26 present the FRT results for the Going Green and Distributed Renewables scenarios respectively. Looking at both figures, it can be seen that the voltages are relatively far from the required LVRT profile, as per RFG. A slight difference between FRT plots representing "Max_Load" and other operational cases is also observed. The FRT response for "Max_Load" (with lower $SNSP$ than other scenarios) has less oscillation resulting in the greater power system stiffness. It is to be noted that the voltage profiles for all SGMs are relatively similar to the results presented here.

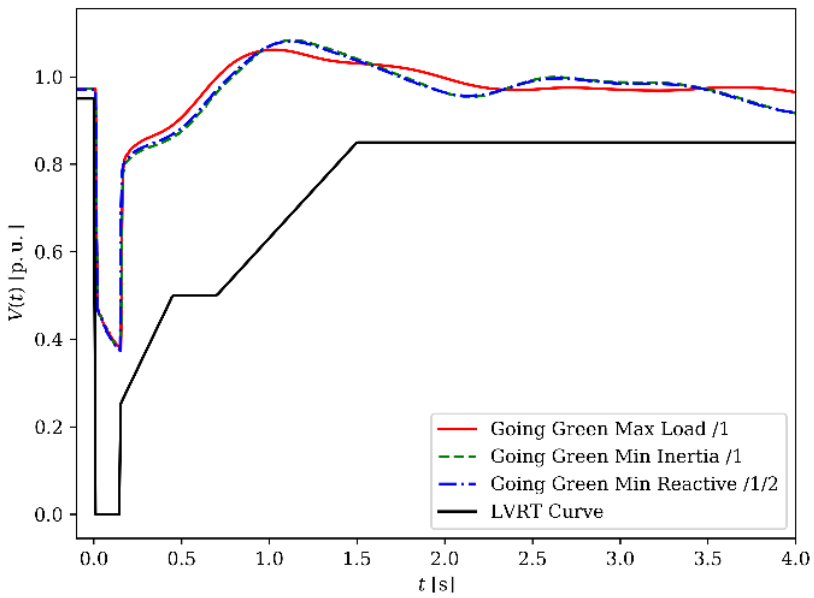

FIGURE 3-25: FRT RESPONSES FOR SGMS (SELECTED EHV BUSBAR OF KOZIENICE POWER PLANT STATION, GOING GREEN SCENARIO, 150 MS SELF-CLEARING 3 PHASE SHORT CIRCUIT).

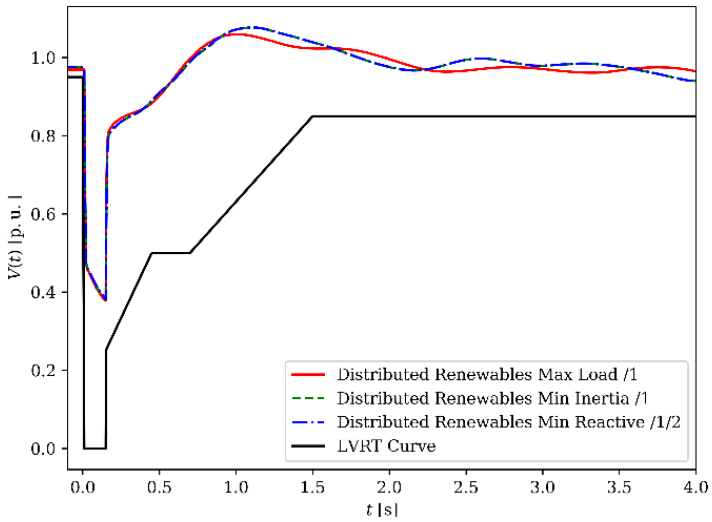

FIGURE 3-26: FRT RESPONSES FOR SGMS (SELECTED EHV BUSBAR OF KOZIENICE POWER PLANT STATION, DISTRIBUTED RENEWABLES SCENARIO, 150 MS SELF-CLEARING 3 PHASE SHORT CIRCUIT).

For PPMs, there is no significant impact of different operational cases (resulting in different SNSP) to FRT responses. For example, the FRT results obtained for the PCC of two of the wind farms are shown in Figure 3-27 and Figure 3-28. The obtained voltage response for the Going Green scenario has a sharper overshoot in comparison to the responses obtained for Distributed Renewables. In Figure 3-27, it can be observed that the FRT curve representing “Max_Load” is steadier than those for “Min_Inertia” and “Min_Reactive” operational cases (higher SNSP). All the FRT responses are within the required LVRT profile. It is also worth emphasising that all the D-type wind farms and active distribution systems (B and C-type PPM generation included) have the FRT capability implemented in their control systems.

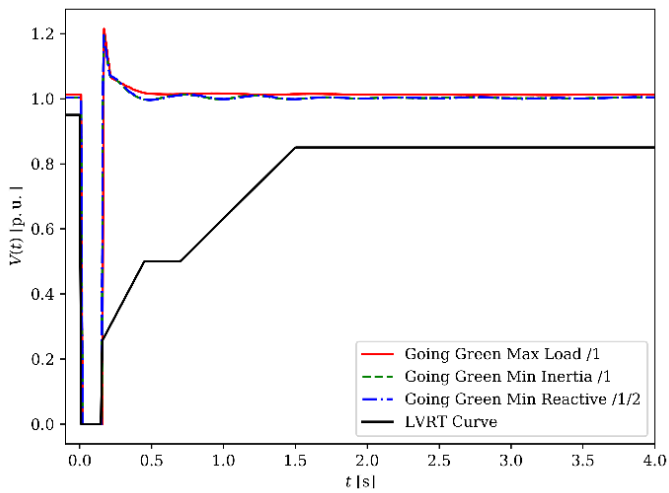

FIGURE 3-27: FRT RESPONSES FOR PPM (SELECTED PCC OF D-TYPE PPM, GOING GREEN SCENARIO).

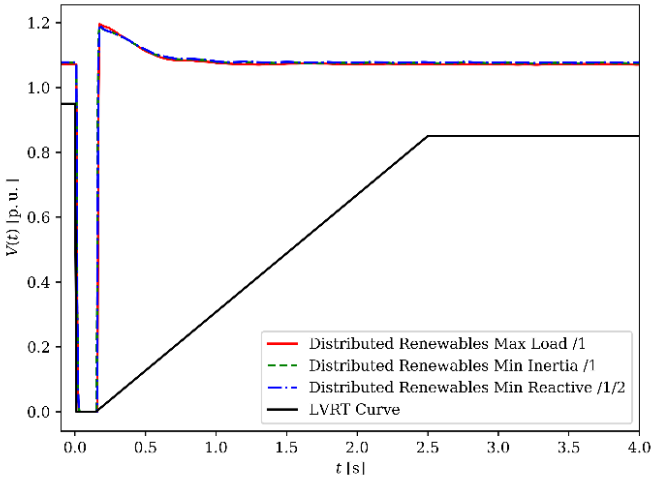

FIGURE 3-28: FRT RESPONSES FOR PPM (SELECTED PCC OF C-TYPE PPM, DISTRIBUTED RENEWABLES SCENARIO).

3.2 IRELAND & NORTHERN IRELAND POWER SYSTEM STATIC VOLTAGE ANALYSIS

3.2.1 VOLTAGE DEVIATIONS

Steady state voltage studies are used to identify instances of reactive power scarcity as levels of non-synchronous variable renewable generation increased. The 2030 Steady Evolution and Low Carbon Living scenarios are utilised in these studies. The respective transmission networks are assessed for voltage deviations as per the Ireland and Northern Ireland Transmission System Security and Planning Standards (TSSPS) [31] [32] documentation; 0.95 p.u. for the intact network and 0.9 p.u. following single contingencies.

3.2.1.1 STATIC VOLTAGE METHODOLOGY

AC load flow analysis is used to assess all transmission network buses that have experienced voltage deviations that fall below 0.9 p.u. AC load flow analysis is performed using PSS®E to assess the impact of increasing levels of non-synchronous variable RES on the 2030 Low Carbon Living and Steady Evolution grid model over the period of a full year (8,760 hours).

An in-house tool has been developed to combine the PLEXOS generated economic dispatches with the PSS®E grid model. LAMDA, or Load-flow & Automated Multi-Dispatch Analysis, takes the generation, interconnection and demand patterns and maps the information into the grid model. The program is developed using the Python programming language. Furthermore, LAMDA finds a solution to create a grid model for each hour and subsequently applies performance tests on the intact (N) grid model and evaluates loss of a single network element (N-1) to identify circuits or stations that have exceeded voltage planning standards limits.

3.2.1.2 STATIC VOLTAGE DEVIATION RESULTS & DISCUSSION

Figure 3-29 presents the analysis of low voltage deviations for the 2030 Steady Evolution scenario over a full year (8,760 hours) plotted against system SNSP. As can be seen, during periods of low SNSP (>25%) there appears to be sufficient steady state reactive power capability on the system due to a higher dispatch of conventional thermal generation. This prevents voltage deviations below planning standards for both N and N-1 conditions. However, as SNSP increases there is a significant lack of steady state reactive capability due to RES displacing conventional generation which results in large increase in both magnitude and occurrences of low voltage deviations under 0.9 p.u.

Analysis of buses experiencing low voltage deviations shown in Figure 3-29 are primarily at 110 kV and are located in areas considered to be weaker parts of the system. These areas typically have little or no stronger transmission network (220 kV and above), have high RES capacities, low local demand and are electrically distant from conventional generation.

As shown in Figure 3-30, analysis of Steady Evolution shows that the impact of increasing SNSP on low voltage deviations is similar to the Low Carbon Living scenario. However, comparing Steady Evolution to Low Carbon Living illustrates that, there is a clear increase in occurrences of low voltage deviations at higher SNSP and a subsequent lack of steady state reactive capability.

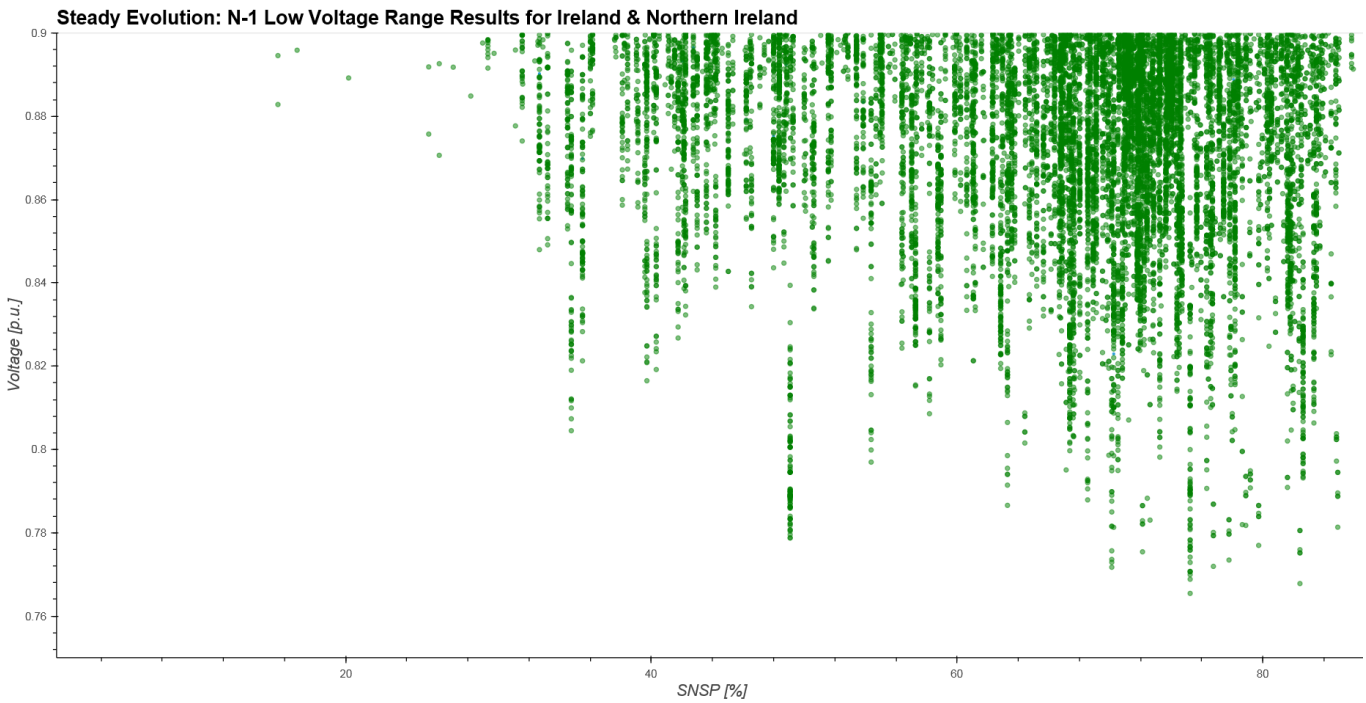

FIGURE 3-29: COMPARISON OF 2030 STEADY EVOLUTION TRANSMISSION BUSSES LOW VOLTAGE DEVIATION AGAINST SNSP

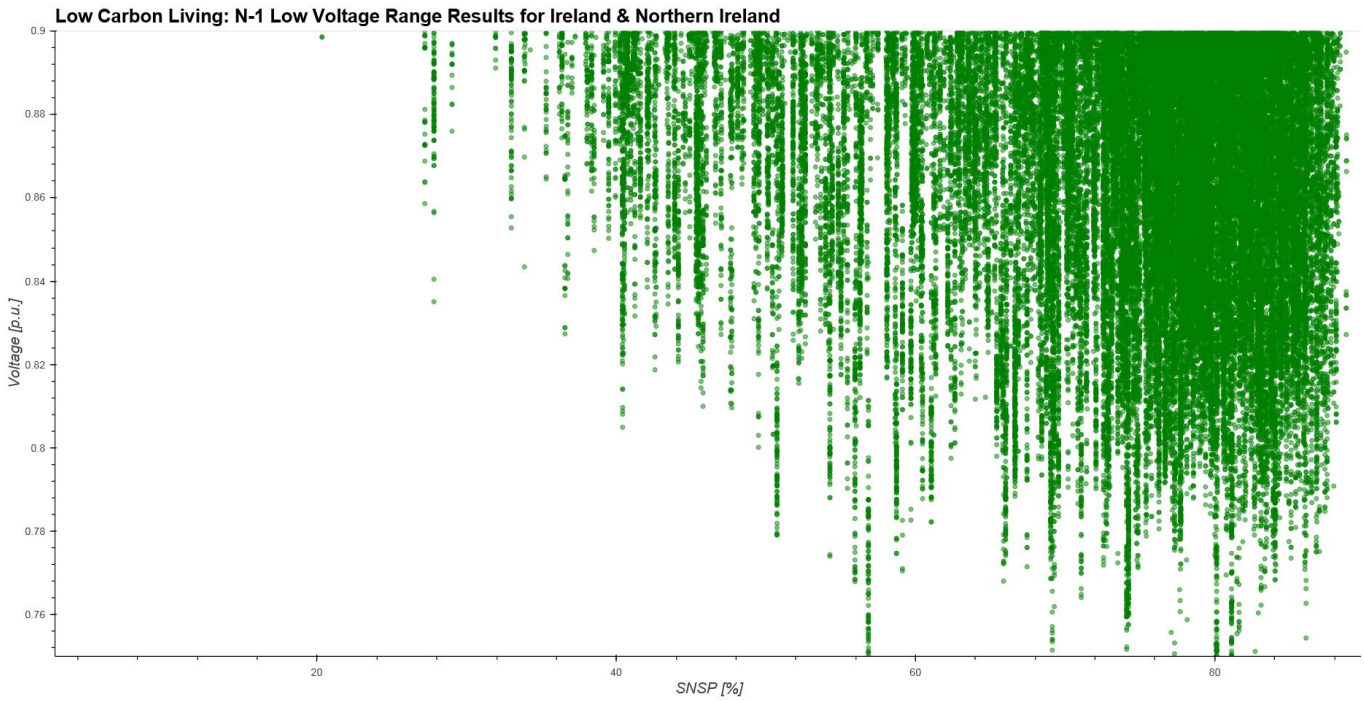

FIGURE 3-30: COMPARISON OF 2030 LOW CARBON LIVING TRANSMISSION BUSSES LOW VOLTAGE DEVIATION AGAINST SNSP

- As SNSP increases the occurrence and magnitude of low voltage deviations are seen to significantly increase, indicating a lack of steady state reactive capability as conventional generation is displaced by RES.
- 110 kV transmission buses located in weaker parts of the system are primarily impacted by the lack of local steady state reactive power at higher levels of SNSP.
- Analysis demonstrates that occurrences of low voltage deviations increased at higher levels of SNSP for Low Carbon Living due to higher RES quantities when compared to Steady Evolution.

3.2.2 QV ANALYSIS

To further study the lack of steady state reactive capability due to increased levels of RES, QV analysis is undertaken. QV analysis is used to determine the reactive power injection required at a bus in order to control the bus voltage to the required value. Although QV analysis yields very local information, a selection of buses have been chosen for closer inspection using QV analysis.

3.2.2.1 QV ANALYSIS METHODOLOGY

QV analysis is performed using a series of AC power flow calculations in PSS®E. An in-house QV tool was developed in Python to automate the PSS®E QV load flow analysis on a selected study bus for each hour of the economic dispatch created for Steady Evolution and Low Carbon Living.

Starting with a specified maximum per unit voltage set point at the study bus, reactive power injection requirements are computed for N and N-1 conditions until the study bus voltage set point is achieved. The QV tool records each reactive power requirement for every N and N-1 condition for each hour and then analysis determines the maximum reactive power requirement at the study bus. As the QV analysis is used to study local phenomenon at a chosen study bus, three study buses are selected to analyse the impact of reduced steady state reactive capability due to increasing levels of RES.

These three study buses are Binbane, Glenree (both 110 kV) and Clonee (220 kV). Binbane and Glenree study buses were selected as both are located in weaker parts of the transmission system and have high levels of RES located within their respective regions. Binbane and Glenree demonstrate significant low voltage deviations with their average low voltage deviation being approximately 0.86 p.u. when compared to buses in a stronger part of the network with high RES experiencing a typical average low voltage deviation of approximately 0.89 p.u.

The third bus, Clonee, is located in the Dublin area which has a strong network, is close to conventional generation and very little RES. It is chosen to act as a comparator to Binbane and Glenree.

3.2.2.2 QV ANALYSIS RESULTS & DISCUSSION

As illustrated in Figure 3-32 to Figure 3-34 both the weak buses, Binbane and Glenree, have steady state reactive requirements that increase with SNSP for both Steady Evolution and Low Carbon Living, reinforcing the results seen during the low voltage deviation analysis. The maximum Mvar requirement for Binbane was 114 Mvar at an SNSP of 79%, while Glenree required 233 Mvar at 86% SNSP. Both the Binbane and Glenree maximum reactive power requirements are recorded in the Low Carbon Living scenario.

It can be observed that the magnitudes of Mvar requirements for both weak buses are quite similar in both scenarios. Based on the results shown in Figure 3-29 and Figure 3-30, it would be expected that the weaker buses in Low Carbon Living would require a greater magnitude of Mvar requirement at higher SNSP due to the increased levels of RES. However, it can be seen that the Low Carbon Living scenario only requires a slightly larger steady state reactive power requirement at high levels of SNSP at the weaker busses. This is particularly evident for one of the weaker buses, Binbane. A contributing factor to this phenomenon is due to the fact that the initial voltage (prior to the loss of a circuit) at the bus is lower in Low Carbon Living when compared to Steady Evolution. Because of the larger levels of RES and demand in Low Carbon Living, the impact on the transmission network's thermal loading is increased which results in the initial voltages in weaker areas tending to be lower than initial voltages in Steady Evolution. Thus Binbane and Glenree buses require similar reactive power in both Low Carbon Living and Steady Evolution to control the bus voltage to 1.0 p.u. as the initial voltage in Low Carbon Living is lower hence producing similar trends as seen in Figure 3-32 to Figure 3-34.

An additional contributing factor is the overall system SNSP value used in Figure 3-32 to Figure 3-34 versus the level of RES in close proximity to Binbane, a weak bus, in both Steady Evolution and Low Carbon Living scenarios. A similar overall value for system SNSP is recorded in Figure 3-32 to Figure 3-34. While this value of SNSP is similar in both Steady Evolution and Low Carbon Living, the system conditions that make up the system SNSP value can vary significantly in both scenarios depending on demand levels, RES generation and conventional generation dispatch. However, at the local bus level the variation of RES levels in close proximity to a weak bus, in this case Binbane, may only differ slightly in both scenarios thus resulting in similar levels of reactive power injection to control the bus's voltage set point to 1.0 p.u.

Figure 3-35 and Figure 3-36 illustrate the steady state reactive power requirement recorded at the strong bus, Clonee 220 kV station, for both Steady Evolution and Low Carbon Living during N and N-1 system conditions. While the trend is not as well defined as the weaker buses, Binbane and Glenree, it can be seen that at higher SNSP there is a significant rise in occurrences when steady state reactive power is required at Clonee.

At SNSP levels in the region of 20% to 60% SNSP, the strong bus, Clonee can experience a large variation in steady state reactive power requirements as the generation mix can also vary significantly. During these periods conventional synchronous generation located in close proximity to the strong bus, Clonee, can be dispatched and will provide sufficient voltage regulation. When this conventional generation is offline the capability for voltage regulation at Clonee is greatly reduced thus the steady state reactive power requirement increases. As the system moves to high levels of SNSP (>70%) it is less likely that conventional generation in close proximity to the strong bus, Clonee is online and therefore there is a definitive rise in number of occurrences when reactive power support is identified. This is especially evident in Low Carbon Living were due to the higher levels of RES it is less likely that conventional generation is dispatched.

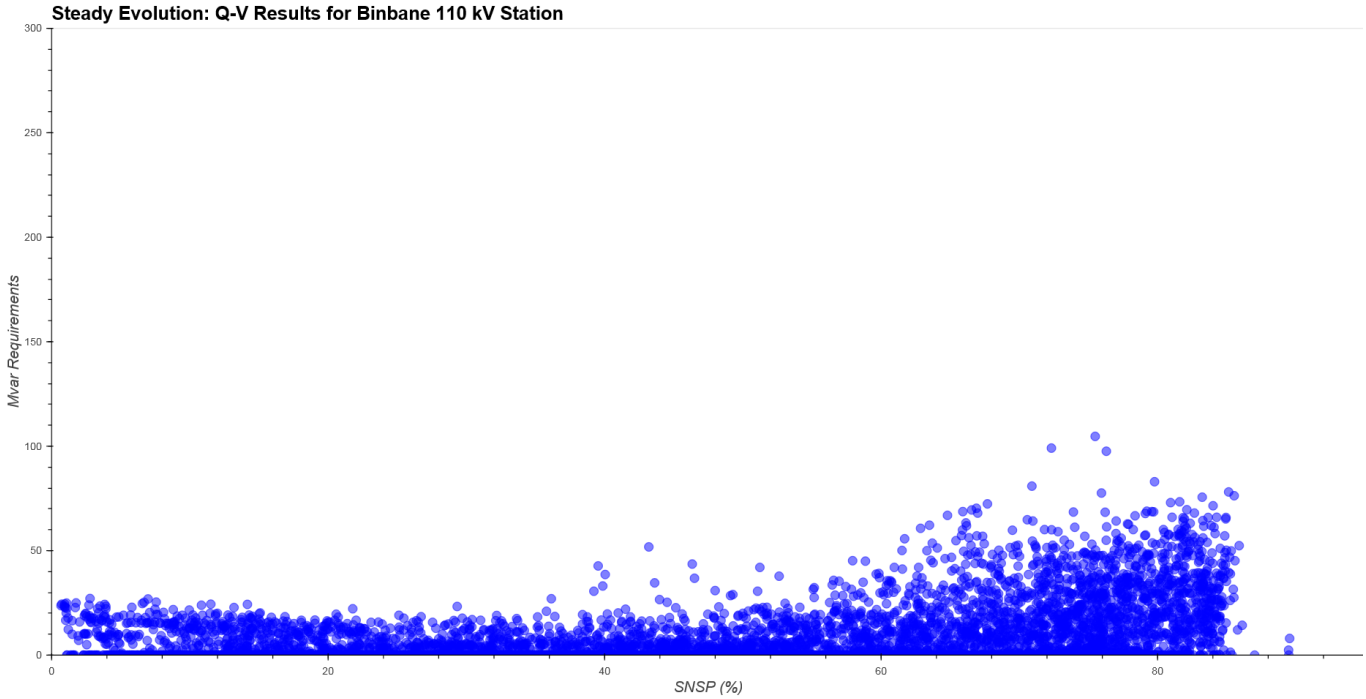

FIGURE 3-31: MVAR REQUIREMENT FOR STEADY EVOLUTION BINBANE 110 KV BUS AGAINST SNSP

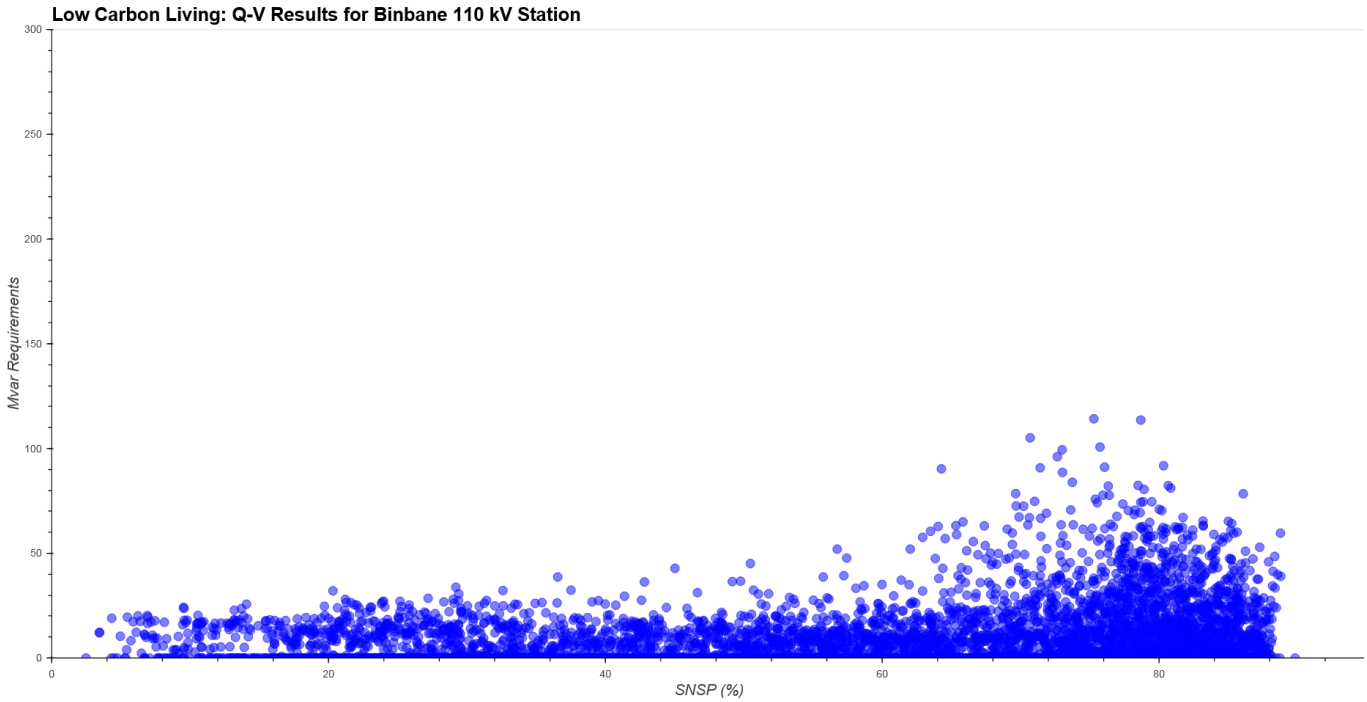

FIGURE 3-32: MVAR REQUIREMENT FOR LOW CARBON LIVING BINBANE 110 KV BUS AGAINST SNSP

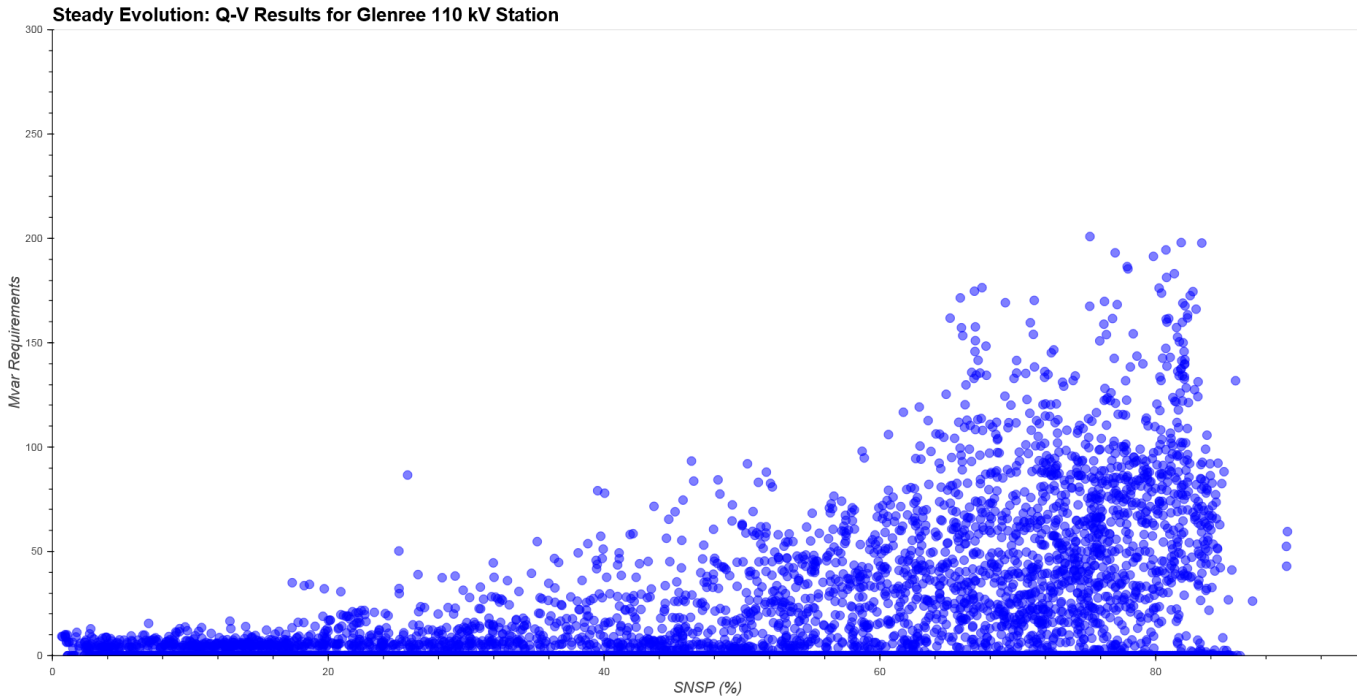

FIGURE 3-33: MVAR REQUIREMENT FOR STEADY EVOLUTION GLENREE 110 KV BUS AGAINST SNSP

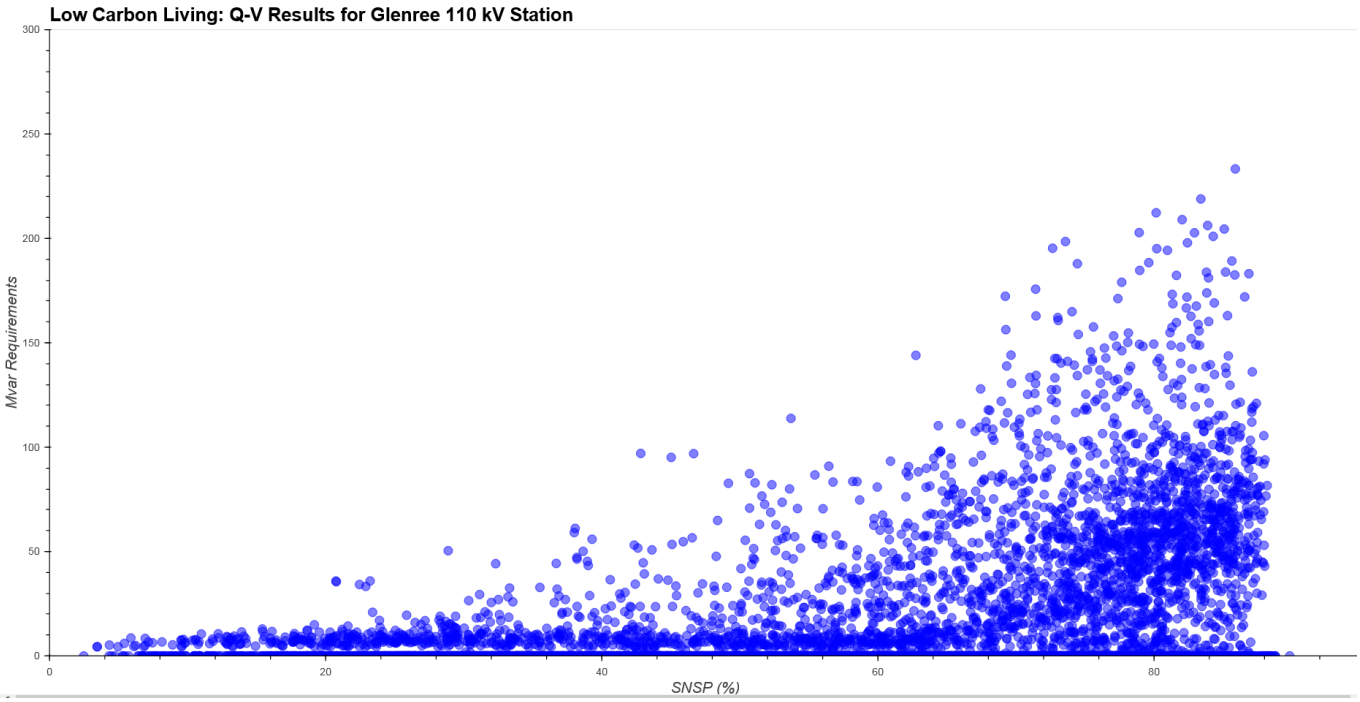

FIGURE 3-34: MVAR REQUIREMENT FOR LOW CARBON LIVING GLENREE 110 KV BUS AGAINST SNSP

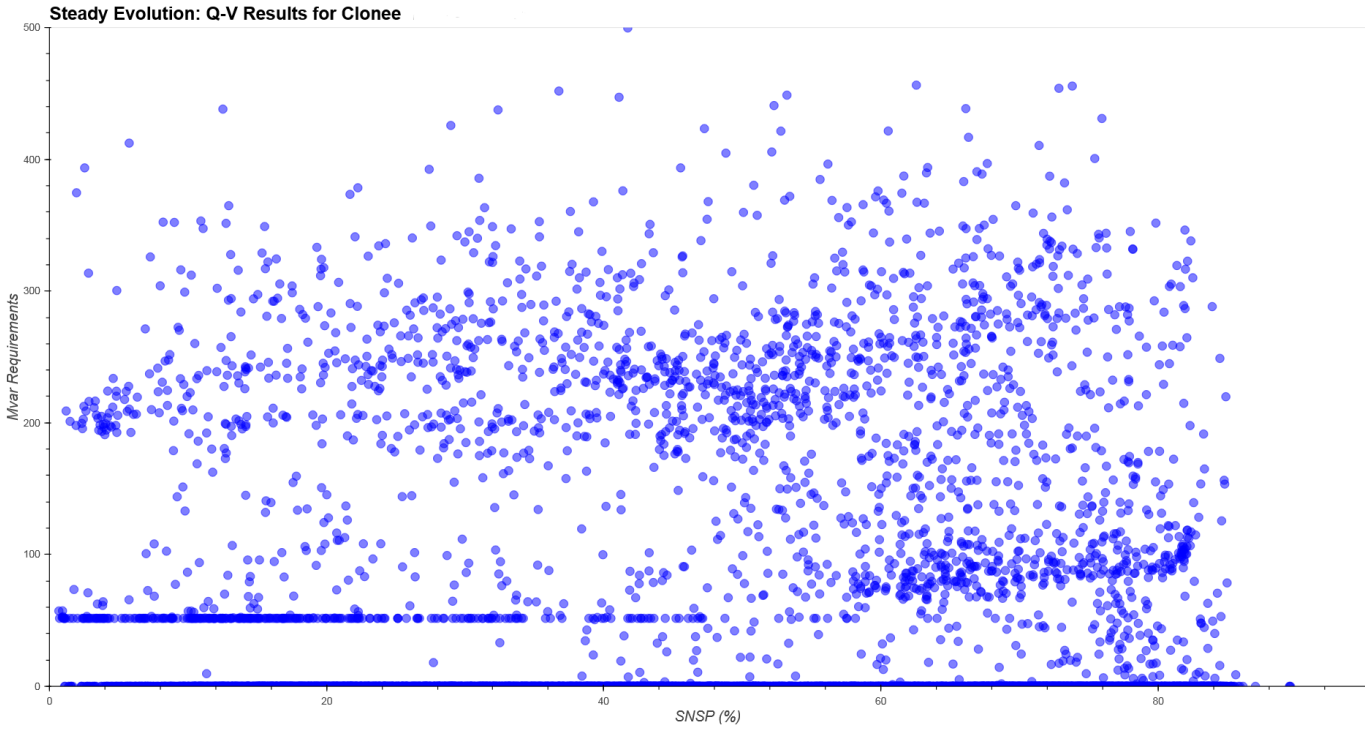

FIGURE 3-35: MVAR REQUIREMENT FOR STEADY EVOLUTION CLONEE 220 KV BUS AGAINST SNSP

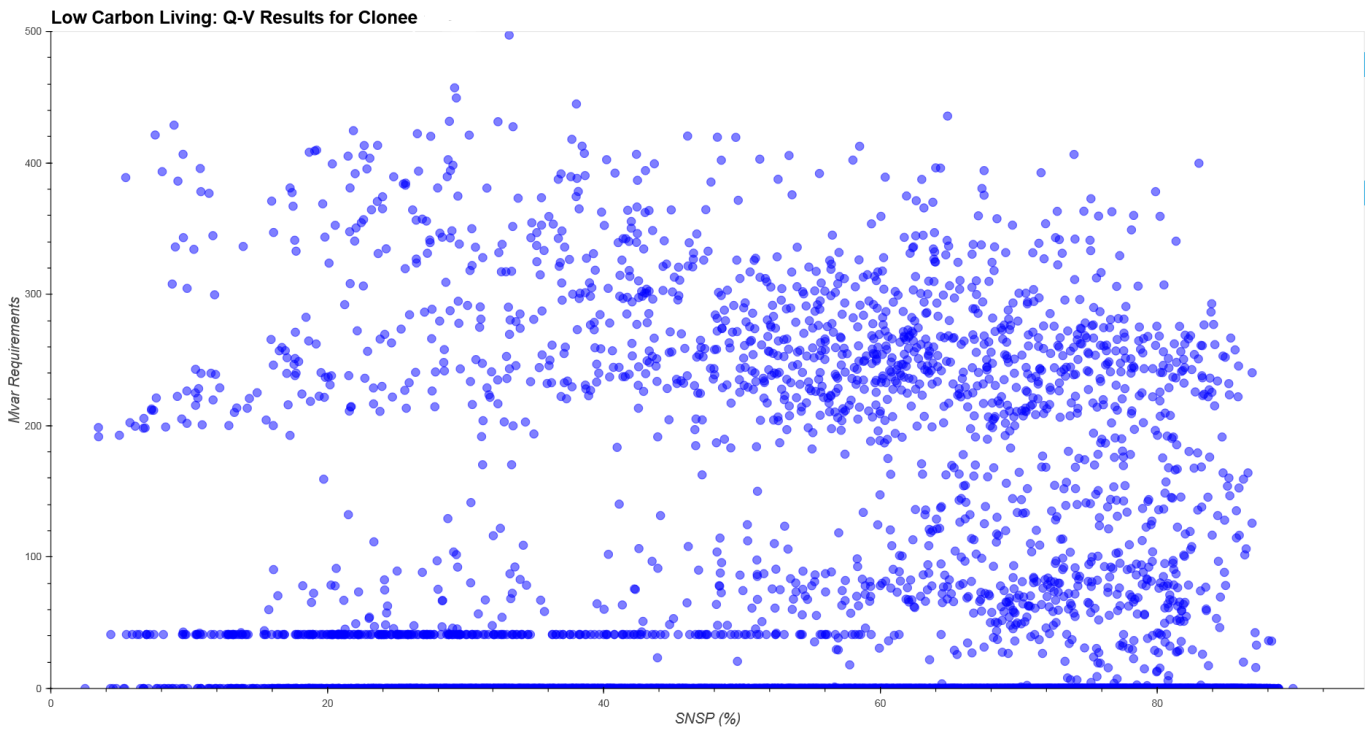

(B)

FIGURE 3-36: MVAR REQUIREMENT FOR LOW CARBON LIVING CLONEE 220 KV BUS AGAINST SNSP

- QV analysis at the study buses further reinforced the results seen during the low voltage deviation analysis.
- As SNSP increased it was observed that steady state reactive power requirements at each of the study buses also increased with the maximum requirements being recorded in Low Carbon Living.
- Although the number of occurrences when steady state reactive power was required was seen to rise at all study busses as SNSP increases, it was observed that busses in weaker parts of the system with higher levels of RES in close proximity were particularly prone to significant rises in steady state reactive power requirements at high SNSP (>70%).

3.2.3 SHORT CIRCUIT LEVELS

Short Circuit (SC) studies are used to determine the impact of increased levels of non-synchronous RES (converter based technology) have on the Short Circuit Power (fault level) at the selected study buses described above. As converter based generation has limited fault current capability (when compared to conventional synchronous generation) and the overall voltage regulation of the system is reduced due to lack of conventional generation available for dispatch, it is anticipated that short circuit power will decrease particularly at higher levels of SNSP.

3.2.3.1 SHORT CIRCUIT METHODOLOGY

Short circuit analysis is carried out using PSSE's automatic sequencing short circuit calculation (ASCC) engine. The ASCC engine calculates short circuit current based on a constant fault infeed from the network sources. The source impedance data to ensure the infeeds are appropriate for generators is based on data submitted by generators. Generators are required under Grid Code to submit model data that must accurately reflect the generator's plant performance during short circuit conditions. An in-house tool was developed in Python in order to automate PSSE's ASCC in order to study each hour of the economic dispatch created for Steady Evolution and Low Carbon Living.

The in-house Short Circuit tool calculates the 3-ph fault current contribution at the study bus using ASCC. This is then multiplied by the recorded bus voltage to obtain an equivalent Short Circuit Power (Fault Level) in MVA.

The Short Circuit tool also calculates the contribution of load to the fault based on the G74 Engineering Recommendation (ER G74) [33]. ER G74 recommends that large industrial motors are modelled explicitly in fault calculations and X/R ratios of 6.67 (up to 1 MW /pole pair), and 10 (for > 1 MW per pole pair) be used to calculate the infeed decrements.

3.2.3.2 SHORT CIRCUIT RESULTS & DISCUSSION

As shown in Figure 3-37 to Figure 3-40 for both the weak buses, Binbane and Glenree, there is a significant overall decrease in short circuit power at higher levels of SNSP (>70%) for both Steady Evolution and Low Carbon Living. It can be observed that Low Carbon Living has a greater impact on reducing short circuit power. This is due to converter based technology dominating the generation portfolio at high levels of SNSP. As the fault current contribution from converter based technology is limited and there is a lack of conventional synchronous generation online to contribute to the fault and regulate system voltage, the overall impact is a reduction in short circuit power.

Initially as SNSP is increasing it can be seen that short circuit power at the weak buses, Binbane and, Glenree gradually increases as well. Both areas contain a significant amount of distributed RES and although converter based technologies fault current contribution is limited, the cumulative impact is to raise the short circuit power at these buses.

It can also be observed that the short circuit power in Steady Evolution is larger than Low Carbon Living particularly in the case of one of the weak buses, Binbane. This is due to the higher initial voltage in Steady Evolution when compared to Low Carbon Living which has levels of RES and demand resulting in higher transmission network thermal loading. Thus the short circuit power calculation is impacted by the lower bus voltage at the weak bus, Binbane, resulting in a lower short circuit power for Low Carbon Living.

Figure 3-41 and Figure 3-42 illustrate the short circuit power recorded at the strong bus, Clonee 220 kV station, for both Steady Evolution and Low Carbon Living. While the trend is not as well defined as the weaker buses, Binbane and Glenree, it can be seen that at higher SNSP there is a significant decrease in short circuit power.

At SNSP levels in the region of 20% to 60% SNSP, the strong bus, Clonee can experience a large variation in short circuit power as the generation mix can also vary significantly. During these periods conventional synchronous generation located in close proximity to the strong bus, Clonee, can be dispatched and raise the short circuit power. When this conventional generation is offline the short circuit power will reduce. As the system moves to high levels of SNSP (>70%) it is less likely that conventional generation in close proximity to the strong bus, Clonee is online and therefore a significant drop in short circuit power is observed.

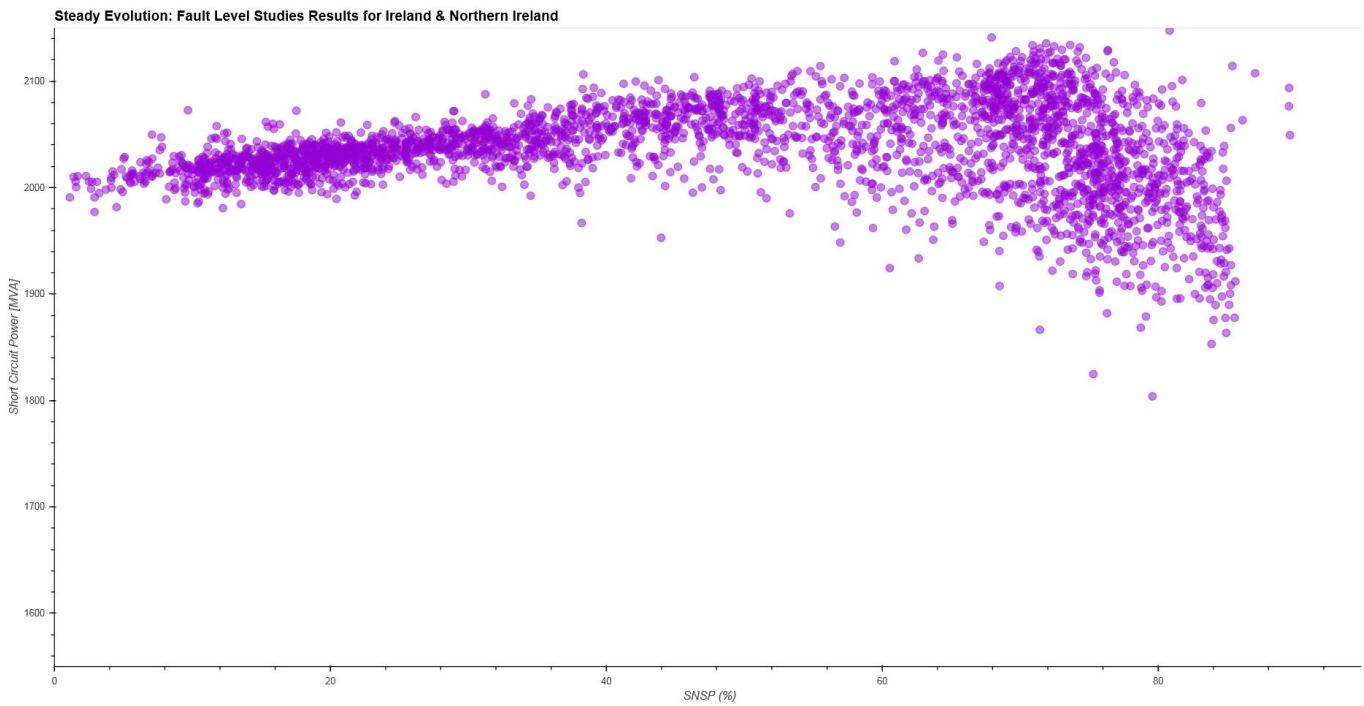

FIGURE 3-37: SHORT CIRCUIT POWER FOR STEADY EVOLUTION BINBANE 110 KV BUS AGAINST SNSP

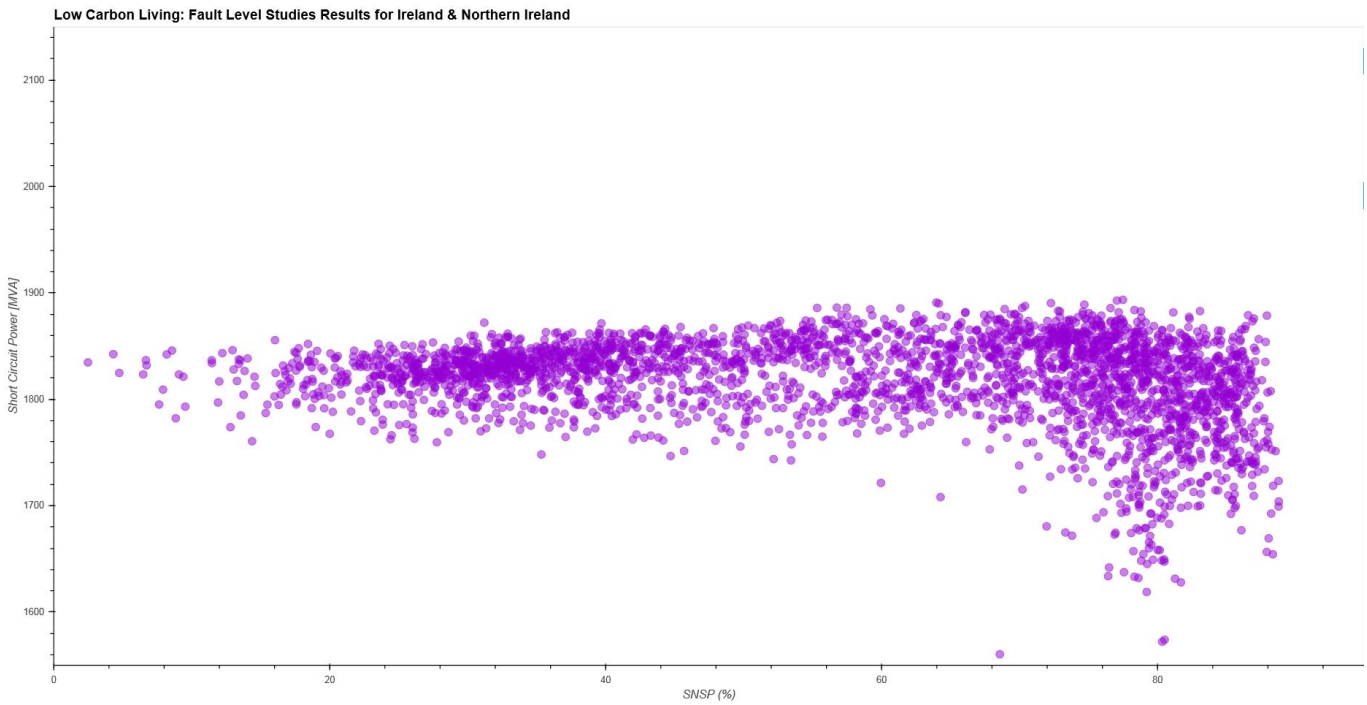

FIGURE 3-38: SHORT CIRCUIT POWER FOR LOW CARBON LIVING BINBANE 110 KV BUS AGAINST SNSP

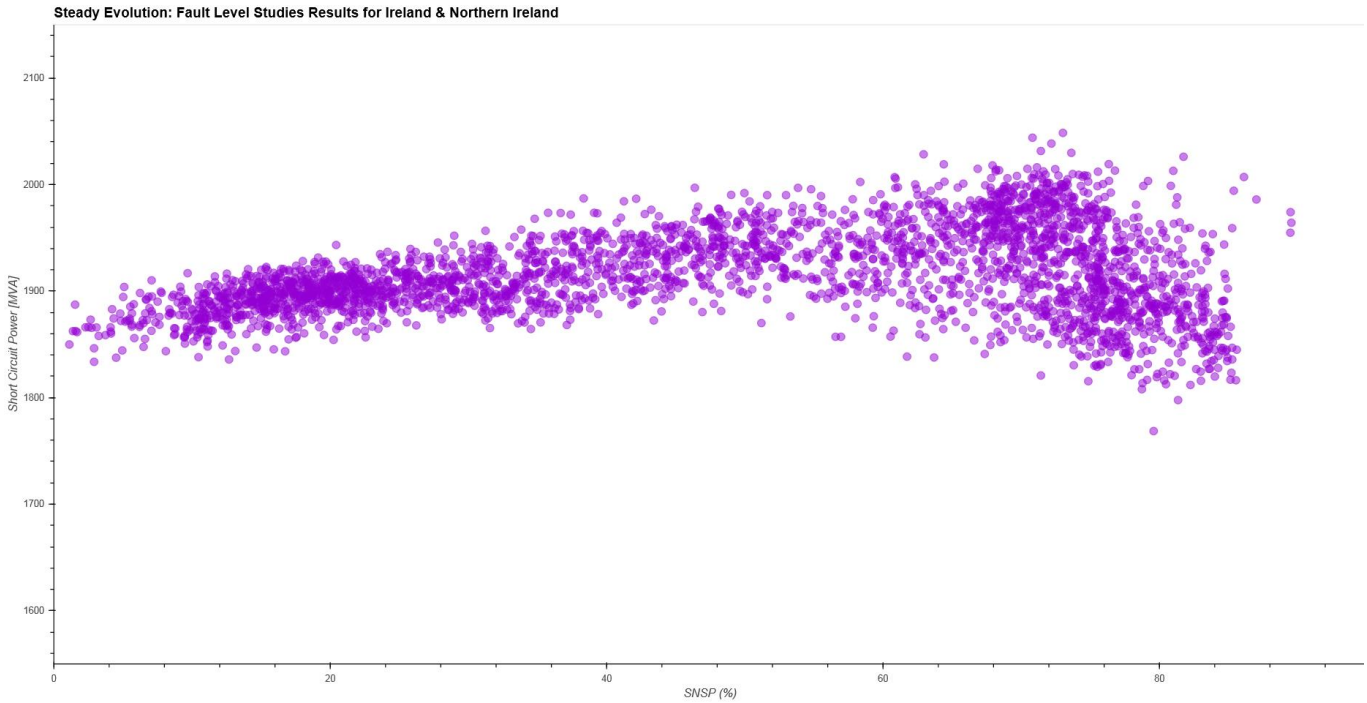

FIGURE 3-39: SHORT CIRCUIT POWER FOR STEADY EVOLUTION GLENREE 110 KV BUS AGAINST SNSP

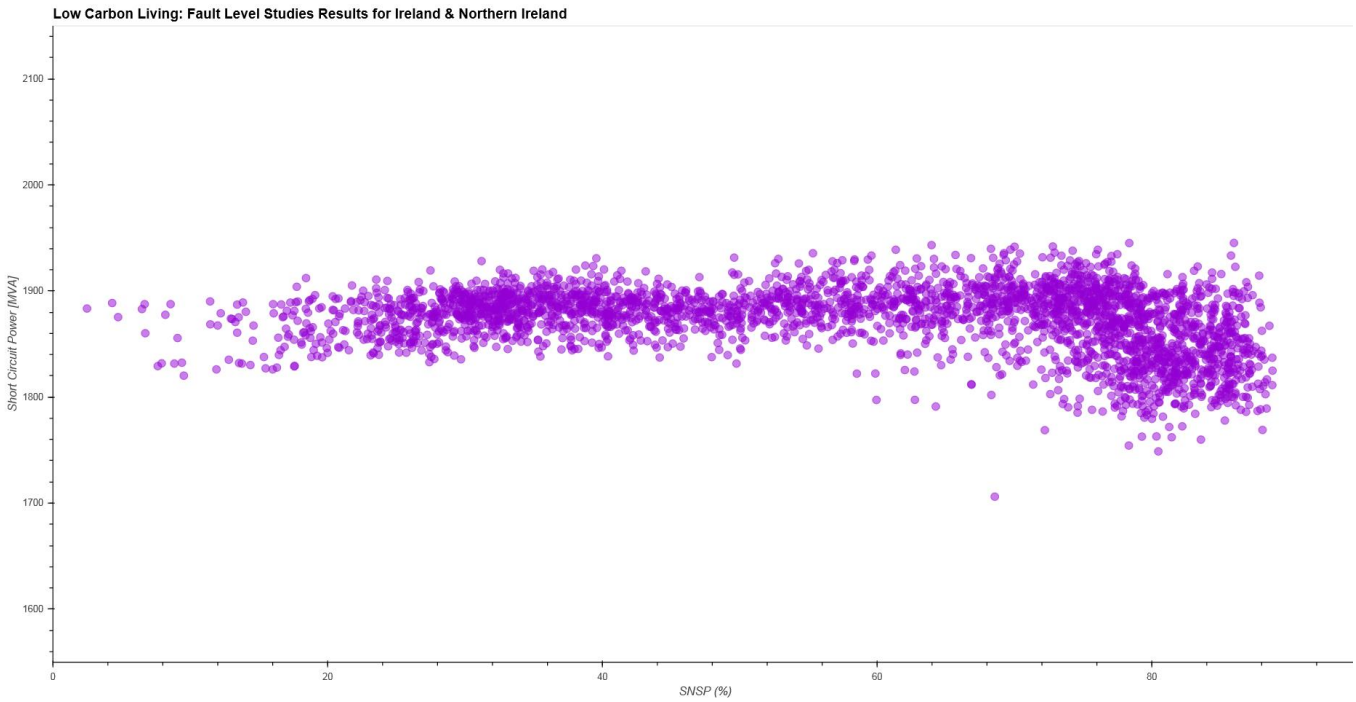

FIGURE 3-40: SHORT CIRCUIT POWER FOR LOW CARBON LIVING GLENREE 110 KV BUS AGAINST SNSP

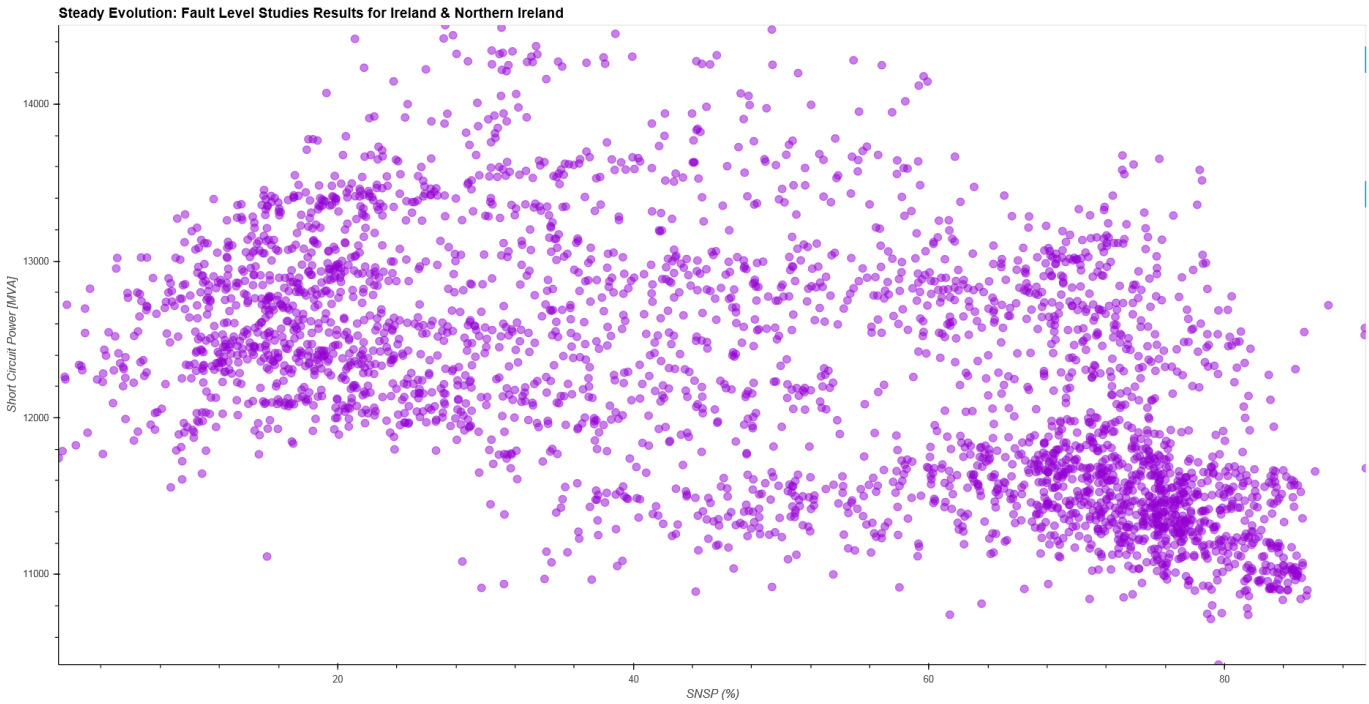

FIGURE 3-41: SHORT CIRCUIT POWER FOR STEADY EVOLUTION CLONEE 220 KV BUS AGAINST SNSP

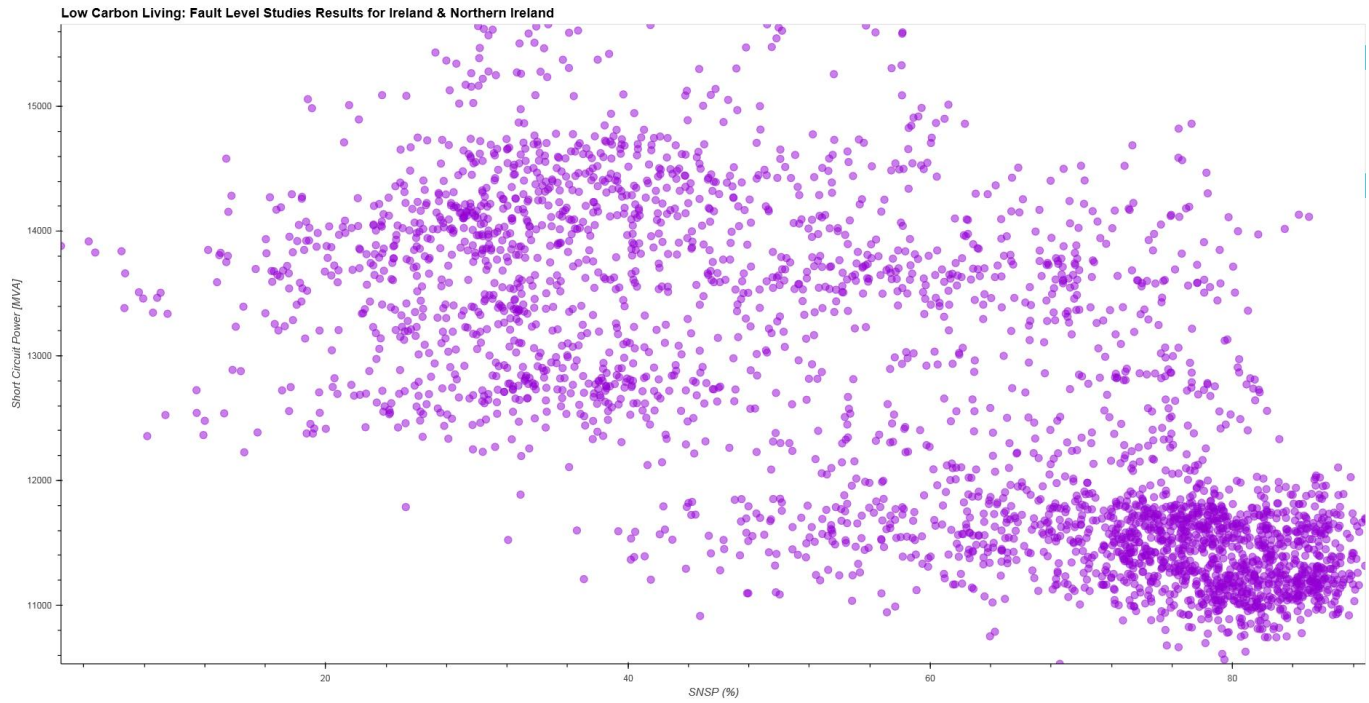

FIGURE 3-42: SHORT CIRCUIT POWER FOR LOW CARBON LIVING CLONEE 220 KV BUS AGAINST SNSP

- As SNSP reaches high levels (>70%) short circuit power at the study buses decreases. This is due to the limited fault current contribution of converter based generation coupled with lack of conventional generation on line to contribute to fault current while also reducing the overall voltage regulation capability of the system.
- Due to the higher levels of RES in Low Carbon Living it was observed that at high SNSP Low Carbon Living had the greater reduction in short circuit power when compared to Steady Evolution.
- Although fault current contribution of converter based generation is limited, in areas with significant levels of distributed RES the cumulative impact can raise the short circuit power in these regions at SNSP levels less than 70%.

3.3 DYNAMIC VOLTAGE CONTROL FOR THE IRELAND AND NOTHERN IRELAND POWER SYSTEM

Dynamic voltage control manages the reactive power imbalance during and after a large disturbance (e.g. for a transmission line fault). The primary sources of this control are, in approximate order of response time: the inherent response from the airgap of synchronous machines, the voltage sensitivity of demand, the control systems of power electronic interfaced generation and the automatic voltage regulators of synchronous machines. The inherent response of synchronous machines is one the fastest and most significant sources of dynamic voltage control and the loss of this response leads to concerns over the emergence of a scarcity in dynamic voltage control either due to the overall volume of response or the geographical distribution of this resource, due to the relatively localised impact of reactive power. As such, this scarcity could manifest in two main forms:

1) a **global scarcity** that results in voltage stability issues for almost all contingencies regardless of location, or
2) a **localised scarcity** that only results in voltage stability issues for contingencies in a specific location or region of the system.

3.3.1 CONTINGENCIES STUDIED

The availability of dynamic voltage control is studied for the snapshot hours described in the Methodology for 306 bolted three phase line fault contingencies. These line faults are in the middle of the line and are cleared by simultaneously opening the breakers at each end of the line, with a clearance time of between 4 and 8 cycles. The contingency locations are defined using the same methodology applied for the existing online dynamic security assessment that is performed every 15 minutes by EirGrid and SONI using the Wind Strength Assessment Tool (WSAT). This means that the line faults considered can result in the separation of HVDC interconnectors from the system (when the line that serves as the HVDC interconnectors AC collector network is lost) but not the separation of synchronous generators.

Note, in the results presented for Low Carbon Living, there are 306 contingencies but for Steady Evolution there are only 305. This is because contingency 1 is for the AC collector network of the Greenlink HVDC project, which is not in place for Steady Evolution. However, the numbering of the contingencies remains the same between these cases for consistency; so, contingency 1 has no results for steady evolution.

3.3.2 DYNAMIC VOLTAGE PROFILE INDEX

The metric used here to assess the availability of dynamic voltage control is the dynamic voltage profile index. This index quantifies the number of buses and the maximum duration of time for which the dynamic voltage profile breaches the permissible voltage range. This index is parameterised as a straight line at 0.5 p.u. for these studies. The parameterisation of this index was selected to focus upon assessing the availability of dynamic voltage control during the fault, as this period is the most essential in determining the dynamic stability of the system. Note, the challenges and scarcities faced when ensuring the post-fault clearance voltage stability of the system should not be discounted but are better captured by the steady state work presented in the previous sections.

The primary measure used is the number of unique violations of the threshold. This simply counts the number of buses for which the voltage went below the threshold and this allows an approximation of how far the fault propagates across the system. The maximum duration for which the violation occurred is not assessed here as it was practically always simply the duration of the fault and thus analysis of this generated little value. However, the duration of the violations were assessed in order to identify buses for which the voltage returned to above 0.5 p.u. prior to the fault clearance time (termed here as early recovery). Furthermore, the minimum observed voltage was primarily a function of the line impedance, with faults on lower impedance (i.e. shorter) lines resulting in lower minimum voltages at the terminal buses of the line.

An illustrative example of the application of this metric is provided in Figure 3-43. This example presents three unique violations (Bus 1, 2 and 3), two of which exhibited early recovery (Bus 2 and 3). Note, the second violation by Bus 3 is not counted as a unique violation and is classed as a repeated violation.

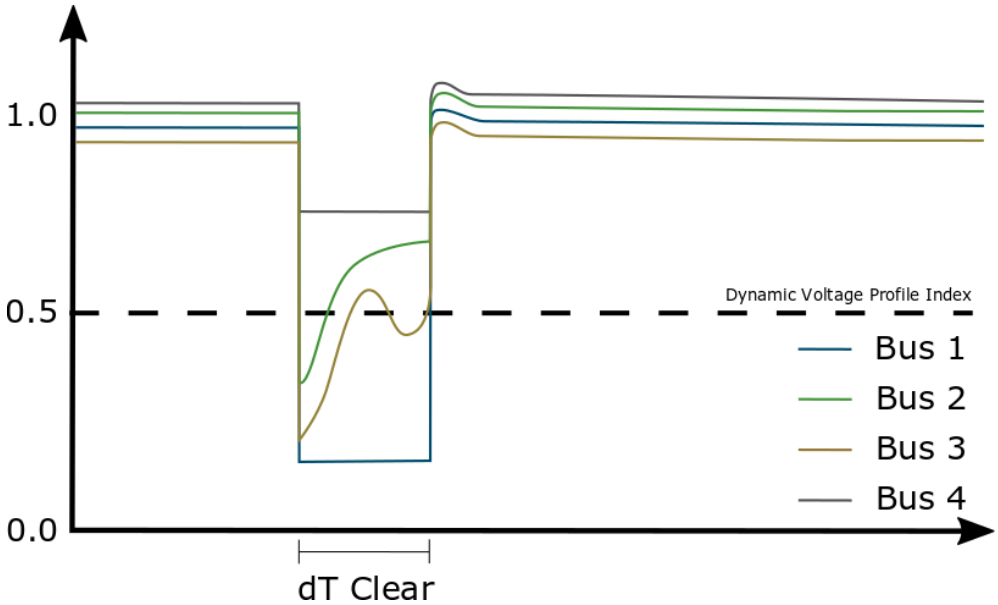

FIGURE 3-43: ILLUSTRATIVE EXAMPLE OF THE DYNAMIC VOLTAGE PROFILE INDEX

It should be noted that the count of unique violations can be skewed by the 'density' of network around the fault, i.e. the number of buses in close proximity to the fault. As such it is not a perfect measure of the propagation of the fault and small differences (e.g. on the order of 25 buses) should not be over analysed but large differences (e.g. on the order of several hundred buses) are meaningful results.

3.3.3 LOW CARBON LIVING SCENARIO

3.3.3.1 ANALYSIS BY SNAPSHOT TYPE

Figure 3-44 presents the results of applying the dynamic voltage profile index to the 36 snapshots selected for the low carbon living scenario. Box plots are used to present the distribution of the unique violation count for each hour (each box plot represents 306 data points, one for each contingency) and the dots on the upper leg each box plot marks the 95th percentile.

From the unique violations reported it can be seen that the fault propagation is significantly worse for the Type 2 cases. This is indicative that these cases exhibit a global scarcity of dynamic voltage control, as the vast majority of faults will cause a wide spread voltage drop. Hour 3013 is the best performing Type 2 hour but the median for this hour is still on the same order as the maximum for Type 1.

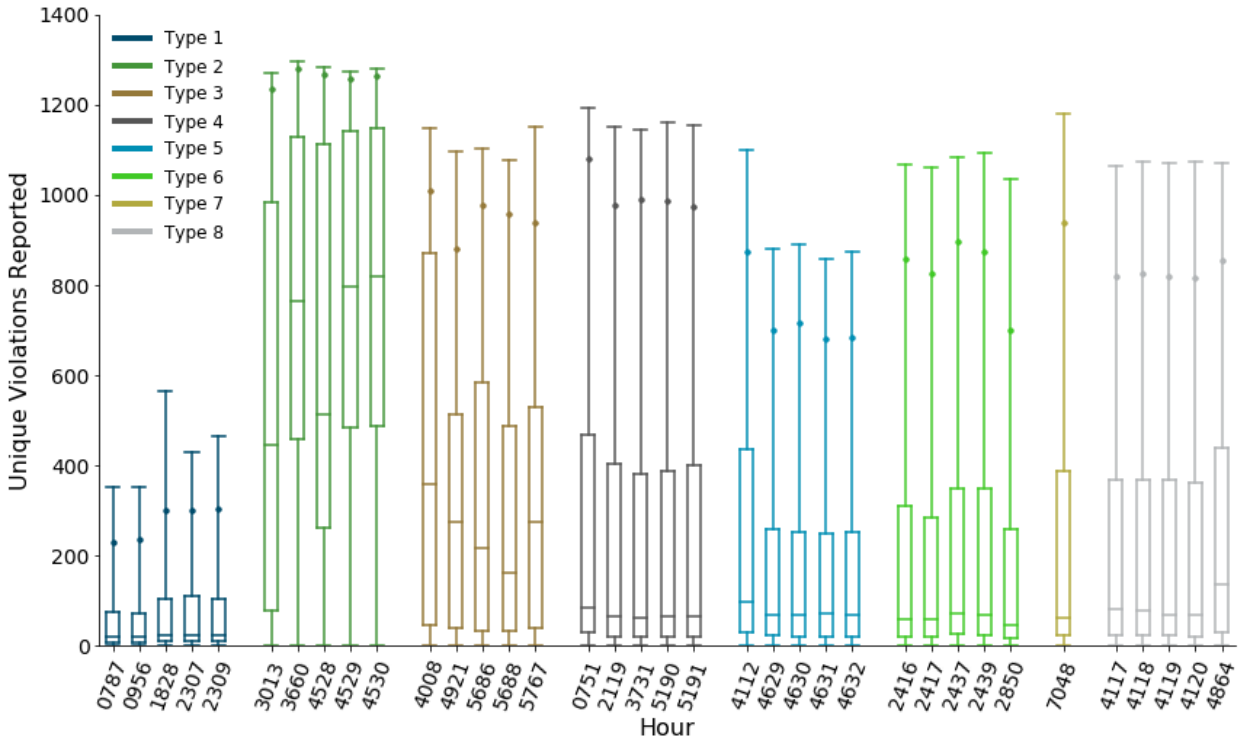

FIGURE 3-44: DISTRIBUTION OF UNIQUE VIOLATIONS REPORTED FOR EACH CONTINGENCY GROUPED BY SNAPSHOT FOR THE LOW CARBON LIVING SCENARIO

A second key feature of the distribution of unique violations is that, with the exception of Type 1, all hours have very large maximum values. This indicates that all of these hours of operation exhibit a localised scarcity of dynamic voltage control, as certain faults will cause wide spread voltage drops for these hours. Furthermore, the relative magnitude of the maximum and the 95th percentile indicates that the maximum values are outliers for all of the types except Type 2 where this localised scarcity is far more common.

It should be noted that the degree of fault propagation observed for this scarcity is sufficiently large that, without mitigation, it would require the impact of certain converter specific phenomena to be studied in significantly more detail in the future. Examples of this would include voltage dip induced frequency deviations and PLL failures, as these results indicate that certain contingencies in the future system may cause severe voltage drops over large parts of the system.

3.3.3.2 ANALYSIS BY CONTINGENCY

Figure 3-44 presents the results of applying the dynamic voltage profile index to the 36 snapshots selected for the low carbon living scenario. Box plots are used to present the distribution of the unique violation count for each contingency (each box plot represents 36 data points, one for each hour studied). Furthermore, Figure 3-46 presents the same data points colour coded base on the Type they belong to.

From these plots a high degree of volatility in the unique violations reported for each contingency can, in general, be observed. Thus, it can be concluded that, in general, the propagation of a fault is mostly dictated by the hour studied, i.e. the localised scarcity of dynamic voltage control varies between hours. This is further reinforced by the fact that for many of the contingencies in Figure 3-46 the violation count is effectively grouped by type (see contingencies 13 to 29 for an example of this).

However, despite this general trend, it can also be seen that certain contingencies have universally low violation counts (coloured blue) and others have universally high counts (coloured orange). These groups are separated by having a maximum count of less than 150 and a minimum count of greater than 150. This is a relatively arbitrary line of separation but it serves to demonstrate that for some contingencies a localised scarcity of dynamic voltage control is a systematic issue that occurs for all hours for some areas of the system while other areas will never observe such a localised scarcity.

Furthermore, from Figure 2-44 it can be observed that certain contingencies have large separation between their maximum and 75th percentile, which is a general indication of outliers – see for example contingencies 104 to 110. Then, from Figure 2-45 it can be seen that these outliers are driven entirely by Type 2 and Type 3 cases. This indicates a very specific localised scarcity that is linked to these specific hours of operation and, in general, this contingency does not demonstrate a localised scarcity.

Thus, the localised scarcities seen here can be separated into systematic localised scarcities, which occur for effectively all hours, and specific localised scarcities, which occur for a small subset of hours. These classifications deal with the when the scarcity occurs and not the severity of the scarcity, although the specific localised scarcities do seem more severe in general. As such, it would be recommended that the systematic localised scarcities be primarily used to target investment based mitigation, as the mitigation measure would be expected to see frequent use, and that the specific localised scarcities be primarily used to develop operational policy based mitigation, as it may be possible to avoid the specific conditions that give rise to the scarcity.

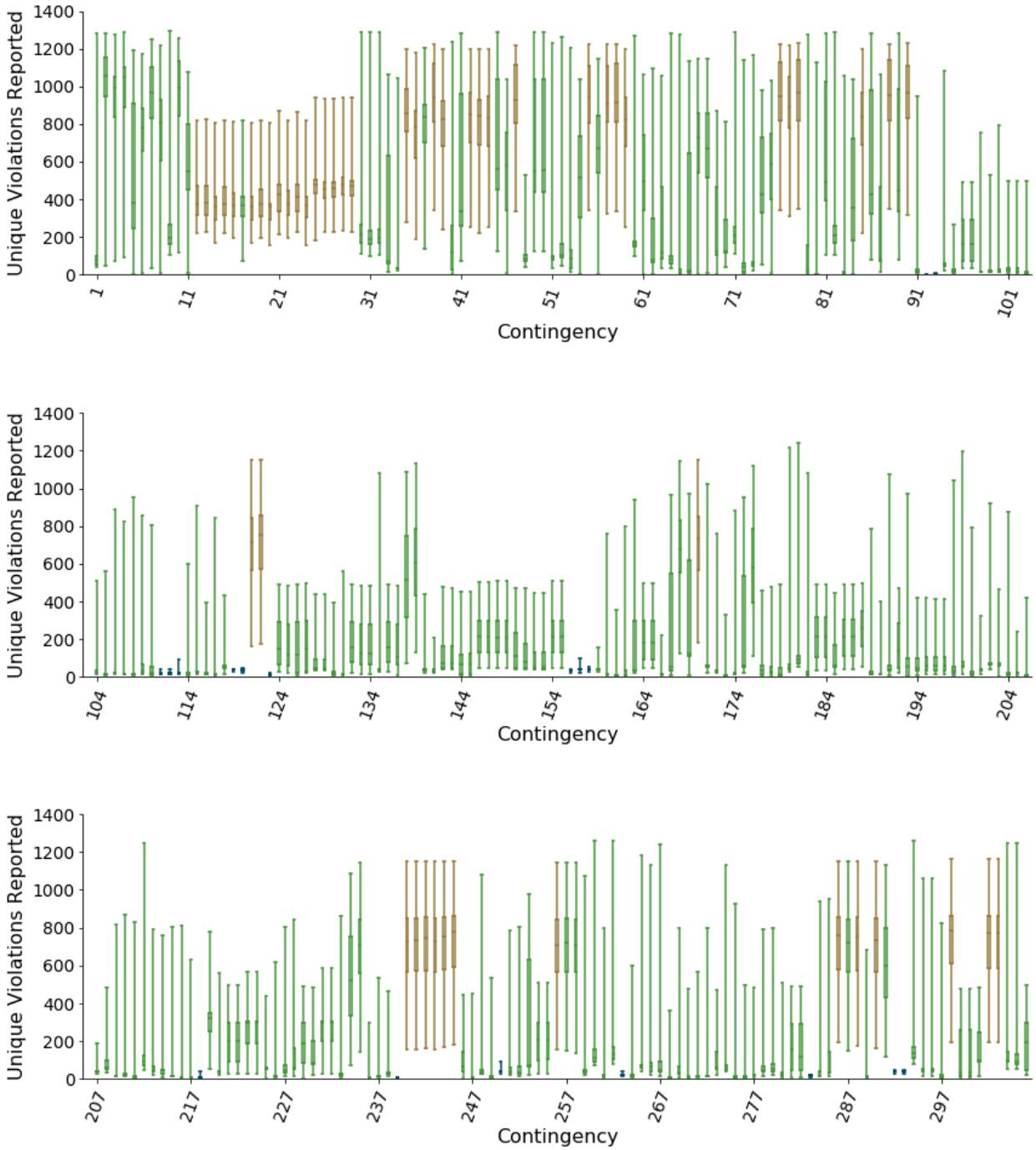

FIGURE 3-45: DISTRIBUTION OF UNIQUE VIOLATIONS REPORTED FOR EACH SNAPSHOT GROUPED BY CONTINGENCY RED BARS DENOTE THOSE CONTINGENCIES WITH ALL VALUES ABOVE 150 AND BLUE BARS THOSE WITH ALL VALUES BELOW 150 FOR THE LOW CARBON LIVING SCENARIO

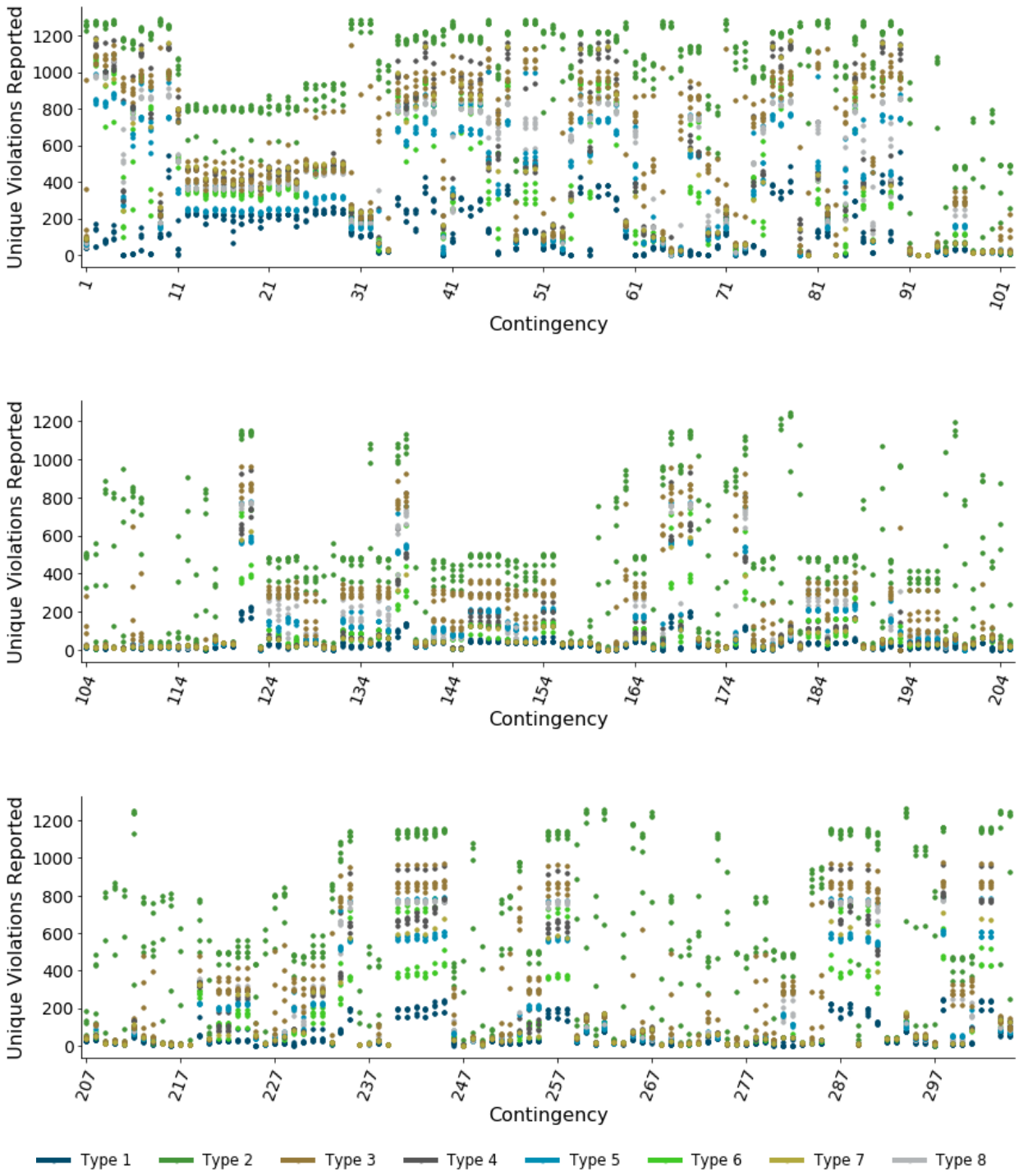

FIGURE 3-46: SCATTER PLOT OF UNIQUE VIOLATIONS REPORTED FOR EACH CONTINGENCY, POINTS ARE COLOURED ACCORDING TO THE TYPE OF SNAPSHOT THEY REPRESENT FOR THE LOW CARBON LIVING SCENARIO

3.3.3.3 EARLY RECOVERY

Figure 3-47 presents the results of applying the dynamic voltage profile index to the 36 snapshots selected for the low carbon living scenario. Box plots are used to present the distribution of the percentage of buses that violated the 0.5 p.u. threshold but recovered to above this value before the fault cleared for each of the 306 contingencies for each hour.

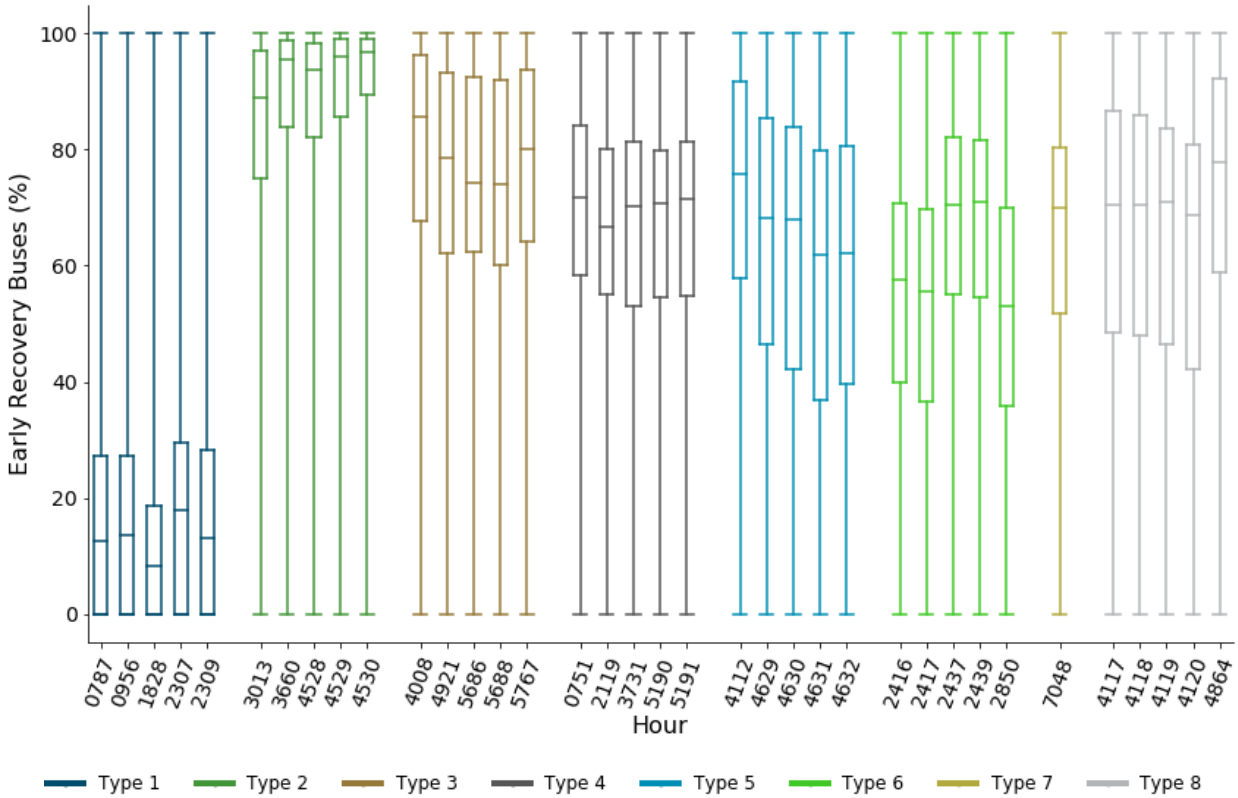

FIGURE 3-47: DISTRIBUTION OF BUSES THAT EXHIBITED EARLY RECOVERY FOR EACH CONTINGENCY GROUPED BY SNAPSHOT FOR THE LOW CARBON LIVING SCENARIO

This measure of early recovery is imperfect, e.g. it heavily influenced by the depth of the voltage drop (i.e. a fault that causes many buses to drop to just below 0.5 will likely have a high percentage of early recoveries regardless of the volume of additional reactive power rejection during the fault) and there is an intrinsic link between system strength (in terms of Q/V sensitivity) and the impact of reactive power injection on the voltage. It should also be noted that early recovery is not intrinsically good or bad but it is valuable in understanding how the voltage during the fault-on period varies in a general sense.

From Figure 3-47 it can clearly be seen that Type 2 exhibits the most significant proportion of early recovery and Type 1 the least significant proportion, with the other types showing levels of recovery more similar to Type 2. This indicates that the deep wide ranging voltage drop that is commonly observed for Type 2 and from the unique violations is a temporary phenomenon.

It should be noted that the measure of early recovery is imperfect, e.g. it heavily influenced by the depth of the voltage drop (i.e. a fault that causes many buses to drop to just below 0.5 will likely have a high percentage of early recoveries regardless of the volume of additional reactive power rejection during the fault) and there is an intrinsic link between system strength (in terms of Q/V sensitivity) and the impact of reactive power injection on the voltage. However, the trend it depicts is valid and is further reinforced by a set of time domain examples in Figure 3-48.

Figure 3-48 shows the bus voltages for three contingencies (283, 278 and 168) for two of the studied hours (1828 a Type 1and 4528, a Type 2). The contingencies were selected to demonstrate cases that had different levels of unique counts and delayed recovery and for both hours plotted contingency 283 was the least sever and 168 was the most severe.

The first noticeable feature of these plots is the oscillatory nature of the post-fault voltage for the Type 2 examples. This oscillation in the voltage is common for Type 2 and can be observed to varying degrees of severity for any non-Type 1 case. In the worst case presented in Figure 3-48 (hour 4528 under contingency 168) the first post-fault swing of the voltage causes a second violation of the 0.5 p.u. threshold, this is rejected by the unique violation assessment but such severe behaviour does call into question the validity of this case for the critical clearing time and angle margin analysis – as the modelling used in this study does not incorporate mechanisms that may cause instability in certain devices connected to the system under such conditions.

Comparing the response to each contingency for each hour shows that the Type 2 cases exhibit significant voltage recovery during the fault across multiple buses, whilst Type 1 only exhibits some limited recovery. This recovery is due to the response of power electronic converter connected generation to the fault and explains the high early recovery proportions observed for the Type 2 and other cases. In effect, the weakness of the system which allows the fault to propagate so far also allows the reactive power injection from the power electronic converter connected generation to cause a significant change in the voltage. Note, a similar injection occurs for the Type 1 cases but it simply has less impact, and this can be observed somewhat for contingency 168 and 278.
It can be seen that the increase propagation of the fault seen for Type 2 cases is actually corrected for, at most buses, within approximately 50 ms by this reactive power injection. Note, this injection does not allow all buses to recover to the voltage levels seen during the fault for Type 1 and at fault clearance it can be seen that more buses remain at low voltages for the Type 2 case presented.

Despite the recovery during the fault-on period, prior to this recovery the Type 2 cases exposes significant parts of the system to large voltage drops. For example for contingency 278 it can be observed that majority of the system for Type 1 experiences a voltage between 0.8 and 1.0 p.u. during this initial period while for Type 2 it is between 0.3 and 0.8 p.u. Another interesting feature of the response for Type 2 under contingency 278 is the fact that the impact of the reactive power injection is noticeably less uniform and a small group of buses appear to register far less impact from this injection. This could indicate a localised scarcity of this reactive injection from converter connected generation under this contingency.

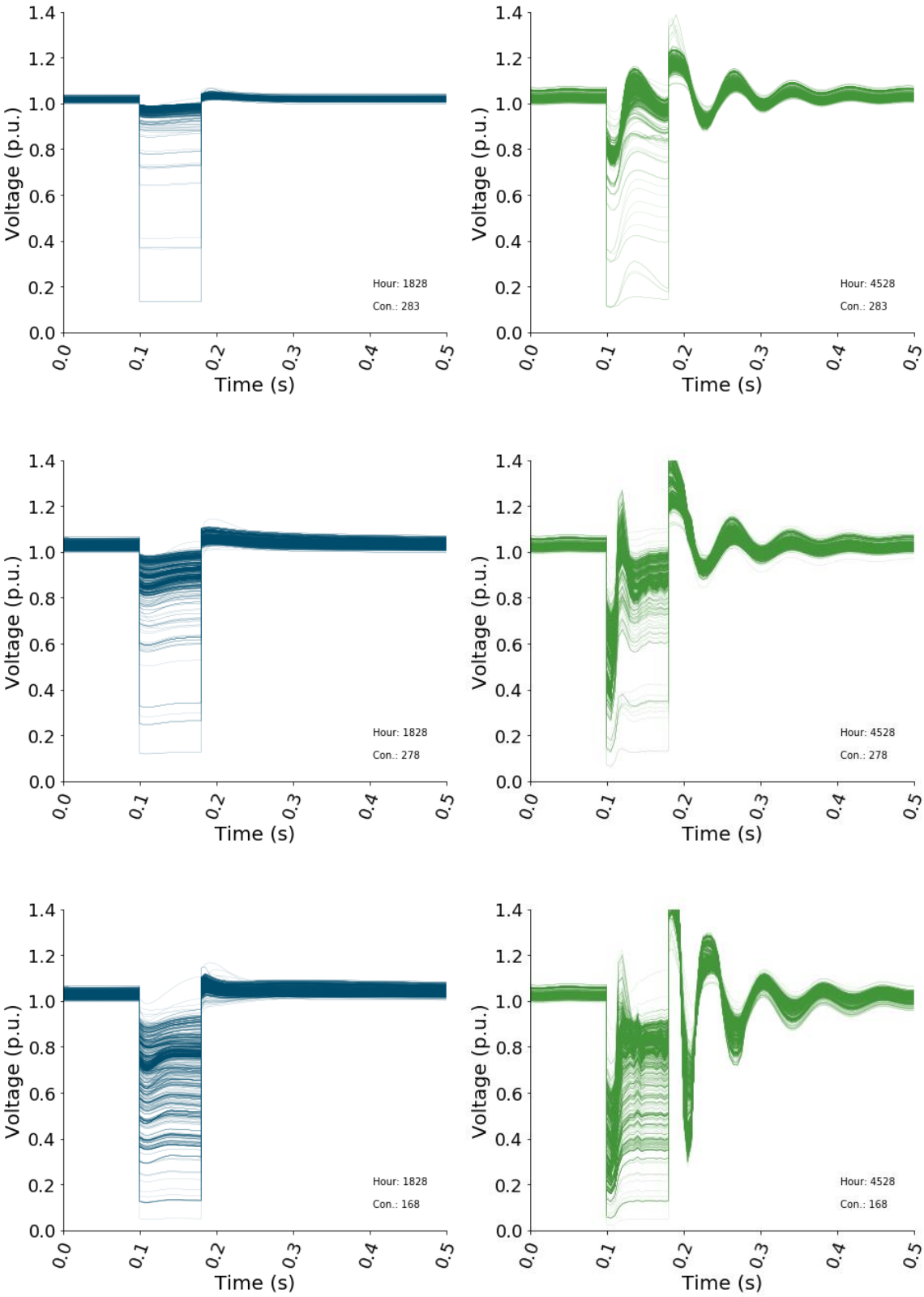

FIGURE 3-48: COMPARISON OF VOLTAGE FOR HOURS 1828 (BLUE) AND 4528 (GREEN) FOR CONTINGENCIES 283, 278 AND 163 FOR THE LOW CARBON LIVING SCENARIO

3.3.4 STEADY EVOLUTION SCENARIO

3.3.4.1 ANALYSIS BY SNAPSHOT TYPE

Figure 3-49 presents the results of applying the dynamic voltage profile index to the 40 snapshots selected for the steady evolution scenario. Box plots are used to present the distribution of the unique violation count for each hour (each box plot represents 305 data points, one for each contingency) and the dots on the upper leg each box plot marks the 95th percentile.

These results demonstrate very similar trends to those observed for low carbon living, with a few key exceptions. The first of these is that three of the Type 1 cases present outliers similar to those observed for the other types in both steady evolution and low carbon living. This indicates that these Type 1 cases also exposed to the specific local scarcities, which was not the case in Low Carbon Living. Another difference is that the medians for the Type 2 cases are significantly lower, indicating a less severe global scarcity occurs in the SE scenario. Finally, the median and upper quartile of the Types 4, 5, 6, 7 and 8 are all significantly lower in steady evolution than they were for low carbon living.

Therefore, the steady evolution scenario has a less severe global scarcity but it is still present and this scenario also still experiences the localised scarcity observed in low carbon living.

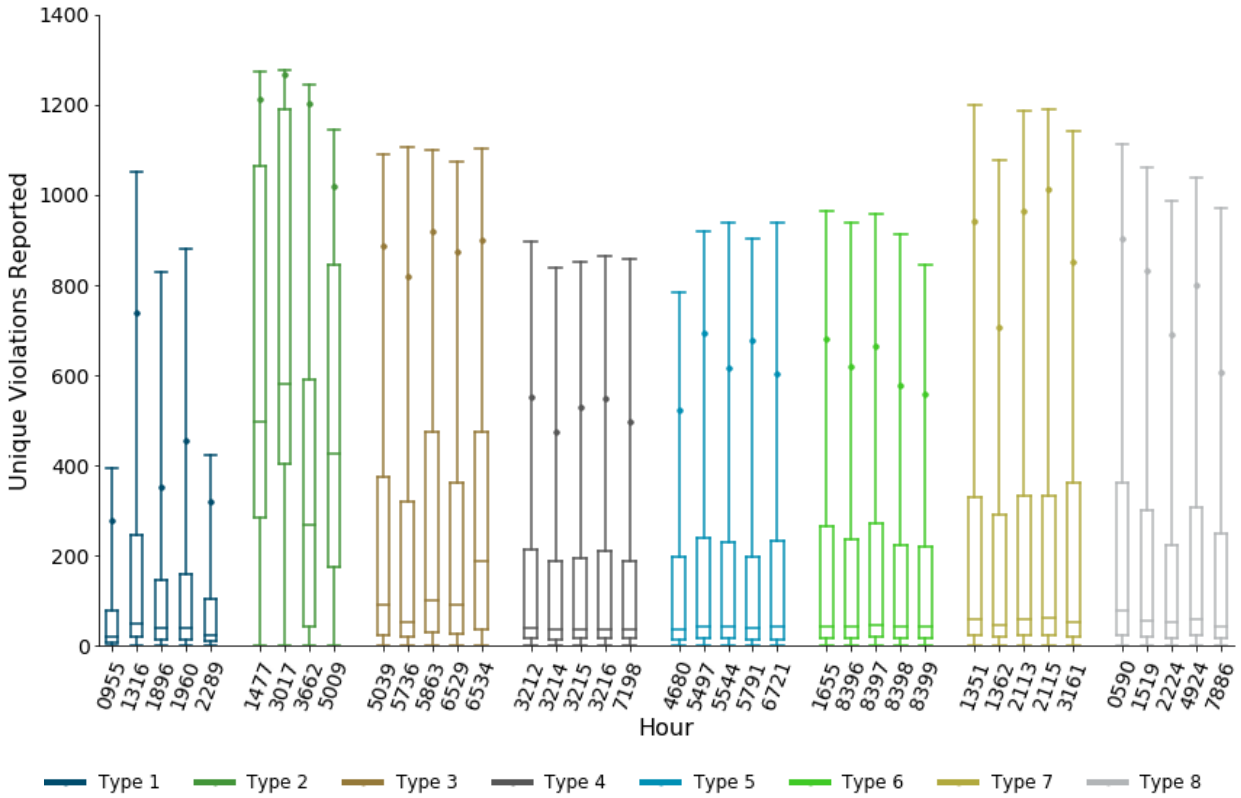

FIGURE 3-49: DISTRIBUTION OF UNIQUE VIOLATIONS REPORTED FOR EACH CONTINGENCY GROUPED BY SNAPSHOT FOR THE STEADY EVOLUTION SCENARIO

3.3.4.2 ANALYSIS BY CONTINGENCY

Figure 2-49 presents the results of applying the dynamic voltage profile index to the 40 snapshots selected for the steady evolution scenario. Box plots are used to present the distribution of the unique violation count for each contingency (each box plot represents 36 data points, one for each hour studied).

Figure 3-51 presents the same data points colour coded base on the Type they belong to.

These results are very similar to those for low carbon living. The most notable difference observed is that maximum value for each contingency tends to be lower in steady evolution than in low carbon living, which concurs with the type level analysis in indicating a less severe global scarcity that was linked to the Type 2 hours. However, many contingencies still have significant outliers which indicates that this scenario is still exposed to the specific local scarcity observed for low carbon living.

It should also be noted that the orange cases which mark a systematic local scarcity correspond closely to those observed for low carbon living, indicating that this form of local scarcity will emerge regardless of the future scenario considered.

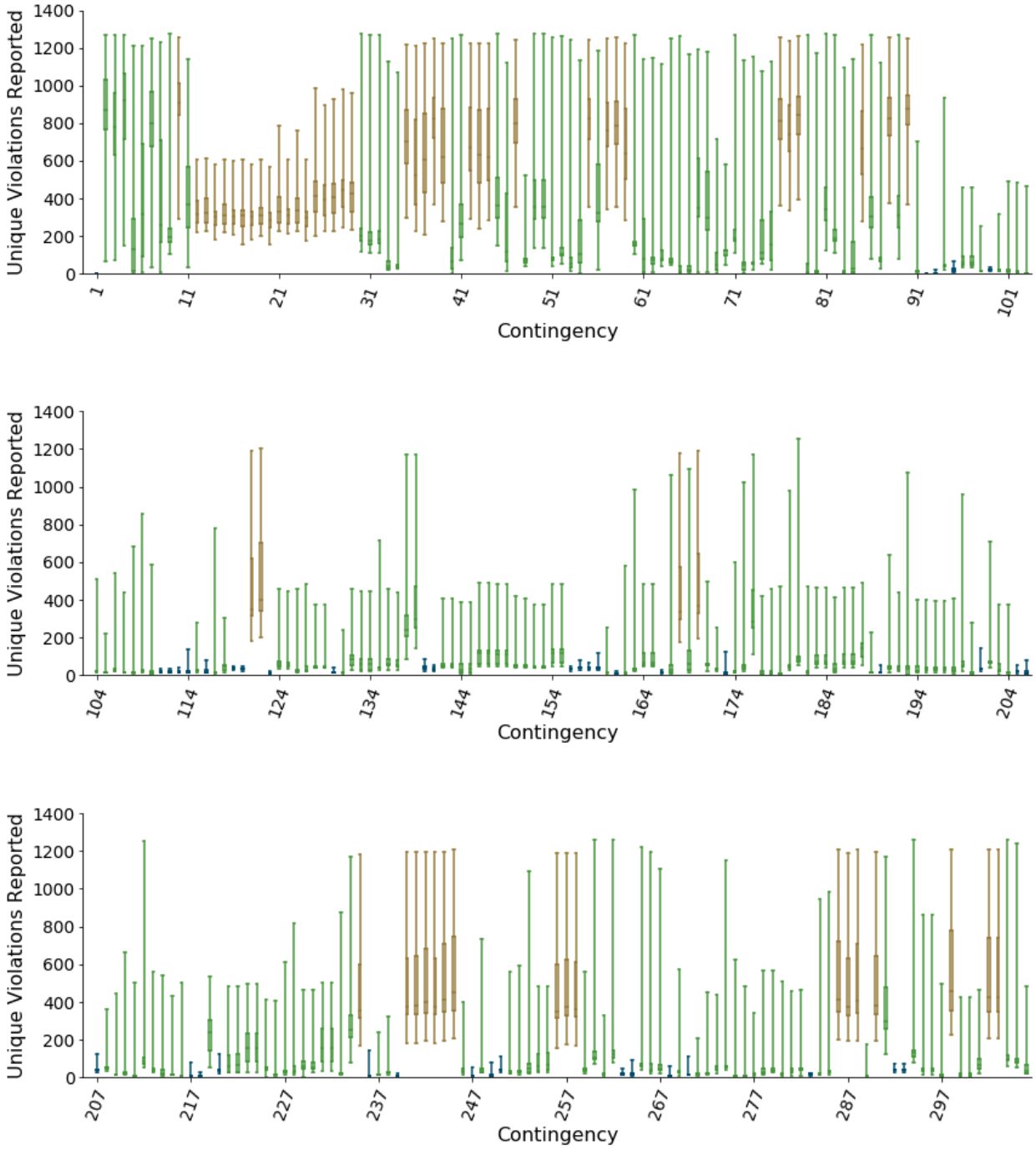

FIGURE 3-50: DISTRIBUTION OF UNIQUE VIOLATIONS REPORTED FOR EACH SNAPSHOT GROUPED BY CONTINGENCY RED BARS DENOTE THOSE CONTINGENCIES WITH ALL VALUES ABOVE 150 AND BLUE BARS THOSE WITH ALL VALUES BELOW 150 FOR THE STEADY EVOLUTION SCENARIO

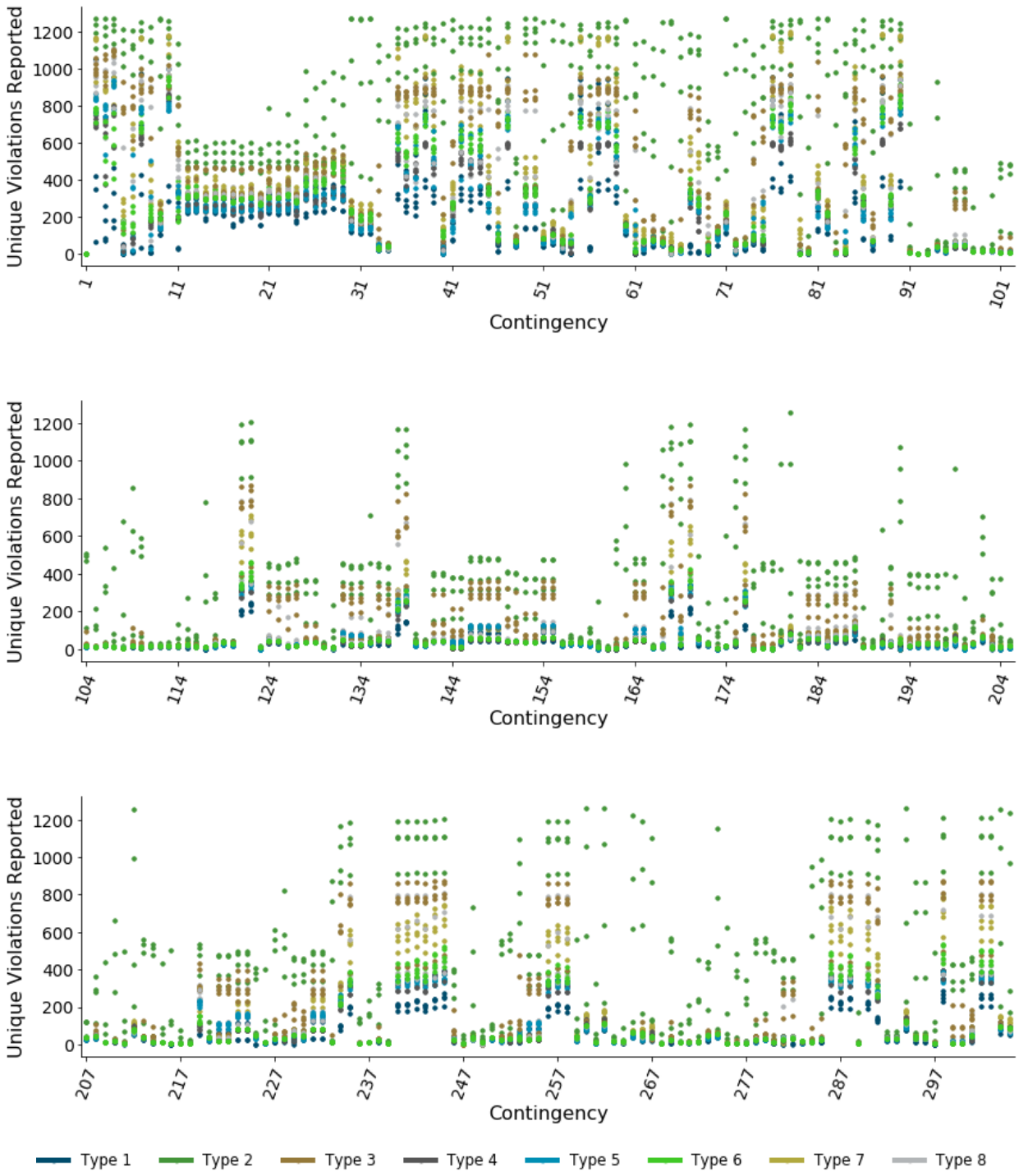

FIGURE 3-51: SCATTER PLOT OF UNIQUE VIOLATIONS REPORTED FOR EACH CONTINGENCY, POINTS ARE COLORED ACCORDING TO THE TYPE OF SNAPSHOT THEY REPRESENT FOR THE STEADY EVOLUTION SCENARIO

3.3.4.3 EARLY RECOVERY

Figure 3-51Figure 3-51 presents the results of applying the dynamic voltage profile index to the 40 snapshots selected for the steady evolution scenario. Box plots are used to present the distribution of the percentage of buses that violated the 0.5 p.u. threshold but recovered to above this value before the fault cleared for each of the 306 contingencies for each hour.

Comparison to the steady evolution results indicates that, with the exception of the Type 1 cases, this scenario has less volatile fault- on voltage behaviour, as indicated by the reduced median recovery rates. In contrast, the Type 1 cases exhibit the opposite behaviour and have a greater tendency toward rising voltages during the fault-on period – indicating that the voltage varies more in response to the reactive power injection from converter connected generation. This concurs with the unique violation count in indicating that the strongest hours in the steady evolution scenario are weaker than their equivalents in low carbon living. This would indicate that, whilst the dynamic voltage control scarcity is less severe in steady evolution, this scarcity will emerge more frequently in steady evolution.

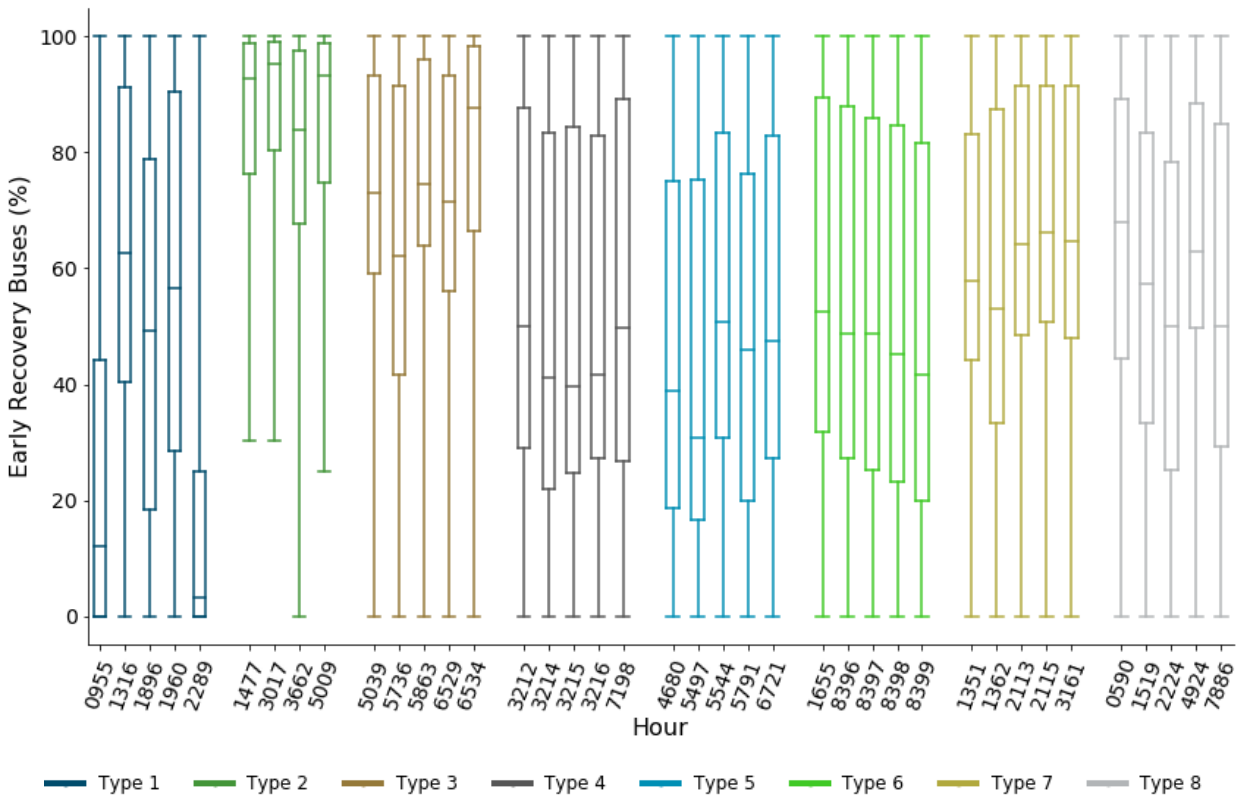

FIGURE 3-52: DISTRIBUTION OF BUSES THAT EXHIBITED EARLY RECOVERY FOR EACH CONTINGENCY GROUPED BY SNAPSHOT FOR THE STEADY EVOLUTION SCENARIO

3.3.5 MANIFESTATION OF SCARCITY

The scarcity of dynamic voltage control observed here is characterised by the voltage drop immediately after a fault being deeper and propagating further when compared to that expected under existing operation. This drop can then be seen to recover during the fault toward the voltage expected under existing operation, primarily due to the injection from power electronic interfaced generation. As such, this scarcity is driven by the reduction in instantaneous dynamic voltage control, which is mostly provided by synchronous generation at this time. Indeed the dynamic voltage control from inverter connected generation is seen to be sufficient to eventually return the fault induced voltage drop to levels similar to those seen for operational cases similar to today, but it is too slow to respond.

It should be noted that the degree of fault propagation observed for this scarcity is sufficiently large that, without mitigation, it would require the impact of certain converter specific phenomena to be studied in significantly more detail in the future. Examples of this would include voltage dip induced frequency deviations and PLL failures, as these results indicate that certain contingencies in the future system may cause severe voltage drops over large parts of the system.

3.3.6 FUTURE ANALYSIS

Having established the presence of a scarcity, the next consideration is the root cause of this scarcity. The successful separation of the good behaviour for Type 1 and the poor behaviour for Type 2 demonstrates that the methodology applied to group the hours can successfully identify the best and worst hour. However it fails to predict the single hours in Types 2, 3 and 5 that have somewhat different behaviour to the other hours in those types and Types 4, 5, 6, 7 and 8 have very similar behaviour. This would indicate that the measures used to separate the hours into types indirectly assesses the root cause in a crude way but does not directly assess the root cause.

The clear separation between Type 1 and Type 2 would indicate that SNSP or inertia could be important determining factors. However, it can be noted that the median reported for Types 4, 5, 6, 7 and 8 are rather similar, but notably higher than for Type 1, whilst Type 3 begins to exhibit similar, but far less severe, behaviour as Type 2. This is an interesting outcome as the range of SNSP for these hours is 27 % to 81 %, which would indicate that SNSP is a particularly poor predictor of a scarcity of dynamic voltage control and the fact that the SNSP is high for all Type 2 hours and low for all Type 1 hours is likely only a symptom of the true root cause of the scarcity.

The outlier hours for Types 2, 3 and 5 (3013, 4008 and 4112 respectively) in LCL have similar inertia and SNSP as the other members of their type but very different unit numbers. However, unit number in itself is a poor predictor. This is possibly due to the localised impact of reactive power not being captured by this measure, or indeed any existing system level measure. Therefore, the best predictor for this scarcity may be derived from the

number of units online (not their total inertia or dispatch) and the geographical spread of these units – with a focus on identifying areas that are remote from any synchronous units.

Low carbon living and steady evolution results both indicate the emergence of a global scarcity of dynamic voltage control in some hours of operation and localised scarcities in the majority of hours. Indeed some of these localised scarcities occur for all hours studied and are classified here as a systematic localised scarcity to separate them from the specific localised scarcities, which occur for only a small subset of hours. It would be recommended that the systematic localised scarcities be primarily used to target investment based mitigation, as the mitigation measure would be expected to see frequent use, and that the specific localised scarcities and global scarcities be primarily used to develop operational policy based mitigation, as it may be possible to avoid the conditions that give rise to the scarcity.

Comparison of the steady evolution and low carbon living scenarios indicates that both scenarios are exposed to the global scarcity and the two forms of localised scarcity. Whilst both the global and local scarcities are less severe in steady evolution, the degree of propagation observed in steady evolution will still prove high problematic if it is not mitigated. It is interesting to note that the systematic local scarcity occurs for the same contingencies in both scenarios – indicating that any actions taken to mitigate these systematic local scarcities would be of benefit regardless of scenario. Finally, a key outcome of this comparison of scenarios is that in steady evolution some of the Type 1 cases exhibit similar behaviour to the other types (wide ranging propagation and voltage oscillations), which is not the case in Low Carbon Living. This means that, whilst the dynamic voltage control scarcity is less severe in steady evolution, this scarcity will emerge more frequently in steady evolution.

In addition to the scarcity in dynamic voltage control during the fault, these results show that post-fault voltage oscillations are quite common in the cases studied and this in itself is indicative of a scarcity in system strength. This scarcity is also evidenced in the static analysis and is reflective of how the low system strength allows the fast injection of reactive power to causes oscillations in the system voltage. This symptom of this scarcity could most likely be best managed by directly mitigating the system strength scarcity or by tuning of the reactive power control loops, although such tuning would prove challenging given the broad and variable demands placed on such tuning in the future system.

Given these voltage oscillation, which can be extreme, and the wide ranging voltage drop and volatile behaviour observed for some of the cases here, it is important to note that certain forms of converter instability (e.g. PLL failure) that could be triggered in reality are not modelled here. This does not invalidate the results here but does mean that the stability results for CCT and angle margin may be optimistic, as converter instability during the fault has been neglected. Future work should explore the potential impact and mitigation of these forms of instability.

3.4 SUMMARY & CONCLUSIONS

Voltage control, both in terms of its steady state and dynamic aspects has been analysed across multiple snapshots & scenarios for the Continental Europe and Ireland & Northern Ireland power system. Multiple analysis methods are used to investigate potential scarcities within the two systems under consideration, as both systems evolve towards higher levels of renewable integration. A potential lack of steady state reactive power has been investigated using steady state voltage deviations, P-V & Q-V analysis while the lack of dynamic reactive injections has been investigated using steady state short circuit analysis, as well as time domain short circuit simulations.

The analysis pertaining to the Continental European system has been carried out using pre-identified system snapshots across the scenarios under consideration. The results are focussed on the Polish system, within the Continental European network. It has been observed that EHV system in Poland remains relatively un-effected by increasing RES levels across the Continental European System. However, the 110 kV Polish system exhibits a lack of steady state reactive power capacity, as demonstrated by deteriorating steady state voltage regulation. The reactive power scarcity becomes most apparent at high load and minimum inertia conditions. Generally, higher levels of RES incorporated in the Going Green scenario; result in a lack of steady state reactive power. P-V analysis across various zones of the Polish system demonstrates that within the subnetworks of the Polish system, regions with higher magnitude of installed renewable capacity, shows a trend towards diminishing stability margins. Similarly the Q-V analysis on the Polish system demonstrates that the scenarios characterised by high RES capacity exhibit a higher risk of potential nodal voltage stability.

Steady state short circuit levels for the Polish system across the considered scenarios remain within minimum operational requirements, pointing to the absence of potential issues regarding dynamic voltage regulation. This is confirmed by the time domain simulations, whereby, it is demonstrated that across all scenarios and snapshots considered; following system faults the voltage profiles encountered by both synchronous machines and power park modules encounter remain within the stipulated fault ride through requirements.

It is to be noted however that the model utilised for Continental European system is characterised by various levels of modelling detail for various component regions, with the Polish system modelled with a high level of detail. Furthermore, the cases analysed have been pre-selected using various criteria such as minimum inertia, minimum reactive margin and maximum load across various component regions, as opposed to analysing all potential system configurations. The levels of RES for a specific system operating condition differ across various sub-systems of the Continental Europe. Therefore a lack of potential scarcity can either be due to the snapshot selection approach, modelling deficiencies or insufficiently high levels of renewable generation. The maximum system wide non-synchronous penetration for the snapshots analysed in this chapter is limited to ~65%.

As opposed to the analysis carried out for the Continental European system, the analysis on Ireland & Northern Ireland power system included every single hourly system snapshot across the two considered scenarios for the static voltage analysis section. For time domain simulations, a snapshot based approach akin to Continental

European analysis was adopted. Detailed model of the Irish power system was used, with some instantaneous SNSP levels being as high as 85-90%.

It has been observed that, there is a significant correlation between increasing renewable generation levels and deterioration of frequency regulation, as evidenced by steady state voltage deviation magnitudes. While the steady state reactive power scarcity has been identified in both the simulated 2030 scenarios, the scarcity is more pronounced in low carbon living scenario which entails higher levels of renewable generation across the year. Steady state reactive power scarcity is further validated by the results of QV analysis whereby, an increased reactive requirement is identified for selected weak buses in the system, to reach target voltages. It has been observed that the weaker parts of the system and areas in the proximity of intermittent renewable generation are particularly prone to significant requirements for steady state reactive power. Dynamic reactive injection scarcity is apparent by the results of fault level analysis. A general trend towards declining fault levels across the system is observed, particularly in the weaker parts of the system. However, in some cases, the local fault levels increase due to the cumulative impact of higher magnitude of renewable generation in the vicinity of the bus under consideration. This is further evidenced by the time domain simulations, which demonstrate a lack of instantaneous dynamic reactive current injection at high renewable levels, resulting in deterioration of dynamic voltage regulation. Low carbon living scenario entailing higher levels of renewable generation, exhibits a more pronounced dynamic reactive current injection scarcity, demonstrating the link between higher levels of renewable generation and reduced dynamic voltage regulation. Furthermore, significant levels of variation in voltage following clearance of faults, indicates reduced system strength and may have implications for phase locked loop control operation and hence warrants further investigation.

The analysis described in this chapter demonstrates that steady state voltage regulation is likely to be significantly effected in the future, for both Continental Europe and Ireland & Northern Ireland power systems. Increased levels of non-synchronous renewable generation are the prime driver of this change. This evident lack of steady state reactive capacity needs to be addressed for secure system operation. While the need for enhanced dynamic voltage regulation capability is clearly demonstrated for the Ireland & Northern Ireland system, a clear indication of a lack of dynamic reactive injection capacity in the Polish system as a subset of the Continental European system is not apparent. It is however to be noted that this can potentially be a function of the difference in the instantaneous renewable generation levels across the Ireland & Norther Ireland and the Continental European system in the considered scenario, among other aforementioned factors. Therefore, an absence of dynamic reactive power scarcity for Continental European system at higher renewable energy levels cannot be concluded.

4. ROTOR ANGLE STABILITY

Rotor angle stability refers to the ability of synchronous machines directly coupled to the grid to remain in synchronism after being subjected to disturbance. This requires that each synchronous machine must maintain the existing equilibrium or reach a new equilibrium between its electromagnetic and mechanical torque whenever a disturbance in power system occurs. Failure to do so will cause a synchronous machine to experience a loss of synchronism and that synchronous generator will be disconnected from the system [4].

The change of the electromagnetic torque of a synchronous machine after a disturbance consists of two components which affect the damping of oscillations:

- Synchronising torque component (in phase with rotor angle deviation)
- Damping torque component (in phase with speed deviation)

Transient stability is concerned with the ability of a power system to maintain synchronism after a severe disturbance, e.g. a three phase line fault. As the system begins to operate with fewer synchronous units, each of the remaining units will be required to contribute more electromagnetic torque during any given fault. Furthermore, a reduction in the number of units may lead to changes in the geographical distribution of units, which could isolate certain units (or groups of units) and expose them to an increased risk of losing synchronism, particularly for faults close to such units or groups (as the torque contribution during the fault is heavily dependent upon electrical distance to the fault).

Therefore, the scarcity under study here is a scarcity of synchronising torque between the remaining synchronous units. Such a scarcity is most likely to manifest itself in one of two ways:

1) a **global scarcity** that results in several groups of generators separating from one another but remaining synchronised to one another, or
2) a **localised scarcity** that results in one generator or a small group of generators separating from the rest of the system.

Note, if a global scarcity were to emerge then this will likely result in system collapse, as the separation of these generators will inevitably lead to electrical centres forming on some of the lines that connect these groups and it is unlikely that this separation of the system will result in the formation of secure, stable or even adequate islands. For a localised scarcity, a system may survive the resulting loss of generation but it would not be classed as secure, as no generation should trip for an N-1 contingency.

4.1 CONTINENTAL EUROPE

4.1.1 METHODS, INDICES AND REQUIREMENTS

For the purposes of the rotor angle stability studies for the Continental European power system, dynamic time-domain simulations representing electromechanical phenomena have been used. Presented calculation results have been obtained using DIgSILENT PowerFactory power system analysis software including RMS package. Critical clearing times t_{cr}, described as the longest clearing times for which a power system will remain in synchronism, have been calculated using a binary search method for a set of assumed network events (disturbances) as well as following protection and control systems response [3]. Fault clearance range for t_{cr} calculations has been specified as $< 0;\ 2\ \mathrm{s} >$. Binary search method will stop if search range is less than a threshold value, which has been determined as 1 ms. Disturbances at the normal fault clearing time will be investigated. These disturbances include:

- close and far 3-phase short-circuit in a single line (labeled as C|K3|1C and F|K3|1C respectively),
- close 3-phase short-circuit in a double-circuit line (C|K3|2C in short) ,
- 3-phase short-circuit in a nearest busbar system (C|K3|B in short).

Schemes for the disturbance events have been presented in Figure 4-1 - Figure 4-4.

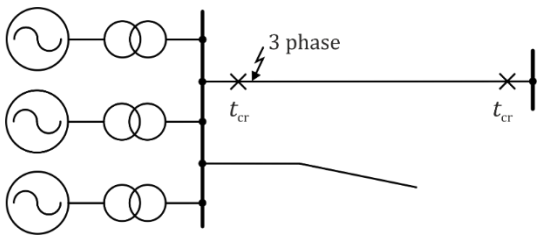

$$k_{\mathrm{t}} = \frac{t_{\mathrm{cr}} - t_{\mathrm{I}}}{t_{\mathrm{I}}} \cdot 100\%$$

FIGURE 4-1: C|K3|1C - CLOSE 3 PHASE SHORT CIRCUIT ELIMINATED BY LINE TRIPPING AT NORMAL CLEARING TIME $\mathrm{t_I} = 100\ \mathrm{ms}$.

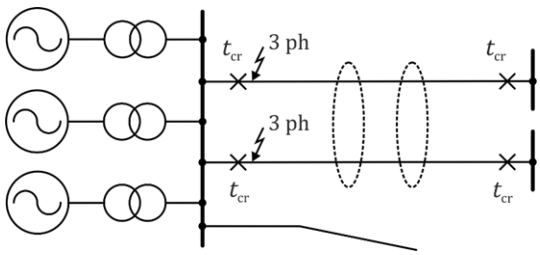

$$k_{\mathrm{t}} = \frac{t_{\mathrm{cr}} - t_{\mathrm{I}}}{t_{\mathrm{I}}} \cdot 100\%$$

FIGURE 4-2: C|K3|2C - CLOSE 3-PHASE SHORT-CIRCUIT IN A DOUBLE-CIRCUIT LINE ELIMINATED BY LINE TRIPPING AT NORMAL CLEARING TIME $\mathrm{St_I} = 100\ \mathrm{ms}$.

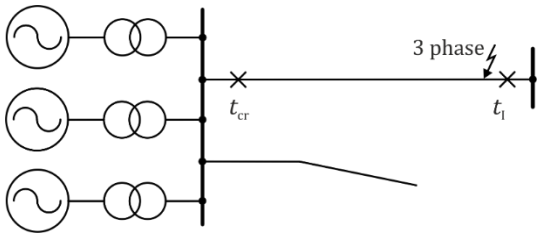

$$k_t = \frac{t_{cr} - t_{I+}}{t_{I+}} \cdot 100\%$$

FIGURE 4-3: F|K3|1C - CLOSE 3 PHASE SHORT CIRCUIT ELIMINATED BY LINE TRIPPING AT IMPEDANCE RELAY II ZONE (85% LINE LENGTH) CLEARING TIME $t_{I+} = 120$ ms FROM THE POWER STATION SIDE OF LINE AND NORMAL CLEARING TIME $t_I = 100$ ms FROM THE OTHER END OF LINE SIDE.

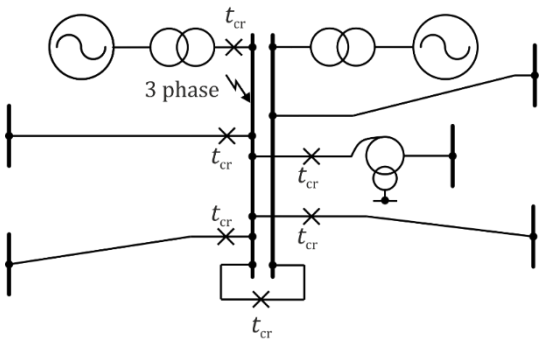

$$k_t = \frac{t_{cr} - t_I}{t_{I+}} \cdot 100\%$$

FIGURE 4-4: C|K3|B - 3 PHASE SHORT-CIRCUIT IN A BUSBAR SYSTEM ELIMINATED AT NORMAL CLEARING TIME $t_I = 100$ ms.

In order to access transient rotor stability in quantitative terms, the use of critical clearing times (CCT) and the following transient stability margin has been proposed:

$$k_t = \frac{t_{cr} - t_f}{t_f} \cdot 100\% \qquad \text{(Eq. 4-1)}$$

where t_{cr} and t_f are the critical and actual clearing times respectively. Presented margins, based on the critical clearing time values k_t have been calculated and compared to the required values, i.e. 20% to 0% depending on pre-fault conditions and the type of simulated disturbance. The required transient stability margins for the disturbances considered, according to the Polish TSO guidelines for stability analysis, have been presented in Table 4-1 below.

TABLE 4-1: PERMISSIBLE TRANSIENT STABILITY MARGIN VALUES FOR CONSIDERED DISTURBANCE EVENTS.

Initial pre-fault system configuration	Fault type	Class of total contingency event	Permissible transient stability margin
N-0	C|K3|1C	probable	≤ 20%
N-1	C|K3|1C	probable	≤ 10%
N-0	C|K3|2C	probable	≤ 20%
N-0	F|K3|1C	probable	≤ 20%
N-0	C|K3|B	probable	≤ 20%

The selected disturbances have been applied on the transmission lines and busbars in the EHV substations transferring power from the biggest conventional Polish power plants (including synchronous generators). Due to the excessive simulation times and the large number of possible outage contingencies that are included in the scope of analysis, simulations are only performed on the base N-0 configuration. Presented transient stability analysis covers 9 operation snapshots for each of the 163 considered fault event contingencies which are under study. The Dynamic CE power system model used for the transient stability studies discussed above is employed for this part of the analysis. More details on the model can be found in Deliverable D2.3 of EU-SysFlex [3].

In order to evaluate electromechanical oscillation damping after severe disturbances, results of time-domain simulation have been also used. For the purposes of oscillatory stability analysis, settling and halving times have been calculated in order to assess the damping of inter-area and inter-plant oscillations. Regulation time indices, which have been described in detail in Deliverable D2.3 of EU-SysFlex [3], can be calculated as time, after which the observed rotor angle signal does not extend beyond an assumed control band. The width of the reference control band is defined as a percent of the first amplitude value, which are 15% for settling time and 50% for halving time, respectively. Small signal stability analysis has not been considered by PSE.

The settling and halving times have been calculated for disturbances in which clearing times are assumed to be 100 ms. For the purposes of the oscillation damping assessment, the same set of close 3-phase short circuit fault events have been assumed. Requirements for damping performance, according to the Polish TSO guidelines for transient stability analysis, are presented in Table 4-2 below.

TABLE 4-2: REQUIREMENTS FOR DAMPING OSCILLATIONS.

Type of oscillations	Frequency	Halving time (50%)	Settling time (15%)
inter-plant	about 1-2 Hz	≤ 5 s	≤ 15 s
Inter-area	about 0,3 Hz	≤ 7 s	≤ 20 s

For the purposes of transient stability studies, all the aforementioned disturbances have been considered in the Polish power system. The initial test simulation results, which have been not shown in the report, proved that there are no apparent discrepancies in terms of observed phenomena and scarcities while comparing results obtained for different sets of countries for which chosen operational snapshots criterions have been applied (see Section 1.6.1.1). Therefore, it is assumed sufficient results can be obtained by performing the simulations only for the Polish TSO's area and applying operational snapshots criterions within it. This succeeds in reducing the simulation time.

4.1.2 CRITICAL CLEARING TIMES ANALYSIS

4.1.2.1 FAULT TYPE: C|K3|1C

Presented transient stability analysis for the C|K3|1C fault event covers 9 operation snapshots for each of the 55 considered fault event contingencies which are under study. As presented in the Figure 4-5 and Figure 4-6 below, for each disturbance C|K3|1C event analysed within the scope of the study, required values of critical clearing times (t_{cr}>=120 ms) and transient stability margins (k_t ≥20%) (see Table 4-1) have been met with sufficient excess. Minimum transient stability margin observed is equal to k_t =72.75%. For each of the analysed scenarios, median values for the CCTs tend to be the highest for the "Max_Load" operational snapshots (which corresponds to relatively low SNSP for those snapshots).

The larger the active power demand is, the larger the number of synchronous generators operating, which leads to the increase of the inertia level in the power system. An increase in the level of inertia augments the power system transient stability margin, which also depends on various factors, i.e. the voltage level at the point of synchronous generator connection. The lower the reactive power generation is, the lower the voltages of generators are, which causes the decrease of transient stability margin. This explains why the median values for "Min_Reactive" and ""Min_Inertia"" operational cases are comparable, but lower than corresponding values for the "Max_Load" operational case. Also, the overall power systems' inertia is being reduced for the "Min_Inertia", and "Min_Reactive" operational cases, due to the higher renewables penetration.

Circles in the box plot figure (Figure 4-6) are described as the outliers, for which apparently higher or lower CCTs have been observed, due to the unusual network configuration (some of the power plants are interconnected to the rest of the system with relatively short transmission lines), higher voltages of the generators caused by high reactive power generation, which was set up in order to perform initial load flow calculation, etc. However, for all of those outliers transient stability margin requirements have been met with a sufficient excess, so there has been no need to perform any remedial actions.

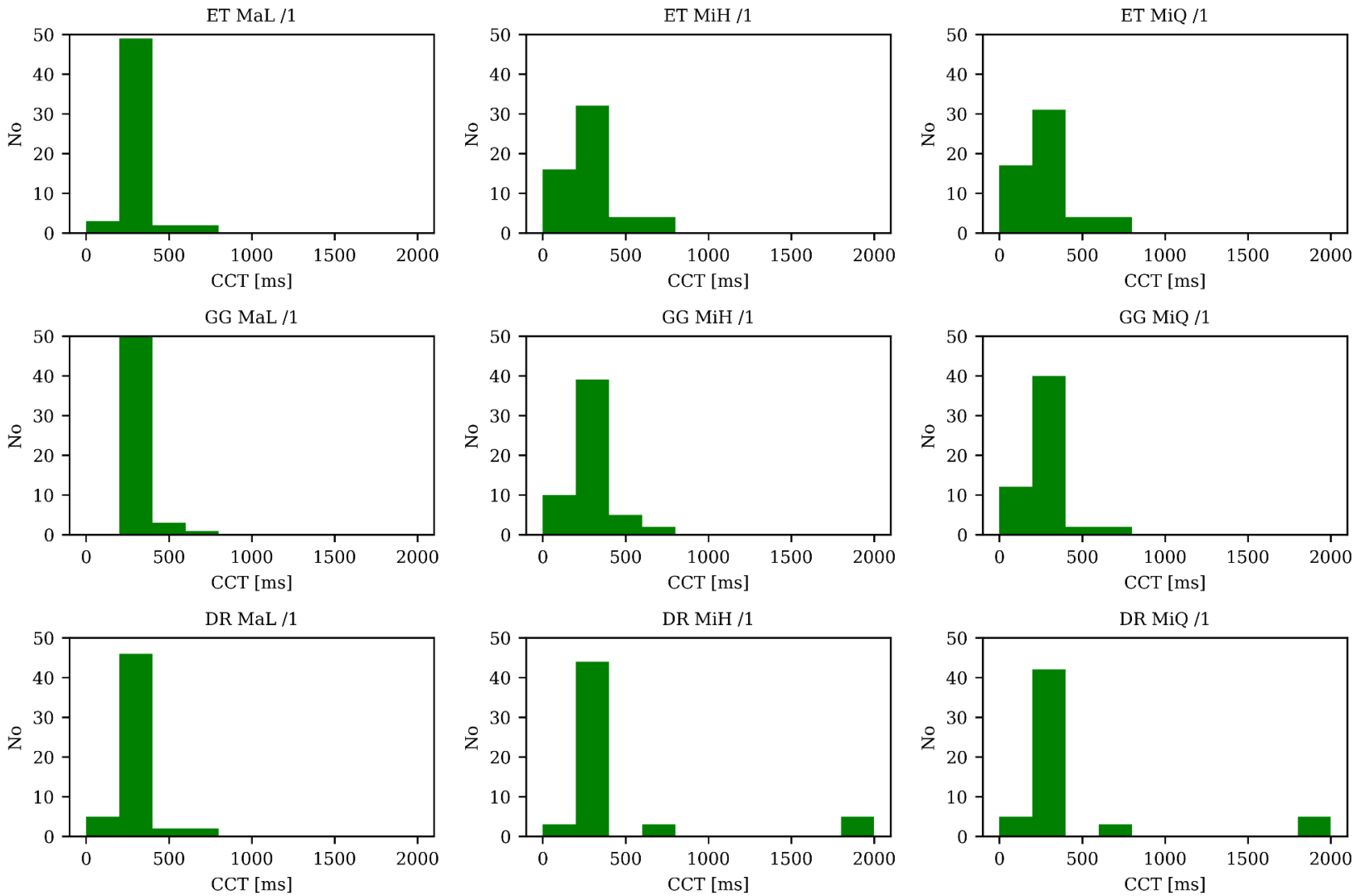

FIGURE 4-5: C|K3|1C CRITICAL CLEARING TIME RESULTS – HISTOGRAMS.

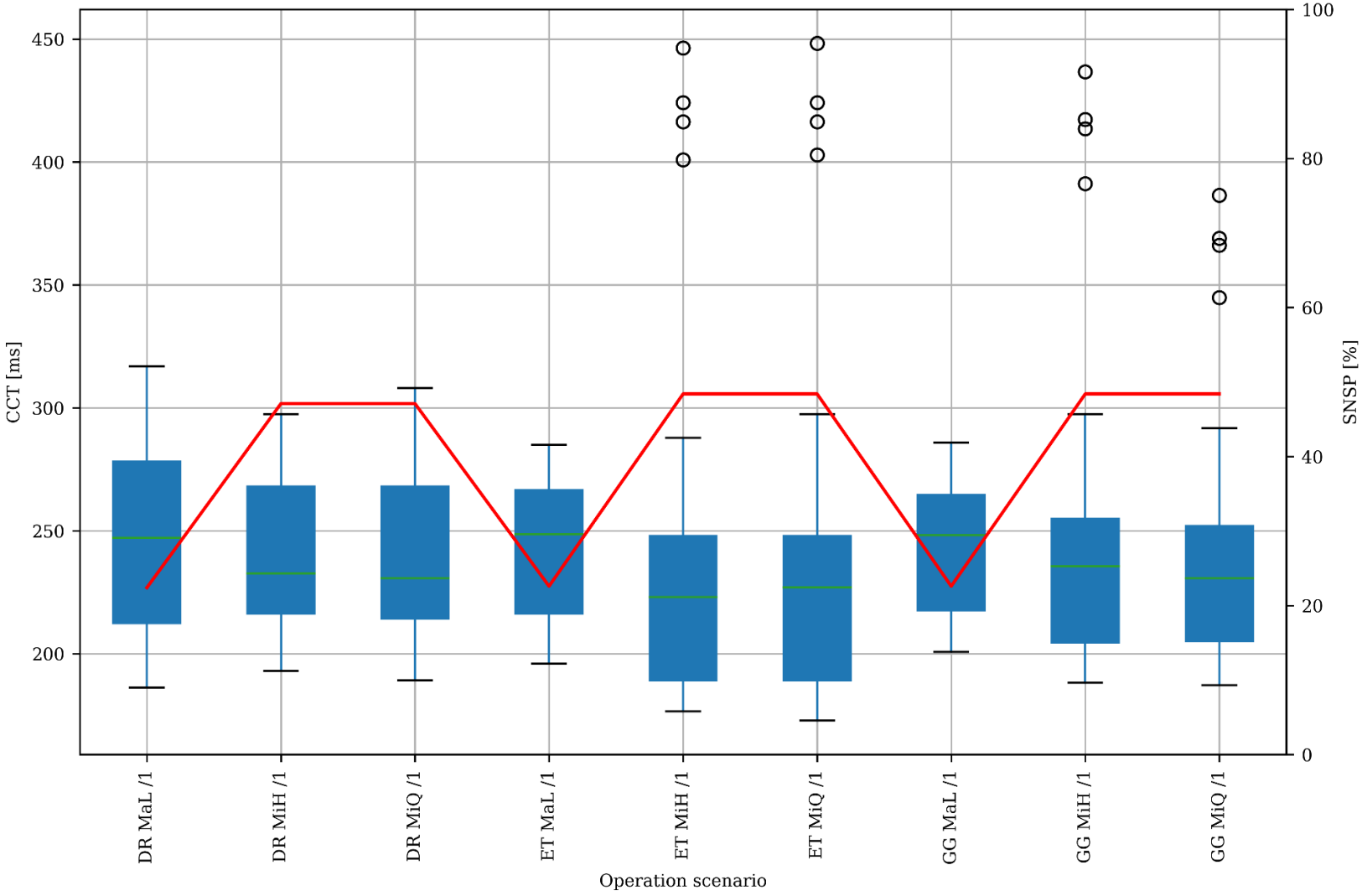

FIGURE 4-6: C|K3|1C CRITICAL CLEARING TIME RESULTS – BOX PLOTS.

4.1.2.2 FAULT TYPE: C|K3|1C – ADDITIONAL CASES

As mentioned in Section 1.6.1.1, an additional case is also analysed. The new operational case meets the criterion of maximum $SNSP$ in the whole CE, when the Distributed Renewables scenario is investigated. For this operational case, CCTs have been calculated for C|K3|1C short circuit events occurring close to the Dolna Odra conventional power plant (located near two Polish-German cross-border transmission lines connecting substations Krajnik (PL) and Vierraden (DE)) starting from N-0 and N-1 prefault conditions. Presented additional transient stability analysis covers 9 for the C|K3|1C fault events for each of the 9 considered N-1 outage contingencies. The obtained distribution of CCTs together with SNSP level is shown in Figure 4-7. Looking at this plot, it can be observed that there is no significant difference between CCTs obtained for Distributed Renewables Min_Inertia /1 and Distributed Renewables Max_SNSP /4 in terms of meeting transient stability margins requirements. Discrepancies observed may have been caused by different initial conditions for both snapshots, although no transient stability scarcities have been observed due to the higher SNSP value. Required values of critical clearing times (t_{cr}>=110 ms) and transient stability margins (k_t ≥10%) (see Table 4-1) have been met with sufficient excess for scenarios being analysed. Minimum transient stability margin observed for both compared scenarios is equal to k_t =148 %.

Additionally, analysis was also conducted to determine how far towards the LV grid it is possible to relocate RES generation whilst still maintaining acceptable CCTs. In order to mimic such effect, artificial impedances on all cross jurisdictional connections in Poland are increased.

The first case of this sensitivity analysis involves taking all the cross border lines on the synchronous connections (PL-DE, PL-CZ and PL-SK) out of service in the CE model. This means that infinite impedance is inserted between Poland and the neighbouring power systems and can be interpreted that all the RES generation is located very far from the investigated power plant (in terms of electrical distance). Such assumptions have been applied to the Distributed Renewables /Max_SNSP/4 case (new case is named Distributed Renewables Max_SNSP /4 InfImp).

Next, the CCTs have been calculated for disturbances C|K3|1C occurring close to Dolna Odra conventional power plant. The impact of the infinite impedance between foreign RES and the fault is shown in Figure 4-8. Presented additional transient stability analysis for the C|K3|1C fault event covers 6 fault events within considered operational snapshot variations. It can be seen that CCTs decrease significantly, but they do not decrease to unacceptable levels. Minimum observed CCT value is equal to 185.3 ms, which corresponds to transient stability margin equal to k_t =85,3%. With these results, there is no need for further sensitivity analysis using finite impedance values.

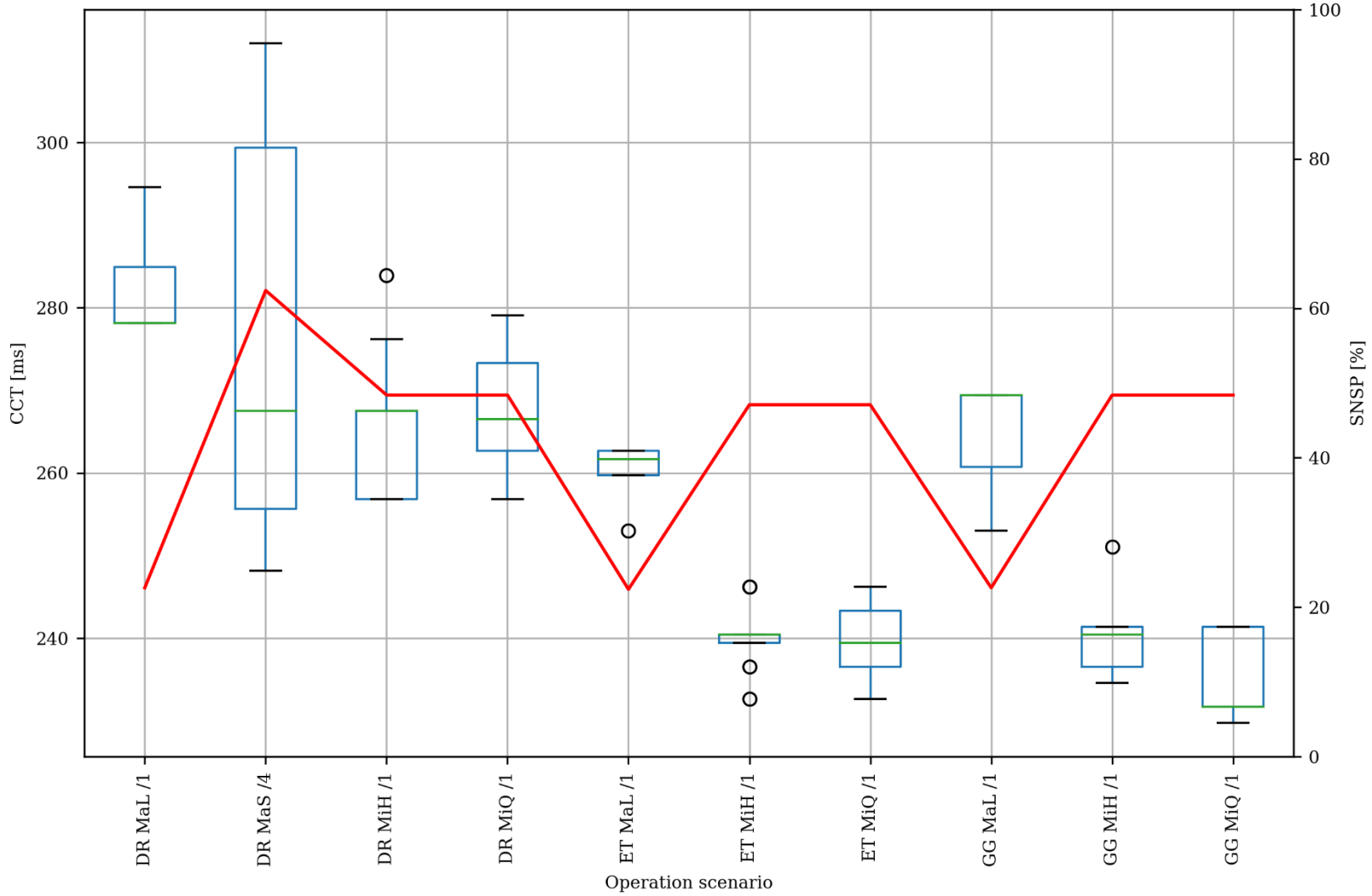

FIGURE 4-7: C|K3|1C CRITICAL CLEARING TIME RESULTS FOR SELECTED POWER PLANT INCLUDING MAX_SNSP OPERATION SCENARIO – BOX PLOTS.

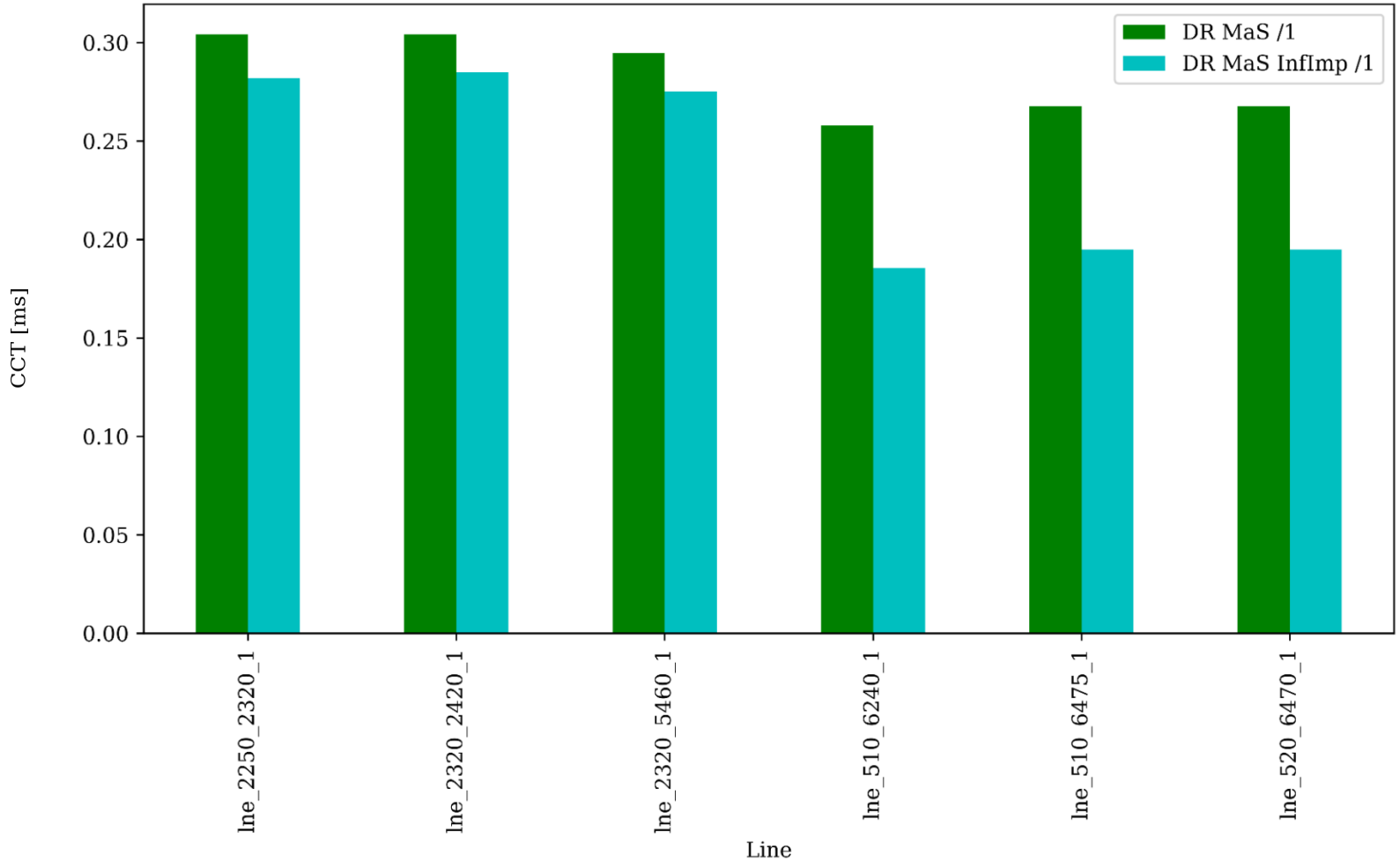

FIGURE 4-8: C|K3|1C CRITICAL CLEARING TIME RESULTS FOR SELECTED POWER PLANT WITH MAX_SNSP OPERATION SCENARIO AND INFINITE IMPEDANCES ON CROSSBORDER CONNECTIONS – BAR PLOTS.

4.1.2.3 **FAULT TYPE: C|K3|2C**

Presented transient stability analysis for the C|K3|2C fault event covers 9 operation snapshots for each of the 21 considered fault event contingencies which are under study. As presented in Figure 4-9 and Figure 4-10 below, for each disturbance C|K3|2C event analysed within the scope of the study, required values of critical clearing times ($\mathrm{t_{cr}} \geq 120$ ms) and transient stability margins ($\mathrm{k_t} \geq 20\%$) (see Table 4-1) have been met with sufficient excess. Minimum transient stability margin observed is equal to $\mathrm{k_t} = 54.38\%$. For each of the analysed scenarios, CCT median values tend to be highest for the Max_Load (relatively low SNSP) operational cases, as was also observed in the previous analysis. CCTs for the C|K3|2C disturbance are shorter than the CCTs for the C|K3|1C disturbance. This is due to the fact that under this disturbance, fault clearing disconnects a double circuit, which leads to lower power system equivalent impedance. According to the following formula for a simplified single machine infinite bus system [22]:

$$P_{\mathrm{e}}(\delta) = \frac{E_{\mathrm{q}} V_s}{x_{\mathrm{d}}} \cdot \sin(\delta) \qquad \text{(Eq. 4-2)}$$

where P_{e} is the active power output of a synchronous generator, E_{q}, V_s are the voltages of generator and infinite bus respectively, x_{d} is the equivalent power system's impedance. As such, the lower x_{d} due to the tripping of two transmission lines instead of one reduces the peak value of the power-angle characteristic and thereby the transient stability margin itself.

For the presented results, the transient stability margin requirements have been met. However, the tripping of a double circuit may cause severe overloads in the rest of the system, which have been not analysed within the scope of the following study.

Circles in the box plot describe the outliers, for which apparently higher or lower CCTs have been observed, due to the unusual network configuration (power plants interconnected to the rest of the system with relatively short transmission lines), higher voltages of the generators caused by high reactive power generation, which was set up in order to perform initial load flow calculation, etc. However, for all of those outliers transient stability margin requirements have been met with a sufficient excess, so there has been no need to perform any remedial actions.

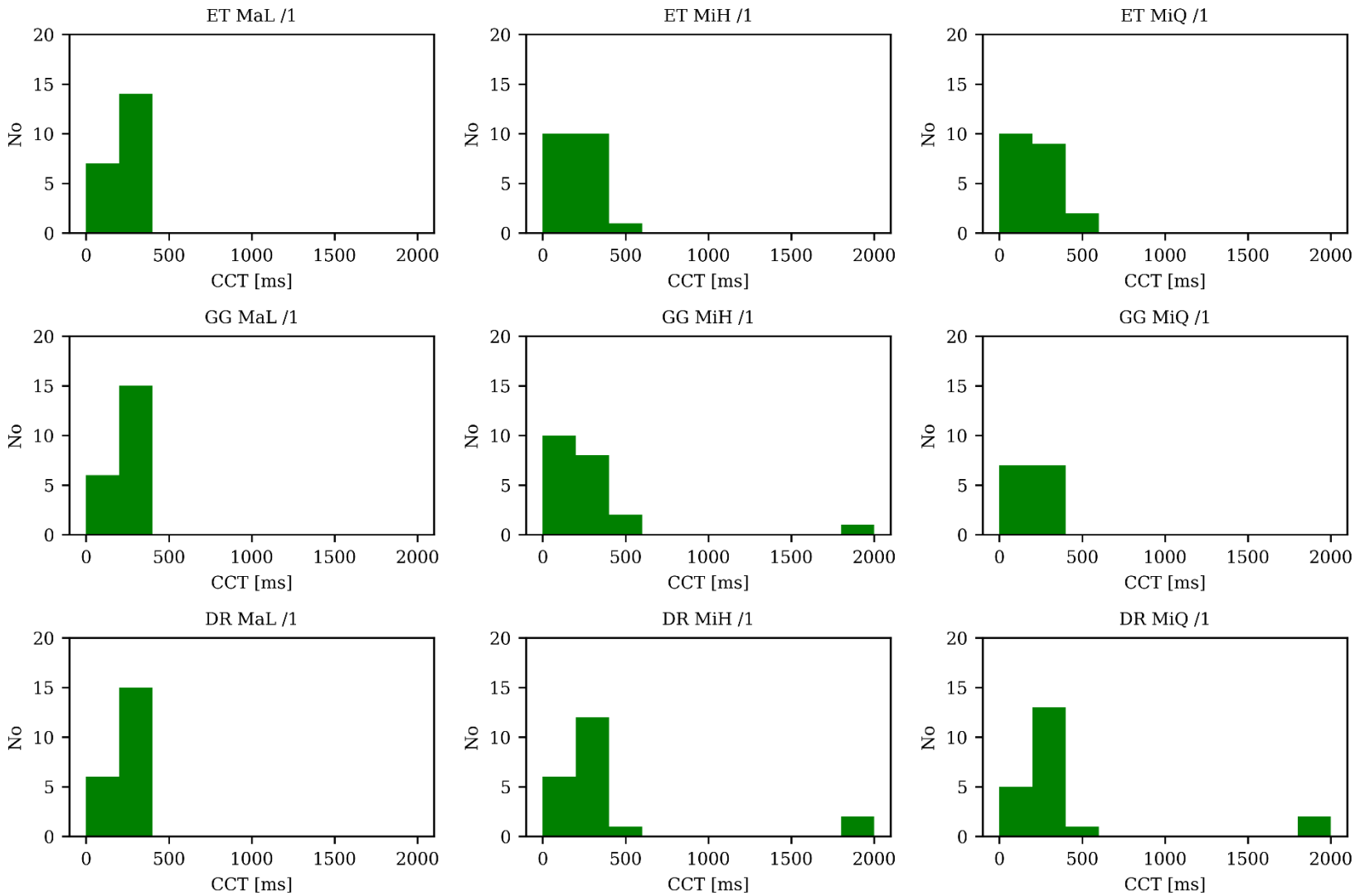

FIGURE 4-9: C|K3|2C CRITICAL CLEARING TIME RESULTS – HISTOGRAMS.

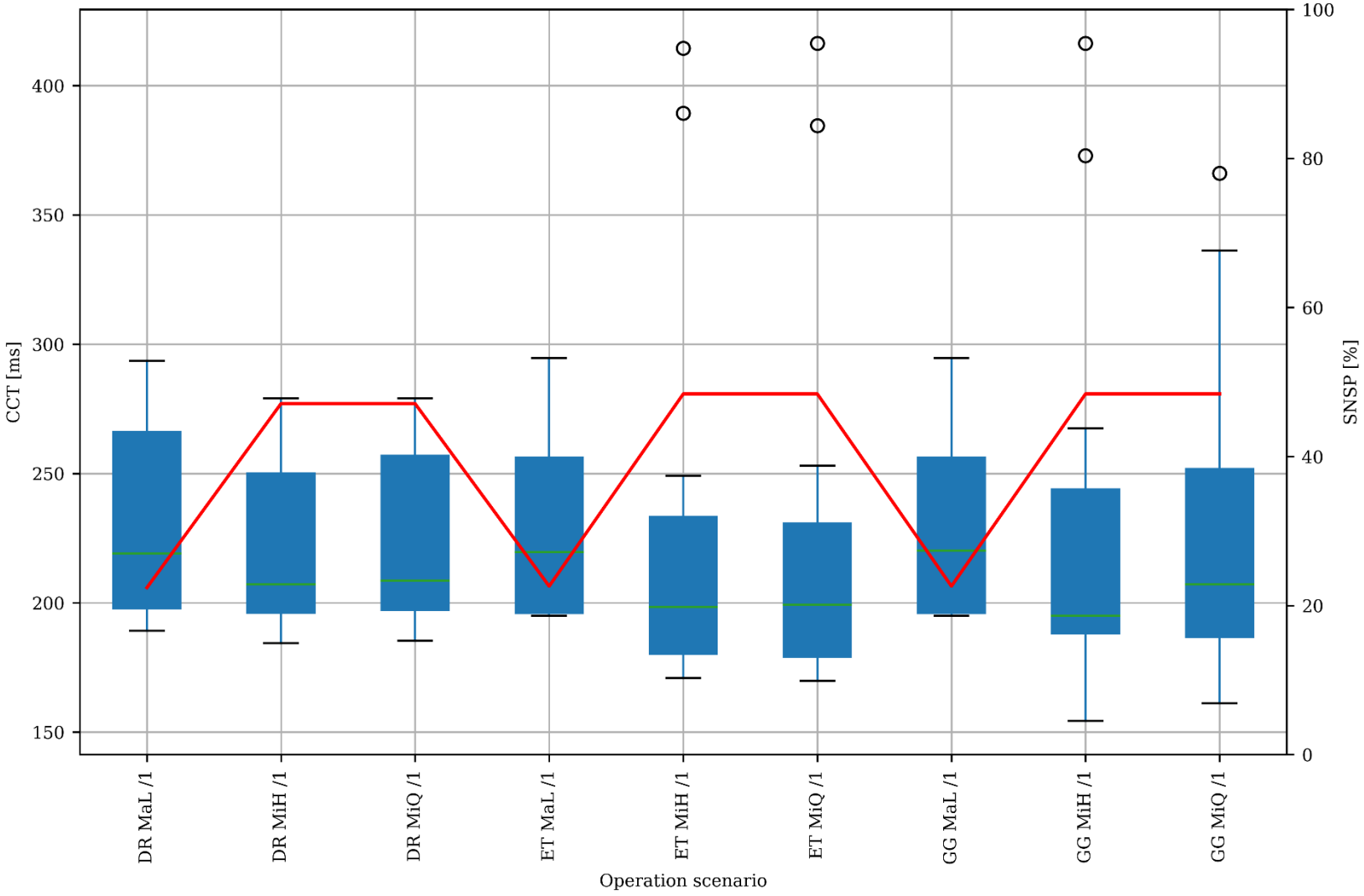

FIGURE 4-10: C|K3|2C CRITICAL CLEARING TIME RESULTS – BOX PLOT.

4.1.2.4 **FAULT TYPE: F|K3|1C**

Presented transient stability analysis for the F|K3|1C fault event covers 9 operation snapshots for each of the 55 considered fault event contingencies which are under study. As presented in the Figure 4-11 and Figure 4-12 below, for each disturbance F|K3|1C event analysed within the scope of the study, required values of critical clearing times (t_{cr}>=120 ms) and transient stability margins (k_t ≥20%) (see Table 4-1) have been met with sufficient excess. Minimum transient stability margin observed is equal to $k_t = 140.43\%$. Due to the fact that analysed short circuit is classified as a far from the power plant, CCTs are relatively high. For a significant number of events, CCT values have been larger than the maximum admissible value for a binary search method.

For these far short circuits power system operation is safe, as they do not have serious influence on transient stability. A more pressing threat to the transient stability is the failure of the fast data exchange fibre connection between the protection devices located at the power stations at the both ends of a line. This may lead to the significant decrease of CCTs and cause instability as any disturbance would be cleared from a power plant side with a delayed 550 ms time due to the backup protection scheme operating on the second zone of an impedance relay. That type of fault event has not been considered in the scope of presented analysis, but it is worth to mention that it may cause a transient stability scarcity.

Circles in the box plot figure are described as the outliers, for which apparently higher or lower CCTs have been observed, due to the unusual network configuration (power plants interconnected to the rest of the system with relatively long transmission lines), higher voltages of the generators caused by high reactive power generation in order to perform initial load flow calculation or short circuits occurring in the transmission lines which interconnect two power plants, meaning that for a one of them, described far fault event is a close disturbance. However, for all of those outliers transient stability margin requirements have been met with a sufficient excess, so there has been no need to perform any remedial actions.

In general, no correlation between CCT and the operational cases (characterised by different $SNSP$ levels) for this type of fault has been observed.

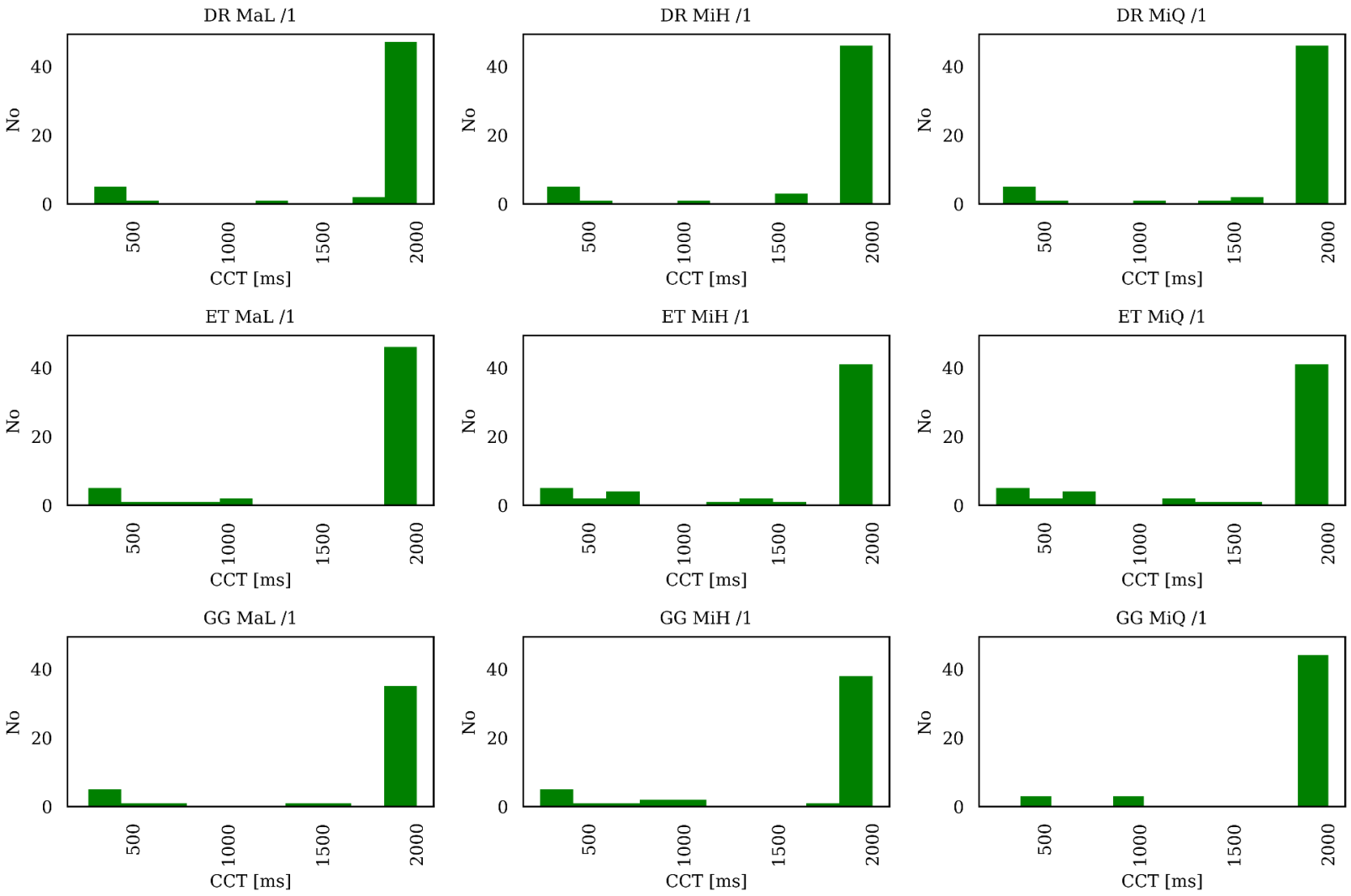

FIGURE 4-11: F|K3|1C CRITICAL CLEARING TIME RESULTS – HISTOGRAMS.

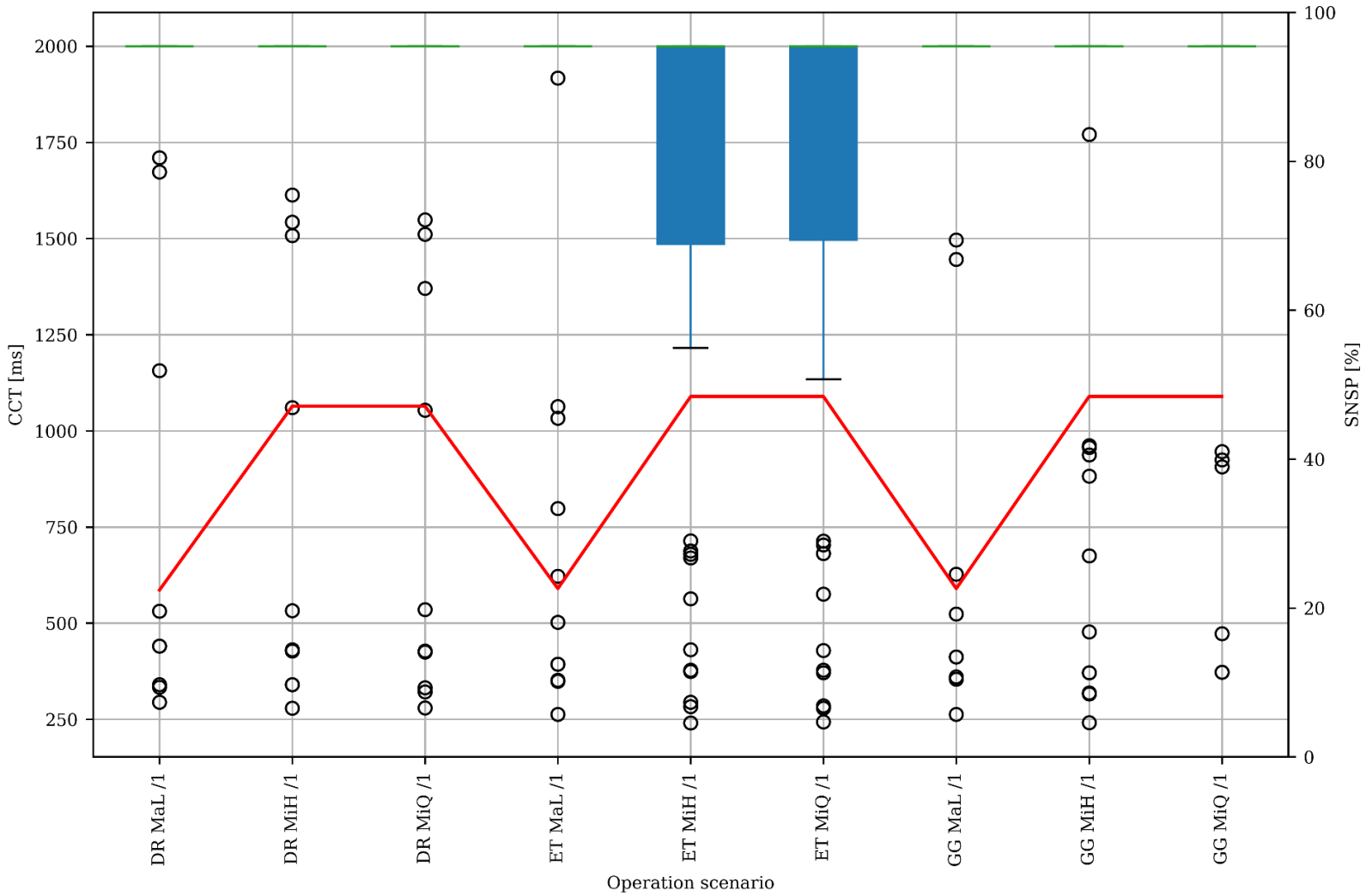

FIGURE 4-12: F|K3|1C CRITICAL CLEARING TIME RESULTS – BOX PLOT

4.1.2.5 **FAULT TYPE: C|K3|B**

Presented transient stability analysis for the C|K3|B fault event covers 9 operation snapshots for each of the 32 considered fault event contingencies which are under study. As presented in the Figure 4-13 and Figure 4-14 below, for each disturbance C|K3|B event analysed within the scope of the study, required values of critical clearing times (t_{cr}>=120 ms) and transient stability margins (k_t ≥20%) (see Table 4-1) have been met with sufficient excess. Minimum transient stability margin observed is equal to $k_t = 31{,}18\%$. For each of analysed capacity scenarios, the median CCT tends to be longest for the Max_Load operational snapshots, as has been observed in the previous sections. For the Min_Reactive operational snapshots, for a noticeable number of power plants reactive power have been slightly increased, in order to allow the correct initial load flow calculation. Due to the fact that analysed short circuit occurs at the busbars of the power plant station, the CCT strongly depends on the voltage. This explains the fact that the CCT values obtained for the Distributed Renewables Min_Reactive case are comparable with those for the Max_Load case, as mentioned changes have been included for that snapshot in order to assure that initial load flow calculation is successful.

Power system operation is secure, as the close short circuits at the power plant busbars as the CCTs observed here exceed the expected clearance time. The main goal to maintain transmission system transient stability is to prevent the failure of the primary power plant busbars protection. Such a failure may lead to the significant decrease of CCTs and cause instability as short circuit would be cleared with a delayed 550 ms time due to the backup protection scheme.

Circles in the box plot are described as the outliers, for which apparently higher or lower CCTs have been observed, due to the unusual network configuration (power plants interconnected to the rest of the system with relatively long transmission lines), higher voltages of the generators caused by high reactive power generation in order to perform initial load flow calculation etc. However, for all of those outliers transient stability margin requirements have been met with a sufficient excess, so there has been no need to perform any remedial actions.

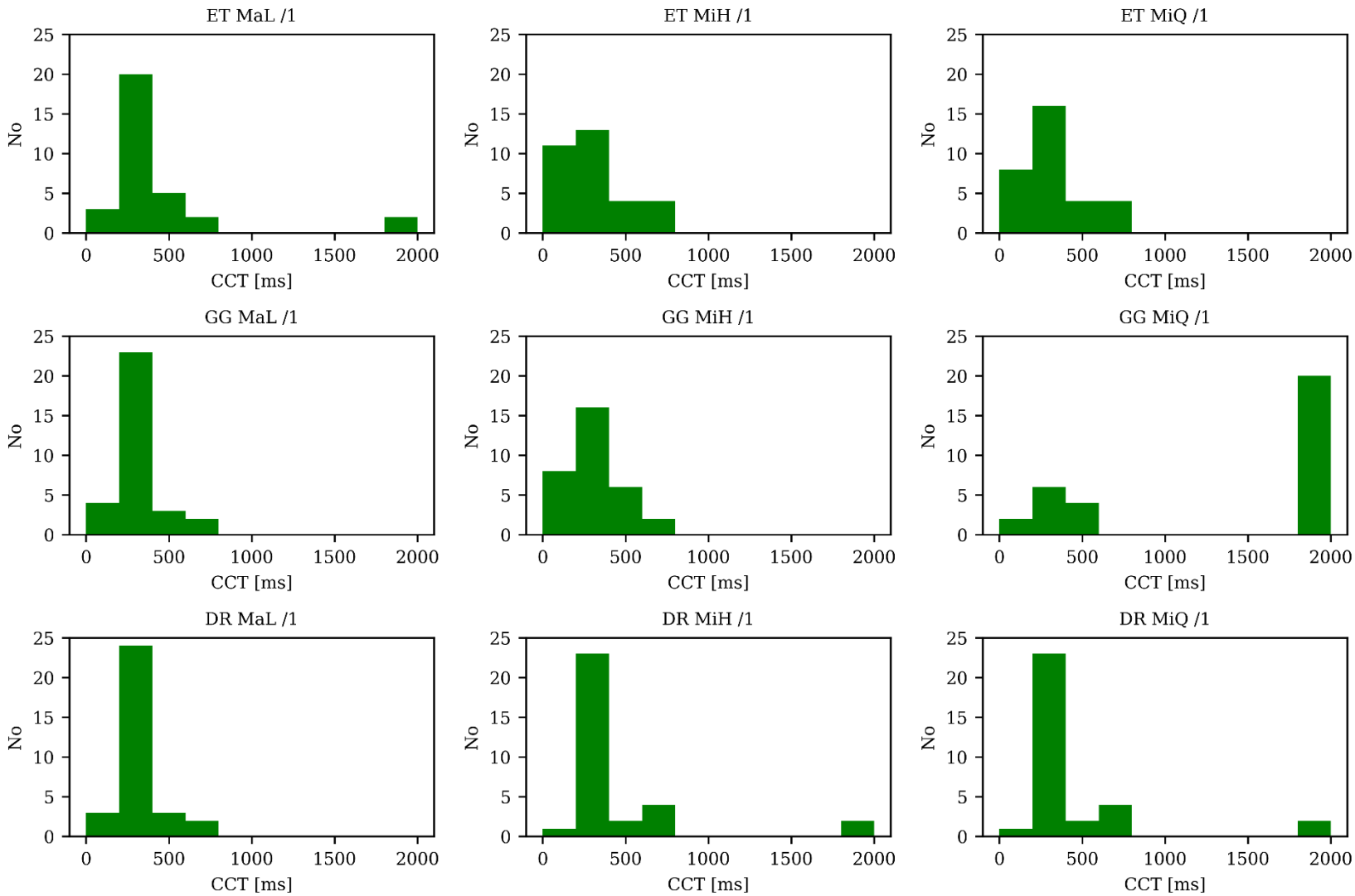

FIGURE 4-13: C|K3|B CRITICAL CLEARING TIME RESULTS – HISTOGRAMS.

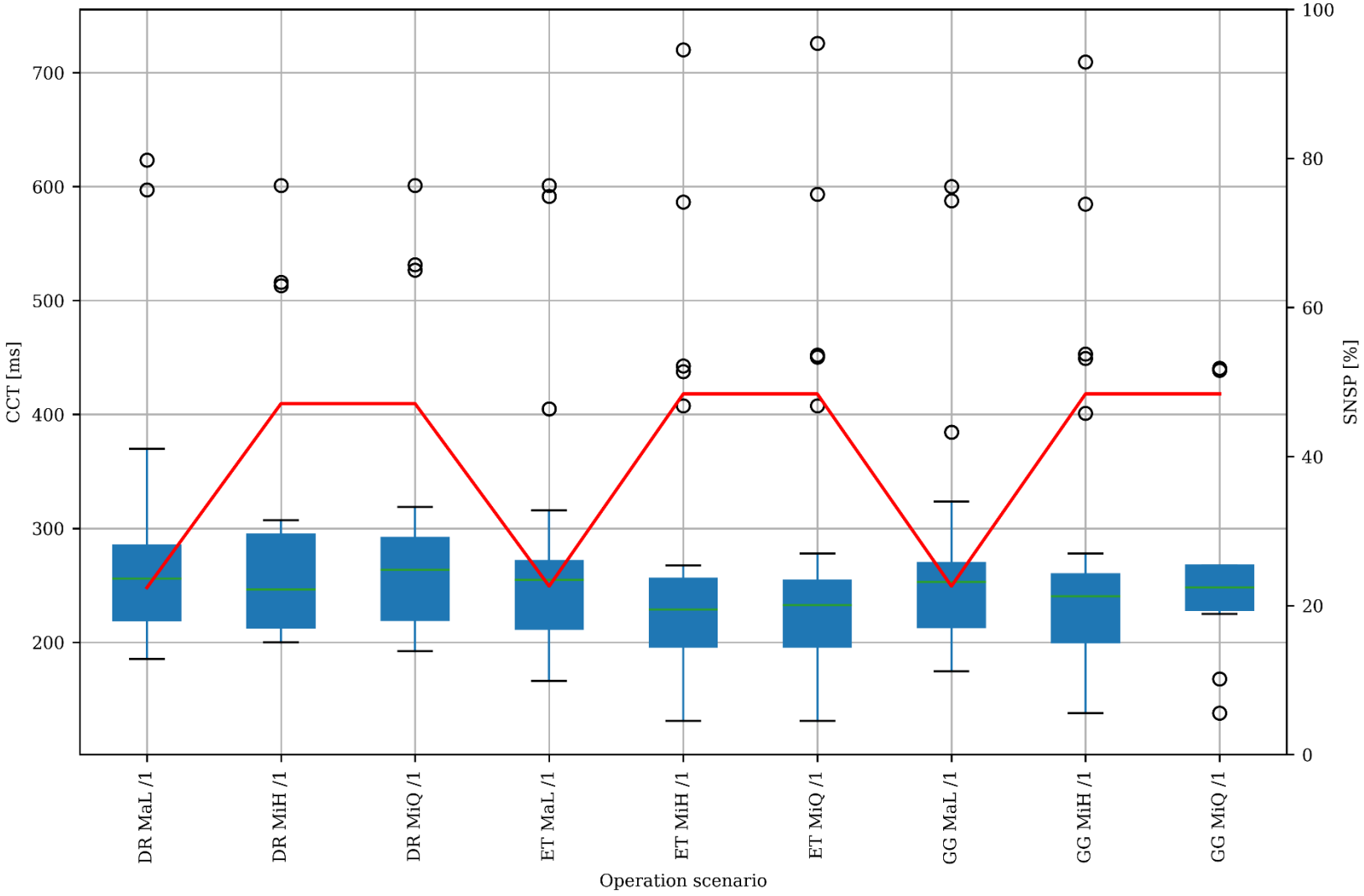

FIGURE 4-14: C|K3|B CRITICAL CLEARING TIME RESULTS – BOX PLOT.

4.1.3 OSCILLATION DAMPING

As presented in the Figure 4-16 - Figure 4-19 below, high penetration of renewables and decrease of the synchronous generation can cause significant issues with an oscillation damping, which may cause the problems with power system instability.

As presented in the histograms, there are a lot more fault cases in the Min_Inertia and Min_Reactive cases in which both regulation times requirements for oscillations damping are not met, showing that cases with high penetration of renewables connected over power electronic converters have poor oscillation damping. There are numerous disturbance events, in which regulation time values have been larger than maximum admissible value of 20 seconds, even for halving time requirements (in GG/Min_Reactive/1), which is less strict than settling time, according to the width of control band.

For each of the analysed capacity scenarios, both halving and settling time median values tend to be lowest for the Max_Load operational snapshots. This is the operation scenario in which $SNSP$ level is relatively low. The larger the active power demand is, also the bigger the number of synchronous generators being operating in the power system is, which indirectly leads to the increase of the inertia level in the power system, leading to the augmentation of the oscillations damping in the power system. Also, the overall power systems' inertia is being reduced for the Min_Inertia and Min_Reactive scenarios, due to the higher renewables penetration, instead of synchronous generation. The lower the reactive power generation is, the lower the voltage of generators connected at the power plant are, which causes reduced damping, explaining why the median values for Min_Reactive and Min_Inertia cases are comparable between themselves and apparently lower than for the Max_Load ones.

Circles in the Box figure describe the outliers, for which excessively high or low regulation times indices values have been observed, due to the unusual network configuration (power plants interconnected to the rest of the system with relatively long transmission lines), higher voltages of the generators caused by high reactive power generation in order to perform initial load flow calculation etc. For the clarity of view for the statistical data presentation in the Box plots, outliers for which regulation time values have been larger than maximum admissible value of 20 seconds, have been not included, as they are presented in the histograms.

Rotor angle plots presented in Figure 4-19 below, represents the influence of operational snapshot's criteria application on the oscillation damping for selected 100 ms close 3-phase short circuit disturbance, applied at the transmission line leading out of one of the largest power plants station in Poland. In order to present the lack of oscillation damping, rotor angle plots for a group of selected power plants synchronous generators and capacity scenario have been presented, as they are comparable to the rest of disturbance events, analysed within the scope of this study.

From the analysis of the rotor angle plots it can be observed that in the first two seconds of the simulation inter-plant oscillation components are more noticeable (approximately 1,42 Hz for all the snapshots), then the nature of the oscillations turns to inter-area values (from 0,63 Hz for Max Load to 0,76 Hz for Min Inertia and Min Reactive). It can be observed, that high penetration of synchronous generation due to the higher active power demand helps to better damp power systems oscillations, as for Min_Inertia and Min_Reactive operational snapshot oscillation damping is apparently worse, caused by higher penetration of renewables and less reactive power generation.

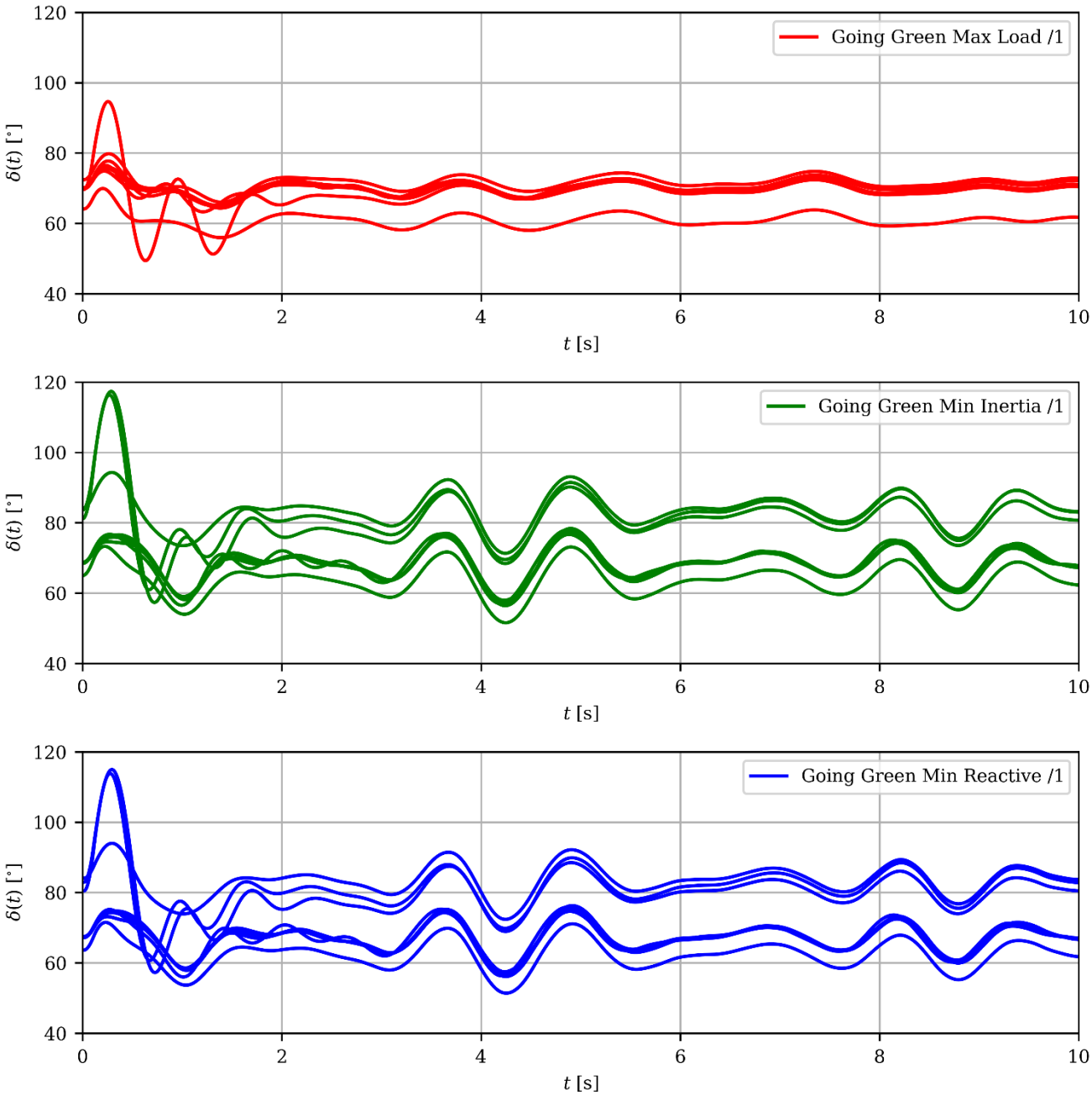

FIGURE 4-15: OSCILLATIONS DAMPING – ROTOR ANGLE PLOTS FOR VARIOUS OPERATION SNAPSHOTS.

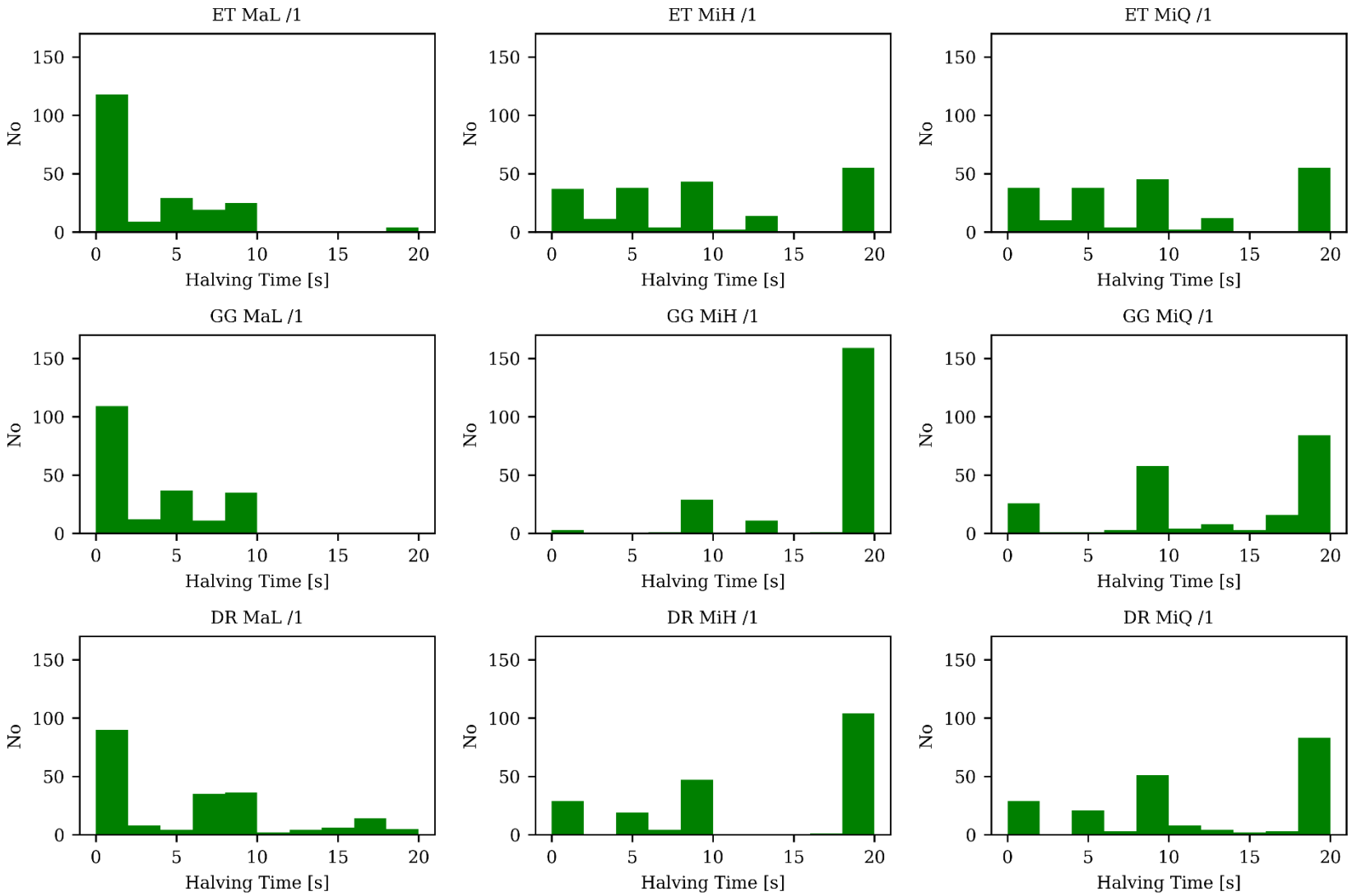

FIGURE 4-16: HALVING TIMES – HISTOGRAMS.

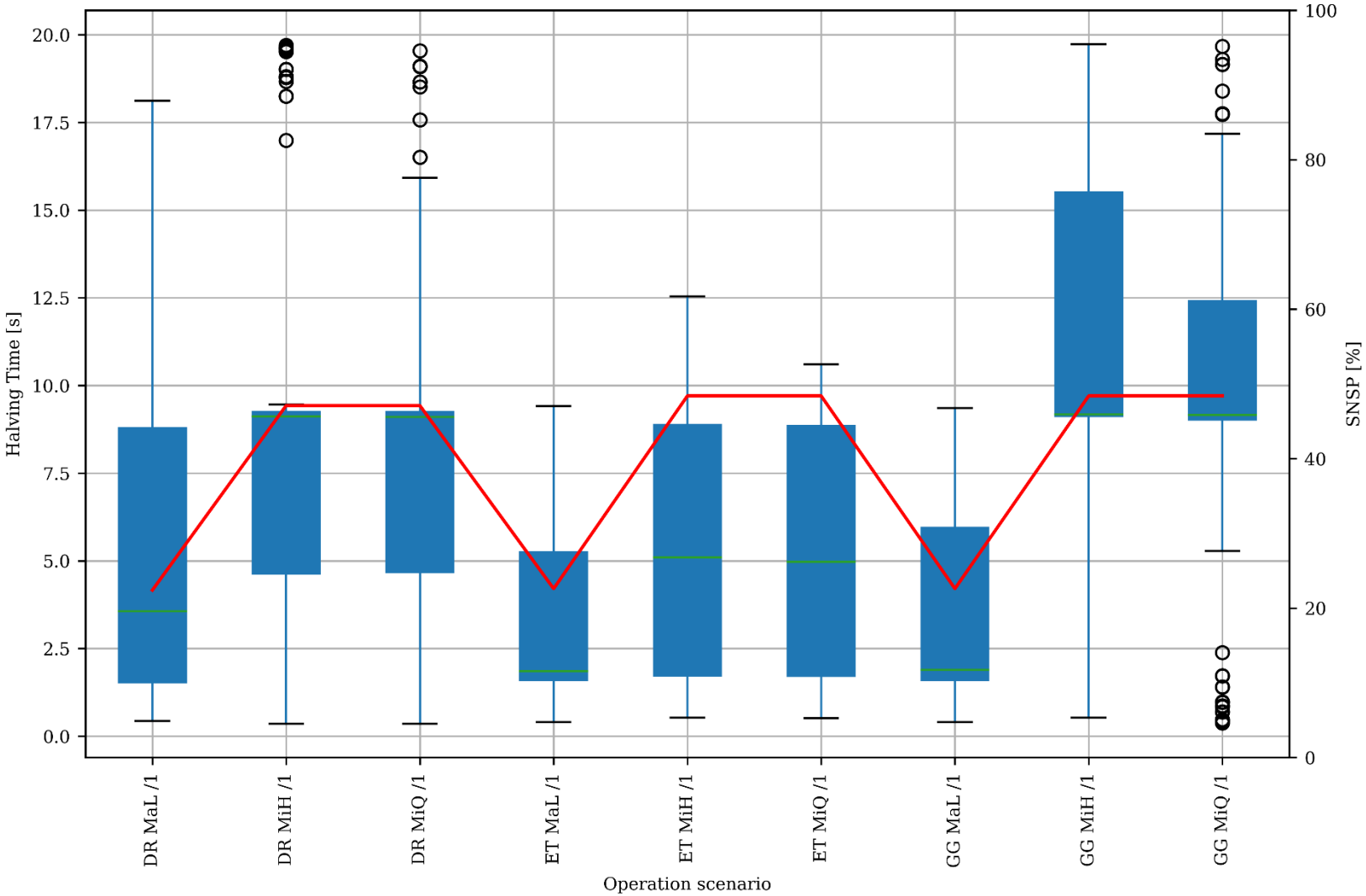

FIGURE 4-17: HALVING TIMES – BOX PLOT.

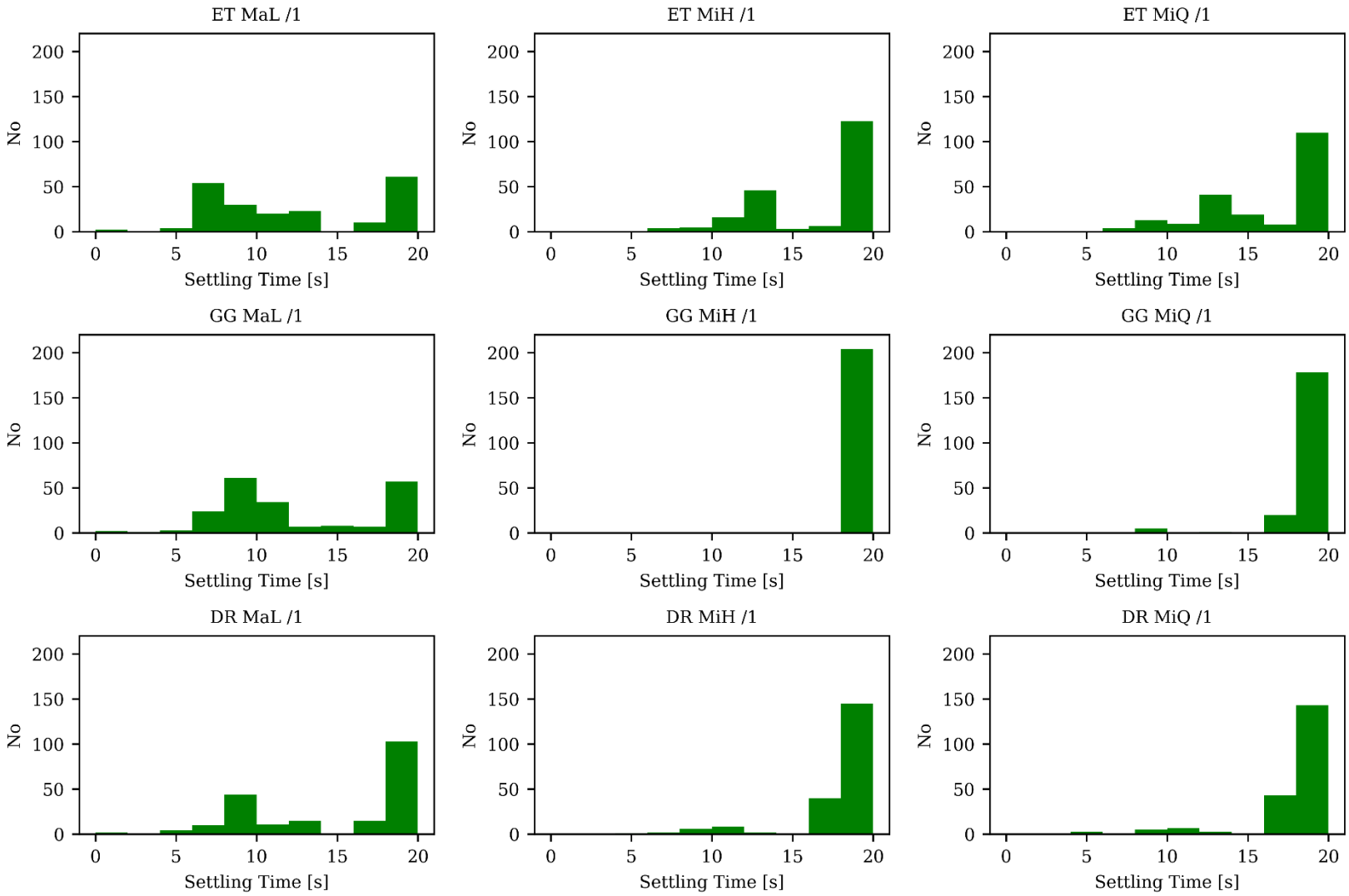

FIGURE 4-18: SETTLING TIMES – HISTOGRAMS.

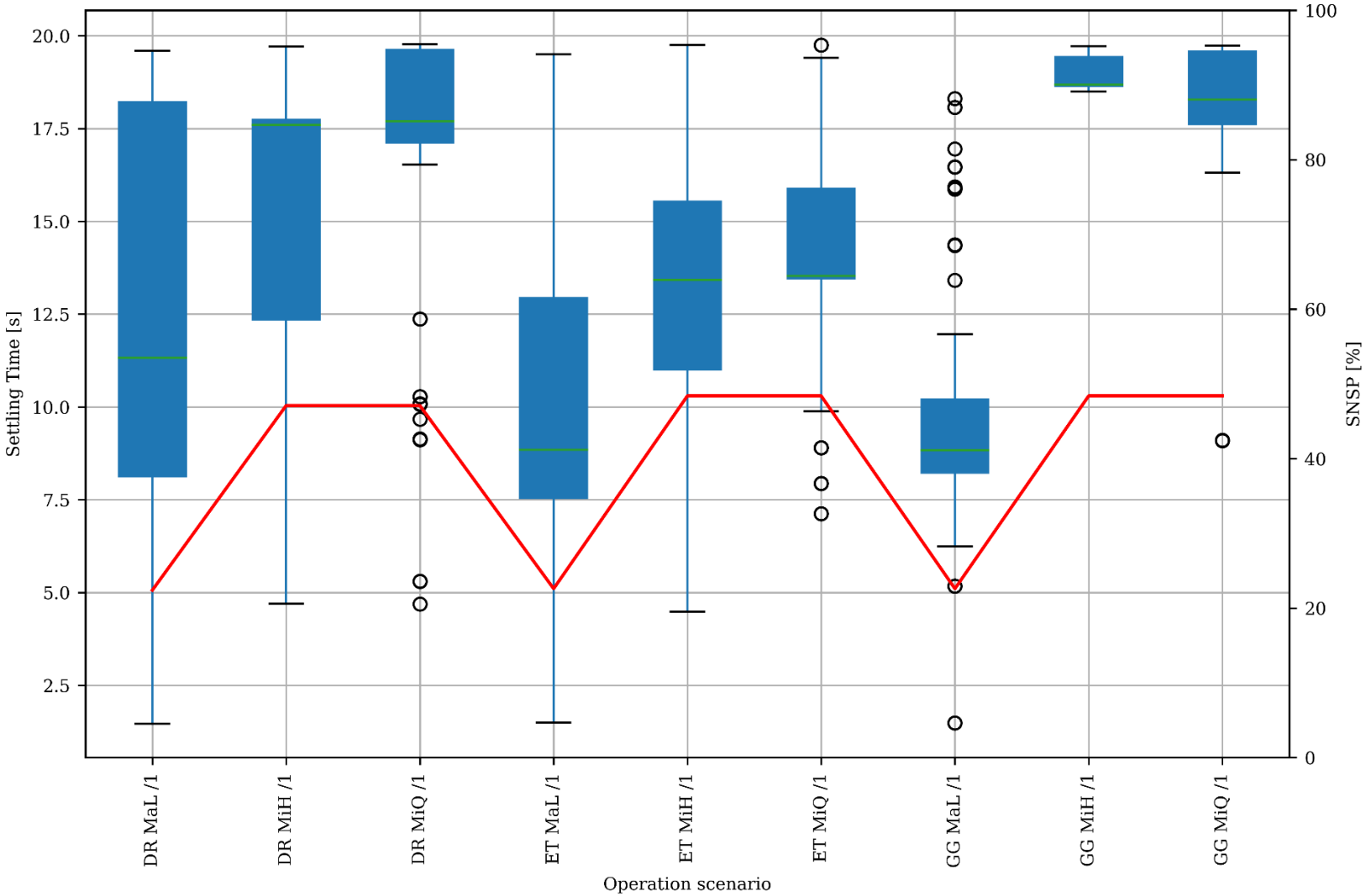

FIGURE 4-19: SETTLING TIMES – BOX PLOT

The analysis of critical clearing time shows no emergence of a localised scarcity in stability margin when assessed in terms of the expected primary protection operation times. However, for both the Energy Transition and Going Green scenarios, the Minimum Inertia and Minimum Reactive Power cases show lower CCTs that may begin to encroach on backup protection operation times for far end faults and busbar faults. This indicates the potential emergence of a localised scarcity in stability margin, under specific operation conditions, which may require detailed assessment of backup protection operation to assess the degree of threat posed by this scarcity.

Oscillation damping presents a global scarcity with poor settling and halving times for all cases and scenarios. Time-domain simulations have identified the poor oscillation damping during severe system disturbances, such as three-phase short-circuit events, with only the maximum load case having any significant number of acceptable settling and halving times. Existing power system stabilisers (PSS) as a supplementary part of voltage controllers usually mitigate these oscillatory problems with electro-mechanical oscillations. However, the PSS tuning has to be carefully coordinated with the power converter controllers located in the power system. Increasing number of power electronic interfaces offers a high level of control potential which among other things can be used for successful oscillation damping but also increase the requirement for greater coordination to avoid controller interactions. This presents a concern moving forward and mitigation should be investigated in future work. Particularly as the nature of the model used and faults studied prevented the assessment of the inter-area modes that are known to exist in the continental system and that may also be impacted by this reduction in damping.

4.2 IRELAND & NORTHERN IRELAND POWER SYSTEM

4.2.1 TRANSIENT ROTOR ANGLE STABILITY

4.2.1.1 CONTINGENCIES STUDIED

The availability of dynamic voltage control is studied for the snapshot hours described in the methodology for 306 bolted three phase line fault contingencies. These line faults are in the middle of the line and are cleared by simultaneously opening the breakers at each end of the line, with a clearance time of between 4 and 8 cycles. The contingency locations are defined using the same methodology applied for the existing online dynamic security assessment that is performed every 15 minutes by EirGrid and SONI using the Wind Strength Assessment Tool (WSAT). This means that the line faults considered can result in the separation of HVDC interconnectors from the system (when the line that serves as the HVDC interconnectors AC collector network is lost) but not the separation of synchronous generators.

Note, in the results presented for low carbon living there are 306 contingencies but for steady evolution there are only 305. This is because contingency 1 is for the AC collector network of the Greenlink HVDC project, which is not

in place for steady evolution. However, the numbering of the contingencies remains the same between these cases for consistency; so, contingency 1 has no results for steady evolution.

4.2.1.2 ANGLE MARGIN INDEX

The evaluation of first swing stability is carried out through an angle margin index. The index compares the relative rotor angles of various generators to evaluate the current level of synchronism in the system and the margin to loss of synchronism. The index is defined as follows [34]:

$$\eta = \frac{360 - \delta_{max}}{360 + \delta_{max}} \times 100 \qquad \text{(Eq. 4-3)}$$

where δ_max is the maximum difference between the relative rotor angles across all generators within the simulation timeframe.

The proposed index value can vary between -100 to 100. For index values of greater than zero the system is stable and higher values indicate the system is more secure. For index values of less than or equal to zero, the system is unstable i.e. at least one generator loses synchronism following a contingency, and larger negative values do not indicate if the system is more or less unstable.

4.2.1.3 LOW CARBON LIVING SCENARIO

4.2.1.3.1 ANALYSIS BY SNAPSHOT TYPE

Figure 4-20 presents the results of applying the angle margin index to each of the 36 snapshots under study for each of the 306 contingencies. Each box plot represents the distribution of the angle margin results for each hour except for unstable results that are excluded from these distributions and plotted as dots.

From Figure 4-20 it can be seen that four unstable cases were reported by these studies. All of these cases are for contingency 9, which is a fault on the AC line connecting the proposed Celtic interconnector to the system and occurred for Type 5, these cases are reviewed in more detail in the following subsection.

Beyond these unstable cases, there is no indication of a consistent trend in angle margin for any of the types. However, certain hours do not exhibit noticeably different angle margin ranges than the other hours in their type. Whilst these hours were stable for every contingency the variation did require further investigation.

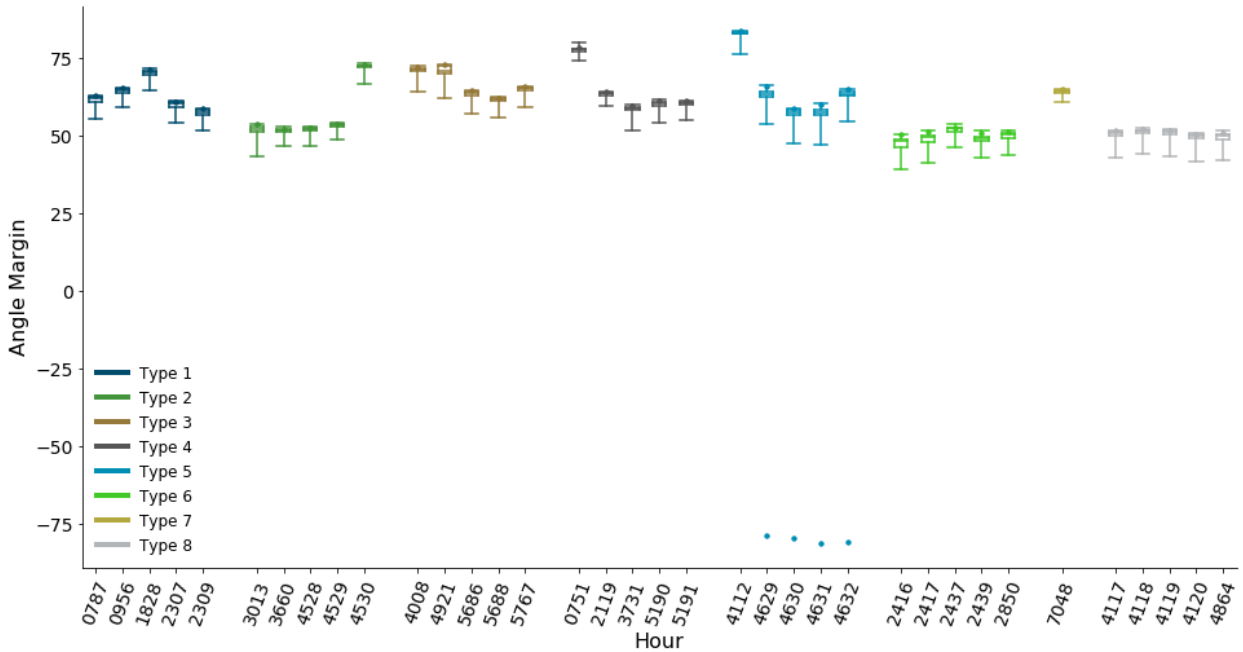

FIGURE 4-20: DISTRIBUTION OF ANGLE MARGINS REPORTED FOR EACH CONTINGENCY GROUPED BY SNAPSHOT FOR THE LOW CARBON LIVING SCENARIO

Table 4-3 summarises the highest and lowest angle margins for Hours 3013 and 4530 while Figure 4-21 shows the simulation results for the relative machine angles. Hour 3013 behaves in a consistent fashion with the other Type 2 hours while 4530 had higher angle margin values for all contingencies.

TABLE 4-3: ANGLE MARGIN EXAMPLES

	Highest Angle Margin		Lowest Angle Margin	
Hour	**Index**	**Contingency**	**Index**	**Contingency**
3013	53.85	270	43.57	68
4530	73.42	48	66.78	10

Comparison of the highest and lowest angle margin results for these hours reveals two key outcomes 1) that notable oscillations emerge in the rotor angles for the high margin cases and 2) that the absolute angle margin is heavily dependent upont the initial angles of the generators.

As such, it is a feature of the angle margin index that, depending upon the iniital angle of the machines certain hours have rather differetn ranges of angle margin index. Whilst the large separation in angles is indicative of a system under more angular strain, it can be seen here that this reduced angle margin has, in this case not indicated that the system is approaching a loss of synchronism due to a scarcity in synchronising torque. Therefore, the fluctiation in angle margin between approximatley 40 and 70 that is observed in Figure 4-20 indicates that there is no global scarcity of sychronising torque for the contingencies considered here.

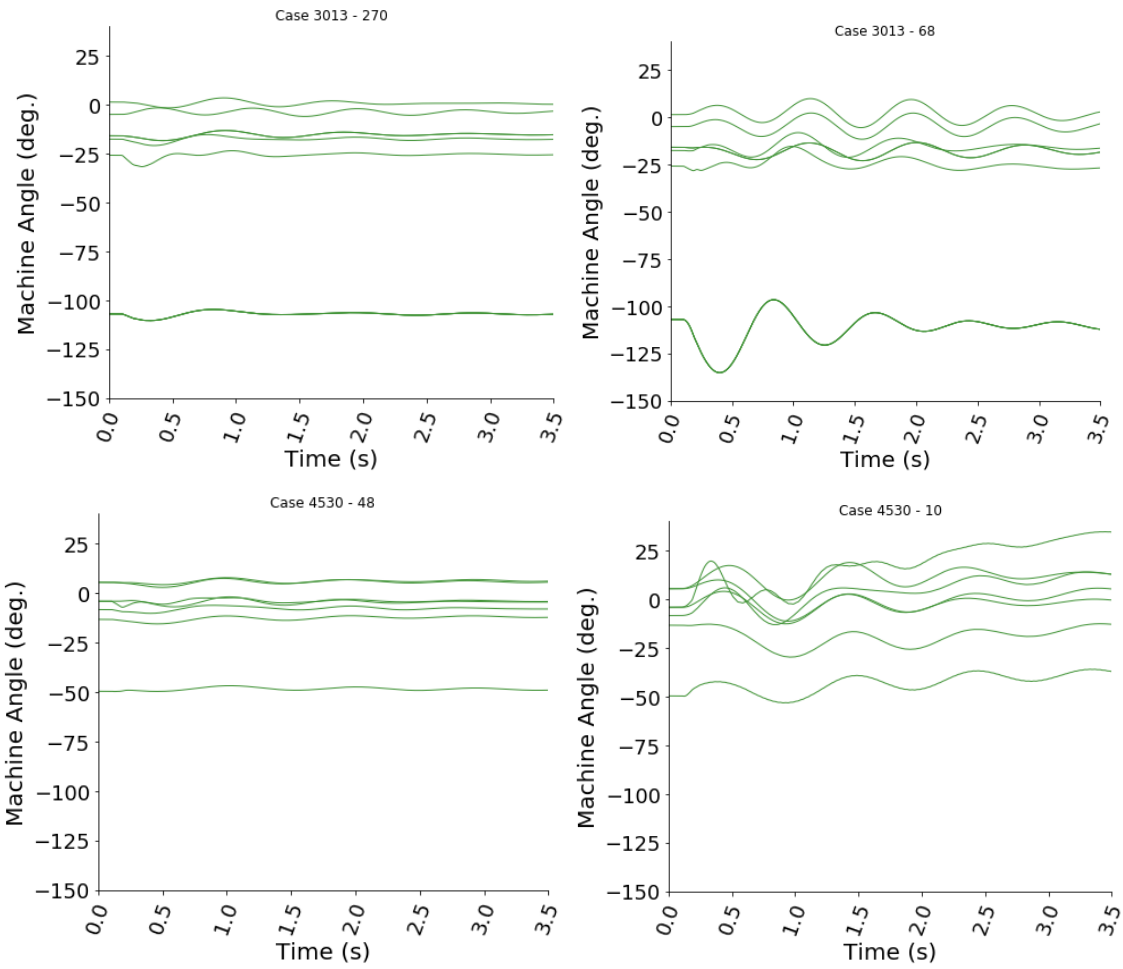

FIGURE 4-21: MACHINE ANGLES FOR HOURS 3013 AND 4530 FOR SMALLEST AND LARGEST ANGLE MARGINS REPORTED

4.2.1.3.2 UNSTABLE CASES

Whilst the results presented in the previous section indicate that there is not a global scarcity of sychronising torque for the contingencies considered here, the unstable cases clearly indicate a localised scarcity as the system is not N-1 secure. This section explores the root cause of these unstable cases in order to illustrate the nature of this localised scarcity. Contingency 9 is a line fault on the AC collector network of the proposed Celtic HVDC interconnector, which is assumed to be in service in both the low carbon living and steady evolution scenarios.The four hours for which contingency 9 is unstable are 4629, 4630, 4631 and 4632 and the instability occurs because a single generator (G1) loses synchronism. G1 is connected close to the proposed Celtic HVDC onshore substation and on review the distinguishing feature of these hours is that the Celtic interconnector is on high import. The only other hour under study for which Celtic is on high import was hour 4864. As such, a comparison of the unstable hours and hour 4864 was performed to understand the nature of the instability. For the sake of brevity only hour 4629 is presented for this comparison, but the similarity of the unstable hours means that the conclusions are drawn.

TABLE 4-4: SUMMARY OF CASES UNDER DETAILED STUDY

Hour	Celtic Import (MW)	SNSP (%)	Inertia (MWs)	G1 Dispatch
4629	700	33	20500	Close to Max
4864	700	80	20400	Close to Min
4864 - HI	700	77	20400	Close to Max

Table 4-4 presents a comparison of high level measures for the two scenarios. It can be seen that the unstable case has lower SNSP and demand but similar inertia. The hours have various differences but the most important is that the dispatch of the unit that was unstable (referred to here as G1) has been reduced in hour 4864. Also a small peaking unit (S5) was synchronised close to the unstable unit in 4864. To accommodate the reduced dispatch of the unstable unit, a new hour was created, 4864 – HI. The demand has been increased to accommodate moving the unstable unit back to close to its maximum generation this reduced the SNSP.

The machine angles for these three cases are presented in figure. From this it can be seen that both versions of hour 4864 are stable, although 4864 – HI experiences larger swings in the machine angle of G1, which is unsurprising given the known link between angular stability and machine loading.
Figure 4-24 and Figure 4-25 present the angles of the large and small synchronous machines in detail. From this it can be seen that G2 and S5 appear to support G1 and prevent it from becoming unstable. Based on this, it can be concluded that the localised scarcity is the synchronising torque between G1 and the rest of the system, which has been exposed by the loss of infeed from Celtic and is sufficiently sensitive that changes to a single unit may be sufficient to mitigate or exacerbate the scarcity.

4.2.1.3.3 MODIFIED CASE WITH CELTIC ON EXPORT

To further investigate the sensitivity to the loss of import, hour 4629 was modified to have the Celtic interconnector exporting power instead of importing power. This was achieved by increasing wind generation. The results of this are presented in Figure 4-22 and it can be seen that the system is stable. Note, the angle margin index is 69.55 here and G1 is marked in dark green.

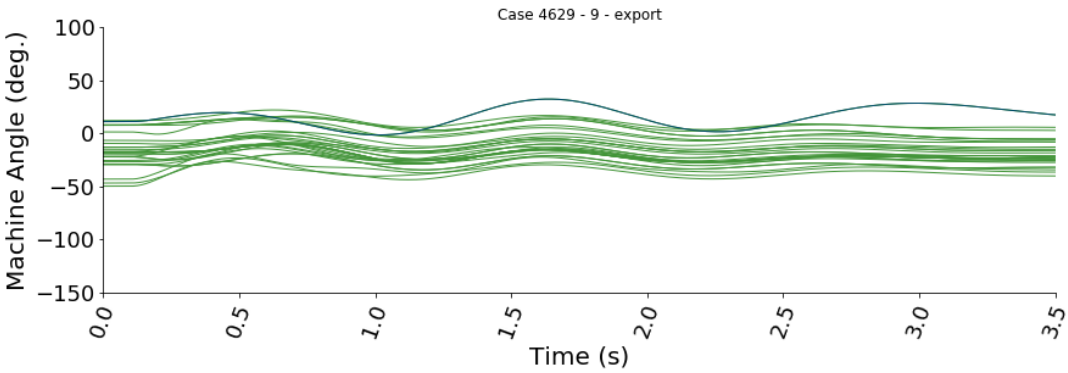

FIGURE 4-22: RELATIVE MACHINE ANGLES FOR CASE 4629 WHEN CELTIC IS ON EXPORT INSTEAD OF IMPORT

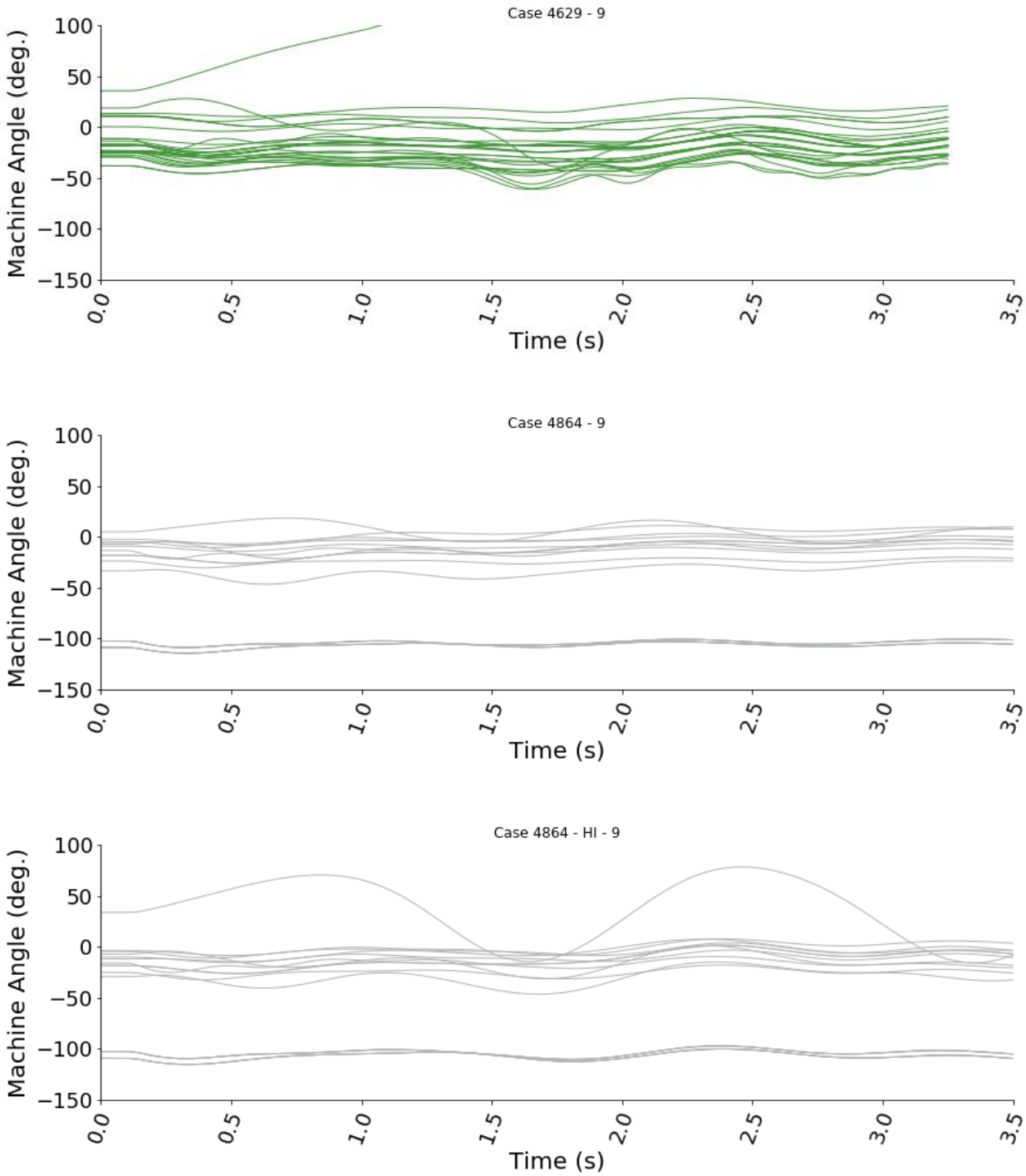

FIGURE 4-23: RELATIVE MACHINE ANGLES FOR CASES UNDER DETAILED STUDY

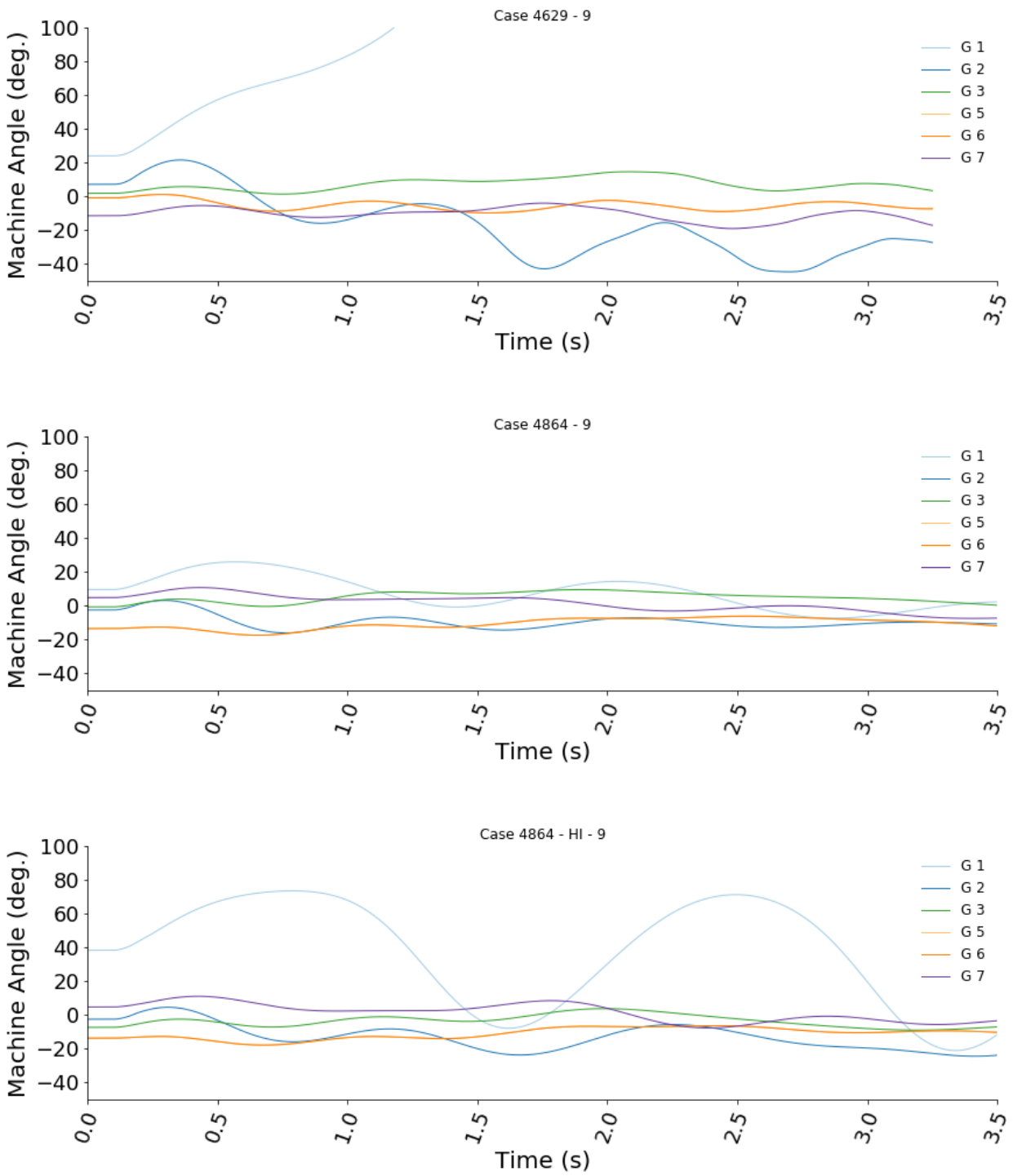

FIGURE 4-24: RELATIVE MACHINE ANGLES FOR LARGE GENERATORS IN CASES UNDER DETAILED STUDY

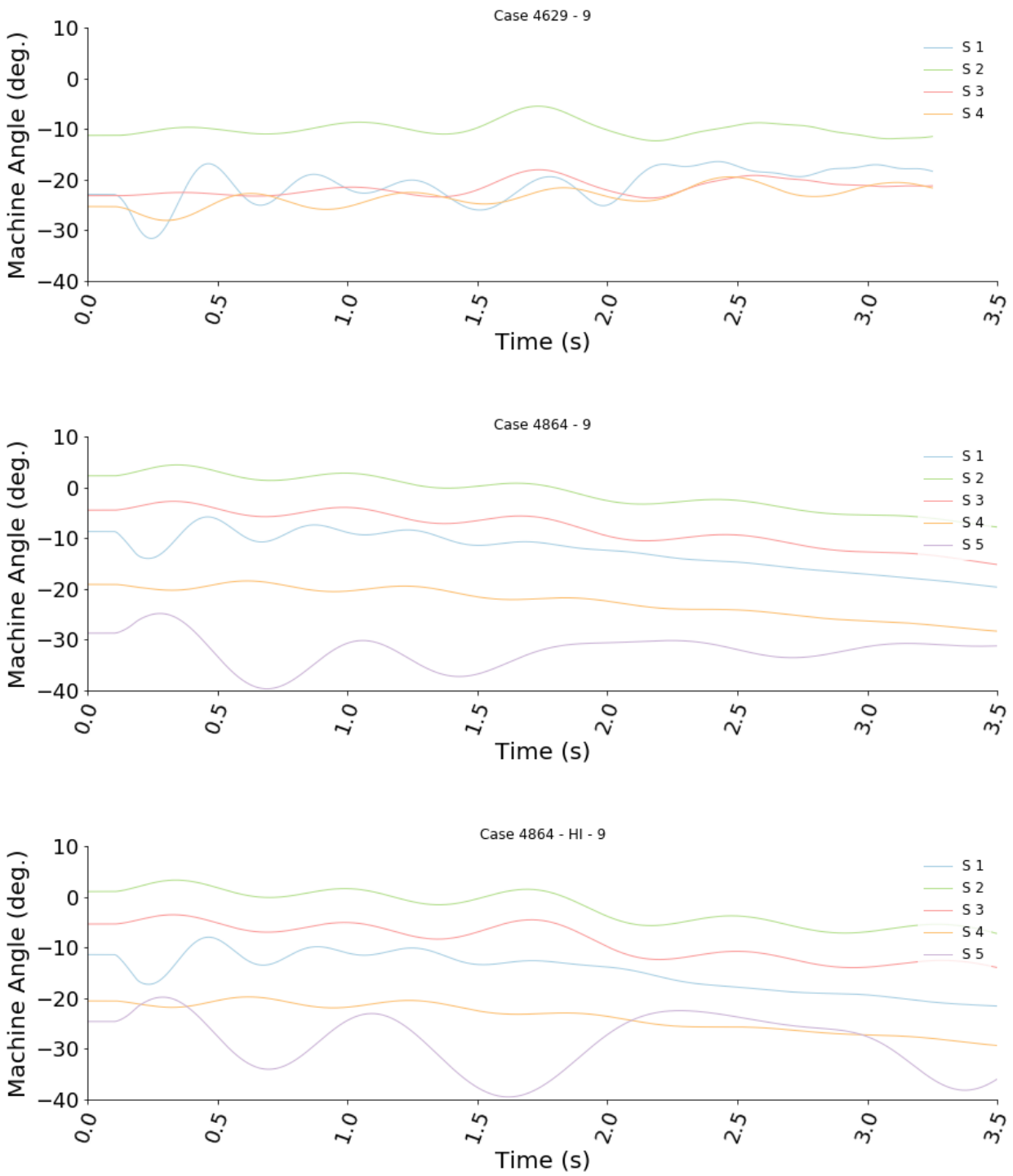

FIGURE 4-25: RELATIVE MACHINE ANGLES FOR SMALL GENERATORS IN CASES UNDER DETAILED STUDY

4.2.1.3.4 ANALYSIS BY CONTINGENCY

Figure 4-26 presents the results of applying the angle margin index to the 36 snapshots selected for the low carbon living scenario. Box plots are used to present the distribution of the angle margin for each contingency (each box plot represents 36 data points, one for each hour studied). The unstable cases related to contingency 9 are omitted here to focus upon any broader trends and these cases are dealt with in detail in the previous section. No real trend is apparent and the angle margin is driven almost entirely by the hour under study. Contingency 9 has no tendency toward lower angle margins even though it generated the only unstable cases. As such it can be concluded that there is no localised scarcity based solely on the location of the contingency and that the localised scarcity observed in the previous section is driven by a combination of the contingency location and the dispatch/commitment of synchronous machines that are close to this location for the hour under study.

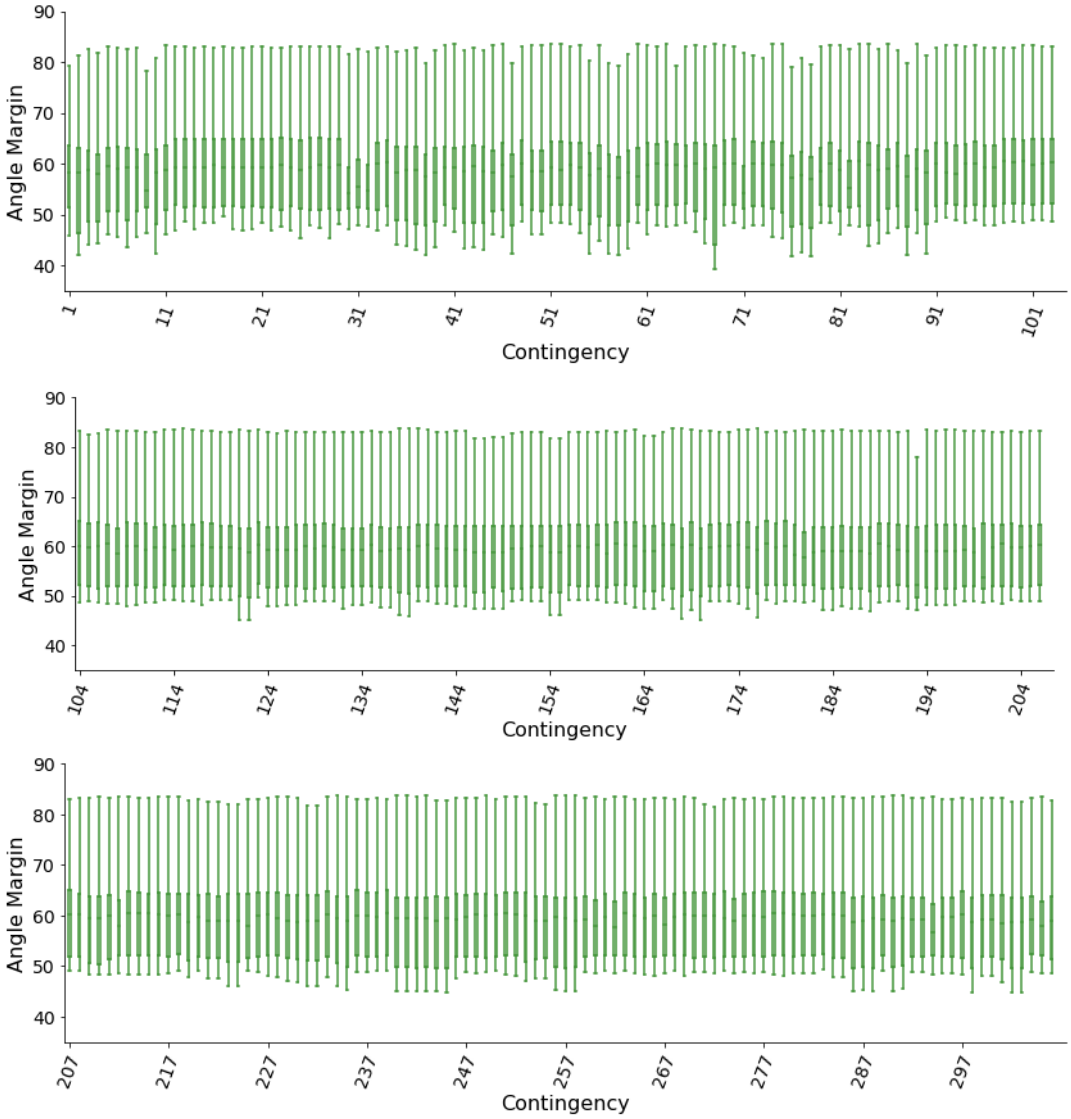

FIGURE 4-26: DISTRIBUTION OF ANGLE MARGIN REPORTED FOR EACH SNAPSHOT GROUPED BY CONTINGENCY FOR THE LOW CARBON LIVING SCENARIO

4.2.1.4 STEADY EVOLUTION SCENARIO

4.2.1.4.1 ANALYSIS BY SNAPSHOT TYPE

Figure 4-27 presents the results of applying the angle margin index to each of the 40 snapshots under study for each of the 305 contingencies. Each box plot represents the distribution of the angle margin results for each hour except for unstable results that are excluded from these distributions and plotted as dots.

From Figure 4-27 it can be seen that five unstable cases were reported by these studies. As in the low carbon living scenario, all of these cases are for contingency 9, which is a fault on the AC line connecting the proposed Celtic interconnector to the system and the unstable hours have high import on Celtic and high dispatch of G1.

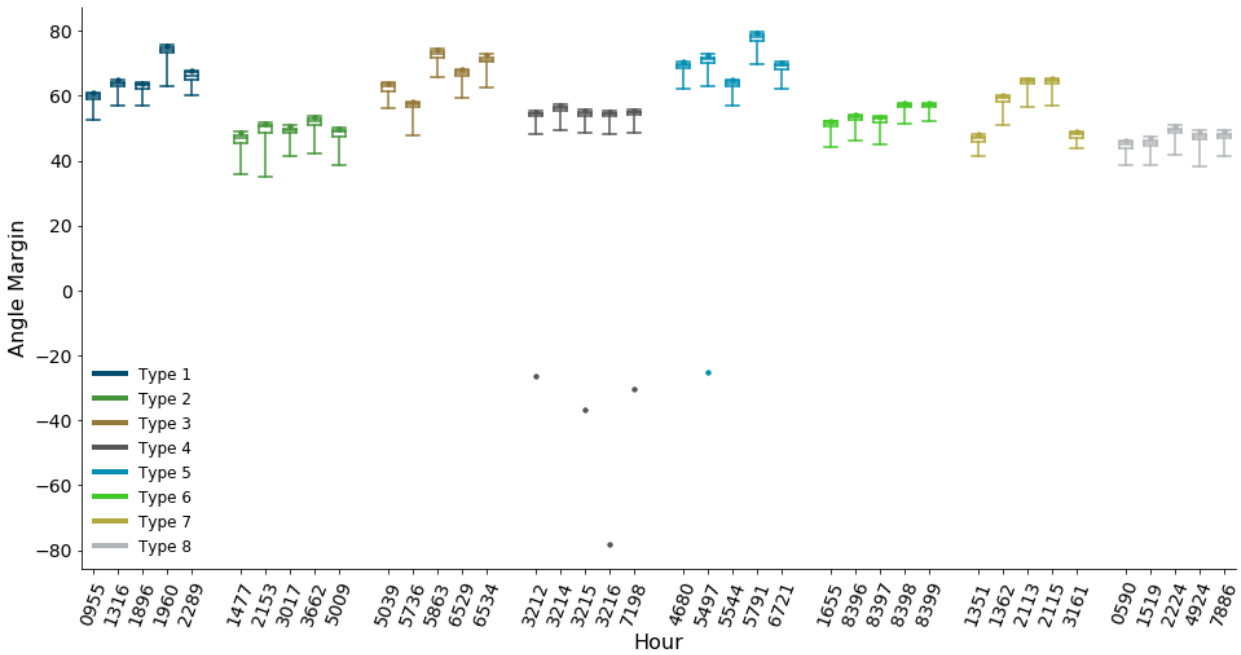

FIGURE 4-27: DISTRIBUTION OF ANGLE MARGINS REPORTED FOR EACH CONTINGENCY GROUPED BY SNAPSHOT FOR THE STEADY EVOLUTIION SCENARIO

4.2.1.4.2 ANALYSIS BY CONTINGENCY

Figure 4-28 presents the results of applying the angle margin index to the 40 snapshots selected for the steady evolution scenario. Box plots are used to present the distribution of the angle margin for each contingency (each box plot represents 36 data points, one for each hour studied). The unstable cases related to contingency 9 are omitted here to focus upon any broader trends and these cases are dealt with in detail in the previous section.
As in the low carbon living scenario these results demonstrate no particular trend or variation between contingencies.

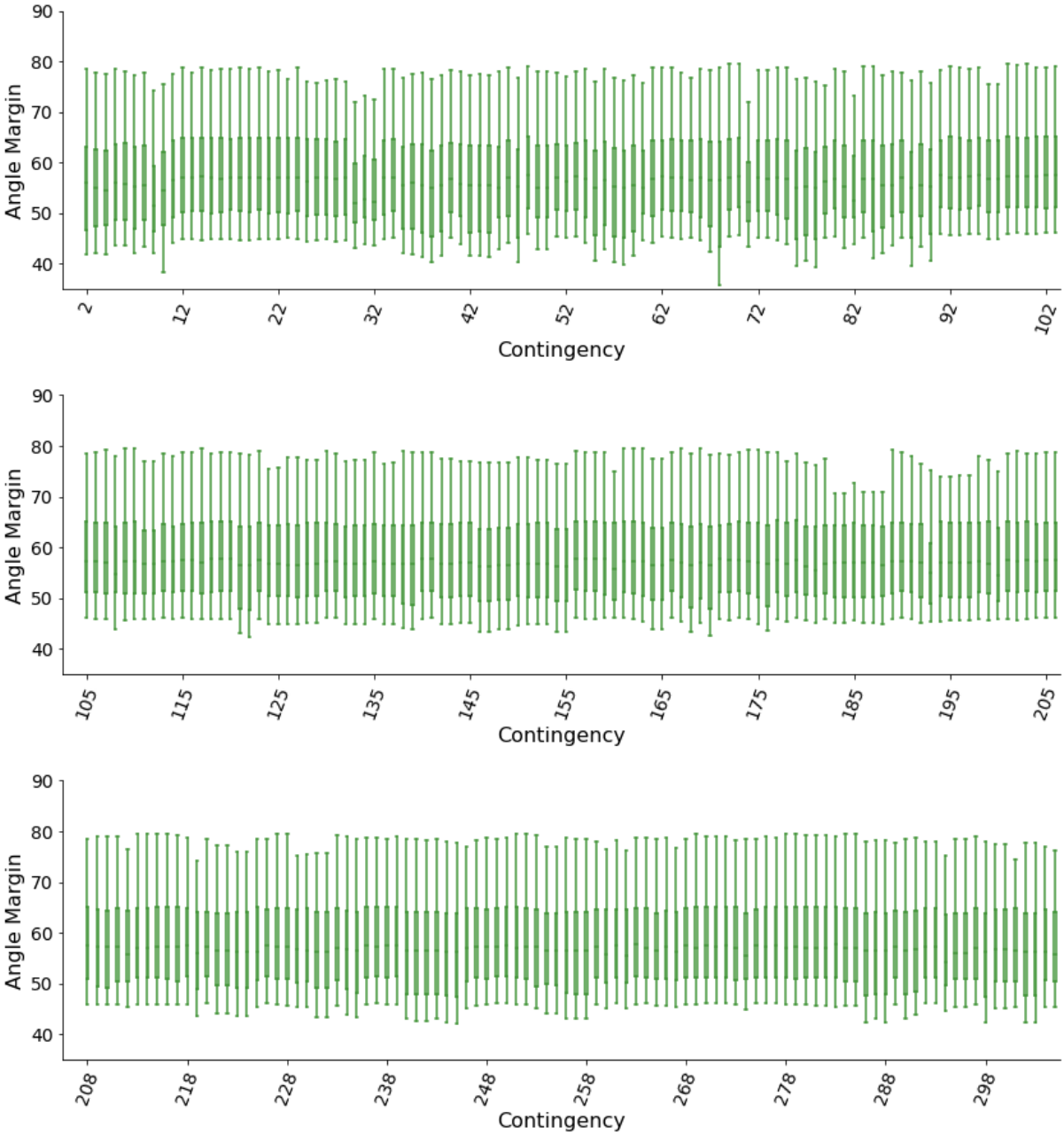

FIGURE 4-28: DISTRIBUTION OF ANGLE MARGIN REPORTED FOR EACH SNAPSHOT GROUPED BY CONTINGENCY FOR THE STEADY EVOLUTION SCENARIO

From the studies presented here for three phase line faults there is no apparent global scarcity of synchronising torque, as there is no hour of operation with particularly poor angle margin. However, a localised scarcity has been identified that caused a generator to lose synchronism when it was heavily loaded and exposed to a large loss of infeed close to its point of connection. Note, outside of these unstable cases the contingency that

triggered the instability and the generator that became unstable showed no particular tendency toward instability.

The specific nature of the localised scarcity observed here indicates that for the All Island system the scarcity of synchronising torque may manifest as highly local issues that are sensitive to specific details of operation, which cannot be identified from the existing system level measures, like SNSP and inertia. In fact, for the localised scarcity identified here these system level measures were found to be misleading (a high SNSP case is stable and a low SNSP case with similar inertia is unstable).

These localised scarcities will likely only emerge for specific combinations of unit commitment and contingency, so the failure for others to be identified here should not be misinterpreted as an absence of similar scarcities. Rather, the snapshot selection process was unable to capture the conditions that may expose the system to such scarcities as metrics for these conditions are not available. As such new metrics should be explored that can predict the potential for localised scarcities and these should likely focus on identifying the proximity of generation assets to the contingency while considered the dispatch and dynamic coupling of these units.
Furthermore, these results indicate that future studies may be advised to consider loss of infeed events when assessing the transient stability of the system, as this appears to have played a pivotal role in exposing the localised scarcity.

The lack of global scarcity, which would manifest as uncontrolled system separation due to generator groups losing synchronism, is not entirely surprising. This is because under current operation the All Island system has no clear inter area mode (a typical indicator of a tendency toward generator groups forming) and both scenarios analysed here included the North-South interconnector project. This project is a proposed 400 kV AC link between Ireland and Northern Ireland which, if constructed, would dramatically reduce the impedance between the generation and load centres in the two jurisdictions (Ireland and Northern Ireland) further reducing the likelihood of any such mode emerging.

4.2.2 TRANSIENT STABILITY MARGINS

The transient stability results presented here assume that the studied contingencies are cleared in the time required under current protection requirements that are based on extensive experience with existing operation. However, the longer it takes to clear a fault the more severe the impact that fault will have on the system. Furthermore, the longer a fault takes to clear the more likely it is that a generator will become unstable, as the accelerating torque applied to it during the fault has caused it to exceed its critical angle and this is commonly assessed using the equal area criterion.

The transient stability margin can be measured by the difference between the existing expected clearance time and the critical clearing time for a given contingency (the clearing time required to ensure system stability). This margin is of interest as operating with reduced numbers of synchronous machines is anticipated to reduce the critical clearing time and thereby the stability margin.

The critical clearing time is determined by the first generator to become unstable and generators are more likely to remain stable if they continue to transfer electrical power to the network during the fault, as the imbalance between mechanical and electromagnetic torque will be reduced and thereby the accelerating torque applied to the machine will be reduced. When a fault is remote from a generator it will have very little impact on the electromagnetic torque of the machine, as it has little impact on the impedance between the machine and the load it is serving. As such, many faults will have long critical clearing times as they are remote from generators and it is unlikely that a global scarcity in stability margin can occur. However, the sensitivity of the critical clearing time to the pre-fault loading of a machine and the proximity of the fault to a generator means that localised scarcities can emerge.

4.2.2.1 CRITICAL CLEARING TIME DETERMINATION

The critical clearing time (CCT) is the longest clearing time for which the system will remain stable. The CCT is obtained through a binary search method, whereby, a fault clearance range and set threshold levels are pre-specified. The stability margin and the threshold applied to check for instability are based on the angle margin index as described above. The binary search applied here was for between 4 cycles and 70 cycles to 1 cycle precision. This means that the maximum CCT result will be 70 cycles and the minimum result will be 4 cycles (even if the case is unstable for a 4 cycle CCT).

Given the current protection design in the All Island system most faults are expected to be cleared within 4 to 8 cycles. The worst case fault clearance time, allowing for a complete failure of primary and redundant communications, the failure of any accelerate tripping schemes and a zone 2 fault, is 25 cycles. This is an extreme worst case that is unlikely to occur but provides a useful reference point for when CCTs may potentially require further study.

4.2.2.2 CONTINGENCIES STUDIED

The availability of dynamic voltage control is studied for the snapshot hours described in the methodology for 306 bolted three phase line fault contingencies. These line faults are in the middle of the line and are cleared by simultaneously opening the breakers at each end of the line, with a clearance time of between 4 and 8 cycles. The contingency locations are defined using the same methodology applied for the existing online dynamic security assessment that is performed every 15 minutes by EirGrid and SONI using the Wind Strength Assessment Tool

(WSAT). This means that the line faults considered can result in the separation of HVDC interconnectors from the system (when the line that serves as the HVDC interconnectors AC collector network is lost) but not the separation of synchronous generators.

Note, in the results presented for Low Carbon Living there are 306 contingencies but for steady evolution there are only 305. This is because contingency 1 is for the AC collector network of the Greenlink HVDC project, which is not in place for steady evolution. However, the numbering of the contingencies remains the same between these cases for consistency; so, contingency 1 has no results for steady evolution.

4.2.2.3 LOW CARBON LIVING SCENARIO

4.2.2.3.1 ANALYSIS BY SNAPSHOT TYPE

Figure 4-29 presents the results of applying the CCT binary search to each of the 36 snapshots under study for each of the 306 contingencies. Each box plot represents the distribution of the CCT results between 4 and 70 cycles and the number of 70 cycle and 4 cycle results for each hour are marked on the plot above and below the box pot. The dots on each box plot leg mark the 5th and 95th percentile.

It was found that, 76% of the contingencies have CCTs of 70 cycles, which indicates that there is no global scarcity in terms of transient stability margin. This, as expected indicates the lack of a global scarcity in stability margin for the contingencies considered. However, the results do indicate the emergence of some localised scarcities. As in other cases there is also some degree of volatility within the types, suggesting that the metrics used to define these types does not assess the details required to faithfully reflect these localised scarcities.

Firstly, the 4 cycle CCTs recorded for hours 4629, 4630, 4631 and 4632 relate to a single contingency that was unstable in the base case. This is dealt with in detail in the section on transient rotor angle stability but does indicate that cases exist with negative stability margins. The box plots show that no hours of operation have a significant number of contingencies for which the CCT is approaching the 4 cycle expected clearing time. However most hours of operation have clusters of outliers that are below 10 cycles and half of the hours studied have a median that is below the absolute worst case clearing time of 25 cycles. As such these results do appear to indicate that a localised scarcity of stability margin is emerging.

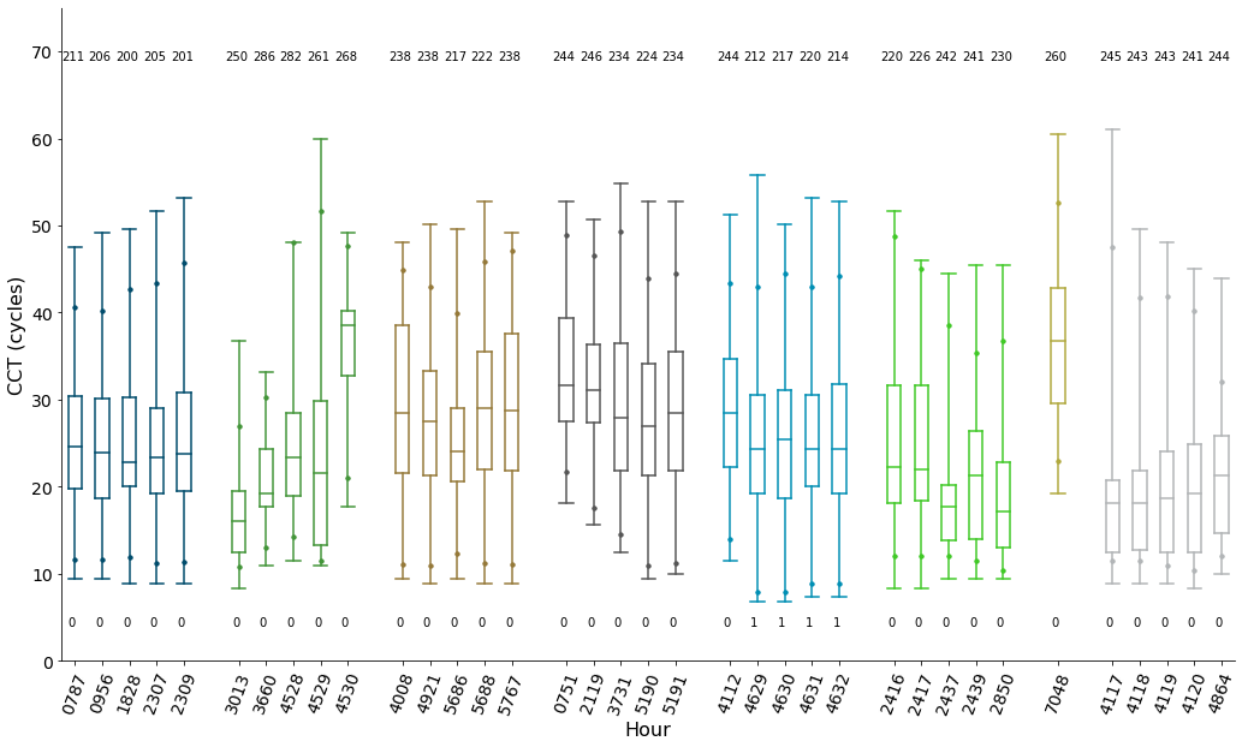

FIGURE 4-29: DISTRIBUTION OF THE CRITICAL CLEARING TIMES BETWEEN 70 AND 4 CYCLES FOR EACH HOUR FOR LOW CARBON LIVING. THE NUMBER OF 70 CYCLE AND 4 CYCLE CRITICAL CLEARING TIMES ARE RECORDED ABOVE AND BELOW EACH BOX PLOT

4.2.2.3.2 ANALYSIS BY CONTINGENCY

Figure 4-30 presents the results of applying the CCT binary search to each of the 40 snapshots under study for each of the 305 contingencies. Each box plot represents the distribution of the CCT results between 4 and 70 cycles. Unlike the analysis by type plot the number of CCTs reported at 70 cycles are not presented on the plot, due to a lack of space.

These plots show that many contingencies had all of their CCTs at 70 cycles (the maximum reported value) and this supports the conclusion that there is no global scarcity (these appear as green dots in the plot). However, as in the analysis by type there are indications of localised scarcities, many of the contingencies have a broad spread of CCT between approximately 10 and 70 indicating that under certain operating conditions they would require further study.

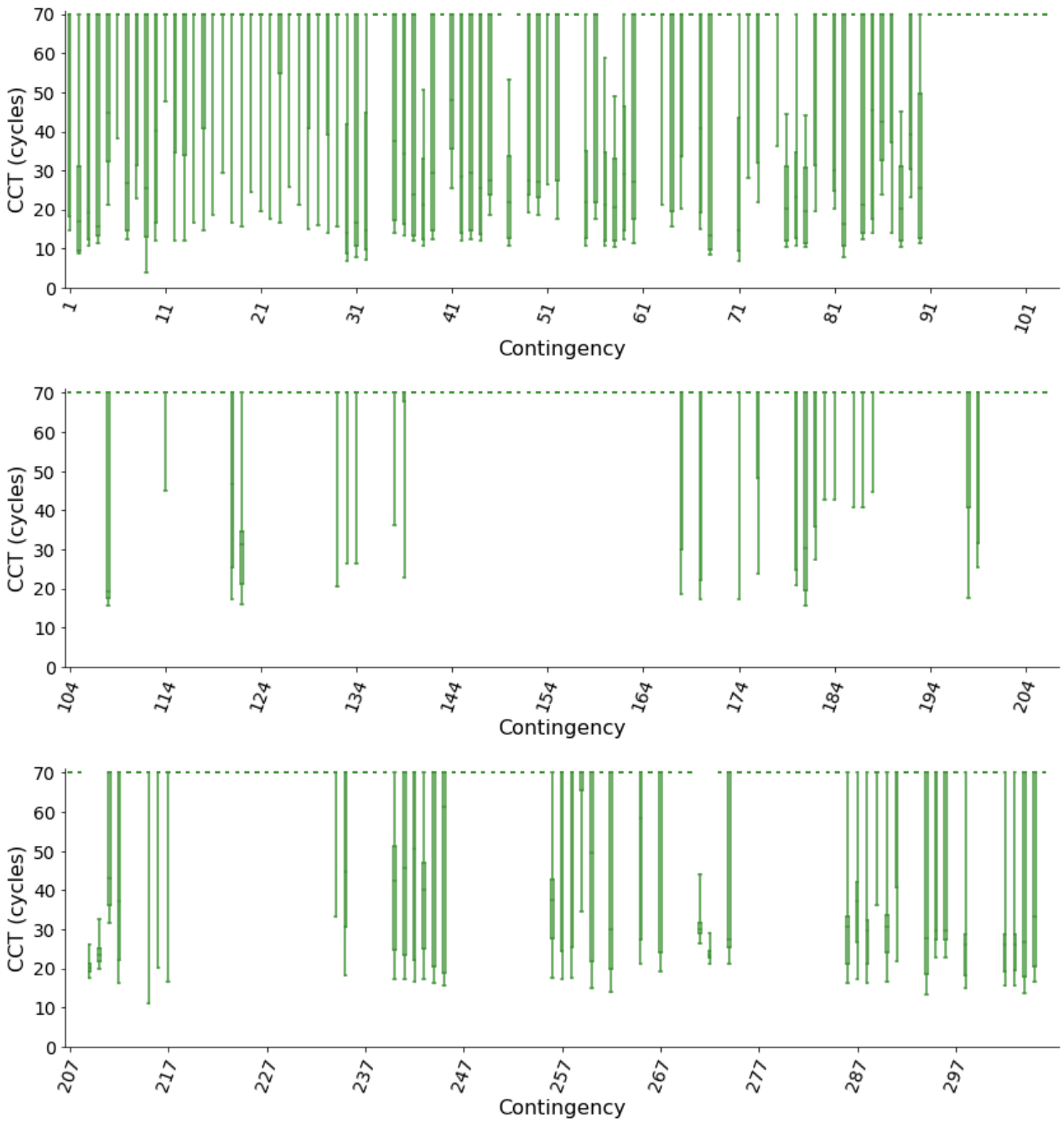

FIGURE 4-30: DISTRIBUTION OF THE CRITICAL CLEARING TIMES FOR EACH CONTINGENCY FOR THE LOW CARBON LIVING SCENARIO

Furthermore, 24 contingencies have medians that are below 25. These contingencies and the small number of contingencies with very little variation in their CCT are for lines that are close to generators that committed in the majority of the snapshot hours and this would indicate that, as may be expected, further study of CCTs and these localised scarcities in stability margin should focus on specific generator and contingency combinations, rather than a system wide approach.

4.2.2.4 STEADY EVOLUTION SCENARIO

4.2.2.4.1 ANALYSIS BY SNAPSHOT TYPE

Figure 4-31 presents the results of applying the CCT binary search to each of the 40 snapshots under study for each of the 305 contingencies. Each box plot represents the distribution of the CCT results between 4 and 70 cycles and the number of 70 cycle and 4 cycle results for each hour are marked on the plot above and below the box pot. The dots on each box plot leg mark the 5th and 95th percentile.

It was found that, 65 % of the contingencies have CCTs of 70 cycles, which indicates that there is no global scarcity in terms of transient stability margin. However, it is a noticeable reduction compared to low carbon living.

As for low carbon living, these results indicate the emergence of localised scarcities. As in other cases there is also some degree of volatility within the types, suggesting that the metrics used to define these types does not assess the details required to faithfully reflect these localised scarcities, a particular example of which is hour 2153.

As for low carbon living, the 5 cycle CCTs relate to a single contingency that was unstable in the base case. This is dealt with in detail in the section on transient rotor angle stability but does indicate that cases exist with negative stability margins.

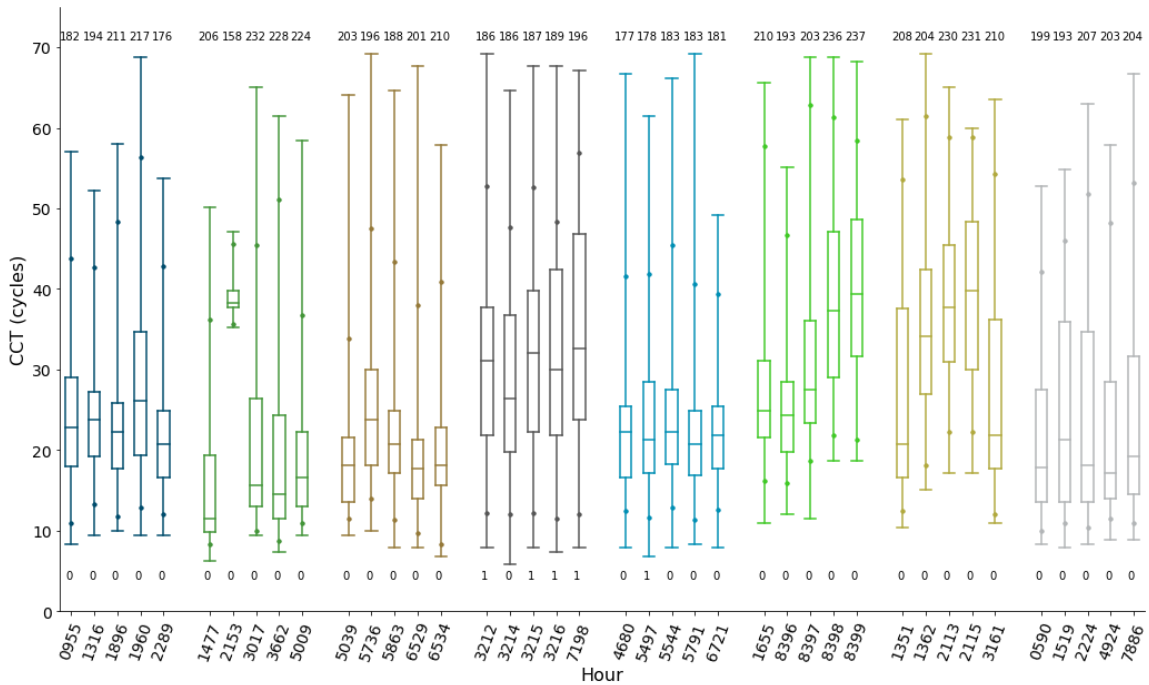

FIGURE 4-31: DISTRIBUTION OF THE CRITICAL CLEARING TIMES BETWEEN 70 AND 4 CYCLES FOR EACH HOUR FOR STEADY EVOLUTION. THE NUMBER OF 70 CYCLE AND 4 CYCLE CRITICAL CLEARING TIMES ARE RECORDED ABOVE AND BELOW EACH BOX PLOT

These results show that hour 1477 has just over 25% of its sub 70 cycle CCTs below 10 cycles. This hour is an isolated case, as the other hours are restricted to a few outliers below 10 cycles, as in low carbon living. Furthermore, two thirds of the hours studied have more than 50 % of their sub 70 cycle CCTs below the absolute worst case clearing time of 25 cycles. As such these results do appear to indicate that a localised scarcity of stability margin is emerging and it is more severe in steady evolution than low carbon living.

4.2.2.5 ANALYSIS BY CONTINGENCY

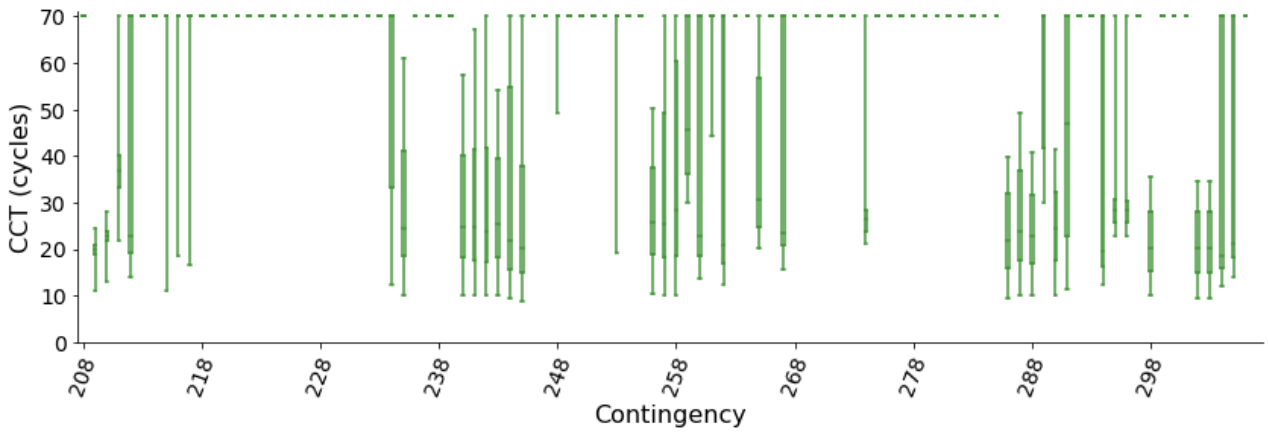

Figure 4-32 presents the results of applying the CCT binary search to each of the 40 snapshots under study for each of the 305 contingencies. Each box plot represents the distribution of the CCT results between 4 and 70 cycles. Unlike the analysis by type plot the number of CCTs at 70 cycles is not presented on the plot, due to a lack of space.

These plots present very similar results as those seen for low carbon living. Many contingencies have no CCTs below 70 cycles and the others mostly have a broad spread of CCT. More contingencies in steady evolution have very concentrated CCTs and 63 of them have medians that are below 25, which is a significant increase when compared to low carbon living. Therefore, these results would indicate that the localised scarcity in angle margin observed here is more severe in the steady evolution scenario than in low carbon living.

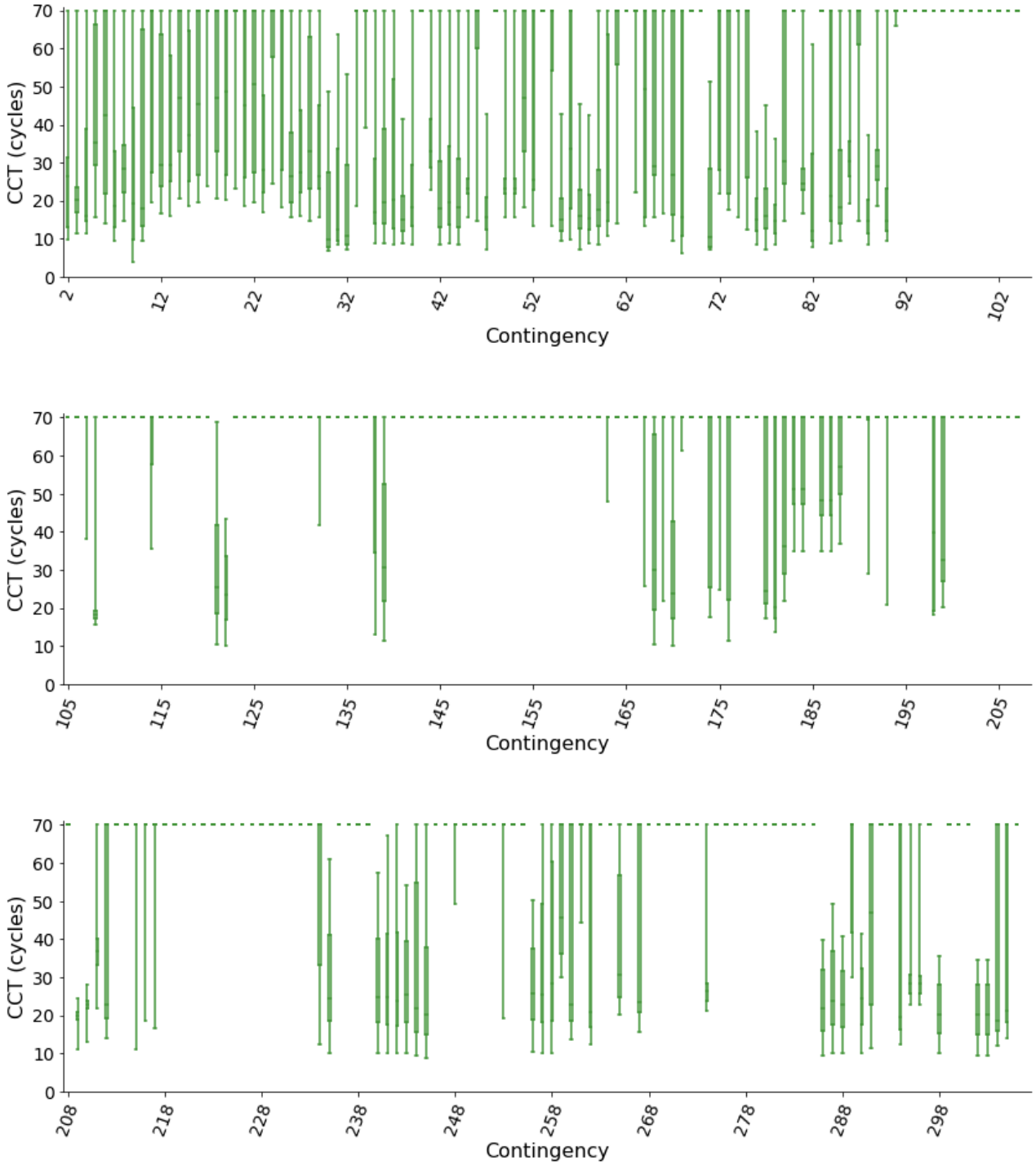

FIGURE 4-32: DISTRIBUTION OF THE CRITICAL CLEARING TIMES FOR EACH CONTINGENCY FOR THE STEADY EVOLUTION SCENARIO

The results presented here indicate that there is no global scarcity of stability margin in either scenario, with both scenarios having more than 65 % of CCTs above the 70 cycle maximum applied for this study. Furthermore, more than half of the CCTs that were below 70 cycles are above the 25 cycle absolute worst case clearing time. As such, most of the contingencies present no indication of any scarcity in angle margin.

However, localised scarcities do appear to be emerging for several combinations of contingencies and generators – when assessed according to the absolute worst case clearing time of cycles. Very few of these localised scarcities are severe enough to have CCTs that encroach upon the 4 cycle expected clearing time. However, a small number of cases for a particular contingency were unstable in the base case, which is a clear indication of a localised scarcity.

Based on the results, future studies addressing the scarcity of critical clearing time may need to be performed; however, they should incorporate the specific study of faults that are close to specific generators for a range of dispatches and system conditions and with proper assessment of the performance of the specific protection in places for those generators for those faults rather than absolute worst case indicator of 25 cycles applied here.

4.2.3 OSCILLATION DAMPING

Some form of oscillation in the rotor angle of machines is almost inevitable after a fault or other disturbance to the system. These oscillations are a natural part of the behaviour of any dynamic system and are not a concern, provided they are sufficiently well damped. In Task 2.3 a settling time of 20 seconds was defined as appropriate, where the settling time is defined here as time required to reach an approximate steady state and an approximate steady state is defined as the peak to peak magnitude of the oscillation remaining below 15 % of its maximum peak to peak magnitude (i.e. the first cycle peak to peak magnitude).

The metric applied here to assess if any oscillation is sufficiently well damped is the decay time. The decay time constant of an oscillation is a function of its natural frequency and damping ratio and is equivalent to the time constant of the exponential decay. Therefore, the oscillation reaches 36.8 % of its initial value after this time. As such, requiring the decay time to be less than a third of the target settling time would seem an effective index for assessing the stability of each oscillatory mode. The decay time is calculated within TSAT using Prony analysis.

Based on these definitions and requirements, the criteria applied here is that the decay time must be less than approximately 7 seconds. Failure to abide by this limit would indicate a scarcity in damping.

4.2.3.1 LOW CARBON LIVING SCENARIO

4.2.3.1.1 ANALYSIS BY SNAPSHOT TYPE

Figure 4-33 presents the results of applying the decay time calculation to the 36 snapshots selected for the low carbon living scenario. Box plots are used to present the distribution of the decay time for each hour (each box plot represents 306 data points, one for each contingency) and the dots on the upper leg each box plot marks the 95th percentile.

A small number of violations can be observed for two Type 1 hours (2307 and 2309); however, it is curious to note that these hours are not dissimilar from 1828 from the system level view. However, they do have the lowest number of synchronous units for Type 1. Indeed, in general, the types with higher medians and outliers would indicate that oscillations are more prevalent in the types with lower levels of inertia but higher numbers of large units, in relative terms (these hours exist in Types 1, 4 and 6).

The results indicate that there is a clear localised scarcity of damping for two hours and an emerging trend of a localised scarcity in other hours.

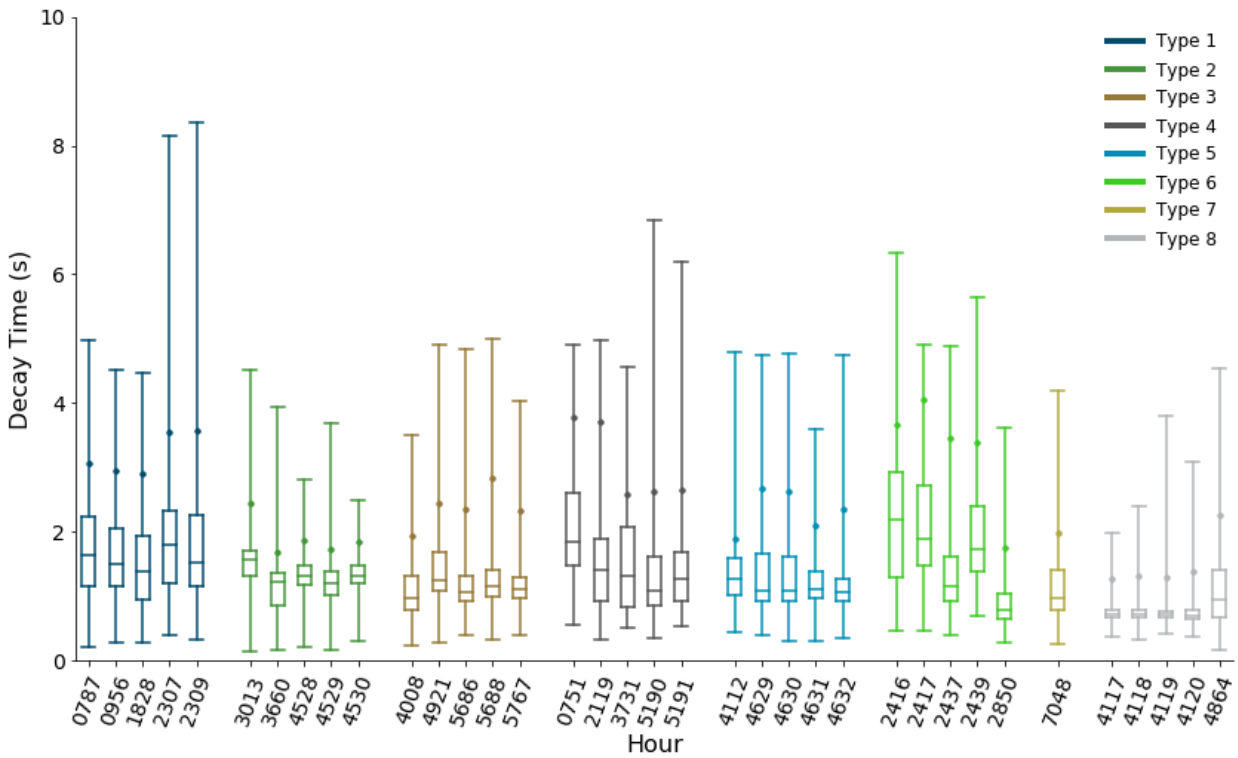

FIGURE 4-33: BOX PLOT OF DECAY TIME FOR LOW CARBON LIVING SNAPSHOTS

4.2.3.1.2 ANALYSIS BY CONTINGENCY

Figure 4-35 presents the results of applying the decay time calculation to the 307 contingencies snapshots selected for the low carbon living scenario. These results indicate that certain contingencies produce the outliers observed in the analysis by type.

Plots for two of these outliers are shown in Figure 4-34 and they reveal that the outliers can be associated with oscillations in specific isolated units. This indicates that certain operating conditions will be exposed to oscillations with poor damping under certain contingencies, which can be characterised as a localised scarcity.

As in the analysis by types most contingencies generate a range of decay times and no contingency has consistently low decay times. Indicating a complex relationship between dispatch and decay time but this is not sufficient to characterise as a global scarcity, as the decay times are sufficiently beneath the 7 second threshold.

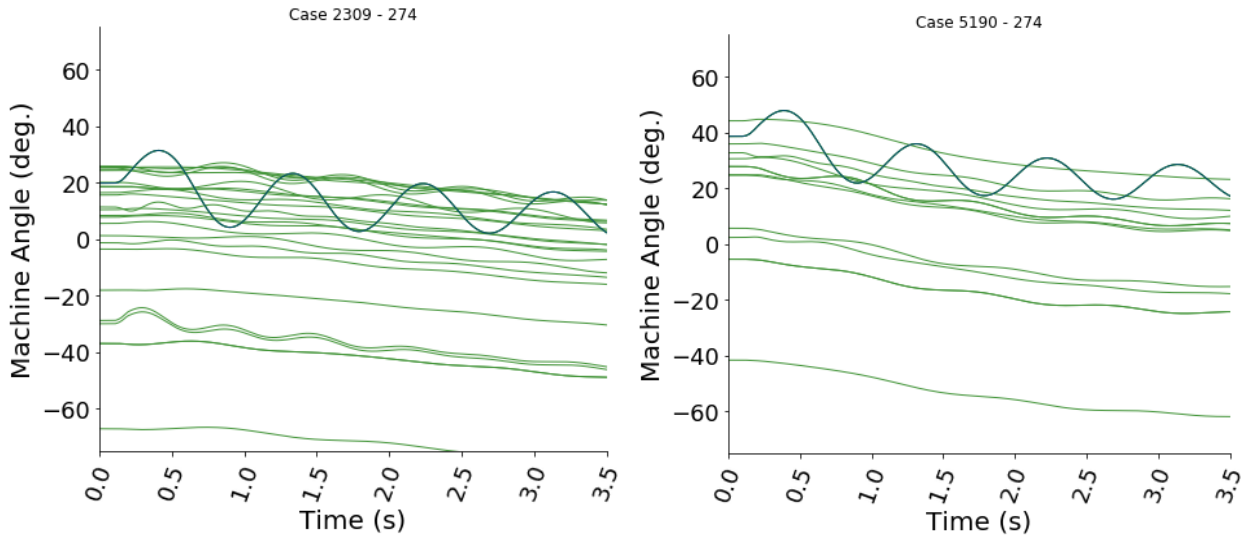

FIGURE 4-34: TIME DOMAIN EXAMPLES FOR OSCILLATION CASE

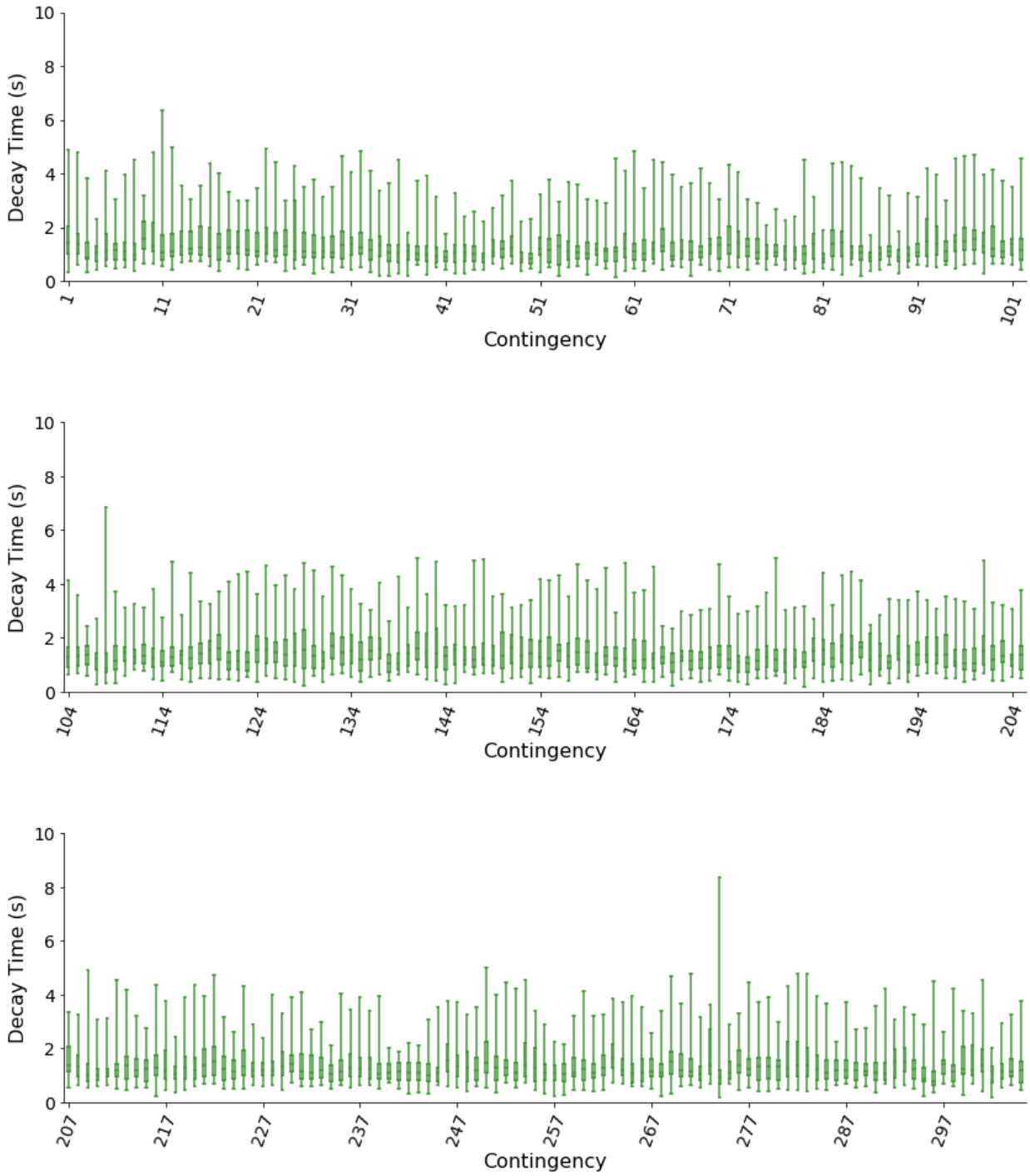

FIGURE 4-35: BOX PLOT OF DECAY TIME BY CONTINGENCY FOR LOW CARBON LIVING SNAPSHOTS

4.2.3.2 STEADY EVOLUTION SCENARIO

4.2.3.2.1 ANALYSIS BY SNAPSHOT TYPE

Figure 4-36 presents the results of applying the decay time calculation to the 40 snapshots selected for the steady evolution scenario. Box plots are used to present the distribution of the decay time for each hour (each box plot represents 306 data points, one for each contingency) and the dots on the upper leg each box plot marks the 95th percentile.

Unlike the low carbon living scenario this reveals that the majority of hours have unacceptable damping, which indicates a potential global scarcity. However, further investigation reveals that these outliers are linked to the same root cause as was observed in low carbon living (isolated units under certain contingencies) and it simply the case that this localised issue emerges more commonly in this scenario.

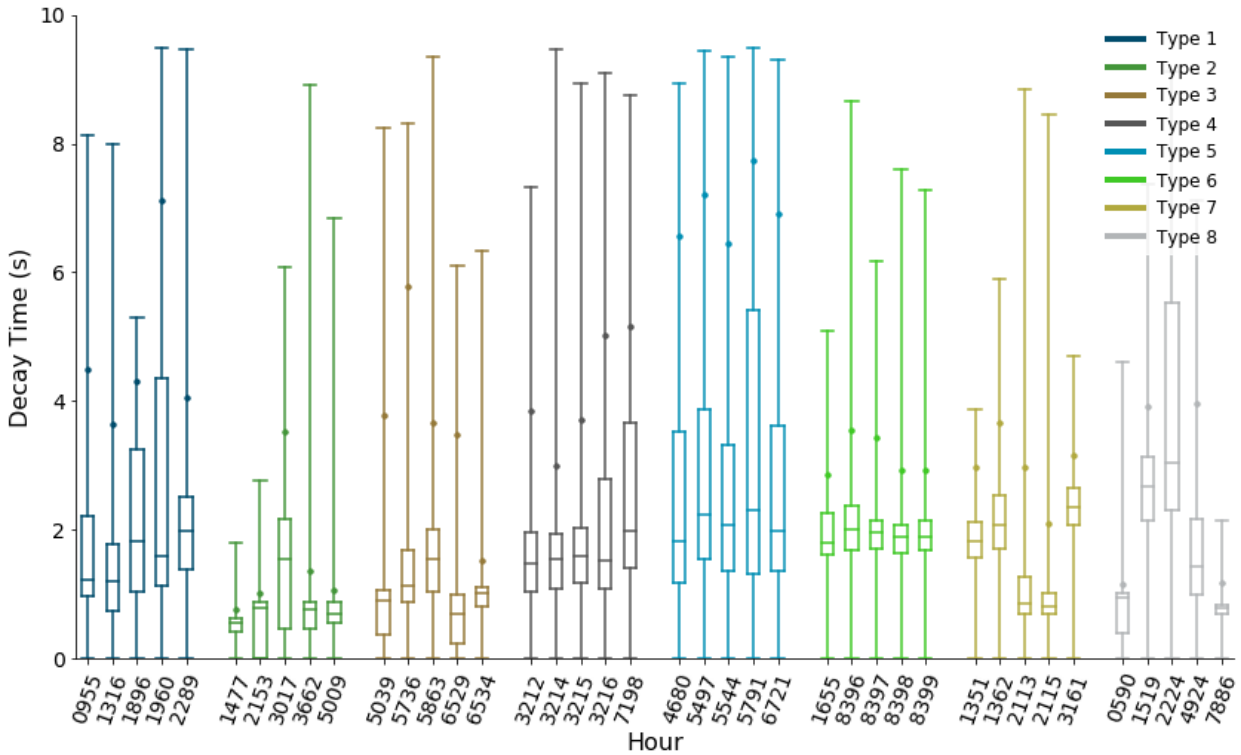

FIGURE 4-36: BOX PLOT OF DECAY TIME FOR LOW CARBON LIVING SNAPSHOTS

4.2.3.2.2 ANALYSIS BY CONTINGENCY

Figure 4-37 presents the results of applying the decay time calculation to the 307 contingencies snapshots selected for the steady evolution scenario. These results indicate that broader range of contingencies produce the outliers observed than was the case in low carbon living. This again can be attributed to specific units, but the broad range of hours and contingencies for which this mechanism occur mean that it should be classified as a global scarcity in this scenario.

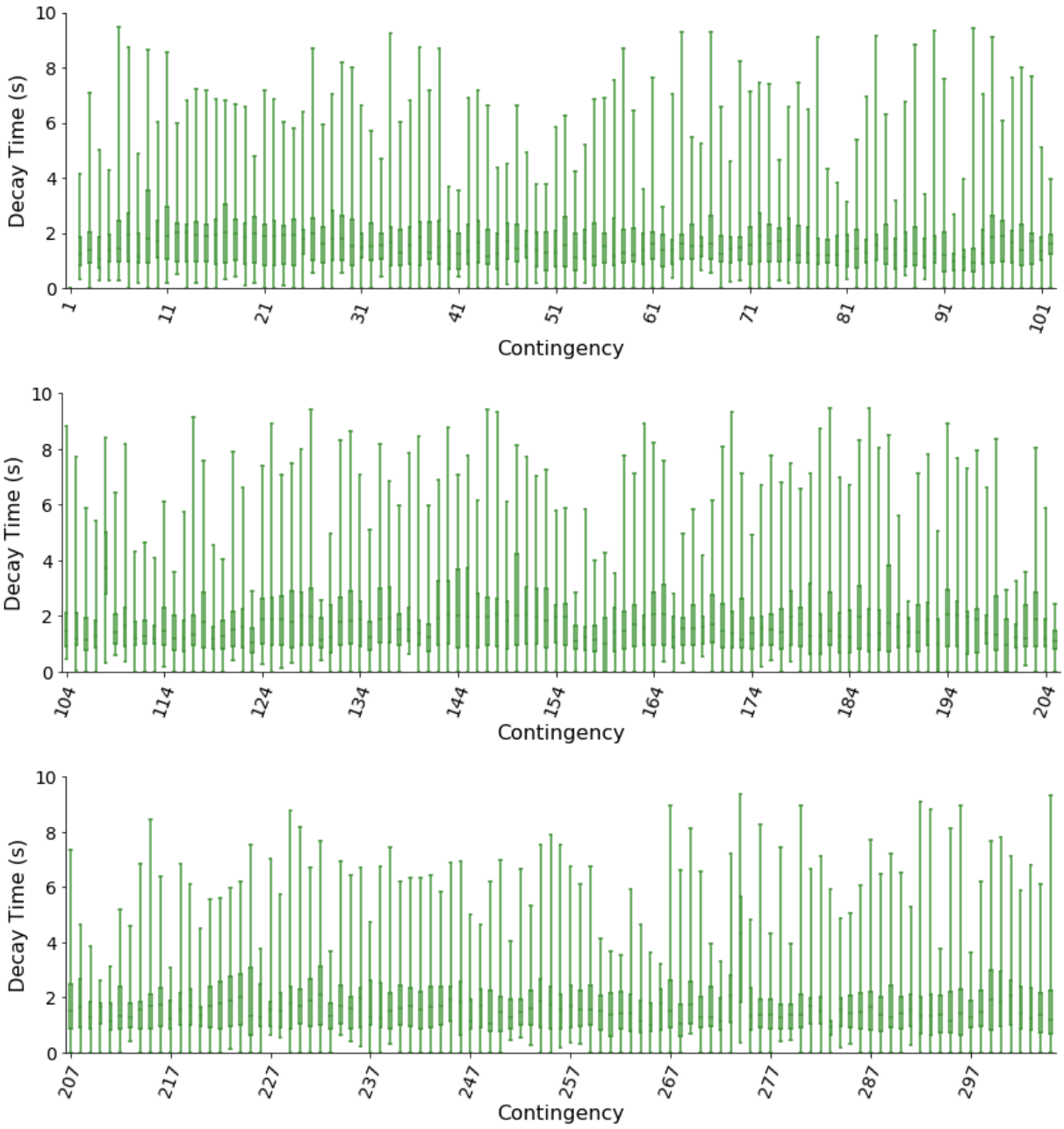

FIGURE 4-37: BOX PLOT OF DECAY TIME BY CONTINGENCY FOR LOW CARBON LIVING SNAPSHOTS

The results presented here indicate a localised scarcity of oscillation damping for low carbon living and a global scarcity of oscillation damping for Steady Evolution. This scarcity can primarily be observed as a local oscillation in one or two units when a contingency occurs close to their point of connection. This conclusion is borne out by the fact that the cases with poor damping are heavily associated with specific contingencies and do not occur in general. As such, the localised scarcity is not driven by SNSP but by the unit commitment schedule and the presence of isolated units that connect through weaker parts of the network, where single contingency can impact the unit most significantly. Whilst these unit commitments with isolated units may be expected to occur more frequently as SNSP increases this does not appear to be the case, as the more severe scarcity is observed for Steady Evolution, which has a lower overall SNSP.

4.3 SUMMARY AND CONCLUSION

Rotor angle stability has been investigated for the continental system, as well as the Ireland & Northern Ireland power system across multiple scenarios and snapshots.

The Ireland and Northern Ireland studies revealed a clear localised scarcity in synchronising torque regardless of scenario that manifested through angular instability of certain generators for certain N-1 contingencies in all scenarios studied. No global scarcity was observed in the Ireland and Northern Ireland studies (which would manifest as inter area oscillations and in the worst case system separation) and the system has no particular recent history of exhibiting such behaviour. This scarcity was not studied for the continental system. This scarcity indicates a need for more detailed study and more specific, localised metrics for assessing the relative security of a case in the future, as the system level measures in use during these studies fail to indicate the presence of this localised scarcity (i.e. it manifested regardless of inertia and SNSP levels). The scarcity would be mitigated by ensuring that any generator synchronised to the system had sufficient level of synchronising torque to the other generators synchronised to the system. This could be resolved through studies to define the sufficient level for each generator and a service through which to incentivise the provision of synchronising torque. Given the nature of the scarcity this service would likely require a locational aspect and the need for the service would be highly sensitive to unit commitment and the contingencies considered, which may have market implications.

A localised scarcity in stability margin (measured through critical clearing time) is emerging for any situation where backup protection is required to operate (e.g. due to protection failures)) in both the Ireland and Northern Ireland studies and the continental system studies. However, there is no global scarcity or localised scarcity in stability margin if primary protection operates as designed. This indicates that more detailed assessment of the performance of backup protection may be required in the future. Furthermore, it should be noted that in these studies it is assumed that the fault current observed would be sufficient for protection relays to pick up. With the scarcity in short circuit current reported in Chapter 3 this assumption should be verified and where necessary

protection settings/design may need to be modified or minimum fault currents ensured. Therefore, based on these results, an effective means by which to ensure that there will be no scarcity in stability margin is to mitigate the scarcity of short circuit current through a system service.

Oscillation damping presents a scarcity in both the Ireland and Northern Ireland studies and the continental system studies. However, it is far more acute in the continental system results and all cases studied exhibit unacceptable damping for most contingencies. In the Ireland and Northern Ireland studies damping was significantly reduced for all cases and at times was outside of acceptable limits, particularly for the steady evolution scenario. This scarcity may be particularly worthy of further study as system models tend to have higher damping than the system will have in reality. Furthermore, the nature of the study performed for the continental system was such that it did not capture the impact of this reduced damping on inter-area oscillations. Therefore, as such modes of oscillation are already known to exist in the continental system, of the impact of this damping scarcity on these modes should be assessed, as poorly damped inter area modes are known to contribute to the occurrence of system separation events. A local or global scarcity can be directly mitigated by developing a damping requirement and associated system service, which would ensure that the system had appropriate damping at a range of frequencies of oscillation. Damping sources could be active (e.g. a converter equipped with a power oscillation damper) or passive in nature (e.g. inertia). Given the nature of the scarcity this could well require a locational aspect and for localised scarcities it may best be managed through a controller tuning policy that places specific damping requirements upon generators.

5. SYSTEM CONGESTION

5.1 CONTINENTAL EUROPE CROSS BORDER MANAGEMENT

Cross-border congestion management entails two processes: market-based allocation of flows and operational remedial actions. The extent of remedial actions required is strongly related to the volume of unscheduled flows (UFs). Regulation 2019/943 from the Clean Energy Package sets the minimal level of cross-border capacities for market exchanges at the level of 70% of interconnectors' thermal capacities. This requirement consequently forces TSOs to reduce a significant amount of UFs by using remedial actions. Additionally, there are other reasons for re-dispatch and these could include market modelling imperfections – Generation Shift Keys (GSK) estimation, DC approximation and errors in the RES forecast. This work focusses on UFs as an indicator of the need for cross-border congestion management in the future scenarios with high penetration levels of renewables.

ENTSO-E categorizes power flow components for selected network elements into four types [32] [35]; internal flows, import-export, transit flows and loop flows. These categories are used to determine the entities responsible for utilisation of the transmission infrastructure. The four aforementioned flow types are defined as follows (Figure 5-1):

a) An internal flow (IN) is the physical flow on a line where the source, sink and the complete line are located in the same zone;
b) A loop flow (LF) is the physical flow on a line where the source and sink are located in the same zone and the line or even part of the tie-line is located in a different zone;
c) An import/export (IE) is the physical flow on a line that belongs completely either to the zone with the source and/or to the zone with the sink;
d) A transit flow (TR) is the physical flow on a line where the source, sink and the line or even part of the tie line are all located in different zones.

Figure 5-1 presents these flow types in a tabular form. First row represents the situation where at least part of the branch is located outside zones with sink (Load, L) or source (Generator, G). Second row describes types with branches located entirely in the zones of transaction sides. Columns distinguish between two cases, (i) sink and source placed in a single zone (i) or (ii) separated by zonal borders. ENTSO-E's document [32] provides additional requirements. In a meshed AC interconnection:

I. Internal Commercial Trade Schedules create internal flows and potentially loop flows,
II. Aggregated Netted External Trade Schedules create transit flows and/or export/import flows.

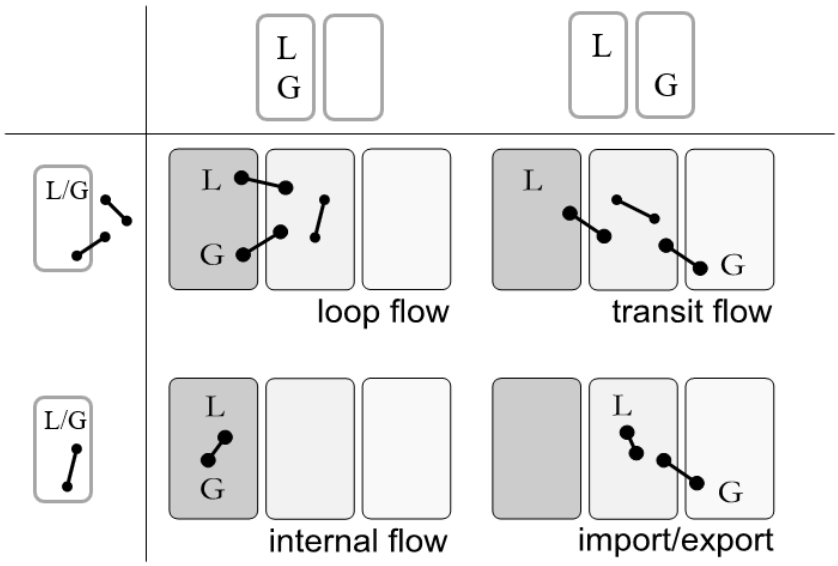

FIGURE 5-1: CLASSIFICATION OF FLOWS ACCORDING TO ZONAL ATTRIBUTION OF GENERATORS (G), LOADS (L) AND BRANCHES

5.1.1 FLOW IDENTIFICATION

A reliable identification and assessment of the flow components on critical network elements requires a robust methodology substantiated by solid numerical evidence. This is done using load flow decomposition approach [35]. In order to decompose power flow it is necessary to identify and process load flow data reflecting power exchanges within and between zones. The method selected for the identification of unscheduled flows is called Power Flow Colouring [36] and is characterized by the following features:

a. It assumes no transmission losses of active power,
b. It is designed to work in the reality of zonal structure of energy market,
c. It identifies all flow components indicated by ENTSO-E [37]

The assumption on loss-free transmission indicates the use of DC power flows as the input data for the method. The fact that this method works for a zonal environment distinguishes this method from other similar approaches [38] [39] which concentrate on inter-nodal exchanges with no regard to inter-zonal exchanges. Once the flow categories are assigned to all flow components, the responsibility of the zones which create the flows needs to be determined. Hence, the following assumptions are made:

1 Zones are exclusively responsible for creating internal flows and loop flows
2 Import/export and transit flows are common responsibility of two areas identified as transaction entities, 50% each.

Power Flow Colouring (PFC) performs the analysis in a top-down approach by using the zonal structure of the energy market and proceeds to power flow analysis on nodal level. The main idea is first to decompose operating points of an analysed system state into the so-called balanced model and model with exchanges. According to PFC, the model with exchanges identifies inter-zonal commercial flows, while the balanced model allows quantifying the loop flows and internal flows.

5.1.2 SCOPE OF OBTAINABLE RESULTS

Decomposition allows identification of flow components and their assignment to zones involved in their creation. The results of zonal decomposition include the following datasets:

a. flow type for an observed branch or border
b. responsibility of particular zones for an observed branch or border
c. responsibility of particular zones for given flow types summed over (selected) branches

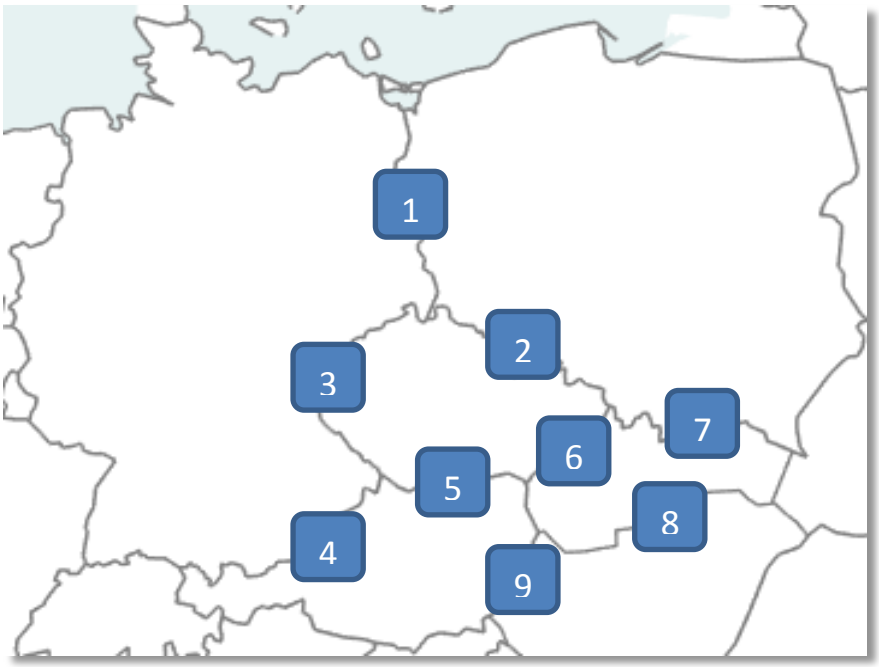

FIGURE 5-2: AREA OF THE ANALYSIS WITH ENUMERATED INTERNAL BORDERS

For the purpose of identification of unscheduled flows, no identification of zonal responsibility is needed, thus the following register of outcomes is limited to dataset (a). Furthermore, due to concentrating on inter-zonal borders, no internal flows are considered in the analysis. The area covered by this numerical study includes Austria, Czech Republic, Germany, Hungary, Poland and Slovakia. Market results, encompassing the whole Europe, were mapped into the subset of the European power system, as defined above. All interactions with the external area (regions not covered by the grid model) are omitted for the purpose of the study. This leads to selecting 9

borders, for which the decomposition results are to be presented (see Figure 5-2). Each decomposition result is provided for one of the aforementioned borders in variants related to 21 timestamps (cases), the names of which follow the convention introduced in Table 1-3.

5.1.3 FLOW DECOMPOSITION FOR DIFFERENT CASES

Borders enumerated in Figure 5-2 are divided into three groups of three. The following tables provide the decomposition outcomes for all borders under investigation. The results are shown in MW by each different category type of power flow (IE – Import/Export, TR – Transit Flow, LF – Loop Flow, SCH – Scheduled Flow) per border and scenario.

TABLE 5-1 :FLOW DECOMPOSITION RESULTS AND SCHEDULED FLOWS [MW] FOR BORDERS 1-3: DE-PL, PL-CZ AND CZ-DE.

	DE-PL				PL-CZ				CZ-DE			
	IE	TR	LF	SCH	IE	TR	LF	SCH	IE	TR	LF	SCH
DR/Max_Load/1	0	-974	1067	2000	-30	-1644	1012	-500	288	2302	361	0
DR/Max_Load/2/3/4	0	-1480	1027	2000	-42	-2043	1010	-500	447	3156	410	0
DR/Min_Inertia/3/4	0	-1491	855	0	488	1746	740	2	-238	303	38	-627
DR/Min_Inertia/1	0	45	1191	1366	0	1119	1049	-500	0	-483	149	0
DR/Min_Inertia/2	0	-1303	493	1742	43	3162	464	0	-108	-282	-106	0
DR/Min_Reactive/1/2	0	45	1193	1366	0	1120	1044	-500	0	-485	150	0
DR/Min_Reactive/3/4	0	-790	1055	1057	131	2859	937	0	-420	-595	49	0
ET/Max_Load/1	0	-1681	979	2000	-5	-1081	1054	-500	163	2812	372	0
ET/Max_Load/2/3/4	0	-2234	936	2000	-8	-1476	1031	-500	350	3705	455	0
ET/Min_Inertia/3/4	0	-225	868	0	156	732	813	2	-149	-491	52	-627
ET/Min_Inertia/1	570	605	1267	1366	-46	-88	1150	-500	0	-1114	206	0
ET/Min_Inertia/2	167	1057	619	1742	0	565	614	0	-222	-1570	-17	0
ET/Min_Reactive/1/2	570	605	1266	1366	-46	-88	1150	-500	0	-1113	206	0
ET/Min_Reactive/3/4	0	816	1117	1057	37	1267	1028	0	-587	-1312	78	0
GG/Max_Load/1	0	-1059	1025	2000	-27	-1584	1030	-500	283	2357	408	0
GG/Max_Load/2/3/4	0	-1565	1036	2000	-39	-1994	1019	-500	444	3219	412	0
GG/Min_Inertia/3/4	0	-1600	683	0	516	1813	689	2	-225	307	-71	-627
GG/Min_Inertia/1	0	-71	1033	1366	0	1236	1019	-500	0	-433	50	0
GG/Min_Inertia/2	0	-1460	339	1742	51	3336	395	0	-118	-202	-205	0
GG/Min_Reactive/1/2	0	-63	1066	1366	0	1238	1034	-500	0	-428	72	0
GG/Min_Reactive/3/4	0	-944	909	1057	143	2984	901	0	-424	-553	-60	0

TABLE 5-2: FLOW DECOMPOSITION RESULTS AND SCHEDULED FLOWS [MW] FOR BORDERS 4-6: DE-AT, CZ-AT AND CZ-SK.

	DE-AT				CZ-AT				CZ-SK			
	IE	TR	LF	SCH	IE	TR	LF	SCH	IE	TR	LF	SCH
DR/Max_Load/1	0	-3973	-706	-1012	1	-1281	582	0	0	-2442	70	115
DR/Max_Load/2/3/4	-2611	-3833	-617	-5958	0	-2312	543	0	0	-2544	57	366
DR/Min_Inertia/3/4	710	1433	-814	7457	0	1426	556	0	-116	-719	146	-886
DR/Min_Inertia/1	2875	1860	-1041	7500	157	2388	730	1200	0	-141	170	-773
DR/Min_Inertia/2	1183	3069	-598	4421	0	2489	459	0	-6	831	111	-287
DR/Min_Reactive/1/2	2876	1860	-1043	7500	156	2388	727	1200	0	-139	167	-773
DR/Min_Reactive/3/4	1898	3164	-1006	5801	0	2562	715	0	-27	411	173	-994
ET/Max_Load/1	0	-4341	-607	-1012	2	-1197	522	0	0	-2579	160	115
ET/Max_Load/2/3/4	-2633	-4171	-481	-5958	0	-2236	465	0	0	-2697	111	366
ET/Min_Inertia/3/4	425	1565	-817	7457	0	844	566	0	-140	-885	194	-886
ET/Min_Inertia/1	3260	1292	-1059	7500	172	1826	757	1200	0	-342	186	-773
ET/Min_Inertia/2	1743	2341	-635	4421	0	1397	500	0	-10	556	130	-287
ET/Min_Reactive/1/2	3259	1292	-1059	7500	172	1826	757	1200	0	-343	186	-773
ET/Min_Reactive/3/4	2387	2487	-1039	5801	0	1828	757	0	-34	198	194	-994
GG/Max_Load/1	0	-3992	-617	-1012	2	-1261	530	0	0	-2462	92	115
GG/Max_Load/2/3/4	-2628	-3855	-624	-5958	0	-2302	516	0	0	-2574	92	366
GG/Min_Inertia/3/4	668	1476	-751	7457	0	1449	540	0	-115	-687	219	-886
GG/Min_Inertia/1	2837	1882	-982	7500	153	2423	711	1200	0	-127	257	-773
GG/Min_Inertia/2	1178	3051	-543	4421	0	2532	440	0	-6	866	161	-287
GG/Min_Reactive/1/2	2836	1879	-993	7500	153	2423	715	1200	0	-130	248	-773
GG/Min_Reactive/3/4	1885	3166	-969	5801	0	2593	709	0	-27	450	252	-994

TABLE 5-3: FLOW DECOMPOSITION RESULTS AND SCHEDULED FLOWS [MW] FOR BORDERS 7-9: PL-SK, SK-HU AND AT-HU.

	PL-SK				SK-HU				AT-HU			
	IE	TR	LF	SCH	IE	TR	LF	SCH	IE	TR	LF	SCH
DR/Max_Load/1	-9	-1441	126	-990	0	-2354	157	-662	-1	-1656	-125	0
DR/Max_Load/2/3/4	-9	-1599	88	-990	1	-2571	64	-398	12	-722	-74	0
DR/Min_Inertia/3/4	0	848	185	0	20	638	240	0	0	-1662	-256	-262
DR/Min_Inertia/1	0	494	212	-990	0	1105	313	-556	-184	-1605	-310	-800
DR/Min_Inertia/2	0	1833	98	-297	9	2244	149	0	0	-563	-139	-48
DR/Min_Reactive/1/2	0	497	220	-990	0	1104	288	-556	-182	-1604	-315	-800
DR/Min_Reactive/3/4	0	1537	188	-220	0	1927	286	-349	-53	-1094	-291	-800
ET/Max_Load/1	-2	-1179	-2	-990	0	-2335	203	-662	-1	-1915	-86	0
ET/Max_Load/2/3/4	-2	-1330	-22	-990	1	-2551	149	-398	18	-984	-16	0
ET/Min_Inertia/3/4	0	57	126	0	27	-3	244	0	0	-1498	-252	-262
ET/Min_Inertia/1	-43	-207	189	-990	0	479	292	-556	-215	-1460	-301	-800
ET/Min_Inertia/2	-5	311	75	-297	12	1063	159	0	0	-188	-134	-48
ET/Min_Reactive/1/2	-43	-207	188	-990	0	479	292	-556	-215	-1460	-301	-800
ET/Min_Reactive/3/4	0	551	160	-220	0	1111	295	-349	-66	-872	-282	-800
GG/Max_Load/1	-8	-1414	66	-990	0	-2361	74	-662	-1	-1702	-87	0
GG/Max_Load/2/3/4	-9	-1577	88	-990	0	-2572	126	-398	6	-760	-109	0
GG/Min_Inertia/3/4	0	854	65	0	21	655	229	0	0	-1671	-209	-262
GG/Min_Inertia/1	0	542	85	-990	0	1126	269	-556	-179	-1634	-271	-800
GG/Min_Inertia/2	0	1874	12	-297	9	2279	126	0	0	-594	-104	-48
GG/Min_Reactive/1/2	0	545	102	-990	0	1126	272	-556	-179	-1636	-278	-800
GG/Min_Reactive/3/4	0	1556	79	-220	0	1949	275	-349	-51	-1112	-260	-800

5.1.4 IDENTIFICATION OF UNSCHEDULED FLOWS

ACER defines Unscheduled Flows (UF) as a sum of loop flows (LF) and unscheduled allocated flows (UAF), which are flows allocated on a given border, but scheduled on a different one. UAF is the result of differences in schedules, which are determined by coupling algorithm or bilateral agreements, and physical allocation of market exchange that is a result of electrical paths of a real power flow. Unscheduled Allocated Flow is defined as:

$$UAF = AF - SCH \qquad \text{(Eq. 5-1)}$$

where AF represents allocated market flows (IE and TR together) and SCH is flow scheduled according to an underlying market solution [10]. Consequently, unscheduled flows are estimated by:

$$UF = LF + UAF = LF + IE + TR - SCH \qquad \text{(Eq. 5-2)}$$

Therefore we can not only estimate the volume of unscheduled flows, but most importantly, UFs can be decomposed into components of different origin and magnitude (LF, UAF), and in case of internal network elements also internal flows. Figure 5-3 present UF levels for each of 21 scenarios under examination.

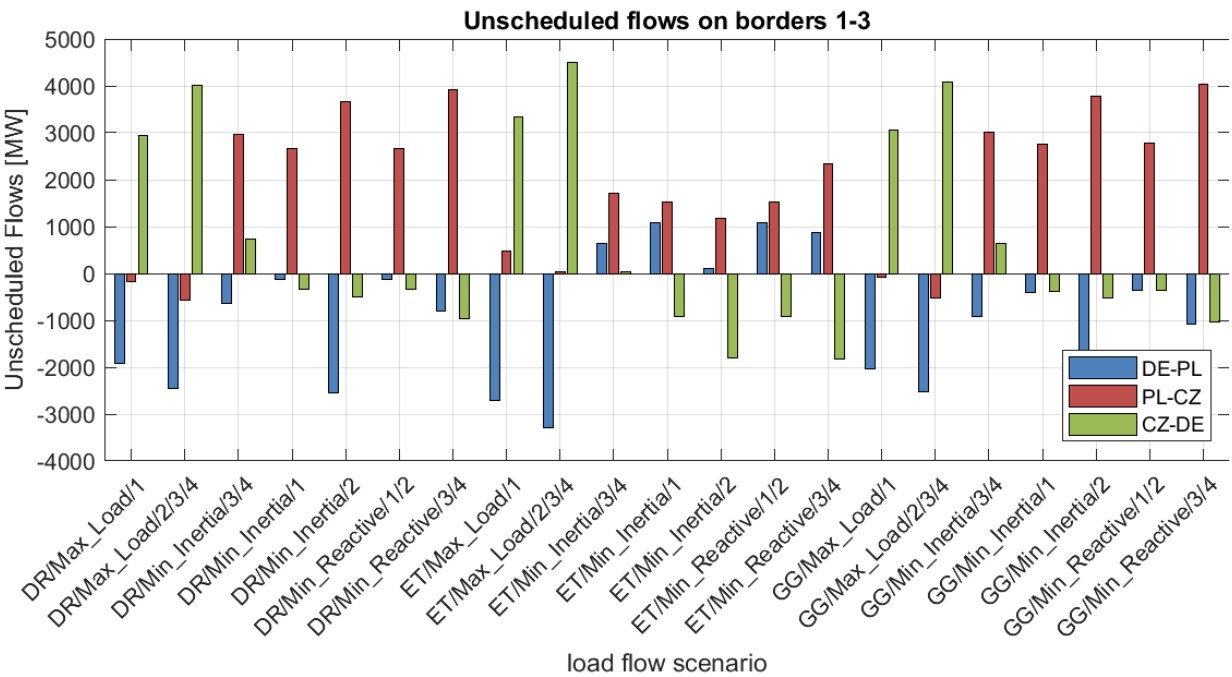

FIGURE 5-3: UNSCHEDULED FLOWS IN BORDERS 1-3

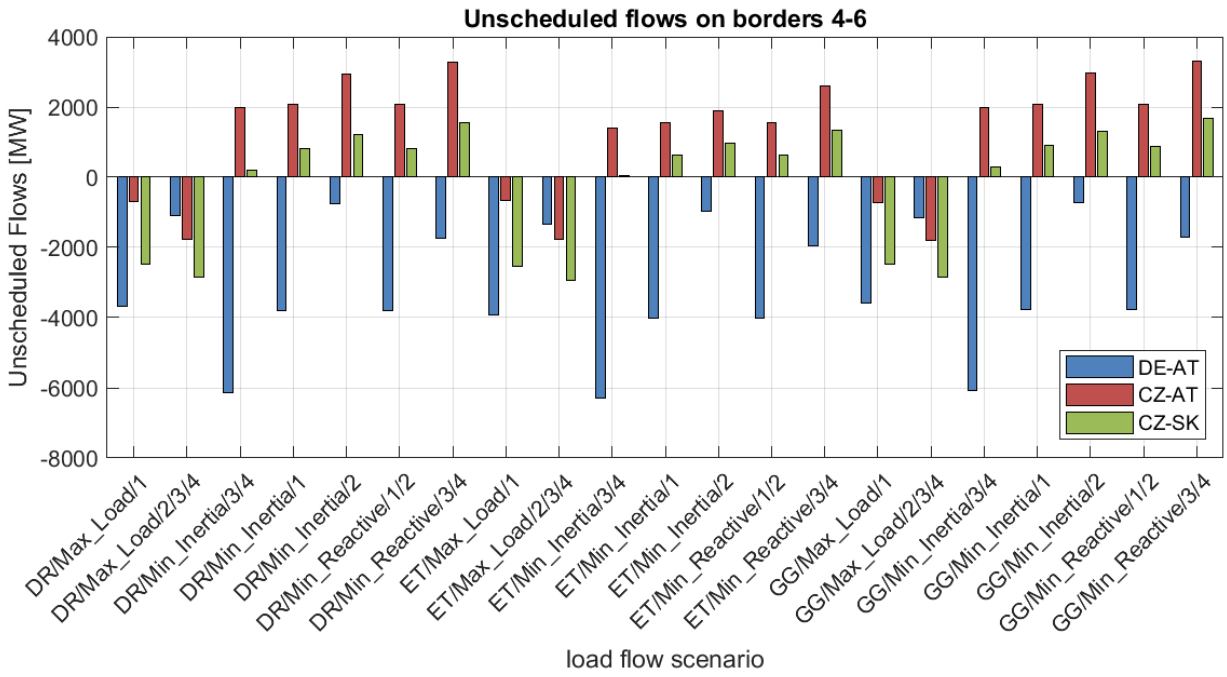

FIGURE 5-4: UNSCHEDULED FLOWS ON BORDERS 4-6

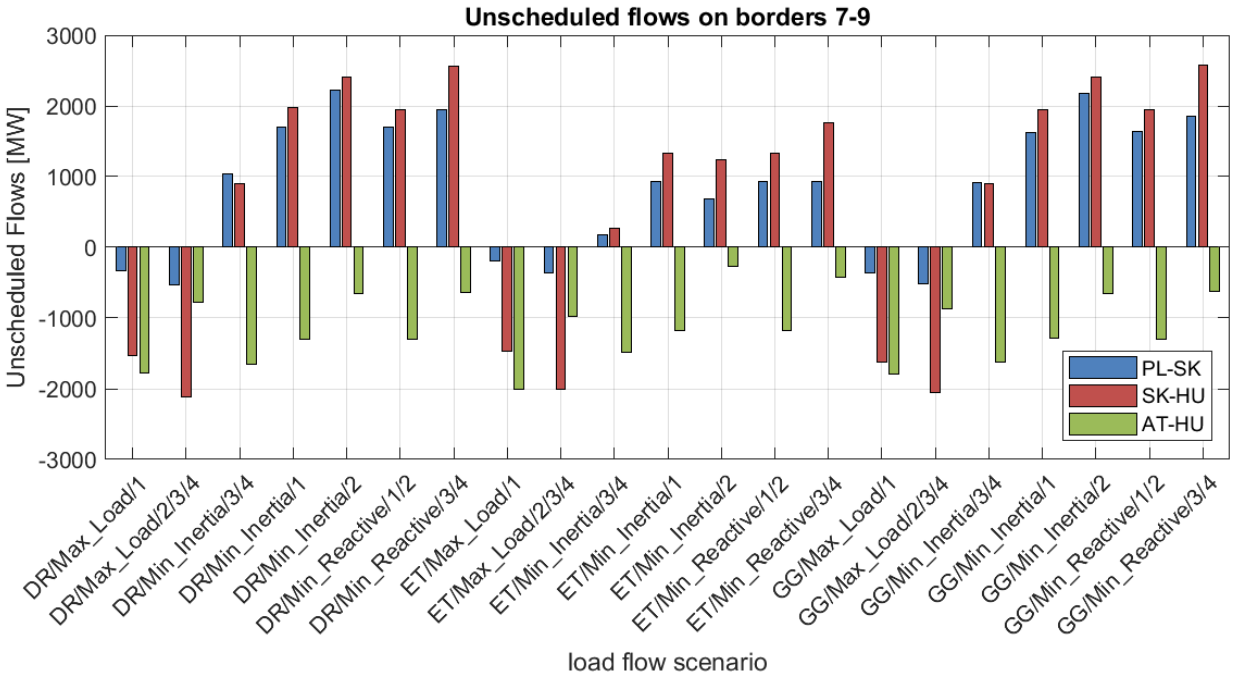

FIGURE 5-5: UNSCHEDULED FLOWS ON BORDERS 7-9

The results indicate that, depending on the case and the border being investigated, the level of unscheduled flows varies, often reaching thousands of megawatts. In extreme cases UFs are beyond 6 GW on DE-AT border. Interestingly, selected sets of unscheduled flows display strong correlation, especially on borders 4-6 and 7-8. This

fact originates from the trans-zonal character of both loop flows and transit flows, i.e. these flow types tend to cross more than one border while flowing from their source to sink.

Nevertheless, high values of UFs resulting from the analysis have to be interpreted critically in respect to limitations of market and grid models used for computations. The estimation of unscheduled flows is prone to at least two errors. First results from using a single set of market results (ET) for constructing various scenarios with different load flow pattern (DR and GG). Second is related to mapping market results to generating units connected to the power system, this mapping was designed for AC load flow calculations (covering losses, among others), whereas the work considered in this section utilises DC power flow for decomposition. First source of error is absent in case of Energy Transition scenario (snapshots 8-14), which makes them the most representative. Indeed, the observed flows, excluding DE-AT and AT-HU display significantly smaller values for ET-related snapshots.

If the outcomes are to be compared with the current situation in continental Europe, the Technical Report of ENTSO-E [40] provides a reasonable reference point. Indicator calculated by ENTSO-E for PL-DE border gives the estimates of annual average 600-800 MW between 2016 and 2018, which is comparable to ET results for this border. The credibility of this reference point is, however, questionable due to different market structure in force in that period (until Q3 2018 Austria and Germany were in the same bidding zone).

It is believed that the flow-based market coupling, designed as a future solution for most of Europe, is able to mitigate significant amounts of the UFs, as the schedules are much closer to physically allocated flows. On the other hand, loop flows are persistently non-negligible components of the UF. Increasing number of renewable installations in Central-Northern Europe along with high demand in the Central-South (exemplified by DE-AT schedules measured in GWs) is expected to create a load flow pattern, which would extensively utilize the capacity of the whole interconnected system. In such a case, effective mitigation of potential overloads can become one of the most significant technical scarcities of the future.

5.2 IRELAND & NORTHERN IRELAND POWER SYSTEM

As opposed to the continental European system, the Ireland and Northern Ireland system is synchronously isolated, therefore any congestion issues are likely to arise within the system as opposed to cross border unscheduled flows. In order to further investigate potential congestion issues, steady state analysis was carried out to evaluate the impact of increasing levels of non-synchronous variable Renewable Energy Sources (RES) as evidenced by transmission line thermal loading (110 kV network and above), coupled with an identification of regions and/or periods where a lack of transmission capacity occurs.

PSSE AC load flow analysis was used to assess network elements that exceed their thermal rating, thereby identifying potential areas of congestion due to increased RES. An in house tool developed in Python (LAMDA, or Load-flow & Automated Multi-Dispatch Analysis) mapped PLEXOS generated economic dispatches for an entire year to the 2030 Steady Evolution and Low Carbon Living transmission network models and evaluated each hour to identify network elements experiencing thermal overloading. This was done for both intact (N) transmission network and loss of a single network element (N-1).

5.2.1 RESULTS & DISCUSSION

Figure 5-6 presents the results of 2030 Steady Evolution transmission network thermal over loading analysis for N-1 system conditions. Thermal overloads above 100% of the networks thermal capability are plotted against SNSP levels. The results shown are for both summer (red) and winter (blue) seasons.

As shown in Figure 5-6, as SNSP increases there is a significant rise in both occurrences and level of overloading above 100% of thermal capability for both summer and winter seasons. The majority of results shown in Figure 5-6 are 110 kV network overloads are associated with the loss of a single circuit in the West of Ireland and Northern Ireland. These regions are typically areas with high geographically distributed RES densities and electrically distant from load centres. As there is not enough local load to absorb the high-levels of RES generation particularly during periods of high SNSP as shown in Figure 5-6, the loss of a circuit in the Western region creates thermal overloads due to power being transferred along the 110 kV network to load centres in the Eastern load centres such as Dublin area. There are a number of 220 kV line overloads recorded in the results shown in Figure 5-6; however, these are primarily located in the Dublin region. As Dublin region has a number of large conventional generator plants along with large offshore wind farms arrays, it can experience thermal overloads on its 220 kV network at both low and high levels of SNSP. Generally the network above 220 kV (e.g. 275 kV, 400 kV) does not experience thermal overloading even at high levels of SNSP.

Furthermore, as expected, the summer period can be seen to have a greater level of overloading when compared to winter. This is due to the lower rating of thermal capability during summer coupled with RES generation levels remaining comparable with winter. While the system load tends to decrease in summer, this is not enough to offset this effect. Lower load levels tend to exacerbate thermal issues in areas with high RES generation which have less local load to absorb and are therefore exporting more RES generated power out of the area using the 110 kV network.

Figure 5-7 presents the results of 2030 Low Carbon Living transmission network thermal over loading analysis for N-1 system conditions. Similar to SE scenario, thermal overloads above 100% of the networks thermal capacity is plotted against SNSP. The results shown are for both summer (red) and winter (blue) seasons. A similar impact of increasing SNSP on thermal overloads as to that of SE can be seen in LCL scenario. However, comparing Steady

Evolution to Low Carbon Living it can be seen that, there is a clear increase in both occurrences and level of overloading above 100% of thermal capability for both summer and winter seasons especially for 110 kV network in the West of Ireland and Northern Ireland. This is due to the increased levels of RES in Low Carbon Living when compared to that of Steady Evolution.

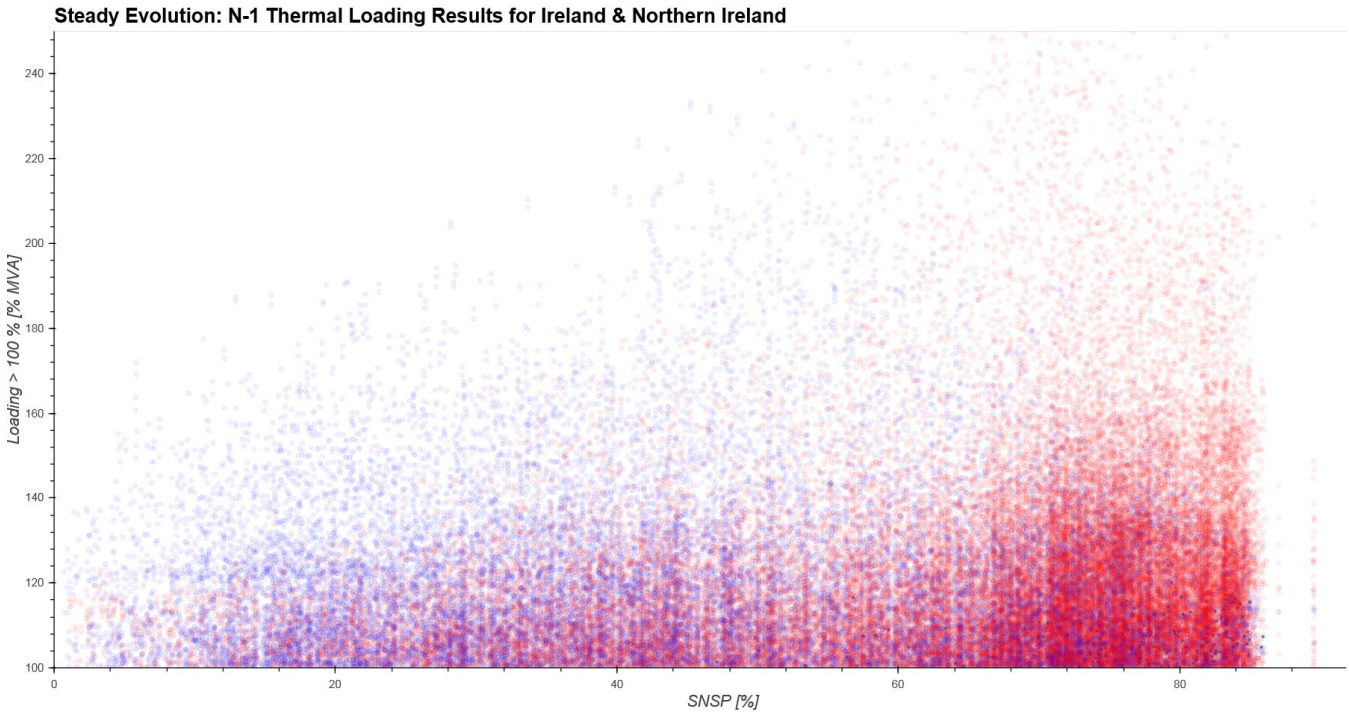

FIGURE 5-6: COMPARISON OF 2030 STEADY EVOLUTION TRANSMISSION NETWORK THERMAL OVER LOADING AGAINST SNSP

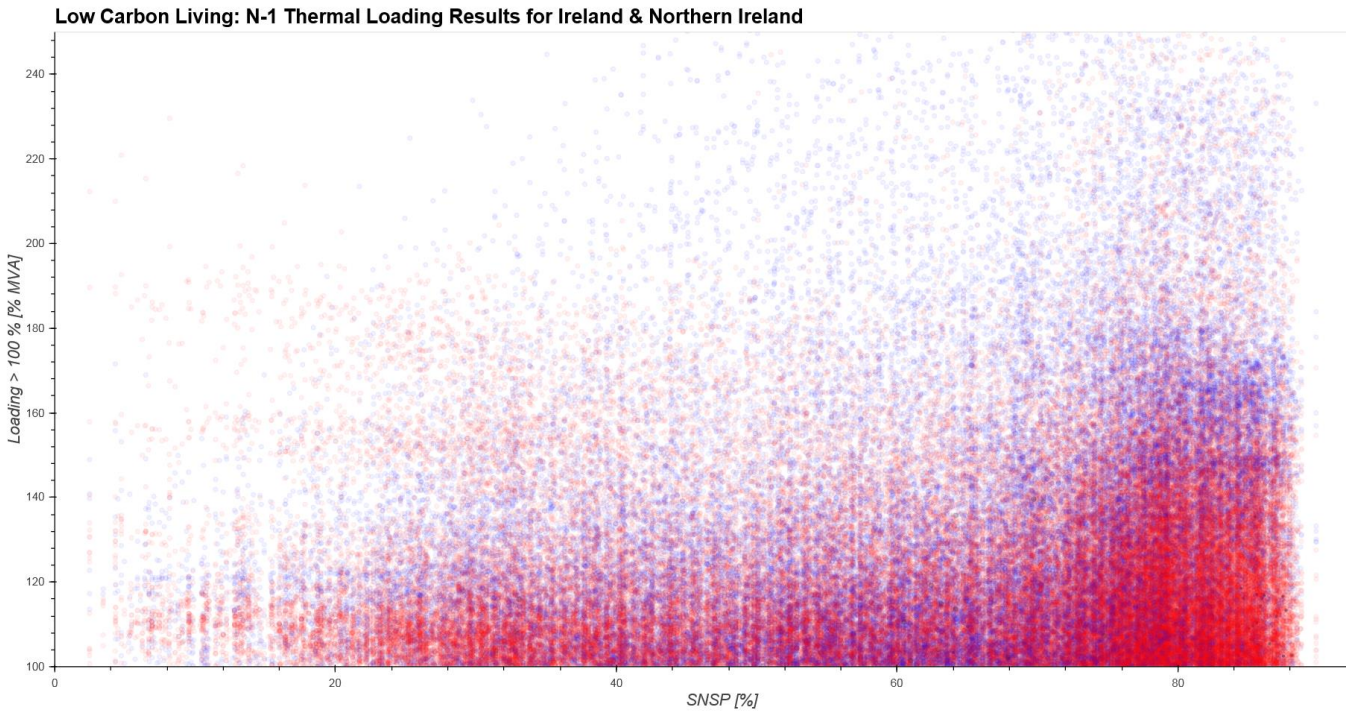

FIGURE 5-7: COMPARISON OF 2030 LOW CARBON LIVING TRANSMISSION NETWORK THERMAL OVER LOADING AGAINST SNSP

5.3 SUMMARY AND CONCLUSIONS

The type of congestion investigated across the two systems is not comparable, and hence the methods used to carry out the analysis also differ substantially. However, both elements of this work have revealed the emergence of global scarcities as renewable penetrations increase. Whilst the congestion of any one line could be viewed as inherently local, congestion is classified here as a global scarcity due to the sheer scale of the congestion issues observed.

For the continental system congestion was studied from the perspective of unscheduled flows, where unscheduled power flows are a concern as they will displace scheduled, market flows and through this manifest a scarcity. The study presented here highlights that an increase in the RES installations in the continental system will increase the severity of this congestion scarcity and this will likely cause unscheduled flows to exceed the acceptable level of 30% of capacity (as allowed under the Clean Energy Package), which will require mitigating actions. This scarcity occurs because, unlike conventional technologies, RES tend to be localized in particular regions of Europe (this refers mostly to wind farms, which benefit from proximity to the North Sea and Baltic). The energy produced by these sources is either exported or consumed domestically. In the latter case, a set of zonal internal exchange is expected to increase the level of loop flows and, consequently, unscheduled flows. Before the implementation of the Clean Energy Package, the capacity calculation process designed for European energy exchange was aimed at adjusting the level of acceptable market flows, so that they complement the

expected level of loop flows. However, the CEP introduced the requirement of offering at least 70% of thermal limits to the inter-zonal market. This legal claim does not change the phenomenon of the increasing amount of loop flows, which drive the observed scarcity. This scarcity could be mitigated through a congestion service that incentivised real-time power flow control devices, geographically dispersed energy storage that can defer the flows, or where justifiable construction of new transmission assets.

The scarcity observed in the Ireland and Northern Ireland power system is a global scarcity that is also driven by the location of new RES. This RES is installed in parts of the system where there was traditionally little generation or demand. Therefore, sufficient transmission infrastructure is not in place to transfer this power to the load centres and the infrastructure that is in place can become heavily overloaded. Overloads are observed at low SNSP and the occurrence and magnitude of thermal overloads increases with SNSP, indicating a lack of transmission network capacity in both Steady Evolution and Low Carbon Living. In general, these overloads are more severe in Low Carbon Living but can be particularly more severe at low SNSP levels. The 110 kV transmission network is most heavily impacted as it this network that is primarily relied upon to connect the distributed RES, particularly in the West of Ireland and Northern Ireland, and this network effectively serves as a collector network for windfarms in these regions. When assessing congestion in the future, a focus should be placed upon how often a specific line or corridor may find itself overloaded and the severity of that overload. This information should be used to guide the selection of asset based and service based solutions, with the more common and severe congestion issues being candidates for asset based solutions. A system service may be required to manage congestion in the future, particularly in view of the barriers faced by onshore, above ground reinforcement, and these results indicate that it is important that this service incorporates elements that allow it to be effective at both high and low SNSP levels. Furthermore, this service would likely require locational aspects to allow focus on the 110kV collector networks but this would need to be complemented by a high degree of coordination to ensure that power flows are routed and deferred effectively.

6. SYSTEM RESTORATION

6.1 IRELAND & NORTHERN IRELAND POWER SYSTEM

6.1.1 THE POWER SYSTEM RESTORATION PLAN

In case of a total or partial system black out, the restoration of continuous supply of electricity as quickly and safely as possible to all generation, transmission, distribution and customers is required. Traditionally, power system operators develop an organised and considered procedure to ensure system restoration, called Power System Restoration Plan (PSRP). The Power System Restoration Plan sets out guidelines and procedures. The principle of the PSRP is to use generation stations that can be started without an external power supply in order to energise other parts of the transmission systems and larger generators called target generators.

With increasing renewable generation levels, provided that the majority of intermittent renewable generation resources (wind/solar PV) entail current source converters to interface with the grid, the number and size of self-starting generating units is likely to significantly decline. Furthermore, as the geographical locations of various generation resources are likely to change with replacement of conventional generation by renewable generation, the pre-existing restoration paths may no longer remain valid. Hence, in view of these factors, the PSRP needs to adapt, incorporating the evolving plant portfolio.

The aim of this section is to assess the existing Ireland and Northern Ireland Power System Restoration Plans in the context of Low Carbon Living (LCL) 2030 scenario. Due to high level of variation between the two 2030 scenarios considered so far and the scenario specific nature of PSRP, the PRSP has been evaluated for one scenario to demonstrate the high level impact of renewable generation resources on the restoration process.

The LCL scenario is the most ambitious scenario, with regards to annual renewable energy production levels. It assumes that by 2030 a high economic growth leading to the creation and rollout of new technologies for low carbon electricity generation. The high levels of renewable generation on the grid are due to a strong public demand to reduce greenhouse gas emissions, as well as high carbon prices and incentives for renewables. In addition, the daily load profile in the LCL scenario is relatively flat; an increased smart demand shifting is assumed.

This evaluation of PSRP entails an examination of the conventional generation units to be decommissioned by 2030, followed by a consideration of the new generation resources, along with various elements that are likely to affect the PRSP, such as synchronising capability and load. Finally the requisite changes and modifications required a reconsidered restoration plan are discussed, in the context of LCL.

6.1.2 REMOVAL OF GENERATION UNITS IN IRELAND

There are currently seven principle generating stations that have Black Start capability in Ireland. These include 6 conventional generation resources and one HVDC link.

In Ireland the transmission system is divided into four subsystems: North, South, West and East (Figure 6-1). Each subsystem has at least one Black Start station and a number of non-Black Start stations which have been identified as primary target generation stations. The restoration path is directly linked to the restoration time frame. In the event of a full or partial blackout, the longer the restoration path the longer it will take for the system to be restored.

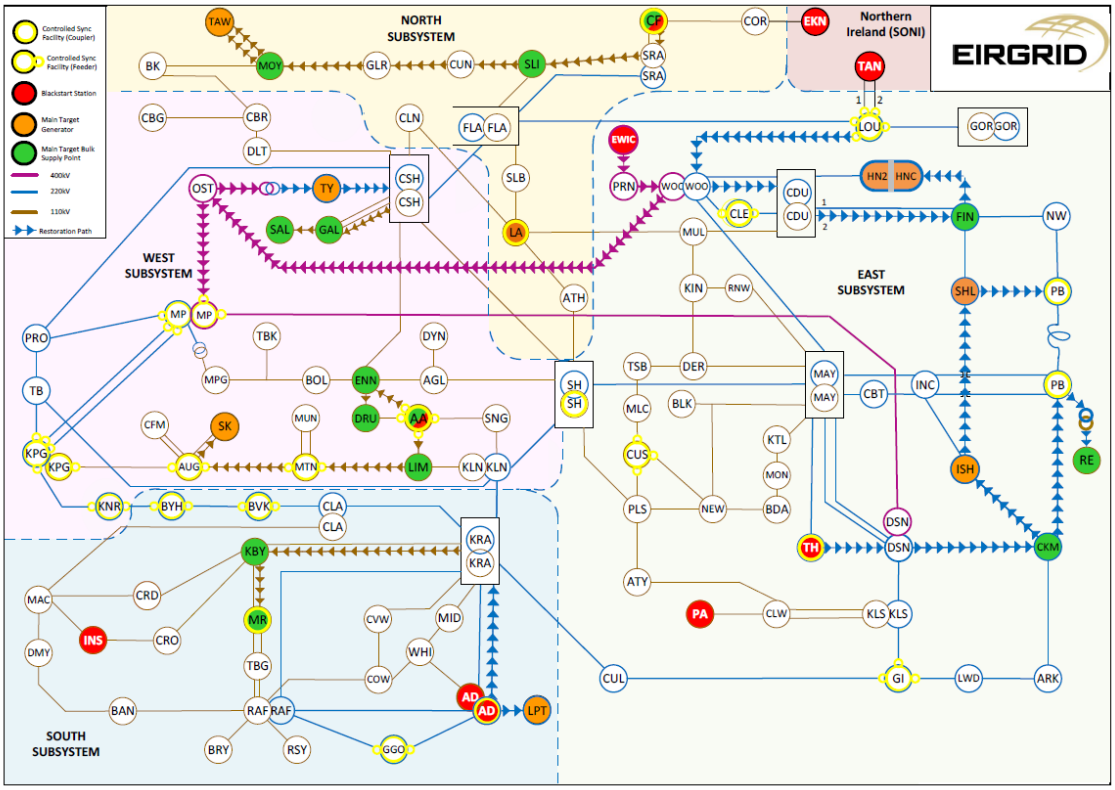

FIGURE 6-1: BLACK START SUBSYTEM MAP OF THE FOUR SUBSYTEMS

6.1.2.1 NORTH SUBSYSTEM

Currently the north subsystem is based on the Black Start capability of the units in Erne hydropower plant (ER1-4).

According to the information summarised in the Table 6-1, the Black Start units in Erne (ER1-4) for the north subsystem will still be present in the LCL 2030 scenario. However most of the target generation stations currently available will be shut down or dismantled. Lough Ree, LR4, will be the only non-Black Start generator left. This

means the power system restoration plan for the north subsystem will need to be reanalysed, and there needs to be more target stations that can be energised by Erne for power restoration to be possible. New wind farms will be implemented in new and existing substations helping mitigate the impact of the conventional generations' shutdown.

TABLE 6-1 GENERATORS IN THE NORTH SUBSYSTEM

Location	Generators	Black Start capability	Technology	Exist in LCL 2030
North	ER1	Yes	Hydroelectric	Yes
North	ER2	Yes	Hydroelectric	Yes
North	ER3	Yes	Hydroelectric	Yes
North	ER4	Yes	Hydroelectric	Yes
North	LR4	No	Thermal ST	No Peat (Still Biomass)
North	TP1	No	OCGT	No
North	TP3	No	OCGT	No

6.1.2.2 SOUTH SUBSYSTEM

Currently the south subsystem is based on the black start capability of the Aghada OCGTs (AT1,2,4) and the Lee hydro station (LE1-2).

TABLE 6-2 GENERATORS IN THE SOUTH SUBSYSTEM

Location	Generators	Black Start capability	Technology	LCL 2030 exist
South	AD2	No	CCGT	Yes
South	AT1	Yes	OCGT	No
South	AT2	Yes	OCGT	Yes
South	AT4	Yes	OCGT	Yes
South	LE1	Yes	Hydroelectric	Yes
South	LE2	Yes	Hydroelectric	Yes
South	LE3	No	Hydroelectric	Yes
South	WG1	No	CCGT	Yes

Table 6-2 shows that the Black Start units, AT1, in Aghada will not exist according to LCL 2030.

The two units of Lee hydro station (LE1, LE2) and the two remaining units of Aghada AT2 and AT4 will be the Black Start units for the south subsystem feeding into AD2, LE3 and WG1. The path to restoration is still possible. Even though a Black Start generator is removed, the south subsystem will not change considerably according to the LCL scenario. However, given that the new Celtic interconnector will be able to provide Black Start Capability and with new wind farms on the grid, the south subsystem is expected to be modified.

6.1.2.3 WEST SUBSYSTEM

There are two Black Start units in the west subsystem, through Ardnacrusha hydro station (AA1-4) or through the EWIC interconnector.

TABLE 6-3 GENERATORS IN THE WEST SUBSYSTEM

Location	Generators	Black Start capability	Technology	LCL 2030 exist
West	AA1	Yes	Hydroelectric	Yes
West	AA2	Yes	Hydroelectric	Yes
West	AA3	Yes	Hydroelectric	Yes
West	AA4	Yes	Hydroelectric	Yes
West	EWIC	Yes	HVDC interconnector	Yes
West	MP1	No	Thermal ST	No
West	MP2	No	Thermal ST	No
West	MP3	No	Thermal ST	No
West	SK3	No	CHP Steam Unit	Yes
West	SK4	No	CHP Steam Unit	Yes
West	TB1	No	Thermal ST	No
West	TB2	No	Thermal ST	No
West	TB3	No	Thermal ST	No
West	TB4	No	Thermal ST	No
West	TYC	No	CCGT	Yes
West	WO4	No	Thermal ST	No Peat (Still Biomass)

According Table 6-3, in the LCL 2030 scenario the Moneypoint (MP1, MP2, MP3) and Tarbert (TB1, TB2, TB3, TB4) thermal units will no longer exist. In addition, West Ofally will no longer generate energy through peat; the only production will be via biomass. There will be no change in the Black Start units according to the LCL 2030 scenario. However there will remain only two target generation stations, Sealrock (SK3 and SK4) and Tynagh (TYC), limiting the paths for power restoration. Restoration time might increase but it is still possible. The system needs to be analysed in more depth to see if there will be new generation sources that can help in the power restoration process.

6.1.2.4 EAST SUBSYSTEM

The East subsystem corresponds to the Dublin area and is probably the most complex of all four with the biggest load. There are currently three Black Start generators, the EWIC interconnector, the Liffey hydro station (LI1-2), and Turlough Hill pumped storage (TH1-4). Due to the location of the Liffey hydro station, its impact is limited as it can only help provide power to Great Island.

TABLE 6-4 GENERATORS IN THE EAST SUBSYSTEM

Location	Generators	Black Start capability	Technology	LCL 2030 exist
East	DB1	No	CCGT	Yes
East	DW1	No	Waste	Yes
East	ED1	No	Thermal ST	No Peat (Still Biomass)
East	ED3	No	OCGT	No
East	ED5	No	OCGT	No
East	EWIC	Yes	HVDC interconnector	Yes
East	GI4	No	CCGT	Yes
East	HN2	No	CCGT	Yes
East	HNC	No	CCGT	Yes
East	IW1	No	Waste	Yes
East	LI1	Yes	Hydroelectric	Yes
East	LI2	Yes	Hydroelectric	Yes
East	LI4	No	Hydroelectric	Yes
East	LI5	No	Hydroelectric	Yes
East	PB	No	CCGT	Yes
East	RP1	No	OCGT	No Gas (Still Distillate)
East	RP2	No	OCGT	No Gas (Still Distillate)
East	TH1	Yes	Pumped storage	Yes
East	TH2	Yes	Pumped storage	Yes
East	TH3	Yes	Pumped storage	Yes
East	TH4	Yes	Pumped storage	Yes

According to Table 6-4, the three Black Start generators will still be running in scenario LCL 2030. However, some of the target generation stations will no longer exist. Edenderry ED3 and ED5 will be shut down, while ED1 will still operate using biomass. Rhode (RP1 and RP2) will only operate using diesel and no longer gas.

The PSRP in the east subsystem will not be affected by the removal of Black Start units according to LCL 2030. However, by removing target generation units, the number of path possible is limited, meaning if one path has an issue such as a breaker that cannot be operated or a line in maintenance, there are fewer alternatives. This is critical considering the load of the east subsystem. Nevertheless, new offshore wind farms and other renewable generation will be implemented on the grid, mitigating the loss of the conventional units.

The location of the Black Start units and the target generation is essential in the case of the east subsystem. Currently there is no generation at the North Wall substation however if this was changed and there was a unit with Black Start capability, it could be very interesting for the PSRP as it is ideally located close to Huntstown, Shellybanks and Irishtown 220 kV stations. This could enable up to 5 CCGTs (HNC, HN2, PBA, PBB and DB1) to be started following a Dublin or a wider area power system incident.

After analysing each subsystem it appears major modifications need to be implemented into the current PSRP. Numerous conventional stations are being shut down in each subsystem and the current restoration path will be compromised.

6.1.3 REMOVAL OF GENERATION UNITS IN NORTHERN IRELAND

The Power System Restoration plan in Northern Ireland is set up into three independent subsystems A, B and C. Each subsystem is based on a power station having Black Start capability.

Currently, in Northern Ireland there are five gas turbines that can be started without a system power supply. These are as follows:

- Coolkeeragh Power Station - GT8 → Black Start source for Subsystem A
- Ballylumford Power Station - GT1 and GT2 → Black Start sources for Subsystem B
- Kilroot Power Station - GT1 and GT2 → Black Start sources for subsystem C

The Black Start plan in Northern Ireland has a considerable advantage, as the Black Start units are in the same plant as the CCGTs. This reduces the restoration path and facilitates the system restoration.

The only change for the North Ireland generation system will be the disappearance of the Kilroot units. This means there is no longer any Black Start source for subsystem C; the subsystems will need to be revised. However, Kilroot substation is located only one substation away from Ballylumford, meaning the restoration path has not been considerably increased. The dismantling of Kilroot does not pose such an issue as the remaining black start units are well spread out geographically with Coolkeeragh to the West and Ballylumford to the East. There is not one part of the system completely lacking Black Start units.

TABLE 6-5 GENERATORS IN NORTHERN IRELAND

Location	Generators	Black Start capability	Technology	LCL 2030 exist
NI	Ballylumford GT1	Yes	GT/peakers	Yes
NI	Ballylumford GT2	Yes	GT/peakers	Yes
NI	Ballylumford BT10	No	Gas/CCGT	Yes
NI	Ballylumford BGT20	No	Gas/CCGT	Yes
NI	Kilroot K1	No	Coal/oil	No
NI	Kilroot K2	No	Coal/oil	No
NI	Kilroot KGT1	Yes	GT/peakers	No
NI	Kilroot KGT2	Yes	GT/peakers	No
NI	Kilroot KGT3	No	GT/peakers	No
NI	Kilroot KGT4	No	GT/peakers	No
NI	Coolkeeragh GT8	Yes	GT/peakers	Yes
NI	Coolkeeragh GS	No	Gas/CCGT	Yes
NI	Coolkeeragh GS	No	Gas/CCGT	Yes
NI	Bombardier	No	Waste	Yes
NI	Lisahally	No	Waste	Yes
NI	Moyle	No	HVCD interconnector	Yes

6.1.4 NEW GENERATION SOURCES

After analysing the generators no longer present in the LCL 2030 scenario, the next step is to look at the elements and generation that have been added into the system, and how they might affect the PSRP in Ireland and Northern Ireland.

6.1.4.1 RENEWABLE GENERATION

In the event a blackout occurs during a period with high renewable penetration, many conventional thermal generators could be offline and cold, hence utilising renewables for Black Start to improve restoration time frame should be considered.

If renewable generation could provide Black Start capability this would add flexibility to the system. The system restoration would be quicker in certain areas because Black Start sources can be closer to a target generator. If the Black Start renewable unit is connected to the distribution network, the path for system restoration may be longer with more transformers to go through and the DSO needs to be involved but it is still an option.

Another approach would be that renewables would be target generators energised by traditional Black Start generators. The renewables could provide a quickly adjustable source of active and reactive power significantly accelerating the restoration of power. The inclusion of renewable energy sources could help maximise the primary operating reserve provided by the Black Start unit while minimising Black Start unit energy usage. However, in the event there is no wind, solar or marine resource at the moment of the blackout, renewables cannot be used. When available renewable sources can be leveraged, but if not the restoration should proceed as normal, hence the PSRP cannot depend entirely on renewables.

WIND: Renewable sources such as wind farms can provide Black Start capability given that they are grid forming; this might imply some changes to existing or new wind farms and incentives. However, due to the variability of renewable resources it is difficult to rely on renewable sources for Black Start capability. Currently in Ireland during the restoration process wind farms are shut down (disconnected) because they have variable outputs, the variability causes unstable generation, a key obstacle to the system restoration. For wind farms to provide black start capability they would need to be curtailed at times of medium or high wind. This would enable them to have a constant output, and a stable generation.

According to the LCL scenario there will be over 10 GW of wind capacity by 2030. In Ireland, wind farms are located in all the country but mainly in the North and West subsystems of Ireland and in Northern Ireland. Wind farms could provide Black Start capability to these subsystems or be energised by other Black Start units.

SOLAR: Similarly to wind, solar energy and solar parks could be curtailed and provide Black Start. With 3.9 GW of solar installed by 2030, certain solar parks will have enough capacity to start up CCGT generators. Potentially solar farms could provide Black Start capability to the Northern Ireland system as well as to the West, South and East subsystems in the Ireland. If they are not Black Start units they can be target generators energised by other Black Start units and help accelerate the restoration process like wind farms.

OCEAN: Ocean wave and tidal resources are will also be present with an estimate of 98 MW. A significant proportion of the tidal and marine current energy resource is to be found on the north and the east coast of Ireland. This means that the generation will most likely be in the east subsystems and Northern Ireland. The advantage of tidal energy is that it is less variable and more predictable than solar or wind resources. However, tidal energy might not provide enough power for the CCGT. In the east subsystem, the Dublin area relies on large CCGTs and the energy provided by the tidal energy might not be sufficient. According to the evolution of the technology this is an element that needs to be considered. Wave resources are also present on the west coast of Ireland, so potentially the west, north and east subsystems of Ireland and the Northern Ireland subsystem could rely on ocean resources in the PSRP.

BIOMASS: The LCL scenario estimated 847 MW of biomass by 2030. Biomass generators have a big capacity and they could be good target generators. However like other thermal generators, their start up time is dependent on the hot or cold state. If the generator was not in use at the time of the blackout and the machine is cold, it will not be able to act quickly and will have no use in the Black Start plan. Biomass plant could also be used as Black Start if for example they added a diesel generator (or some other mechanism) to their system. This could be possible if they are incentivised to do so.

6.1.4.2 BATTERY STORAGE

LCL 2030 anticipates 500 MW of small scale and 1200 MW of large scale battery storage. Potentially these sources of energy will be spread out in all of Ireland. A large number of these batteries will be utilised for data centres. These data centres could potentially provide Black Start capability. According to the graph Figure 6-2, there will be almost 2,000 MVA of datacentres connected on the system. As most of them are located in the Dublin area, if they provide Black Start it could help strengthen greatly the east subsystem.

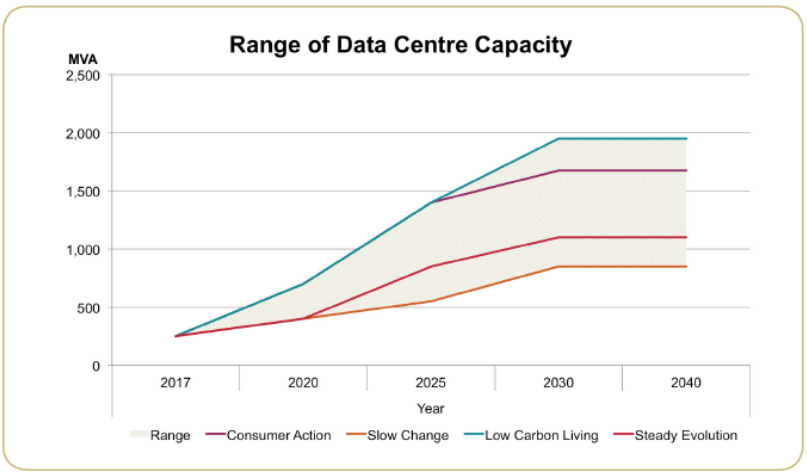

FIGURE 6-2: DATA CENTRES CONNECTED TO THE POWER SYSTEM FOR THE FIVE SCENARIOS

For example, a large energy company has a data centre based in Clonee substation. Currently there is more battery capacity installed than needed for their Data Centre. In addition, Clonee is just one substation away from Huntstown which is a major power station in Dublin. If the battery provided power to Huntstown it could help with the power restoration of the Dublin area. There needs to be an incentive and an agreement for the Data Centres and their batteries to help support the network as this could considerably help simplify and improve the PSRP.

6.1.4.3 DC INTERCONNECTION

Two new interconnections are planned in LCL 2030 scenario; the Celtic Interconnector between France and Ireland with 700 MW, and the Greenlink between Wales and Ireland with 500 MW.

The Celtic Interconnector will be connected near Cork on the Irish side. This suggests that the interconnector will be able to provide Black Start capability to the south subsystem, like EWIC does for the east and west subsystems. The connection point has not yet been defined, depending on the final location of the substation; the Celtic interconnector could also provide Black Start to other subsystems.

Greenlink will be close to the Great Island substation in Ireland. This means that the interconnector will be able to provide Black Start capability to the east subsystem.

6.1.5 SYNCHRONISING CAPABILITY

Synchronising capability is also a very important element that needs to be examined. In the event of a total blackout, once the subsystems are up and running they need to be synchronised. This is possible through only certain stations that have controlled synchronising facility, this is called Paralleling Check. The paralleling check is used for synchronising two or more power 'islands' and have tight requirements on frequency, voltage and phase angle difference. They differ from energising check used in power stations for synchronous generators that only have voltage requirements (fewer constraints). There are over 230 substations in Ireland and only about 30 have Paralleling Check synchronising schemes. It would be a great advantage, provide more flexibility, and as well as help decrease the restoration time, if additional substations were to be set up with such capabilities. If in the event of a blackout the restoration path needs to go through 5 additional substations to be able to synchronise this will make the restoration more difficult and longer. For example there could be an issue on the path like a breaker not able to operate.

Synchronising capability is essential, and with new generation at new locations the substations equipped with such capability need to be revised. A few additional synchronising schemes would enhance considerably the flexibility of the system and the restoration time which is critical in the PSRP.

6.1.6 LOAD AND LOAD RESTORATION

The change in the generation comparing today's system with the LCL 2030 scenario have been discussed; but the demand will also change in 2030. The demand will increase in 2030 according to the LCL scenario; this means more generation will be needed to support the increasing load. Demand side management, electric vehicles, data centres, and heat pumps contribute to a change in the load. For example, electric vehicles can potentially be

regulated in the PSRP; the electric vehicle can potentially be restricted during the restoration process to avoid overloading and collapsing the system. A blackout during moments of peak is problematic, because when some load will be connected back households might add even more elements on the circuit making it more unpredictable.

In the 2030 LCL scenario, the DSO will have a greater role to play; it will need to be highly involved in load restoration. The DSO will also have a role to play with regard to DSM and solar/wind plants connected to the distribution system.

6.1.7 ELEMENTS OF THE REVISED/FINAL RESTORATION PLAN

The current Power System Restoration Plan sets a framework for the restoration. However as the network is changing it is not perfect and cannot account for all the possible cases. For the LCL 2030 scenario it will need to be revised accordingly. As more loads are connecting and multiple generators decommissioned, more Black Start units should be added to the system; this can be done in different ways.

One element as described previously is to enable renewables, such as wind, solar and ocean energy sources, to provide Black Start capability. They can have the ability to start without any external generation and the advantage of being closer to some target generation. To integrate the renewables in the PSRP, new regulations should be put in place as currently wind farms are shut down. However, renewables are heavily dependent on the weather conditions, so the PSRP cannot rely entirely on them.

Another solution is to incentivise existing generators to provide Black Start. Some OCGT could potentially have such capability. Other generators like CCGTs or biomass pants could add diesel generators (or similar mechanism) to their system to provide such capability. There are a number of different sites where this is possible. It is essential to add incentives for generators to be interested in doing so, as it could help strengthen the network considerably. But when doing so, it is essential to consider the location of the plants as the distance between Black Start units and target generation is crucial for the restoration time.

Similarly batteries could also be used as Black Start units in the PSRP. Some batteries are located very strategically to provide power to the system, if incentivised correctly this could be a key element for the future restoration plan.

The new interconnectors will also play an essential role in the future PSRP, given that they have Black Start capability.

For better flexibility in the restoration process additional synchronising capability should be considered.

Finally the current PRSP is split into different subsystems, however these should be revised.

There is a wide range of solutions potentially available and they should be considered to make the Black Start plan stronger and more reliable than it already is. As the network is increasing, new connections and substations are being built; this will improve the system stability but can also provide shorter path for PSRP.

6.1.8 EXAMPLE OF RESTORATION PATH

In what is currently the north subsystem of Ireland, due to the changes in LCL 2030 the current restoration path will no longer be feasible; there will only be one traditional target generator left Lough Ree in the subsystem.

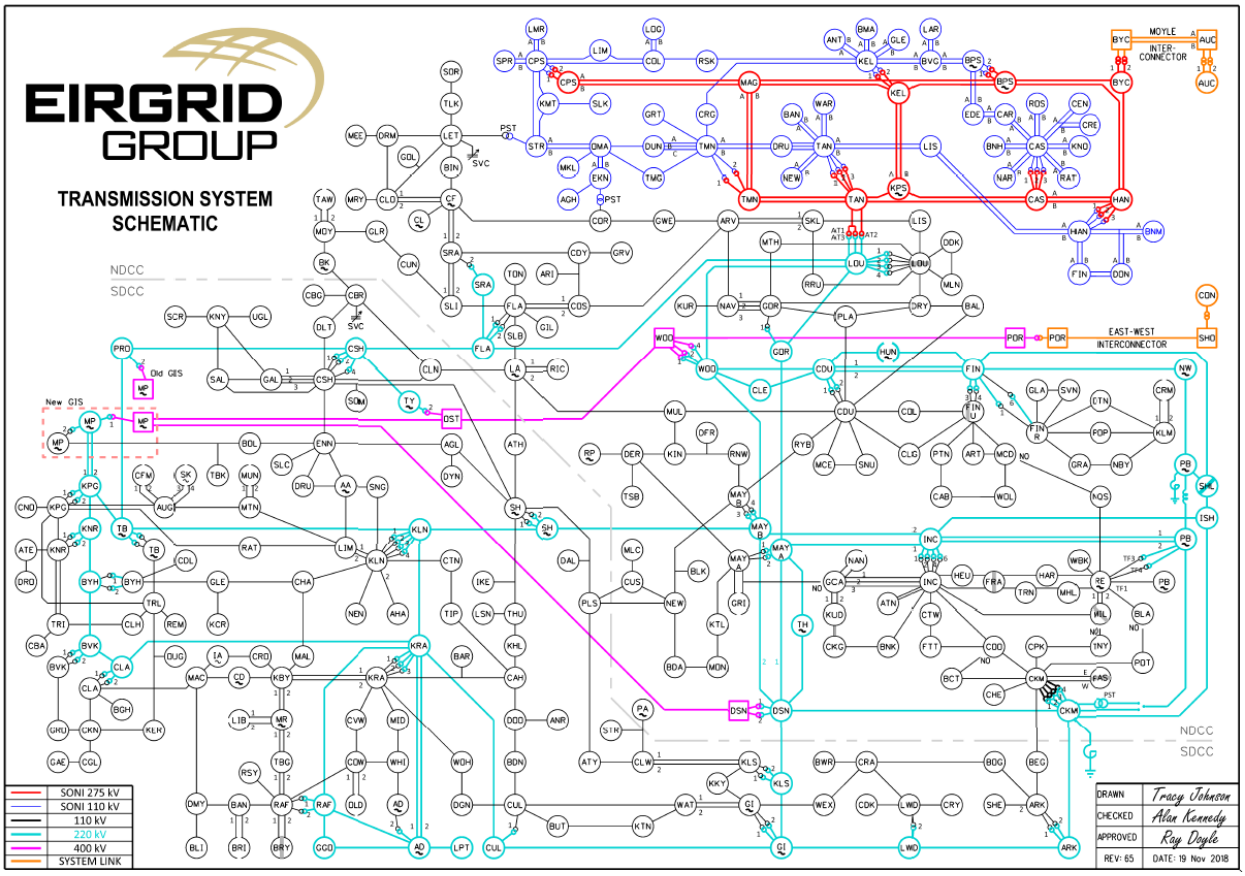

FIGURE 6-3: TRANSMISSION SCHEMATICS MAP OF IRELAND AND NORTHERN IRELAND

In the current PSRP there are two main restoration paths:

1. Cathaleen's Fall (or Cliff) → Srananagh → Sligo → Cunghill → Glenree → Moy → **Tawnaghmore**
2. Cathaleen's Fall (or Cliff) → Srananagh → Sligo → Flagford → Lanesboro → **Lough Ree Power**

In LCL 2030 the power plants in Tawnaghmore will be gone; meaning path 1 is no longer a possibility. However there is a wide range of possible path as described below:

- Cathaleen's Fall (or Cliff) → Tawnaghmore : there will be a new power plant in Tawnaghmore Biomass Mayo 49 MW.
- Cashala→ Tawnaghmore: there will be Shantallow Sloar, a 35 MW solar plant in Cashla that can energise Biomass Mayo.
- Shannonbridge → Lough Ree: the subsystems can be reconfigured; there is no reason why Shanonbridge cannot help the northern area in the power restoration.
- Northern Ireland → North subsystem: in case of partial blackout if the Northern Ireland Subsystem is still intact it could provide power to the north region through Letterkenny. Coolkeragh Power station is just one substation away from Letterkenny.

6.1.9 SUMMARY & CONCLUSION

The Low Carbon Living 2030 scenario plans for numerous changes in the current grid with the reduction of conventional generation sources and thus decommissioning of certain units. As it has been showed, the current restoration plan will need to be revised. There are a number of different ways to adapt and improve the PSRP. Many generation units can provide Black Start generation with the right incentives and changes. There potentially could be a lot of possible ways to restore power, but the key will be to choose to best units based on their location and their capacity.

As the system evolves, it entails a higher geographical dispersion of distributed renewable energy resources. This change can also result in the availability of a larger number of potential restoration paths. The future restoration plan will need to be robust and precise to cover all the different conditions, such as the availability of distributed renewable energy resources to participate in the restoration, either by providing a black-start service or providing a more suitable path for the black start. It is to be noted that due to the variability of renewable energy sources, the restoration paths are likely to change very frequently and hence may complicate the management of the restoration.

With regards to the installed black start capacity magnitude, although it appears to be unaffected as only a couple Black Start units are being decommissioned (in the analysed scenario) and new black start sources such as the interconnectors are becoming available; the availability of the black start magnitude is not always guaranteed.

For example, at the times of high renewable generation most black start conventional generation is likely to be either off or cold. In such circumstances, the Black Start conventional generators will take longer to start up thereby increasing the Black Start restoration time.

7. CONCLUSIONS & DISCUSSION

The analysis conducted under Task 2.4 was focussed on investigating potential system levels scarcities that may develop at high RES level operation. The analysis was conducted for several power systems e.g. Continental European, Nordic and Ireland & Northern Ireland power system. Multiple aspects of system operation that may be influenced by the development of potential scarcities at high RES level are analysed using purpose built models and analysis methods, suitable for bulk power system analysis. The details of analysed scenarios, snapshots, stimuli and models were finalised in Task 2.2 & Task 2.3 and are briefly reproduced in Chapter 1. The conclusions & discussion pertaining to individual categories of system operational stability are described below:

7.1 FREQUENCY STABILITY & CONTROL

Frequency stability analysis has been carried out for the Continental European, Nordic and Ireland & Northern Ireland power systems. Time domain frequency stability simulations, informed by least cost dispatch optimisation have been carried out for all systems, while the stimuli and operational assumptions have been varied to focus on the most relevant aspects of frequency stability for each of the power systems under consideration.

A direct consequence of increasing non-synchronously connected generation (PV and Wind RES technologies) is a decline in power system rotational energy or system inertia, leading to higher RoCoF values. An inertia scarcity has therefore been investigated across the various systems under consideration.

Different operating conditions for the pan-European power system were explored, including interconnected system operation and system split conditions. It has been shown for the Continental system that with higher SNSP and lower inertial response, there is a tendency towards higher local RoCoF values. The impact of SNSP levels on RoCoF values is observed in every zone considered, and this impact is only visible above a certain level of penetration in the strongest zones (70% to 75%). There is an indication that RoCoF values as high as 1.3 Hz/s could be reached in the Iberian Peninsula. System inertia levels, for the Ireland and Northern Ireland system exhibit a similar albeit a more serious inertia problem. It was found that in a 2030 power system with SNSP levels approaching 90%, RoCoFs can be so excessive, so as to prohibit any meaningful analysis of frequency deviations in time domain simulations. Consequently, it was decided to put a mitigation in place early in the study; a 1 Hz/s RoCoF constraint was included in the system scheduling. Therefore reducing inertia levels has clearly been identified as a scarcity for the Ireland & Northern Ireland system, which if left unmitigated is likely to severely impact future system operation at high RES levels. For the Nordic power system, it was observed that upon increasing the operational levels of RES in the system, the minimum system inertia shows a declining trend. However, the RoCoF was deemed not to be a serious issue for the Nordic power system in 2030 for the considered scenarios, for which a high share of synchronous machines are still connected, with RoCoF values never rising above 0.4 Hz/s. It is to be noted that during some hours, typically at night and during the summer

when demand is low and depending on the dispatch schedule, the Nordic power system could experience inertia levels that are lower than current inertia levels due to displacement of conventional generation by non-synchronous resources. A trend towards declining system inertia levels was observed across all the power systems analysed, with this scarcity being most onerous for Ireland & Northern Ireland power system, due to higher variable renewable energy levels, smaller size and synchronously isolated nature of the system. The nature of the inertia scarcity is more locational in the Continental Europe system, due to its comparatively larger size, interconnected nature and the share of low-carbon synchronous generation connected in some areas.

In addition to RoCoF, system frequency deviations following a sudden energy imbalance (infeed/export loss or system split) are a key measure of system frequency stability. In addition to increased RoCoF values, reducing system inertia contributes to large frequency deviations following a sudden energy imbalance. However, another key contributing factor determining the largest frequency deviations following a sudden energy imbalance (frequency nadirs & zeniths), is the nature, magnitude and speed of response of contingency reserve portfolio. Increased RES levels imply that the contingency reserve should theoretically be required to be quicker. In the simulations, contingency reserve provision for the Continental European system represents the current system operational policies, as is the case for the Ireland & Northern Ireland system. However, for Ireland & Northern Ireland system a FFR service is currently deployed to cater for faster frequency dynamics. It should therefore be noted that the Ireland & Northern Ireland system results presented entail an inherent representation of fast contingency reserves. The composition and magnitude of this fast reserve varies across the considered scenarios and the snapshots within those scenarios. Similarly, the FFR provision is assumed to be active for the Nordic power system.

For an intact Continental power system, it has been shown that frequency nadirs following the loss of a large generating unit in each jurisdiction decline as SNSP levels in that jurisdiction increase. It should be noted, however, that all the frequency nadirs recorded for the intact system are above the threshold for activation of load shedding. The Iberian Peninsula is the worst affected, where, for the highest renewable scenario, the loss of 2 GW of generation in the peninsula has been shown to lead to nadirs around 49.35 Hz. This is a result of the fact that the Iberian Peninsula is weakly interconnected with the rest of the Continental power system and has low system inertia due to the high penetration of variable renewable generation. It has also been observed that with increasing RES levels; the frequency in the Continental European system becomes more locational, implying a generally looser electrical coupling among various parts of the Continental European system. System split events for the Continental power system were also examined. Unsurprisingly, the frequency stability indicators are much more extreme than for interconnected incidents and the traditional frequency control mechanisms are insufficient to cope with such incidents. Under system split conditions, the system stability relies on LFSM-O/U and load shedding. It was observed that, for all three Continental power system split events studied, the frequency stability of the system is endangered. However, for example, in the case of the Iberian Peninsula disconnecting from the remainder of the Continental system, frequency nadirs in the peninsula could fall as low

as 46 Hz, well under the load shedding threshold, and such a situation corresponds to a blackout event as generators are not obliged to remain connected at such low frequencies. Similarly, extreme frequency zeniths of 53 Hz in the Iberian Peninsula could be possible if the Iberian Peninsula is disconnected, while RoCoF values greater than 2 Hz/s are more likely, also leading to generator disconnections. The probability of such extreme events is however very low and should be assessed in future work. Moreover, the split events simulated in that study assume that DC links also disconnect, which is questionable. Again this is an area that requires further detailed analysis.

Similar to the Continental system results, the majority of cases examined for Ireland & Northern Ireland system experience nadirs above the load shedding threshold. It is interesting to note that there is no clear correlation between SNSP levels and frequency nadirs. This is because as SNSP levels increase there is a trend towards smaller dimensioning incidents, in order to satisfy the RoCoF constraint. While it was found in the Ireland and Northern Ireland analysis that there are some frequency nadirs below load shedding levels, there is mitigation currently available such as carrying sufficient reserve. The results indicate that the higher the fast reserve magnitude that is available, the higher the frequency nadirs. A general finding is that to maintain frequency stability, the volume of fast acting reserves should at least be equal to the magnitude of the dimensioning incident. In cases where there is insufficient fast acting dynamic reserve capability in the generation portfolio, lower frequency nadirs for the Ireland and Northern Ireland power system are observed. This is because, as the portfolio changes, there is increasing reliance on non-conventional generators (batteries, IC and demand-side units). These resources provide precisely their contracted volumes and no more and the result is that the dimensioning incident causes lower frequency nadirs that can only be arrested by load shedding. This indicates that the current practice of scheduling 75% of largest infeed loss (dimensioning incident) as the fastest contingency reserve category, no longer guarantees system security, due to changing reserve portfolio in the future.

For the Nordic system, reducing inertia levels at certain operating conditions lead to lower frequency nadirs similar to the other systems examined. That being said, even in the highest variable renewable scenario tested here, these nadir levels are never below the load shedding threshold. It is acknowledged however, that there are certain measures that could be implemented to improve nadir margin above the critical level. This includes the Fast Frequency Reserve, which is already being adopted

It has been observed that increased RES levels result in a trend towards reducing system inertia, increasing RoCoF and generally high frequency deviations following the sudden loss of an infeed/export, across all the examined systems. Furthermore, the importance of fast reserves is clearly demonstrated for the Ireland and Northern Ireland power system, it should be noted that the analysis for the Continental European power system did not consider fast reserves. Consequently, no overarching conclusions about fast reserves in Continental Europe can be drawn. What can be concluded, however, is that future analysis, potentially EU-SysFlex Task 2.6, should

explore the need for fast reserves, particularly for the Iberian Peninsula, where low frequency nadirs and high RoCoF values are observed. Another interesting outcome of the analysis as evidenced by the Ireland and Northern Ireland system is that the scenario with higher RES level (LCL) exhibits better frequency stability than the scenario with lower RES level (SE). This occurs due to a number of factors such as higher magnitudes of infeed loss in SE and smaller magnitude of available fast reserve from batteries and HVDC interconnection in SE scenario. It can therefore be inferred that the transitory phase from relatively smaller to very high levels of RES can be very challenging from a frequency stability viewpoint.

7.2 VOLTAGE CONTROL

Voltage stability analysis has been carried out for the Continental European and Ireland & Northern Ireland power systems. Both steady state voltage control and dynamic voltage regulation have been investigated so as to reveal any potential scarcities regarding steady state reactive capacity and dynamic reactive regulation capability. Multiple analysis methods including steady state voltage deviations, P-V & Q-V analysis, fault level analysis and time domain simulation are carried out. The Polish power system, as a representative network of the Continental European system, is the focus of the initial part of the analysis, followed by the Ireland & Northern Ireland power system.

The analysis shows that the 110 kV Polish system exhibits a lack of steady state reactive power capacity, as demonstrated by deteriorating steady state voltage regulation. The reactive power scarcity becomes most apparent at high load and minimum inertia conditions. Generally, higher levels of RES incorporated in the Going Green scenario; result in a lack of steady state reactive power. P-V analysis across various zones of the Polish system demonstrates that within the subnetworks of the Polish system, regions with higher magnitude of installed renewable capacity show a trend towards diminishing stability margins. Similarly the Q-V analysis on the Polish system demonstrates that the scenarios characterised by high RES capacity exhibit a higher risk of potential nodal voltage stability. Steady state short circuit levels for the Polish system across the considered scenarios remain within minimum operational requirements, pointing to the absence of potential issues regarding dynamic voltage regulation. This is confirmed by the time domain simulations, whereby, it is demonstrated that across all scenarios and snapshots considered; following system faults the voltage profiles encountered by both synchronous machines and power park modules encounter remain within the stipulated fault ride through requirements.

For the Ireland & Northern Ireland system it has been observed that there is a significant correlation between increasing renewable generation levels and the deterioration of voltage regulation, as evidenced by steady state voltage deviation magnitudes. While the steady state reactive power scarcity has been identified in both the simulated 2030 scenarios, the scarcity is more pronounced in the low carbon living scenario, which entails higher

levels of renewable generation across the year. Steady state reactive power scarcity is further validated by the results of QV analysis; where, it was found that selected weak buses in the system required increased reactive power required to reach their target voltage. It has been observed that the weaker parts of the system and areas in the proximity of intermittent renewable generation are particularly prone to significant requirements for steady state reactive power. A dynamic reactive injection scarcity is apparent from the results of fault level analysis. A general trend towards declining fault levels across the system is observed, particularly in the weaker parts of the system. However, in some cases, the local fault levels increase due to the cumulative impact of higher magnitude of renewable generation in the vicinity of the bus under consideration. This is further evidenced by the time domain simulations, which demonstrate a lack of instantaneous dynamic reactive current injection at high renewable levels, resulting in deterioration of dynamic voltage regulation. The low carbon living scenario, which entails higher levels of renewable generation, exhibits a more pronounced dynamic reactive current injection scarcity, demonstrating the link between higher levels of renewable generation and reduced dynamic voltage regulation. Furthermore, significant levels of variation in voltage following the clearance of faults, indicates reduced system strength and may have implications for phased lock loop control operation and hence warrants further investigation.

The Polish and Ireland & Northern Ireland power system exhibit a steady state voltage regulation scarcity as the system evolves towards higher levels of renewable generation. The Ireland & Northern Ireland system exhibits a clear deterioration of fault levels, and a dynamic voltage regulation scarcity, these issues are not observed for the Polish system. However, it is to be noted that the model utilised for the Continental European system is characterised by various levels of modelling detail for various component regions, with the Polish system modelled with a high level of detail. Furthermore, the cases analysed have been pre-selected using various criteria such as minimum inertia, minimum reactive margin and maximum load across various component regions, as opposed to analysing all potential system configurations. The levels of RES for a specific system operating condition differ across various sub-systems of the Continental Europe. Therefore a lack of potential scarcity can either be due to the snapshot selection approach, modelling deficiencies, choice of the representative system within the Continental European system or insufficiently high levels of renewable generation considered.

7.3 ROTOR ANGLE STABILITY

Rotor angle stability analysis has been carried out for the Continental European and Ireland & Northern Ireland power systems. The analysis focussed on time domain simulations following a system short circuit event. The levels of stability have been categorised using multiple indicators such as rotor angle deviations, critical clearing times & oscillation damping quantification indices.

The studies performed for the Continental System focused upon the detailed model of the Polish system and showed no scarcity in stability margin, when assessed through critical clearing times for a range of busbar and single and double circuit faults that are cleared by primary protection operation. However, a localised scarcity is observed when close end line faults or busbar faults are cleared by backup protection. The required stability margin is 20 % and the lowest margin for a line fault is 72 %and for a busbar fault it is 31 %. No particular, significant variation in margin was observed between the cases analysed with a marginal reduction in median margin for the Energy Transition minimum inertia and minimum reactive power cases being the most notable outcomes. In the Polish system the primary protection will clear a fault in at most 120 ms and backup protection, where required, would clear the fault in 550 ms. Given the results presented, this primary operation time ensures that there is no scarcity but if the operation of backup protection were required then many of the close end and busbar faults studied would not be cleared quickly enough.

The studies performed for Ireland and Northern Ireland studied the range of fault contingencies used in WSAT, the online dynamic security assessment tool used in the control room. In these studies it was found that 65 % of critical clearing times exceeded the 70 cycle maximum search value applied (primary operation time in Zone 1 is 4 cycles and backup protection operation time is 25 cycles). As such there is no global scarcity of stability margin; however, a localised scarcity does emerge for several cases when assessed according to the absolute worst case backup protection clearing time and for a very small set of cases when assessed against the 4 cycle expected clearing time. These cases are driven by specific combinations of contingencies, unit commitments and the generator's pre-fault conditions and not the overall SNSP level.

Therefore, a localised scarcity of stability margin (measured through critical clearing time) is emerging for any situation where backup protection is required to operate (e.g. due to protection failures) in both the Continental system studies and the Ireland and Northern Ireland studies. However, there is no scarcity of stability margin if primary protection operates as designed. This indicates that more detailed assessment of the performance of backup protection may be required in the future. Furthermore, it should be noted that in these studies it is assumed that the fault current observed would be sufficient for protection relays to pick up, i.e. the protection relay is not modelled and breakers are simply opened by predefined simulation events. With the scarcity in short circuit current reported in Chapter 3 this assumption should be verified and where necessary protection settings/design may need to be modified or minimum fault currents ensured. Therefore, based on these results, an effective means by which to ensure that there will be no scarcity in stability margin is to mitigate the localised scarcity of short circuit current through a system service.

Oscillation damping in the Continental European system was studied for the detailed model of the Polish system. This study indicated that oscillation damping presents a global scarcity with poor settling and halving times for almost all cases and scenarios, with only the maximum load case having any significant number of acceptable settling and halving times. However, it should be noted that the nature of the model developed for this study is

not appropriate for the study of inter-area oscillations on the Continental system and that this conclusion is only applicable to the local modes observed within the detailed model of the Polish system. In contemporary operation power system stabilisers (PSSs) that are installed as a supplementary part of voltage controllers usually mitigate these oscillatory problems and this appears to no longer be the case. This is not entirely surprising, as PSS tuning can be quite sensitive and may have to be carefully coordinated with the power converter controllers located in the power system.

Oscillation damping in the Ireland and Northern Ireland system was studied for the same contingencies and hours of operation for which stability margin was assessed. The results presented indicate a localised scarcity of oscillation damping for low carbon living and a global scarcity of oscillation damping for Steady Evolution. This scarcity can primarily be observed as a local oscillation in one or two units when a contingency occurs close to their point of connection. This conclusion is borne out by the fact that the cases with poor damping are heavily associated with specific contingencies and do not occur in general. As such, the scarcity is not driven by SNSP but by the unit commitment schedule and the presence of isolated units that connect through weaker parts of the network, where single contingency can impact the unit most significantly. Whilst these unit commitments with isolated units may be expected to occur more frequently as SNSP increases this does not appear to be the case, as the more severe scarcity is observed for Steady Evolution, which has a lower overall SNSP.

Oscillation damping presents a scarcity in both the Ireland and Northern Ireland studies and the Pan-European system studies. However, it is far more acute in the Continental Europe system results and all cases studied exhibit unacceptable damping for most contingencies and all scenarios. In the Ireland and Northern Ireland studies damping was significantly reduced for all cases and at times was outside of acceptable limits, particularly for the steady evolution scenario. This makes it a local scarcity compared to the global scarcity observed for the continental system, where poor settling and halving times occurred for almost all cases and scenarios. This scarcity does not correlate to SNSP and may be particularly worthy of further study as system models tend to have higher damping than the system will have in reality. Furthermore, the nature of the study performed for the continental system was such that it did not capture the impact of this reduced damping on inter-area oscillations. Therefore, as such modes of oscillation are already known to exist in the continental system, the impact of this damping scarcity on these modes should be assessed, as poorly damped inter area modes are known to contribute to the occurrence of system separation events. A local or global scarcity can be directly mitigated by developing a damping requirement and associated system service, which would ensure that the system had appropriate damping at a range of frequencies of oscillation. Damping sources could be active (e.g. a converter equipped with a power oscillation damper) or passive in nature (e.g. inertia). Given the nature of the scarcity this could well require a locational aspect and for localised scarcities it may best be managed through a controller tuning policy that places specific damping requirements upon generators.

Angle margin was used to determine if a scarcity of synchronising torque was present in the Ireland and Northern Ireland system. This scarcity was not studied for the continental system. In general there were no angular stability issues, with almost all hours and contingencies having very similar ranges of angle margins and the variation that was observed between hours being attributed primarily to the initial angular positions. However, a small subset of contingencies exhibited angular instability that caused a generator to slip a pole. This reveals a clear localised scarcity in synchronising torque and occurred regardless of scenario and manifested through angular instability of certain generators for certain N-1 contingencies. No global scarcity was observed in the Ireland and Northern Ireland studies (which would manifest as inter area oscillations and in the worst case system separation) and the system has no particular recent history of exhibiting such behaviour. This scarcity indicates a need for more detailed study and more specific, localised metrics for assessing the relative security of a case in the future, as the system level measures in use during these studies fail to indicate the presence of this localised scarcity (i.e. it manifested regardless of inertia and SNSP levels). The scarcity would be mitigated by ensuring that any generator synchronised to the system had sufficient level of synchronising torque to the other generators synchronised to the system. This could be resolved through studies to define the sufficient level for each generator and a service through which to incentivise the provision of synchronising torque. Given the nature of the scarcity this service would likely require a locational aspect and the need for the service would be highly sensitive to unit commitment and the contingencies considered which may have market implications.

7.4 SYSTEM CONGESTION

The type of congestion investigated across the systems is not comparable, and hence the methods used to carry out the analysis also differ substantially. However, both elements of this work have revealed the emergence of global scarcities as renewable penetrations increase. Whilst the congestion of any one line could be viewed as inherently local, congestion is classified here as a global scarcity due to the sheer scale of the congestion issues observed.

For the Continental European system congestion was studied from the perspective of unscheduled flows, where unscheduled power flows are a concern as they will displace scheduled, market flows and through this manifest a scarcity. The study presented here highlights that an increase in the RES installations in the continental system will increase the severity of this congestion scarcity and this will likely cause unscheduled flows to exceed the acceptable level of 30% of capacity (as allowed under the Clean Energy Package), which will require mitigating actions. This scarcity occurs because, unlike conventional technologies, RES tend to be localized in particular regions of Europe (this refers mostly to wind farms, which benefit from proximity to the North Sea and Baltic). The energy produced by these sources is either exported or consumed domestically. In the latter case, a set of zonal internal exchange is expected to increase the level of loop flows and, consequently, unscheduled flows. Before the implementation of the Clean Energy Package, the capacity calculation process designed for European energy exchange was aimed at adjusting the level of acceptable market flows, so that they complement the

expected level of loop flows. However, the CEP introduced the requirement of offering at least 70% of thermal limits to the inter-zonal market. This legal claim does not change the phenomenon of the increasing amount of loop flows, which drives the observed scarcity. This scarcity could be mitigated through a congestion service that incentivised real-time power flow control devices, geographically dispersed energy storage that can defer the flows, or where justifiable construction of new transmission assets.

The scarcity observed in the Ireland and Northern Ireland power system is a global scarcity that is also driven by the location of new RES. RES are installed in parts of the system where there was traditionally little generation or demand. Therefore, sufficient transmission infrastructure is not in place to transfer this power to the load centres and the infrastructure that is in place can become heavily overloaded. Overloads are observed at low SNSP and the occurrence and magnitude of thermal overloads increases with SNSP, indicating a lack of transmission network capacity in both Steady Evolution and Low Carbon Living. In general, these overloads are more severe in Low Carbon Living but are particularly more severe at low SNSP levels. The 110 kV transmission network is most heavily impacted as this network is primarily relied upon to connect the distributed RES, particularly in the West of Ireland and Northern Ireland, and this network effectively serves as a collector network for windfarms in these regions. When assessing congestion in the future, a focus should be placed upon how often a specific line or corridor may find itself overloaded and the severity of that overload. This information should be used to guide the selection of asset based and service based solutions, with the more common and severe congestion issues being candidates for asset based solutions. A system service may be required to manage congestion in the future, particularly in view of the barriers faced by onshore, above ground reinforcement, and these results indicate that it is important that this service incorporates elements that allow it to be effective at both high and low SNSP levels. Furthermore, this service would likely require locational aspects to allow focus on the 110kV collector networks but this would need to be complemented by a high degree of coordination to ensure that power flows are routed and deferred effectively.

7.5 SYSTEM RESTORATION

System restoration analysis has only been studied for the Ireland & Northern Ireland power system. The analysis takes a critical view of the current system restoration plan for Ireland & Northern Ireland power system, against the backdrop of the displacement of conventional black start capable units by renewable generation sources. The analysis has been carried out on for the LCL scenario.

The black start restoration plan (BSRP) will need to be re-inspected. There are a number of different ways to adapt and improve the BSRP. Many generation units can provide Black Start generation with the right incentives and changes. There potentially could be a lot of possible ways to restore power, but the key is to choose the best units based on their location and capacity.

As the system evolves, it entails a higher geographical dispersion of distributed renewable energy resources. This change can also result in the availability of a larger number of potential restoration paths. The future restoration plan will need to be robust and precise to cover all the different conditions, such as the availability of distributed renewable energy resources to participate in the restoration, either by providing a black-start service or providing a more suitable path for the black start. It is to be noted that due to the variability of renewable energy sources, the restoration paths are likely to change very frequently and hence may complicate the management of the restoration.

With regards to the installed black start capacity magnitude, although it appears to be unaffected as only a couple Black Start units are being decommissioned (in the analysed scenario) and new black start sources such as the interconnectors are becoming available; the availability of sufficient black start magnitude is not always guaranteed. For example, at the times of high renewable generation most black start conventional generation is likely to be either off or cold. In such circumstances, the Black Start conventional generators will take longer to start up thereby increasing the Black Start restoration time.

It is therefore concluded that against the backdrop of increasing renewable generation, the system restoration plan cannot remain un-effected. The black start installed capacity for the analysed scenario doesn't necessarily decline in magnitude by the addition of renewable generation, however at times of high renewable generation the black start restoration time may be negatively influenced. Over-all the black start plan is required to be more flexible, so as to incorporate the variable nature of renewable generation resources.

Overall, the scarcities are more clearly apparent for the Ireland & Northern Ireland power system, when compared to the Continental European power system; however, it must be noted that this does not imply absence of technical scarcities in the Continental European system. The appearance (or otherwise) of scarcities for the Continental European system is highly influenced by the focus area (Poland in this Task), snapshots, renewable energy levels and the stimuli used. A further complicating factor, for example, is the complex interaction between the focus area (e.g. Poland for rotor angle stability) and the rest of the Continental European system for certain parts of the analysis presented.

It is also to be noted that the analysis carried out in this report has been done using Root Means Squared (RMS) models for various components of the system. However, the extent of the validity of RMS models at very low system strength conditions is still a matter of debate within the industry. The extent of fidelity of PLL tracking at low system strength conditions is also considered a potential area of concern. A key consideration with regards to the limitations of RMS models is the comparatively limited frequency ranges for model validity, as opposed to electromagnetic transient (EMT) models. The EMT models are considered more suitable to represent the sub-synchronous frequency range transients associated with power electronics based converters used as interface between renewable energy resources and the power system. With this limitation in view, in this report, the power oscillation damping is assessed only with regard to the lower frequency electro-mechanical oscillations and not any resonances or control interactions that may occur. Further work is required towards establishing the extent of the validity of RMS models for bulk system stability evaluation at significantly low system strength conditions and PLL fidelity. While, Task 2.6 will re-examine, and if required modify, the assumptions made in the initial system stability assessment carried out in Task 2.4, in light of information provided by the demonstration projects and areas of further consideration identified in Task 2.4, additional work is likely to be required beyond the remit of EU-SysFlex.

It can be concluded that the analysis on the Continental European and Nordic system, clearly demonstrates technical scarcities associated with certain domains of system stability (e.g. voltage control), while highlighting increasing areas of concern for others (e.g. frequency control & congestion). An indication of the evolution of system needs (characterised by scarcities) due to a potential change in the system generation portfolio is evident for the Continental European system. The Ireland & Northern Ireland system clearly demonstrates technical scarcities across multiple categories of system stability for the scenarios analysed. Across all the considered systems, it is evident that some technical scarcities require mitigation measures to enable secure system operation. These mitigation measures can be implemented through designing appropriate and targeted system services, underpinned by appropriate financial and regulatory arrangements, and. the extent of their effectiveness will be examined in Task 2.6.

8. COPYRIGHT

This project has received funding from the European Union's Horizon 2020 research and innovation programme under EC-GA No 773505.

9. BIBLIOGRAPHY

[1] EU-SysFlex, "EU-SysFlex – Deliverable D2.1 - State-of-the-Art Literature Review of System Scarcities at Hi Levels of Renewable Generation," 2018.

[2] EU-SysFlex, "EU-SysFlex - Deliverable D2.2 - EU-SysFlex Scenarios and Network Sensitivities," 2018.

[3] EU-SysFlex, "EU-SysFlex - Deliverable D2.3 - Models for Simulating Technical Scarcities on the European Pow System with High Levels of Renewable Generation," 2018.

[4] P. Kundur, Power System Stability and Control, McGraw-Hill, 1994.

[5] ENTSO-E, "Dispersed Generation Impact on Continental Europe Region Security," 2014.

[6] ENTSO-E, "Frequency Stability Evaluation Criteria for the Synchronous Zone of Continental Europe Requirements and impacting factors," 2016. [Online]. Availabl https://docstore.entsoe.eu/Documents/SOC%20documents/RGCE_SPD_frequency_stability_criteria_v10.pdf.

[7] UCTE, "Continental Europe Operation Handbook Policy 1: Load-frequency control and performance, Appendi 2004.

[8] ENTSO-E, "IGD - Rate of Change of Frenquency withstand capability," 2018.

[9] EU-Turbines, "EU Turbines Statement on Frequency Requirements," 2018.

[10] UCTE, "Final Report of the Investigation Committee on the 28 September 2003 Blackout in Italy," 2003.

[11] UCTE, "Interim Report, System Disturbance on November 2006," 2006.

[12] J. Morin, "Probabilistic estimation of the aFRR requirement in the future European power system with high R penetration," Wind Integration Workshop, 2019.

[13] "Data Platform - Load, wind and solar, prices in hourly resolution for 37 European Countries," [Onlin Available: https://data.open-power-system-data.org/time_series/ .

[14] L. Hirth and I. Ziegenhagen, "Balancing power and variable renewables: Three links," *Renewable a Sustainable Energy Reviews,* vol. 50, pp. 1035-1051, 2015.

[15] K. De Vosa, N. Stevensb, O. Devolderb, A. Papavasiliouc, B. Hebba and J. Matth, "Dynamic dimensioni approach for operating reserves: Proof of concept in Belgium," *Energy Policy,* 2019.

[16] ENTSOE, "Deterministic frequency deviations – Root Causes and Proposals for Potential Solutions," 2011.

[17] EirGrid, "Tomorrow's Energy Scenarios 2017: Planning our Energy Future," EirGrid Plc, Dublin, 2017.

[18] EirGrid and SONI, "Operational Constraints Update," 2019.

[19] EirGrid and SONI, "Annual Renewable Energy Constraint and Curtailment Report 2016: Non-Technic Summary," 2017.

[20] ENTSO-E, "Technical Requirements for Frequency Containment Reserve Provision in the Nordic Synchrono Area - draft," 2017.

[21] Fingrid, "Nopean taajuusreservin (FFR) teknisten vaatimusten todentaminen ja hyväksyttämisprosessi," 201 [Online]. Available: https://www.fingrid.fi/sahkomarkkinat/reservit-ja-saatosahko/nopea-taajuusreservi/.

[22] J. Machowski, J. Bialek and J. Bumby, Power system dynamics: Stability and Control. Second Edition, John Wil & Sons, Ltd., 2008.

[23] E. Agneholm, S. Meybodi, M. Kuivaniemi and P. Ruokola, "FCR-D design of requirements – phase 2.," ENTSO- 2019.

[24] Statnett, Fingrid, Energinet.dk, Svenska Kraftnät, "Challenges and Opportunities for the Nordic Power System 2016.

[25] E. Ørum, M. Kuivaniemi , A. Bruseth, E. Jansson, A. Danell and N. Modig, "Future System Inertia," 2015.

[26] E. Ørum, L. Haarla, M. Kuivaniem, M. Laasonen, A. Jerkø, I. Stenkløv, F. Wik, K. Elkington, R. Eriksson, N. Moc and P. Schavemaker, "Future System Inertia 2," 2017. [Online]. Availabl https://www.statnett.no/globalassets/for-aktorer-i-kraftsystemet/ut.

[27] ENTSO-E, "Fast Frequency Reserve - Solution to the Nordic inertia challenge," 2019.

[28] PSE S.A., "Standard functional specification: Polish Power System (in Polish)," Konstancin-Jeziorna, 2015.

[29] IEC 60909, "Short-circuit currents in three-phase a.c. systems (series)," (2000-2016).

[30] T. Van Cutsem and C. Vournas, Voltage stability of electric power systems, Springer Science & Business Medi 2007.

[31] EirGrid, "Transmission System Security and Planning Standards," 2016. [Online]. Availabl http://www.eirgridgroup.com/site-files/library/EirGrid/EirGrid-Transmission-System-Security-and-Planning-Standards-TSSPS-Final-May-2016-APPROVED.pdf.

[32] SONI, "Northern Ireland Transmission System Security and Planning Standards Security and Quality of Supp Standard," 2015. [Online]. Available: http://www.soni.ltd.uk/media/Northern-Ireland-TSSPS-Septembe 2015.pdf.

[33] Energy Networks, "Engineering Recommendation G74 (ER G74)," [Online]. Availabl https://www.energynetworks.org/.

[34] Powertech, "Transient Security Assessment Tool User Manual," DSATools, 2016.

[35] M. Kłos and K. Wawrzyniak, "Comparing Load Flow Decomposition Methods for Cost Sharing of Coordinate Redispatch," National Centre for Nuclear Research: European Energy Markets 2019, Lublana, 2019.

[36] FutureFlow, "Cross-border balancing and redispatching mechanisms tailored to congested borders situati and design of a Common Activation Function," 2016.

[37] ENTSO-E, "Joint Task Force Cross Border Redispatch Flow Definitions".

[38] J. Bialek, "Tracing the flow of electricity, IEE Proceedings on Generation, Transmission and Distribution".

[39] I. Chychykina, C. Klabunde and M. Wolter, "Redispatch with power flow decomposition and power transf

distribution factors methods," International Universities Power Engineering Conference, 2016.

[40] ENTSO-E, "ENTSO-E, Bidding zone configuration, Technical Report 2018," 2018.

[41] S. Nouri and S. Jadid, "Transmission network loss allocation via equivalent bilateral exchanges principle ar genetic algorithm," IEEE 2nd International Power and Energy, 2008.

[42] N. Fulgêncio, C. Moreira, L. Carvalho and J. Peça, Aggregated dynamic model of active distribution networks f large voltage disturbances, Electr. Power Syst. Res., vol. 178, p. 106006, 2020.

[43] European Commission, "Establishing a Network Code on Requirements for Grid Connection of Generators 2016.

[44] D. Chakravorty, B. Chaudhuri and S. Hui, "Rapid frequency response from smart loads in Great Britain pow system," 2017. [Online]. Available: https://doi.org/10.1109/TSG.2016.2517409.

10. ANNEX1: SNAPSHOT SELECTION FOR IRELAND & NORTHERN IRELAND SYSTEM

10.1 LOW CARBON LIVING SCENARIO

For the low carbon living scenario the following ranges were selected for the three measures:

Low SNSP – SNSP < 75%, High SNSP – SNSP > 80%
Low inertia – Inertia < 15.5 GWs, High inertia – Inertia > 20 GWs
Low Units – No units in NI & Dublin, High Units > 1 unit in NI & Dublin

The hours selected for low carbon living are scatter plotted against all of the hours in the scenario in Figure 1-3.

TABLE 10-1: SNAPSHOT HOURS TO STUDY FOR LOW CARBON LIVING

Type ID	SNSP level	Units in NI & Dublin	Inertia	Hours to analyse
Type 1	Low	High	High	956,2307,2309,787,1828
Type 2	High	Low	Low	4530,3017,4528,4529,3660
Type 3	Low	Low	Low	4008,5767,5686,5688,4921
Type 4	Low	High	Low	751,2119,3731,5190,5191
Type 5	Low	Low	High	4631,4632,4112,4630,4629
Type 6	High	High	High	2416,2417,2437,2439,2850
Type 7	High	High	Low	7048
Type 8	High	Low	High	4864,4117,4118,4119,4120

10.2 STEADY EVOLUTION SCENARIO

For steady evolution, the high, low criteria for everything have been based on the median value. Anything above median is high, anything below it is low.

- SNSP median = 48%
- Inertia median = 23,000
- Dublin&NI unit median = 3

The hours selected for low carbon living are scatter plotted against all of the hours in the scenario in Figure 1-4.

TABLE 10-2: SNAPSHOT HOURS TO STUDY FOR STEADY EVOLUTION

Type ID	SNSP level	Units in NI & Dublin	Inertia	Hours to analyse
Type 1	Low	High	High	955, 2289, 1896, 1960, 1316
Type 2	High	Low	Low	2151, 2149, 3017, 1477, 5009
Type 3	Low	Low	Low	6529, 6534, 5039, 5736, 5863

Type 4	Low	High	Low	7198, 3215, 3216, 3212, 3214
Type 5	Low	Low	High	6721, 5544, 5791, 4680, 5497
Type 6	High	High	High	8396, 8397, 8398, 8399, 1655
Type 7	High	High	Low	1351, 1362, 3161, 2113, 2115
Type 8	High	Low	High	590, 1519, 4924, 7886, 2224

10.3 COMPARISON OF TYPES BY SCENARIO

Types are defined here in order to separate the hours based on similarity and then select a subset from each type. The types are separated by the three binary measures described above and the following is a brief summary of the hours selected and how this may impact the analysis.

To support this analysis the cumulative sum of the inertia, SNSP and NI & Dublin units is presented for each scenario in Figure 10-1 and the range in these parameters is presented in plot for each type separated by scenario in FIGURE 10-2.

The comparison of the scenarios and snapshots indicates that, in general: LCL has lower inertia and lower SNSP; SE has lower demand in many of the snapshots selected and SE has a tendency to have more units on in NI & D. Beyond these tendencies and with the exception of a cluster of very low inertia points that emerge for low carbon living (See type 2 in Figure 1-3, the two scenarios are not intrinsically very different.

From the comparison of the hours in each type it would appear that the most valuable points of comparison in the study results will be:

- Type 1 is expected to be the most secure type.
    - Two clear sub types emerge:
        - Very high inertia and higher demand: 787 and 956 and 955 and 2289
        - Medium Inertia and lower demand 1828, 2307 and 2309 and 1896 and 1960 Noting that the SE hours have notably higher SNSP
    - Greater variation will be observed for SE than LCL, as the hours are less uniform, particularly 1316 that has much lower inertia and higher SNSP
- Type 2 is expected to be the least secure hour and this should be less of an issue for SE than in LCL (as SE has higher inertia and more units in NI & D).
    - The LCL hours are all similar but will only be truly comparable to 2153 as the other SE hours have notably higher inertia
- Types 3 to 8 have very similar inertia but Types 3,4 and 5 have lower SNSP in general than 6, 7 and 8. Therefore, if these types exhibit similar behaviour it would suggest inertia is a more dominant factor than SNSP.

- Type 4 for LCL has two distinct sub types a higher demand sub type (751, 2119 and 3731) and lower demand sub type (5190 and 5191).
- The high variation in SNSP between LCL and SE for Types 3, 4 and 5 may highlight the inherent impact of SNSP.
- Equally, if inertia is treated as a proxy for the total number of units then relative impact of NI & Dublin units can be assessed by comparing Types 3 to 8.

One challenge posed by the analysis between types is that it has been observed that multiple factors vary between the types, which will make definitive conclusions on the root cause of any change in behaviour challenging. Furthermore, the general tendency for the LCL types to have higher SNSP, lower inertia and fewer NI & Dublin units than the SE types may limit the extent to which any analysis can distinguish the relative impact of these factors in each scenario.

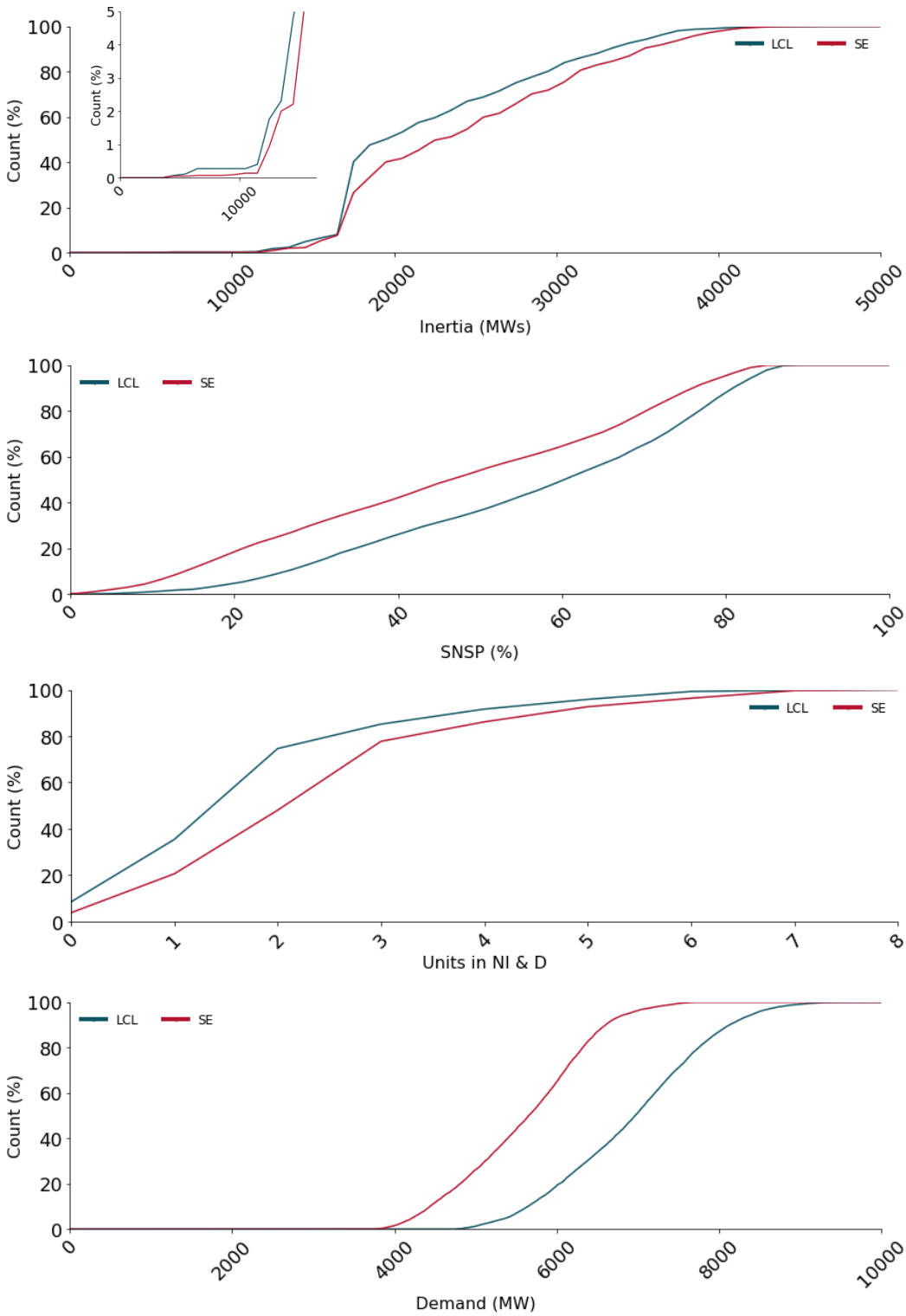

FIGURE 10-1: CUMULATIVE DISTRIBUTION OF INERTIA, SNSP, UNITS IN NI & DUBLIN AND DEMAND FOR LOW CARBON LIVING AND STEADY EVOLUTION

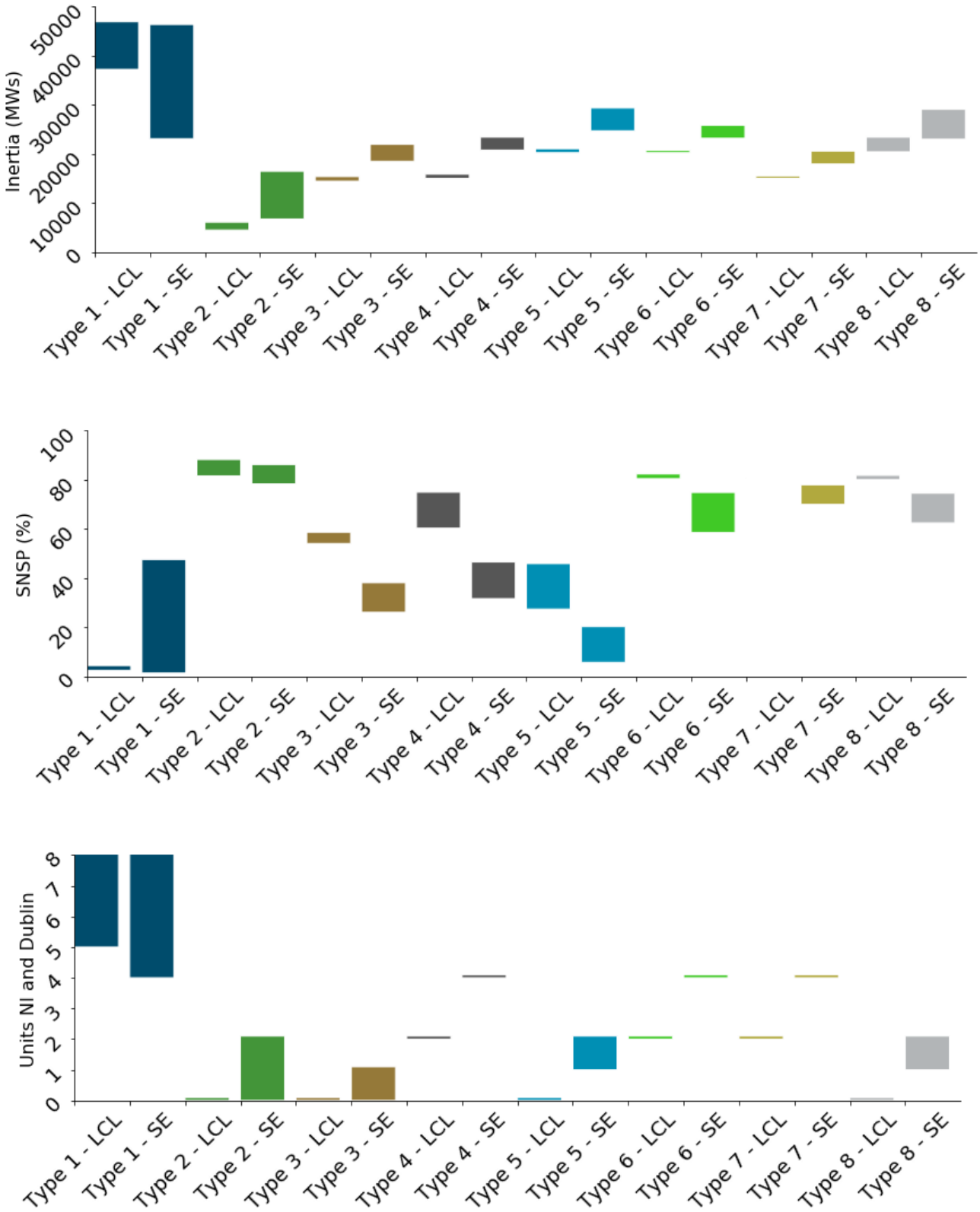

FIGURE 10-2: PARAMETER RANGES FOR EACH TYPE IN LOW CARBON LIVING AND STEADY EVOLUTION

10.3.1 TYPE 1 – HIGH INERTIA AND MULTIPLE NI & DUBLIN UNITS

a. Type 1 contains hours that have the highest inertia, lowest SNSP and the most NI & Dublin units. As such, these hours would be expected to be the most secure.

TABLE 10-3 presents the value of the three measures used and the demand. The demand is included as it provides context to the SNSP and inertia values. The LCL hours are quite similar but SE has several hours with high SNSP, which should serves as a useful comparison point.

These hours can be further sub typed as follows with colour denoting scenario:

b. Very high inertia and higher demand: 787 and 956 and 955 and 2289
c. Medium Inertia and lower demand 1828, 2307 and 2309 and 1896 and 1960 (Note, the steady evolution hour has high SNSP. So may be an interesting comparison point.)

TABLE 10-3: SUMMARY OF TYPE 1 HOURS FOR EACH SCENARIO

Type 1	Low Carbon Living						Steady Evolution				
Hour	**787**	**956**	**1828**	**2307**	**2309**		**955**	**1316**	**1896**	**1960**	**2289**
Inertia (GWs)	46	46	37	38	38		46	23	38	34	42
SNSP (SNSP)	4	2	4	3	3		5	48	28	39	1
Units NI & D	8	8	5	6	6		8	4	6	5	7
Demand (GW)	8.6	8.5	5.6	5.5	5.4		7.6	6.9	5.6	6.7	6.2
Sub Type	a	a	b	b	b		a	x	b	b	a

10.3.2 TYPE 2 – LOW INERTIA AND HIGH SNSP

This type contains hours with high SNSP and low numbers of Units in NI & D. A distinct difference can be observed between LCL and SE in that, while the SNSP levels are similar, the snapshots for SE mostly have units connected in NI & D, which also results in higher inertia. This occurs because of the lack of very low inertia hours in SE.

These hours can be further sub typed as follows with colour denoting scenario:

a. Very high SNSP and very low inertia: all LCL hours and 2153
b. Very high SNSP and low Inertia, with units in NI & D: 1477, 3017 and 3662
c. Hour 5009 is an interesting case, as it has the highest inertia of Type 2 but no units in NI & D.

TABLE 10-4: SUMMARY OF TYPE 2 HOURS FOR EACH SCENARIO

Type 2	Low Carbon Living						Steady Evolution				
Hour	**3013**	**3660**	**4528**	**4529**	**4530**		**1477**	**2153**	**3017**	**3662**	**5009**
Inertia (GWs)	6	5	5	5	5		14	7	10	14	16
SNSP (SNSP)	82	88	82	87	84		79	86	82	84	78
Units NI & D	0	0	0	0	0		1	1	1	2	0
Demand (GW)	7.9	7.6	7.2	6.7	6.2		7.0	6.5	5.4	6.1	5.9
Sub Type	a	a	a	a	a		b	a	b	b	c

10.3.3 TYPE 3 – LOW DEMAND WITH LOW NI & DUBLIN UNITS

Type 3 captures hours were all three measures are low. These hours are similar, from a high level and reflect the relative properties of their scenarios (e.g. SE has higher inertia and lower SNSP). An interesting feature is that the demand is also notably lower in the SE hours than in the LCL hours. The hours are very similar within each scenario but the differences between the hours for each scenario will make direct comparison of results challenging.

TABLE 10-5: SUMMARY OF TYPE 3 HOURS FOR EACH SCENARIO

Type 3	Low Carbon Living						Steady Evolution				
Hour	**4008**	**4921**	**5686**	**5688**	**5767**		**5039**	**5736**	**5863**	**6529**	**6534**
Inertia (GWs)	15	15	14	15	15		21	20	19	20	19
SNSP (SNSP)	54	59	55	56	54		31	38	27	26	26
Units NI & D	0	0	0	0	0		0	1	1	0	0
Demand (GW)	5.8	5.6	6.4	5.8	5.5		4.7	4.6	4.2	4.7	4.1
Sub Type	x	x	x	x	x		x	x	x	x	X

10.3.4 TYPE 4 – MEDIUM DEMAND WITH HIGH NI & DUBLIN UNITS

Type 4 captures hours with low inertia and SNSP but a higher number of units in NI & D. It is similar to Type 3 in that the hours reflect the relative properties of their scenarios (e.g. SE has higher inertia and lower SNSP). The differences between the hours for each scenario will make direct comparison of results challenging.

For LCL two sub types can be formed; a higher demand sub type (751, 2119 and 3731) and lower demand sub type (5190 and 5191). Any variation in the results between these subtypes may be of interest and it is worthwhile

to note that it is quite common for the system to serve a range of demand levels whilst having similar Inertia and SNSP.

TABLE 10-6: SUMMARY OF TYPE 4 HOURS FOR EACH SCENARIO

Type 4	Low Carbon Living						Steady Evolution				
Hour	**751**	**2119**	**3731**	**5190**	**5191**		**3212**	**3214**	**3215**	**3216**	**7198**
Inertia (GWs)	15	15	15	15	15		23	22	21	21	22
SNSP (SNSP)	74	73	75	61	60		42	32	39	35	46
Units NI & D	2	2	2	2	2		4	4	4	4	4
Demand (GW)	6.8	6.5	6.4	4.7	4.8		5.3	5.3	5.1	4.8	5.9
Sub Type	a	a	a	b	b		x	x	x	x	X

10.3.5 TYPE 5 – MEDIUM DEMAND WITH LOW NI & DUBLIN UNITS

Type 5 contains hours with low SNSP, low units in NI & Dublin and high inertia. It is interesting to note that both scenarios offer cases with similar inertia and demand but quite high variation in SNSP.

Hour 5497 from SE may be a useful comparison point within the scenario as it has notably higher SNSP than the other SE hours. However, the scope for worthwhile comparison between scenarios is limited as the hours have little in common.

TABLE 10-7: SUMMARY OF TYPE 5 HOURS FOR EACH SCENARIO

Type 5	Low Carbon Living						Steady Evolution				
Hour	**4112**	**4629**	**4630**	**4631**	**4632**		**4680**	**5497**	**5544**	**5791**	**6721**
Inertia (GWs)	20	21	21	20	20		29	25	26	27	26
SNSP (SNSP)	46	33	27	42	37		7	20	10	6	8
Units NI & D	0	0	0	0	0		2	1	1	2	1
Demand (GW)	6.1	6.5	6.4	6.2	5.9		4.7	4.4	4.6	4.4	4.7
Sub Type	x	x	x	x	x	x	x	x	x	x	x

10.3.6 TYPE 6 – HIGH DEMAND WITH HIGH NI & DUBLIN UNITS

Type 6 represents the case where all measures are high. Thus it is a useful case for analysis in terms of the inherent impact of high SNSP, as opposed to the impact of SNSP in terms of reduced inertia or displaced generation units.

Both scenarios have a remarkable degree of similarity within their hours but, as with the other cases notable differences between the scenarios (LCL has lower inertia, higher SNSP, fewer units and higher demand). Hour 2850 for LCL has slightly lower demand than the other hours, so may be of value for comparison.

TABLE 10-8: SUMMARY OF TYPE 6 HOURS FOR EACH SCENARIO

Type 6	Low Carbon Living						Steady Evolution				
Hour	**2416**	**2417**	**2437**	**2439**	**2850**		**1655**	**8396**	**8397**	**8398**	**8399**
Inertia (GWs)	20	20	20	20	20		25	24	23	24	24
SNSP (SNSP)	81	82	80	81	82		59	59	65	69	75
Units NI & D	2	2	2	2	2		4	4	4	4	4
Demand (GW)	8.3	8.7	8.2	8.4	7.4		5.9	6.5	6.2	5.9	5.8
Sub Type	x	x	x	x	x	x	x	x	x	x	x

10.3.7 TYPE 7 – LOAD SERVED BY RENEWABLES AND A FEW LARGE UNITS

Type 7 requires high SNSP, a high number of units in NI & Dublin and low inertia. The conflicting demands of these requirements have meant that only one suitable hour was found for LCL. This is likely due to LCL's tendency to have fewer units on in NI & D. This limits the value of any comparison for this type but is an outcome in itself and the presence of one hour does allow some analysis.

The hours found for SE are very consistent in nature with some variation in the demand, so similar results would be expected.

TABLE 10-9: SUMMARY OF TYPE 7 HOURS FOR EACH SCENARIO

Type 7	Low Carbon Living						Steady Evolution				
Hour	7048						1351	1362	2113	2115	3161
Inertia (GWs)	15						18	20	18	18	20
SNSP (SNSP)	80						78	70	72	76	78
Units NI & D	2						4	4	4	4	4
Demand (GW)	7.1						4.9	6.2	5.2	5.0	6.0
Sub Type	x	x	x	x	x	x	x	x	x	x	x

10.3.8 TYPE 8 – HIGH DEMAND WITH HIGH SNSP

Type 8 requires high SNSP and high inertia, with low numbers of NI & Dublin units. This implies high demand as inertia and non-synchronous penetration are high. This is true for LCL but less so for SE, where hour 1519 and 4924 have lower than anticipated demand. While the SNSP level and demand is lower in SE it could expected that LCL and SE should exhibit similar behaviour, with the exception of 2224 which has notably higher inertia. Such an outcome would indicate limited impact from the units in NI & Dublin measure.

TABLE 10-10: SUMMARY OF TYPE 8 HOURS FOR EACH SCENARIO

Type 8	Low Carbon Living						Steady Evolution				
Hour	**4117**	**4118**	**4119**	**4120**	**4864**		**590**	**1519**	**2224**	**4924**	**7886**
Inertia (GWs)	23	23	23	23	20		23	23	29	23	23
SNSP (SNSP)	80	82	82	81	80		68	69	74	62	71
Units NI & D	0	0	0	0	0		1	2	2	1	2
Demand (GW)	8.0	8.9	8.7	8.3	8.1		7.0	5.0	6.5	4.4	6.1
Sub Type	x	x	x	x	x	x	x	x	x	x	x

11. ANNEX II: DETAILED RESULTS FOR CE VOLTAGE AND TRANSIENT STABILITY MODEL

TABLE 11-1: DISPATCHING RESULTS OF GROUP OF SCENARIOS: ENERGY TRANSITION AND "MIN_INERTIA".

Parameter/Country	PL	DE	CZ	SK	AT	HU	Rest in CE
/1 – 2030-01-13, 01:00[6] ($SNSP = 47{,}1\%$)							
Kinetic energy in SGMs (MVA·s)	42815,9	85103,2	53151,3	27924	42513,6	35501,3	849049,3
Load (MW)	19257,5	55481,6	7522	3590,6	6914,1	4798,1	232865,7
Power exchange (MW)	-3455,5	10398,3	927,5	1078,9	-6676,5	791,6	-12709,3
Hydro pumping in SGMs (MW)	0	0	1043	0	6139	0	9993
Generation in SGMs (MW)	10316,8	21125,7	9291,5	4661	5018,6	5458,4	165450,5
Generation in PPMs (MW)	5485,2	44754,2	201	8,5	1358	131,3	64698,8
Wind (MW)	5485,2	44754,2	201	8,5	1358	131,3	64691
Solar (MW)	0	0	0	0	0	0	7,8
/2 = /3 – 2030-06-23, 13:00 ($SNSP = 59{,}0\%$)							
Kinetic energy in SGMs (MVA·s)	45071,6	77822	31661,9	20209,8	33148,5	26307,6	633291,9
Load (MW)	19475,1	59167,3	7310,9	3572	7174,2	4710,1	212531,3
Power exchange (MW)	-2638,7	15268	-286,7	583,8	-2813,9	-516,4	-10220,4
Hydro pumping in SGMs (MW)	0	0	0	0	6139	0	13817
Generation in SGMs (MW)	9403,8	17409,3	5520,6	3778,2	6711,7	3942,7	127832
Generation in PPMs (MW)	7432,6	57026	1503,6	377,6	3787,6	251	88295,5
Wind (MW)	7379,3	18722,7	130,8	4,3	1695,4	192,5	19210,2
Solar (MW)	53,3	38303,3	1372,8	373,3	2092,2	58,5	69085,3
/4 – 2030-06-22, 05:00 ($SNSP = 51{,}5\%$)							
Kinetic energy in SGMs (MVA·s)	57538,3	75322	34019,5	20209,8	33148,5	23374,3	638903
Load (MW)	16558,9	51097,9	6299,9	3013,2	5967,5	3830,5	181763,6
Power exchange (MW)	-597,6	2105	-1515,1	886,1	-4364,8	-301,7	-10024,2
Hydro pumping in SGMs (MW)	0	0	1043	0	6139	0	12214
Generation in SGMs (MW)	10903,8	17111,3	5281,5	3778,2	6711,7	3462,7	128359,2
Generation in PPMs (MW)	5057,5	36091,6	546,3	121,1	1030	66,1	55594
Wind (MW)	5048,8	29851,6	121,2	5,1	689,4	47,9	48539,6
Solar (MW)	8,7	6240	425,1	116	340,6	18,2	7054,4

[6] UCT time

TABLE 11-2: DISPATCHING RESULTS OF GROUP OF SCENARIOS: ENERGY TRANSITION AND MAX_LOAD.

Parameter/Country	PL	DE	CZ	SK	AT	HU	Rest in CE
/1 – 2029-11-28, 16:00 ($SNSP = 22{,}4\%$)							
Kinetic energy in SGMs (MVA·s)	106949,2	268389,9	55692,8	26778,3	36639,5	40534,6	1246352,1
Load (MW)	31442,2	97873,8	12658,1	5226,3	11573,9	6779,2	301017,7
Power exchange (MW)	-4090	-17354,4	614,6	213,9	-173,4	97,5	7831,2
Hydro pumping in SGMs (MW)	0	0	0	0	0	0	0
Generation in SGMs (MW)	25997,8	70818,7	13253,4	5439,6	11388,1	6866,4	268519,9
Generation in PPMs (MW)	1354,4	9700,7	19,3	0,6	12,4	10,3	40329
Wind (MW)	1354,4	9700,7	19,3	0,6	12,4	10,3	37145,8
Solar (MW)	0	0	0	0	0	0	3183,2
/2 = /3 = /4 – 2029-11-28, 17:00 ($SNSP = 22{,}4\%$)							
Kinetic energy in SGMs (MVA·s)	106949,2	270618,6	55692,8	26874,7	40883,1	40534,6	1252670,8
Load (MW)	31451,7	101216,8	12403,2	5322,4	11601,7	7045	310638,5
Power exchange (MW)	-4090	-20091,6	866,1	226,1	4573,4	-166,2	7655,7
Hydro pumping in SGMs (MW)	0	0	0	0	0	0	0
Generation in SGMs (MW)	25997,8	71013,5	13253,4	5548	16162,2	6866,4	277665,4
Generation in PPMs (MW)	1363,9	10111,7	15,9	0,5	12,9	12,4	40628,8
Wind (MW)	1363,9	10111,7	15,9	0,5	12,9	12,4	40289,5
Solar (MW)	0	0	0	0	0	0	339,3

TABLE 11-3: DISPATCHING RESULTS OF GROUP OF SCENARIOS: ENERGY TRANSITION AND MIN_REACTIVE.

Parameter/Country	PL	DE	CZ	SK	AT	HU	Rest in CE
/1 = /2 – 2030-01-13, 01:00 ($SNSP$ = 47,1%)							
Kinetic energy in SGMs (MVA·s)	42815,9	85103,2	53151,3	27924	42513,6	35501,3	849049,3
Load (MW)	19257,5	55481,6	7522	3590,6	6914,1	4798,1	232865,7
Power exchange (MW)	-3455,5	10398,3	927,5	1078,9	-6676,5	791,6	-12709,3
Hydro pumping in SGMs (MW)	0	0	1043	0	6139	0	9993
Generation in SGMs (MW)	10316,8	2112 5,7	9291,5	4661	5018,6	5458,4	165450,5
Generation in PPMs (MW)	5485,2	44754,2	201	8,5	1358	131,3	64698,8
Wind (MW)	5485,2	44754,2	201	8,5	1358	131,3	64691
Solar (MW)	0	0	0	0	0	0	7,8
/3 = /4 – 2030-03-24, 04:00 ($SNSP$ = 46,5%)							
Kinetic energy in SGMs (MVA·s)	42815,9	86597,7	37629,1	25258,4	37623,1	26701,3	748021
Load (MW)	17566	50781,1	6818,2	3481,3	6090,5	3915,2	188240,2
Power exchange (MW)	-677,6	15927,2	-994,2	865,5	-4226,4	584,7	-12211,9
Hydro pumping in SGMs (MW)	0	296,6	1043	0	6139	0	8357
Generation in SGMs (MW)	10316,8	21583,7	6593,2	4335,2	5833,8	4306,4	136907,5
Generation in PPMs (MW)	6571,6	45421,2	273,8	11,6	2169,3	193,5	47478,1
Wind (MW)	6571,6	45421,2	273,8	11,6	2169,3	193,5	47468,4
Solar (MW)	0	0	0	0	0	0	9,7

TABLE 11-4: DISPATCHING RESULTS OF GROUP OF SCENARIOS: ENERGY TRANSITION AND MAX_SNSP.

Parameter/Country	PL	DE	CZ	SK	AT	HU	Rest in CE
/4 – 2030-06-22, 12:00 ($SNSP$ = 62,4%)							
Kinetic energy in SGMs (MVA·s)	59738	100439	30195	20210	33149	23374	671669
Load (MW)	22746	69111	7759	3829	8182	5124	233270
Power exchange (MW)	4090	-9430	851	-330	4816	1535	7565
Hydro pumping in SGMs (MW)	0	6850	0	0	6139	0	18941
Generation in SGMs (MW)	11970	17111	5293	3778	6712	3463	135163
Generation in PPMs (MW)	6686	68280	1616	381	2794	127	109482
Wind (MW)	6645	38652	251	9	1175	69	38809
Solar (MW)	41	29628	1365	371	1619	58	70673

TABLE 11-5: REQUIRED FCR AND AFRR VLUES IN ALL THE CONSIDERED GROUPS OF SCENARIOS.

Parameter/Country	PL	DE	CZ	SK	AT	HU	Rest in CE
Annual FCR (MW)	159	607	81	26	68	28	1988,2
Annual aFRR (MW)	560	2050	360	140	200	250	4430

TABLE 11-6: RESULTS FOR SIMPLIFIED VOLTAGE STABILITY ANALYSIS FOR (N-0) STATE.

Scenario name	Busbar ID and nominal voltage	S_{load} [MV·A]	$\cos\varphi$	S''_{k} [MV·A]	$2k_v(1+\sin\varphi)\,S_{\mathrm{load}}$ [MV·A]
ET/Max_Load/1	45270 (110 kV)	19,8	0,981	378,7	52,0
ET/Max_Load/2/3/4	45270 (110 kV)	17,3	0,981	378,7	45,4
ET/"Min_Inertia"/1	45270 (110 kV)	12,6	0,981	375,8	33,0
ET/"Min_Inertia"/2/3	45270 (110 kV)	12,8	0,981	375,5	33,5
ET/"Min_Inertia"/4	53150 (110 kV)	5,9	1	359,1	13,1
ET/Min_Reactive/1/2	45270 (110 kV)	12,6	0,981	375,8	33,0
ET/Min_Reactive/3/4	53150 (110 kV)	6,3	1	359,1	13,9
GG/Max_Load /1	42505 (110 kV)	9,7	0,986	157,8	24,9
GG/Max_Load/2/3/4	42505 (110 kV)	9,7	0,986	157,8	24,9
GG/"Min_Inertia"/1	42505 (110 kV)	6,1	0,986	157,5	15,7
GG/"Min_Inertia"/2/3	42505 (110 kV)	6,2	0,986	157,5	15,9
GG/"Min_Inertia"/4	42505 (110 kV)	5,2	0,986	157,6	13,5
GG/Min_Reactive/1/2	42505 (110 kV)	6,1	0,986	157,5	15,7
GG/Min_Reactive/3/4	42505 (110 kV)	5,6	0,986	157,6	14,3
DR/Max_Load/1	42505 (110 kV)	9,7	0,986	247,0	24,9
DR/Max_Load/2/3/4	42505 (110 kV)	9,7	0,986	247,0	24,9
DR/"Min_Inertia"/1	42505 (110 kV)	6,2	0,986	246,9	15,9
DR/"Min_Inertia"/2/3	42505 (110 kV)	6,3	0,986	246,9	16,1
DR/"Min_Inertia"/4	42505 (110 kV)	5,3	0,986	246,9	13,6
DR/Min_Reactive/1/2	42505 (110 kV)	6,2	0,986	246,9	15,9
DR/Min_Reactive/3/4	42505 (110 kV)	5,6	0,986	246,9	14,5

TABLE 11-7: RESULTS FOR SIMPLIFIED VOLTAGE STABILITY ANALYSIS FOR (N-1) CONTINGENCY STATE.

Scenario name	Contingency	Busbar ID and nominal voltage	S_{load} [MV·A]	$\cos\varphi$	S''_{k} [MV·A]	$2k_v(1+\sin\varphi)\,S_{\mathrm{load}}$ [MV·A]
ET/Max_Load/1	1070 (busbar 220 kV)	45270 (110 KV)	19,8	0,981	378,7	52,0
	170 (busbar 400 kV)	45270 (110 KV)	19,8	0,981	378,5	52,0
	2200 (busbar 220 kV)	45270 (110 KV)	19,8	0,981	378,7	52,0
	2370 (busbar 220 kV)	45270 (110 KV)	19,8	0,981	377,2	52,0
	2460 (busbar 220 kV)	45270 (110 KV)	19,8	0,981	378,7	52,0
	2470 (busbar 220 kV)	45270 (110 KV)	19,8	0,981	378,6	52,0
	2620 (busbar 220 kV)	45270 (110 KV)	19,8	0,981	378,5	52,0
	550 (busbar 400 kV)	45510 (110 KV)	3,7	0,997	222,1	8,8
	560 (busbar 400 kV)	45270 (110 KV)	19,8	0,981	378,1	52,0
	570 (busbar 400 kV)	45270 (110 KV)	19,8	0,981	378,7	52,0
	580 (busbar 400 kV)	45270 (110 KV)	19,8	0,981	378,7	52,0
	6210 (busbar 400 kV)	45270 (110 KV)	19,8	0,981	378,7	52,0
	680 (busbar 400 kV)	45270 (110 KV)	19,8	0,981	378,4	52,0
	740 (busbar 400 kV)	53150 (110 KV)	10,9	1	290,0	24,0
	980 (busbar 400 kV)	45270 (110 KV)	19,8	0,981	378,7	52,0
ET/Max_Load/2/3/4	1070 (busbar 220 kV)	45270 (110 KV)	17,3	0,981	378,7	45,4
	170 (busbar 400 kV)	45270 (110 KV)	17,3	0,981	378,5	45,4
	2200 (busbar 220 kV)	45270 (110 KV)	17,3	0,981	378,7	45,4
	2370 (busbar 220 kV)	45270 (110 KV)	17,3	0,981	377,2	45,4
	2460 (busbar 220 kV)	45270 (110 KV)	17,3	0,981	378,7	45,4
	2470 (busbar 220 kV)	45270 (110 KV)	17,3	0,981	378,6	45,4
	2620 (busbar 220 kV)	45270 (110 KV)	17,3	0,981	378,5	45,4
	550 (busbar 400 kV)	45510 (110 KV)	3,8	0,997	222,1	8,9
	560 (busbar 400 kV)	45270 (110 KV)	17,3	0,981	378,1	45,4
	570 (busbar 400 kV)	45270 (110 KV)	17,3	0,981	378,7	45,4
	580 (busbar 400 kV)	45270 (110 KV)	17,3	0,981	378,7	45,4
	6210 (busbar 400 kV)	45270 (110 KV)	17,3	0,981	378,7	45,4
	680 (busbar 400 kV)	53150 (110 KV)	11,0	1	352,9	24,2
	740 (busbar 400 kV)	53150 (110 KV)	11,0	1	290,0	24,2
	980 (busbar 400 kV)	45270 (110 KV)	17,3	0,981	378,7	45,4
GG/Max_Load /1	1070 (busbar 220 kV)	42505 (110 KV)	9,7	0,986	157,8	24,9
	170 (busbar 400 kV)	42505 (110 KV)	9,7	0,986	157,8	24,9
	2200 (busbar 220 kV)	42505 (110 KV)	9,7	0,986	157,8	24,9
	2370 (busbar 220 kV)	42505 (110 KV)	9,7	0,986	157,6	24,9
	2460 (busbar 220 kV)	42505 (110 KV)	9,7	0,986	157,6	24,9
	2470 (busbar 220 kV)	42505 (110 KV)	9,7	0,986	157,6	24,9
	260 (busbar 400 kV)	42505 (110 KV)	9,7	0,986	157,8	24,9
	2620 (busbar 220 kV)	42505 (110 KV)	9,7	0,986	157,8	24,9
	550 (busbar 400 kV)	42505 (110 KV)	9,7	0,986	157,7	24,9
	560 (busbar 400 kV)	42505 (110 KV)	9,7	0,986	157,5	24,9

Scenario name	Contingency	Busbar ID and nominal voltage	S_{load} [MV·A]	$\cos\varphi$	S''_{k} [MV·A]	$2k_v(1+\sin\varphi)\,S_{\mathrm{load}}$ [MV·A]
	570 (busbar 400 kV)	42505 (110 KV)	9,7	0,986	157,8	24,9
	580 (busbar 400 kV)	42505 (110 KV)	9,7	0,986	157,8	24,9
	6210 (busbar 400 kV)	42505 (110 KV)	9,7	0,986	157,8	24,9
	680 (busbar 400 kV)	42505 (110 KV)	9,7	0,986	157,7	24,9
	740 (busbar 400 kV)	42505 (110 KV)	9,7	0,986	157,8	24,9
	980 (busbar 400 kV)	42505 (110 KV)	9,7	0,986	157,8	24,9
GG/Max_Load /2/3/4	1070 (busbar 220 kV)	42505 (110 KV)	9,7	0,986	157,8	24,9
	170 (busbar 400 kV)	42505 (110 KV)	9,7	0,986	157,8	24,9
	2200 (busbar 220 kV)	42505 (110 KV)	9,7	0,986	157,8	24,9
	2370 (busbar 220 kV)	42505 (110 KV)	9,7	0,986	157,6	24,9
	2460 (busbar 220 kV)	42505 (110 KV)	9,7	0,986	157,6	24,9
	2470 (busbar 220 kV)	42505 (110 KV)	9,7	0,986	157,6	24,9
	260 (busbar 400 kV)	42505 (110 KV)	9,7	0,986	157,8	24,9
	2620 (busbar 220 kV)	42505 (110 KV)	9,7	0,986	157,8	24,9
	550 (busbar 400 kV)	42505 (110 KV)	9,7	0,986	157,7	24,9
	560 (busbar 400 kV)	42505 (110 KV)	9,7	0,986	157,5	24,9
	570 (busbar 400 kV)	42505 (110 KV)	9,7	0,986	157,8	24,9
	580 (busbar 400 kV)	42505 (110 KV)	9,7	0,986	157,8	24,9
	6210 (busbar 400 kV)	42505 (110 KV)	9,7	0,986	157,8	24,9
	680 (busbar 400 kV)	42505 (110 KV)	9,7	0,986	157,7	24,9
	740 (busbar 400 kV)	42505 (110 KV)	9,7	0,986	157,8	24,9
	980 (busbar 400 kV)	42505 (110 KV)	9,7	0,986	157,8	24,9
GG/"Min_Inertia"/1	2370 (busbar 220 kV)	42505 (110 KV)	6,1	0,986	157,3	15,7
	6240 (busbar 400 kV)	42505 (110 KV)	6,1	0,986	157,5	15,7
	700 (busbar 400 kV)	42505 (110 KV)	6,1	0,986	157,5	15,7
GG/"Min_Inertia"/2/3	2370 (busbar 220 kV)	42505 (110 KV)	6,2	0,986	157,3	15,9
	660 (busbar 400 kV)	42505 (110 KV)	6,2	0,986	157,5	15,9
	700 (busbar 400 kV)	42505 (110 KV)	6,2	0,986	157,5	15,9
GG/"Min_Inertia"/4	680 (busbar 400 kV)	42505 (110 KV)	5,2	0,986	157,5	13,5
GG/Min_Reactive/1/2	2370 (busbar 220 kV)	42505 (110 KV)	6,1	0,986	157,3	15,7
	6240 (busbar 400 kV)	42505 (110 KV)	6,1	0,986	157,4	15,7
	700 (busbar 400 kV)	42505 (110 KV)	6,1	0,986	157,5	15,7
GG/Min_Reactive/3/4	2370 (busbar 220 kV)	42505 (110 KV)	5,6	0,986	157,3	14,3
	680 (busbar 400 kV)	42505 (110 KV)	5,6	0,986	157,5	14,3
DR/Max_Load/1	1070 (busbar 220 kV)	42505 (110 KV)	9,7	0,986	247,0	24,9
	2200 (busbar 220 kV)	42505 (110 KV)	9,7	0,986	247,0	24,9
	2370 (busbar 220 kV)	42505 (110 KV)	9,7	0,986	246,9	24,9
	2460 (busbar 220 kV)	42505 (110 KV)	9,7	0,986	246,9	24,9
	2470 (busbar 220 kV)	42505 (110 KV)	9,7	0,986	246,9	24,9
	2620 (busbar 220 kV)	42505 (110 KV)	9,7	0,986	247,0	24,9
	560 (busbar 400 kV)	42505 (110 KV)	9,7	0,986	246,9	24,9

Scenario name	Contingency	Busbar ID and nominal voltage	S_{load} [MV·A]	$\cos\varphi$	S''_{k} [MV·A]	$2k_v(1+\sin\varphi)\,S_{\text{load}}$ [MV·A]
	570 (busbar 400 kV)	42505 (110 KV)	9,7	0,986	247,0	24,9
	6210 (busbar 400 kV)	42505 (110 KV)	9,7	0,986	247,0	24,9
	740 (busbar 400 kV)	42505 (110 KV)	9,7	0,986	247,0	24,9
	980 (busbar 400 kV)	42505 (110 KV)	9,7	0,986	247,0	24,9
	34710 30037 (transformer 400/110 kV)	42505 (110 KV)	9,7	0,986	247,0	24,9
DR/Max_Load/2/3/4	1070 (busbar 220 kV)	42505 (110 KV)	9,7	0,986	247,0	24,9
	2200 (busbar 220 kV)	42505 (110 KV)	9,7	0,986	247,0	24,9
	2370 (busbar 220 kV)	42505 (110 KV)	9,7	0,986	246,9	24,9
	2460 (busbar 220 kV)	42505 (110 KV)	9,7	0,986	246,9	24,9
	2470 (busbar 220 kV)	42505 (110 KV)	9,7	0,986	246,9	24,9
	2620 (busbar 220 kV)	42505 (110 KV)	9,7	0,986	247,0	24,9
	560 (busbar 400 kV)	42505 (110 KV)	9,7	0,986	246,9	24,9
	570 (busbar 400 kV)	42505 (110 KV)	9,7	0,986	247,0	24,9
	6210 (busbar 400 kV)	42505 (110 KV)	9,7	0,986	247,0	24,9
	740 (busbar 400 kV)	42505 (110 KV)	9,7	0,986	247,0	24,9
	980 (busbar 400 kV)	42505 (110 KV)	9,7	0,986	247,0	24,9
DR/"Min_Inertia"/4	2370 (busbar 220 kV)	42505 (110 KV)	5,3	0,986	246,8	13,6
	560 (busbar 400 kV)	42505 (110 KV)	5,3	0,986	246,8	13,6
	lne 630 6240 1 (line 400 kV)	42505 (110 KV)	5,3	0,986	246,9	13,6
	lne 6320 6455 1 (line 400 kV)	42505 (110 KV)	5,3	0,986	246,9	13,6

TABLE 11-8: CRITICAL ZONES IDENTIFIED FOR EACH CAPACITY AND OPERATION SCENARIO.

Scenario name	Critical zone	Critical contingency (type and busbar no.)
ET/Max_Load/1	17	busbar 400 kV (6210)
	41, 42	busbar 400 kV (560)
	49	busbar 220 kV (2370)
	51, 52, 56, 57	busbar 400 kV (680)
	53, 54	busbar 400 kV (740)
ET/Max_Load/2/3/4	41,42	busbar 400 kV (560)
	49	busbar 220 kV (2370)
	16, 17, 51, 52, 55, 56, 57	busbar 400 kV (680)
	53, 54	busbar 400 kV (740)
ET/"Min_Inertia"/1	-	-
ET/"Min_Inertia"/2/3	-	-
ET/"Min_Inertia"/4	-	-

Scenario name	Critical zone	Critical contingency (type and busbar no.)
ET/Min_Reactive/1/2	-	-
ET/Min_Reactive/3/4	-	-
GG/Max_Load /1	13	busbar 220 kV (1070)
	17	busbar 400 kV (6210)
	41, 42	busbar 400 kV (560)
	49	busbar 220 kV (2370)
GG/Max_Load/2/3/4	13	busbar 220 kV (1070)
	17	busbar 400 kV (6210)
	41	busbar 400 kV (560)
	49	busbar 220 kV (2370)
GG/"Min_Inertia"/1	54, 57	busbar 400 kV (6240)
	55	busbar 400 kV (700)
GG/"Min_Inertia"/2/3	49	busbar 220 kV (2370)
	57	busbar 400 kV (660)
GG/"Min_Inertia"/4	17, 55	busbar 400 kV (680)
GG/Min_Reactive/1/2	54, 57	busbar 400 kV (6240)
	55	busbar 400 kV (700)
GG/Min_Reactive/3/4	12,16,17,42,45,51,52,57	busbar 400 kV (680)
DR/Max_Load/1	49	busbar 220 kV (2370)
	54	busbar 400 kV (740)
DR/Max_Load/2/3/4	49	busbar 220 kV (2370)
	54	busbar 400 kV (740)
DR/"Min_Inertia"/1	-	-
DR/"Min_Inertia"/2/3	-	-
DR/"Min_Inertia"/4	42	line 400 kV (lne_630_6240_1)
	43	busbar 400 kV (560)
	49	busbar 220 kV (2370)
	51, 52, 53, 54 ,55, 57	line 400 kV (lne_630_6240_1)
DR/Min_Reactive/1/2	-	-
DR/Min_Reactive/3/4	-	-

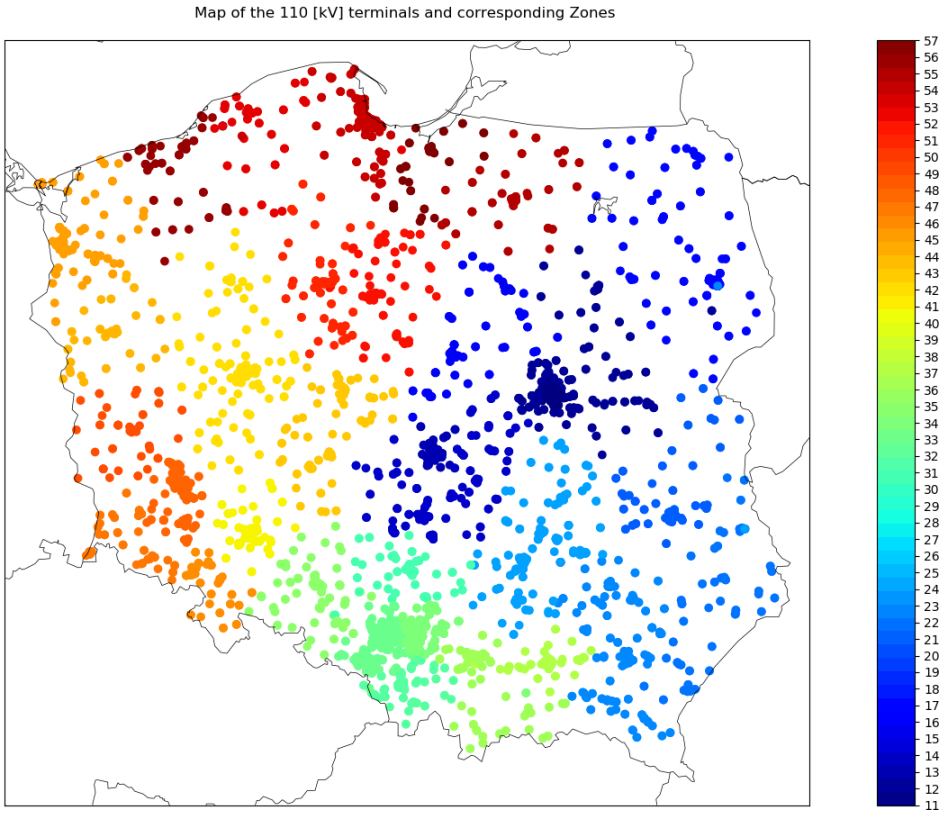

FIGURE 11-1: MAP OF 110 KV NODES AND CORRESPONDING NETWORK ZONES.

12. ANNEX III: SENSITIVITY ANALYSIS – IMPACT OF ACTIVE DISTRIBUTION SYSTEM IMPEDANCE TO THE VOLTAGE STABILITY RESULTS

Further analysis focuses on the active distribution system (ADS) equivalents. The purpose is to study how the change of impedance Z_{GEN} located between the main distribution transformer and RES converters impact on the voltage level in 110 kV nodes (see Figure 12-1). For basic steady-state analysis, Z_{GEN} has been assumed to be equal to 0.15 Ω which corresponds to a capacity ratio of 2/3 in MV network and 1/3 in LV network.

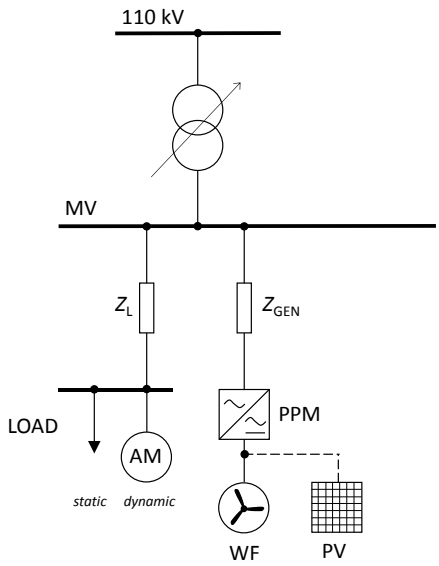

FIGURE 12-1: SIMPLIFIED DIAGRAM OF ACTIVE DISTRIBUTION SYSTEM EQUIVALENT CONNECTED TO 110 KV NODE.

The sensitivity analysis has been performed for the critical zones during the worst contingency (N-1). In the designated critical zone all the impedances Z_{GEN} were increased up to 4.5 Ω, which can be interpreted as moving RES into LV network level. Then, voltage levels at all 110 kV nodes in the investigated zones have been obtained from load flow calculation. Differences between voltage level before and after the change of impendence have been recorded for the weakest nodes. Table 12-1 presents the results obtained for all scenarios and operational cases.

In general, increasing impedance results in lower voltage levels at the analysed nodes. Looking at the results presented in Table 12-1, it can be observed that there is a relatively low voltage difference before and after the impedances are increased when the Energy Transition and Going Green scenarios are considered. On the other hand, there are significant voltage differences in Distributed Renewables/ ""Min_Inertia"" /2/3 and Distributed Renewables / "Min_Reactive" /3/4 scenarios, for which 3% and 4% difference values have been obtained, respectively. This means that the impedance between the power grid and voltage source is more significant if more DER capacity is considered in the model.

Additionally, the same kind of analysis has been performed for the area of Poland. In this case, the impedances Z_{GEN} were increasing up to 4.5 Ω for all ADS equivalents in the Polish power system. The voltage levels before and after the changes are similar in comparison to the results presented in Table 12-1. The maximum observed difference in voltage levels is 0.02 p.u.

TABLE 12-1: RESULTS OF IMPACT OF ACTIVE DISTRIBUTION SYSTEM IMPEDANCE TO VOLTAGE LEVELS IN 110 KV NODES.

Scenario name	Critical zone	Critical contingency	Busbar 110 kV	Voltage before change [p.u.]	Voltage after change [p.u.]	Difference [p.u.]
ET/Max_Load/1	43	560 OSR414	43580 PSZ114	0.8067	0.8066	0.0001
ET/Max_Load/2/3/4	43	560 OSR414	43500 OPL124	0.7995	0.7993	0.0001
ET/"Min_Inertia"/1	4	530 MIK414	6475 BCS1XX	0.9371	0.9367	0.0004
ET/"Min_Inertia"/2/3	4	530 MIK414	6475 BCS1XX	0.976	0.9753	0.0007
ET/"Min_Inertia"/4	53	740 ZRC415	53150 SLH115	0.9992	0.993	0.0062
ET/Min_Reactive/1/2	4	530 MIK414	6475 BCS1XX	0.9366	0.9362	0.0004
ET/Min_Reactive/3/4	4	530 MIK414	6475 BCS1XX	0.9574	0.9568	0.0006
GG/Max_Load /1	53	740 ZRC415	53150 SLH115	0.7762	0.7759	0.0003
GG/Max_Load/2/3/4	43	560 OSR414	43500 OPL124	0.7707	0.7706	0.0001
GG/"Min_Inertia"/1	57	6240 MON424	57170 PTC115	0.9346	0.9324	0.0022
GG/"Min_Inertia"/2/3	57	660 GBL425	57170 PTC115	0.9489	0.9451	0.0039
GG/"Min_Inertia"/4	57	680 GRU415	57170 PTC115	0.974	0.9728	0.0013
GG/Min_Reactive/1/2	57	6240 MON424	57170 PTC115	0.9399	0.9375	0.0025

GG/Min_Reactive/3/4	17	680 GRU415	17970 FIL121	0.9106	0.908	0.0026
DR/Max_Load/1	43	560 OSR414	43500 OPL124	0.8638	0.8571	0.0067
DR/Max_Load/2/3/4	43	560 OSR414	43500 OPL124	0.8612	0.8544	0.0068
DR/"Min_Inertia"/1	17	lne 6320 6455 1	17865 GOD121	1.0038	0.9967	0.0072
DR/"Min_Inertia"/2/3	56	750 ZRC425	56350 KCO115	1.0426	1.0118	0.0309
DR/"Min_Inertia"/4	56	lne 630 6240 1	No convergence in the load flow			
DR/Min_Reactive/1/2	17	700 OLM415	17520 SEJ111	1.0147	1.0089	0.0058
DR/Min_Reactive/3/4	56	lne 630 6240 1	56350 KCO115	1.0048	0.959	0.0457

13. ANNEX IV: POWER FLOW DECOMPOSITION METHOD – POWER FLOW COLOURING

13.1 CREATING SUB-MODELS

The analysed initial load flow model is divided into two sub-models. The division is aimed at separating the amount of power injected or withdrawn in each node into two groups:

(i) For the purpose of intra-zonal power exchange

(ii) Inter-zonal commercial power exchange.

The balanced model can be created by decreasing the net position of exporting zones or increasing the net positions of importing zones. The procedures leading to establishing new operational points, related to the balanced model, can use e.g. merit order, Generation Shift Keys provided by the TSOs or proportional scaling up/down of nodal injections/withdrawals. Table 13-1 introduces an example for transforming quantities of generation and demand into a balanced model and a model with exchanges.

TABLE 13-1: EXAMPLE OF BALANCED MODEL AND MODEL WITH EXCHANGES

	Initial		Balanced		Exchanges	
	Generation	Demand	Generation	Demand	Generation	Demand
Zone A	300	200	200	200	100	0
Zone B	50	50	50	50	0	0
Zone C	100	200	100	100	0	100

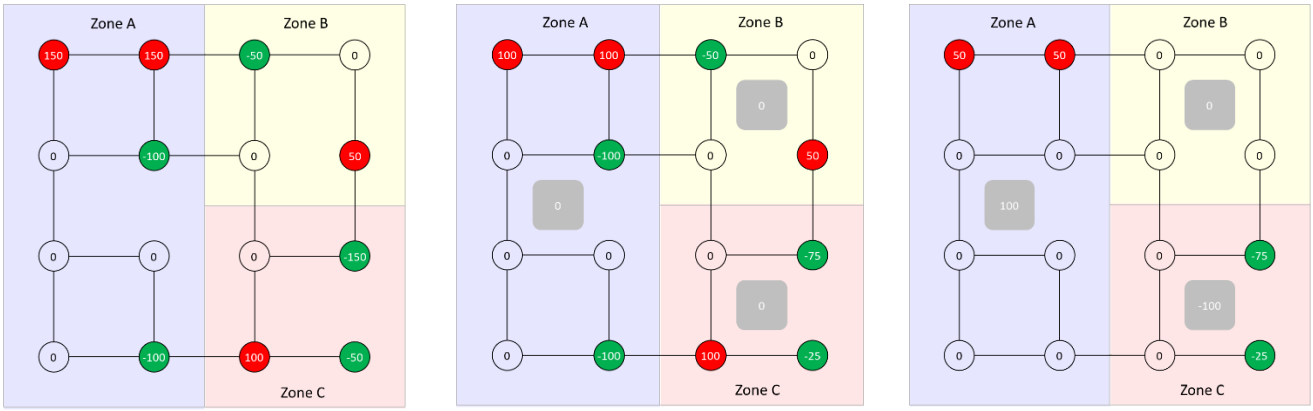

(A) Original Model (B) Balanced Model (C) Model with Exchanges

FIGURE 13-1: EXAMPLE INVOLVING GRID: DECOMPOSITION OF ORIGINAL MODEL (A) INTO A BALANCED MODEL (B) AND A MODEL WITH EXCHANGES (C)

13.2 GROUPING NODES FOR POWER EXCHANGE

The sub-models are further utilised for identifying flow components. Power flow is performed for each zone of the balanced model separately, i.e. assuming no demand or generation for all other zones. A different procedure takes place for the model with exchanges. A process called Equivalent Bilateral Exchange (EBE) [41] is used to assess the amount of power exchanged between zones. EBE states that each power source sends energy to each sink (regardless of the distances between the nodes). Moreover, the quantity of the power exchanged between any source i and sink j is proportional to the generation at the source and load at the sink (further normalized by the inverse sum of the overall power exchange is the power system). A rigorous description of this phase is as follows: assume that a vector of nodal power injections in a DC paradigm ($\mathbf{p} = \mathbf{B\theta}$, where $\mathbf{B}$ stands for susceptance matrix and $\boldsymbol{\theta}$ - voltage angles) can be expressed by $p = p^{+} - p^{-}$, so that non-negative nodal injections ($\mathbf{p}^{+}$) and non-negative nodal withdrawals ($\mathbf{p}^{-}$) represent all the exchanges in the grid. Then power exchange between nodes i and j (PEX_{ij}) is calculated as:

$$SPEX_{ij} = \frac{p_i^{+} \cdot p_j^{-}}{\sum_k p_k^{-}}, \qquad \text{(Eq. 13-1)}$$

where in the denominator, the sum indicates the total demand (or total generation, as lossless transmission is assumed).

13.3 CATEGORIZING FLOWS

Flow components derived from the balanced model lead to identification of internal flows and loop flows, whereas components provided by the model with exchanges give the results in terms of inter-zonal commercial flows (import/export and transit flows).

14. ANNEX V: DISTRIBUTION NETWORK EQUIVALENT MODEL FOR FREQUENCY DISTURBANCES

In order to support the analysis of technical shortfalls of the European system, an extension of the dynamic equivalent model for active distribution networks considering voltage related disturbances (task T2.3, reported in the deliverable D2.3 [3]) has been developed, taking in consideration frequency-related disturbances' representation. The model structure, the respective methodology and important considerations/limitations are extensively discussed in D2.3 and in the following publication [42]. In the present report, only a brief overview of the overall methodological approach is presented, focusing mainly on the additional functionalities the model incorporates.

The dynamic equivalent model aims to a significant reduction of the network representation complexity, in comparison to a fully detailed approach considering the overall network structure and connected elements. This is achieved by adopting an equivalent structure that considers the lumped aggregation of the main components that actively contribute to the grid's overall response. Due to the characteristics of the task, intending to explore the challenges system operators will face in scenarios with massive integration of renewable-based generation; only converter-connected generation has been considered. Additionally, the most recent grid codes requirements for the connection of generators [43] were adopted, to increase the solution's adequacy regarding the applicability domain.

In line with this view, the adopted equivalent model structure is presented in Figure 14-1. It is composed by the connection of a composite load – accounting for a static, voltage dependent load model, in parallel to an induction motor to represent the dynamic part of the load – and two equivalent power converters – representing the RES connected to the grid. The two separated generation units allow the (disaggregated) representation of units able to comply with limited frequency sensitivity modes (LFSM); either only over-frequency (LFSM-O), or both LFSM-O and under-frequency (LFSM-U). These components are connected to the transmission/distribution power substation through an impedance to represent the voltage drop along the grid.

Additional modelling details of the aforementioned equivalent structure are extensively presented in this paper [42]. The most significant improvement to the solution presented in D2.3 is the control of active power of the equivalent power converters, through the implementation of the LFSM functionality, for the purpose of being compliant with the ability of providing frequency containment support. In Figure 14-2 is presented an overview of the power converter's active and reactive power decoupled control loops.

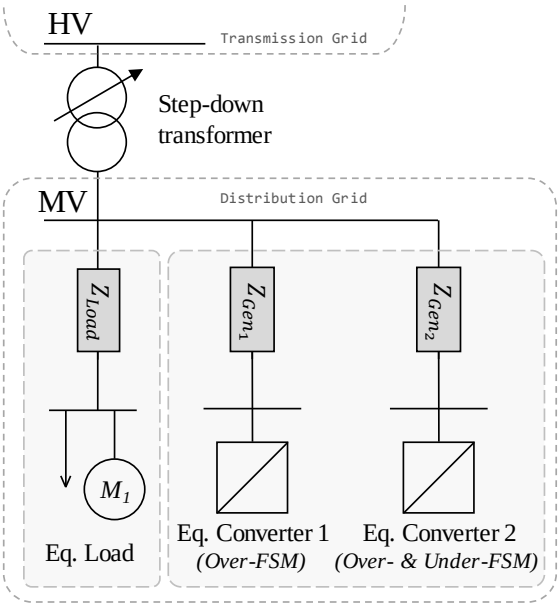

FIGURE 14-1: DISTRIBUTIONDISTRIBUTION NETWORK'S EQUIVALENT MODEL STRUCTURE.

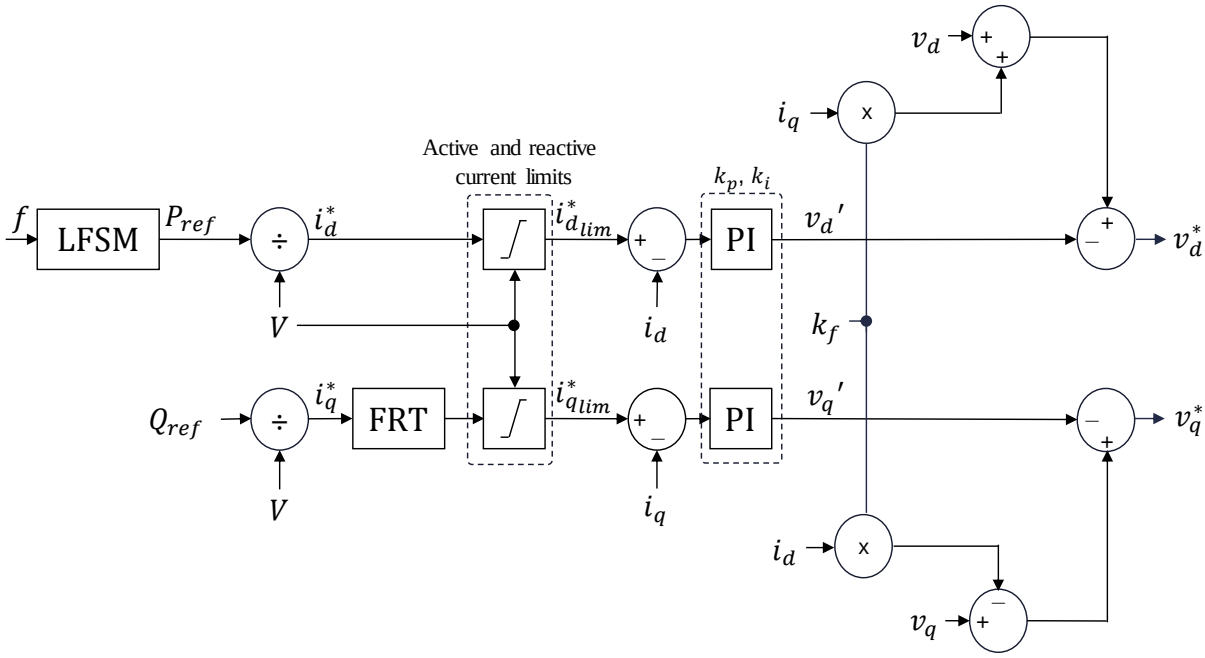

FIGURE 14-2: EQUIVALENT CONVERTERS' ACTIVE AND REACTIVE POWER CONTROL STRUCTURES.

The modelling structure lays on a standard *dq* representation, controlling the voltage components (v_d^*, v_q^*) to be fed to a controlled voltage source, responsible of providing the interface to grid (not represented in the scheme). The voltage set-points are controlled in order to follow active and reactive power references (P_{ref}, Q_{ref}). In this case, P_{ref} results from the new LFSM module, which aims to control the system frequency (f). Figure 14-3,

depicts the control structure of this module. According to the regulatory requirements for the connection of new generation units, and as it will be following depicted in the presented test case, the units may be required to provide only LFSM-O, both LFSM-O and LFSM-U, or simply none depending on the unit's size and voltage level where it is connected. The separation of the over- and under-frequency related phenomena on the control structure is then inevitable. For both cases, frequency excursions are contained using a proportional control with a gain of R_{LFSM-O} or $R_{LFSM-\mathrm{U}}$ (respectively for over- and under-frequency episodes), similar to the conventional generation's droop, and a first-order filter with a time constant of T_g. Also, in line with the regulatory requirements, the units are intended to be unresponsive to small frequency deviations (for up to ±0.5Hz, but considered to have a ±0.2Hz dead-band in this study), meaning a dead-band and respective limits are considered.

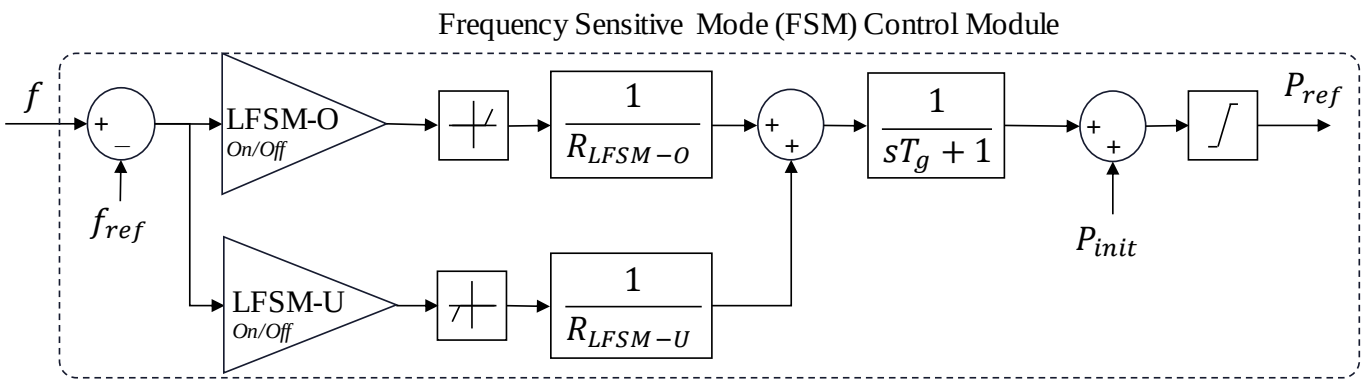

FIGURE 14-3: FREQUENCY SENSITIVE MODE CONTROL STRUCTURE, FOR OVER- AND UNDER-FREQUENCY MODES.

14.1 METHODOLOGICAL APROACH – AN OVERVIEW

Based on the methodological approach presented in D2.4, the proposed equivalent model was designed using a fully detailed distribution network model. The idea is to provide the detailed model with a set of frequency disturbances and record the dynamic behaviour of the active and reactive $(P_{det}(t), Q_{det}(t))$ power at the equivalency point (transmission to distribution power substation). The resultant timeseries are then fitted by the equivalent model, recurring to a heuristic-based optimization method, in this case an evolutionary particle swarm optimization (EPSO) algorithm. A schematic representation of the overall methodology is depicted in Figure 14-4.

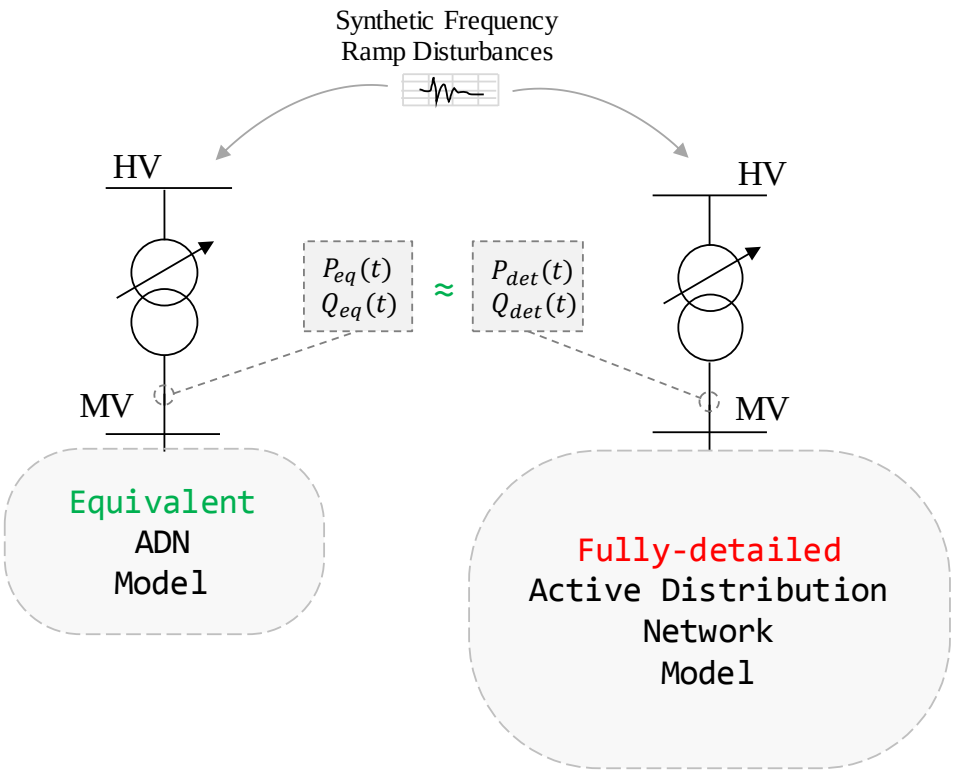

FIGURE 14-4: SCHEMATIC FOR THE DETAILED VS EQUIVALENT IMPLEMENTED APPROACH.

The equivalent model's state-variables under identification accounted for 33 parameters (summarized in Table 14-1). These proved to be efficient when adjusting the aggregated model's dynamic responses, as it is shown in the following section, while maintaining the computational time within acceptable limits. The selection of the variables' boundaries followed a trial-and-error approach.

TABLE 14-1 PAREMETERS PARAMETERS FOR EQUIVALENT MODEL FITTING.

Model	Description	Variable	No. of variables
Converters 1 & 2	Initial active and reactive power set-point	P_{ref}, Q_{ref}	4
	Share of converter 1 vs converter 2	$Share_{TUV}$	1
	Total generation apparent power	$S_{n_{gen}}$	1
	Droops (for over and under-frequency control)	R_{LFSM-O}, R_{LFSM-U}	4
	LFSM module time constant	T_g	2
	LFSM module dead-band for LSFM-O and LFSM-U	db_{LFSM-O}, db_{LFSM-U}	4
Impedances	Rate between resistance vs inductance	RL_{rate}	3
	Lines lengths	$LineLength$	3
Load	Static and dynamic loads initial power factor	$P_{SL_{pu}}, Q_{SL_{pu}}, P_{DL_{pu}}$	3
	Static load exponents, for load nature definition	n^p, n^q	2
	Dynamic load resistances and inductances	$R_s, L_{l_s}, R_r', L_{l_r}', L_m$	5
	Dynamic load inertia constant	H	1

14.2 TEST CASE DEFINITION

The test cases presented in this report were achieved using a fully detailed 72-buses distribution network, presented in Figure 14-5. The distribution network is operated radially at the MV level (30kV) and sums a total of 6.725MVA of load power and 30MVA of installed capacity from the generation units. Loads are divided into static and dynamic types, considering different parametrizations for improved diversity [44], being distributed randomly throughout the grid. The generation portfolio includes eleven converter-connected units (C1 to C11), also randomly connected to the grid. Due to their sizes and voltage level to which they are connected, all the units are LFSM-O compliant, agreeing with the required by the European grid codes (considered to be of type B generation [43]). Additionally, generator C1, which is directly connected to the MV side of the power substation, is also set to be able to provide LFSM-U (considered to be laying on the type C category [43]). For increased diversity, unit's LFSM control droops (see R_{LFSM-O} and $R_{LFSM-\mathrm{U}}$ in Figure 14-3) range from 2% to 9%, randomly defined for all the eleven units. Additional modelling details on the generation units, loads and lines can also be found in the previous mentioned documents [42] [43]. The HV network equivalent, upstream to the substation, was modelled as a constant voltage source at the 110 kV level, with a 3-phase short-circuit level, at base voltage, of 500MVA, and a X/R ratio of 5. The test system was implemented using the simulation platform of MATLAB®/Simulink ®.

The replicability of the responses of the detailed model by the proposed equivalent was assessed by imposing a set of ramps of synthetic frequency excursions. These synthetic frequency excursions were selected in order to reproduce a set of frequency excursion tends in face of a scenario where no detailed information on real system frequency excursions due exists. The maximum and minimum nadirs, respectively for over- and under-frequency, were kept constant and equal to 1.03pu (51.5 Hz) and 0.97pu (48.5Hz), respectively. The time to achieve the limit varied from nearly zero (simulation of a fast, step-like effect) to 6 seconds, every 1-second intervals. The six cases for over- and under-frequency episodes are depicted in Figure 14-6.

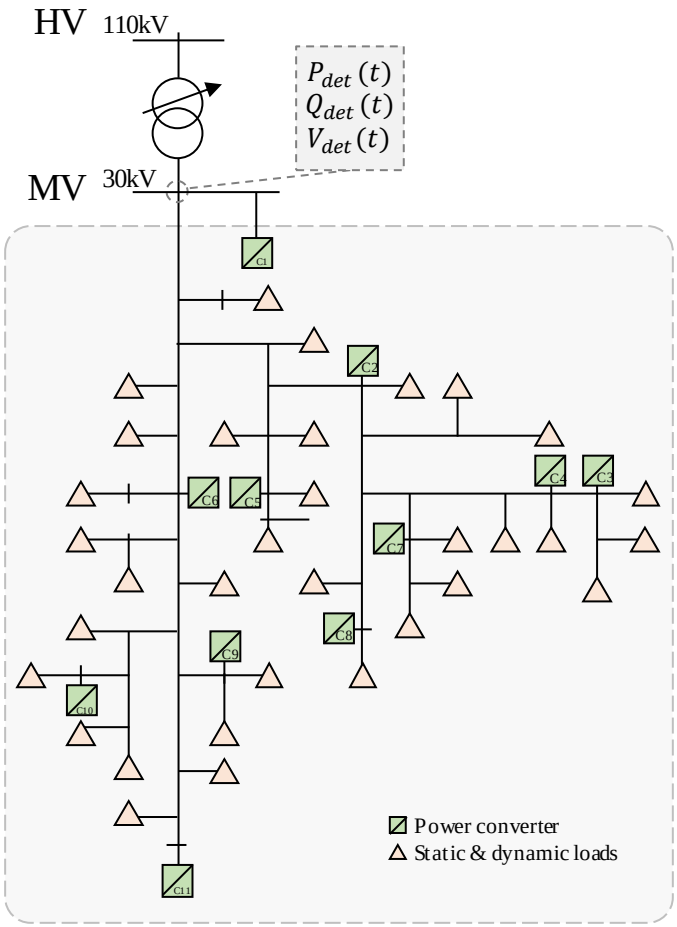

FIGURE 14-5: FULLY DETAILED DISTRIBUTION NETWORK CONFIGURATION.

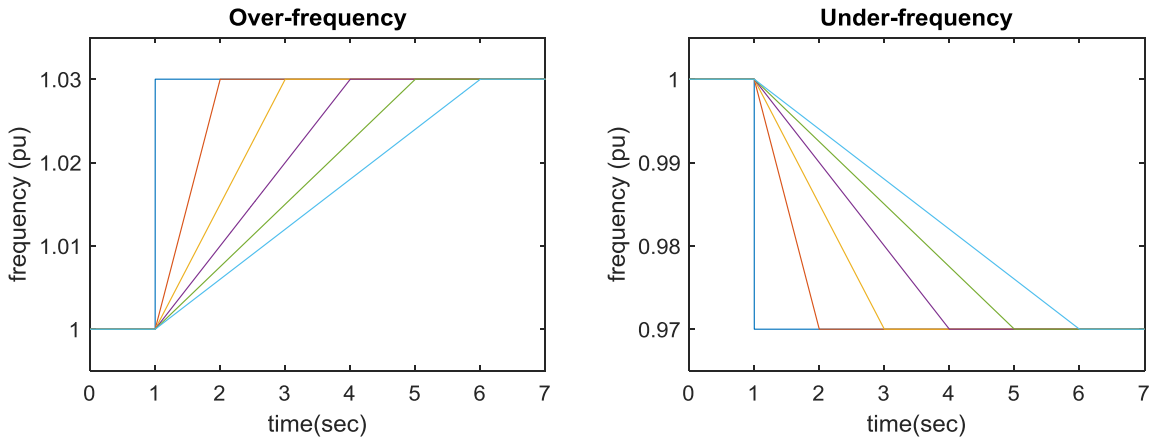

FIGURE 14-6: TEST CASES' OVER- AND UNDER-FREQUENCY VARIATION RAMPS.

14.3 RESULTS

The test cases and respective results were separated into two main sections, considering either over- or under-frequency cases. According to the previously presented methodology, the equivalent model was fitted to adhere to the detailed model responses, and it is important to stress that all the six frequency variations (see Figure 14-6) were considered at once per case, resulting in a single parametrization that suits all. Moreover, the methodology considered the aggregated fitting of both active and reactive power.

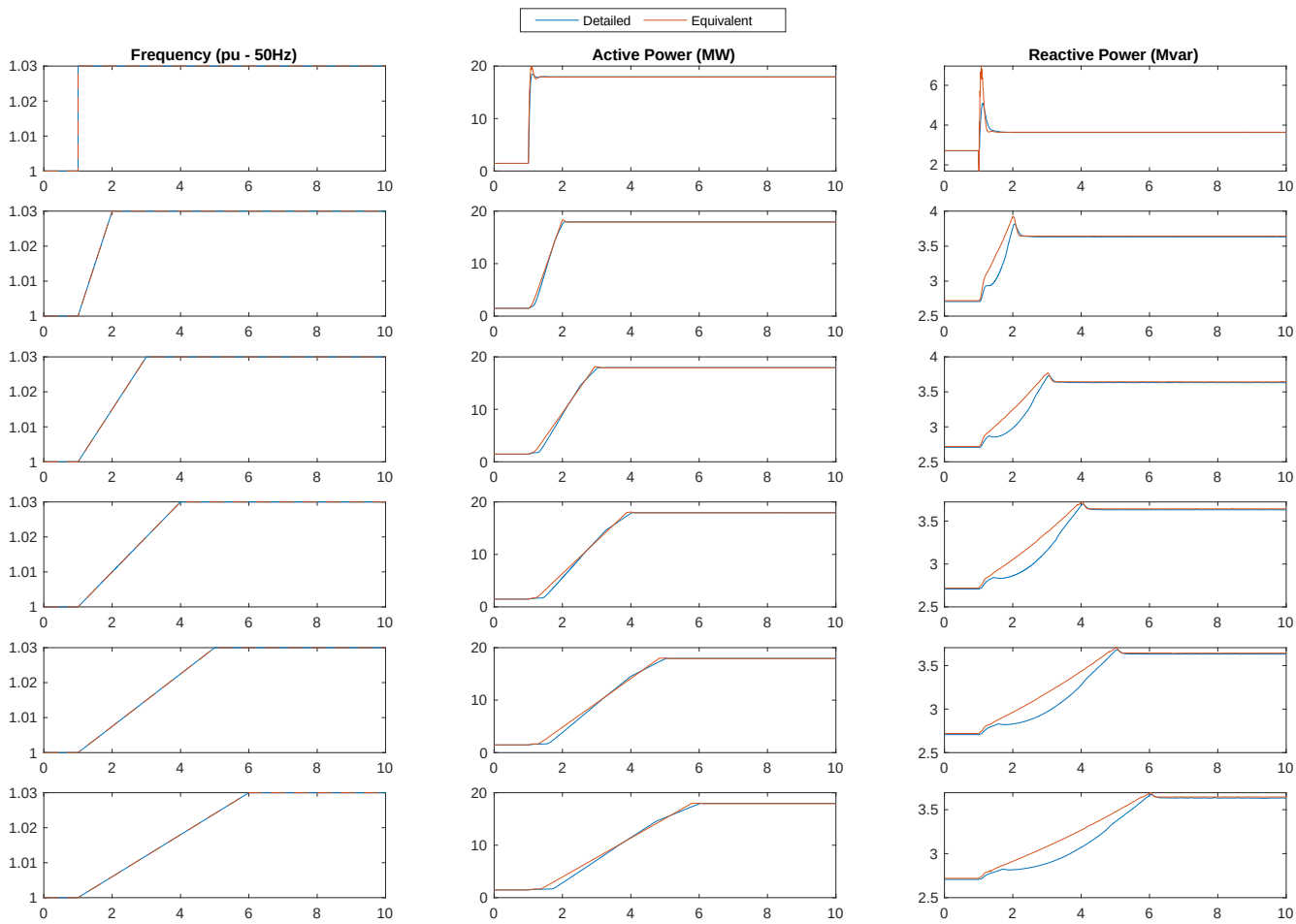

FIGURE 14-7: DETAILED VERSUS EQUIVALENT MODELS FOR OVER-FREQUENCY CASES.

Figure 14-7 and Figure 14-8 depict the results for over- and under-frequency, respectively, presenting vertically each of the frequency disturbance cases (see Figure 14-6), and horizontally the frequency case associated: active and reactive power. Both cases present a high level of adherence of the equivalent to the detailed model. For the over-frequency case, in Figure 14-7, the equivalent model almost fully captured the active power response for all the disturbances. The aggregated reactive power is also properly represented in its main tendencies – initial and final values, and overshoot before the final value is achieved, however, during the ramp, a slight delay was not

fully captured. The presence of voltage-dependent loads (both static and dynamic loads used in the detailed model) lead to a more complex dynamic behaviour that is not fully considered with this model reduction. Since the focus of this case is on frequency-related disturbances, a high adherence of active power is privileged.

A similar performance is achieved for under-frequency variations. For this case, as previously mentioned, only the power converter connected directly to the power substation is providing an active support to the frequency containment, meaning all the other units are operating at a constant-power mode. In this case, both active and reactive power present a high level of adherence from the equivalent model (Figure 14-8), being able to almost fully capture the whole aggregated responses from the detailed cases.

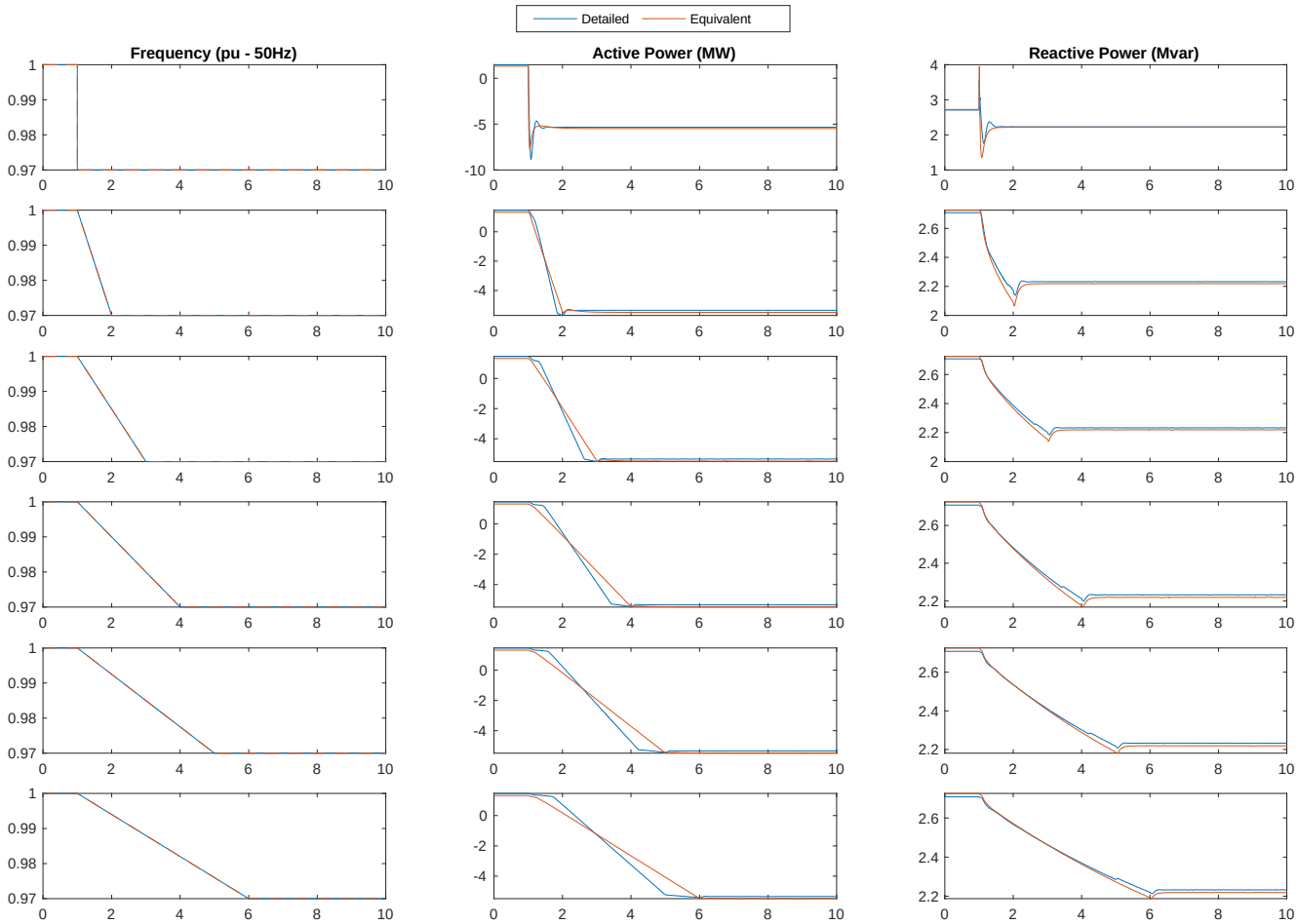

FIGURE 14-8: DETAILED VERSUS EQUIVALENT MODELS FOR UNDER-FREQUENCY CASES.